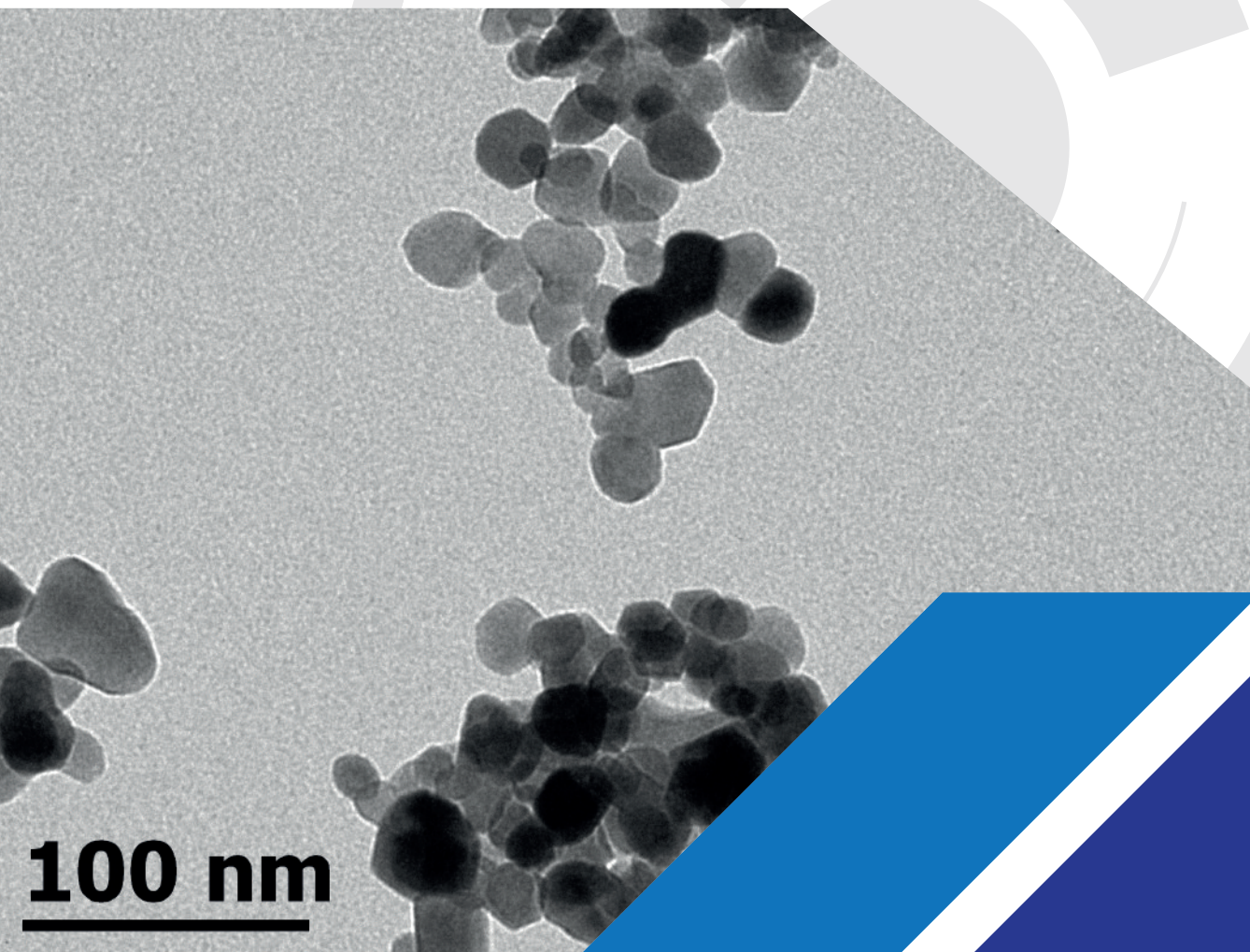




UNIVERSIDAD
AUTÓNOMA DE
QUERÉTARO

CONIIN

LOOKING FOR SOLUTIONS WITH APPLIED ENGINEERING



100 nm

FACULTAD DE INGENIERÍA



CONCYTEQ

CONIIN

LOOKING FOR SOLUTIONS WITH APPLIED ENGINEERING



CONACYT
Consejo Nacional de Ciencia y Tecnología



UNIVERSIDAD
AUTÓNOMA DE
QUERÉTARO

CONIIN

LOOKING FOR SOLUTIONS WITH APPLIED ENGINEERING

Directorio

Dr. Gilberto Herrera Ruiz
Rector

Dr. Irineo Torres Pacheco
Secretario Académico

Dra. María Guadalupe Flavia Loarca Piña
Directora de Investigación y Posgrado

Dr. Aurelio Domínguez González
Director de la Facultad de Ingeniería

MDM Carmen Sosa Garza
Secretaria Académica de la Facultad de Ingeniería

CP Guadalupe del Carmen Molinero González
Secretaría Administrativa de la Facultad de Ingeniería

Dr. Manuel Toledano Ayala
Jefe de Investigación y Posgrado de la Facultad de Ingeniería

Dra. Karen Esquivel Escalante
Director de la Publicación

Dr. Eduardo Arturo Elizalde Peña
Sub director de la Publicación

Consejo Editorial

Dr. Aurelio Domínguez González

Dra. Karen Esquivel Escalante

Dr. Eduardo Arturo Elizalde Peña

Dr. Carlos Guzmán Martínez

CONIIN: Looking for solutions with applied engineering, es una publicación anual de la Facultad de Ingeniería de la Universidad Autónoma de Querétaro, con arbitraje interno y externo (revista publicada desde el año 2016)

CONIIN: Looking for solutions with applied engineering, año 2, No. 1, (2017), es una publicación anual publicada por la Universidad Autónoma de Querétaro, por medio de la Facultad de Ingeniería, con domicilio en el Edificio A de la Facultad de Ingeniería, Cerro de las Campanas S/N, Col. Las campanas, C.P. 76010.

Editores Responsables:

Karen Esquivel Escalante, Eduardo A. Elizalde Peña y Carlos Guzmán Martínez.

Reserva de derechos al título exclusivo: en trámite

ISSN: en trámite

Certificado de Licitud y contenido otorgado por la Comisión calificadoras de Publicaciones y Revistas Ilustradas de la Secretaría de Gobernación (en trámite).

Se distribuye actualmente mediante descarga electrónica.

Informes y correspondencia: Edificio A, Facultad de Ingeniería, Universidad Autónoma de Querétaro, Cerro de las Campanas s/n, Col. Las Campanas, C.P. 76010, Querétaro-México. Tel: +52 (442) 192 1200 ext. 6016 y 65401.

GENERAL INDEX

General Index.....	i
<i>A New Approach to Estimate Fat and Protein in Cow’s Milk</i>	<i>1</i>
<i>Modal Model of Gas Turbines: Modal Model Using Measurements of Vibrations and Acoustic.....</i>	<i>4</i>
<i>A Literature Review of Different Ways to Perform a Pitch Control in Wind Turbines</i>	<i>9</i>
<i>Thermosolar temperature control system for aquaculture breeding</i>	<i>15</i>
<i>Graphs and Trees with Prototypes and Object Delegation</i>	<i>18</i>
<i>Detection System to Analyze Modulated Light Signals.....</i>	<i>24</i>
<i>Metaheuristic algorithms: Review and comparison.....</i>	<i>27</i>
<i>Synthesis of Hydroxyapatite Nanostructures by Hydrothermal Microwave Assisted Method and Characterization</i>	<i>36</i>
<i>ACI’s technology transference for arsenic and pathogens removal to supply safe drinking water</i>	<i>40</i>
<i>Phenotypical responses and DNA methylation changes on transgenic tobacco to CchGLP exposed to heavy metal stress.....</i>	<i>46</i>
<i>Chitosan electrospun nanofibers with Au/Ag Nanoparticles: Synthesis and Characterization</i>	<i>51</i>
<i>Molecular determination of Glomerella cingulata Penz in avocado Hass</i>	<i>57</i>
<i>Application of Entropy and Fractal Dimension for Automatic Diagnosis in Induction Motors.....</i>	<i>60</i>
<i>Timbe methanolic pod extract Acaciella angustissima’s Properties</i>	<i>65</i>
<i>Development of a particle swarm optimization algorithm applied to atmospheric pollutants.....</i>	<i>67</i>
<i>Bonding analysis for composite beams (mdf wood and steel) which are test by bending stresses: REVIEW</i>	<i>71</i>
<i>Comparison of traditional protein sources, soybean meal and fishmeal, with house cricket (Acheta domesticus): Review about proximate analysis and amino acids content.....</i>	<i>76</i>

<i>Design of a domestic irrigation system for a green roof</i>	84
<i>Biological System Modelling: Breast Cancer Marker Electrics Properties</i>	91
<i>Optimization of scheduling problems by coloring Planning Time Slots for Courses offered by the School of Engineering: A case study</i>	96
Estimating the basic reproductive number, using differential equations, for Dengue.....	101
Uses and applications of expanded polystyrene in construction	105
Production of Bean Straw Pellets with Maximum Energy Content.....	110
Electrostatic fermentation system for the production of bioethanol	114
Simulation and Assessment of Cable Tension Forces in a Cable-Stayed Bridge	118
Freight Trip Generation in Querétaro City, Mexico.....	124
Random Number Generator based on electrical noise and implemented on FPGA	130
Effect of density in leopard frog tadpoles (<i>Lithobates forreri</i>) under greenhouse	137
A hydroinformatics tool for data management and IDW interpolation	141
Effect of grazing time and natural feed additives on the quality of Ross 308 chicken meat	145
Antimicrobial activity of habanero pepper extracts under the influence of hydrogen peroxide	148
Sustainability in the Construction Industry: A Review of Recent Developments in Modular Systems	152
Diagnostic Methodology Based on Extraction of Statistical Indicators for Detection of Bearing Fault in Induction Motors	157
Analysis of Spatial Variability of Short-duration Storms for the Northwest Region of Querétaro City and the Metropolitan Area	163
Characterization of Mortar with Mineral Additives	168
Living walls: A little review trough this technology and the opportunities to innovate.....	171
Estimation of a probabilistic model for the count rate of a two stages outbound call center	176
Test of Lightweight Panel based on non-standard steel profiles under AISC-05LFRD and ANSI-01 LRFD	182

Physical properties analysis of strawberry grown in aquaponic culture.....	193
Mathematical modeling of leptospirosis in multiple hosts.....	197
Tour Planning for the Small Unmanned Meteorological Observer	203



A new approach to estimate fat and protein in cow's milk

Abraham Gastélum-Barrios

PhD Biosystems Engineering Student
Facultad de Ingeniería, Universidad Autónoma de Querétaro
Querétaro, México
abraham.gastelum@uaq.mx

Genaro Martín Soto-Zarazúa

Cuerpo Académico de Sistemas Embebidos y Aplicaciones
Facultad de Ingeniería, Universidad Autónoma de Querétaro
Querétaro, México
soto_zarazua@yahoo.com.mx

Daniel Járegui-Vázquez

Electronic Department DICIS, Universidad de Guanajuato
Salamanca, México
jaureguid3@gmail.com

Abstract—In this work, we present a new method to determine fat and protein content in cow's fresh raw milk. The new technique involves image processing and artificial neural networks. We are proposing different types of light used as primary source for the image processing in the ultraviolet, visible and infrared wavelengths. This advance, shows the methodology proposed to reach the primary objective: a new system to determine fat and protein using image processing.

Keywords—milk; protein; fat; determination; system

I. INTRODUCTION

Milk is a diluted emulsion formed by two phases, fat and oil dispersed, and a colloidal continual aqueous phase [1]. Is a worldwide consumed and nutritive food, its quality directly affects human health and its consume is increased every year [2]. México produces above 11.3 million of tons of raw milk every year, with an increasing index of 2.5% [3]. In average, cow's milk is composing of water (87%), fat (3.8%), protein (3.4%), lactose (4.5%) and other solids like minerals, vitamins and enzymes (1.3%) [4]. The compound analysis in foods has been the key in industrial processes improvement [5]. To keep an online monitoring system of the processes is indispensable for food industry, becoming in one of the principal targets in automated system development using artificial intelligence.

There are several systems for raw milk quality analysis, principally for fats and proteins. For the protein determination we can point from Dumas [6], Kjeldahl and Lowry method [5].

To determine total fat, we can use the Gerber [7] and Soxhlet method; also we can use techniques based in spectroscopy of near and medium infrared [8]. Commercial systems [9, 10] have been using, with these, we can perform rapid analysis of the milk samples in laboratory.

Currently, there are developing new techniques to estimate fat and protein indirectly, helping from image processing based in light scattering. Some new techniques are using temperature sensor and electric resistance [11], somatic cell count using a new biosensor [12]. Using CIELAB color space, developers found the relationship between viscosity and color in low fat milk [13]; the representation of every change in the color of raw milk [14]; related with the fat and protein content. A first approach to perform a quantitative analysis of fat and protein particles was using RGB color space [15], and months later, was improved using a different camera [16].

As we can observe, the development goes towards non-invasive systems to estimate food quality. In this work we present a new methodology to determine fat and protein content in raw milk using image processing techniques and Artificial Neural Networks (ANN)

II. MATERIALS AND METHODS

The project is being carried out in the experimental field of Amazcala Campus of the Engineering Faculty (20°42'23.0"N, 100°15'39.7"W, 1920 m a.s.l.). The methodology is separated in three blocks (Fig. 1).

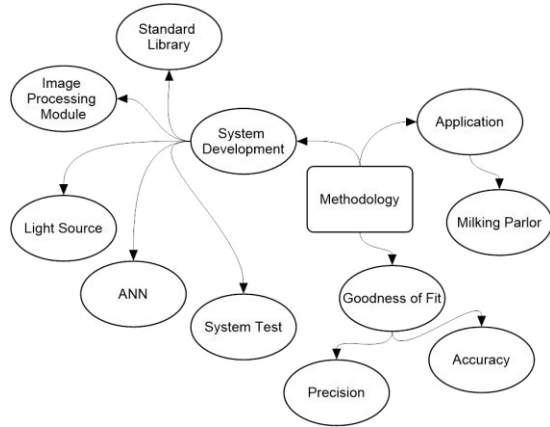


Fig. 1. Mental map of the methodology.

A. System development

The first stage of the present work, is to develop a new fat and protein analysis system, to get images from the milk samples and process it using image processing techniques and ANN.

1) Standard library

To have a standard library of known concentrations of fat and protein in milk, we are going to buy a standard solution (QSE GmbH and/or Eurofins DQCI), to obtain multiple solutions for system calibration, and validation steps. To get the standard curve, we are based in the method proposed in [15].

2) Image processing module

Since we are developing a unique platform, is necessary to have a special image capture system, where we can put the milk samples and the light source, besides the digital camera. We propose to use different types of cameras: ultraviolet (UV), light visible spectrum and infrared (IR) camera. Therefore, the image processing systems must have equipped a multiple camera support. The image processing module, has get communication with a personal computer, the cameras should have USB interface protocol, at least.

We propose a small cabin were we can add different types of light sources like UV; red, green and blue visible light spectrum (RGB), and IR.

3) Light source

A critical stage of the project, is the light source, and the image processing depends of the type selected. We were working initially with RGB lights, using light emitter diodes (LED), in the three basic colors: red (630 nm), green (536 nm) and blue (465 nm). Later, we are going to design a UV system in order to observe the variation in the perception of fat and protein globules, expecting to find relationships with this two phenomenon. A third approximation is the design and develop of two wide specter source, in collaboration with the Optic Laboratory of the Universidad de Guanajuato Campus Salamanca. The first, has the hypothesis that the biological elements reacts on wavelengths in the visible light, proposing

the scheme by [17] shown in the Fig. 2. The method includes a microchip laser generating pulses at 650 ps in a wavelength of 532 nm, the emitted light is polarized and focused by a quart of wave delay and a microscope objective. The light travels inside a solid core photonic crystal fiber (PCF), this interaction (light and fiber), produces a supercontinuum spectrum; inducing the emitted light onto the milk sample.

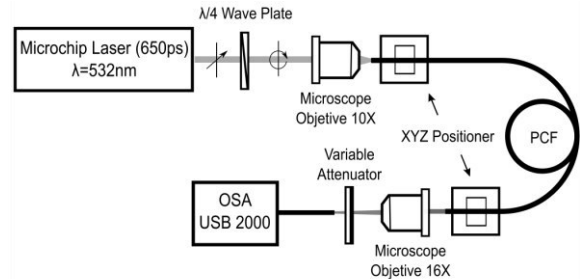


Fig. 2. Experimental scheme of the supercontinuum spectrum [17].

The second design, is to generate a medium IR laser, using the system shown in Fig. 2, we are going to change the microchip laser by a 1064 nm generator. With this proposed experiments we are expecting to analyze several options to select the best light source for the application we need.

4) Artificial Neural Network development

The previous experiment delivers a lot of data related with the content of fat and protein in raw milk. In order to process it, we are going to design an ANN. We are to train the network with the standard library data build previously. The ANN is having as entry signals the data exported from the image processing module.

5) System test

Once the ANN is trained, simulated and tested, we are going to test the system with the different milk samples in order to determine the functionality. In this part of the project, we expecting to establish the best method to determine the content of fat and protein in cow's raw milk.

B. Application

The second part of the proposed methodology is the installation of the system inside a parlor. In this point it will be necessary to design a special container with the capacity to have all the necessary elements determined in the previous step. The new cabin must be design and develop according to the safety of the present animals and has to sees indifferent to they.

C. Application

Once the ANN is trained, we are going to test the entire system to determine the goodness of fit, stablishing the accuracy and precision.

To finish the tests of the new method, we are get random samples of fresh cow's milk and tested by the system and the laboratory test in order to stablish statistical parameters.

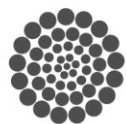


ACKNOWLEDGMENT

We thank to the CONACyT for the scholarship that make possible the present work.

REFERENCES

- [1] P. F. Fox, T. Uniacke-Lowe, P. L. H. Mcsweeney, and J. A. O'Mahony, *Dairy Chemistry and Biochemistry*, Second., vol. 1542, no. 9. 2015.
- [2] R. Alves da Rocha, I. M. Paiva, V. Anjos de Carvalho Dos Anjos, M. A. M. Furtado, and M. J. V. Bell, "Quantification of whey in fluid milk using confocal Raman microscopy and artificial neural network.," *J. Dairy Sci.*, pp. 3559–3567, 2015.
- [3] SIAP, "Boletín de Leche," 2016.
- [4] M. Pinto, E. Carrasco, L. Fraser, A. Letelier, and P. Dörner, "Composición química de la leche cruda y sus variaciones a nivel de silos en plantas lecheras de la VIII, IX y X regiones de Chile. Parte I. Macromoléculas," *Agro Sur*, vol. 26, no. 2, pp. 97–109, 1998.
- [5] A. O'Sullivan, B. O'Connor, A. Kelly, and M. McGrath, "The use of chemical and infrared methods for analysis of milk and dairy products," *J. Dairy*, vol. 52, no. 4, pp. 139–148, 1999.
- [6] X. Fu, M. Kim, K. Chao, J. Qin, J. Lim, H. Lee, A. Garrido-Varo, D. Pérez-Marín, and Y. Ying. "Detection of melamine in milk powders based on NIR hyperspectral imaging and spectral similarity analyses," *J. Food Eng.*, vol. 124, pp. 97–104, 2014.
- [7] X. Zhu, Z. Zhao, K. Qian, L. Wang, and X. Lan, "A rapid method for measuring fat content in milk based on W-type optical fibre sensor system," *Trans. Inst. Meas. Control*, pp. 1–9, 2015.
- [8] W. Xu, J. Bai, J. Peng, A. Samanta, Divyanshu, and Y.-T. Chang, "Milk quality control: Instant and quantitative milk fat determination with a BODIPY sensor-based fluorescence detector," *Chemical Communications*, 2014.
- [9] B. Aernouts, R. Van Beers, R. Watté, T. Huybrechts, J. Lammertyn, and W. Saeys, "Visible and near-infrared bulk optical properties of raw milk.," *J. Dairy Sci.*, vol. 98, no. 10, pp. 6727–38, 2015.
- [10] D. Wu, S. Feng, and Y. He, "Infrared spectroscopy technique for the nondestructive measurement of fat content in milk powder.," *J. Dairy Sci.*, vol. 90, no. 8, pp. 3613–9, Aug. 2007.
- [11] M. Sharifi and B. Young, "Milk total solids and fat content soft sensing via electrical resistance tomography and temperature measurement," *Food Bioprod. Process.*, vol. 90, no. 4, pp. 659–666, 2012.
- [12] W. Li, S. Liao, and C. Tsou, "Sensors and Actuators A : Physical A novel sensing chip with dual-coil inductance for determining raw milk quality," *Sensors Actuators A. Phys.*, vol. 241, pp. 96–103, 2016.
- [13] L. G. Phillips, D. M. Barbano, M. Lou McGiff, and H. T. Lawless, "The Influence of Fat Substitutes Based on Protein and Titanium Dioxide on the Sensory Properties of Lowfat Milks," *J. Dairy Sci.*, vol. 80, no. 11, pp. 2726–2731, 1997.
- [14] G. Grigioni, A. Biolatto, M. Irurueta, A. M. Sancho, R. Páez, and N. Pensel, "Color Changes of Milk Powder Due To Heat Treatments and Season of Manufacture Cambios En El Color De Leche En Polvo Debido a Tratamientos Térmicos Y Estación De Elaboración," *Cienc. y Tecnol. Aliment.*, vol. 5, no. 5, pp. 335–339, 2007.
- [15] S. Kucheryavskiy, A. Melenteva, and A. Bogomolov, "Determination of fat and total protein content in milk using conventional digital imaging," *Talanta*, vol. 121, pp. 144–152, 2014.
- [16] P. Jain and S. E. Sarma, "Light scattering and transmission measurement using digital imaging for online analysis of constituents in milk", *Proceedings of SPIE*, vol. 9525, 2015.
- [17] F. J. Valle-Atilano, J.M. Estudillo-Ayala, J.D. Filoteo-Razo, J.C. Hernández-García, D. Jáuregui-Vázquez, J.M. Sierra-Hernández, R. Rojas-Laguna, R.I. Mata-Chavez, and L.F. Samano-Aguilar. "Generation of supercontinuum light in micro-structured fiber and polarization study at different wavelengths", *Pocceedings of SPIE*, vol. 9958, p. 995817. 2016.



CONACYT

Consejo Nacional de Ciencia y Tecnología



CONCYTEQ



MODAL MODEL OF GAS TURBINES

MODAL MODEL USING MEASUREMENTS OF VIBRATIONS AND ACOUSTIC

X. H. Herrera

National Laboratory of Investigations and Cold
Technologies

Engineering Center for Industrial Development CIDESI
Querétaro, Qro. México
xherrera@posgrado.cidesi.edu.mx

E. E. Rodríguez

National Laboratory of Investigations and Cold
Technologies

Engineering Center for Industrial Development CIDESI
Querétaro, Qro. México
eloy.rodriguez@cidosi.edu.mx

Abstract— Grounded into the hypothesis that the airflow behavior into the gas turbine cycle excites pressure waves that can be monitored by the use of microphones and induces vibrations in solids that also can be measured by accelerometers; this work proposes a mathematical model for the pressures, temperatures and rotor speed. The mathematical model considers four modal models from: the acoustic behavior of the combustion chamber, as well as the modal vibrations from the rotor, and from two disks of blades one located at the compressor and the second one at turbine stage. The model proposed was fed with the experimental data gotten from a speed step test with a defined load torque. The simulation and comparison shows that proposed model works properly to predict the stabilization time and the magnitude of variables at steady state.

Keywords— *Gas turbine, modal model, vibrations, acoustics.*

I. INTRODUCTION

The gas turbine behavior as the Brayton thermodynamic cycle has been studied since this technology was invented. Several research works have implemented more efficient thermodynamic cycles for gas turbines by adding subsystems or increasing the components capabilities [1 – 3]; nevertheless, the dynamic modeling of gas turbines to synthesize and tune the control algorithms of commercial engines are simple according to the entire physical phenomenology that occurs while the energy transformation is realized through the thermodynamic system of the gas turbines [4, 5].

Due to the thermodynamic and mechanical nature of the gas turbine as dynamic system, its performance depends for much on the control algorithm definition and it is tuning in situ. Nowadays the controller tuning for gas turbines consider dynamic but spatially punctual measurements of the more important physical variables to protect the health of its

components, so that the control algorithm works like a kind of supervisor instead of a dynamic regulator [6 - 10].

It is not new that computational electronics has great data processing capabilities, which thanks to the advanced manufacturing and production process is increasing its availability and reliability and is also reducing its cost and size [11 - 13]. In this point, more capable electronic technology can be used on industrial controllers to regulate gas turbines behavior. Of course better performance needs optimization of resources use, and implies more robust and adaptable control algorithms which also need more accurate mathematical models like the one proposed here.

The hypothesis for the proposed model can be summarized as: "the dynamic performance of the gas turbines can be monitored by the use of vibrational and acoustic models from the compressor, rotor, combustion chamber and turbine." because the air flow behavior excites pressure waves that induce vibrations in solids or can be detected by microphones.

The proposed mathematical model here calculates the flow pressure and rotor speed magnitudes by considering a set of vibrational and acoustic modal models from: A disk of blades from the compressor stator and also from the turbine [14], the acoustic performance of the flame into the combustion chamber [15] and the lateral vibration of the rotor-bearing system [16]. This mathematical model has been fed with the numerical results gotten from an experimental characterization of a microturbine, which sustained a 300 N-m load.

The numerical results of the simulations model are compared with the ones gotten from the mentioned characterization test, which were acquired in real time by the means of an optical tachometer and pyrometer.

II. MATHEMATICAL MODEL

The Brayton cycle for pressure and temperature can be expressed as Fig 1.

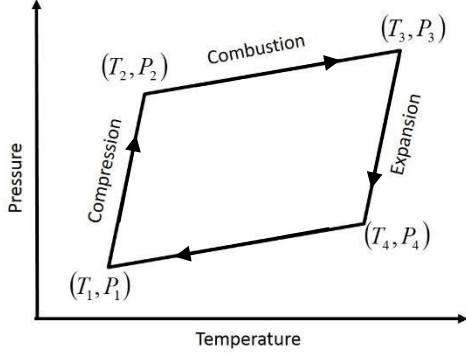


Fig. 1. Bryton cycle.

The dynamical model proposed was formulated from a single rotor microturbine, which is schematic is on Fig. 2. And its main objective is to follow the Brayton cycle, by solving the flow pressure and rotor speed based on the modal models that has been gotten experimentally [14 – 16].

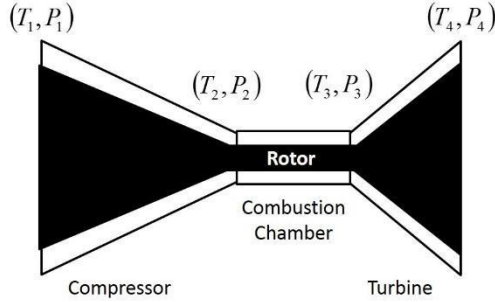


Fig. 2. Microturbine schematic.

The mathematical algorithm follows this steps:
The initial conditions from external ambient

$$\begin{aligned} P_0(t) &= P_1(t) = P_{atm} \\ T_0(t) &= T_1(t) = T_{amb} \end{aligned} \quad (1)$$

where: $P_1(t)$ is the input pressure and $T_1(t)$ the input temperature at the compressor, $P_{atm}(t)$ is the atmospheric pressure and $T_{amb}(t)$ is the ambient temperature.

The modal model for the output pressure from the compressor in terms of the vibrations from a special mounted blade disk

$$\mathbf{P}_2(t) = \mathbf{M}_1 \mathbf{x}_1(t) + \mathbf{B}_1 \dot{\mathbf{x}}_1(t) + \mathbf{K}_1 \mathbf{x}_1(t) \quad [14], \quad (2)$$

where: $\mathbf{x}_1(t)$ is the vibrations of the blade disk, $P_2(t)$ the output pressure from the compressor.

The thermodynamic relationship between pressure and temperature into the compressor

$$\frac{|\mathbf{P}_2(t)|}{P_1(t)} = K_c(t), \quad (3)$$

$$T_2(t) = K_c(t)T_1(t), \quad (4)$$

where: $T_2(t)$ is the output temperature of the airflow from the compressor.

The modal model of the lateral vibrations from the gas turbine rotor

$$\boldsymbol{\tau}_R(t) = \mathbf{M}_R \ddot{\mathbf{x}}_R(t) + \mathbf{B}_R \dot{\mathbf{x}}_R(t) + \mathbf{K}_R \mathbf{x}_R(t) \quad [15], \quad (5)$$

$$\boldsymbol{\omega}_R(t) = \cos^{-1} \left(\frac{\boldsymbol{\tau}_R(t)}{m_R g d} \right) \quad (6)$$

where: $\boldsymbol{\tau}_R(t)$ and $\boldsymbol{\omega}_R(t)$ are the rotor torque and speed respectively, $m_R g$ the rotor weight and d the rotor unbalance.

The air flow $q_A(t)$ control in terms of the rotor speed

$$q_A(t) = K_A |\boldsymbol{\omega}(t)|. \quad (7)$$

The fuel flow $q_c(t)$ need for a good combustion,

$$q_A(t) = K_C q_c(t) \quad 0.1 < K_C \leq 0.5. \quad (8)$$

The acoustic modal model from the combustion chamber

$$\mathbf{P}_3(t) = \mathbf{M}_2 \ddot{\mathbf{a}}_2(t) + \mathbf{B}_2 \dot{\mathbf{a}}_2(t) + \mathbf{K}_2 \mathbf{a}_2(t) \quad [16], \quad (9)$$

where: $\mathbf{a}_1(t)$ is the acoustic magnitude of the combustion chamber, $P_3(t)$ the output pressure from the combustion chamber.

The pressure relationship into the combustion chamber.

$$K_{Com}(t) = \frac{|\mathbf{P}_3(t)|}{|\mathbf{P}_2(t)|}. \quad (10)$$

The energy need to sustain the load torque $\boldsymbol{\tau}_C(t)$

$$Q_3(t) = \frac{K_{Com}}{K_{Com} - 1} |\boldsymbol{\omega}_R(t)| [|\boldsymbol{\tau}_R(t)| + \boldsymbol{\tau}_C(t)]. \quad (11)$$

The heat transfer into the combustion chamber,

$$Q_3(t) = C_3 \frac{d}{dt} T_3(t) + R_3 \{T_3(t) - T_0(t)\} \quad (12)$$

where: C_3 and R_3 are the heat capacitance and resistance of the combustion chamber thermal system.

The modal model from the vibration of a blade disk into the turbine,

$$\mathbf{P}_4(t) = \mathbf{M}_3 \mathbf{x}_3(t) + \mathbf{B}_3 \dot{\mathbf{x}}_3(t) + \mathbf{K}_3 \mathbf{x}_3(t) \quad [16], \quad (13)$$

where: $\mathbf{x}_3(t)$ is the vibrations of the blade disk at the turbine, $P_4(t)$ the output pressure from the turbine.

And the Pressure and temperature relationships into the turbine.

$$K_T(t) = \frac{P_4(t)}{P_3(t)} \quad (14)$$

, and

$$T_4(t) = K_T(t) T_3(t), \quad (15)$$

III. NUMERICAL SIMULATIONS

As above mentioned the mathematical model proposed was fed with the numerical results are from the experimental characterization, which was tested to sustain a 300 N-m torque load. These numerical simulations are compared with the experimental data acquired in real time by the means of an optical tachometer for the rotor speed and a pyrometer for the combustion chamber internal temperature.

The simulation results and their comparison with the experimental ones are shown in Figs. 3 to 9.

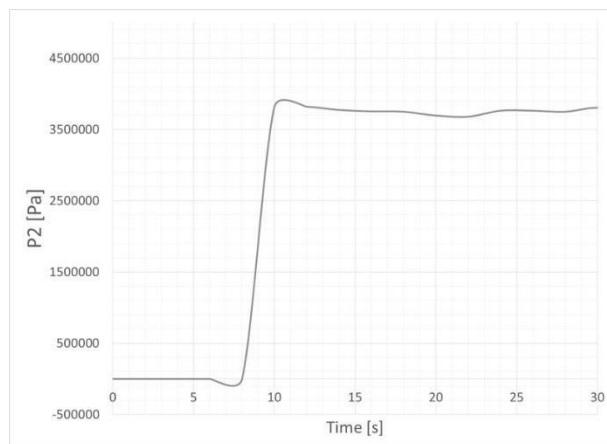


Fig. 3. P2 simulation.

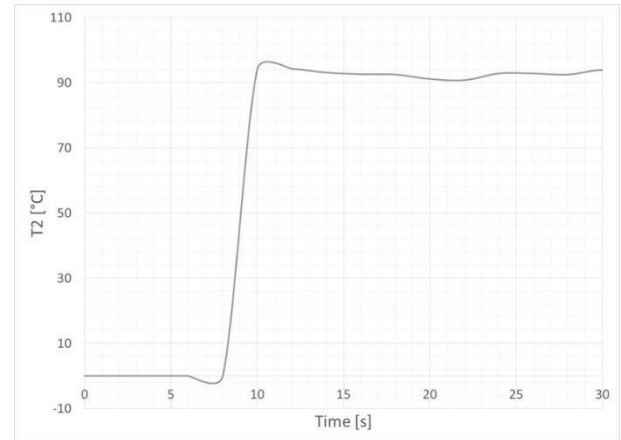


Fig. 4. T2 simulation.

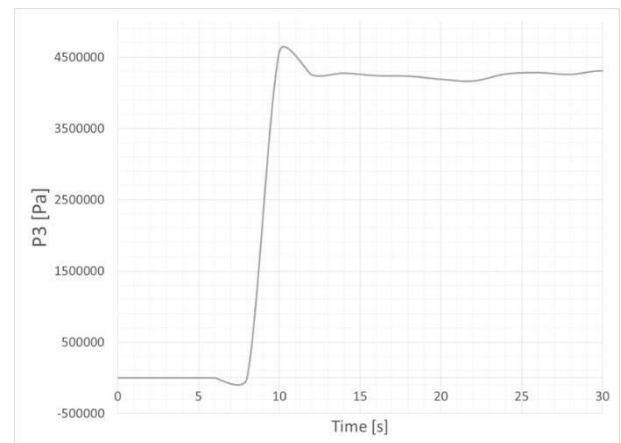


Fig. 5. P3 simulation.

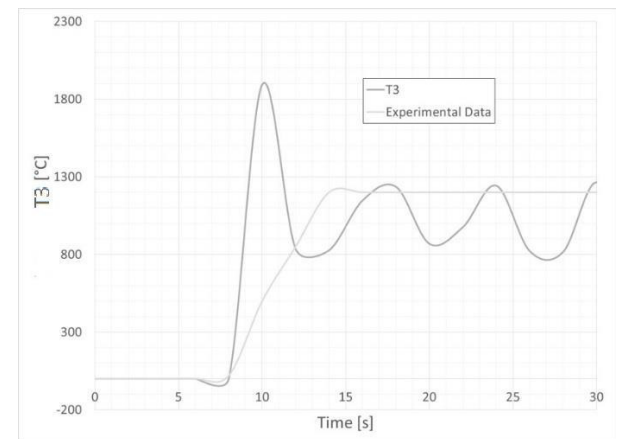


Fig. 6. T3 comparison.

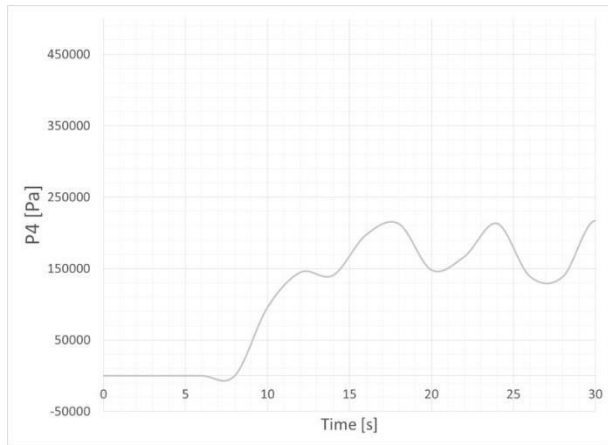


Fig. 7. P4 simulation.

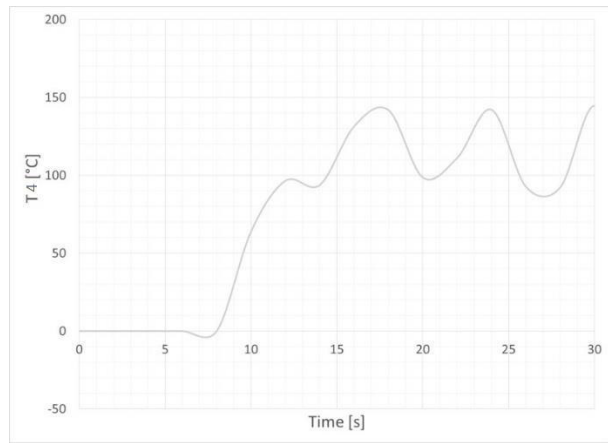


Fig. 8. T4 simulation.

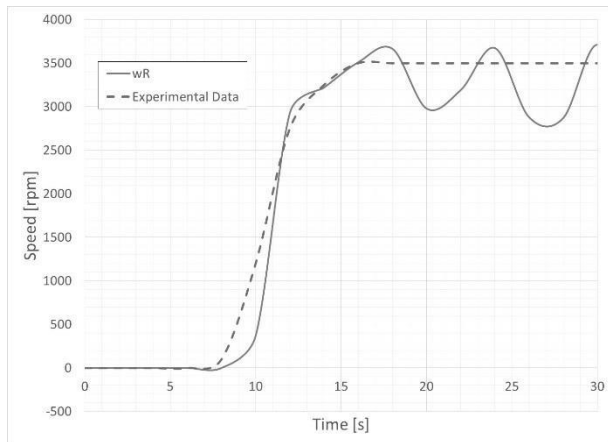


Fig. 9. Rotor speed comparison.

IV. RESULT ANALYSIS

As can be predicted, the linear domain for the variable relationships into the model, for a speed step of 3500 rpm the proposed model reacts as a linear system. Also due to the magnitudes of the calculated variables in steady state it looks that the model is working properly at least by considering the magnitude order.

At the beginning, most of the variables have constant behavior in steady state, but it looks like the performance of T_3 and ω_R make oscillate the rest of the model. So it is shown that the lateral vibrations of the rotor and the acoustic behavior of the combustion chamber have more height for this model prediction.

Considering the limitations of instrumentation to measure the dynamic evolution of the concerned variables during this test, Figs 3 and 9 show that the stabilization time is almost the same.

V. CONCLUSIONS

The numerical simulations of this model have shown that it works properly to predict the stabilization time and the magnitudes into the steady state for the speed rotor, pressures and temperatures. Then the hypothesis that the dynamical behavior of the gas turbine can be monitored by the use of vibrations has been validated.

Of course there is a lot of work to do to diminish the oscillations into the steady state prediction, and it looks like, the acoustic modal model from the combustion chamber and the modal model from the rotor vibrations have to be adjusted through more tests of dynamical performance.

ACKNOWLEDGMENT

The preferred spelling of the word “acknowledgment” in America is without an “e” after the “g”. Avoid the stilted expression “one of us (R. B. G.) thanks ...”. Instead, try “R. B. G. thanks...”. Put sponsor acknowledgments in the unnumbered footnote on the first page.

REFERENCES

- [1] P. Chiesa, E. Macchi, “A Thermodynamic Analysis of Different Options to Break 60% Electric Efficiency in Combined Cycle Power Plants”, ASME Turbo Expo 2002: Power for Land, Sea, and Air, Vol. 1: Turbo Expo 2002, ASME, GT2002-30663, pp. 987-1002.
- [2] B. Facchini, L. Innocenti, E. Carnevale, “Evaluation and Comparison of Different Blade Cooling Solutions to Improve Cooling Efficiency and Gas Turbine Performances”, ASME Turbo Expo 2001: Power for Land, Sea, and Air, Vol.3: Heat Transfer; Electric Power; Industrial and Cogeneration, 2001-GT-0571, pp. V003T02A025.
- [3] A. Simpson, C. Aalborg, M. B. Schmitz, R. Pannekeet, V. Michelassi, F. Larisch, “Application of Flow Control in a Novel Sector Test Rig”, Journal of Turbomachinery, 136(4), 041002, Sep 26, 2013, TURBO-12-1249.
- [4] M. Sunar, S. S. Rao, “Recent Advances in Sensing and Control of Flexible Structures Via Piezoelectric Materials Technology”, Applied Mechanics Reviews, Vol.52, Issue 1.
- [5] J. Bordeneuve-Guibe, C. Vaucoret, “Robust multivariable predictive control: an application to an industrial test stand”, Control Systems IEEE, Vol. 21, Issue 2.
- [6] D.W. Clarke, “Application of generalized predictive control to industrial processes”, Control Systems Magazine IEEE, Vol. 8, Issue 2,
- [7] S. Ziaran, M. Musil, O. Chlebo, “Determination of the Bearing Quality by Means of Vibroacoustic Response”, ASME 2015 Noise Control and Acoustics Division Conference at InterNoise 2015, , NCAD2015-5910, pp. V001T01A004.

- [8] C. Ozsoy, A. Duyar, ; R. Kazan, R. Kilic, “Power turbine speed control of the GE T700 engine using the zero steady-state self-tuning regulator”, Intelligent Engineering Systems, 1997. INES '97. Proceedings, 1997 IEEE International Conference on.
- [9] J. Frischbier; G. Schulze; M. Zielinski; G. Ziller; C. Blaha; D. K. Hennecke, “Blade Vibrations of a High Speed Compressor Blisk-Rotor: Numerical Resonance Tuning and Optical Measurements”, Proc. ASME. 78767; Vol. 5, V005T14A007,1996.
- [10] U. Haupt, K. Bammert, M. Rautenberg, “Blade Vibration on Centrifugal Compressors: Fundamental Considerations and Initial Measurements”, 85-GT-92, pp. V004T13A006, ASME 1985 International Gas Turbine Conference and Exhibit, Vol. 4.
- [11] J. A. Reed, A. A. Afjeh, “Computational Simulation of Gas Turbines: Part 1—Foundations of Component-Based Models”, Journal Eng. Gas Turbines Power 122 (3), pp. 366-376, 2000.
- [12] M. Amundarain, M. Alberdi, A.J. Garrido, Garrido, I., “Modeling and Simulation of Wave Energy Generation Plants: Output Power Control”, Industrial Electronics IEEE Transactions on Vol. 58, Issue 1.
- [13] L. Chi-Huang, T. Ching-Chih, “Adaptive Predictive Control With Recurrent Neural Network for Industrial Processes: An Application to Temperature Control of a Variable-Frequency Oil-Cooling Machine, Industrial Electronics IEEE Transactions on, 04/2008; 55(3):1366 - 1375.
- [14] Zúñiga H. J.(2015), Modelo modal para las vibraciones de un disco de alabes de un compresor de turbinas de gas en función del comportamiento dinámico del flujo de aire, Tesis de doctorado “draft”, CIDESI – PICYT.
- [15] Montoya L. A. (2015), Modelo modal sobre-muestreado en 3D para un rotor de una microturbina, Tesis de doctorado “draft”, CIDESI – PICYT.
- [16] Mejia I. (2015), Modelos modal termo-acustico de un compresor desarrollado para un microturbina de gas, Tesis de doctorado “draft”, CIDESI – PICYT.

A Literature Review of Different Ways to Perform a Pitch Control in Wind Turbines

Hugo Torres Salinas
Engineering school
UAQ
Querétaro, México
thugos@outlook.com

Dr. Juvenal Rodríguez Reséndiz
Engineering school
UAQ
Querétaro, México

Abstract— Currently finding efficient ways to generate electricity through renewable energy is one of the objectives pursued in many areas of study. The use of a wind turbine to transform the kinetic energy of the wind into mechanical energy which in turn will be transformed into electrical energy is one of the most popular ways to achieve this goal. In horizontal axis wind turbines a control method called pitch control is used, which consists in modifying the angle at which the wind affects the blades of the wind turbine, thus being able to control the speed of rotation of the generator as well as the output power when is connected to the mains. In this article we review different methods to perform the pitch control, using different ways from conventional PIDs to neural networks, fuzzy control, and genetic algorithms.

Keywords—pitch control, wind turbine, kinetic energy, generator

I. INTRODUCTION

In recent years there has been an increase in the generation of electrical energy from renewable energy sources, one of which is wind energy. In Mexico, for example, the generation of electricity through this renewable source increased more than 36% from 2014 to 2015 [1].

The conversion of wind kinetic energy into electrical energy is done by means of wind turbines, which transform this energy into mechanical energy which drives a generator that is in charge of producing electric energy. There are two types of them, of horizontal axis and vertical axis, being the first one that has gained more popularity.

Horizontal-axis wind turbines (HAWT) are those in which the axis of rotation of the equipment is parallel to the ground. This technology has advantages such as:

- Greater efficiency than vertical axis wind turbine (VAWT).
- Ability to adapt to different powers.
- They do not require connection to the electric network to be able to start.

However, the HAWT have the disadvantage that they require a control system to constantly change their position on the direction of the wind [2].

Due to the need to modify the position of the HAWT, the pitch control is implemented. The design of controlled wind turbines by pitch requires a highly developed engineering, to ensure that the blades rotate exactly the desired angle. In this type of wind turbine, the controller rotates the blades a little degrees each time the wind changes, to maintain an optimum angle that provides the maximum performance at all wind speeds.

Different ways to implement the control pitch have been developed, and in this work, the review of some of them is done. In the current literature there are many works that deal with pitch control, however it is not easy to find some that make a revision on the different ways of doing it, that is to say they focus mainly on a single one, which can be fuzzy logic, genetic algorithms, PID; that is why it was decided to perform this work which deals with all the techniques mentioned above and not only one, which will facilitate future researchers to have a quick access to information that would otherwise review each of the papers to obtain it.

II. LITERATURE REVIEW

In this section, we have presented a literature review of different authors in various domains. We have ordered the articles in chronological order regardless of the technique used to perform the pitch control, for this reason, it is possible to present in several sections the work of several authors even when they use similar techniques.

Zhang Xin-fang, XU Da-ping, and LIU Yi-bing presented a work where they showed an adaptive optimal fuzzy control that can fit all input and output sample data at arbitrary prescribing precision. These authors work with a controller consisting of two parts, a fuzzy identifier, and a fuzzy controller. Fuzzy identifier approximates the unknown nonlinear function using the adaptive fuzzy system. The system shown uses the algorithm of the nearest neighbour clustering learning. The results showed by simulations demonstrated that this algorithm can realize smooth and asymptotic rotor speed reference tracking. At low wind speed, captured power is maximized, and at high wind speed, output power is kept at nominal value [3].

Lin Yonggang, Li Wei, Cui Baoling, and Liu Hongwei presented a work in 2006, they based their work on two models switched predictive pitch control algorithm for wind turbine. They use support vector regression (SVR) for identifying the model of the wind turbine. Nevertheless, the model can change in fieldwork, so the authors adopted an incremental learning algorithm for SVR online identification. They compared the performance of their controller with that of a conventional Proportional-Integral-Derivative (PID), and the results showed that the maximum tolerance of power output decreased from 10% to 3% [4].

Amêndola and Gonzaga used a fuzzy logic control system [5]. They justified the use of this controller because the fuzzy logic-based controllers have shown better performance in applications where the systems can show non-linear behavior, which is precisely what the wind turbine does, in addition to the stochastic nature of the wind which is another factor in selecting this controller. The eolic-energy capture controller determines the pitch angle variations " $\Delta\alpha$ " from the turbine output power " P_g ," from output power variations " ΔP_g ," and from the pitch-angle " α ." Also, they implemented another controller based on fuzzy logic too; this additional controller has the objective of controlling the speed of the wind turbine, unlike the first controller whose objective is to control the generated power. The results that they obtained demonstrated that the presented control system permits a smooth and stable operation to the turbine, under several wind regimes, since the weak winds, until those most intense and turbulent winds.

Feng Gao, Daping Xu, and Yuegang Lv presented in 2008 a work in where they showed the performance of a controller that uses the combination of fuzzy logic with a Proportional-Integral (PI) control [6]. Fuzzy control can not depend on the mathematical model, so it solves the problem of modeling wind turbine system including feed forward control. And PI control was introduced to promote the control precision of the compound system. The investigators erase the influence on control quality because of variable wind speed because they

use the wind speed as forwarding feed signal. The controller enhances rapidity and anti-interference capability of pitch system. The simulations showed high performance and produced a good response in cases of highly nonlinear systems such as wind turbine systems, in spite of the existence of the random and unacceptable disturbance such as wind speed.

Unlike the works presented in this paper until this moment, in 2008 [7] proposed a control with independent blade pitch regulation and a self-tuning regulator (STR) for generator torque control. The control proposed by them is exercised through two schemes: independent blade pitch control, and generator torque control. The devised strategy ensures active power control for optimal conversion and alleviation of torsional loads on the power train. The goal of individual pitch control concept is that the pitch of each blade is adjusted individually in response to measured loads, with the added advantage that the failure probability of the system is significantly reduced even if one of the blades failed. The researches want to reduce asymmetric loads that emanate from wind speed fluctuations across the rotor disc that are significant due to increased size of blades and turbulent eddies.

Xin-yan Zhang, Jing Cheng, and Wei-qing Wang used a technique in 2008 that uses a combination of fuzzy control (FC) and neural networks (NN) to control the blade of wind turbine generator system (WTGS) [8]. They use NN to get the proper pitch angle under large wind speed and so to get the proper power coefficient C_p . The control proposed by the authors is showed in Fig. 1. The results showed that variable speed WTGS can obtain smooth, steady output power and generator rotation speed. Under low wind speed, the rotation speed of wind turbine can be controlled to trace the optimum power and so the wind turbine can get the biggest energy by using FC. Under high wind speed, the output power can be controlled not to exceed the rated power by using two NN.

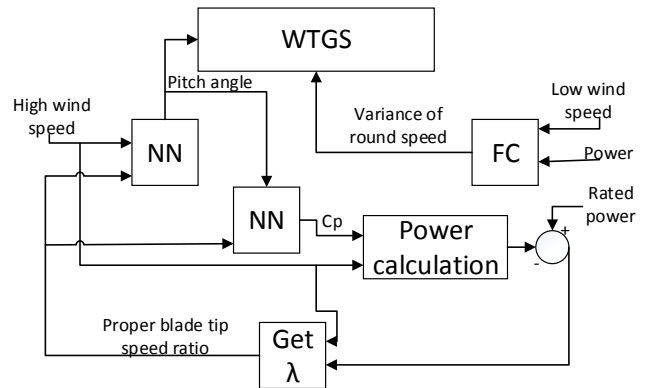


Fig. 1. Simulation block diagram of variable speed WTGS.

Also in 2008 Yanping Liu, Shuhong Liu, Hongmei Guo, and Huajun Wang used an artificial neural network to obtain more accurate pitch angle reference value, this angle can be predicted by trained neural network model. The corresponding pitch angle value can be identified as long as input the immediate wind speed. They used three methods of neural calculation; those methods are back-propagation (BP) algorithm, Radial Basis Function Network (RBF) and Levenberg-Marquard (LM) algorithm. The results showed that

the neural network based on LM algorithm is better than the neural network based on BP algorithm in the training speed and precision approach, and RBF neural networks is better than BP network in the ability of generalization. The Fig. 2 shows the scheme of the control proposed by [9].

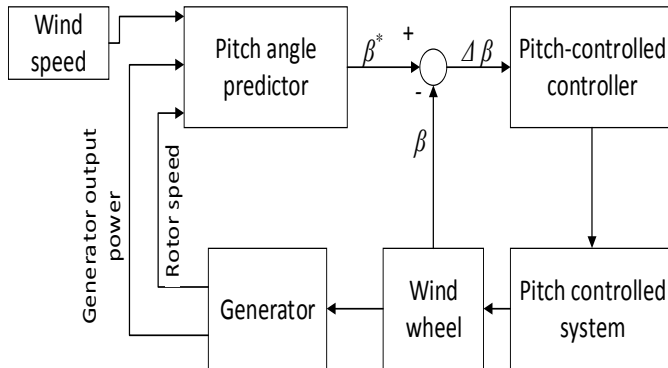


Figure 2. Control diagram of the pitch-controlled wind turbine

Hitoshi Takaai, Yuichi Chida, Kimi Sakurai, and Takashi Isobe proposed in 2009 a less conservative robust control [10]. The authors propose a robust control method based on the H_∞ , that is used in control theory to synthesize controllers achieving stabilization with guaranteed performance. However, it is well known that designed controllers by using the standard H_∞ design provide conservative performances and that is why the authors proposed a less conservative robust control. The control performances were evaluated by the authors based on numerical simulations by using the non-linear simulator “Bladed”. They verified that the proposed method provides superior performances under the allowable loads on a wind turbine to a standard H_∞ control. And also, the performances of the proposed method are almost equivalent to those of a gain scheduling PI control.

Another work using a neural network was presented in 2009 by [11], this time in combination with PID control. The method proposed uses a BP algorithm like in [10], and the goal of the control is to solve non-linear, parameter time changing, anti-disturb and time-lag problems. The technique used by the authors is an improved neural network control method applied to PID control and combined with traditional PID control. It is a kind of improvement and optimization of traditional PID control. The results obtained showed that wind turbine with neural network controller significantly improves the flexibility of transmission system and stability of output at high wind speed. The diagram of the control used by the authors is shown in Fig. 3. The researchers also concluded that the control system becomes more complicated with Neural Network Controller, but it is still considered a reasonable and preferable choice with the dynamic characteristic.

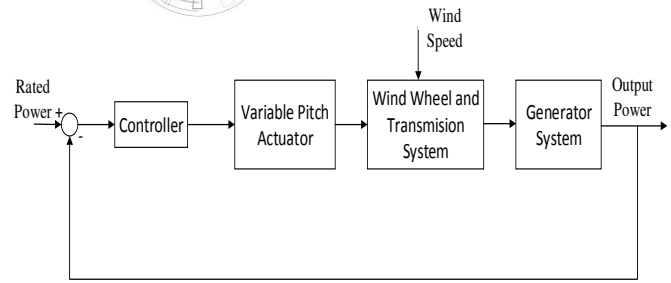


Fig. 3. Block diagram of Neural Network control system.

In 2009, Xingjia Yao, Changchun Guo, and Zuoxia Xing presented a control scheme based on fuzzy logic for adjusting the turbine speed so as to track the maximum power point. In this work, the researchers propose a controller that apply small changes in the speed command at regular intervals, and monitors the corresponding changes in the actual speed ($\Delta\omega_m$) and generator output power (ΔP_G) the scheme is showed in Fig. 4 [12]. In this paper optimum fuzzy control of wind turbine to extract maximum power is described and verified through the simulation. The main goal of implemented fuzzy controller is to continuously adapt the rotational speed of the generator to the wind speed in a way that the turbine operates at its optimum level of aerodynamic efficiency. The results obtained through simulation showed that the implemented system had satisfactory static and dynamic performances.

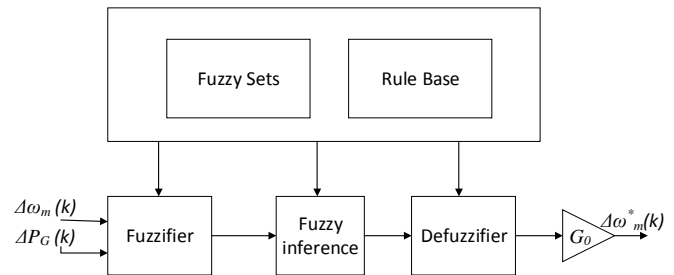


Fig. 4. Block diagram of the fuzzy controller.

In 2010 Guo Peng changed the conventional PID by adding a non-linear feedforward controller [13] the systems is showed in Fig 5, where β_r is the pitch angle setpoint. They used numerical calculation and least square polynomial fit to create the nonlinear model between pitch angle and wind speed according to the rotor’s aerodynamic characteristic. Then they add feed forward pitch controller based on the nonlinear model obtained previously. The simulation showed that this new pitch control strategy could quickly compensate the disturbance of wind speed and reduce the overshoot and regular time.

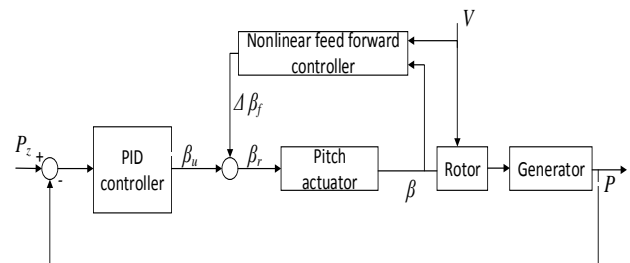


Fig. 5. Diagram of new control pitch strategy.

Mina Zaher and Hani Hagrass presented in 2010 [14] a method to generate a type-2 fuzzy logic model entirely from data to provide a dynamic footprint of uncertainty for the generated fuzzy set. They used the fuzzy model for predicting the wind speed experienced by a wind turbine without the use of sensors. This estimated wind speed is then passed to another fuzzy controller that changes the pitch angles of the wind turbine blades in order to track the maximum power available. They choose type-2 fuzzy logic because of it provides robust control performances when there exists a high level of uncertainty. The results displayed the importance and role of the footprint of uncertainty. They found that that as the footprint of uncertainty size decreases, the type-2 fuzzy logic model will act similar to type-1 fuzzy models. The type-2 fuzzy logic model systems are described in Fig. 6.

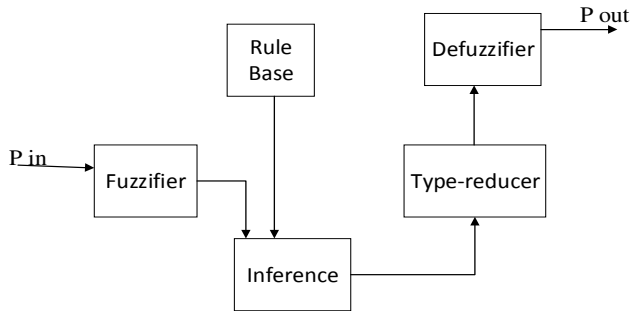


Fig. 6. The Type-2 Fuzzy Logic System.

In 2011 Maurizio Cirrincione and Marcello Pucci proposed a maximum power point tracking (MPPT) technique for variable pitch wind generators, which can suitably be adopted in both the maximum power range and the constant power range of the wind speed [15]. The proposed methodology had been verified both in numerical simulation and experimentally on a properly devised test set-up. The authors obtained results that showed the good behavior of the system, permitting the maximum generable power to be extracted at low wind speeds and making the system work at the machine rated power at high wind speed with proper control of the blade pitch actuators.

Also in 2011 Andrew Kusiak and Zijun Zhang presented a technique where data-mining algorithms were utilized to generate models of wind turbine power generation and the wind power prediction model. An integrated model with a linear combination of weighted objectives was created. The weights associated with the objectives were estimated based on the predicted power and demand. The demand was generated from two simulation models [16]. In this work, a wind turbine is an optimized subject to the following two objectives: power maximization and minimization of the torque ramp rate. A weighted linear combination of the two objectives is used in the bi-objective optimization model. Three models, the wind turbine power generation, the wind power prediction, and the electricity demand are established to realize the adaptive control framework in Fig. 7 the structure of the control is shown.

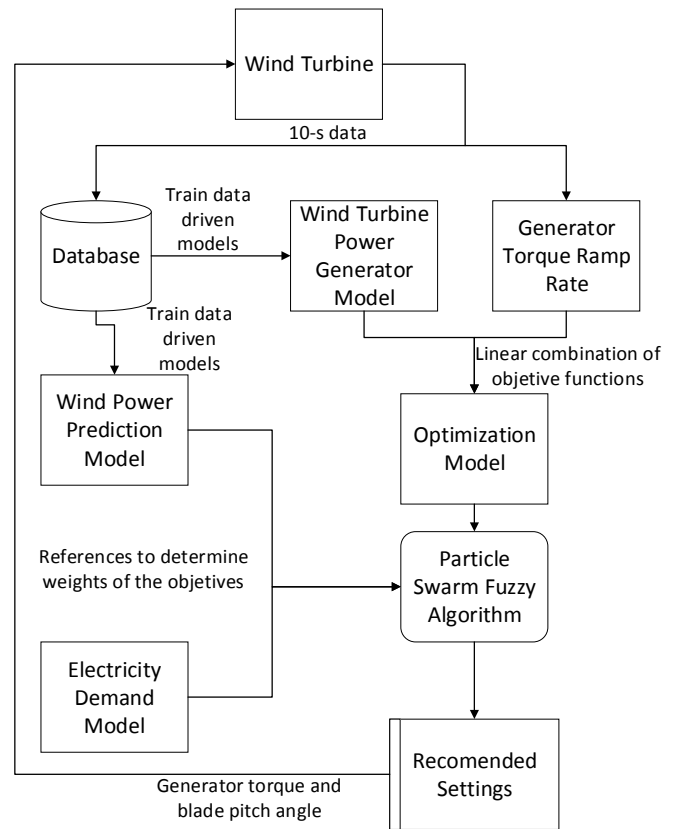


Fig. 7. The structure of adaptive wind turbine control.

Just like in [7] Feng Gao presented in 2012 a technique of individual pitch control [17]. In this work, the Pitch angle was distributed by weight coefficient to realize individual pitch control. The weight coefficient was computed according to the computed axial load based on blade element theory, at the same time the blade elements were divided by weight coefficient to ensure the real-time request for control algorithm. The advantage that the authors mentioned is that unlike the collective pitch control, the individual pitch control allows to optimize the angle of pitch individually depending on the speed that is present in each blade of the wind turbine, therefore reducing also the load in these blades, this is achieved because the collective pitch control works under the premise that the wind speed is the same throughout the rotor, ie the same in each blade, while the individual pitch control works considering a different speed in each blade.

A combination of fuzzy logic with PI to perform pitch control was used in 2014 by [18]. The paper proposed a new fuzzy logic for pitch control considering its effect on the grid. The prime step is to change the angle of the pitch so that it helps to produce maximum energy underrated speed, but at the same time it is to observe that the pitch variation is not so rapid to induce oscillation in the supplied power. The authors compared the result of fuzzy-PI with a typical PI controller, and they found that fuzzy-PI provides a better operating condition for wind turbines integrated with the short transmission line. The transient response provided by the

fuzzy-PI control system was found to be better than classical PI control.

Another combination of fuzzy logic, this time, with PID, was used in 2014 by [19]. In the paper, the authors developed a mathematical model for pitch control system and proposed a fuzzy adaptive PID controller to deal with the control of pitch system with disturbances and uncertain factors. The auto tuning of proportional, integral and derivative constants are performed using a fuzzy controller for optimum response. The Fig. 8 shows the structure of fuzzy-PID control. By using fuzzy adaptive PID controller, where the PID gains are tuned by using fuzzy logic concepts, the results showed that this design could effectively suppress the steady state error and the system has a minimum delay time, fast rising, quick settling, and stability. The investigators conclude that their controller can provide a fast response to a step unit input and can guarantee the stability of wind turbine output power.

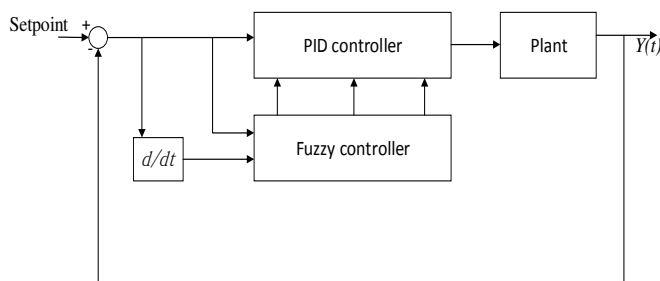


Fig. 8. The structure of fuzzy-PID.

A technique of pitch control of wind turbine based on RBF neural network was presented in October 2014 by [20]. This work gets the original nonlinear system model of the global linearization first, then by radial function neural network to approach uncertainties, combined sliding mode control with backstepping method to designed back stepping sliding-mode controller. The designed controller was compared with traditional sliding mode controller, the results obtained with simulation indicated that their designed controller could stabilized the output power of wind turbines and improved the performance of wind turbines variable pitch system effectively.

The last work to be reviewed in this paper is the one presented in 2016 by [21]. In their study, a new Intelligent Genetic Algorithm (IGA) algorithm approach has been suggested for the PID parameter setting optimization of the blade pitch controller. The authors chose IGAs because they are optimization methods and they have an ability to look for multi-point solutions. After testing the controller using MATLAB/Simulink, they observed that the IGA was better than Ziegler-Nichols GA being classic PID parameter calculation method in the PID parameter optimization. The final results showed the system optimized by the IGA gave a better efficiency about 17% than the system optimized by the GA.

III. CONCLUSION

Given the need to control the position in the HAWT, a technique called control pitch is developed, which modifies the angle of the blades of the wind turbine to modify the way in which the wind affects them, for this reason, the control can control the speed in the wind turbine as well as regulate the output power.

The approach in this paper is to deal with works of both collective pitch control and individual pitch control. The first works under the premise that the airflow is the same in each of the wind turbine blades, so the blades move the same angle, and the second consider a specific angle for each blade depending on the characteristics presented in which and is because of this that collective pitch control has the advantage of load reduction in the blades.

Several methods were approached but all of them uses the peculiarity of using a technique to predict the model of the wind turbine and thus be able to overcome its non-linear behavior. For this case fuzzy logic was one of the techniques preferred by the authors thanks to its good behavior on systems that present a high degree of uncertainty, although other methods such as genetic algorithms, neural networks, and combinations of these showed a very good behavior.

It was demonstrated in each of the works that the PID control is not a method that guarantees a good performance in comparison to the methods used by the researchers, mainly due to the inability to overcome the uncertainty that presents the behavior of the wind turbine.

REFERENCES

- [1] S. de Energía, "Reporte de avance de energías limpias 2015." p. 21, 2016.
- [2] R. Howell, N. Qin, J. Edwards, and N. Durrani, "Wind tunnel and numerical study of a small vertical axis wind turbine," *Renew. Energy*, vol. 35, no. 2, pp. 412-422, 2010.
- [3] Z. Xin-fang, X. Da-ping, and L. Yi-bing, "Adaptive optimal fuzzy control for variable speed fixed pitch wind turbines," *5th World Congr. Intell. Control Autom. (IEEE Cat. No.04EX788)*, vol. 3, pp. 2481-2485, 2004.
- [4] Y. Lin, W. Li, B. Cui, and H. Liu, "Two models switched predictive pitch control for wind turbine based on improved incremental SVR," in *Proceedings of the World Congress on Intelligent Control and Automation (WCICA)*, 2006, vol. 2, pp. 7498-7502.
- [5] C. A. M. Amêndola and D. P. Gonzaga, "Fuzzy-logic control system of a variable-speed variable-pitch wind-turbine and a double-fed induction generator," in *Proceedings of The 7th International Conference on Intelligent Systems Design and Applications, ISDA 2007*, 2007, no. Point D, pp. 252-257.
- [6] F. Gao, D. Xu, and Y. Lv, "Pitch-control for large-scale wind turbines based on feed forward fuzzy-PI," in *Proceedings of the*

- World Congress on Intelligent Control and Automation (WCICA), 2008, pp. 2277–2282.
- [7] E. B. Muhando, T. Senjyu, E. Omine, T. Funabashi, and C. H. Kim, “Design for MW-class variable speed WECS with independent blade pitch regulation,” in *PECon 2008 - 2008 IEEE 2nd International Power and Energy Conference*, 2008, no. PECon 08, pp. 413–418.
- [8] X. Zhang, J. Cheng, and W. Wang, “The intelligent control method study of variable speed wind turbine generator,” *2008 IEEE Int. Conf. Sustain. Energy Technol.*, pp. 173–177, 2008.
- [9] Y. Liu, S. Liu, H. Guo, and H. Wang, “The estimation of wind turbine pitch angle based on ANN,” in *ICINIS 2009 - Proceedings of the 2nd International Conference on Intelligent Networks and Intelligent Systems*, 2009, pp. 581–584.
- [10] H. Takaai, Y. Chida, K. Sakurai, and T. Isobe, “Pitch Angle Control of Wind Turbine Generator using Less Conservative Robust Control,” *Science (80-.)*, pp. 542–547, 2009.
- [11] Z. Xing, Q. Li, X. Su, and H. Guo, “Application of BP Neural Network for Wind Turbines,” in *Second International Conference on Intelligent Computation Technology and Automation*, 2009, pp. 42–44.
- [12] X. Yao, C. Guo, Z. Xing, Y. Li, and S. Liu, “Variable Speed Wind Turbine Maximum Power Extraction Based on Fuzzy Logic Control,” in *2009 International Conference on Intelligent Human-Machine Systems and Cybernetics*, 2009, vol. 2, pp. 202–205.
- [13] P. Guo, “Nonlinear feed forward pitch controller for wind turbine based on rotor’s aerodynamic characteristic,” in *2010 International Conference on Machine Learning and Cybernetics, ICMLC 2010*, 2010, vol. 2, no. July, pp. 879–883.
- [14] M. Zaher and H. Hagrass, “Data generated type-2 fuzzy logic model for control of wind turbines,” in *Intelligent Systems Design and Applications (ISDA), 2010 10th International Conference on*, 2010, pp. 80–85.
- [15] M. Cirrincione and P. Marcello, “Neural MPPT of variable pitch wind generators with induction machines in a wide wind speed range,” *2011 IEEE Energy Convers. Congr. Expo.*, pp. 857–864, 2011.
- [16] A. Kusiak and Z. Zhang, “Adaptive Control of a Wind Turbine With Data Mining and Swarm Intelligence,” *Sustain. Energy, IEEE Trans.*, vol. 2, no. 1, pp. 28–36, 2011.
- [17] F. Gao, “Individual Pitch Control of Large-scale Wind Turbine Based on Load Calculation,” *Proc. 10th World Congr. Intell. Control Autom.*, pp. 3384–3388, 2012.
- [18] S. Ahmed, M. A. Rashid, S. B. Yaakob, and A. Yusof, “Pitch angle control of a grid connected wind turbine,” *2014 5th Int. Conf. Intell. Adv. Syst.*, vol. 5, no. 1, pp. 1–6, 2014.
- [19] K. V. Lakshmi and P. Srinivas, “Fuzzy adaptive PID control of pitch system in variable speed wind turbines,” *2014 Int. Conf. Issues Challenges Intell. Comput. Tech.*, pp. 52–57, 2014.
- [20] L. Qian, X. Jiang, and R. Wang, “Variable Pitch Control of Wind Turbine Based on RBF Neural Network,” *2014 Int. Conf. Power Syst. Technol.*, vol. 22, no. Powercon, pp. 20–22, 2014.
- [21] Z. Civelek, E. Çam, M. Lüy, and H. Mamur, “Proportional–integral–derivative parameter optimisation of blade pitch controller in wind turbines by a new intelligent genetic algorithm,” *IET Renew. Power Gener.*, vol. 10, no. 8, pp. 1220–1228, 2016.



Thermosolar temperature control system for aquaculture breeding

H. Aguirre-Becerra^{a*}, J. F. García Trejo^b, G. A. Peña-Herrejón^b

^a Doctorado en Ingeniería de Biosistemas de la Facultad de Ingeniería (FI) del Campus Amazcala (CA) de la Universidad Autónoma de Querétaro (UAQ), ^b Cuerpo Académico de Biosistemas de la FI de la UAQ Querétaro, México

*Corresponding author: humberto.aguirreb@uaq.mx

Abstract — A thermosolar temperature control system for aquaculture breeding that uses a solar collector as source of heat is presented. The objective of this work was to evaluate the thermal performance and efficiency of the overall system. A temperature control of $26^{\circ}\text{C} \pm 1^{\circ}\text{C}$ (value used for tadpole breeding) and an efficiency of 86% were achieved. 13.77% of the energy is lost to the environment through the recirculation tank and pipeline.

Keywords—Thermosolar, solar collector, temperature control

I. INTRODUCTION

Despite the technological progress in frog farming, equipment that minimize environmental effects are frequently neglected by farmers [1]. Feeding, electricity and fuel represent more than 90% of the total energy requirement in intensive aquaculture [2]. New culture technologies that minimize environmental pollution are required in aquaculture [3]. Active solar systems, where a solar collector is used as the main heat generator, have been used to maintain water temperatures recirculation aquaculture systems [4]. The aim of this work was to design and evaluate a temperature control system for intensive tadpole rearing that uses a solar collector as source of heat.

I. SYSTEM DESIGN

Figure 1 describes the temperature control system designed for the experiment. Hot water enters from a solar collector into the recirculating tank (RT) inside the greenhouse. Hot water of the RT flows through the pipeline to the heat exchanger installed inside the incubation tank (IT) which is covered with a plastic material. The RT contains a digital temperature sensor, so when the water of the RT cools, it returns to the general reservoir outside the greenhouse and new hot water refills the system. The controller turns on and off the pump and electrovalves for controlling temperature in the ITs. The RT, where hot water is received, has a capacity of 300 L. The system was designed for controlling the temperature of four ITs, each with a digital temperature sensor and an electrovalve. The user can select the temperature set point (SP) of each tank with a capacitive touchscreen (CP) in the control panel. The user can access the temperature records by subtracting a micro-SD located in the back part of the CP and inserting it in a computer. The controller is programmed to turn on if the temperature of the IT is below a degree Celsius of the SP, and to stop if the temperature is above a degree Celsius of the SP.

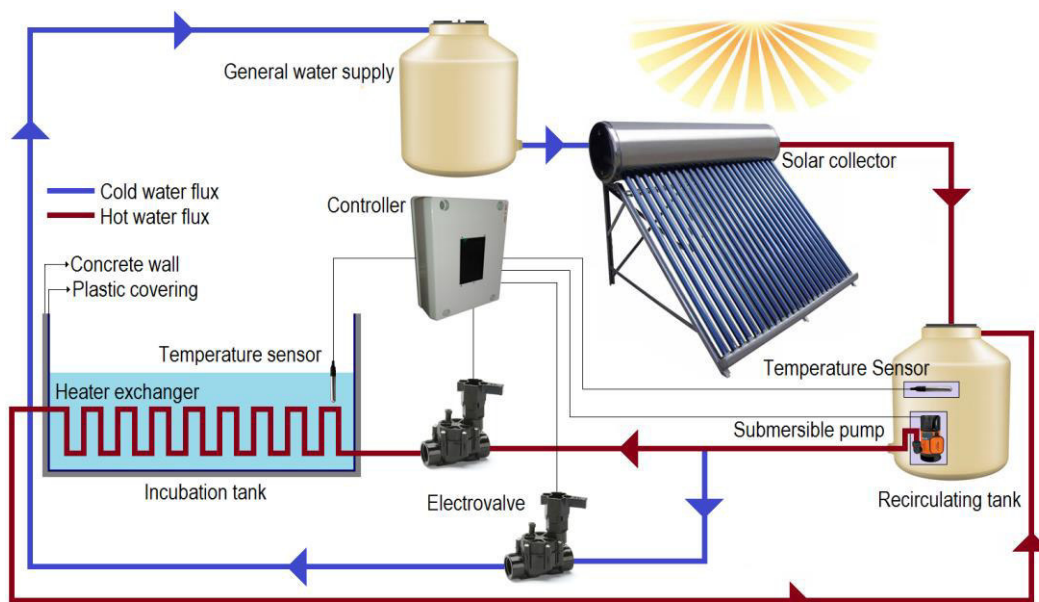


Figure 1. Temperature control system for intensive tadpole rearing that uses a solar collector as source of heat

II. INSTALLATION

The system was installed in four ITs at the bullfrog production and research greenhouse (Fig. 2) at the UAQ, FI, Campus Amazcala, located in the municipality of El Marqués, Querétaro. The greenhouse has concrete ponds of 400 L each for tadpole farming.

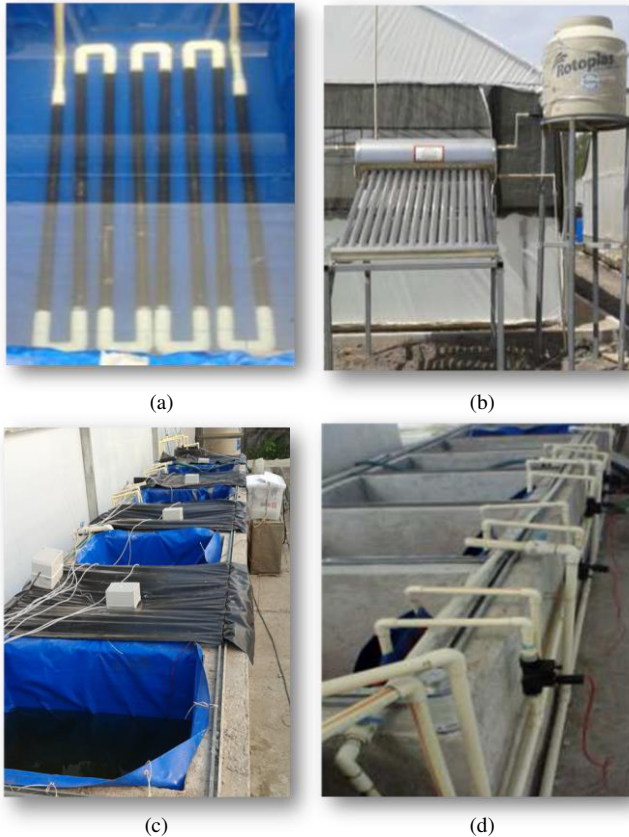


Figure 2. Installation of the temperature control system for intensive tadpole rearing. (a) Heat exchanger. (b) Solar collector and general water reservoir. (c) Ponds. (d) Piping and electrovalves

III. TEST 1 – SYSTEM EFFICIENCY

The results of the first operation test are shown in Table 1. For this test, rearing ponds were filled with 216 L (half of its capacity), and the recirculating tank and recirculating pipeline was filled with 76 L (a quarter of its capacity). Then, the pump inside the RT and one electrovalve were activated to heat one IT and determine the energy loss. This test was run until the temperature of the RT and the IT achieved a static value during 30 minutes. This test indicates that 13.77% of the thermal energy of the hot water is lost to the environment through the recirculation tank and pipeline. Fig. 3 shows the dynamics of the system. It is observed how the hot water of the recirculation tank decreases its temperature while that of the pond increases until a balance point between 27 °C and 30 °C.

Table 1. System thermal analysis

Variable	Value
Initial pond temperature [°C]	21.2
Final pond temperature [°C]	32.2
Initial recirculating tank temperature [°C]	72.8
Final recirculating tank temperature [°C]	35
Water volume of rearing pond [L]	216.68
Water volume or recirculating tank and recirculating pipeline [L]	73.12
Total system energy [J]	11556.96
Energy acquired by the rearing pond [J]	9965.95
Energy loss [J]	1591.01
Energy efficiency[%]	86.23
Time of test [min]	100

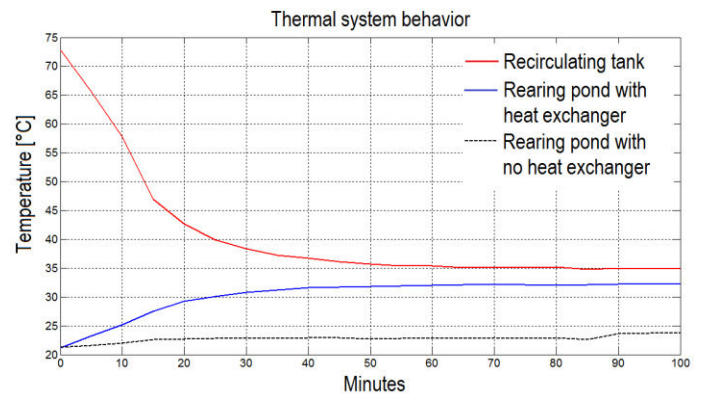


Figure 3. Thermal system behavior

IV. TEST 2 – SYSTEM OPERATION

The second test consisted on ensuring that the system works properly during a tadpole cultivation cycle. Fig. 4 shows the temperature behavior of two ponds were the system was installed. SP of 26°C was selected. It can be observed that temperature was in a range of 26°C ± 1°C. Temperature of pond 02 has a lower variation than pond 01 because it was covered with black plastic.

V. CONCLUSION

The thermosolar temperature control system for aquaculture breeding was programmed to work at 26°C ± 1°C. This proposal uses solar energy as source of heat and worked for four ponds of 400 L. However for a bigger pond, where fish are grown, it would be necessary to resize the heat exchanger and solar collector, but the controller would work properly.

VI. ACKNOWLEDGMENT

We want to thanks the members of the Bioengineering Laboratory at Campus Amazcala of Universidad Autónoma de Querétaro. This work was partially financed by CONACYT for awarding the scholarship 332171 for Master Degree studies and FOPER 2012 projects.

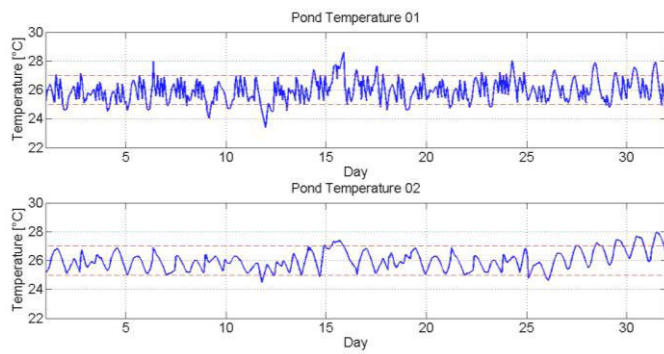
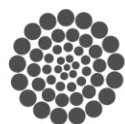


Figure 4. Temperature control of one month cultivation cycle

REFERENCES

- [1] Mello, S. C. R. P., Oliveira, R. R. D., Pereira, M. M., Rodrigues, E., Silva, W. N., and Seixas Filho, J. T. D. "Development of a water recirculating system for bullfrog production: technological innovation for small farmers". *Ciência e Agrotecnologia*, 40(1), 67-75. Troell, M., P. Tyedmers, N. Kautsky, and P. Rönnbäck, *Aquaculture and energy use*, Encyclopedia of energy 1: 97-108, 2016.
- [2] Troell, M., P. Tyedmers, N. Kautsky, and P. Rönnbäck, *Aquaculture and energy use*, Encyclopedia of energy 1: 97-108, 2004.
- [3] Munguia-Fragozo, P. V., Alatorre-Jacome, O., Aguirre-Becerra, H., García-Trejo, J. F., Soto-Zarazúa, G. M., and Rico-García, E. "Growth and Metabolic Effects of Stocking Density in Bullfrog Tadpoles (*Rana catesbeiana*) under Greenhouse Conditions". *International Journal of Agriculture and Biology*, 17(4), 711-718, 2015.
- [4] Fuller, R., Solar heating systems for recirculation aquaculture. *Aquacultural engineering* 36: 250-260, 2007.



Graphs and Trees with Prototypes and Object Delegation

Gutiérrez-Velázquez Luis David
Facultad de Informática
Universidad Autónoma de Querétaro
Querétaro, México
david@golemcode.com

González-Gutiérrez Fidel, Gonzalez-Gutierrez
Arturo, Tovar-Arriaga Saul
Facultad de Ingeniería
Universidad Autónoma de Querétaro
Querétaro, México
{fglez, aglez, saul.tovar}@uaq.mx

Abstract— In this paper we present the OLOO (Objects Linking to Other Objects) paradigm provided by polymorphism to show that it is possible to optimize computing resources when using data structures defined as trees and graphs, in the context of ubiquitous technologies. We also present some case studies to explore the capacity and reliability of a library developed in JavaScript/ECMAScript 6, making strong use of prototyping and object delegation system.

Keywords—graphs; trees; JavaScript/ECMAScript 6; polymorphism; object delegation; OLOO Paradigm.

I. INTRODUCTION

This work consists in developing a software tool that we will refer to it as a software library, or simply a library, that is able to implement efficiently data structures such that trees and graphs, with two objectives in mind:

- The tool must be light and flexible to allow decentralized use by computer entities commonly referred as customers;
- It must be robust enough to solve a series of problems that are modeled by trees and graphs such as the Minimum Cost Spanning Tree (MCST) problem, the Pre-order and Post-order Tree Traversing, the Shortest Path between two vertices problem, and the Traveling Salesperson (TSP) problem.

In order to reach these objectives, the library has been built in a software paradigm different from the traditional ones, since it does not make use of classes nor generate chains of inheritance. Instead, the construction of the tool favors polymorphism and object delegation.

II. STATE OF THE ART

At present, the implementation of complex data structures through the development of programming languages has

evolved [1]. However, this kind of implementations has focused on centralized systems with special attention to traditional back-end languages such as C, C++, C#, Java, and Python. They, although robust and stable, lack the ability to transparently distribute the operations related to data structures across clients. Finally, they end up causing an overload to the central systems by requiring centralized resolution of all data requirements, preventing the correct performance of these systems.

The approach proposed in this work addresses the construction of a library supported by the technologies that make possible to transparently be in the majority of client type systems. Thus, this approach makes use of requirements about the data and their relationships so that they can be solved locally, reducing the number of requests to the servers.

The representation of information in the form of lists and tables has been a common way in which the web systems have addressed data organization since the emerged of the Internet [1]. While providing more robust implementations of data structures, allows us to address problems more efficiently [2]. To do so by using JavaScript, we will show not only that the language is powerful and sufficiently capable of solving complex data organization problems [2], but also to show that object composition by polymorphism as opposed to inheritance is an alternative and an efficient way of implementing data structures such as trees and graphs [3].

In order to achieve the objectives presented in the introduction, the JavaScript programming language, according to the ECMAScript 6 specification [4], was chosen. This selection is based on two fundamental aspects:

- The programming paradigms that JavaScript supports reduce the complexity of the abstraction required for building libraries. These are OLOO, functional programming

• This material is based upon work supported by a grant from the Autonomous University of Queretaro according to the program FOFI-UAQ-2015.

- As demonstrated in several works [5] this programming language allows a robust generation of tools, which are able to execute transparently in the full-stack of the systems. This is possible due to the stable implementations of the web browsers as well as to the development of technologies such as *node.js*. These technologies allow the developed library to be deployed in servers, client applications and IoT (Internet of Things) systems.

Breakdown of the paradigm used.

As mentioned above, one of the main characteristics of the developed library is the programming paradigm used in its construction called OLOO. Although this paradigm as its name indicates it is based on structures known as objects, it has important differences with the traditional paradigm OOP (Object-oriented programming). The differences that matter most in this work are presented in the following paragraphs:

In OOP objects are created from previously declared "blueprints" known as Classes. These classes can copy (inherit) the operation of other classes which produces hierarchies which can contain several levels; This form of composing objects allows the use of polymorphism mechanism. In this architecture, each created object and declared class must have an exact copy of all previous classes in their genealogy, this may require memory allocation in an inefficient way; it also generates a strict relationship between the elements that conforms the system, since each class and object must know not only the existence of the elements that compose them but also the fundamental implementation of those elements [6], this creates two problems:

- The abstraction of the developed system becomes complex, which greatly complicates the development of the system and subsequent updates, causing the systems to become monolithic and prone to the typical "Banana and Jungle" problem [7].
- The system is tied to the definitions given in development time, being difficult to adapt or understand a new operation during runtime; although this can generally be considered a positive feature, there are solutions that benefit from flexible systems at runtime [6].

In contrast, in the OLOO paradigm there are no classes, objects are literally declared [8], once created these objects can link to each other, these links generate a structure known as prototype chain; In turn this composition of objects is called composition by prototyping; This composition can be declared at development time, or happen during the runtime. This allows:

- Through the chain of prototypes, it is possible to delegate different activities in different objects, which allow the construction of weakly coupled structures. This is because objects link together do not need to be aware of implementations of other objects, only a result containing a certain generic form is expected.
- It gives flexibility to the system allowing the complexity of abstraction to be reduced, composing objects selectively with functions of other objects (mixing) and

allowing them to change at runtime without affecting the operation of other objects in the prototype chain [6].

As we have shown OLOO paradigm allows a much simpler and more robust abstraction of the implemented data structures, allowing a solid and highly flexible development. In this implementation, the final objects of the prototypal chain depend on the base objects to which they are linked (OLOO) to be able to perform operations on the states they have.

III. DATA STRUCTURES: GRAPHS AND TREES

The structures implemented in the library are known as complex data structures because they are forms of data representation that allow not only to organize the data but also make use of mathematical concepts to solve problems related to the data and their relationships. Thus, the structures implemented are:

- **Graphs:** A graph is a data structure that allows us to model the data present in a system so that we can respond elegantly and efficiently to questions about the data itself and its relationships. A formal definition is: "A graph G consists of a non-empty set V of objects called vertices (Vertex) and a set E of two elements subsets of V called Edges. So, a graph is a set (an ordered set) of two sets V and E. For this reason, it can be defined as $G = (V, E)$ "[1].
- **Trees:** Trees are a type of connected graphs that do not contain cycles, are widely used to sort data and facilitate their search. A form definition is: "A tree is an acyclic connected graph [1].

The main structures implemented in the library and its prototyping chains are shown in Table I.

TABLE I. TABLE OBJECT INSPECTION

Object	Prototype	Description
Node	Object	Implementation of the vertices that conform V (G)
Edge	Object	Implementation of the edges that make up E (G)
Graph	Object	Implementation of the structure known as graph
Undirected Graph	Graph	Implementation of a graph with no direction in elements of E (G)
Trees	Graph	Implementation of the structure known as tree
Directed Graph	Graph	Implementation of a graph with direction in elements of E (G)

^a This is the main components and their links of the developed library.

As a prototype model, none of these objects has the attributes that make up the description of the structures they represent, instead those attributes are created in new objects when the factory function contained in the objects to which they are linked created with the Object.create directive, are called. That means, none of the final objects that represent the structures actually have the functionality to do the operations described in the

library, therefore, they delegate the work to their prototypes; This way you can compose new functionalities at runtime and even change the prototype chain without affecting the final objects or the main objects.

IV. ALGORITHMS

Our library contains utilities to solve the following problems, which use graphs and trees and data structures:

A. Trees

Tree traversal

- **Pre-Order:** In a pre-order traversing, the root node is visited first, then recursively traverse the left sub-tree in preorder, followed by a recursively traversing of the right sub-tree [9].
- **Post-Order:** In a post-order traversing, a recursive traverse is made on the left sub-tree, then a recursive traverse on the right sub-tree followed by visiting the root node [9].

Our library includes utilities that support operations on vertices such as insertion, update and deletion, as well as some search operations in order to streamline the construction and simplify the management of the structures created.

B. Graphs

Dijkstra Algorithms: The Dijkstra algorithm is an iterative algorithm that provides the shortest path from a particular node to all other nodes in the graph [10]. This operation will result in one array. The algorithm is described in Fig. 1.

- **Minimum Cost Spanning Tree (MCST):** The problem is defined as finding the tree T contained in G where the subset $V(T)$ is equal to the subset $V(G)$ and it has the lowest possible cost which is defined by the weight of its edges. If G is a Tree, then it is assumed that the MST is the same tree. To find a solution there are different algorithms that address the problem. The research and implementation of this project was based on two:

1. **Prim Algorithm:** An algorithm attributed to Robert Prim in 1957. In this algorithm, we start by considering a set S to which we assign an element of $V(G)$. We explore the set S and add to the MST the edge with the lowest weight whose opposite vertex is outside S [11]. The algorithm is described in Fig. 2.

Algorithm 1: Dijkstra's Algorithm

Input : A weighted graph G with nonnegative edge weights, and a distinguished vertex s of G .

Output: The shortest path from s to v for each vertex v of G .

```

1 function Dijkstra ();
2 Let  $S$  be the set of explored nodes;
3 Initially,  $S = \{s\}$  and  $d[s] = 0$ ;
4 while  $S \neq V(G)$  do
5     Select  $v$  not in  $S$  with an edge into  $S$  satisfying:
6     |  $D[v] = \min (e=(u, v), u \text{ in } S) d[u] + w[e]$  is as small as possible;
7     | Add  $v$  to  $S$  and set  $d[v] = D[v]$ ;
8 end
9 return  $d[]$ ;

```

Fig. 1. Dijkstra's Algorithm

Algorithm 2: Prim's Algorithm

Input : An undirected, weighted, connected graph G with n vertices and m edges

Output: A minimum spanning tree MST for G

```

1 function Prim ();
2 Choose a start vertex,  $s$ ;
3 Initially,  $S = \{s\}$  and  $MST = \{\}$ ;
4 while  $S \neq V(G)$  do
5     Find an edge  $e$  such that:
6     | 1.  $e$  starts in  $S$  and ends out of  $S$ ;
7     | 2.  $e$  has the minimal weight of edges satisfying 1;
8     | Add  $e$  to  $MST$ ;
9     | Add the vertex at the end of  $e$  to  $S$ ;
10 end
11 return  $MST$ ;

```

Fig. 2. Prim's Algorithm

Algorithm 3: Kruskal's Algorithm

Input : An undirected, weighted, connected graph G with n vertices and m edges

Output: A minimum spanning tree MST for G

```

1 function kruskal ();
2 Initially, sort  $E(G)$  in order by ascending weight;
3 Set  $MST = \{\}$ ;
4 for  $e$  in  $E(G)$  do
5     if  $G = (V(G), MST \cup e)$  does not contain a cycle then
6     | Add  $e$  to  $MST$ ;
7     end
8 end
9 return  $MST$ ;

```

Fig. 3. Kruskal's Algorithm

2. **Kruskal Algorithm:** An algorithm designed by Joseph Kruskal in 1956. In this algorithm, we start from considering $E(V)$ in ascending order of weight; add an edge to the MST if and only if it doesn't break the definition of tree which is to be an acyclic graph [11]. The algorithm is described in Fig. 3.

- **The Traveling Salesperson Problem (TSP):** This problem is composed of a salesperson and a set of locations. The salesperson must visit each of the locations from a certain start point and returning to the same location after visiting all the other locations. The fundamental part of the problem is that the salesperson wants to minimize the total cost of the trip. It is a problem closely related to the problem of the Hamiltonian circle [1]. This problem is addressed in the library with different heuristics that allow a satisfactory result to be approximated; since this is not a library developed to make an exhaustive use of

computational resources, the approximations given may not be the best.

In addition to implementing the graphs, we also implemented and used "peripheral" data structures that allow a better control and abstraction of the graphs and their elements. Examples of these are: Sets, Disjoint set, Queues, Empty object without a prototype chain. These peripheral structures are implemented with the ECMAScript 6 specification and can be used in the same form as the main data structures, although their separate use has not been thoroughly tested.

Finally, we also add some basic functions to know the properties of the created graph and to manipulate the existing elements in $V(G)$ and $E(G)$ sets with the operations of add, delete, disconnect and search.

V. RESULTS

The result of this work is the creation of a software library that allows a robust implementation of the data structures: Graphs and Trees; as revised in this work the implementation is done under the JavaScript programming language using the mechanics of the language known as object composition by prototype and object delegation, making use of the OLOO paradigm. These relationships and structure can be seen in Fig. 6 where the dotted line marks a prototype chain that is different in order and complexity to a chain of inheritance

The creation of this library make it possible to verify if we can optimize computational resources, so to properly perform the necessary tests, two case studies were constructed with the purpose of evaluating the capacity of the library. These case studies were developed in web platforms that allow us to deploy them in a large number of client-type systems [12]. These two case studies are presented below:

- Use of graphs to search for the best possible path using Dijkstra's algorithm. As demonstrated in Fig. 4 and 5
- The second case of study allows the free construction of trees and graphs providing the tools to obtain the MST and the construction and traversal of any given tree. This application demonstrates the stability of the library up to 5,000 nodes and 10,000 edges, therefore we can conclude that we can use the computational resources of the clients for solving data related problems instead of using the central systems; If the central systems provide JSON-like structures to provide the clients with the information needed to solve some questions about the data, the use of the central resources in these types of problems will be reduced to the sending of information to the client systems. See Fig. 7 and 8, the order and size of the graph presented has been lightly edited for length and clarity.

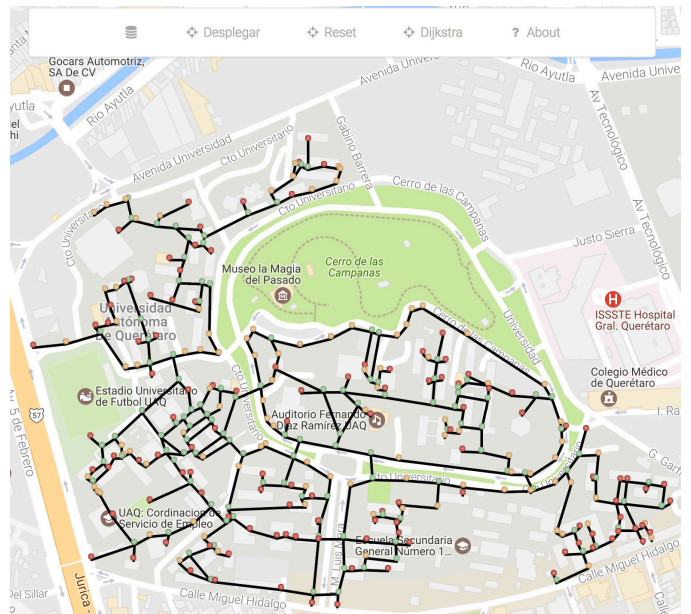


Fig. 4. Graph of the pedestrian walkway system of the central campus of Autonomous University of Queretaro (UAQ).

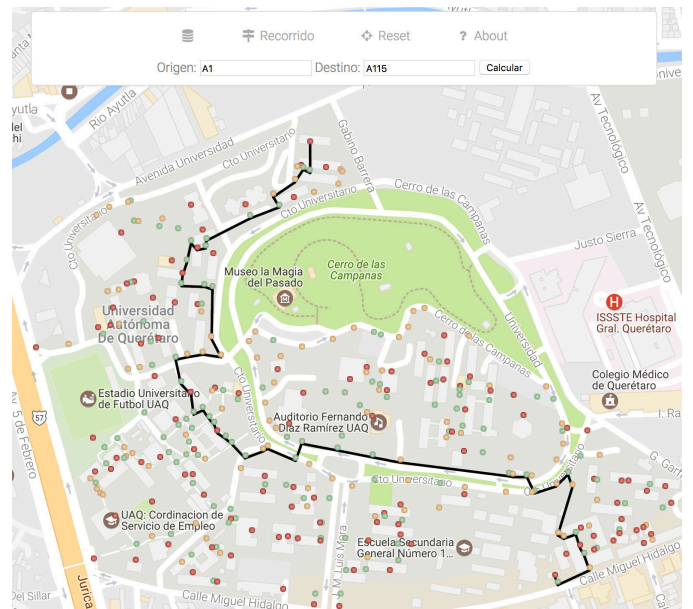


Fig. 5. Shortest path between two vertices on central campus of UAQ generate with Dijkstra's algorithm.

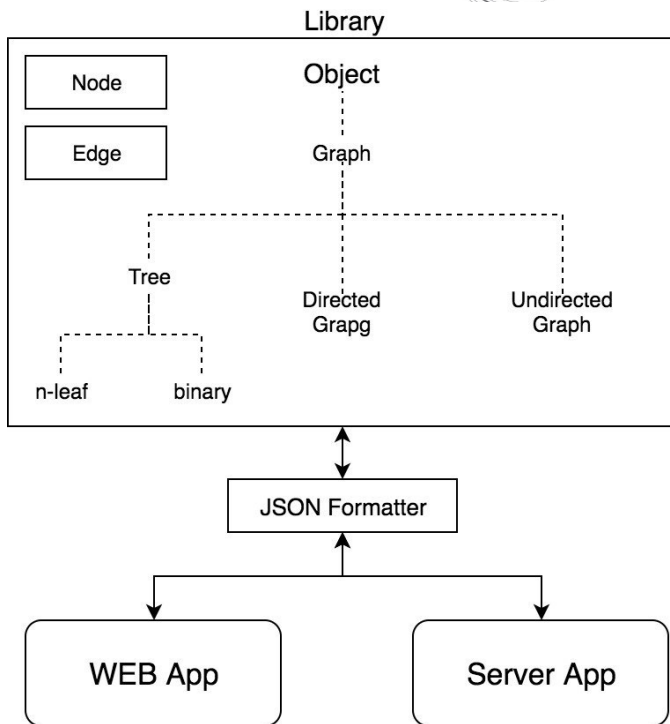


Fig. 6. Blocks Diagram

VI. CONCLUSIONS

The library is able to delegate satisfactorily part of the mainstream data related problems to the client systems. However, being a fairly new implementation it merits a great deal of work in order to reach a more robust development of the data structures. Two of the job opportunities that will be addressed in subsequent work will be:

- The development of new functionalities associated with binary trees, AVL, graph coloring [13], balancing and more robust searching and ordering algorithms.
- The exploration of the implementation of the library in the central systems with technologies such as node.js to allow a transparent use of the data throughout the system stack. Also, the implementation of the developed library in IoT devices in order to address routing problems in embedded systems.

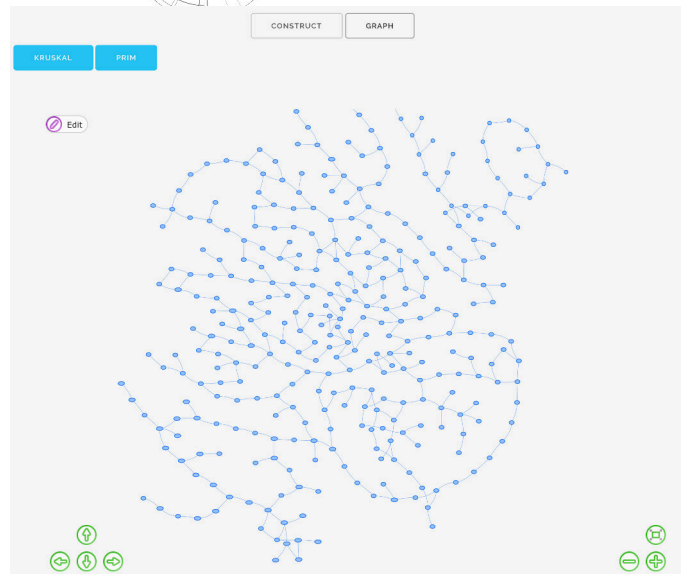


Fig. 7. Graph of the central campus of UAQ using the Vis.js graphical utility.

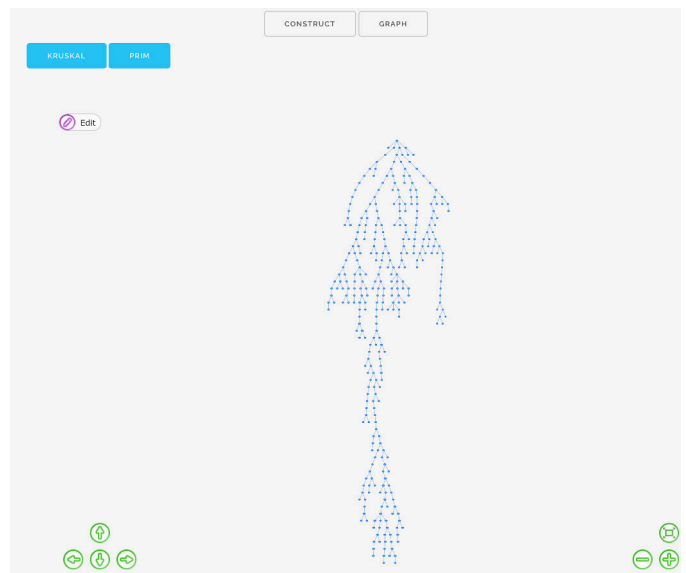


Fig. 8. The minimum cost spanning tree of the graph in Fig. 6 produced by kruskal's algorithm

ACKNOWLEDGMENT

The visual display of the data structures created in the two case studies are provided by the tools of Google Maps API and Vis.js. G.V.L.D thanks the support of the engineer Alfaro Cruz Marco A. for his recommendations, comments and constant support.

REFERENCES

- [1] G. Chartrand, P. Zhang. "A First Course in Graph Theory". Mineola, New York, USA: Dover Publications 2012.
- [2] M. MCMillan. Data Structures and Algorithms with JavaScript. United States of America: O'Reilly books, 2014.
- [3] D. Crockford, "JavaScript: The World's Most Misunderstood Programming Language" 2001, unpublished.
- [4] ecma International Standard ECMA-262 ECMAScript 2015 Language Specification 2015
- [5] Tipling B., "Advanced objects in JavaScript" 2014, unpublished.
- [6] Simpson Kyle "You don't know JavaScript – this and Object Prototypes" O'Reilly books, 2015.
- [7] Simpson Kyle "You don't know JavaScript – Up and Going" O'Reilly books, 2015.
- [8] Simpson Kyle "You don't know JavaScript – Scope and Closures" O'Reilly books, 2015.
- [9] Bradley N. Miller and David L. Ranum "Problem Solving with Algorithms and Data Structures Using Python" Franklin, Beedle and Associates Inc, 2013.
- [10] Goodrich Michael T., Tamassia Roberto and Goldwasser Michael H. "Data Structures and Algorithms in Python" Wiley, 2013.
- [11] Cormen Thomas H., Leiserson Charles E., Rivest Ronald L., Clifford Stein "Introduction To Algorithms" The MIT Press, 2009.
- [12] HTML5 Game Development Insights: Efficient javaScript data structures, Duncan Tebbs. 2014, pp 59-68.
- [13] Excursions in Modern Mathematics, Peter Tannenbaum, 2017, pp B1-B14



Detection System to Analyze Modulated Light Signals

Mario A. Hernández-Martínez
Alternative Energies department
CICATA-IPN, Queretaro
mario_hernandez_mtz1993@hotmail.com

Jorge A. Huerta-Ruelas
Alternative Energies department
CICATA-IPN, Queretaro
jhuertar@ipn.mx

Omar Rodríguez-Zalapa
Automatization Technology department
UTEQ, Queretaro
omar.rodriguez.2013@ieee.org

Enrique Augusto García-Guerrero
Alternative Energies department
CICATA-IPN, Queretaro
eaggro@gmail.com

Abstract—This work shows a Detection System to analyze light signals. Optical system was designed and built with the purpose of obtain useful information from samples using a light beam, where Scattering, absorption, reflection and/or transmission of light in noisy environments. To achieve this purpose, it is needed to apply filters and processing techniques. Phase-Sensitive Detection (PSD) technique was applied in this work showing main benefits obtained. Preliminary results are shown comparing a commercial equipment with designed electronics.

Keywords—Light; Optical Detection; Signal to noise ratio; Phase-Sensitive Detection.

I. INTRODUCTION

Signal processing is a matter widely used in applications like control systems, industries, militia, research between others. The evolution of the signal processing produced different techniques to obtain desired information. Signals can be classified in analog and digital [1], [2], which determines the methodology to process the message information. There are three essential parts of any communication system: the transmitter, transmission channel, and receiver. Each part has a function in the message transmission, and any of them produce some noise added to final signal. Hence, our approach look to quit or filter the noise in any system stage. In first instance, we modulated the intensity of probe light beam to an specified frequency. For decoding the signal, there are many techniques, like channel coding, but it is bandwidth limited. Other option, take advantage of the statistical knowledge of the source signal to enable efficient encoding known like source-coding. Another option to process signals, is a Phase-Sensitive Detection (PSD), that allows recover signals in noisy environments[3], [4]. This instrument extract features of a sinusoidal component of a known frequency from a signal that is noisy[4]. This technique was used to recover optical signals in the detection system. The optical detection systems have had many applications in research to characterize surface, particles

in solution, position objects, forms, etc. Light is collected through a photodetector, that allows obtain a data in a magnitude and phase, which can be correlated to sample properties. System interface show us information to monitor sample evolution.

To show system performance, an optical system with three detectors was built according to ISO 7027[5].

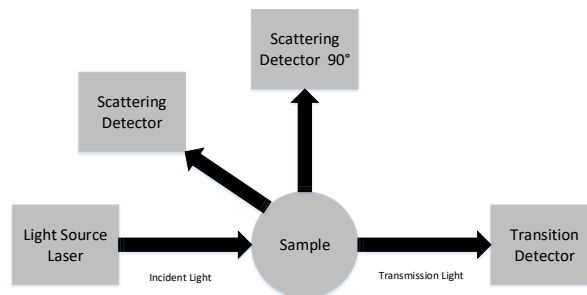


Fig. 1. The optical arrangement in a turbidimetric system diagram [5].

II. MOTIVATION FOR THE APPROACH

The aim to build an Optical Detection System arises from the necessity of characterize, processing, visualize and control the data that measure light intensity to determine: Absorption, Transmission and Scattering. The main aim was:

- To design and built a system to process optical signals through PSD technique.

Others specific aims considered to visualize the data of Optical Detection System are:

- Design an electronic hardware based on analog signals.
- Processing the data in a Analog Device chip AD630.

- Design an interface to visualize and control the data of optical system.
- Save the data for the analysis of system behavior.
- Validation of technique PSD compared with a commercial equipment.

III. PHASE-SENSITIVE DETECTION

The Principle of operation of Phase-Sensitive Detection technique consist on the use of a multiplier as shown in Fig. 2. The two-state switch is controlled electronically from the reference voltage. The switch changes position between point A and B as the reference changes polarity. This action gives a systematic change of gain between +1 and -1, or 1 and 0, in the signal [6], [7].

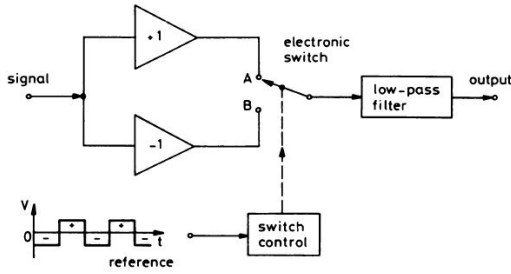


Fig. 2. Phase-Sensitive Detection: Principle of operation [6].

Consider a continuous test signal made up of signal components of the form:

$$V^{\text{sig}} = A_{\text{sig}} \sin(\omega_{\text{sig}}t + \theta_{\text{sig}}) \quad \omega_{\text{sig}} = 2\pi f_{\text{sig}} \quad (1)$$

And of reference signal in X components of the form:

$$V^{X,\text{ref}} = A_{\text{ref}} \sin(\omega_{\text{ref}}t + \theta_{\text{ref}}) \quad \omega_{\text{ref}} = 2\pi f_{\text{ref}}. \quad (2)$$

Multiply the test signal by reference signal to give output signal with component of the form:

$$V^X = A_{\text{sig}} A_{\text{ref}} \sin(\omega_{\text{sig}}t + \theta_{\text{sig}}) \sin(\omega_{\text{ref}}t + \theta_{\text{ref}}) \quad (3)$$

Using trigonometric identities allow to components be expressed as:

$$V^X = \frac{1}{2} A_{\text{sig}} A_{\text{ref}} [\cos((\omega_{\text{sig}} - \omega_{\text{ref}})t + (\theta_{\text{sig}} - \theta_{\text{ref}})) - \cos((\omega_{\text{sig}} + \omega_{\text{ref}})t + (\theta_{\text{sig}} + \theta_{\text{ref}}))] \quad (4)$$

Apply a Low-pass filter it is obtained the respective DC components:

$$X = \frac{1}{2} A_{\text{sig}} A_{\text{ref}} \cos(\theta_{\text{sig}} - \theta_{\text{ref}}) \quad (5)$$

This quantity represents the signal in a vector relative to reference oscillator. X is called the “in phase” component, this is because $\Theta = 0$ [4], [8], [9].

IV. HARDWARE IMPLEMENTATION

The PSD system built consist in a CMOS AD630 [9] from analog device. A general structure of a Lock-In Amplifier (LIA) (see Fig. 3), produce a system able to measure light coming from an object of study, in a noisy environment (Fig. 4).

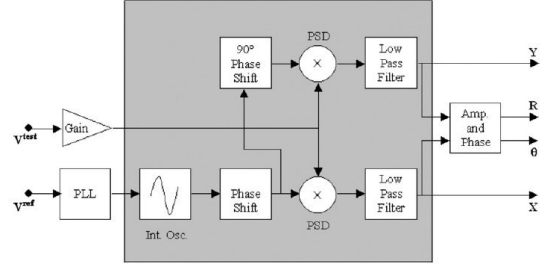


Fig. 3. Lock-In Amplifier general diagram [4].

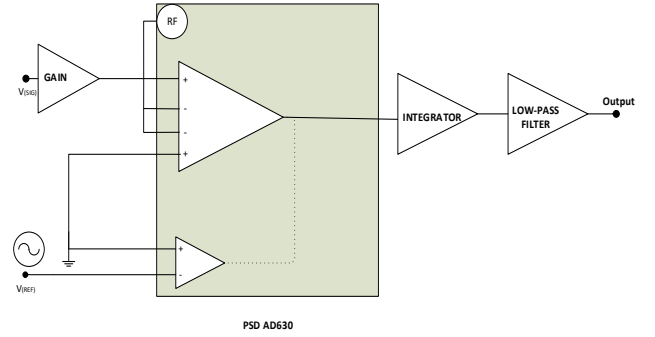


Fig. 4. PSD filter AD630 system built

Analog system produce as output an analog DC signal proportional to intensity of modulated light coming from sample. Data acquisition is made with a FPGA MyRIO1900®, [10]. To data visualization a VI interface was programed in LabVIEW® (Fig. 5). We did a comparison between a commercial equipment (Stanford research Systems, RS830) and our own system designed, with the purpose to check the correct performance of developed system. The results can be observed in Fig. 6, where it is compared the response of both systems. The output signal represents the light intensity which get through a Titania sample diluted in methanol. Our prototype and commercial equipment has the same response of scattered light due to substance sedimentation which provokes proportional light changes as it is absorbed or not. In this comparison, the transmitted light increased while the substance enters to sedimentation state.

V. CONCLUSION AND FUTURE WORK

In this paper, a developed PSD system was presented and compared with a commercial equipment, for the use in an Optical Detection System. To validate the system a turbidimetry setup was used to measure transmission, absorption and scattering, using photodetectors at three different angles.

The characteristics of our own instrumentation design will allow to build a system with better portability and will allow to process more signals at different environments and/or conditions.

REFERENCES

- [1] A. B. Carlson and P. B. Crilly, *Communication Systems*.
- [2] J. G. Proakis and M. D. G., *Digital Signal Processing*, Third Edit. United States of America: Prentice Hall, 1996.
- [3] J. Aguirre, N. Medrano, B. Calvo, and S. Celma, "A 3V single supply LIA for portable sensing systems," *Proc. IEEE Sensors*, vol. 47, no. 21, pp. 1866–1869, 2011.
- [4] P. Clarkson, T. J. Esward, P. M. Harris, A. A. Smith, and I. M. Smith, "Software simulation of a lock-in amplifier with application to the evaluation of uncertainties in real measuring systems," *Meas. Sci. Technol.*, vol. 21, no. 4, p. 45106, 2010.
- [5] M. M. F. Tirado Guerrero, "Effect of the sedimentation kinetic in suspensions of titanium dioxide particles treated by atmospheric plasmas MICHELLE MARIA FERNANDA TIRADO GUERRERO A," Mexico, 2016.
- [6] M. M.L., *Lock-in amplifiers: Principles and applications*. London UK: Peter Peregrinus Ltd., 1983.
- [7] G. Yang, J. F. Barry, E. S. Shuman, M. H. Steinecker, and D. DeMille, "A low-cost, FPGA-based servo controller with lock-in amplifier," *J. Instrum.*, vol. 7, no. 10, pp. P10026–P10026, 2012.
- [8] Srs, "About Lock-In Amplifiers," *Appl. Note*, no. 408, pp. 1–9, 2011.
- [9] G. B. Armen, "Phase sensitive detection : the lock-in amplifier," *Lect. Notes*, pp. 1–40, 2008.
- [10] U. Guide, "NI myRIO-1900," 1900.

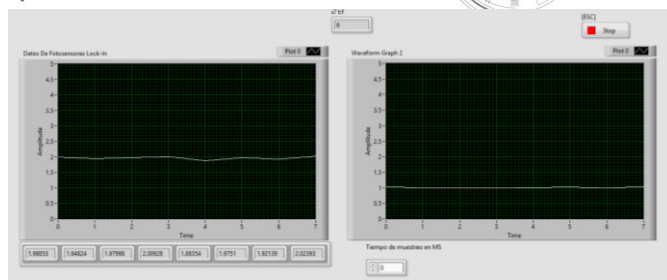


Fig. 5. Interface in LabVIEW

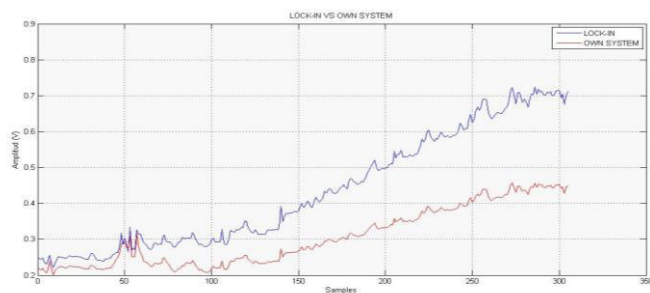


Fig. 6. Prototype vs. Commercial Equipment.

In Fig. 7., we show signals from our prototype, from three sensor at different angles, using the configuration showed in Fig. 1. We obtained different light intensity of Scattered Light, and Transmission. The signals were obtained using a multiplexer to allow read three analog channels sequentially.

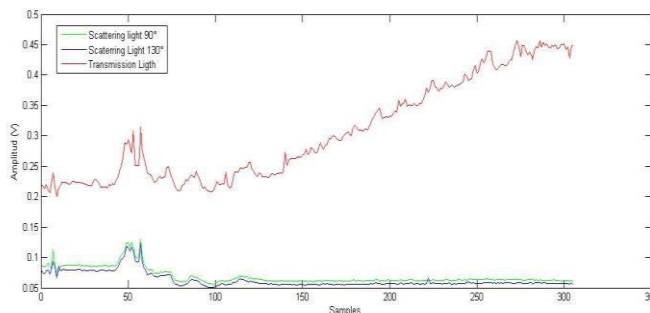


Fig. 7. Result in different angles

Metaheuristic algorithms

Review and comparison

S. V. Camacho Gutierrez, J.R. Alanis Gomez, G. Diaz de Leon Piña, J.A. Lopez, A. Dominguez

Division de Investigacion y Posgrado, Facultad de Ingenieria
Universidad Autonoma de Queretaro
Queretaro, Mexico

Abstract— Optimization is the process to do something better, chosen between potential solutions. However, when the optimization problems are multivariable, with inequalities restrictions or have a complex domain, the classical deterministic optimization algorithms like complex method, Newton or quasi-Newton do not work. On other hand, with the metaheuristic algorithms is possible to find a solution that meets our necessities. This paper have the goal of summarize and compare some of the most popular metaheuristic algorithms as differential evolution, bee colony, simulate annealing and tabu search.

Keywords— optimization, differential evolution; bee colony; simulate annealing; tabu search

I. INTRODUCTION

Optimization is the process to improve something. To achieve these it is necessary to convert the optimization problem into a function (called objective function, cost function or fitness function). Then, the inputs are adjusted to find the optimum value (minimum or maximum result). However, when the fitness function is subject to multiple inputs (variables), which could be discrete or continues or both, and it is constrained to boundary or variable equalities or inequalities, the optimization process becomes complex.

There optimization algorithms that work very well with the fitness function described above are the metaheuristic algorithms which use the randomization to reach global optimum, also they are outstanding because of the easy implementation and high quality results. According to their characteristics, they can be classified in: algorithms based on nature, algorithms based on trajectories, and algorithms based on population or single-point search [1].

Among the optimization algorithms based on nature are evolutionary and swarm intelligence algorithms. The evolutionary algorithms are derived from evolution theory proposed by Charles Darwin, the survival of the fittest. The main idea is: the best “individuals” (candidate solutions for the objective function) are selected to reproduce and using mutation and recombination operators, the next children generation is created, and the iterative cycle is repeated until a stop criterion is met [2]. In this subcategory are found genetic algorithms, evolution strategies, evolutionary programming and differential

evolution. As for the swarm intelligence algorithms, they are based on collective behavior and properties of complex, self-organized, decentralized systems with social structure as fish schools, bird flocks, ant colonies, animal herds or any type of swarm which have the ability to react to environmental changes and decision-making capacities [3].

Regarding to algorithms based on trajectory, they are characterized for following a single path, corresponding to a closed walk on the neighborhood graph, to avoid local optima they allow worse solutions (under certain rules); simulated annealing and tabu search are the most representative of this category [1]. As regards with other categories of optimization, as based on population or single-point search it could include all the algorithms based on nature in the first and based on trajectory in the second.

Likewise, all these algorithms have been applied to a diversity of optimization problems as design of mechanical elements [4] [5] [6], design of electric and electronic elements [7] [8] [9], control design, process improvement [10] [11], path planning [12] [13] [14] [15] [16] [17] [18] [19], building design [20], saving energy consumption [21], and many more applications.

This article summarizes and compare some of the metaheuristic algorithms more representative: differential evolution, bee colony, simulate annealing and tabu search. This review is structured as follow: section II deal with algorithms based on nature: differential evolution and bee colony; section III focus on algorithms based on trajectories: tabu search and simulate annealing, section IV shows and discusses the results of implementation of metaheuristic algorithms on a test function. Finally, section V gives the conclusion of this work.

II. METAHEURISTIC ALGORITHMS BASED ON NATURE

A. Differential evolution

Differential Evolution, DE, is an algorithm created by Kenneth Price and Rainer Storn in 1995 and is defined as a Continuous Function Optimization that is at the same time, an evolution strategy optimization method fast and robust, as well as working in a parallel direct search. DE has the capacity of

running nonlinear, non-differential and multimodal objective functions [22]. The DE global process includes two main parts. The first one is the initialization, and the second one is the evolution that includes iterations between differential mutation, crossover and selection.

The main idea of differential evolution is the difference between two randomly selected parameter vectors as the basis of random variations for a third parameter vector. The parameters of this algorithm are: dimension of problem (Dim), size of population (N_{pop}), maximum generation number (K), generation number g , solution vector X of Dim size and trial vector V of Dim size, likewise there is an important factor which affects the performance of the algorithm: the scale factor F , between 0 and 1, that denotes the rate in which the population evolves and crossover factor Cr . The flowchart of differential evolution could appreciate at Fig. 1.

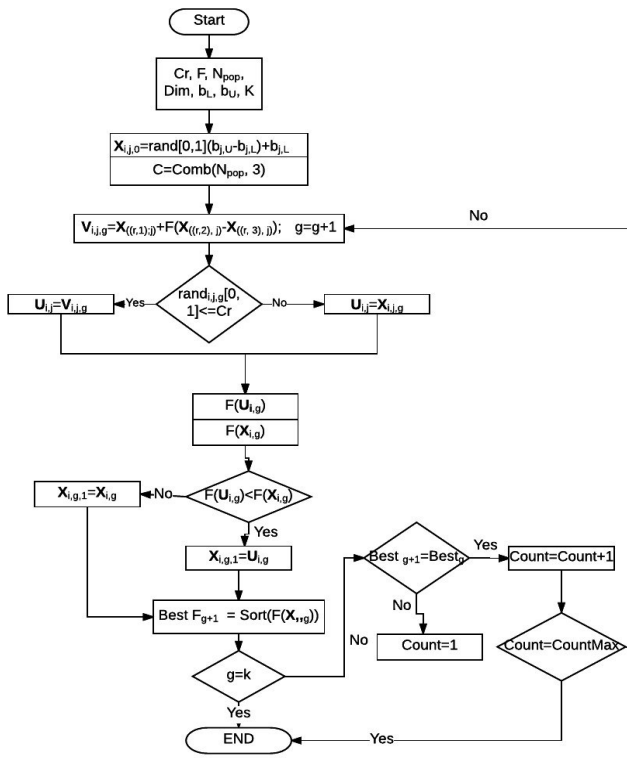


Fig. 1 Flowchart of differential evolution

As the evolutionary algorithms, DE works with a population of solutions, so the first step is initialize randomly the values of the population between the boundaries of problem variables (1), the lower and upper boundary are expressed by $x_{j(U)}$ and $x_{j(L)}$.

$$P_{(0)} = X_{j,i,0} = x_j(l) + \text{rand}_j[0,1] * (x_{j(U)} - x_{j(L)}) \quad (1)$$

The second step is to create trial vectors V using (2):

$$V_{j,i,g} = X_{j,i,g} + F * (X_{j,r2,g} - X_{j,r3,g}) \quad (2)$$

Where $i \in [1, Dim]$, $F > 0$, and $r1, r2, r3 \in [1, Dim]$, they are randomly selected and they should be mutually different. This part of the algorithm is known as mutation.

In order to increase the diversity of the population a crossover is carry out through u vector:

$$u = (u_1, u_2, \dots, u_{Dim}) \quad (3)$$

With:

$$V_{j,i,g} \text{ if } \text{rand}[0,1] < Cr$$

$u =$

$$X_{j,i,g} \text{ if } \text{rand}[0,1] > Cr$$

To decide if the new u vector will become in a new member of the population, the objective function evaluated at u will be compared with the value of the objective function at $X_{j,g}$. If is better, $X_{j,g}$ will be set to u , otherwise the old value of $X_{j,g}$ will remain. The algorithm would stop if the maximum number of generations is reached or stop criteria is met.

B. Bee colony

The optimization of a function inspired by bees swarming behavior is based on the studies of J. Kennedy (social psychologist) and R. Eberhart (electrical engineer) in 1995. The artificial bee colony algorithm (ABC) has shown provide adequate solutions to the problems of maximizing functions; similar to real bees, the algorithm involves "virtual bees" that combine the best solutions of each individual particle and with the best positions as an organized swarm. That means, each bee is directed through the space of solutions, and each individual optimal solution represents in the system a candidate value to represent the general solution to the proposed function; Bees continue flying in search of the value to maximize until finally finding a steady state [23].

The operation of the ABC algorithm is composed of a position equation (x_i) which represents the position of a particle i at time t ; and a velocity equation (v_i) which represents the velocity of a particle i at time t (4) and (5).

$$v_i(t+1) = \emptyset v_i(t) + C_1 R_1 [Pbest - x_i(t)] + C_2 R_2 [Gbest - x_i(t)] \quad (4)$$

$$x_i(t+1) = v_i(t+1) + x_i(t) \quad (5)$$

Thereby the speed equation is formed by three components that are:

- i. Inertial, composed by the velocity of the particle before being updated, factor inertial \emptyset , which is between the values $0 < \emptyset < 1.2$. \emptyset is a value that represents a balance between diversification and intensification. In terms of real bees, they are exploring bees and colonizing bees.
- ii. Cognitive, composed of the coefficients $C1$ called acceleration constant and rewards personal experience; $R1$, is a random value $0 < R1 < 1$, $Pbest$ is the best solution of particle i at time t , and it remains in force in the equation until that particle locates a new best solution $Pbest$.
- iii. Social, composed of the coefficients $C2$ called acceleration constant and rewards personal experience; $R1$, is a random value $0 < R2 < 1$, $Gbest$ is the best solution of the swarm at

time t , and it remains in force in the equation until that swarm locates a new best solution G_{best} .

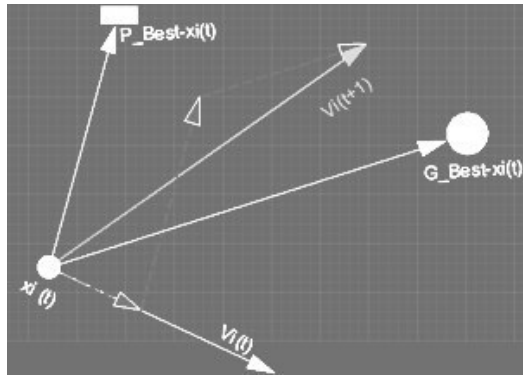


Fig. 2 Movement of an artificial bee

Once the value of the velocity of the particle i is obtained, from (4) and it updates the own position with (5). The velocity and position equations are represented in Fig. 2 by a simple array of vectors. The above figure indicates that the position of the particle i at time t is moving at a velocity through the solutions space, each of the particles i is storing at each iteration the information of the best individual position in which it has remained (P_{best}), also the set of particles holds the information of the best global position (G_{best}). The vector of the position of the particle i to the best position that it has visited corresponds to the expression:

$$P_{Best-x_i(t)} \quad (6)$$

Similarly, the vector of the position of the particle i to the best global position corresponds to the expression:

$$G_{Best-x_i(t)} \quad (7)$$

The inertial factor, as well as the cognitive and social coefficients initiate to vectors parallel to the velocity vector and the cognitive and initial components. Finally the vector in the next iteration corresponds to the sum of the vectors of the three components previously calculated and is named in the new iteration $v_i(t+1)$.

Initially the algorithm chooses solutions randomly in the solution domain, and successively after several iterations the particles reach a stable state in the optimized value. The flowchart of bee colony could be appreciate at **Fig. 2**

III. METAHEURISTIC ALGORITHMS BASED ON TRAJECTORIES

A. Simulate annealing

Simulated annealing copies a phenomenon in nature--the annealing of solids to optimize a complex system. Annealing refers to heating a solid to a liquid state and then cooling it slowly so that thermal equilibrium is maintained. Atoms then assume a nearly globally minimum energy state [24].

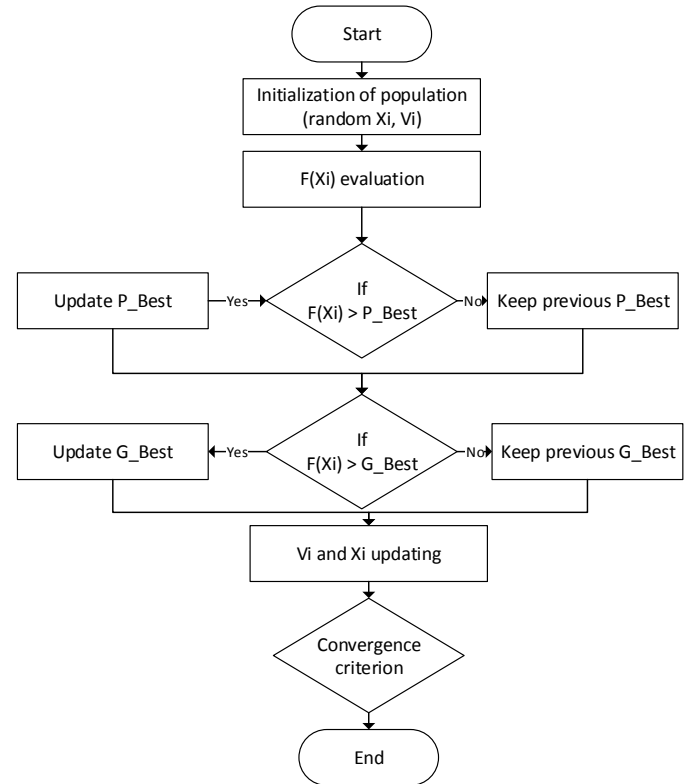


Fig. 3 Flowchart of Artificial Bee Colony

In 1953 Metropolis created an algorithm to simulate the annealing process. The algorithm simulates a small random displacement of an atom that results in a change in energy. If the change in energy is negative, the energy state of the new configuration is lower and the new configuration is accepted. If the change in energy is positive, the new configuration has a higher energy state; however, it may still be accepted according to the Boltzmann probability factor (8). Where k_b is the Boltzmann constant and T is the current temperature [25]. The algorithm of simulated annealing is shown at **Fig. 4**

$$P = \exp(-\Delta E / (k_b T)) \quad (8)$$

B. Tabu search

The tabu search was introduced officially by Fred Glover in 1989 as a metaheuristic method which guides a local heuristic search procedure to explore outside local optima [26]. This method is based in the artificial intelligence, a short and long term memory.

In contrast with others optimization algorithms, the tabu search is not inspired in the nature. The base of this algorithm is the tabu list which have the objective of save the best solutions and prevent that same solutions would be re-visited. This list is also known as short-memory. The long memory save

information as frequency of a value is saved in the tabu list, this allow intensify the search or diversified it.

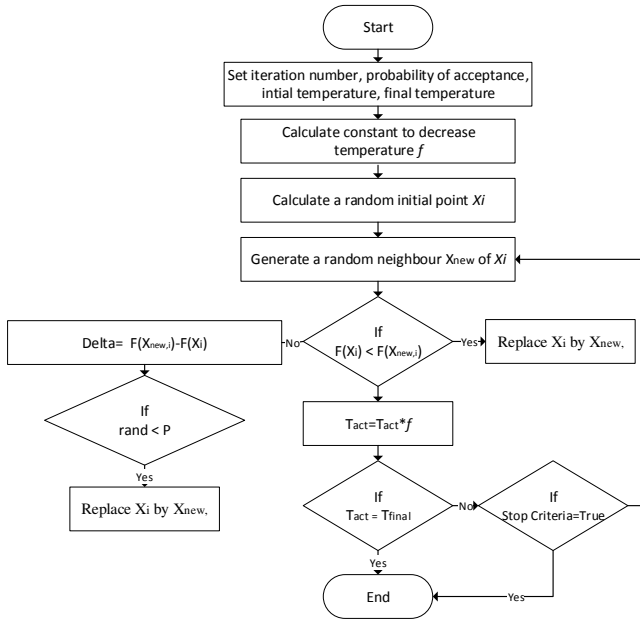


Fig. 4 Flowchart of Simulate annealing

The basic structure of the tabu search could be observed at Fig. 5 and 6. The tabu search starts defining the size of tabu list and neighborhood, the global bounds of optimization problem variables and the local bounds (which corresponds to the range around of a point S_n which would be used as limits of the neighborhood). Likewise, the maximum number of iterations (K). In this study case, the algorithm could be stopped if the best value ($\pm 5\%$) of each iteration (S_n) is repeated at least n iterations.

The second step is generate a random point S_n between the global bounds. The third step consist on generate a neighborhood around this point S_n (between the local bounds). Next, the sub-routine of figure 2 is executed. Each neighbor is evaluated in the objective function and by each restriction would be infringed a penalization is applied. Following, these results are sorted and the best is chosen as S_n , however, if this new value of S_n is inside of tabu list, the next best value should be selected.

If the actual iteration is 10 multiple, then “diversification” occurs. The diversification consist on generate randomly a S_n point between the global limits. Finally, the new value of S_n is added to tabu list and the oldest is let free, to be evaluated.

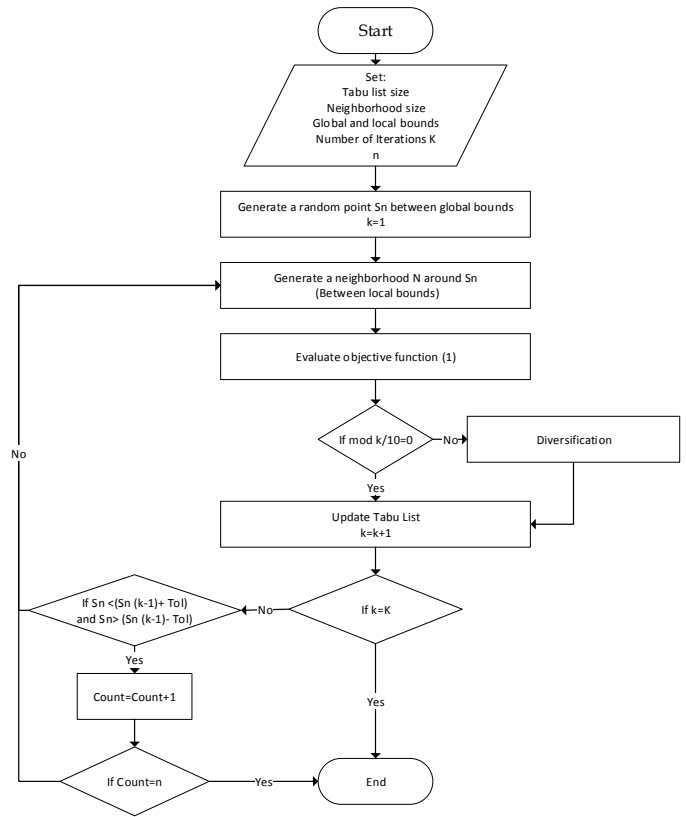


Fig. 5 General flow diagram of tabu search.

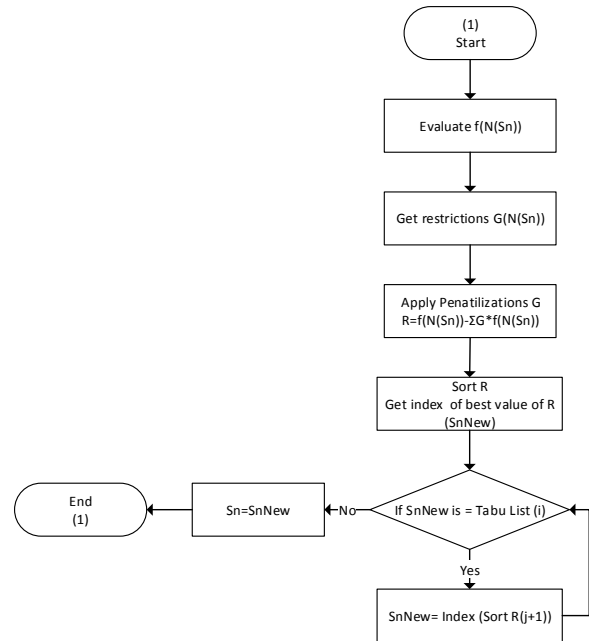


Fig. 6 Sub-routine, tabu search.

This cycle is executed until the stop conditions would be accomplished.

IV. RESULTS

In order to probe the performance of each optimization algorithm explained in section 1 and 2, an objective test function was chosen to minimize it (9), which have two continuous variables:

$$f(x)=(x_1-10)^3+(x_2-20)^3 \quad (9)$$

With the restrictions:

$$G_1=-(x_1-5)^2-(x_2-20)^2+100 \leq 0 \quad (10)$$

$$G_2=(x_1-6)^2+(x_2-5)-82.81 \leq 0 \quad (11)$$

And bound limits:

$$13 \leq x_1 \leq 100 \quad (12)$$

$$0 \leq x_2 \leq 100 \quad (13)$$

A. Differential evolution

To execute the differential evolution algorithm, this parameters were chosen:

- $C_r=0.5;$
- $F=0.7;$
- $N_{pop}=20;$
- $Dim=2;$
- $Lb=[13 \ 0];$
- $Ub=[100 \ 100];$
- $Gen=300;$
- $Countmax=10;$

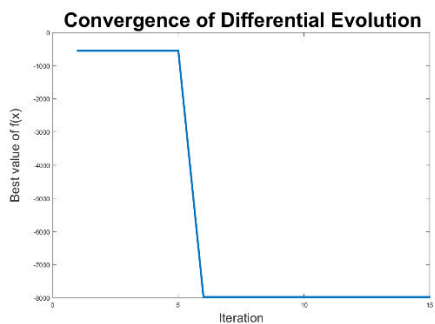


Fig. 7 Convergence of DE.

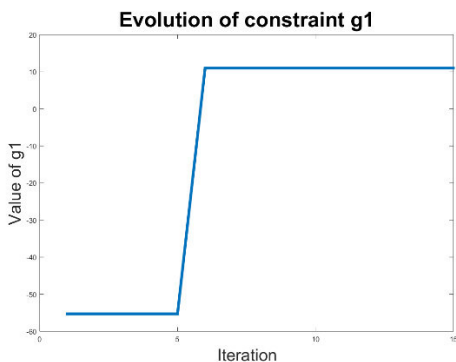


Fig. 8 Evolution of constraint G1 of DE

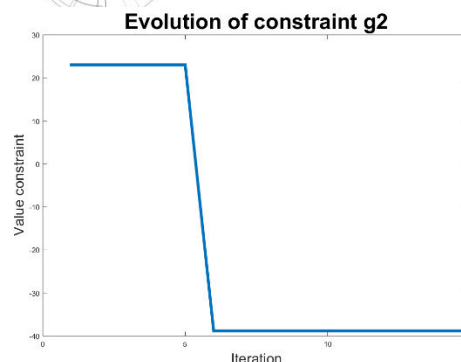


Fig. 9 Evolution of constraint G2 of DE.

In figure 7 could observe the convergence of differential evolution algorithm, it this figure is graph the best value of the population each iteration. The algorithm converges in the 6th iteration, going from a low negative value to large negative value (From -548.80 to -7973). Likewise, the program stops when the best value is repeated during 10 iterations. The evolution of value restrictions g1 and g2 is shown at Fig. 8 and 9, respectively. The restriction g1 starts with a negative value and it becomes positive, in contrast to value of g2 restriction, with starts with a positive value and finishes with a negative value. So, to reach the most negative value of the objective function trying to comply both restrictions, it is sacrificed the negativity of g1. Finally, the program finishes after 1.19 seconds. The best values for x1 and x2 are 13 and 0, respectively.

B. Bee colony

The parameters to run the bee colony algorithm are:

- $C_1=0.5;$
- $C_2=0.5;$
- $Inertia=0.5;$
- $Swarm_{size}=50;$
- $Iter_{max}=200;$

The boundary values (Lb and Ub) are the same that used at DE.

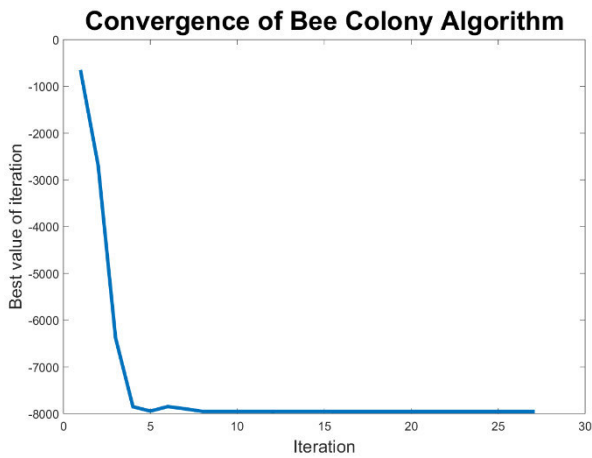


Fig. 10 Convergence of Bee Algorithm

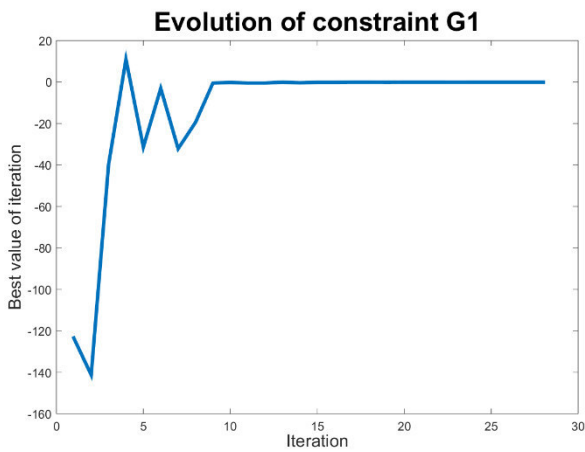


Fig. 11 Evolution of constraint G₁ of bee algorithm

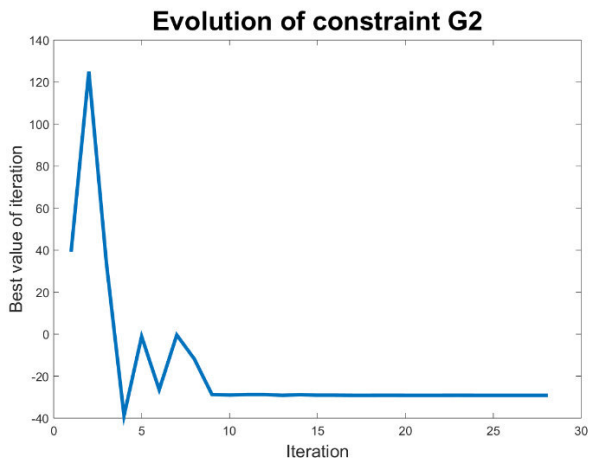


Fig. 12 Evolution of constraint G₂ of bee algorithm

At Fig. 10 can be seen the convergence of bee algorithm, compared with DE there are more oscillations and the bee algorithm converges at iteration 18, going from 138.20 to -7950.9. The changes of restrictions are shown at Fig. 11 and 12, the values of restrictions have the same behavior that shows

in DE, however, the bee algorithm restrictions have many oscillations throughout at beginning. The program finish after 28 iterations or 0.19 seconds. The best values are 13.661 for x_1 and -0.0 for x_2

C. Simulate annealing

For executing this algorithm, the next values were set:

- n= 50; (Probe points to reach T0)
- m=50; (Probe points for each Celsius or Fahrenheit grade)
- Pi= 0.7; (Initial probability)
- Pf=0.001; (Final probability)
- lowLimNex= [5 5]; (Low limit around X_i)
- upLimNet=[5 5]; (Upper limit around X_i)

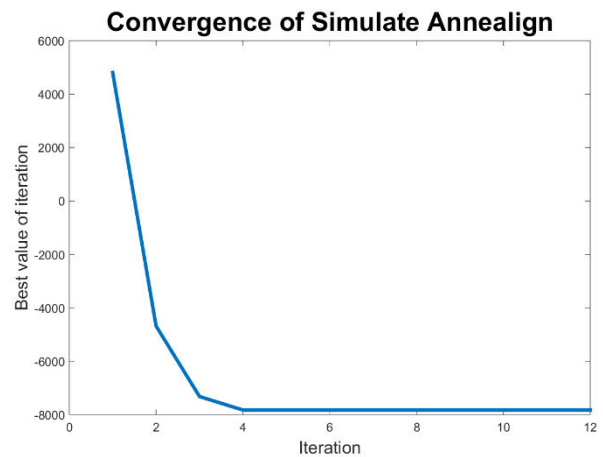


Fig. 13 Convergence of simulate annealing.

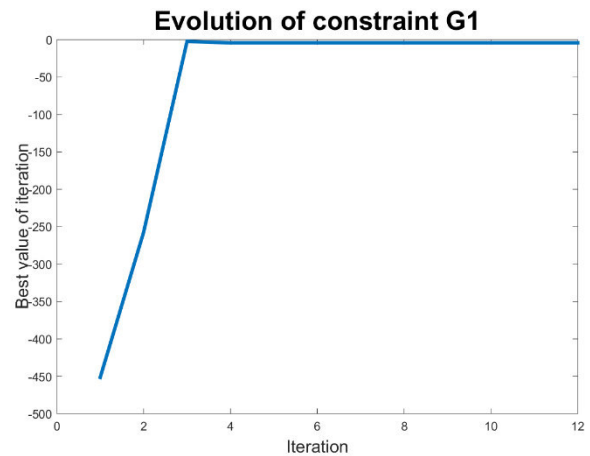


Fig. 14 Evolution of constraint G₁ of simulate annealing

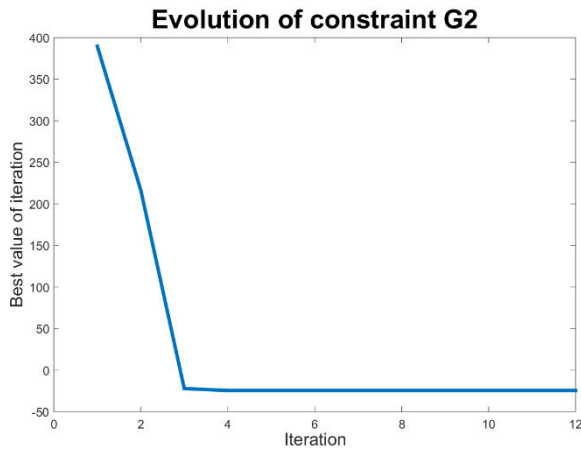


Fig. 15 Evolution of constraint G₁ of simulate annealing

In fig. 13 is shown the convergence of simulate annealing, the initial best value is significantly positive (4808.87) and the last value is as negative as the best value found by the two previous algorithms (-7823.58). The best values for x_1 and x_2 were 13.953 and 0.096, respectively. The time of execution of the program was 0.249 seconds. The restrictions follow the behavior of the DE and Bee Colony, with the slight difference that G₁ is almost zero at early stage.

D. Tabu search

The next values were used to run the tabu search algorithm:

```
Tabusize=4;
Neighborsize = 30;
lowLimNex= [3 3]; (Low limit around Xi)
upLimNet=[3 3]; (Upper limit around Xi)
K= 500;
```

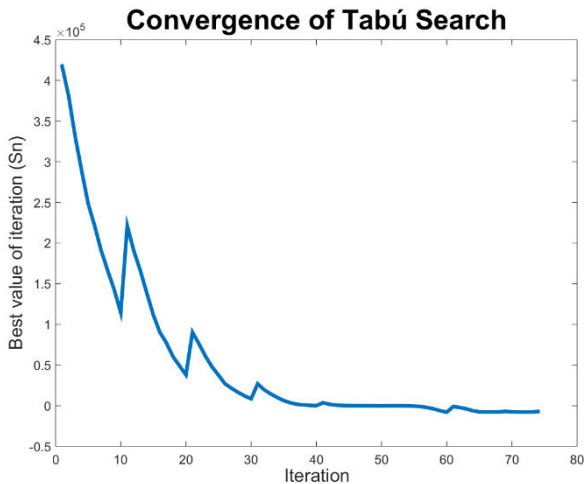


Fig. 16 Convergence of tabu search

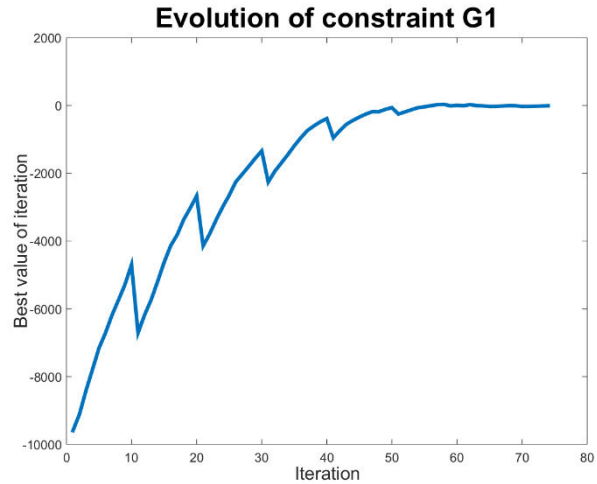


Fig. 17 Evolution of constraint G₁ of Tabu search

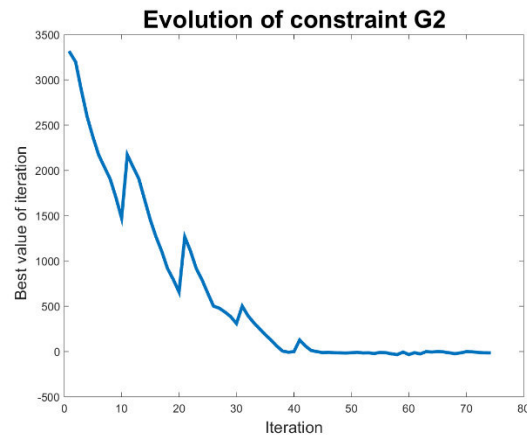


Fig. 18 Evolution of constraint G₂ of Tabu search

Figure 16 shows the convergence of tabu search, in comparison with the previous algorithms, the iterations required to optimize is greater (74 iterations), however, the time elapsed is .20 seconds, probably because it requires fewer operations to optimize. The abrupt changes observed at figure are due to diversification. The best value of the objective function is -7737.02 taking on account the values trapped at tabu list and the variable values are 4.91 and 0.12 for x_1 and x_2 , respectively and g_1 and g_2 are -22.09 and 20.45. The last best value is -7066.24 with $x_1=14.48$ and $x_2=0.72$ with g_1 and g_2 equal to zero. The evolution of constraints showed at Fig. 17 and 18 matches with the behavior of previous algorithms and almost.

V. CONCLUSION

All the optimization algorithms described at this works arrived to similar results. According to nature of each algorithm, it could be observed the differences between them.

For example, the algorithm which had the best results was the differential evolution but the constraints were not entirely fulfilled, it converged with less iterations but took longer processing time. Respect to bee colony, the restrictions were met although the iteration number to converge was higher than DE but with less machine time.

Simulated annealing also complied with the restrictions but the optimized value was worse than that obtained by previous algorithms, also the time elapsed was much less than required by DE. Regarding to tabu search, it required more iterations to reach an optimum, even though the constraints had acceptable values and the time was significantly lower than required by differential evolution.

In conclusion, if the most important is to get the best value of function objective without taking into account time, differential evolution is ideal. If good values are required and the machine time is a factor to consider, bee colony matches with this problem. If the values optimized do not require to be global optima, simulated annealing and tabu search are the options. So, to select an optimization algorithm it is necessary to consider what type of result is expected: a local optimum or a global one, which consumes less iterations to converge or consumes less machine time.

ACKNOWLEDGMENT

The authors thank to CONACYT and the engineering faculty for their support.

REFERENCES

- [1] M. Birattari, L. Paquete, T. Stützle and K. Varrentrapp, "Classification of metaheuristics and design of experiments for the analysis components," Darmstadt, 2001.
- [2] G. Jones, "Genetic and Evolutionary Algorithms," in *Encyclopedia of computational chemistry*, John Wiley & Sons, 2002.
- [3] K. E. Parsopoulos and M. N. Vrahatis, *Particle swarm optimization and intelligence: Advances and applications*, Hershey: IGI Global, 2010.
- [4] C. Gologlu and M. Zeyveli, "A genetic approach to automate preliminary design of gear drives.," *Computers & Industrial Engineering*, vol. 57, pp. 1043-1051, 2009.
- [5] K. S. K. Rajiv Tiwari, "An optimum design of crowned cylindrical roller bearings using genetic algorithms," *Journal of mechanical design*, vol. 131, Mayo 2009.
- [6] S. Corbera, J. L. Olazagoitia and J. A. Lozano, "Multi-objective global optimization of a butterfly valve using genetic algorithms," *ISA Transactions*, no. 63, pp. 401-412, 2016.
- [7] K.-S. Low and T.-S. Wong, "Optimization of a Hard Disk Drive Using Multiobjective Genetic Algorithm," *Cybernetics and Intelligent Systems, 2004 IEEE Conference on*, vol. 2, pp. 706 - 711, 2004.
- [8] J. Zhao, F. Yao, H. Wang, Y. z. Mi and Y. i. Wang, "Research on application of genetic algorithm in optimization design of transformer," *IEEE*, pp. 955-958, 2011.
- [9] E. M. Bates, W. J. Birmingham and C. Romero-Talamás, "Design optimization of nested bitter magnets," *IEEE Transaction on magnetics*, vol. 53, no. 3, 2017.
- [10] E.-N. Dragoi, S. Curteanu, A.-I. Galaction and D. Cascaval, "Optimization methodology based on neural networks and self-adaptive differential evolution applied to an aerobic fermentation process," *Applied soft computing*, no. 13, pp. 222-238, 2013.
- [11] Y. Wang, G. Bu, Y. Wang, T. Zhao, Z. Zhang and Z. Zhu, "Application of a simulated annealing algorithm to design and optimize a pressure-swing distillation process," *Computers and chemical engineering*, no. 95, pp. 97-107, 2016.
- [12] M. Roca-Riu, M. Estrada and C. Trapote, "The design of interurban bus networks in city centers," *Transportation Research Part A*, no. 46, pp. 1153-1165, 2012.
- [13] A. Mahapatro and P. Mohan Khilar, "Detection and diagnosis of node failure in wireless sensor networks: A multiobjective optimization approach," *Swarm and Evolutionary Computation*, no. 13, pp. 74-84, 2013.
- [14] K. V. Narasimha, E. Kivelevitch, B. Sharma and M. Kumar, "An ant colony optimization technique for solving min-max multi-depot vehicle routing problem," *Swarm and evolutionary computation*, no. 13, pp. 63-73, 2013.
- [15] P. Das, H. Behera and B. Panigrahi, "A hybridization of an improved particle swarm optimization and gravitational search algorithm for multi-robot path planning," *Swarm and evolutionary computation*, no. 28, pp. 14-28, 2016.
- [16] J. Wu, H. Wu, Y. Song, Y. Cheng, W. Zhao and Y. Wang, "Genetic algorithm trajectory plan optimization for EAMA: EAST articulated maintenance arm," *Fusion engineering design*, vol. 109, no. 111, pp. 700-706, 2016.
- [17] R. Alvizu, X. Zhao, G. Maier, Y. Xu and A. Pattavina, "Energy efficient dynamic optical routing for mobile metro-core networks under tidal traffic patterns," *Journal of lightwave technology*, vol. 35, no. 2, pp. 325-333, 2017.
- [18] K. K. Fung, G. F. Lewis and X. Wu, "The optimisation of low acceleration interstellar relativistic rocket trajectories using genetic algorithms.," *Acta Astronautica*, no. 133, pp. 258-268, 2017.
- [19] P. V. Silvestrin and M. Ritt, "An iterated tabu search for the multi-compartment vehicle routing problem,"



Computers and operations research, no. 81, pp. 192-202, 2017.

[20] F. Bre, A. Santos Silva, E. Ghisi and V. D. Fachinotti, "Residential building design optimisation using sensitivity analysis and genetic algorithm," *Energy and buildings*, no. 133, pp. 853-866, 2016.

[21] X. Li, K. Xing, Y. Wu, X. Wang and J. Luo, "Total energy consumption optimization via genetic algorithm in flexible manufacturing systems," *Computers & industrial engineering*, no. 104, pp. 188-200, 2017.

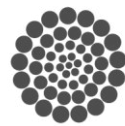
[22] G. Onwubolu and B. Babu, *New optimization techniques in engineering*, Springer, 2013.

[23] M. Muñoz, J. Lopez and E. Caicedo, "Inteligencia en enjambres: sociedades para la resolución de problemas," *Ingeniería e Investigación*, vol. 28, no. 2, pp. 119-130, 2008.

[24] S. Moins, "Implementation of a simulated annealing algorithm for Matlab," Linköping Institute of Technology, 2002.

[25] P. van Laarhoven and E. Aarts, *Simulated annealing: Theory and Applications*, 1987, p. 198.

[26] F. Glover and E. Taillard, "An user's guide to tabu search.," *Annals of operations research*, vol. 41, pp. 3-28, 1998.



CONACYT

Consejo Nacional de Ciencia y Tecnología



CONCYTEQ

Synthesis of Hydroxyapatite Nanostructures by Hydrothermal Microwave Assisted Method and Characterization

Luis Armando Baltazar-Montoya, Susana Alonso-Sierra, Rodrigo, Rafael Alanis-Gómez, and Rodrigo Rafael Velázquez-Castillo

División de Investigación y Posgrado, Facultad de Ingeniería,
Universidad Autónoma de Querétaro, Cerro de las Campanas s/n, C.P. 76010 Querétaro, Qro., México.
Querétaro. Qro.

luis.armandoo10@gmail.com, alonso.susana@yahoo.com.mx, j.rafael.alanis@gmail.com,
rodrigo.velazquez@uaq.mx

Abstract— Hydroxyapatite (HAp) nanostructures have been synthesized by microwave heating using $\text{Ca}(\text{NO}_3)_2$, glutamic acid, K_2HPO_4 and KOH were used as precursors. The precursor concentration was the same in all experiments; also temperature, heating time, the ramp and the reaction time were varied in each reaction. Quartz vessels were used to place the precursor mixture to microwave heating, which made it easier to obtain such HAp nanostructures. X-ray Diffraction (XRD), X-ray fluorescence (XRF), Scanning Electron Microscopy (SEM) and Transmission Electronic Microscopy (TEM) were used to assess the HAp crystalline phase obtained, the Ca/P ratio, morphology and nanostructure of the synthesized structures were used.

Keywords— *Hydroxyapatite; microwave heating; nanofiber; nanostructure*

I. INTRODUCTION

Synthetic Hydroxyapatite (HAp), $\text{Ca}_{10}(\text{PO}_4)_6(\text{OH})_2$, is a bioactive material that is chemically compatible with biological apatite in both, composition and structure [1]. This is the main mineral constituent of hard human tissues such bones and teeth, and possesses excellent biocompatibility and bioactivity, HAp has been widely used in health-related fields as a material for damaged bones or teeth, important implant and scaffold materials and drug delivery agents [2, 3]. Bioactivity is influenced by several factors such as the Ca/P ratio, content of carbonate or other ions, crystal size, morphology and sample texture [1-3].

Natural bone minerals are nanostructured non-stoichiometric Hap of dimensions 20 nm in diameter and 50 nm long [4]. Nanocrystalline HAp has proved to be of greater biological efficacy in terms of osteoblast adhesion,

proliferation, Osseo-integration and formation of new bone on its surface [1,3].

Different methods have been used for nanocrystalline HAp synthesis such as hydrothermal, mechanochemical, electrospinning, chemical precipitation, and microwave irradiation can be effectively used for fabrication of Nanostructures HAp. Depending upon the technique, materials with various morphology, stoichiometry, or level or crystallinity have been obtained [2-4].

Even though various synthesis methods have been used to fabricate nanosized HAp structures, there are intensive interests to find mild and rapid ways for synthesis of pure HAp nanoparticles [1, 2]. Microwave synthesis is a fast, simple and efficient method to prepare nanosized inorganic materials. Compared with conventional methods, microwave synthesis has the advantages of rapid growth, small particle size and narrow particle size distribution due to fast homogenous nucleation [3-5].

Microwaves play an important role in reactions in aqueous media, increasing the yield of precipitations, and have been used for preparing HAp in less than 45 min. Precipitation of nanosized HAp using microwave irradiation has also been reported [6,7]. The thermal stability of microwave synthesized HAp increases with increases in the aging time, microwave irradiation time and power.

Many efforts have been aimed to produce HAp with controlled morphology and dimension using this type of energy source. In addition, the used of pressured Teflon or quartz

vessels in combination with a heating by microwaves helps maintaining homogeneous temperature and pressure in the whole reacting mixture bulk and as a consequence, the crystal growth is easier to control obtaining HAp nanostructures with controlled dimension and with a preferential crystal orientation [3-5].

The mains objectives of this research are the obtaining of HAp nanofiber with diameters in the order of nanometers and lengths of micrometers [7]. The HAp nanostructures will be use on the synthesis of a composite biomaterial which a potential applications in medicine and odontology [3, 4, 7].

II. MATERIALS AND METHODS

A. Synthesis

For the synthesis of HAp by hydrothermal microwave assisted method, the reacting mixtures were prepared in two steps. Initially, one solution was prepared with glutamic acid [$C_5H_9NO_4 \cdot H_2O$] and calcium nitrate [$Ca(NO_3)_2 \cdot 4H_2O$] in 200 ml tri-distilled water. The two components were dissolved by mechanical agitation during 2 hours at 60° C. Also, other solution of monobasic potassium phosphate [KH_2PO_4] was mixed with potassium hydroxide [KOH] in 200 ml tri-distilled water

Finally, both solutions were mixed and this reacting mixture was spilled inside quartz vessels at once. Each vessel contained 50 ml of the mixture, which were closed immediately and placed within a microwave oven (Synthos 3000 by Anton Paar). The power used in the Microwave was 1200 W. All synthesis reactions were carried out at 170° C. The concentration of all reagents remained constant in the reacting mixture in order to evaluate the possible effect of these conditions in the morphology as well as in the microstructure of HAp nanostructures. The Table I summarize the chemical composition of the different reacting mixtures used in this research.

Moreover the heating rate, the reaction and the cooling times are showed in Table I, these conditions were varied to observe possible changes in the morphology of the HAp nanostructures. After heat treatment the samples were dried at room temperature for 24 h.

In order to know how is the growth of the structures a second part reaction time was varied between 5 to 40 minutes and the others conditions were remained same Table II.

B. Characterization

For identify which HAp crystal phase was obtained, each of the HAp nanostructures synthesized were analyzed by X-Ray Diffraction by powder (XRD) using a D8 Advance diffractometer built by Bruker. The operation conditions in the diffractometer were 30 kV and 30 mA using CuK_{α} radiation with a wavelength of $\lambda = 1.5406 \text{ \AA}$. The measurements were made from 10° through 90° on a 2 θ scale with a step size of 0.05°.

TABLE I. FORMULATION OF REACTING MIXTURES AND REACTION CONDITIONS

Reacting	Quantity (gr)	Heating rate (min)	Cooling time (min)
Glutamic acid	1.144	15	10
Calcium nitrate	4	10	15
Monobasic potassium phosphate	0.9272	15	15
Potassium hydroxide	0.736	15	10

TABLE II. DIFFERENT TIMES THAT WERE USED.

Reaction	Temperature (°C)	Power (watts)	Reaction time (min)
HAp-1	170	1200	5
HAp-2	170	1200	15
HAp-3	170	1200	20
HAp-4	170	1200	30
HAp-5	170	1200	40

In addition, observations of the morphology and microstructure of the samples were made using a Scanning Electron Microscope JEOL JSM-6390 LV. The accelerating voltage employed in the microscope was 20 kV and all the images were formed from secondary electrons.

Microstructure was observed using a Transmission Electron Microscope (TEM) JEOL JEM-2100F using 120 kV as accelerating voltage. Moreover most of the images were analyzed using the software Digital Micrograph by Gatan for analyze the HAp nanostructure of nanofibers

Furthermore, XRF analysis was performed to determine the Ca / P ratio of HAp samples and the presence of any impurity substance or residual precursors. The samples were dispersed in 1 ml of isopropyl alcohol as dispersing agent and iron was added as internal standard.

The XRD results confirmed the obtaining of synthetic HAP crystals. Phases identification were made by comparison with some powder diffraction files (PDF's) corresponding to different synthetic HAP phases. The more similar phases were those corresponding to the PDF's 86-1199 and 86-1203.

All samples synthesized produced alike XRD results, which showed in the Fig. 1. The most relevant is the signal at 32.65° of 2θ which is related to the planes (300). This signal is more intense than that at 31.60° corresponding to the planes (211) which is the most intense signal in the PDF's. As a consequence, the abundance of planes (300) is indicative that there is a preferential crystal orientation in the [300] direction in the HAP nanostructures.

In the second part also similar phases were found and corresponding to PDF's previously mentioned. It is observed that the most relevant is the signal at 32.65° of 2θ degrees which is related to the planes (300), 10 minutes after the reaction started these planes began to arise Fig. 2 and Fig. 3.

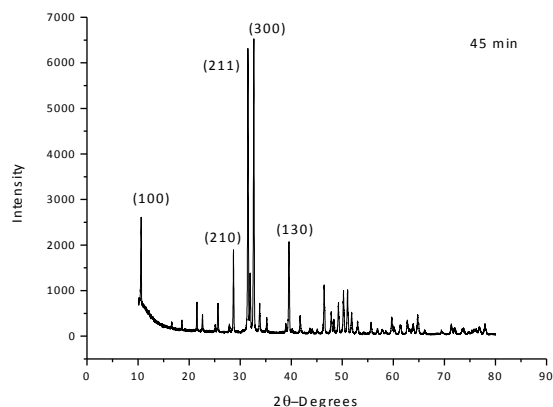


Fig. 1 X-Ray diffraction pattern by powders of the HAP samples by identification of the HAP phases.

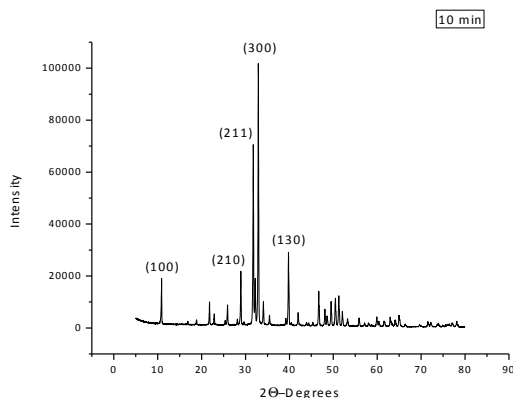


Fig. 2 X-Ray diffraction pattern by powder of the sample HAP at 10 minutes.

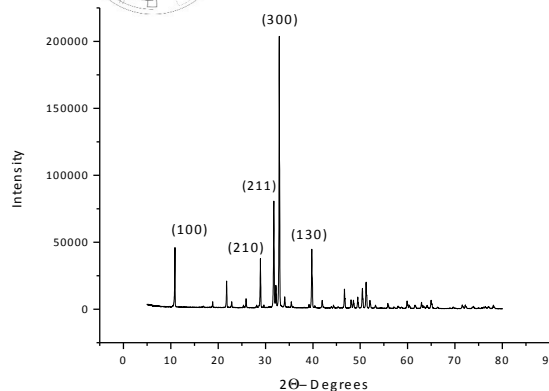


Fig. 3 X-Ray diffraction pattern by powder of the sample HAP at 20 minutes.

Observations through SEM revealed that from all the synthesis reactions, nanofiber structures were obtained with a homogeneous diameter as could be seen in Fig. 4. The length of the nanofibers varied as a function of reaction time, the longer of reaction time, the larger of length in the nanofibers. The thickness also showed a small variation with the reaction time.

Samples of HAP nanofibers were observed by TEM. It is possible to see a periodic arrangement of lines, which correspond, to the HAP crystal structure. The regularity in the lines distribution is an evidence of a high crystallinity structure. Using the software Digital Micrograph by Gatan it was possible to determinate the distance between lines in the images and they were of 2.72\AA which corresponds to the interplanar distance among the (300). This result agrees to that found in the X-Ray diffraction Fig. 5.

The samples were analyzed by XRF to determine the Ca / P ratio, which is important in HAP structures. All the samples analyzed showed similar Ca / P ratios as those elements in Table III.

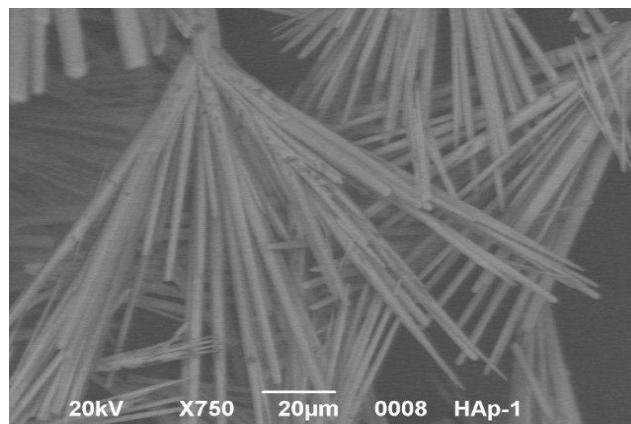


Fig. 4 Micrograph of nanofibers obtained by SEM, showing morphology and topology of nanofibers.

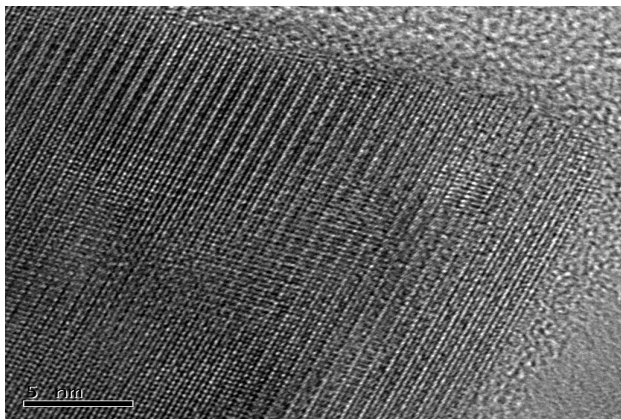


Fig. 5 Micrograph of nanofibers obtained by: HRTEM showing the atomic array of the HAp crystal structure and a detail of one nanofiber morphology.

TABLE III. CA/P RATIO OF THE SYNTHESIZED SAMPLES

# Sample	%P	%Ca	Ca/P ratio
1	32.54	67.46	2.073
2	33.20	66.80	2.012
3	33.02	66.98	2.091
4	34.04	65.92	1.934

IV. CONCLUSIONS

HAp nanostructures were synthesized using the microwave assisted method. The reaction conditions used in the synthesis processes helped to obtain a reproducible structure (nanofibers) and a preferential crystal orientation in the (300). The Ca / P ratio present in all synthesized samples was similar and the average is about 2, indicating that the variations on the synthesis reactions conditions didn't affect the Ca / P ratio.

ACKNOWLEDGMENT

The authors thank the financial support of Fond of Health CONACyT-IMSS-ISSSTE-SSA 2013-1 201329. The authors also acknowledge to José Luis Cabrera Torres for the technical assistance on Electron microscopy.

REFERENCES

- [1] Siddharthan, A., Seshadri, S.K. y Sampath, T.S., "Influence of microwave power on nanosized hydroxyapatite particles", India, Scripta Materialia, Vol. 55, pp. 175–178, May 2006..
- [2] Cabrera, J.L., Velázquez, R. y Rivera, E.M., "Synthesis of Hydroxyapatite Nanostructures Using Microwave Heating", Qro., Mx., Journal of Nanoscience and Nanotechnology, Vol.11, pp. 1 –7, Jun.2011.
- [3] Arami, H., Mohajerani, M., Mazlounia, M., Khalifehzadeh, R., Laka, A. y Sadrezhaad, S.K., "Rapid formation of hydroxyapatite nanostrips via microwave irradiation", Iran, Journal of Alloys and Compounds Vol.469, pp. 391–394, Mar. 2009.
- [4] Eric M. Rivera-Muñoz, R. V.-T., "Morphological analysis of hydroxyapatite particles". Materials Science Forum ,Vol. 638, pp. 681-686, Jan.2010.
- [5] Agrawal, P. C., "Sol-gel derived hydroxyapatite coatings on titanium substrates". Surface & Coatings Technology ,Vol. 206, pp. 360–365, Jul. 2011.
- [6] Šupován, M., "Substituted hydroxyapatites for biomedical applications: A review", Ceramics International , Vol 41, pp. 9203–9231, Mar. 2015.
- [7] Xu Lijuan, J. L., "Effect of different synthesis conditions on the microstructure", Advanced Powder Technology, Vol. 25, pp. 1142-1146, Mar. 2014.

ACI's technology transference for arsenic and pathogens removal to supply safe drinking water

Marcela S. Duhne-Ramírez, Luis E. García
Hernández, Gustavo A. Oliván López, Zaira
Valverde Barragán, José M. Velasco Ramírez, Hilda
Romero Zepeda
Facultad de Ingeniería
UAQ
Queretaro, Mexico
marcela.duhne@uaq.mx

Jay VandenBrink, Harry J. Knopke
Aqua Clara International
Holland, MI, USA

Abstract— Arsenic is one of the top ten chemicals of public health concern and which continuous consumption alters ones health affecting the respiratory, gastrointestinal, cardiovascular and nervous systems. This may be found in water due to natural or anthropogenic causes. Nonetheless, in the world there are communities who depend on arsenic in toxic levels, which are usually located far away from urban areas. The objective of this research was to transfer a low cost filtering system designed by Aqua Clara International (ACI) to remove arsenic and pathogens. This system requires no external sources of energy to treat the water and remove heavy metals and pathogens. Four systems were installed in 2016 in the municipality of Pinal de Amoles, Querétaro. The team was made by faculty members and students of the Department of Engineering at the Universidad Autónoma de Querétaro (UAQ), members of the Council for Water at the State of Queretaro (Comisión Nacional del Agua, CONAGUA), members of the Health Council at the State of Queretaro (Secretaría de Salud del Estado de Querétaro, SESEQ) and representatives for Aqua Clara International (ACI, USA). Water samples were analyzed in the field using a Rapid Arsenic Testing Kit and were compared against the analysis made to the samples in a certified Laboratory. Results indicate that ACI's filters work properly in the field, there was no presence of arsenic once the water was treated by the installed systems, and the Rapid Arsenic Testing Kit may be used in the field because its sensitivity and precision for arsenic concentration..

Keywords— *water treatment; hollow membrane and media filters; rural communities; Sierra Gorda; filtration*

I. INTRODUCTION

In the world, the concern about the water quality has grown; in addition, there has been a decrease of water available for human consumption. The polluted water and sanitation deficit are linked to disease transmission like the cholera, diarrheas, dysentery, hepatitis A, typhoid fever, and the poliomyelitis, among others. These diseases are directly attributed to the presence of pathogens in water. When the

water services and sanitation are insufficient or inappropriately managed or nonexistent, the population is exposed to preventable risks to their health [1]. Therefore, methods to remove pathogens have been studied such as the use of chlorine, ceramic filters, biosand filters, the combination of filtration and chlorine application, use of chlorine and flocculation, use of colloidal silver, solar disinfection, and membranes with different pore sizes [2; 3; 4]. The present research pretends to show the efficiency for arsenic removal.

Heavy metals represent a considerate risk for the health and environment, because they cause neurological and renal damage. In 2015, the World Health Organization (WHO) [1] declares that the presence of heavy metals in food is mainly due to the air, water, and soil pollution.

One of the most dangerous metals is the arsenic, listed among the top ten chemicals of public health concern [5]. Also, arsenic is considered carcinogenic for humans. On certain regions, there exists epidemiological evidence of health alterations because the constant water consumption polluted with arsenic that affects the respiratory, the gastrointestinal, the cardiovascular, and the nervous systems [6].

Reference [5] showed that inorganic arsenic is naturally present at high levels in various countries, but among them, Argentina, Bangladesh, Chile, China, India, Mexico, and the United States of America (USA) [7; 8]. Particularly, Mexico is one of the main countries where arsenic is present in water, some states at the Mexican Republic have shown data for arsenic concentrations above standard levels: Nayarit, Chihuahua, Veracruz, Puebla, San Luis Potosí, Hidalgo, and Nuevo León [9; 10]. Regrettably, as it is indicated by Francisca y Carro-Perez [11], in many places the only source of drinking water available contains dissolved arsenic (As), so it is necessary to study its removal mechanisms.

There are various methods used to remove or reduce arsenic levels based on chemical processes applied alone, simultaneously, or sequentially. Among them are: oxidation

reduction, coagulation-filtration, coagulation-flocculation, precipitation, electrocoagulation, adsorption, ion exchange, liquid and solid phase separation, physical exclusion, membrane technologies, and biological processes [11; 12; 13]. These methods have been developed and applied in different locations and circumstances; regrettably, those that have been applied and evaluated in the field are located in rural or urban populations with a centralized water supply system.

In Latin American countries, among them Mexico, part of its inhabitants depend on water that contains arsenic in toxic levels; these communities are generally located in rural or peri-urban areas. These places are highly or very highly marginalized areas, in addition they have dispersion among its members. References [14] and [15] have worked with solutions of coagulation-flocculation, adsorption, and ion exchange in laboratory. They concluded, in their respective researches, that the reliability of the technology and the laboratory analysis are mandatory, before the field application.

In the previous studies mentioned although they have not been applied successfully in the field, some of the most relevant results are presented as follows. Up to 98% removal of arsenic concentration is obtained with bentonite and ferric chloride as coagulant at the lab and prepared solutions, but its efficiency is reduced to 71-85%, at the lab, using natural waters [11]. More than 99% of arsenic removal was obtained with a pilot plant of electrocoagulation in La Comarca Lagunera, Torreón, Mexico, the initial concentration ranged from 5 to 25 ppb, and after a 1 minute residence time, a voltage of 20-30 V and a current of 5 A, a final concentration of less than 2 ppb was obtained [13]. Finally, solar radiation and zerovalent iron in the form of steel wool and lemon juice is used in Chile and Argentina, with initial concentrations of arsenic up to 1300 ppb, the removal was 99.5%, but this technology has not been deployed and residues need to be studied [15].

The arsenic contamination in Mexico and Querétaro has been documented [16]. Concluding that some aquifers of the state are naturally polluted, while others are anthropologically polluted due to mining; but future research is required to determine which the case of each aquifer is. Whereby, it becomes imperative to implement local systems of purification that allow the population access to drinking water in order to be used to drink, cook and basic hygiene at a lower cost than the commercial.

The purpose of this project was the installation of hydraulic systems developed by Aqua Clara International (ACI), a non-governmental organization (NGO) of the USA. These systems do not require external sources of energy to purify water, removing mainly arsenic and pathogens present in the water. This research, presents the results of four of the five installations carried out in the municipality of Pinal de Amoles, Querétaro during 2016.

This work describes the technology implemented, the team that made possible this project, and the results obtained through the analysis of raw water and purified water. Likewise,

a testing arsenic kit used in the field was used and its results are compared against results obtained in a laboratory.

II. MATERIALS AND METHODS

A. Study Zone

Querétaro has 18 municipalities, with 2 038 372 habitants, of which 70% correspond to the urban area and 30% to the rural area. The 51% of the state's surface has a dry and semi-dry climate located in the central region. The 24.3% of the state has a sub-humid warm climate and is located in the Sierra Madre Oriental. The 23% of its surface has sub-humid temperate climate located in the south, center and northeast of the state. Finally, 1% has humid warm climate and 0.7% has humid temperate climate these are both located at the northeast of the state [17].

The state of Querétaro is in 16th place at levels of marginalization. This represents 17,601 people living in 215 municipalities. Most of these places have problems with drinking water shortages, due to the isolation between these, and the developing cities. Also, the water available is usually polluted.

The communities that received this technology from ACI, belong to the municipality of Pinal de Amoles (Fig. 1). This municipality is part of the mountainous region known as the Sierra Gorda. This is located at 153 kilometers from the state's capital, at north of the State, in a mountainous area with steep slopes, and small plains and plateaus. It has an extension of 705.4 km², which represent the 6.04% of the state's surface.

B. Technology of Aqua Clara International (ACI)

The Universidad Autónoma de Querétaro (UAQ) and Aqua Clara International (ACI) operating in Holland, Michigan,

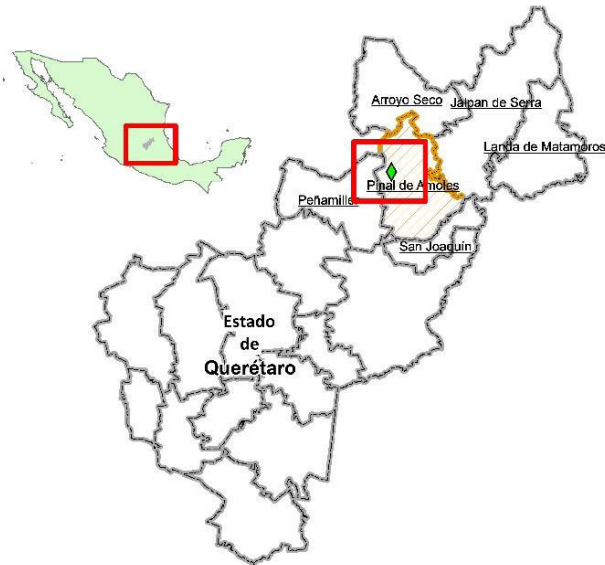


Fig. 1. Location of the municipality of Pinal de Amoles

USA, have an agreement that promotes the transfer of ACI technology to the UAQ so its members: teachers, technical personnel, and students, have the possibility of providing drinking water to the inhabitants of the state of Querétaro.

This technology is the result of four years of laboratory experimentation followed by validation studies in the field. Aqua Clara's laboratory is contained in the Michigan State University Bio-economy Institute; the university assigns an analytical chemist to the Aqua Clara team. The initial formulation of the technology's media was developed in the Aqua Clara laboratory and confirmed by field testing in Nicaragua [18], removing from 45 ppb to 0-1 ppb. Further laboratory refinement of the technology, based on these field studies, resulted in subsequent field testing through systems installed in schools in the Nalbari region of Assam, India [19], where arsenic concentrations found were up to 150 ppb, obtaining final concentrations of 0-1 ppb. Finally, the partnership of Aqua Clara and UAQ led to field tests of revised systems in Queretaro, resulting in household units now being installed in multiple locations in Mexico and Nicaragua, with Aqua Clara responding to requests for this technology from additional countries.

The systems for arsenic and pathogen removal installed in this research, have three stages: The first stage is the pretreatment, where by means of a pre filter the coarse particles and parasites are retained, and turbidity is reduced. Due to the quality of the incoming water source, it was only needed to be installed in one of the communities. The second stage consists of the removal of pathogens. In here, water passes through a roughing filter of 75 microns, and then through two hollow membrane filters 250mm-long of 0.1 microns which retain microorganisms (Fig. 2). These have a pore diameter smaller than the typical size of the bacteria, which is 1-3 microns, obtaining a removal efficiency of 99.9999% of bacteria.

In the third stage, the water passes through a volume of



Fig. 2. Second stage: pathogen removal through hollow membrane filters.

0.02 or 0.04m³ of an adsorbent media, which consists of nanoparticles of titanium dioxide (TiO₂), supported on silicon dioxide (Fig. 3). The TiO₂ traps the arsenic or any heavy metal and retains it while the water passes through the media. Also, this compound is used to disinfect and could remove bacteria too, but it is sought to focus its use on the removal of arsenic. Finally, the water flows by gravity to a storage tank, which has a faucet at the bottom for filling clean and dry containers.

The amount of sand that is placed in the system depends on the concentration of arsenic in the water. This system has demonstrated that can remove arsenic amounts up to 1000 ppb by laboratory testing designed by ACI and Michigan State University.

The filter media is calibrated to be used during two years. At the end of this period, the media can be replaced and will not leach out the arsenic retained. Once used, it can be placed in landfills and even used as sand in asphalt mixture.

This project was feasible with the support of teachers and students of the Faculty of engineering, and Scientifics of Aqua Clara International. Besides them, personnel of Comisión Nacional del Agua (CONAGUA) served as witnesses of the systems installed, and personnel of the Secretaría de Salud del Estado de Querétaro (SESEQ) were responsible of the first contact with the communities and follow-up visits to the installed systems in Pinal de Amoles, Querétaro.

III. RESULTS

The four systems were installed at locations in Pinal de Amoles of 500 habitants or less, installing two systems per visit in May and October 2016 (Table 1). Due to confidentiality of data, the names of the communities are not presented in this article.

In these communities alternative sources of water are available; however, its habitants have identified that they are intermittent or due to the dispersion of the households, it is not feasible to supply all the houses with such sources.

Once installed each of the systems. Samples of water before and after treatment were taken. In field the Quick Rapid

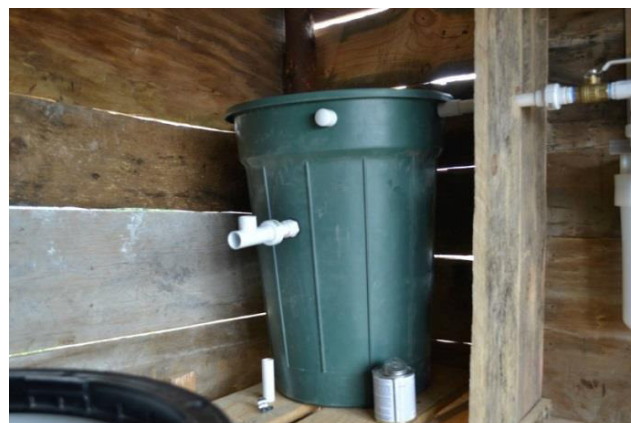


Fig. 3. Third stage: arsenic removal (while installing).

Arsenic Test Kit was used in order to obtain results in 12 minutes. This kit has been used in the field by ACI's Scientists and is manufactured by Industrial Test Systems, Inc., an American company located in South Carolina. Another sample was analyzed in a laboratory, which is certified by the Entidad Mexicana de Acreditación, A.C. (EMA): Ingeniería y Estudios Ambientales, S.A, de C.V. (INESA) of Querétaro.

Table 2, shows the results obtained by the two analysis methods. The Rapid Arsenic Test Kit has a strip which is colored and compared against a table of colors Easy-Read where white is 0 and 0.005 mg/L is the first color, so the results table was written a value of <0.004 mg/L if the strip was not colored. For the community B, due to the color was slightly greater than 0.010 mg/L, the researchers opted for a value of 0.011 mg/L. The correct operation of the removal of arsenic in the last locations could not be detected. In C, due the filling tank was connected to an alternate spring instead of that is allegedly contaminated. While in D, water is stored in an open storage dam and there was rain the week prior to the installation.

The UAQ researchers responsible for the technical implementation of the systems, developed with their experience and through ACI training a series of steps as part of the transfer and adoption process of the technology from ACI in Querétaro. The list of those steps, the actors involved and a brief description of them are presented in the following paragraph.

TABLE I. INSTALLATION DATES OF THE SYSTEMS AND POPULATION PER COMMUNITY

Community	Installation date	Population
A	May 2016	185
B	May 2016	280
C	October 2016	180
D	October 2016	500

TABLE II. ARSENIC CONCENTRATION RESULTS

Community	Inflow (mg/L)		Outflow (mg/L)	
	Kit	Lab	Kit	Lab
A	0.020	0.017	< 0.004	< 0.005
B	0.011	0.012	< 0.004	< 0.005
C	< 0.004	< 0.005	< 0.004	< 0.005
D	< 0.004	< 0.005	< 0.004	< 0.005

1. Identification of the affected communities.

Approach of the UAQ researchers with the SESEQ and the CONAGUA, allowed to define the priority of the communities to benefit with the systems' installation and transference of water filters technology.

2. Training.

ACI provided at least twice a year, training on the installation, use and maintenance of the filtration systems to the

UAQ staff and members of the communities who were benefited.

3. First visit to de community.

3.1. Introductory talk.

With support of SESEQ is made the first approach to the community, in which the purpose, benefit, and how to work on the project is explained. Cooperation of the inhabitants to define the location and construction of the enclosed area for the installation of the filters is required, and a supply water pipeline is requested in this first approach.

3.2. Preliminary diagnosis.

The purpose of this visit is to sample and analyze the arsenic levels and pathogens in water used for daily consumption. Usually, no information is available; therefore, the use of the rapid arsenic testing kit allows the scientists to measure in the field the levels of arsenic. An additional sample is sent for analysis in the laboratory according to the official requirements for arsenic in Mexico.

3.3. Design and installation of the system.

According to turbidity and arsenic concentration that has water, the design of the system is made. First the size of the arsenic's reactor (0.02 m³ or 0.04 m³) is defined. Subsequently, the installation of each of the parts of the system is made. Its components are pre-filter (if needed), roughening filter, two hollow membrane filters, the arsenic reactor and a clean water storage tank. And all components are connected through polyvinyl chlorine (PVC) schedule 40 pipelines to provide safe drinking water to the residents of the community.

3.4. Final diagnosis.

To evaluate the correct functioning, samples are taken to be evaluated with the rapid arsenic testing kit and at the laboratory. Therefore, confirming that the arsenic levels have decreased and they are within the guidelines set by the WHO and the Mexican Standards.

3.5. Corrections.

When it was the case that the arsenic levels did not decrease as much as it was needed to reach the international standards or guidelines, the researchers proceed to review all the installation connections, from the beginning to the final storage tank. If the above does not show problems, the used amount of sand is increased by placing another arsenic reactor next and afterwards the one installed initially.

3.6. Community training.

Finally, to ensure the transfer of the system to the community, their members are trained on how to correctly use the system and for them to know the correct maintenance, which consists in the backwash of the filters located in the second stage of the treatment.

4. Follow-up evaluation.

Again, the water analysis is carried out after three, six, or eight months of the filter's installation in order to warranty the

functioning of the system. If necessary, the appropriate corrections are made to ensure the quality of drinking water.

IV. CONCLUSIONS

The researchers identify that the ACI technology is implemented and properly running in four communities of the state of Querétaro, since they were installed. ACI's filters work properly even the high concentration level for Arsenic at the water samples, because that there was no presence of arsenic once the water was treated by the installed system, and the Rapid Arsenic Testing Kit may be used in the field because its sensitivity and precision for Arsenic concentration. This project depends on the inter-institutional team that allows the problem to be approached from different areas of expertise, and witnesses the correct functioning of the systems. Therefore, it is possible to have new sources of funding and scale the impact to benefit even more people with low-cost technologies, and without the need for external power sources.

ACKNOWLEDGMENT

We thank to the local management of the Comisión Nacional del Agua in Querétaro and the Dirección de Protección contra Riesgos Sanitarios of the Secretaría de Salud del Estado de Querétaro by the logistical support and contact with staff of the locations and municipal authorities. We thank the facilities and support from the government representatives at the Municipality of Pinal de Amoles throughout the reception of the installed systems and commitments acquired to give follow-up to the project.

The authors of the UAQ thank from ACI Bob McDonald for his vision, Marcia Buck for their work and logistical support, and Head for ACI Harry Knopke, and Jay VandenBrink for their work, training, visits to Queretaro and humanity commitment. We thank the financial support from ACI and their financing granted by the West Foundation. Dr. Eusebio Ventura, thank you for collaborating in the project when needed.

Marcela S. Duhne thanks to CONACYT for the scholarship to perform her PhD degree studies.

REFERENCES

- [1] World Health Organization (WHO) (2015). Agua (Water). Available: <http://www.who.int/mediacentre/factsheets/fs391/es/>
- [2] Amin, M. T. y M.Y. Han (2009). "Roof-harvested rainwater for potable purposes: application of solar disinfection (SODIS) and limitations". *Water Science and Technology*, Vol. 60, No. 2, pp. 419-431.
- [3] Lantagne, D. S., R. Quick y E. D. Mintz (2006). "Household Water Treatment and Safe Storage Options in Developing Countries: Review of Current Implementation Practices". *Water Stories: Expanding Opportunities in small-scale Water and Sanitation Projects*, M. Parker, A. Williams & C. Youngblood (eds.), Woodrow Wilson International Center for Scholars. Washington, DC, USA, pp. 17-38.
- [4] Rangel Hernández, J.G. (2015). Proceso de filtración de aguas pluviales a base de plata coloidal (THESIS). Universidad Tecnológica de Querétaro, Santiago de Querétaro, Querétaro.
- [5] World Health Organization. (2011). Arsenic in drinking water: background document for development of WHO guidelines for drinking water quality. WHO/SDE/WSH/03.04/75/Rev/1.
- [6] Campos, V. (2003). "Estudio de un método alternativo para la purificación de arsénico del agua". *Journal of the Mexican Chemical Society*, Vol. 47, No. 3, Julio-Septiembre 2003, pp. 283-286.
- [7] U.K. Chowdhury, B.K. Biswas, T.R. Chowdhury, G. Samanta, B.K. Mandal, G.C. Basu, C.R. Chandra, D. Lodh, K.C. Saha, S.K. Mukherjee, S. Roy, S. Kabir, Q. Quamruzzaman y D. Chakraborti (2000). "Groundwater arsenic contamination in Bangladesh and West Bengal, India". *Environmental Health Perspectives*. Vol. 108, No. 5, mayo 2000, pp. 393-397.
- [8] Bundschuh, J., M.I. Litter, F. Parvez, G. Román-Ross, H.B. Nicolli, J.S. Jean, C.W. Liu, D. López, M.A. Armienta, L.R.G. Guilherme, A. Gómez Cuevas, L. Cornejo, L. Cumbal, R. Toujaguez (2012). "One century of arsenic exposure in Latin America: A review of history and occurrence from 14 countries". *Science of the Total Environment*, Vol. 429, pp. 2-35.
- [9] Cebrian, Mariano E., Arnulfo Albores, Manuel Aguilar, Enrique Blakely. Chronic arsenic poisoning in the north of Mexico. (1983). *Human Toxicology*. 2: 121-133.
- [10] Rico-Rodríguez, M.A., F. Prieto-García, A.D. Roman-Gutiérrez, E.M. Otazo-Sanc y O.A. Acevedo-Sandoval (2013). "Characterization of three soils in Hidalgo and Queretaro, Mexico: availability effects on arsenic in chickpea". *FCA UNCUIYO*, Vol. 45, No. 1, pp. 225-246.
- [11] Francisca, F. M. y M. E. Carro Pérez (2014). "Remoción de arsénico en agua mediante procesos de coagulación-floculación". *Revista internacional de contaminación ambiental*, Vol. 30, No. 2, Mayo 2014, pp. 177-190.
- [12] Litter, Marta I., María E. Morgada Jochen Bundschuh. Possible treatments for arsenic removal in Latin American waters for human consumption. *Environmental Pollution* 158 (2010) 1105-1118.
- [13] Parga, J.R., D.L. Cocke, J.L. Valenzuela, J.A. Gomes, M. Kesmez, G. Irwin, H. Moreno y M. Weir (2005). "Arsenic removal via electrocoagulation from heavy metal contaminated groundwater in La Comarca Lagunera Mexico". *Journal of Hazardous Materials*, Vol. 124, pp. 247-254.
- [14] Bundschuh, J., M. Litter, V.S.T. Ciminelli, M. E. Morada, L. Cornejo, S. Garrido Hoyos, J. Hoinkis, M.T. Alarcón-Herrera, M. A. Arrieta y P. Bhattacharya (2010). "Emerging mitigation needs and sustainable options for solving the arsenic problems of rural and isolated urban areas in Latin America. A critical analysis". *Water Research*, Vol. 44, pp. 5828-5845.
- [15] Litter, Marta I, María Teresa Alarcón-Herrera, María J. Arenas, María A. Armienta, Marta Avilés, Roberto E. Cáceres, Henrique Nery Cipriani, Lorena Cornejo, Luiz E. Diasi, Alicia Fernández Cirelli, Elsa M. Farfán, Sofía Garrido, Liliana Lorenzo, María. E. Morgada, Mario A. Olmos-Márquez, Alejo Pérez-Carrera. Small-scale and household methods to remove arsenic from water for drinking purposes in Latin America. *Science of the Total Environment* 429 (2012) 107-122. Litter et al., 2011b
- [16] Armienta, M.A., C.R. Rodríguez, L.K. Ongley, H. Brust, F. Morales, A. Aquayo, O. Cruz y N. Ceniceros (2007). "Origin and fate of arsenic in a historic mining area of Mexico". Chapter 18 in Bhattacharya et al., (eds) *Trace metals and other contaminants in the environment*, Vol. 9, pp. 473-498.
- [17] INEGI (2015). Cuéntame INEGI. Obtenido de <http://www.cuentame.inegi.org.mx/monografias/informacion/queret/territorio/clima.aspx?tema=me&e=22>
- [18] Alvarez, Gema Daday Rivas, Perez, Eddysson Jamir Flores, Meza, Javier Ramirez. (2003). Potabilización domiciliar de agua de pozo, utilizando filtros de Bioarena y de medio adsorbente de dióxido de titanio para la comunidad rural «La Corona». Universidad Nacional de Ingeniería, Facultad de Ingeniería Química Managua, Nicaragua (April 2003)
- [19] Bhuyan, R. (2013). Test Report of the Three Completed Schools for Rotary Global Grant #25607. Guwahati, India. (May 24, 2013).





Phenotypical responses and DNA methylation changes on transgenic tobacco to *CchGLP* exposed to heavy metal stress

Diana SÁENZ DE LA O, Mariela MARTÍNEZ RESÉNDIZ, Ramón GERARDO GUEVARA GONZÁLEZ, Germán CÁRDENAS MANRÍQUEZ

Biosystems Engineering Group, School of Engineering
Autonomous University of Queretaro
Queretaro, Mexico
sadedi.95@gmail.com

Abstract— The development of heavy metal-tolerant crops represents an alternative to ensure agricultural production in contaminated regions. The objective of this study was to investigate the cadmium and aluminium stress responses of transgenic *Nicotiana tabacum* plant expressing *CchGLP* gene, during germination and early stages of root development. Seeds of this model organism from two highly expressing lines (L8 and L26) as well as an azygote line (L1), were exposed to three concentrations of cadmium chloride (100, 300 and 500 μM) and aluminium chloride (50, 150 and 300 μM). Phenotypic responses were evaluated in terms of germination percentage and root length. The effects of Cd and Al treatments on the DNA methylation level were analysed using 5-mC DNA ELISA Kit. Transgenic line L8 was the line that phenotypically demonstrated to have greater tolerance to the stress since plants showed a higher percentage of germination under both Cd and Al treatments and the root length showed to be significantly higher too. The transgenic line L8 showed a higher percentage of methylation in its natural state (without stress) comparing to azygote line L1, which might be due to the transgene expression. However, under all treatments, line 1 showed higher methylation compared to its control, unlike L8 which, compared to its control, showed less methylation, except for cadmium treatment at 100 μM concentration. The tolerance of L8 against cadmium and aluminium was attributed to the endogenous and uniform production of hydrogen peroxide that these plants exhibit and to the induction of genes related to the systemic acquired resistance. DNA methylation did not show to be the molecular mechanism that determines this resistance.

Keywords—*Nicotiana tabacum* c.v. *Xanthi nc*, aluminium resistance, cadmium resistance, DNA-methylation.

I. INTRODUCTION

Soil contamination with toxic levels of heavy metals is one of the main abiotic stresses that affects crop yield. Cadmium (Cd) and Aluminium (Al) contamination in soils is a major

ecological concern since they are two of most widespread heavy metals in terrestrial environments [1]. Acidic soils are the result of the indiscriminate discharge of heavy metals generated mostly by anthropogenic activities such as industrial processes, modern agricultural practices, acid mine drainage and human wastes. Natural geological activities, such as soil erosion and volcanoes, constitute also an important source of these elements in soils [2,3].

Cd is a non-essential element for plants which is highly toxic to all species even at very low concentrations. Its absorption is carried out easily by plant roots and translocated to the aerial organs causing chlorosis, leaf roll, browning of root tips and inhibition of growth due to the reduction in some processes such as photosynthesis, respiration and water and nutrient uptake [1,4]. Soils often also contain toxic concentrations of Aluminium (Al) ions (10 to 100 μM), therefore Al toxicity is considered as the most important factor limiting plant growth in acidic soils [5,6,7]. Interestingly, experimental works in this respect report a very wide variety of results, depending on the plant species, Al concentration used, duration of exposure, and growth conditions, but most of them agree in that the primary effect under aluminium stress in plants result in gross changes in root morphology and root growth inhibition [8,9]. The reduced and damaged root system results in swollen root apices, root thickening, poor or no root-hair development, disturbances of root peripheral tissues and initiation of lateral roots closer to the root tip, altering the water balance and nutrient assimilation [5,9]. It has also been reported that low concentrations of Al may have some physiological role in some plants, especially in accumulator species, considering it as a beneficial element but not an essential nutrient for plants [10].

Heavy metal-induced effects also include genotoxicity which is studied by epigenetics. In this subject, DNA methylation has been extensively studied, mainly in mammals, and consists in that cytosine nucleotides can be methylated at

carbon 5 of the pyrimidine ring [5-methylcytosine (5-mC)] by DNA methyltransferases, if methylation is excessive this may lead to gene silencing [11]. Reference [1] study in which *Posidonia oceanica* plants were exposed to Cd treatments demonstrate that this element induced a DNA hypermethylation through the involvement of a specific methyltransferase.

In previous work in our laboratory, *Nicotiana tabacum* Xanthi nc expressing the gene *CchGLP* was engineered as an ideal expression model for studying the elements involved in molecular defence networks in plants. The *CchGLP* gene, which was identified and characterized from a collection of habanero chilli plant (*Capsicum chinense* Jacq BG-3821), codes for a germin-like protein (GLP) which showed superoxide dismutase activity (SOD) [12]. GLPs belong to the cupin superfamily and their expression has been associated with a variety of specific stages of plant development but particularly with different types of biotic and abiotic stress [13,14]. It was also identified that *CchGLP* is part of the salicylic acid and ethylene signalling pathways, so it has an active role in the defence response of the plant [15]. In fact, this transgenic tobacco has shown to have tolerance to stress caused by geminivirus, *Pseudomonas silyngae* pv tabaci and *Fusarium oxysporum* infections [16,17]. This experiment was carried out adopting a molecular approach in combination with phenotypical parameters.

The aim was to evaluate the responses of seed germination and growth of *N. tabacum* Xanthi nc expressing *CchGLP* against cadmium and aluminium toxicity.

II. MATERIALS AND METHODS

A. Plant Material and Germination Assay

Two highly expressing *CchGLP* transgenic lines of *N. tabacum* xanthi nc (L8 and L26) and an azygote line (L1), which was used as control, were generated in previous work and seeds were obtained by self-pollination [17]. Seeds were surface-sterilized by incubation for 1 min in 95% ethanol, 7 min incubation in 10% bleach and 0.1% Tween 20 solution and finally five washes with sterile distilled water in laminar flow cabinet. Seeds were sown directly in 90-mm sterilized Petri dishes, containing 20 to 25 seeds each one, in Murashiage-Skoog medium with addition of cadmium chloride (CdCl_2) and aluminium chloride (AlCl_3) at three different concentrations: 100, 300 and 500 μM and 50, 150 and 300 μM respectively. Seeds were kept at room temperature (22 °C) under a photoperiod of 16-h light/8-h dark. Each treatment was replicated three times.

B. Effect of Cd and Al on Germination Percentage and Root Length

Germinated seeds were recorded every day after sowing until no further radicle emergence was observed (day 7) and germination percentage was then calculated. At 16 d after sowing, 10 plants of each treatment were sampled for the determination of primary root length using a digital caliper.

C. DNA-Methylation Assays

Seedlings tissues, from one of the transgenic lines (L8) and control plants (L1), that were exposed to concentrations 100,

150 and 300 μM of AlCl_3 and 100 and 500 μM of CdCl_2 were collected, frozen in liquid nitrogen and subsequently stored at -80 °C. Genomic DNA was then isolated essentially as follows: 100 mg of each treated sample was grind to a fine powder in a mortar using liquid nitrogen and then mixed with 750 μl of CTAB buffer. Samples were vortexed and incubated for 5 min at room temperature. Then 750 μl of chloroform-isoamylalcohol (24:1) were added followed by vortex and a centrifugation at 12,000 RPM for 5 min at 4° C. The top layer or aqueous phase was removed with a micropipette, transferred into a new polypropylene conical tube and mixed with 2/3 of its volume of isopropanol 100% and 1/10 of its volume of sodium acetate 5 M. After incubation for 10 min at room temperature, samples were centrifuged at 12,000 RPM for 5 min at 4 °C. Then the supernatant was discarded and the obtained DNA pellet was washed with 1 ml of chilled 70% ethanol and a gentle vortex. Samples were again centrifuged at 7,500 RPM for 5 min at 4°C and the supernatant was discarded. Pellets were air dried and suspended in 50 μl of DEPC-treated distilled water. The methylation percentage test was carried out following the protocol included in the instruction manual of the 5-mC DNA ELISA Kit from ZYMO RESEARCH which basically works by detecting and quantifying 5-methylcytosine in the DNA samples by a monoclonal antibody (Anti-5-Methylcytosine). The ratio CpG dinucleotides density/genome length utilized was that for *Arabidopsis thaliana*, 0.022, giving a fold difference of 3.409.

D. Statistical Analyses

Differences between values of phenotypical and molecular assays were calculated using two-way analysis of ANOVA with Tukey's multiple comparisons test at a significance level of 0.05 in GraphPad PRISM 6 software. All results are presented as means \pm standard error (SE) of three replicates.

III. RESULTS AND DISCUSSION

A. Germination Percentage and Root Length

Results showed that the germination rate of both transgenic lines was higher than control line under all the three different concentrations of cadmium (Cd) (Fig. 1). Differences were highly significant specially for line 8.

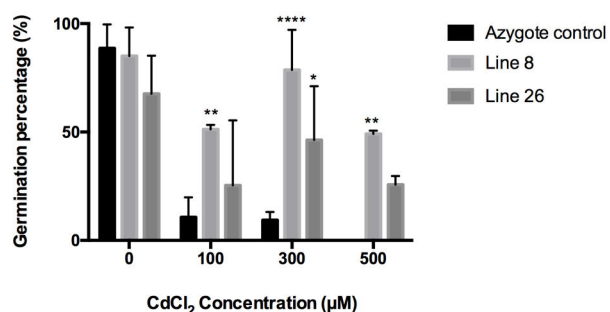


Fig. 1. Percentage of germination of the azygote control and of the transgenic lines to the gene *CchGLP* L8 and L26 of *N. tabacum* cv, xanthi nc at day 2, after sowing, in medium with different concentrations of Aluminium Chloride. Results were considered significant (*) when $P \leq 0.05$ and highly significant (**) when $P \leq 0.01$ and (***) $P \leq 0.001$ according to the Tukey test.

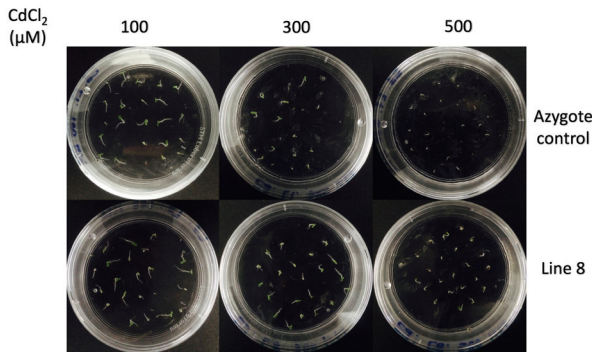


Fig. 2. Azygote control (L1) and transgenic line (L8) under cadmium stress at day 5 after sowing.

Increases in cadmium concentration in the medium resulted in dramatically decreased germination rate in control plants and the inhibition of plant growth and development in germinated seedlings was evident under concentrations 300 and 500 μM . Fig. 2 shows that L8 seedlings were more vigorous than control plants at day 5 after being sowed. Root length of transgenic plants was higher than that of control plants 16 days after being sowed (Fig.3). Under the cadmium concentration of 100 μM , the development of transgenic plants was normal and without symptoms of stress, some of the plants already had true leaves. Fig. 4 confirms this fact, however, by increasing the concentration to 300 and 500 μM , we began to notice symptoms of stress in transgenic plants, especially darkening and malformation of the roots was evident in some of them. The damage was worse for the azygote line, in this same figure it can be observed that under the concentration 100 and 300 μM of the salt, growth is severely retarded with many rolled leaves and malformed root tips and at the concentration of 500 μM plants showed complete growth arrest. Results of germination under Aluminium (Al) stress showed a behaviour which has been already reported which is that aluminium in the medium promoted the acceleration of radicle emergence. On day 2 after sowing there wasn't any germinated seeds on plates with 0 μM concentration, however under 100, 150 and 300 μM all lines showed already radicle emergence on this day.

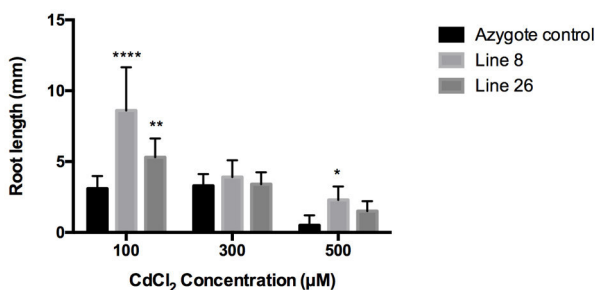


Fig. 3. Root length (mm) of the azygote line (control) and transgenic lines (L8 and L26) at day 16 after sowing in medium with different concentrations of Cadmium Chloride (100, 300 and 500 μM). Results were considered significant (*) when $P \leq 0.05$ and highly significant (**) when $P \leq 0.01$ and (****) $P \leq 0.001$ according to the Tukey test.

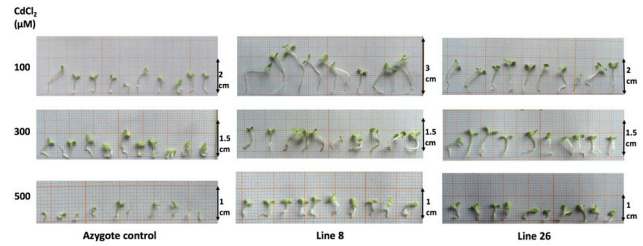


Fig. 4. Stem and root length of azygote (control) and transgenic lines (L8 and L26) at day 16 after sowing in medium with different concentrations of Cadmium Chloride (100, 300 and 500 μM).

Among them, transgenic line L8 showed higher germination rates under the different concentrations (Fig. 5). Root length was not a factor that showed significant differences between control and transgenic plants, except for L8 under the concentration of 100 μM (Fig. 6). We decided to study under microscopic observation the roots of the plants of line 1 and line 8 that grew under the lowest (100 μM) and highest concentrations of Al (300 μM). We found no great differences under 100 μM concentration between the two lines, however, the roots of L1 showed to have malformations in the tip, swelling of the same and null presence of root hairs. L8 roots under the same concentration were more vigorous and showed normal growth of root hair (Fig. 7). We confirmed that even if transgenic lines L8 and L26 both suffered the transformation process and highly express the transgene CchGLP, they behave different under adverse growth conditions.

This translates to us that the transgene acts of different form, depending on the site to which it has been inserted in the genome of the plant. At least under Cd and Al stress, L8 is more tolerant than L26. It was also clearly shown that the effect of Cd on the germination and development of seedlings is dependent on its concentration and differed greatly among the transgenic and the control lines, being transgenic lines more tolerant under this type of stress. This was not necessarily true for aluminium stress, at least at root length, however differences in root vigour were found, with transgenic plants being healthier.

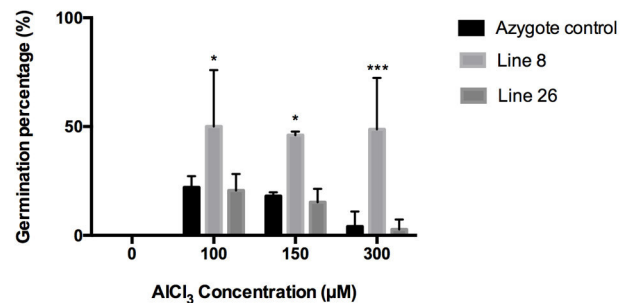


Fig. 5. Percentage of germination of the azygote control and of the transgenic lines to the gene CchGLP L8 and L26 of *N. tabacum* cv, xanthi nc at day 2, after planting, in medium with different concentrations of Aluminum Chloride. The results were considered significant (*) when $P \leq 0.05$ and highly significant (**) when $P \leq 0.01$ and (****) $P \leq 0.001$ according to the Tukey test.

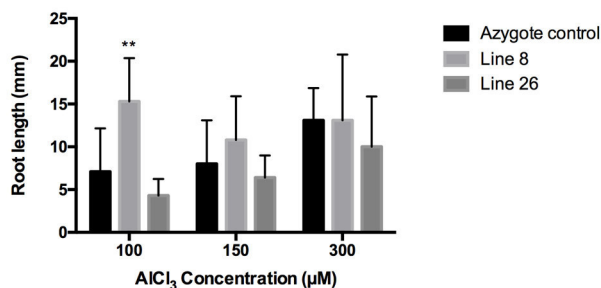


Fig. 6. Root length (mm) of the azygote line (control) and transgenic lines (L8 and L26) at day 16 after sowing in medium with different concentrations of Aluminum Chloride (100, 150 and 300 μ M). The results were considered significant (*) when $P \leq 0.05$ and highly significant (**) when $P \leq 0.01$ according to the Tukey test.

Definitely Cd stress was found to be more aggressive to plants than Al stress and L8 transgenic plants tolerate it better.

B. Methylation Percentage

We decided to quantify the DNA methylation percentage of lines 1 and 8, since this last line showed to be the most resistant between the two transgenic lines used in the phenotypical assays in this experiment. The results obtained showed very small percentages of methylation that varied between 3% and 10%, therefore the differences were not significant, however certain patterns were found. The methylation percentage of the azygote line tended to be higher in plants under Cd and Al stress, comparing with its control in salt-free medium. In contrast, plants of the L8 transgenic line were more methylated in its natural state (without stress) than under Cd and Al stress, except for 100 μ M concentration of Cd, which was the only significant difference throughout the assay. Hypermethylation has already been reported by reference [1] in *Posidonia oceanica* under Cd stress.

In salt-free medium, the transgenic line presented a higher percentage of methylation than the control line, which was to be expected because in their natural state these plants present continuous production of hydrogen peroxide and therefore greater induction and repression of genes related to the defense mechanism of plants.

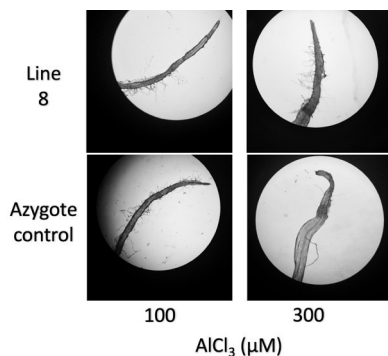


Fig. 7. Root tips of azygote control and transgenic line L8 under aluminum stress 16 days after sowing.

These results give us the clue that the heavy metal stress tolerance of the transgenic line is not due to hyper or hypo methylation of the DNA.

IV. CONCLUSIONS

We consider that the transgenic plants used in this study are naturally under a stress state because of the fact that they are constantly producing hydrogen peroxide due to the transgene expression. During this experiment we exposed them to an additional stress, specifically heavy metal toxicity, and it appeared that these transgenic plants were more prepared to tolerate it compare to their azygote control. According to the results it could be concluded that cadmium has an adverse effect on the non-transgenic tobacco cultivar, while transgenic plants were more resistant. Aluminium stress turned out to be much less aggressive and under the used concentrations in this experiment, none of the lines showed total deterioration in vegetative development, however the roots of the azygote line showed much more damage than those of line 8. With these results we confirm what has been frequently reported in the literature that aluminum stress, under certain concentrations, mainly affects plant roots and cadmium stress to both vegetative and root development.

Our goal in measuring the percentage of DNA methylation was to determine whether this molecular mechanism is key in the tolerance of transgenic plants under heavy metal stress. However, this type of stress appeared to have no major effect on DNA methylation in the plants used in this experiment. Even if methylation of transgenic line under 100 μ M of cadmium showed a significant difference compared to azygote line we still not assume that this is considered hypermethylation because it is only 9% of the DNA methylated. It would be very useful for us to know the *N. tabacum* specific parameters that indicates hyper or hypo methylation, as they have been established for another species. However, there is still very little information on this subject.

Results provide new insights that can lead to a better understanding of the molecular basis of heavy metal responses of seeds at the germination stage as studying the DNA methylation patterns and the expression of genes can lead to understand plant immunity. Additionally, these breakthroughs will provide new molecular resources for improving crop tolerance via both molecular-assisted breeding and biotechnology. Line 8 distinguished as the most resilient so it's a target cultivar to be studied. The next step includes studying Al and Cd effects on the vegetative stage of these plants, which is essential for the mentioned purposes and study of miRNAs which will complement the molecular findings.

ACKNOWLEDGMENT

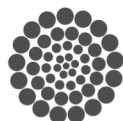
We thank the Autonomous University of Queretaro and CONACYT for the support to carry out this research.

REFERENCES

- [1] Greco, M., Chiappetta, A., Bruno, L., Bitonti, M.B., 2012. In *Posidonia oceanica* cadmium induces changes in DNA methylation and chromatin patterning. *J. Exp. Bot.* 63, 695–709. doi:10.1093/jxb/err313



- [2] Alloway, B.J., 2013. Introduction, in: Alloway, B.J. (Ed.), *Heavy Metals in Soils: Trace Metals and Metalloids in Soils and Their Bioavailability*. Springer Netherlands, Dordrecht, pp. 3–9. doi:10.1007/978-94-007-4470-7_1
- [3] Singh, S., Parihar, P., Singh, R., SINGH, V.P., Prasad, S.M., 2015. Heavy metal tolerance in plants: Role of transcriptomics, proteomics, metabolomics and ionomics. *Front. Plant Sci.* 6, 1–36. doi:10.3389/fpls.2015.01143
- [4] Yue, R., Lu, C., Qi, J., Han, X., Yan, S., Guo, S., Liu, L., Fu, X., Chen, N., Yin, H., Chi, H., Tie, S., 2016. Transcriptome Analysis of Cadmium-Treated Roots in Maize (*Zea mays* L.). *Front. Plant Sci.* 7, 1–11. doi:10.3389/fpls.2016.01298
- [5] Ciamporova, M., 2002. Morphological and structural responses of plant roots to aluminium at organ, tissue, and cellular levels. *Biol. Plant.* 45, 161–171.
- [6] Kochian, L. V., Hoekenga, O.A., Piñeros, M.A., 2004. How Do Crop Plants Tolerate Acid Soils? Mechanisms of Aluminum Tolerance and Phosphorous Efficiency. *Annu. Rev. Plant Biol.* 55, 459–493. doi:10.1146/annurev.arplant.55.031903.141655
- [7] Zhao, X.Q., Chen, R.F., Shen, R.F., 2014. Coadaptation of Plants to Multiple Stresses in Acidic Soils. *Soil Sci.* 179, 503–513. doi:10.1097/SS.0000000000000086
- [8] Delhaize, E., Ryan, P.R., 1995. Aluminum Toxicity and Tolerance in Plants. *Plant Physiol* 107, 315–321. doi:10.72/315 [pii]
- [9] Kochian, L. V., Piñeros, M.A., Hoekenga, O.A., 2005. The physiology, genetics and molecular biology of plant aluminum resistance and toxicity. *Plant Soil* 274, 175–195. doi:10.1007/s11104-004-1158-7
- [10] Hajiboland, R., 2012. Effect of micronutrient deficiencies on plants stress responses, in: Ahmad, P., Prasad, M.N.V. (Eds.), *Abiotic Stress Responses in Plants: Metabolism, Productivity and Sustainability*. Springer, pp. 283–329. doi:10.1073/pnas.0703993104
- [11] Andresen, E., Hendrik, K., 2013. Cadmium toxicity in plants, in: Sigel, A., Sigel, H., Sigel, R.K.O. (Eds.), *Cadmium: From Toxicity to Essentiality*. Springer, pp. 395–413. doi:10.1007/978-94-007-5179-8
- [12] Barrera-Pacheco, A., Joaquín-Ramos, A.D.J., Torres-Pacheco, I., González-Chavira, M.M., Pérez-Pérez, M.C.L., Guevara-Olvera, L., Guevara-González, R.G., 2008. Análisis de la expresión transcripcional inducida Bajo condiciones de estrés biótico y abiótico en *Capsicum chinense* BG-3821. *Agrociencia* 42, 95–106.
- [13] Davidson, R.M., Reeves, P.A., Manosalva, P.M., Leach, J.E., 2009. Germins: A diverse protein family important for crop improvement. *Plant Sci.* 177, 499–510. doi:10.1016/j.plantsci.2009.08.012
- [14] Dunwell, J.M., Gibbings, J.G., Mahmood, T., Saqlan Naqvi, S.M., 2008. Germin and germin-like proteins: evolution, structure and function. *CRC. Crit. Rev. Plant Sci.* 27, 342–375. doi:10.1080/07352680802333938
- [15] León-galván, F., Joaquín-ramos, A.D.J., Torres-pacheco, I., 2011. A Germin-Like Protein Gene (CchGLP) of *Capsicum chinense* Jacq . Is Induced during Incompatible Interactions and Displays Mn-Superoxide Dismutase Activity 1200, 7301–7313. doi:10.3390/ijms12117301
- [16] Guevara-Olvera, L., Ruíz-Nito, M.L., Rangel-Cano, R.M., Torres-Pacheco, I., Rivera-Bustamante, R.F., Muñoz-Sánchez, C.I., González-Chavira, M.M., Cruz-Hernandez, A., Guevara-González, R.G., 2012. Expression of a germin-like protein gene (CchGLP) from a geminivirus-resistant pepper (*Capsicum chinense* Jacq.) enhances tolerance to geminivirus infection in transgenic tobacco. *Physiol. Mol. Plant Pathol.* 78, 45–50. doi:10.1016/j.pmpp.2012.01.005
- [17] Ruiz Nito, M., 2009. EXPRESIÓN TRANSGÉNICA DE CchGLP (*Capsicum chinense* GLP) en *Nicotiana Tabacum* Xanthi nc PARA EVALUAR RESISTENCIA A GEMINIVIRUS.



CONACYT

Consejo Nacional de Ciencia y Tecnología



CONCYTEQ

Chitosan electrospun nanofibers with Au/Ag Nanoparticles

Synthesis and Characterisation

Adrián Roca Aranda

Laboratory of Nanostructured
and Functional Materials
Autonomous University of
Querétaro

Querétaro, México

AdrRocaA@gmail.com

Eduardo A. Elizalde P.

Laboratory of Nanostructured
and Functional Materials
Autonomous University of
Querétaro

Querétaro, México

eelizalde@uaq.edu.mx

Susana Meraz Dávila

CINVESTAV

Querétaro, México

smeraz@cinvestav.mx

Rafael Ramirez Bon

CINVESTAV

Querétaro, México

rrbon@cinvestav.mx

Abstract— Chitosan solutions in acetic acid were studied for electrospinning process. Thus, we are looking for establish a method of synthesis that generates a stable blend of chitosan and poly (ethylene oxide) with gold and silver nanoparticles. In order to reduce the surface strength and becomes the electrospinning process into an easy one we incorporate Triton X-100 into the blend. The results obtained for the synthesis of gold and silver nanoparticles by separately are consistent with the literature and we show that is possible to add nanoparticles into the fibers, but this research is still in process to obtain a better distribution of the nanoparticles.

Keywords—Chitosan; Silver; Gold; Nanoparticles; Nanofibers, Electrospinning.

I. INTRODUCTION

Advances in the medicine have been paralleled by increased interactions among multiple disciplines such as biology, material sciences, and engineering. The origin of tissue engineering stems from the demands by surgeons in regenerating functionally active tissue to replace those lost due to trauma, congenital malformations, or various disease [1].

It is already known that tissues are conformed by cells that interact between them. These cells need a kind of support such as spatial and physicochemical given by a structure known as extracellular matrix (ECM) where they are guided through their growing and differentiation (in the case of stem cells), therefore the ECM provides a substrate with specific ligands for cell adhesion and migration, and regulates cellular proliferation and function by providing various growth factors [2, 3].

In order to mimic the structure and biological function of native ECM and generate functional tissues to biomedical

applications, engineers have been developing new biodegradable and biocompatible synthetic or natural polymer structures called scaffolds [4]. The supporting scaffold temporarily replaces the function of the ECM, in general should impart a 3D geometry, have appropriate mechanical properties, enable cell attachment, and facilitate the development of a functional tissue [1]. At the microscopic level, a highly porous structure is needed for diffusion of nutrients and waste products through the scaffold. Finally the scaffold should have good mechanical properties, enabling handling during cultivation in bioreactors and transplantation into the patient [2].

In our body, the natural ECMs are mainly conformed by two kind of extracellular macromolecules: (1) Proteoglycans and (2) Fibrous proteins with diameters ranging from 50 to 500 nm depending on the tissue type [5]. For example, collagen is a natural ECM component of many tissues, such as skin, bone, tendon, ligament, and other connective tissues and exists in a three-dimensional network structure composed of multi-fibrils in the nanofiber scale [6, 4].

As was explained, it is needed a material that can replace for a while the ECM, thus it should be chosen a process which allows to create a structure with nanometric characteristics. In fact, there are a lot of techniques for this task but there is one in particular that has been used more frequently in the recent years by researchers because of it actually generates a fibrous structure like the ECM [7]. For this technique, it is used an electrospinning which generates fibers at the submicron scale, yielding a three-dimensional porous network (a random mat) of nanofibers with high aspect ratio and a large specific surface area by utilizing electrostatic forces to create these fibers [8]. In the electrospinning process, a polymer solution is advanced through a syringe with a needle on the end to form a Taylor

cone (a conically shaped volume of fluid). A voltage drop is created between the needle and collector. When the electrostatic force is able to overcome the surface tension force, and a thin jet will form and thin out over the course of three stages: jet initiation and extension in a straight line, whipping instability, and jet solidification and fiber collection [9].

We focused on chitosan as a polymer for electrospinning instead of collagen because the second one isn't enough available in nature as chitosan and it has a poor immunogenicity [10]. Thus, Chitosan is a linear polymer, the partially deacetylated form of chitin, obtained from crustaceans [11]. It's biocompatible, biodegradable, and antimicrobial nature has resulted in significant research activity in fields such as drug delivery, tissue engineering scaffolds, and wound healing dressings [12, 13]. It also is insoluble in water, alkali, and most mineral acidic systems. However, though its solubility in inorganic acids is quite limited, chitosan is in fact soluble in organic acids, such as dilute aqueous acetic, formic, and lactic acids [14].

Additionally, to improve the engineering-tissue properties that provides by itself the chitosan nanofibers, other compounds are added into the chitosan solution such as silver nanoparticles (AgNPs) and gold nanoparticles (AuNPs) [15, 16]. The reason that AgNPs were selected is that they have long been a broad spectrum and highly effective antimicrobial agent in biomedical applications for treating wounds and burns on the benefit of its surface plasma resonance. Since AgNPs are relatively stable, electrospun AgNP-containing membranes were recognized as safe materials with strong inhibitory and bactericidal effects, in comparison with those containing ionic Ag which may cause the discoloration of ultrafine fibers and the skin [17]. Because of the unique cationic-polyelectrolyte character and gel-forming ability, chitosan could bind metal ions by electrostatic attraction [18]. It has been widely accepted that protonated amine and hydroxide sites are the main reactive sites for interaction with metal ions. AgNPs in a good dispersion state could be synthesized with the aid of chitosan [19]. Moreover, we include AuNPs as their excellent biocompatibility and especially because it was found that chitosan-AuNPs nanocomposites enhance the proliferation of human fibroblasts on chitosan. This significant enhancement of biocompatibility may be due to the altered surface morphology. The size of the surface nanometric domains could have an impact on the cellular response [20].

But there is an obstacle in the process to create fibers via electrospinning with this chitosan solution and it is its high viscosity [10]. Consequently, has been introduced the polyethylene oxide (PEO) to resolve this viscosity problem taking advantage of its biocompatibility and that it is one of the few synthetic polymers approved for internal use in food, cosmetics, personal care products and pharmaceutical. It had been studied that spinnability of chitosan solutions depends strongly on the mass ratio of chitosan to PEO, and nanofibrous structures with fiber diameters ranging from 80 to 180 nm were achieved from the solution with a PEO-to-chitosan mass ratio of 1:1 [21].

Hence, we show as a first part of the whole research a study about the preparation and characterization of a stable chitosan-

Ag/Au-NPs blend suitable for electrospinning once that PEO was introduced into the solution

II. EXPERIMENTAL SECTION

A. Materials

We used Chitosan low molecular weight [Deacetylated chitin, Poly(D-glucosamine)], Poly (Ethylene Oxide), Glacial Acetic Acid, Triton X-100, Dimethyl Sulfoxide, Silver Nitrate (AgNO_3) and Chloroauric Acid, all of these purchased from Sigma Aldrich.

B. Synthesis of a suitable solution of Chitosan to contain Au and Ag Nanoparticles

Solutions of chitosan 2 and 3 wt% were prepared in acetic acid 2% as a stock. Then a solution of HAuCl_4 and chitosan 2% were mixed in a volume ratio of 3:1 at 100 °C for a while until the solution turns into a pink-red color.

At this moment two different methods were followed just with a little change between them to synthesize the AgNPs.

Therefore, a solution 0.05M of AgNO_3 was incorporated into the chitosan 3% solution and after that a fresh solution of NaBH_4 was added to reduce the AgNO_3 and by this reaction get the AgNPs. It is necessary ensure that AgNO_3 reacts completely. A continuous stirring was needed at any time of the synthesis. Then the solution of chitosan-AgNPs was mixed with a little amount of chitosan-AuNPs solution.

In the other method, a chitosan 3 wt% solution was added into the blend of chitosan-AuNPs in a volume ratio of 4:1. And the AgNPs were synthesized in the resulting solution following the same steps using AgNO_3 and NaBH_4 previously.

So, we have two final solutions with nanoparticles, one of this is a blend by a final mixing and the other one is a blend of chitosan and Au-AgNPs by a continuous synthesis.

C. Synthesis of a suitable solution for electrospinning process

1) Preparation of Chitosan/PEO solution (CsPEO)

Chitosan and PEO were dissolved in 2% Acetic Acid to obtain a 2, 4, 6 wt% solution with a mass rate of 5:1 between them. Then a little amount of Triton X-100 was added into the solution and finally 2.7 ml of Dimethyl Sulfoxide (DMSO) was incorporated into the solution. The final solution was stirred overnight to ensure its well mixing.

2) Preparation of AuNPs Solution

It was used a solution of HAuCl_4 2.193 mM in order to get in the final solution a concentration of AuNPs of 60 ppm. Subsequently Chitosan 2 wt% and HAuCl_4 were mixed in a volume rate of 3:1 at 90 °C with constant stirring until the solution turn its color into pink.

3) Preparation of Chitosan/PEO solution with Au and Ag Nps (CsPEO-NPs)

From the AuNPs solution 5 ml were added into the Chitosan/PEO solution at constant stirring, then 1 ml of AgNO_3 0.03M was mixed into this solution and after a while finally 1 ml of NaBH_4 was added drop by drop.

D. Electrospinning process

A certain amount of the CsPEO-NPs solution was loaded in a 10-ml syringe with 0.6 mm inner capillary diameter and flat-tipped tip. The capillary was connected with a high voltage power supply which could generate positive DC voltages up to 30 kV. The flow rate of the solution was controlled by a syringe pump which could adjust the flow rate. A grounded piece of aluminum foil was placed in front of the capillary tip.

The parameters used in the electrospinning system were different for each solution but we placed the aluminum foil at 15 cm from the capillary tip for every experiment. We used a range voltage from 10 to 25 kV and a flow rate from 0.04 to 5.00 ml/hr. When we found what were the correct parameters, that produce a continuous jet and the formation of the Taylor's cone, we used them for the electrospinning process with the solutions that contain nanoparticles. These final parameters were a voltage of 15 kV and a flow rate of 0.5 ml/hr.

E. Characterization

The morphology of the electrospun fibers of CsPEO and CsPEO-NPs was observed under a scanning electron microscope. The fiber diameter of the electrospun fibers was measured by ImageJ software. In order to confirm the presence of Ag and Au nanoparticles in the fibers, ultraviolet-visible spectrophotometry was performed with a system used for solids. Finally to verify the presence of Ag and Au nanoparticles in the fibers, TEM observations were carried out at room temperature using a Cu grid with a thin layer of fibers deposited previously on it.

III. RESULTS & DISCUSSES

A. Synthesis process of Chitosan-AgNPs

We could observe that AgNPs synthesis using NaBH₄ must be controlled at any time, adding the NaBH₄ drop by drop and at moderate stirring because it could show aggregate easily as we see in Figure 1a. Using the half or a low concentration of NaBH₄ the AgNO₃ is possible (Fig. 1) but it couldn't be obtained the maximum yield from the reaction also there will

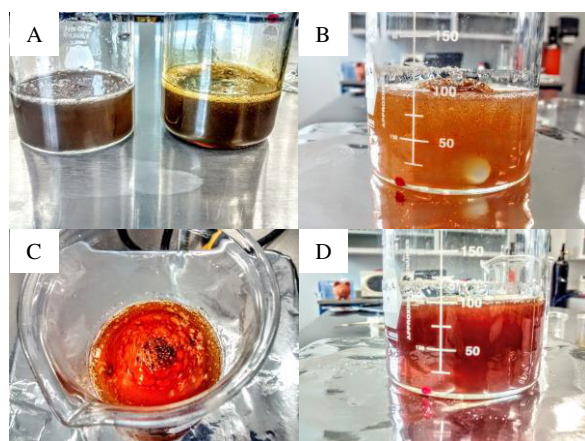


Fig. 1. Samples of AgNPs preparation with NaBH₄. (A) NaBH₄ added too fast into CS 2% & 3%. (B) Using the half concentration of NaBH₄ into CS 2%. Using the complete concentration of NaBH₄ into (C) CS 2%. (D) CS 3%.

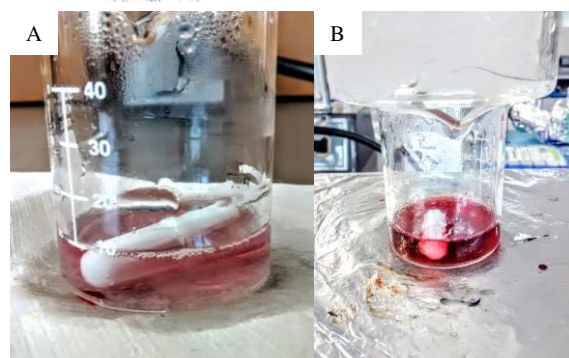


Fig. 2. Solution of Chitosan-AuNPs (A) first color change and (B) final color change after a few minutes.

be either AgNO₃ as AgNPs and the literature indicates that if it is used a low concentration of NaBH₄ it would be aggregate easily with the pass of time [22]. The color showed by the sample with AgNPs will depend of the concentration of AgNO₃ used but we could observe that in the same way the concentration of CS could influence in the final color showed (Fig. 1C & D).

B. Synthesis process of Chitosan-AuNPs

The solution generated via this method has a characteristic pink-red color, but we observed that the reaction didn't finish immediately when it began to turn pink because after a few minutes it got a pink-red color (Fig. 2) but it doesn't mean that AuNPs were collapsing in spite of this, it is just because chitosan hadn't finished to reduce the entire solution of HAuCl₄ yet.

C. Continuous Synthesis of AgNPs from a blend of chitosan AuNPs

This method give us more control over the reduction of AgNO₃. In this manner, there wasn't observed aggregating and the color of solution was like purple that looked translucent that is a good indicator of NPs could be well disperse (Fig. 3).

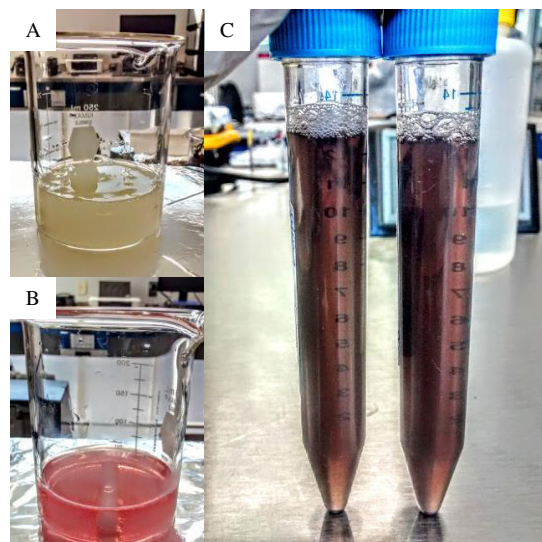


Fig. 3. Continuous Synthesis of AgNPs. (A) Chitosan in acetic acid. (B) Chitosan with AuNPs. (C) Chitosan with Au/Ag-NPs blend.

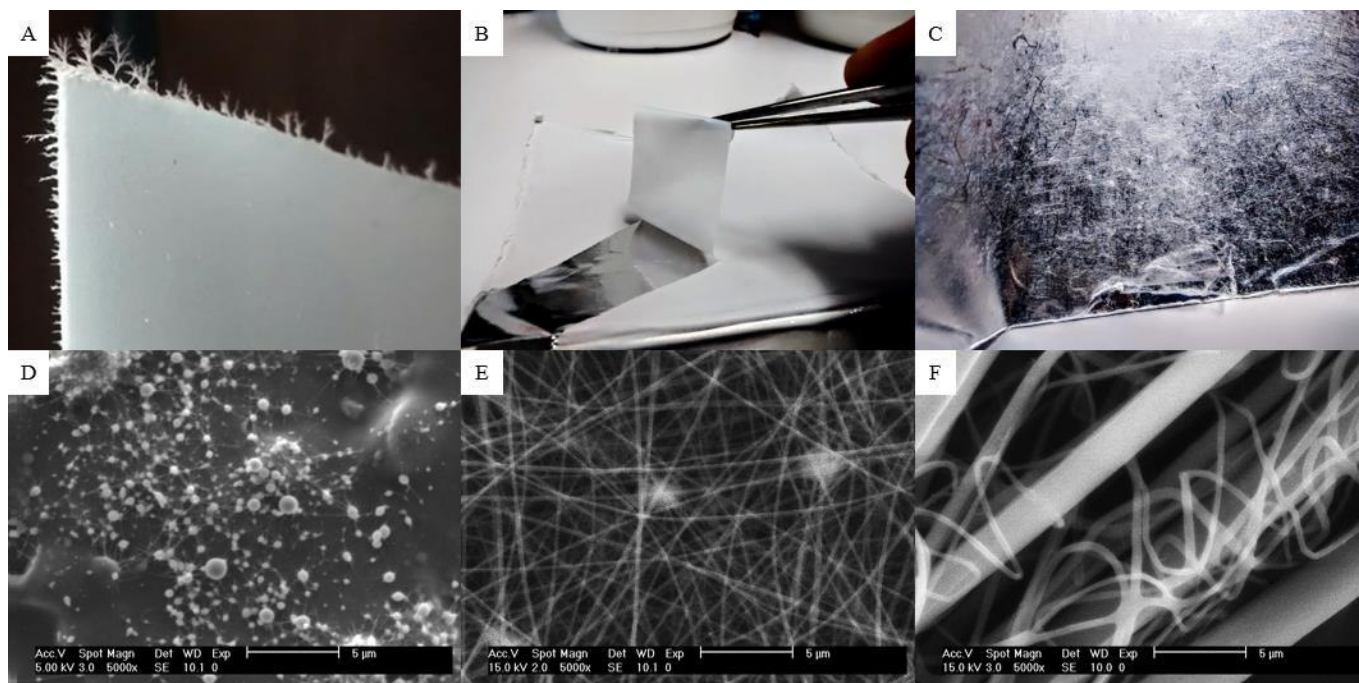


Fig. 4. Morphology observed after electrospinning process from solutions of CsPEO 2, 4 and 6 wt%; A, B and C on the aluminum foil; D, E and F images obtained by SEM.

It was the same result in both cases using CS 2% and CS 3% the difference is in the consistence of the final solution compared with the chitosan dissolved only in acetic acid it could help in case of chitosan 3% that is too viscous initially. According to this results and literature about Chitosan Fibers it was proposed the synthesis method of a suitable solution with Nanoparticles for electrospinning using Poly (Ethylene Oxide), Triton X-100 and DMSO to improve the spinnability of Chitosan.

D. Fiber Morphologies

Firstly the solutions of CsPEO with different concentration were studied in Fig. 4 to identify which one could generate fibers using the electrospinning process before to add the nanoparticles at macroscale and microscale.

It was observed that solution with a concentration of 2 wt% generated a thin film without enough integrity so it could be removed as a frail powder Fig. 4A and as result it couldn't be handled easily, using SEM we corroborated the lack of continues fibers instead of this we could identified in the Fig.

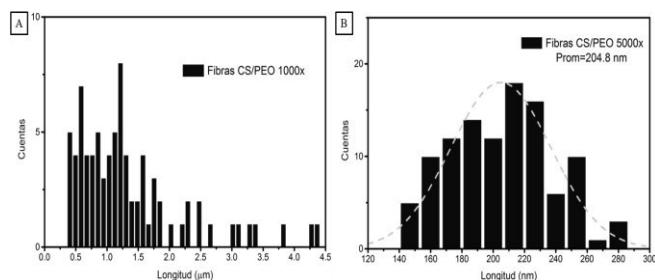


Fig. 5. Distribution of fiber diameters from solution (A) 6 wt% and (B) 4 wt%.

4D several beads the reason of the appearance of powder on the aluminum foil.

In case of 6 wt% solution the electrospinning process wasn't enough to generate fibers by itself because the drop on the capillary tip didn't form the Taylor cone because the surface tension was too strong due to the high viscosity of the solution and only when the tip was cleaned the drop elongated and a kind of strand was ejected to the aluminum foil. As a result of this we could observe a mat of fibers with a naked eye in Fig. 4C so it implicated that fibers were too thick and we checked this on SEM image in Fig. 4F with different diameter sizes ranging from 400 nm up to 4.4 μm as we can observe in Fig 5A.

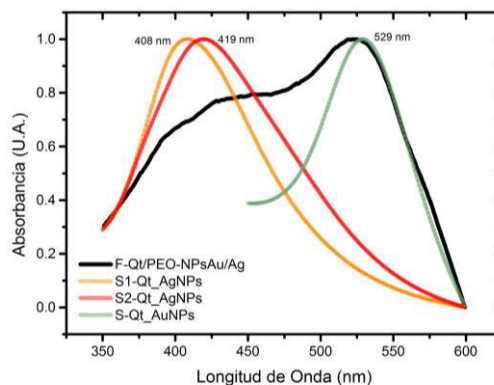


Fig. 6. Absorption spectrum from silver nanoparticles (red and orange lines), gold nanoparticles (green line), fibers with Ag and Au Nanoparticles (black line).

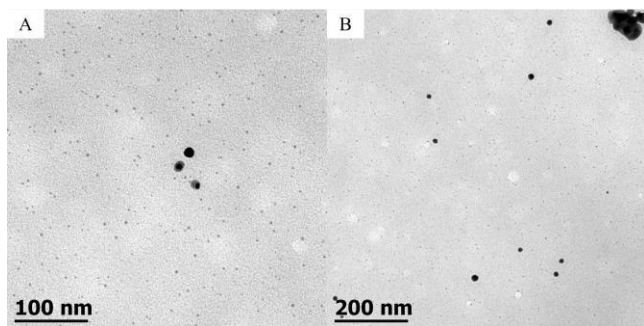


Fig. 7. TEM image of Ag and Au nanoparticles in fibers

Finally the information obtained from the solution with a concentration of 4 wt% demonstrated that this should be used when nanoparticles were added because it can generate a thin film that could be recovered and handled easily from aluminum foil (Fig. 4B) it could be observed the presence of several fibers in Fig. 4E with homogenous structure, these fibers just showed a slight difference between its diameters and they display an average diameter of 204.8 nm (Fig. 5B) that is good enough for the purpose of this research.

E. UV-Vis Spectra

In order to confirm the presence of Au and Ag NPs in fibers resulted from electrospinning process the absorption spectrum was measured and compared with the known spectrums of these nanoparticles Fig. 6. In case of gold nanoparticles, it could be inferred its presence in fibers because the absorption spectrum shows approximately at the same wave length an absorption peak very well defined. In the other case at the range of absorption range of silver nanoparticles it is observed an absorption curve that indicate the possible presence of this nanoparticles.

F. Nanoparticles images

The presence of nanoparticles was confirmed via TEM images that exhibit small particles with average size of 5 nm that are well disperse between them and another group of particles that show agglomeration with a bigger average size (Fig. 7 A and B). At first sight, according with literature, it is assumed that the smallest particles correspond to the Ag nanoparticles and the bigger ones correspond to the Au nanoparticles.

IV. CONCLUSION

The first part of this research showed that Chitosan could be electrospun using Poly (Ethylene Oxide) in addition of Triton X-100 and DMSO, but it is possible only when the concentration of the final solution has enough polymer to generate continuous fibers without overload the solution with a high concentration that makes the electrospinning process too hard (because of its high viscosity and surface strength). The addition of nanoparticles is possible without compromise the fiber formation but it should be studied a little more to

ensure their complete dispersion without exhibit agglomeration.

ACKNOWLEDGMENT

This work was supported by Autonomous University of Queretaro. And we would also like to thanks CINVESTAV, Queretaro division, to provide us the electrospinning equipment and all the characterization facilities during this research.

REFERENCES

- [1] T. L. Cato and S. N. Lakshmi, *Nanotechnology and Regenerative Engineering: The Scaffold*, Second edition ed., New York: CRC Press, 2015.
- [2] D. Tal, T.-G. Orna y C. Smadar, «"Designer" Scaffolds for Tissue Engineering and Regeneration,» *Israel Journal of Chemistry*, vol. 45, pp. 487-494, 2005.
- [3] M. Zuwei, K. Masaya, I. Ryuji y R. Seeram, «Potential of Nanofiber Matrix as Tissue-Engineering Scaffolds,» *Tissue Engineering*, vol. 11, n° 1/2, pp. 101-109, 2005.
- [4] S. R. Kyong, J. Lim, L. Gene, S. Byoung-Moo, J. P. Yoon, H. Seong-Doo, R. Sangho, J. C. Jae, H. P. Won and M. Byung-Moo, "Electrospinning of collagen nanofibers: Effects on the behavior of normal human keratinocytes and early-stage wound healing," *Elsevier*, vol. 27, pp. 1452-1461, 2006.
- [5] T. Elsdale and J. Bard, "Collagen Substrata for Studies on Cell Behavior," *The Journal of Cell Biology*, vol. 54, pp. 626-637, 1972.
- [6] J. A. Matthews, G. E. Wnek, D. G. Simpson y G. L. Bowlin, «Electrospinning of Collagen Nanofibers,» *American Chemical Society*, vol. 3, pp. 232-238, 2002.
- [7] S. S. Ojha, D. R. Stevens, T. J. Hoffman, K. Stano, R. Klossner, M. C. Scott, W. Krause, L. I. Clarke and R. E. Georgia, "Fabrication and Characterization of Electrospun Chitosan Nanofibers Formed via Templating with Polyethylene Oxide," *American Chemical Society*, vol. 9, pp. 2523-2529, 2008.
- [8] K. Sun and Z. H. Li, "Preparations, properties and applications of chitosan based nanofibers fabricated by electrospinning," *EXPRESS Polymer Letters*, vol. 5, no. 4, pp. 342-361, 2011.
- [9] J. D. Schiffman y C. L. Schauer, «Cross-Linking Chitosan Nanofibers,» *American Chemical Society*, vol. 8, pp. 594-601, 2007.
- [10] N. Bhattarai, D. Edmondson, O. Veisoh, F. A. Matsen and M. Zhang, "Electrospun chitosan-based nanofibers and their cellular compatibility," *Elsevier*, vol. 26, pp. 6176-6184, 2005.
- [11] A. Precot, C. Viton and A. Domard, "Optimization of Chitin Extraction from Shrimp Shells," *Biomacromolecules*, vol. 4, no. 1, pp. 12-18, 2003.
- [12] J.-K. F. Suh and H. W. Matthew, "Application of chitosan-based polysaccharide biomaterials in cartilage tissue engineering: a review," *Biomaterials*, vol. 21, no. 24, p. 2589-2598, 2000.
- [13] A. Matsuda, G. Kagata, R. Kino and J. Tanaka, "Preparation of Chitosan Nanofiber Tube by Electrospinning," *Journal of Nanoscience and Nanotechnology*, vol. 7, no. 3, pp. 852-855, 2007.
- [14] H. Homayoni, S. A. Hosseini Ravandi y M. Valizadeh, «Electrospinning of chitosan nanofibers: Processing optimization,» *Carbohydrate Polymers*, vol. 77, p. 656-661, 2009.
- [15] J. An, H. Zhang, J. Zhang, Y. Zhao y X. Yuan, «Preparation and antibacterial activity of electrospun chitosan/poly(ethylene oxide) membranes containing silver nanoparticles,» *Colloid Polym Sci*, vol. 287, p. 1425-1434, 2009.
- [16] E. Yan, X. Li, C. Wang, Z. Sun, L. Ni y D. Zhang, «Electrospun

polyvinyl alcohol/chitosan composite nanofibers involving Au nanoparticles and their in vitro release properties,» *Materials Science and Engineering C*, vol. 33, p. 461–465, 2013.

- [17] D. Lee, R. E. Cohen and M. F. Rubner, "Antibacterial Properties of Ag Nanoparticle Loaded Multilayers and Formation of Magnetically Directed Antibacterial Microparticles," *Langmuir*, vol. 21, no. 21, p. 9651–9659, 2005.
- [18] H. Huang and X. Yang, "Synthesis of polysaccharide-stabilized gold and silver nanoparticles: a green method," *Carbohydrate Research*, vol. 339, no. 15, p. 2627–2631, 2004.
- [19] Y.-K. Twu, Y.-W. Chen and C.-M. Shih, "Preparation of silver nanoparticles using chitosan suspensions," *Powder Technology*, vol. 185, no. 3, p. 251–257, 2008.

- [20] S.-h. Hsu, Y.-B. Chang, C.-L. Tsai, K.-Y. Fu, S.-H. Wang y H.-J. Tseng, «Characterization and biocompatibility of chitosan nanocomposites,» *Colloids and Surfaces B: Biointerfaces*, vol. 85, p. 198–206, 2011.

- [21] B. Duan, C. Dong, X. Yuan y K. Yao, «Electrospinning of chitosan solutions in acetic acid with poly(ethylene oxide),» *Journal of Biomaterials Science, Polymer Edition*, vol. 15, n° 6, pp. 797-811, 2013.



Molecular determination of *Glomerella cingulata* Penz in avocado Hass

¹Vázquez-Hernández Ma Cristina, ¹Guevara-Gonzalez Ramón G. ¹Alvarado-Mariana Aurora, ¹Aguirre-Becerra Humberto, ¹Macias-Bobadilla Israel, ¹Rico-García Enrique.

¹Biosystem group. School of Engineering. Amazcala Campus. Querétaro Autonomous University, C.U. Cerro de las Campanas, S/N, colonia Las Campanas, C.P 76010, Santiago de Querétaro, Querétaro, México. * Corresponding author. crisedi3@hotmail.com, *ramongg66@gmail.com

Abstract — Avocado has been characterized based on its chemical composition and phenotype. The sensory aspect is not used in quality control, but is an important variable for final consumer. Anthracnosis is a disease caused by the teleomorph fungus *Glomerella cingulata* of *Colletotrichum gloeosporioides* that promotes fruit rot and generates losses for producers of until a 90%. The main objective of this research was to provide an early diagnostic tool for *G. cingulata* to avoid fruit contamination and reduce economic losses for producers. Avocados from Michoacan were sanitized and infected with the pathogen for further microbiological analysis. Polymerase Chain Reaction (PCR) analysis with specific box initiators of high mobility was used, with amplification of the HMG domain of the high mobility box of mating genes MAT 1-2. The presence of the pathogen in infected fruits was confirmed by the amplification of a 238 bp band corresponding to gen MAT 1-2.

Keywords— *Avocado*, *sensory aspects*, *anthracnosis*

I. INTRODUCTION

Avocado (*Persea americana* Mill) var. Hass has become an important international product with a steadily economic growth, ceasing from being an exotic fruit to be part of the diet of many countries population [1, 2]. At the international level, the commercial activity of avocado in Mexico has intensified in the last decades, producing 1,230,973 metric tons per year, where 326.12 thousand metric tons were exported mainly to The United States, Europe and Asia [2]. The main producing Mexican states are Nayarit, Puebla, Mexico State, Morelos and Michoacán, where the latter is the largest producer at international level with an estimated annual production of 950 thousand metric tons [1, 2].

Avocado is a native species cultivated in subtropical climate areas in Mexico that belongs to the Lauracéas family and *Persea* genus [1]. It is a single-seeded berry with a smooth or rough surface and a high nutritional content due to the presence of fatty acids (palmitic and oleic), vitamins A, C, and E, fiber, protein, carbohydrates and minerals [1]. Anthracnosis is an avocado disease caused by the infection of the pathogenic fungus *Glomerella cingulata*, whose spores penetrate the fruit in conditions of high relative humidity (RH) (50-53%) and temperature of approximately 28°C, germinating and forming appressoria that invade the fruit [3]. This disease causes necrotic (melanized) lesions with subsequent rotting of the fruit [3]. Infection progresses faster when the fruit presents lesions

caused by other microorganisms, insects, or mechanical damage occurred during harvesting or postharvest, generating large economic losses to producers and in most cases the total loss of shipment [2].

The PCR is a molecular detection tool which amplifies a gene of interest using specific oligonucleotides [4, 5]. Researchers have reported the use of mating-type genes of *G. cingulata* (MAT 1-2) which amplify a band of approximately 238 bp that is a highly conserved region of its genome which can be used as tool to identify this fungus [3]. Avocados were sanitized, inoculated with the fungus spores, and stored at different maturation times (0, 7, 14 and 21 days), under controlled conditions (53% RH and temperature of 4°C [1]. Microbiological analysis and PCR were used as tools of early detection of this pathogen.

II. MATERIALS AND METHODS

A. Biological material

Avocados from Michoacan orchards were stored for 21 days at 4 ° C and 53% RH, sanitized with a solution of sodium hypochlorite at 150 ppm concentration [6], and infected with fungus spores. Using a climate chamber, morphological studies of the fungus were carried out. To determine the presence of the pathogen amplification of the HMG domain of the high mobility box mating genes MAT 1-2 [5] were performed.

B. Isolation of *G. cingulata*

A monoconidial strain of *G. cingulata* (CT-100) was isolated from an avocado from Uruapan, Michoacán. Avocado was selected based on the lesions presented in the fruit [7]. Infected sample was microscopically examined, and a spore of the fungus was selected and seeded in potato and a dextrose solid medium (PDA) to obtain a pure culture, which was replaced each month, stored at room temperature and at 4°C in medium PDA [1].

C. Morphological studies

Pieces of infected pulp and control sample pulp (not infected) and three pieces of peel (approx. 1 cm²) were cut. From the first piece a sample was placed on a microscope

slide to observe the presence of *G. cingulata* spores. The second piece was incubated at room temperature on a slide in a wet chamber, and was observed under microscope at 0, 24, and 48 hours. From the third piece the extraction of genomic DNA was performed to be used as pattern in the amplification by PCR to identify the presence of the pathogen [7, 8]. Sample was analyzed randomly for triplicate.

D. Extraction of genomic DNA (mycelium of the fungus, peel and avocado pulp)

Modified Dellaporta protocol was used. Sample was grinded with liquid nitrogen and placed in a 1.5 ml Eppendorf tube where 1 ml of Dellaporta regulator was added and vortexed. 50 µl of SDS 20X was resuspended by inversion and incubated at 65°C for 20 min. 300 µl of 5M potassium acetate was added, and rested on ice for 20 min for posterior centrifugation at 12000 rpm for 10 min.

Two extractions of supernatant were performed with phenol: chloroform, and homogenized by vortexing during 2 min. Supernatant was centrifuged and decanted. A volume of isopropanol was added, and rested on ice for 10 min for centrifugation at 12000 rpm during 10 min. After supernatant removal, pellet was resuspended in 50 µl sterile deionized distilled H₂O [8].

E. Molecular diagnosis of *Glomerella cingulata*

PCR reactions were incubated in a BIORAD thermocycler with a reaction volume of 25 µl (100 ng genomic DNA, 1.5 mM MgCl₂, 2.5 U / µl Taq polymerase DNA (Platinum), 0.2 mM of each dNTP, 0.1 µM of each oligonucleotide (sense and antisense), 2.5 µl of PCR Buffer (Minus)). Amplification cycle consisted of denaturation at 95°C for 5 min, followed by 40 cycles of 30 s at 95°C, 30 s at 55°C and 1.5 min. At 72°C. PCR products were separated by electrophoresis on a 1.2% agarose gel stained with ethidium bromide and visualized on a UV transilluminator [3, 5].

Specific oligonucleotides were used to amplify MAT 1 and MAT 2 mating genes, synthesized by INVITROGEN life technologies, according to the sequence reported in 2005[3], for phylogenetic studies of species identification of this fungus, because these genes are mating-type specific for *G. cingulata*. For the sense oligonucleotide (5'-3'): CCTAATGCGTACATTCTCTACC, and for antisense oligonucleotide (5'-3'): CCTAATGCGTACATTCTCTACC.

III. RESULTS AND DISCUSSION

Morphological studies showed that using a climate chamber in 48 hours positive results were obtained from samples inoculated with monoconidial strain of *G. cingulata* (CT-100) (Fig. 1). It was observed under microscope the particular characteristics of this fungus such as cottony mycelium and salmon spore generation [3]. An economical and

easy to use tool for field detection of infected avocados was generated.



Fig. 1. Identification of *G. cingulata* in avocado peel using a wet chamber.

Using Dellaporta's modified protocol for the extraction of genomic DNA satisfactory results were obtained by gathering good quality genetic material for subsequent PCR analysis (Fig. 2), which is consistent with the results obtained in *C. annum* [8].

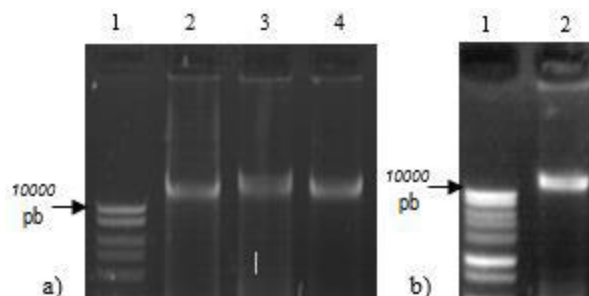


Fig. 2. Extraction of genomic DNA. a) Line 1 Molecular size marker (MSM). Line 2-4 Mycelium of *G. cingulata*. b) Line 1 MSM. Line 2 avocado pulp.

Presence of *G. cingulata* in inoculated avocados was determined by analyzing the genomic DNA of infected and healthy avocado samples against a negative control which is phylogenetically very distant from the inoculated pathogen (genomic DNA of *Aspergillus Niger*) (Fig. 3). Products of PCR showed a band of interest (that amplifies to 238 bp) presented in infected samples, which is consistent with the analysis carried out [3]. This indicates that mating genes, besides of being determinants of sexual compatibility, can be used for pathogen identification.

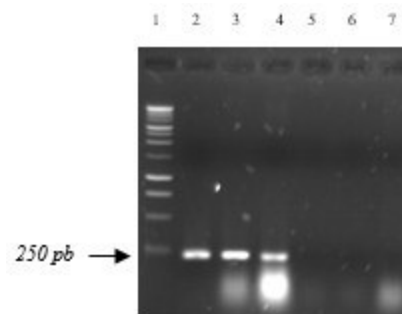


Fig. 3. Products of PCR. Line 1 MSM. Line 2 Positive control. Mycelium of *G. cingulata*. Line 3 infected pulp. Line 4 peel infected. Line 5 uninfected pulp. Line 6 uninfected peel. Line 7 negative control. Mycelium of *A. niger*.



IV. CONCLUSIONS

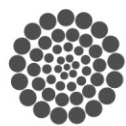
Using a climate chamber for sample incubation, correlating with microscopic observations of the morphological characteristics of *G. cingulata* and making PCR analysis with primers that amplify the HMG domain of MAT 1-2 mating genes, a diagnostic tool was achieved for an early confirmation of anthracnosis disease in order to take the necessary control measures (physical, chemical or biological), offering to farmers a quick methodology and avoiding loss of production.

ACKNOWLEDGMENT

Our most sincere thanks to DGEST for the financing of this project, to CONACYT for the scholarship granted, and to Dr. Raúl Rodríguez Guerra of INIFAP Bajío campus.

REFERENCES

- [1] L. Morales. Caracterización del perfil del aroma de aguacate Hass a diferentes estados de maduración empleando el método OSME. Tesis. Instituto Tecnológico de Celaya. Cap. 2. 2007.
- [2] INEGI. Available in <http://cuentame.inegi.org.mx/economia/primarias/agri/default.aspx?tema=&E>. 2009, 2010.
- [3] M. Du, C. Schardl, E. Nuckles, L. Vaillancourt. "Using mating-type gene sequences for improved phylogenetic resolution of *Colletotrichum* species complexes". *Mycologia*, 97(3).Pp.641-658. 2005.
- [4] N. Palacios, D. del Burtin, M. Leech. "Molecular biology, a tool for bioprospection of plants secondary metabolism in Colombia". *Revista Colombiana de Biotecnología*. Vol. VI. No. 2. 67-77. Diciembre 2004.
- [5] R. Rodríguez., M. Ramírez, M. Cabral, M. García, Z. Lira, R. Guevara, J. Simpson. Heterothallic mating observed between Mexican isolates of *Glomerella lindemuthiana*. *Mycologia*, 97(4), 793-803. 2005.
- [6] G. Garmendia & S. Vero. "Métodos para la desinfección de frutas y hortalizas". *Horticultura. Tecnología Poscosecha*. 197. 2006.
- [7] Y. Chen. & G. Séguin. "A rapid method for assessing the viability of fungal spores". *Canadian journal of plant pathology*, 24(2), 230-232. 2002.
- [8] A. Joaquín. "Análisis de la expresión del ADN complementario R100 de *Capsicum chinense*, obtenido durante la Interacción con Virus Huasteco del Chile (PHV), Bajo estrés biótico". Tesis de Licenciatura. Instituto Tecnológico de Celaya. Pp.43-49. 2005.



CONACYT
Consejo Nacional de Ciencia y Tecnología



CONCYTEQ

Application of Entropy and Fractal Dimension for automatic diagnosis in induction motors

Lisbeth Dayanne Giorgi-Ortiz, Yulimar Lorena Roa-Teran, Arturo Garcia-Perez, Rene de Jesus Romero-Troncoso, David Camarena Martínez
Departamento de Ingeniería Electrónica
DICIS, Universidad de Guanajuato
Salamanca, Guanajuato, México

Carlos Andres Perez-Ramirez, Juan Pablo Amezcua-Sanchez, Martin Valtierra-Rodriguez
Facultad de Ingeniería, Campus San Juan del Río
Universidad Autónoma de Querétaro
San Juan del Río, Querétaro, México

Abstract— Several approaches appear in literature to make a reliable diagnosis of the condition of induction motors. The most popular approaches are based on current or vibration signal analysis. In this paper, it is presented a comparative study about the application of different complexity parameters that allow the classification of multiple and combined faults in induction motors. For this, it is extracted the vibration signals from an induction motor and then is calculated several complexity features such as Entropy- and Fractal dimension-based parameters, later, these extracted features are passed through a neural network to do an automatic classification. The effectiveness of classification using different complexity parameter shows a reliable methodology for diagnosing faults in induction motors.

Keywords—induction motor, fractal dimension, entropy, diagnosis

I. INTRODUCTION

Induction motors are the most important source of mechanical power in industries due to robustness and simplicity of construction. However, induction motors are susceptible to faults decreasing its performance and increasing the possibility of damage and accidents. Therefore, the performance of the induction motors depends on correct condition monitoring techniques to avoid failures during their operation. These failures increment the unwanted downtimes and maintenance costs. Most techniques used in condition monitoring are based on the study of electrical or vibrational signals. In general, the methods based on the analysis of vibration signals have demonstrated to be reliable methods for assessing the overall health of a rotor system. Also, most of the methods for vibration signal analysis can be applied in either time domain or frequency domain, increasing their versatility. Regarding frequency domain analysis techniques, many reported studies in literature have used from the classical Fourier transform to the high resolution spectral analysis such as MUSIC [1], Hilbert-Huang transform [2], synchrosqueezing transform [3], among others, in order to find frequencies related to the faults. With respect to time domain techniques, a

simple detection of fault signature data in a diagnosis approach consists of monitoring specific parameters of the vibration signals (e.g., statistical parameters). In recent years, new parameters that measure the complexity of the signals such as entropy and fractal dimension have been used. These parameters have proved to be effective tools to detect and classify different features in a signal; for instance, in applications of ECG [4], pattern recognition [5], [6], motor condition monitoring [7]–[9], etc.

In this work, a comparison to classify several faults in induction motors from a fusion of feature extraction-based methods and neural networks is presented. The used features extraction-based methods are Higuchi fractal dimension, Katz fractal dimension, Shannon entropy, and permutation entropy; these features allow to know the “complexity” of the signal. The features along with a neural network are tested individually to know their capability to classify the faults.

II. THEORETICAL BACKGROUND

Feature extraction is used on measured data with the aim of describing or giving relevant information from the obtained values. Fractal dimension and entropy are different parameters used to measure chaotic systems, both approaches have been used as features to identify different conditions of the systems. This section will give a brief explanation of the parameters used in this work.

A. Fractal Dimension

A fractal can be defined as the measurement of regularity of the structure of a physical phenomenon, so for those geometric objects that have an irregular structure, a more appropriate geometry than the classic one is needed to be able to describe its irregularities. Therefore, the fractal dimension value serves to define different geometries found in signals, which can be associated to faults of a system.

Katz fractal dimension

Katz's method calculates the fractal dimension of a sequence of data by making the summation of the Euclidean distances between the successive points of the sample, which is the total length of the curve, the average step size, a , of the curve and the diameter of the curve, d , between the first point of the sequence and the farthest point. The resultant equation of Katz fractal dimension is:

$$FD = \frac{\log(L/a)}{\log(d/a)} \quad (1)$$

Higuchi fractal dimension

Other way to calculate the fractal dimension is the Higuchi's method, which calculates the fractal dimension of the dataset X of N data points, by extracting $m \in [1, k]$ sub-sample sets (X_k), where $k \in [1, k_{\max}]$ as follows:

$$X_k^m = \{X + ik\}_{i=0}^{\lfloor (N-m)/k \rfloor} \quad (2)$$

Later, the length of each X_k (L_m) is calculated as:

$$L_m(k) = \frac{\sum_{i=1}^{\lfloor (N-m)/k \rfloor} |X(m+ik) - X(m+(i-1)k)|}{\lfloor (N-m)/k \rfloor \lfloor k/(m-1) \rfloor} \quad (3)$$

Finally, the fractal dimension of the sample (D) is solved from

$$\langle L(k) \rangle \propto k^{-D} \quad (4)$$

Where $\langle L \rangle$ is the average of L_m .

B. Entropy

Entropy was defined by Kolmogorov in the 1950's, it is defined as a nonlinear measurement by a functional that maps probability distributions or, equivalently, random variables, to real numbers. This notion is derived from first principles as the only 'reasonable' way to measure the 'average amount of information conveyed when an outcome of the random variable is observed'. Therefore, entropy can be considered as a measure of the disorder in physical systems, or an amount of information that may be gained by observations of the disordered systems.

Shannon Entropy

The Shannon entropy of a time series was proposed as a measure of disorder in physical systems. Entropy, E , is an additive cost function described as:

$$E(0) = 0 \text{ and } E(s) = \sum_{i=0}^n E(s_i) \quad (5)$$

Where s is the time series and s_i the coefficients of s in an orthonormal basis. Therefore, the non-normalized Shannon entropy is

$$E(s) = - \sum_{i=0}^n s_i^2 \log(s_i)^2 \quad (6)$$

Permutation Entropy

As Shannon entropy, permutation entropy quantifies the disorder of a system. The permutation entropy of a time series x is calculated as a function of the scale factor s . To calculate the permutation of a new time vector X_j , $S_i = [X_{t_i}, X_{t_{i+1}}, \dots, X_{t_{i+m-1}}]$ is generated with the embedding dimension m and then arranged in an increasing order: $[X_{t_{+j_1-1}} \leq X_{t_{+j_2-1}} \leq \dots \leq X_{t_{+j_n-1}}]$. Given m different values, there will be $m!$ possible patterns π , also known as permutations. If $f(\pi)$ denotes its frequency in the time series, its relative frequency is $p(\pi) = f(\pi) / (L/s - m + 1)$ [10]. The permutation entropy is then defined as:

$$PE = \sum_{i=1}^{m!} p(\pi_i) \ln p(\pi_i) \quad (7)$$

Summarizing, permutation entropy refers to the local order structure of the time series, which can give a quantitative measure of complexity for dynamical time series.

C. Feed Forward Neural Network

The feedforward neural network is the simplest type of artificial neural network devised, where the information moves in only one direction, forward, from the input nodes, through the hidden nodes and, finally, to the output nodes. There is not feedback between layers.

III. METHODOLOGY AND EXPERIMENTAL SETUP

The experimental setup shown in Fig. 1 is composed by a 1-hp three-phase induction motor (model WEG00136APE48T), which has two poles, 28 bars, and receive a power supply of 220 Vac at 60 Hz. The mechanical load is an ordinary alternator. To generate the treated faulty conditions, the rotor, bearing, and arm of the motor were modified synthetically; for broken bar conditions, the bar of the motor was gradually broken by drilling a hole of 10 mm depth for one broken bar (1BB) condition and two holes of 10 mm depth in two bars for two broken bars (2BB) condition, respectively (Fig. 2a-b). The unbalance condition (UNB) was produced by attaching a mass to one arm of the motor pulley as shown in Fig. 2c. To carry out the faulty bearing defect (BRN) test, the bearing was artificially damaged by drilling a hole with 1.191 mm of diameter on its outer race using a tungsten drill bit. Fig. 2d shows the artificially damaged bearing. In order to acquire the 3-axis vibration signals (A_x ,

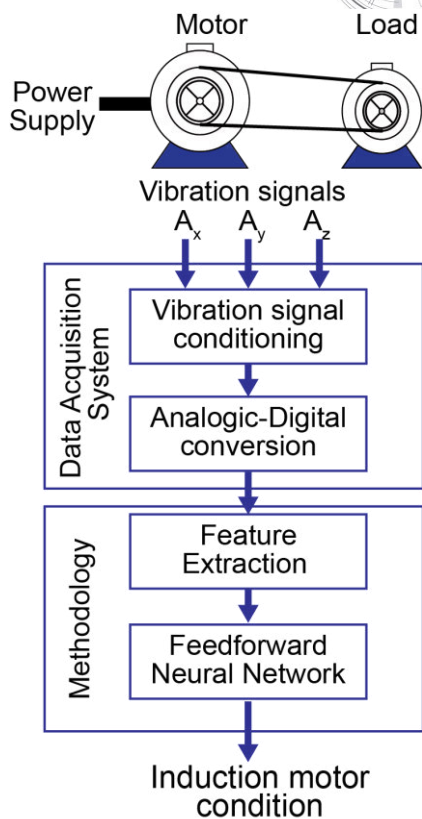


Fig. 1. Methodology of the motor diagnosis system

A_y , and A_z) is used a MEMS-based triaxial accelerometer (model LIS3L02AS4) from STMicroelectronic.

The acquisition data system takes 4096 samples at a sampling frequency of 1500 Hz, taking 4096 samples during the steady state of the motor. Then, the information of the vibration signals is transferred to a personal computer to apply the methodology for motor diagnosis. The methodology (shown in Fig. 1) takes the vibration signals in order to obtain characteristics of complexity, Katz fractal dimension (KFD), Higuchi fractal dimension (HFD), Shannon entropy (SE) and Permutation entropy (PE), the extracted information of each vibration signal (A_x , A_y , and A_z) are sent to a FFNN for automatic diagnosis.

The FFNN designed has three input nodes, one hidden layers, and five output nodes. The three inputs receive one of the characteristic of complexity from the 3 axes vibration signals (A_x , A_y , and A_z) of the induction motor. The one hidden layers has ten nodes and the five output nodes are selected to function as flags that indicate each induction motor condition (HLT, 1BB, 2BB, BRN, and UNB). For the stage of the FFNN training, 20 real trials using the same induction motor are carried out for each condition. These conditions include single faults (1BB, 2BB, UNB, and BRN), the combinations of the single faults (1BB & BRN, 1BB & UNB, BRN & UNB, 1BB & BRN & UNB, 2BB & BRN, 2BB & UNB, and 2BB & BRN & UNB), and HLT condition; then,

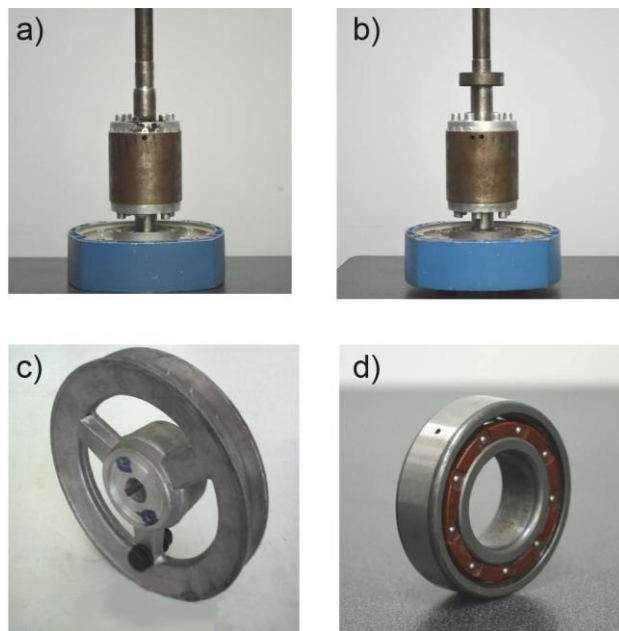


Fig. 2. Treated faults.

new twenty trials are taken to obtain twenty complexity values of each axis from each condition, which are used to synthetically obtain 100 new values by randomly producing values within the range $[\mu - \sigma, \mu + \sigma]$ for each condition, where μ is the mean and σ is the standard deviation of real complexity values, which are used as validation sets.

IV. DISCUSSION AND RESULTS

The results of the values of mean (μ) and standard deviation (σ) of calculated complexity parameters of the 20 test for each operational condition and axis are shown as a boxplot graphic (the central mark is the median, the edges of the box are the 25th and 75th percentiles, the whiskers extend to the most extreme data points not considered outliers) in Fig. 3, this figure is used to know the statically properties to design the FFNN in order to identify each operation condition. From Fig. 3, it can be observed that the range of values varies for each of the complexity parameter values, also for each condition the variation of the complexity values overlap for other condition, therefore, to help the identification through the FFNN, each complexity value of the three vibration signals obtained, A_x -axis, A_y -axis and A_z -axis, is used, allowing a better classification of the faulty conditions.

The effectiveness percentages of classification results for each used complexity parameter are shown in Table 1. 100 tests in all treated cases are used. The results include the identification of healthy condition (HLT), single isolated faults (1BB, 2BB, BRN, and UNB), and the combination of two or three faulty conditions at same time (1BB & BRN, 1BB & UNB, BRN & UNB, 1BB & BRN & UNB, 2BB & BRN, 2BB & UNB, and 2BB & BRN & UNB). From Table 1 can be observed that the best parameters to make a viable classification are the HFD

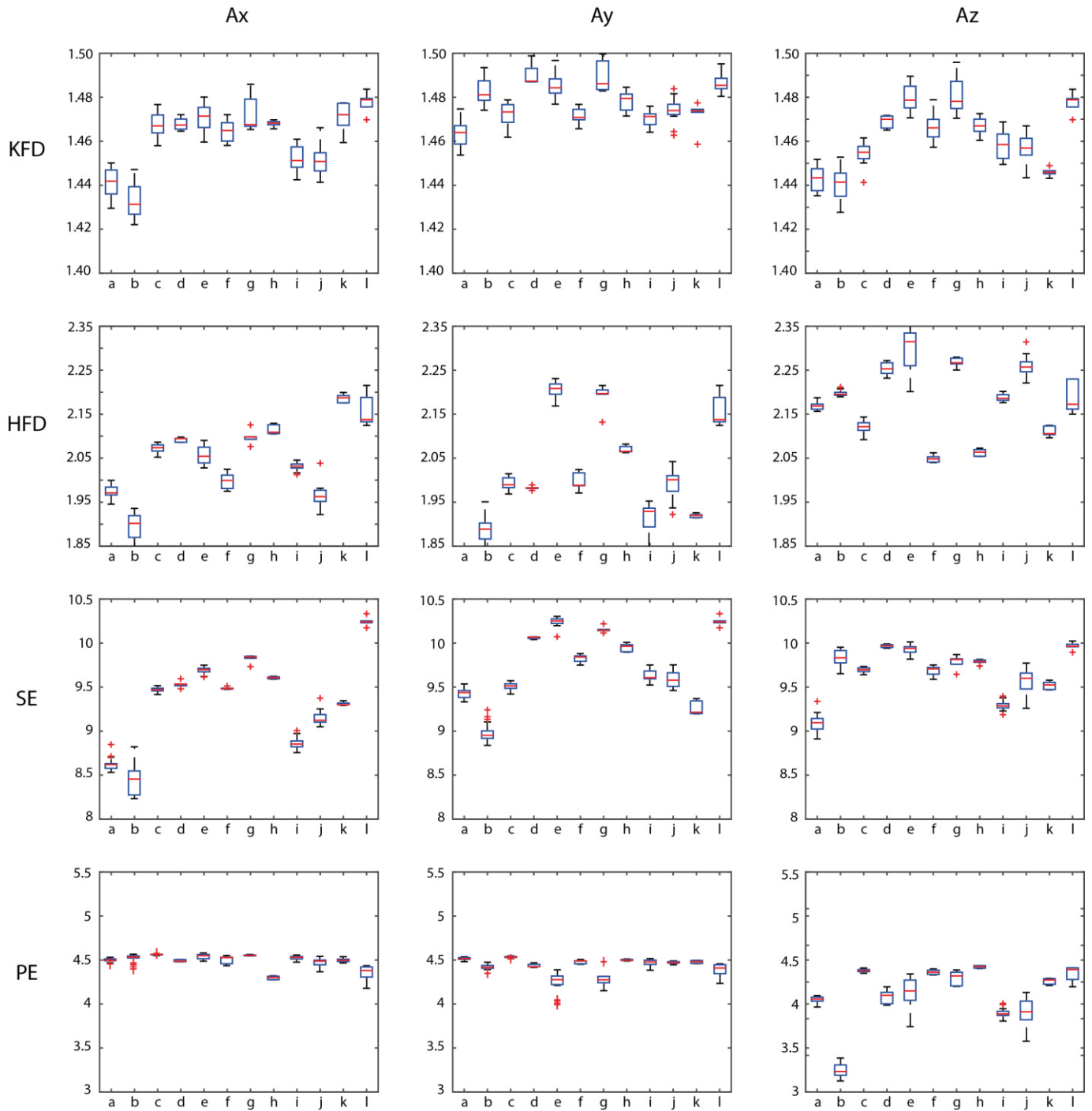


Fig. 3. Boxplots of the values of KFD, HFD, SE and PE of each axis of the twenty real tests.

and SE, both can classify almost all the condition; for HFD parameter the worst obtained effectiveness percentages is for 1BB & UNB condition with 78% and 2BB & BRN & UNB with 82%, whereas SE the worst effectiveness percentage is for 2BB & UNB condition with 81%. The other conditions have an effectiveness percentage above 93% and 95% for HFD and SE, respectively. The KFD and PE parameters have a low effectiveness percentage for many faulty conditions, for that reason they do not allow a good classification. It is clear

to see that with the fusion of a complexity parameter with a simple FFNN is possible to obtain good results in the classification of multiple and combined faults.

V. CONCLUSIONS

In this work, the application of several complexity parameters to allow a classification methodology for induction motor condition monitoring is presented. Firstly, there is a

TABLE I
CLASSIFICATION EFFECTIVENESS PERCENTAGE FOR EACH COMPLEXITY PARAMETER

	Complexity Parameter				
	KFD (%)	HFD (%)	SE (%)	PE (%)	
Motor condition	HLT	91	100	100	96
	1BB	94	94	100	100
	UNB	64	98	97	99
	BRN	74	100	97	84
	1BB & UNB	33	78	98	56
	1BB & BRN	49	100	98	90
	BRN & UNB	50	93	99	84
	1BB & BRN & UNB	65	100	99	100
	2BB	55	99	100	88
	2BB & UNB	46	97	81	65
	2BB & BRN	81	100	95	96
	2BB & BRN & UNB	65	82	97	85
	Mean (%)	64	95	97	87
	Maximum (%)	94	100	100	100
Minimum (%)	33	78	81	56	

stage of feature extraction, where different fractal dimension and entropy values are calculated. Secondly, they are used as input features to an FFNN-based classifier to obtain an automatic diagnostic of the induction motor faults. The values of classification effectiveness percentage show that the parameters HFD and SE present the best results for classification of multiple and combined faults. These parameters could be used as an effective and simple way, without sophisticated analysis, for detecting other fault conditions on induction motors. For future works, new parameters or a fusion of them will be used to allow a better classification. Also, it will be studied other classification methods, which could improve the results.

REFERENCES

- [1] A. Garcia-Perez, R. J. Romero-Troncoso, E. Cabal-Yeppez, R. a. Osornio-Rios, J. D. J. Rangel-Magdaleno, and H. Miranda, "Startup current analysis of incipient broken rotor bar in induction motors using high-resolution spectral analysis," *SDEMPED 2011 - 8th IEEE Symp. Diagnostics Electr. Mach. Power Electron. Drives*, pp. 657–663, 2011.
- [2] J. a. Antonino-Daviu, M. Riera-Guasp, M. Pineda-Sanchez, and R. B. Perez, "A critical comparison between DWT and Hilbert-Huang-based methods for the diagnosis of rotor bar failures in induction machines," *IEEE Trans. Ind. Appl.*, vol. 45, no. 5, pp. 1794–1803, 2009.
- [3] C. Li and M. Liang, "Timefrequency signal analysis for gearbox fault diagnosis using a generalized synchrosqueezing transform," *Mech. Syst. Signal Process.*, vol. 26, no. 1, pp. 205–217, Jan. 2012.
- [4] W. Klonowski, E. Olejarczyk, and R. Stepien, "Sleep-EEG Analysis Using Higuchi 's Fractal Dimension," in *International Symposium on Nonlinear Theory and its Applications*, 2005, pp. 222–225.
- [5] Y. Tao, E. C. M. Lam, and Y. Y. Tang, "Extraction of Fractal Feature for Pattern Recognition," pp. 527–530, 2000.
- [6] J. Florindo and O. Bruno, "Local fractal dimension and binary patterns in texture recognition," *Pattern Recognit. Lett.*, vol. 78, pp. 22–27, 2016.
- [7] H. Heidari Bafroui and A. Ohadi, "Application of wavelet energy and Shannon entropy for feature extraction in gearbox fault detection under varying speed conditions," *Neurocomputing*, vol. 133, pp. 437–445, 2014.
- [8] S. Pan, T. Han, A. C. C. Tan, and T. Ran, "Fault Diagnosis System of Induction Motors based on Multi-scale Entropy and Support Vector Machine with Mutual Information Algorithm," *Shock Vib.*, vol. 2016, pp. 1–21, 2015.
- [9] Z. Zheng, W. Jiang, Z. Wang, Y. Zhu, and K. Yang, "Gear fault diagnosis method based on local mean decomposition and generalized morphological fractal dimensions," *Mech. Mach. Theory*, vol. 91, no. 438, pp. 151–167, 2015.
- [10] H. Eguiraun, K. López-de-Ipiña, and I. Martinez, "Application of entropy and fractal dimension analyses to the pattern recognition of contaminated fish responses in aquaculture," *Entropy*, vol. 16, no. 11, pp. 6133–6151, 2014.

Timbe methanolic pod extract *Acaciella angustissima*'s Properties

Formulation of seed pods *Acaciella angustissima* methanolic extract

I. Parola-Contreras, Ana A. Feregrino-Pérez, Ramón
G. Guevara-González
Facultad de Ingeniería
Universidad Autónoma de Querétaro
México
ix.parola@gmail.com

María C. García-Barrera
Facultad de Química
Universidad Autónoma de Querétaro
México

Abstract— The acquisition of new anticancer products is a way of innovation for the cosmeceutical industry. Due to phenolic compounds in medicinal plants, *Acaciella Angustissima* is a promising candidate for use in cosmetic formulations. Interest in the use of this species is due to its rapid growth, ability to fix nitrogen and restoration of the soil in high densities [1]. Flavonoids of this genus have been reported by Feregrino-Pérez [2] and by Vargas-Hernández [3]. Flavonoids are responsible for antimutagenic activity in the crude methanolic extract, and are known to have the ability to trap free radicals and anticancer activities. For this reason the methanolic extract of Timbe pods is the ideal compound to be part of various formulations and applications.

Keywords—*Acaciella angustissima*; sunscreen; antioxidant, antimutagenic and antimicrobial activity

I. INTRODUCTION

Until a few years ago the scientific knowledge of the chemical and biological activities of medicinal plants [4]. *A. angustissima* is a species found from the southern United States to Argentina, where it occupies a wide range of habitats from sea level up to 2500 m [5]. This tree has been reported as a promising source of bioactive compounds such as phenolic compounds; the pods being a sustainable exploitation [2].

II. MATERIALS AND METHODS

A. Plant material

Fig. 1 The Timbe pods (*A. angustissima*) was collected in February 2017 from the trees located in the Amazcala campus of the UAQ Engineering Faculty 100 ° 15 '33.87' west longitude at 2,272 msnm with the geostatistical key 220110005 (INEGI, 2017).



Figure 1 The Timbe pod.

B. Extracts preparation

Reported the procedure the extraction with methanol by maceration. The methanolic extract from *A. angustissima* (MEA) should be evaporated to dryness in vacuum. The extract should be stored at 4°C in sealed amber jars [6].

C. Total phenolic compounds

Vargas-Hernández [3] describe this method for MEA. Total phenolics of MEA were determined according to Folin-Ciocalteu colorimetric method [7] and flavonoids were determined as reported Liu [8] They found in MEA using maceration extraction method: total phenolics, 88.87 mg equivalent of gallic acid/g extract; and total flavonoids, 127.19 mg equivalent of (+)-catechin/g extract. And according to statistical test, the extraction method did not affect the phenolic compounds content ($p < 0.05$). The flavonoids content found in the work of Vargas-Hernández [3] is higher to those reported in *A. pennatula* pods by Feregrino-Pérez [2].

D. HPLC analysis

The data obtained by Vargas-Hernández [3] showed MEA contain various phenolic compounds from Timbe pods, among which can mention: gallic acid, (+)-catechin and luteoline in high concentrations.

The latter has a high antioxidant capacity, besides being an agent in the prevention of inflammatory processes and modulators of the immune system.

E. Antioxidant activity

Lab data determined a high antioxidant capacity of 110.3 μ g/ml by ABTS technique, while DPPH technique obtained an inhibitory concentration of 349.1 μ g/ml and 2.77mmol FeSO₄ /g extract [3].

F. Mutagenicity and antimutagenicity tests

By AMES test against aflatoxin B1 (AFB1) using a strain of *Salmonella typhimurium* [9] for the evaluation of the antimutagenic capacity of the extract. Samples will be tested in triplicate for each experiment. The results obtained by Vargas-Hernández [3] indicate that MEA showed medium antimutagenic activity in concentrations 0.077, 0.155 and 0.31 mg/ml, while concentration 0.625–5 mg/ml antimutagenic activity was strong. According to scientific literature, if the percent range of inhibition is 25–50%, the antimutagenic activity in sample is medium, but when the antimutagenic activity in sample is higher than 40%, means that antimutagenic activity is strong [10].

G. Antimicrobial activity

Vargas-Hernández [3] proved the antifungal properties of MEA *in vitro*, according to the poisoned-food technique by evaluating concentrations of 50, 100 and 200, 300 and 400 mg gallic acid equivalents/ml dissolved in potato dextrose agar (Invitrogen Corporation, Carlsbad, CA, USA) [6]. The fungistatic–fungicidal nature of MEA after be tested by observing revival of growth of the inhibited mycelial disk following its transfer to non-treated potato dextrose agar. In this sense, extract was classified as fungistatic if any mycelial growth was observed after 10 days. In *A. angustissima* against *P. capsici* it was showed inhibition of 15.5% for 300 mg/ml of extract and the maximum concentration tested reached 28% of inhibition. These results demonstrate that *A. angustissima* phenolics displayed fungistatic activity, which suggest that these extracts were either unable or poorly absorbed by the pathogen cells and that corresponded to surface contact actions likely on several proteins, as reported for other phenolics [3,6]

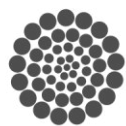
III. CONCLUSION

Methanolic extracts of *A. angustissima* pods showed biological activity such as antioxidant, antimicrobial and

antimutagenic activity, which could be related to their phenolic compounds content; thus, these results suggest a potential use of *A. angustissima* pods in different industrial areas. Endangered species that are harvested sustainably with added value. With the advancement of this research, other cosmeceutical and industrial products will be harnessed to the maximum of all the benefits of bioactive substances. The preliminary studies show that the seedpods of *A. angustissima* can be used in the manufacture of a cosmeceutical product like sunscreen lotion.

REFERENCES

- [1] R. Rincón-Rosales and F. A. Gutiérrez. “Características biológicas de *Acaciella angustissima* (mill.) Britton & Rose en su hábitat natural y evaluación de su potencial cortical en Chiapas, México/Biological characteristics of *Acaciella angustissima* (mill.) Britton & Rose in its natural habitat and assessment of its bark potential in Chiapas, México”. *Agrociencia* 42, 129–137. 2008.
- [2] A.A. Feregrino-Pérez, I. Torres-Pacheco, M. Vargas-Hernández, P. V. Munguía-Fragozo, V. Loarca-Piña, G. F. Mendoza-Díaz, S. O. Ocampo-Velázquez, E. Rico-García, R. G. Guevara-González. “Antioxidant and antimutagenic activities of *Acacia pennatula* pods”. *J. Sci. Ind. Res.* 70, 859–864. 2011.
- [3] M. Vargas-Hernandez, P. V. Munguia-Fragozo, A. Cruz-Hernandez, B. Z. Guerrero, M. M. Gonzalez-Chavira, A. A. Feregrino-Perez, S. O. Mendoza-Diaz, G. Loarca-Pina, I. Torres-Pacheco, M. Hernández-Salazar, R. G. Guevara-Gonzalez, “Bioactivity and gene expression studies of an arbutive Mexican specie *Acaciella angustissima* (Timbe)”. *Ind. Crops Prod.*, 52, pp. 649–655. 2014.
- [4] S. F. van Vuuren. “Antimicrobial activity of South African medicinal plants”(2008), *J Ethnopharmacol* 119: 462 - 472.
- [5] M. L. Rico-Arce and S. Bachean. “A taxonomic revision of *Acaciella* (Leguminosae, Mimosoideae)”. *An. Jardín Bot. Madrid* 63: 189–244. 2006.
- [6] DM Maron and GN Ames, “Revised methods for *Salmonella* mutagenicity test” (1983), *Mutat Res* 113: 173-215.
- [7] V. Dewanto, X. Wu, K. K. Adom, R. H. Liu. “Thermal processing enhances the nutritional value of tomatoes by increasing total antioxidant activity”. *J Agric Food Chem.* 8;50(10): 3010-4. 2002.
- [8] M. Liu, X. Qi, C. Weber, C. Yong, J. Brown, R. Hai. “Antioxidant and antiproliferative activities of raspberries”. *J. Agric. Food Chem.* 50, 2926–2930. 2002.
- [9] D. M. Maron and G. N. Ames. “Revised methods for *Salmonella* mutagenicity test”. *Mutat Res* 113: 173-215. 1983.
- [10] M. Entezari, A. Majd, F. Falahian, S. Mehrabian, M. Hashemi, A. Lajimi. “Antimutagenicity and anticancer effects of citrus medica fruit juice”. *Acta Med. Iran.* 47, 373–377. 2009.



CONACYT
Consejo Nacional de Ciencia y Tecnología



CONCYTEQ

Development of a particle swarm optimization algorithm applied to atmospheric pollutants

Ing. Bruno Ordóñez De León

School of engineering
Universidad Autónoma de Querétaro UAQ
Querétaro, México
ordonez.bruno@gmail.com

Dr. Marco Antonio Aceves Fernández (*Author*)

School of engineering
Universidad Autónoma de Querétaro UAQ
Querétaro, México
marco.aceves@gmail.com

Abstract— Nowadays, the issue of environmental pollution has become very important. One of the factors that greatly affects and that is of utmost importance is the air quality, because in this are immersed small particles (particles ≤ 10 microns, Pm_{10} , and particles ≤ 2.5 microns, $Pm_{2.5}$). This kind of particles cause respiratory diseases that can become deadly. So the need to determine the concentration of these particles in the air in a given area and find a model capable of predicting such concentration in future days has been increased. Find a mathematical model is practically impossible due to the complexity of the phenomenon. It is necessary to use an intelligent algorithm that learn the pollutant particles behavior and give the possible behavior of the concentration in the future. In this project will be used the algorithm "Particle Swarm Optimization (PSO)".

Keywords— *Environmental pollution, Airborne particle, particle swarm, intelligent algorithm, Optimization*

I. INTRODUCTION

In recent years, the environment has been affected by the presence of pollutants such as ozone (O_3), nitrogen oxide (NO_2), carbon monoxide (CO), sulfur dioxide (SO_2) and particles smaller than 10 Microns (PM_{10}) and particles smaller than 2.5 microns ($PM_{2.5}$). For this reason, pollutant monitoring has been necessary in large cities with high concentration of population and industries [1]. The figure 1 shows the concentration of the particles in the state of Querétaro according to the page of the secretariat of sustainable development.

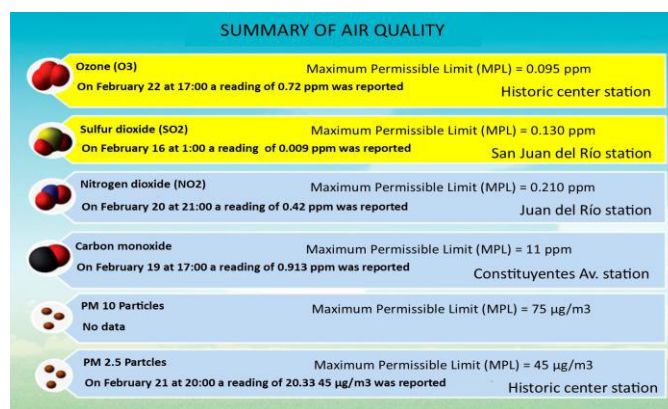


Fig. 1. Summary of air quality in Querétaro, SEDESU

The toxicity of the particles is determined by their physical and chemical characteristics. The particle size, which is measured in aerodynamic diameter, is an important parameter for the characterization of its behavior. This parameter is very important due to the penetration and retention capacity in the respiratory system, further defining the residence time in the atmosphere [2]. In the figure 2 is shown the particles concentration in Querétaro.

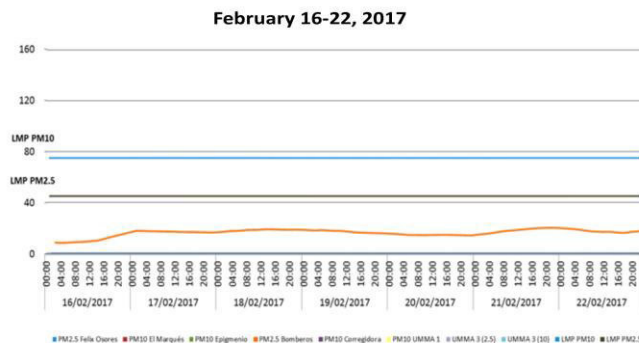


Fig. 2. Airborne particles concentration, Querétaro

A. Particle Swarm Optimization.

Particle swarm optimization is a type of algorithm based on collective animal intelligence, which emulates the behavior of a swarm. This type of algorithm looks for an optimal local solution by using the memory of each particle as well as the memory of the swarm. Its properties of low restrictions on the continuity of the objective function together with the search space and the ability to adapt to the dynamic environment makes PSO one of the most important methods of swarm intelligence and algorithms of evolutionary computation [3].

In this project, the PSO algorithm will be used to find the model of the behavior of suspended particles in the air, using its benefits to find a good solution. In this case, the particles social behavior will help with a global search, exploring good areas in the search space, and the individual behavior will help to find good solutions in the promising areas found by the swarm.

The main objective is to improve the performance of the previously obtained models using Fuzzy logic, ANFIS and ACO, on the behavior of PM₁₀ and PM_{2.5} particles suspended in the air through the implementation of the PSO algorithm for a better Description of the behavior of said particles and use a raspberry pi 3 card for the processing of said analysis.

II. METODOLOGY

A. The original PSO Algorithm

In the original PSO algorithm, each particle globally compares its fitness to the entire swarm population and adjusts its velocity towards the swarm's global best particle. There are, however, recent versions of local/topological PSO algorithms, in which the comparison process is locally performed within a predetermined neighborhood topology. The original PSO is designed to optimize real-value continuous problems, but the PSO algorithm has also been extended to optimize binary or discrete problems [4].

$$v_{id}(t+1) = v_{id}(t) + c_1 R_1(p_{id}(t) - x_{id}(t)) + c_2 R_2(p_{gd}(t) - x_{id}(t)) \quad (1)$$

$$x_{id}(t+1) = x_{id}(t) + v_{id}(t+1) \quad (2)$$

Where:

a) v_{id} represents the rate of the position change (velocity) of the i th particle in the d th dimension, and t denotes the iteration counter.

b) x_{id} represents the position of the i th particle in the d th dimension. It is worth noting here that x_i is referred to as the i th particle itself, or as a vector of its positions in all dimensions of the problem space. The n -dimensional problem space has a number of dimensions that equals to the numbers of variables of the desired fitness function to be optimized.

c) p_{id} represents the historically best position of the i th particle in the d th dimension (or, the position giving the best ever fitness value attained by x_i).

d) p_{gd} represents the position of the swarm's global best particle (x_g) in the d th dimension (or, the position giving the global best fitness value attained by any particle among the entire swarm).

e) R_1 and R_2 are two n -dimensional vectors with random numbers uniformly selected in the range of [0.0, 1.0], which introduce useful randomness for the search strategy. It worth noting that each dimension has its own random number, r , because PSO operates on each dimension independently.

f) c_1 and c_2 are positive constant weighting parameters, also called the cognitive and social parameters, respectively, which control the relative importance of particle's private experience versus swarm's social experience (or, in other words, it controls the movement of each particle towards its individual versus global best position [4].

B. Limiting the Maximum Velocity.

In the velocity update equation (1), when $x_{id}(t) \ll p_{id}(t)$ and $x_{id}(t) \ll p_{gd}(t)$, the new velocity will have a very large positive value and the algorithm will force to the current position of the i -th particle is significantly adjusted forward to approximate its best historical position and the best overall position of the swarm. In the opposite case, the new velocity will have a very large negative value of velocity and the algorithm will force the current position of the i -th particle to go back to its best historical position and the best overall position of the swarm. It has been observed that by greatly increasing or decreasing the velocity values of particles, it has led to what is known as a "swarm explosion" in early versions of PSO, this refers to the uncontrollable increase in the magnitude of the velocity of each Particle $|v_{id}(t+1)|$, which could lead to divergence of the swarm [4]. If the result of equation (1) to update the velocity violates the rule $|v_{id}(t+1)| > V_{max}$ then the velocity values of the violated particles are subject to:

$$v_{max} = \frac{x_d^{max} - x_d^{min}}{k} \quad (3)$$

C. Inertial Weight

Inertial weight is introduced to control the global exploration ability of the PSO and to obtain a balance between local and global search. It has been observed that PSO yields a better result when the global exploration is more favored in the early stages of optimization allowing the exploration of many promising areas of the search space. Almost at the end of the optimization process, it is better that the local exploration is favored, this allows a more refined search around the best detected areas. This is possible by reducing the change of position or the velocity of the particles in the later objectives. A linear decrease in inertial weight (w) multiplied by the

previous velocity was introduced by Shi and Eberhart, this is shown in equation (6).

$$v_{id}(t+1) = wv_{id}(t) + c_1 R_1(p_{id}(t) - x_{id}(t)) + c_2 R_2(p_{gd}(t) - x_{id}(t)) \quad (4)$$

$$x_{id}(t+1) = x_{id}(t) + v_{id}(t+1) \quad (5)$$

A possible definition of inertial weight is:

$$\omega(t) = \omega_{hi} - (\omega_{hi} - \omega_{low}) \frac{t}{T_{max}} \quad (6)$$

Where t is the iteration, ω_{hi} and ω_{low} are the upper and lower limits of the inertial weight and T_{max} is the maximum number of iterations before the algorithm ends [5].

D. Algorithm Description

The algorithm itself consists of 6 essential steps, described in the flowchart of figure 3. First, there is the initialization: In this step the limits of the position and velocity of the particles, the number of particles, the parameters as weight (w), the individual and social learning parameters (c_1 and c_2) And the randomness parameters for a better search (R_1 and R_2). In the second step the information of the position and velocity of each particle is accessed, in the first iteration this is going to be the same that we introduced as initial values. As a third step, the initial population is evaluated comparing the cost of each particle with the objective function and selecting the best overall particle. The fourth step consists of the update of position and speed, these are updated by equations 6 and 7, if they exceed the corresponding limits, and they conform to the established limits. The fourth step is to evaluate the updated population, this is similar to step two, where the updated positions are evaluated with the objective function and if necessary, the variables p_{id} and p_{gd} will be updated. In the fifth step a check is made to see if the stop condition has been fulfilled, in case this condition has not been fulfilled, the algorithm is repeated from step three, otherwise the optimization process is concluded. Finally, the best solution obtained during the optimization process (p_{gd}) is shown [6].

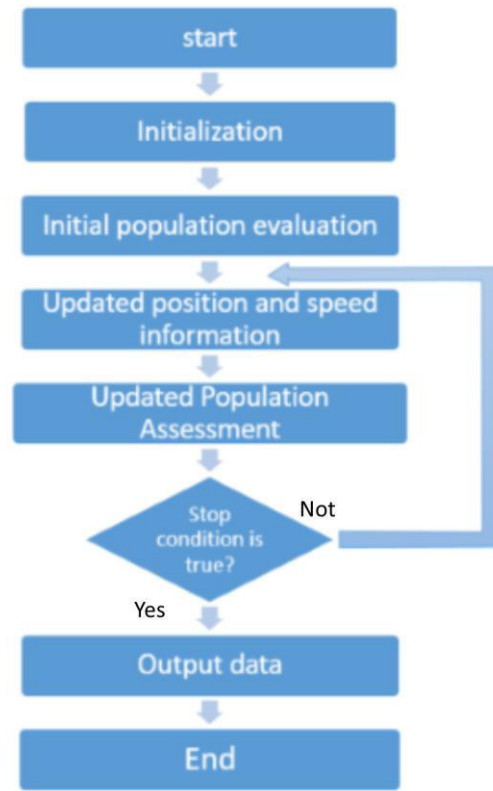


Fig. 3. PSO algorithm Flowchart

E. Process

Figure 4 shows a diagram of the methodology to be used, to initiate the acquisition of data, the research project does not focus on this stage, since it is not focused on the acquisition or measurement of data, goes Dedicated to the processing and analysis of the data. In the second port, the implementation of the PSO algorithm is carried out in a raspberry pi 3, in this stage the algorithm and the error that exists between the output of the algorithm and the actual data are evaluated. In the third block the results of the algorithm are shown, in this case the graph of the prediction of the concentration of the particles. The fourth block is a feedback to the system, which by means of statistical algorithms, at the moment it is not contemplated which algorithm will be used, will obtain the error that exists between the actual data and those obtained by the algorithm PSO to later adjust parameters to reduce this error.

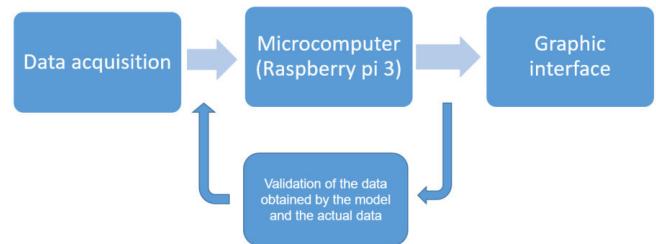


Fig. 4. Process diagram description

III. DISCUSSION

Different types of algorithms, fuzzy logic, Anfis, Ant Colony Optimization [1] among others, have been used to find a model that is efficient and reliable to predict the behavior of particle concentration, these methods have achieved satisfactory results, in the figure 5 are shown the algorithms result, but there is still a large area of opportunity because there are still different algorithms that have not been implemented and due to their ability to adapt and learn, better results can be obtained.

At this point, the original PSO algorithm is proposed as a better alternative to be able to find a model that improves the results of the algorithms mentioned above, supporting this conjecture based on the aforementioned advantages of this type of algorithm[1].

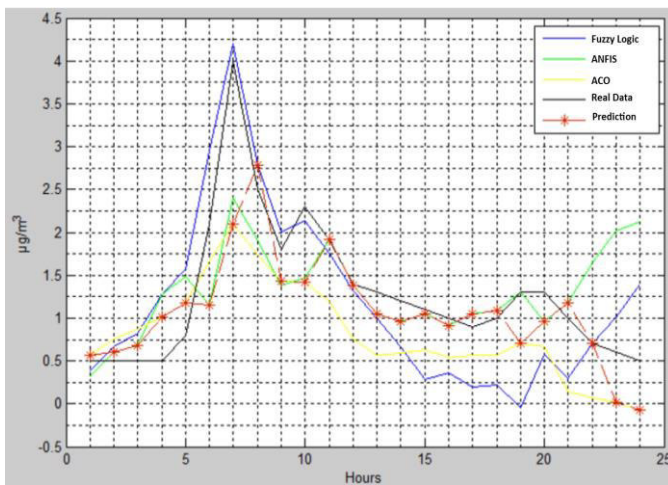


Fig. 5. Different models response comparison

- [1] E. Martinez-zeron, M. A. Aceves-fernandez, E. Gorrostieta-hurtado, A. Sotomayor-olmedo, and J. M. Ramos-arreguín, "Method to Improve Airborne Pollution Forecasting by Using Ant Colony Optimization and Neuro-Fuzzy Algorithms," no. October, pp. 81–90, 2014.
- [2] A. L. Estrada, "Design and Implementation of Ant Colony Algorithms to Enhance Airborne Pollution Models," vol. 3, no. 2, pp. 22–28, 2015.
- [3] H. Vennila and T. R. Deva Prakash, "Particle Swarm Optimization Technique for Solving Economic Emission Dispatch Problems," *Procedia Eng.*, vol. 38, pp. 2009–2021, 2012.
- [4] H. Ahmed and J. Glasgow, "Swarm Intelligence: Concepts, Models and Applications Technical Report 2012-585," *Tech. Rep.*, vol. 585, no. February, pp. 1–50, 2012.
- [5] C. Blum and D. Merkle, *Swarm Intelligence Introduction and Applications*, vol. 1. Berlin: Springer, 2008.
- [6] J. Quiroga, "Algoritmo PSO para identificación de parámetros en un motor DC System identification of a DC motor using PSO algorithm," pp. 116–124, 2010.
- [7] Secretariat of Sustainable Development, Suspended particles <http://www.queretaro.gob.mx/sedesu/contenido.aspx?q=0P7Np1eT MwzKx4t1luGNSxKe8AMHKnDRpJpA3zCAa9s=>



Bonding analysis for composite beams (mdf wood and steel) which are test by bending stresses.

REVIEW

Miguel Angel Sandoval-Morfin
Queretaro State University (UAQ)
DIPFI
Queretaro, Mexico
mr.sandoval26@gmail.com

Jose Luis Reyes-Araiza
Queretaro State University (UAQ)
DIPFI
Queretaro, Mexico
araiza@uaq.mx

Abstract— This paper shows an analysis of other jobs that have been developed on the bonding (adhesion) of wood with steel, which have been used for the development, strengthening and testing of structural beams subjected to bending with the intention to propose a new methodology for calculating the adhesion between wood particle board and steel, so that it can subsequently ensure working together in a composite material where tensile stresses will be absorbed by the steel while compression stresses are absorbed by the wood. Therefore it was observed that Soriano and Parvez works showed the best results using epoxy adhesives to produce beams and obtaining interesting results in terms of flexural strength and adhesion between both materials.

Keywords— *adhesion, bending, composite material.*

I. INTRODUCTION

A. *Uses of wood composites for construction purposes.*

The use of wood for construction in any type of structure (light or heavy) in Mexico is scarce compared to neighboring countries such as the United States of America and Canada, but the use of lumber, for example in dwellings, is Practically null, due to its low resistance to the tension of the agglomerated wood even though studies have been carried out on elements reinforced with steel, carbon fiber among others, where although the resistance of the element is improved in addition to the systems are lightened Of the mezzanine favoring the structure of an earthquake, the incompatibility of adhesion between these materials has proved to be the main limiting factor for the compound to develop its maximum resistance when used in structural elements (Anders et al., 1980; Mc Neil and Witold , 2002).

B. *Wood composites reinforced by several mecanisms.*

The use of internal metal reinforcement for wooden beams has been beneficial to repair elements that have been overloaded, being an economical solution that allows to preserve the existing structure, where the use of tempered steel turns out to be the most frequent for these cases due to its resistance And rigidity (Parvez et al., 2012).

On the other hand the use of non-reinforced chipboard (LVL / Laminated veneer lumber) has shown that the orientation of the wood sheets is decisive for improving the mechanical properties of the material. In this case, in order to improve the tensile strength of the material, it has been shown that if the wood sheets are oriented parallel to the longitudinal axis of the element, unlike agglomerates where the orientation is random, there is an increase in the tensile strength, Which although this represents an improvement in the capacity of the material, does not surpass the increase in resistance that an extra reinforcement of steel can provide (Anders et al., 1980).

It has also been shown that the use of reinforcing steel in LVL or agglomerated lumber elements subjected to bending as shown in figure 1 increases its stiffness by up to 48% and its strength by 25 to 45% To the stress of the element, in comparison with non-reinforced elements, in addition to that the amount of reinforcement near the neutral axis represents a small benefit to the element (Parvez et al., 2012, Morales-Conde and Rodriguez-Liñan, 2014).

Of the above, one of the most worrisome external agents for the engineer when choosing wood as a construction material is the risk that the material faces against any fire inside the building, so it is important to define in what type of structure would be

used The material, so that the occupants of the structure can evacuate it quickly and easily in the event of a disaster of this magnitude (McNeil and Witold, 2002).

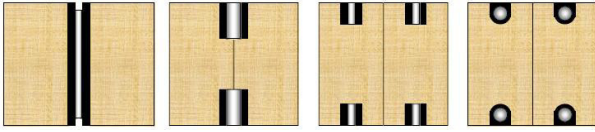


Fig 1. Longitudinal steel configurations in reinforced wood beams tested by Parvez Alam (Parvez et al., 2012).

C. Bonding mechanism wood-steel.

The adhesion mechanism between the materials involved in the cross section of the beam is vital to ensure that both materials work evenly. For example, in reinforced concrete, the chemical adhesion provided by the concrete to be set as well as the corrugations of the rods embedded in the concrete act as a mechanism of mechanical adhesion between both materials.

In the case of reinforced wood, the use of epoxy adhesive, such as Guomin amylum, produced by Henkel or Rotafix® CB10TSS, has been shown to give good results in order for the material to work properly and guarantee increases in resistance up to 45% (Neubauerova , Yushun Li et al., 2000), where although the incompatibility of adhesion between the materials involved has been the main problem for the development of composites, studies have been carried out to reinforce wooden beams with steel bars where the calculations Analytical studies show an increase in resistance of up to 53.1% applying a reinforcement steel amount up to 4% in beams, and in which the use of chemical adhesives has shown that the theoretical analysis of stress resembles in more than a 90 (2), which means that the adhesion between the two materials is ideal for the transformed section theory to be valid (Soriano et al., 2016, Parvez et al., 2012).

In addition to the use of chemical adhesives, different methods of mechanical adhesion have been used among them, which is observed in figure 3, which works with the fixing of a metal plate on the side faces of the element by means of the placement of a pairs arrangement Metallic flat head which are embedded in the wood and provide a good fixation of the metal plate without the use of chemical adhesives. The mechanism has not been published in scientific articles but patent US81666721B1 explains its operation and the way in which it is used to reinforce agglomerated wood beams although in this case the steel reinforcement is placed on the side faces of the cross section And not in the lower or upper bed of the section as in the cases mentioned above (DiGirolamo et al, 2012).

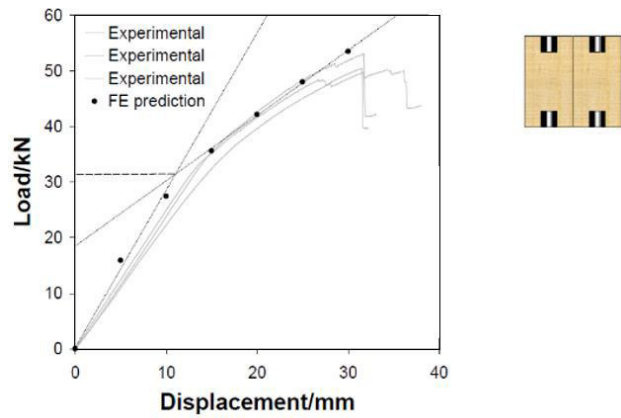


Fig 2. Load-strain test on a steel member reinforced with steel bars in the upper and lower bed. It is observed with points the computer prediction of the load-strain curve (Image: Parvez et al., 2012).

Unlike chemical adhesion, the use of mechanical devices for the joining of two materials benefits the system since the incompatibility of materials is reduced since the mechanical adhesion is not crucial and therefore an increase in the resistance to Flexion of the composite section (McNeil and Witold, 2002; Hassanieh et al., 2016, Piazza M., 2002).

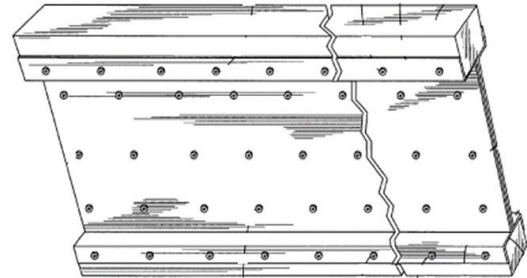


Fig. 3 Fixture arrangement for fixing metal reinforcement for a beam subjected to bending (Image: DiGirolamo et al., 2012).

II. MATERIALS AND METHODS OF STUDY

A. Types of wood composites

Of the studies that have been cited in the present work, the tests with lumber of LVL type pine and the use of elements formed by veneers of wood (glulam), as in the case of Julio Soriano, where the beams were reinforced with bars Of steel with $f_y = 4200\text{kg / cm}^2$ and adhered to the plated wood and from where they obtained to obtain last loads superiores to three tonnes and average. The specimens presented by Julio Soriano are shown in Figure 4, where it can be seen that the wood beams were longitudinally milled to give a cavity to the corrugated steel bar and these cavities were filled with 501® PUR epoxy adhesive for Guarantee the adherence of materials.



Fig. 4 Specimens reinforced by steel bars inserted into the cavity that was milled into the wood (Image: Soriano et al., 2016).

On the other hand Parvez Alam emphasizes the use of LVL type wood, steel $f_y = 4200 \text{ kg/cm}^2$ and Rotafix® adhesive for the test of its elements to flexion with which it obtains last loads superior to four tons in addition to having corroborated that the data of its Experimentation well enough coincide the strain-versus-deformation curve obtained from analysis using specialized software (ANSYS 5.7®).

B. Bending test.

The type of test to determine the flexural strength of the elements used in the various related articles is based on the ASTM D198 standard "Standard Test Methods of Static Testing of Lumber in Structural Size". The dimensions of the test specimen as well as the configuration of loads to be applied to the specimen are shown in figure 5 where it can be seen that both Soriano and Parvez used the same geometric configuration in the specimens they tested.

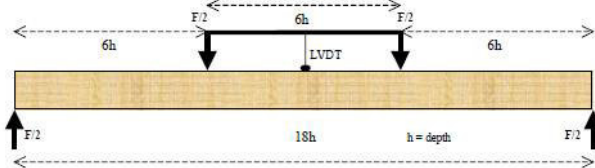


Fig. 5 Load configuration for 4-point test according to ASTM D198 (Image: Parvez et al., 2012).

C. Specimens manufacturing.

The fabrication of the specimens to be tested will depend on the type of wood selected for working as well as on the geometric distribution of reinforcing steel in the cross-section of the elements. In addition, it is important to mention that the specimens can be manufactured by reference to the dimensions indicated by ASTM D198.

III. RESULTS

A. Results analysis from Parvez Alam work.

From Parvez Alam's study of sawn timber, last loads of more than four tons were reported depending on the geometric configuration of the steel. In Table 1 we can see the experimental results obtained by Parvez Alam applying

Rotafix® adhesive to its elements to guarantee adhesion between steel and wood.

From the results obtained, it is worth noting that the variations with respect to the load - strain curve obtained with the use of ANSYS® (Figure 2), did not vary by more than 8%, which is an indicator of the excellent adherence that the Adhesive used in the present test and therefore can be considered in future studies to be carried out with wood and steel.

TABLE I. LAST LOAD ACCORDING TO THE GEOMETRIC CONFIGURATION OF THE STEEL IN THE STUDY OF PARVEZ ALAM.

Configuración acero	Carga Última (kg)
I	4170
II	3360
III	4280
IV	3567

From Figure 1 it can also be analyzed that the distribution of the steel for the configuration III and IV is very similar, only changes the geometry of the reinforcement that in case III is used sheet or steel hearth and in the case IV circular bars Corrugated) and as shown in table 1, configuration III improves the performance of the reinforcement giving an increase in resistance with respect to IV of 20%, this will probably be due to the increase of moment of inertia provided by the steel hearth Placed in that direction.

B. Results analysis from Julio Soriano work.

The study presented by Soriano shows very similar results to those of Parvez in terms of final load, which still refers to the fact that the wood used in each work is different, since it should be remembered that one type of LVL wood was used and the other elements formed by Wood veneer

Figure 6 shows the last load data obtained by Soriano from his experiment, in which he formed three groups of beams to be tested, the first group three beams without reinforcement, the second were three beams with a reinforcement value of 2 % and the third group were three beams with an amount of 4% longitudinal reinforcement.

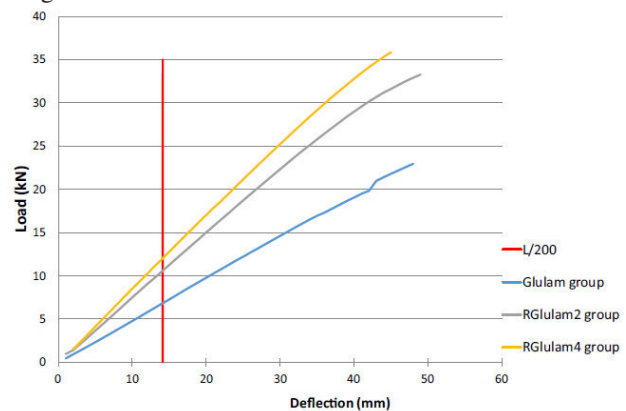


Fig. 6 Load - strain graph where three groups of specimens, Glulam group, RGlulam 2 group (2% reinforcement) and RGlulam 4 group (4% reinforcement) were tested, the L / 200 arrangement represents the

deformation limit per service In construction regulations (Image: Soriano et al., 2016).

Table 2 shows the numerical results at point L / 200 (service limit) and at the point of failure obtained from the graph shown in figure 6, the first ones are of great interest since they are the maximum loads that they support For the condition that marks the regulation of construction where the excessive deformations in the element are limited and it is where greater emphasis must be made to look for to reduce the deformations and to increase the last load.

TABLE II. FINAL LOAD FOR DIFFERENT REINFORCEMENT CONDITIONS IN THE BEAMS TESTED BY J. SORIANO.

Configuración acero	Carga (kg) L/200	Carga última (kg)
Glulam Group	680	1800
RGlulam Group 2	1100	2750
R Glulam Group 4	1250	3350

From the results shown in Table 2, it can be seen that the strength in conditions of serviceability (L / 200) of a beam reinforced with a 4% of steel area represented an increase of 84% of load compared to non-reinforced beams.

As for reinforced beams with only 2% steel and 4%, it was observed that increasing the steel area doubled only by an increase of 13.6%

Under the ultimate load conditions the non-reinforced beams compared to the 4% steel reinforcement, a resistance increase of 86% was observed.

As for beams with a value of 2% and 4%, only an increase of 21% was observed, which almost doubled in comparison to the increase obtained for service conditions (L / 200), which represents that Event of failure in the structure, increase of the amount of steel if it represents a significant benefit to benefit the element resistance.

C. Type of failures obtained.

The failures obtained in the studies that have been analyzed are the fragile failure and the ductile failure. The first one is observed in figure 7a where the destruction of the wood veins of the elements without longitudinal reinforcement of steel is observed. Figure 7b shows a ductile failure that occurred in the reinforced elements with 2 and 4% steel, where the cracks of the wood are very light compared to those of the fragile failure.



Fig. 7 A) Fragile fault in beam without reinforcement. B) Ductile failure in reinforced beam with 2% steel (Image: Soriano et al., 2016).

Soriano his experimentation comments that the difference between theoretical and experimental rigidity differ somewhat because the adhesion between steel and wood is not effective in a hundred percent and that is why there are variations.

D. Stiffness specimen determination.

For the calculation of the experimental rigidity of the elements tested Soriano does this by means of the increase of load, the vertical displacement and the length of the clearing, see equation (1).

$$E_w I_{eq} = \frac{23 \cdot \Delta P \cdot L^3}{1296 \cdot \Delta u} \quad (1)$$

Where E_w is the modulus of elasticity, I_{eq} is the moment of inertia of the section, L represents the clearing of the beam, ΔP represents the increase of load and Δu is the increase of the vertical displacement to the center of the clearing.

The stiffness data obtained in the Soriano study are shown in Table 3 and an increase of up to 72% with respect to the specimens not reinforced with steel can be observed.

TABLE III. STIFFNESS OF THE ELEMENTS TESTED IN FLEXION WHERE THE ELEMENTS ARE NOT REINFORCED AND REINFORCED WITH 2 AND 4% OF LONGITUDINAL STEEL.

Configuración acero	$E_w I_{eq} (kNm^2)$
Glulam Group	197
RGlulam Group 2	299
R Glulam Group 4	340

Therefore, in case of wanting to reduce deformation and increase the service load (L / 200), the geometry of the cross section can be modified to increase the rigidity of the element and reduce the deformations that are the Limiting the elements to provide the condition of adequate service.

IV. CONCLUSIONS

From the present work we could compare two experimental studies that have to do with the test of structural elements constructed from wood and reinforced with steel in order to increase the strength and rigidity of the elements. In the first case that was the study made by Parvez Alam, we can conclude the following:

- The longitudinal steel reinforcement shown in prototype III proved to be the one with the highest flexural strength, and that the prototype IV, even having a similar reinforcement geometry (common reinforced concrete), showed a lower resistance to III. This can be a cause of poor adhesion between steel and wood, so we should go into that analysis.
- The use of Rotafix® epoxy adhesive in the tested elements provides perfect adhesion for all configurations tested, since the theoretical results

were more than 90% similar to the experimental ones.

In the second case, where the study of Julio Soriano was analyzed, it can be concluded that:

- The steel reinforcement from 2 to 4% better in more than 84% load bearing capacity of the beam.
- The failure mechanism was modified from a brittle to a ductile failure due to the steel reinforcement that was given to the element, which is a good indicator of sufficient adhesion provided by the 501® PUR adhesive used in the specimens tested.

In general, both authors described in the present work have lacked to emphasize more in depth on the measurement of the adhesion that is generated between the materials and that allows a homogenous behavior of the composite material under study. That is why it is of great interest to introduce ourselves beyond this shallow analysis to identify the possible adhesion mechanisms that can lead us to obtain greater resistance or ultimate loads while reducing the deformations to comply with the conditions of service that mark the construction regulations in force.

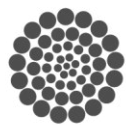
What is the new proposal?

The main objective of the analysis of the previous documents has been to forge a basis for a new model that is proposed to create, a model no longer built with sawn or veneered wood since these materials have already been studied in a wide way and we must go to areas of study that have not been developed and therefore it is proposed to carry out the study with wood of a particleboard such as MDF boards, and to reinforce this material with steel as has been done in the studies shown here,

but as it is of the utmost importance to be able to guarantee the adhesion between both materials and that is why different ways of joining the materials have been analyzed, which have guaranteed excellent flexural strength.

(1) REFERENCES

- [1] Anders E. Lund, Gordon P. Krueger, Darrell D. Nicholas, Roy D. Adams. Structural members of composite wood material and process for making same. U.S., 4241133. (CI. 428/326), Dec. 23, 1980. Appl. 26095, Apr. 2, 1979.
- [2] DiGirolamo R., et al., Metal-wood structural member. US. 8166721B1. (CI. 52/455), Mayo 1, 2012. Appl. 11/358,758, Feb. 21, 2006.
- [3] Hassanieh A., Valipour H., Bradford M., 2016. Experimental and numerical study of steel-timber composite (STC) beams. Elsevier Journal of Constructional Steel Research.
- [4] Mc Neil Brian F., Witold Krassowski D., Composite I-beam having improved properties. U.S. 6460310B1. (CI. 52/729.1), Oct. 8, 2002. Appl. 09/670088, Sep. 26, 2000.
- [5] Morales-Conde M.J., Rodríguez C., Rubio-de Hita P., 2014. Bending and shear reinforcements for timber beams using GFRP plates. Elsevier Construction and Building.
- [6] Neubauerova P., 2012. Timber beams strengthened by carbon – fiber reinforced lamellas. Elsevier Procedia Engineering.
- [7] Parvez A., Ansell M., Smedley D., 2012. Effects of reinforcement geometry on strength and stiffness in adhesively bonded steel – timber flexural beams. J. of buildings. 231 (Abstr).
- [8] Soriano J., Piva B., Tadeu N., 2016. Mechanical performance of flued-laminated timber beams symmetrically reinforced with steel bars. Elsevier Composite Structures.
- [9] Yushun L., Wei S., Huangying S., Zhen Z., Junzhe L., 2015. Bending resistance of I-section bamboo-steel composite beams utilizing adhesive bonding. Elsevier Thin Walled Structures.



CONACYT

Consejo Nacional de Ciencia y Tecnología



CONCYTEQ



Comparison of traditional protein sources, soybean meal and fishmeal, with house cricket (*Acheta domesticus*): Review about proximate analysis and amino acids content.

Pérez Rosas José Alberto, García Trejo Juan Fernando
División de Investigación y Posgrado de la Facultad de Ingeniería.
Universidad Autónoma de Querétaro, UAQ.
Querétaro, México
alberto_japr@hotmail.com

Abstract—In the early twenty-first century it was worldwide banned the use of meat bone meal as a source of protein in the diet of animals for human consumption, which forced to search for new sources of high quality protein, making the soybean meal and flour fish the most used around the world; as result, this brought problems of seas overexploitation it also caused deterioration in the ecosystems where soy is cultivated. Recently the world has turned his gaze to the insects in search of new sources of high quality protein, and so, numerous studies have been conducted with a variety of insects from different families as *Blattaria*, *Coleoptera*, *Diptera*, *Lepidoptera*, *Orthoptera*; including the house cricket (*Acheta domesticus*). The main purpose of this work is to make a review of the main features of the house cricket and compare it with traditional protein sources such as soybean meal and fishmeal; the results of the house cricket's chemical composition are, for raw protein around 550-736 g kg⁻¹, raw fat oscillating from 79 to 230 g kg⁻¹, ashes 50-140 g kg⁻¹ and gross energy 17-23 MJ kg⁻¹; the reviewed data of the soybean meal and fishmeal protein contents show a high similarity with the one found in the house cricket.

Keywords—house cricket; quality protein; chemical composition; soybean meal; fishmeal.

I. INTRODUCTION

Currently world's population is around 7000 million people. This number is growing day by day and with it, so does the need to supply the food's requirements of each individual, which represents a real challenge for the future. Food production must have two main guidelines: quantity and quality [1].

Fishes produced under aquaculture, monogastric livestock, poultry and even reptiles need to consume high-quality protein in order to become nourishment which satisfies the nutritional needs and quality to be consumed by humans [2].

Inland aquaculture is growing strongly, according to statistics from the Fisheries Department of Food and

Agriculture Organization (FAO), the total world production of species produced under this system doubled between 2004 and 2012. The main species produced worldwide are grass carp (*Ctenopharyngodon idellus*), silver carp (*silver carp*), common carp (*Cyprinus carpio*), Nile tilapia (*Oreochromis niloticus*) and channel catfish (*Ictalurus punctatus*) [3].

In Mexico the behavior is not equal to that followed worldwide, just between 2010 and 2012 there was an increase of 13 thousand tons in total aquaculture production of any kind, being the capturing aquaculture production the most predominant in the total national production, with 1.5 million tons in 2012. The three species most commonly grown in Mexico are tilapia (*Oreochromis spp.*), channel catfish (*Ictalurus punctatus*) and common carp (*Cyprinus carpio*). Tilapia is the most cultivated specie; nearly 24 thousand tons were produced in 2012, while only 2 thousand tons of channel catfish were produced in the same year [3] The states with the largest aquaculture production are Sinaloa, Jalisco, Veracruz; but Queretaro is not among the 10 states with the largest aquaculture production [4].

Since 2000 it is forbidden using bone meal in the diets of animals for human consumption [5]. Therefore soybean meal and fish meal are the most used protein source in animal feed. But obtaining these proteins can be translated to overexploitation of seas, where fishes are usually obtained from to produce fishmeal, or deterioration of the ecosystem where soy is produced.

In regard to the production of fishmeal, global production over the last 50 years has fluctuated between 4 and 7 million tons per year [3]. Fish production by aquaculture is still growing by leaps and bounds: just in the last decade, aquaculture production grew 96% Fig. 1, consumption of fishmeal in aquaculture systems grew by 800 thousand tons in the same period, and consumption of fish oil is maintained,

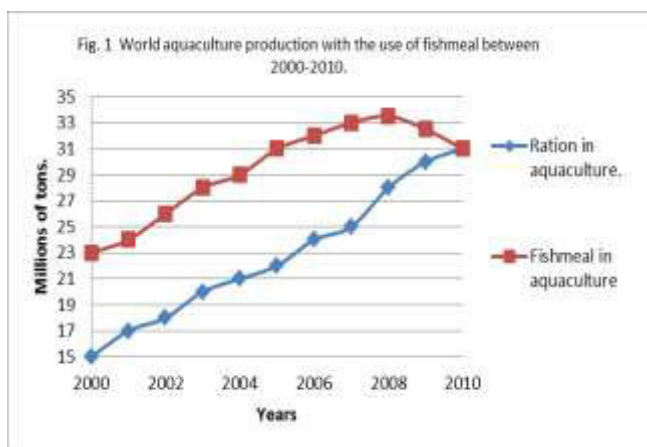


Fig. 1 World aquaculture production with the use of fishmeal between 2000-2010.

showing a slight drop in recent years. It can be assumed that the decrease in the consumption of fish meal is caused by the novel balanced foods, which present greater efficiency due to they replace part of the protein provided by fish meal with vegetable proteins.

The cost of feeding in intensive aquaculture production systems represents between 35 -45% of the total cost of production [6]. Protein is the most expensive component in fishes' feeding [7]. Insect flours may be a feed option in aquaculture systems thanks to its protein content.

Recently insects have got special attention as potential new sources of high quality protein because they have high feed conversion, require little space for breeding and they can be produced in industrial quantities using wastes [8]. One of these insects is the common domestic cricket or house cricket (*Acheta domesticus*), which is an insect from the family of Orthoptera.

II. MATERIALS AND METHODS

The aim of this review is to compile information on the chemical and nutritional composition (DM – dry matter, CP - crude protein, CF - crude fat, NFE – nitrogen free extracts, ADF – acid detergent fiber, NDF – neutral detergent fiber, BE – gross energy, amino acid composition) of flour house cricket (*Acheta domesticus*), soybean meal and fishmeal. Information of the chemical composition about other insects that also have feed interests for their proteic content, is also described and compared, and even those from the same order of house cricket (*Acheta domesticus*).

III. RESULTS

A. Soybean meal

Balanced foods currently used in aquaculture contain soybean meal as protein source, necessary for the development

and growth of fishes. Below are mentioned the main characteristics of soybean meal.

Soy is considered the main source of vegetable protein for animal and human consumption because the 40-45% of the soybean is protein; it also contains considerable amounts of energy and essential amino acid [9]. The protein in soybean meal can be compared in nutrition quality with those present yolk's eggs and casein [10].

Soybean meal contains the best vegetable protein taking into consideration the relationship between quality and quantity. Notwithstanding it is deficient in methionine and tryptophan, is rich in the following essential amino acids: isoleucine, leucine, lysine, methionine, cysteine, phenylalanine, tyrosine, threonine, tryptophan, valine and histidine [1].

World production of soybean in 2010 was around 260 mln ton, being the main producers USA, Brazil, Argentina and China, which produce about 90% of total world production [11].

B. Chemical and nutritional composition of soybean meal

Initially we can mention that soybean meal contains between 5.5 - 12% water, 5-7% crude fiber, which is little when compared with other seeds; contains as well between 32-45% crude protein, which could reach up to 50% and 15.5 to 25% of fats. Contains lots of lysine (6.2g / 16gN) while the value of cystine is (2.9g / 16gN) [12].

Table 1 shows the basic nutrients in soybeans and soy flours with low protein content (44%) and high protein content (49%), the content of nitrogen-free extract and starch [13]. In which we can see that the protein content of the flour is higher than in the seed, while the fat content is higher in seeds (18.38%).

TABLE 1. BASIC NUTRIENTS IN SOYBEAN SEEDS AND MEAL.[13]

Nutrient	Soybean seeds % DM	Soybean meal	
		44%CP %DM	49%CP %DM
Crude protein	37.1	44-50	53-56
Crude ash	4.9	5.6-7	5.2-9
Crude fat	19.4	0.5-3	1-3.3
Crude fiber	5.1	4.3-7	3.1-4.1
NDF	13	12.1-19	7.4-12
ADF	7.2	8.9-12	5.2-6.7
N-free-extractive	24	34	33
Starch	4.7	5.5	5.5

C. Fishmeal

The use of fishmeal manifested an increase in early XXI century because it has a good quality protein and it is relatively easy to obtain, by the exploitation of the seas and oceans; global production of fishmeal is 7 million tons per year [3]

Fishmeal is produced from catching low-demand fishes for human, in some situations fish meal is made from fish's wastes generated during processing, viscera, blood and bones. Between 13% and 18 % of world's fishmeal is produced from wastes. Normally fish meal is used as an ingredient in animal feed, poultry, pigs, cattle and fish farming, because it contains high protein percentage [14].

D. Chemical and nutritional composition of fishmeal

Fishmeal is brown-colored, with a content of protein between 65% and 75%, between 5% and 12% fat and 10%-20% ash. In Table 2, can be found the characteristics of fishmeal with low and high protein contents, the first one containing approximately 47% in dry matter (DM), meanwhile fishmeal high protein contains 75%; crude fiber for both flours is varied 10-11%, the average gross energy is 20 Mj / kg [15].

E. House cricket (*Acheta domesticus*)

It is an insect from the family of the Orthoptera, of the superfamily of Grylloidea, members of this family are commonly known as crickets [16]. They are mostly yellowish-brown, with nocturnal habits. Originating in southern Europe, northern Africa, and Asia, crickets are distributed around the

world (except at the poles), especially in temperate zones but also found in tropical areas [17].

Due to it belongs to the family of the orthopterans, it has similar characteristics with grasshoppers. The legs of crickets, like those of grasshoppers, are adapted to perform jumps; however they achieve less height on their jumps, what is offset by their ability to run fast on the ground [18]. They measure between 2.5 and 3 centimeters, their antennae can reach a similar length; its activity is nocturnal and crepuscular, remain hidden during the day and prefer high temperatures. Their diet is omnivorous; they consume fruit, smaller insects, and almost any kind of organic waste. Within cities can be easily found in areas near garbage dumps [19].

They present sexual dimorphism, this is, male and female are differentiated: males are smaller in size, and females are darker in color, have smooth wings and possess an appendix, known as ovipositor at the end of their abdomen, with which they put their eggs underground [19]. It is a territorial insect, can become aggressive with their peers either for protecting their territory or females, as far as dismember the opponents; when food is scarce, the eggs laid by females are eaten when food is scarce.

Currently they are bred in captivity to feed insectivorous animals, but studies have tried to prove that the cricket's protein is high quality and can partially or completely replace the animal protein and / or vegetable that are currently used [20].

TABLE 2 CHEMICAL COMPOSITION OF HOUSE CRICKET, SOYBEAN MEAL, FISHMEAL. (SOURCES ARE SHOWN IN TABLE).

name	scientific name	stage	DM (g/Kg)	CP (g/Kg)	CF (g/Kg)	Ash (g/Kg)	NFE (g/Kg)	BE (Mj/Kg)	references
House cricket	<i>Acheta domesticus</i>	adult	268	644	228	51	N/A	N/A	Barker et al., 1998
		adult	310	649	138	138	N/A	22.4	Bernard et al., 1997
		adult	N/A	706	177	53	N/A	N/A	Bosch et al., 2014
		adult	308	666	221	35.7	26	N/A	Finke, 2002
		adult	292	736	123	N/A	N/A	19.16	Yi et al., 2013
		nymph	332	550	98	62	N/A	N/A	Barker et al., 1998
		nymph	229	673	144	48	39.3	N/A	Finke, 2002
		mix	N/A	654	79	48.5	N/A	17.5 Nagasaki and DeFoliart. 1987	
Soybean meal		44%	N/A	460	15	68	398	N/A	Banaszkiewicz, 2011
		low prot.	879	518	20	71	94	19.7	Heuzé et al., 2015
		high prot.	881	535	18	72	106	19.7	Heuzé et al., 2015
Fish meal		high prot.	921	754	110	136	N/A	21.9	Heuzé et al., 2015
		low prot.	925	484	103	352	N/A	19	Heuzé et al., 2015

F. Chemical and nutritional composition of house cricket (Acheta domesticus)

Several authors have performed and reported analysis of the chemical composition of common cricket, where the crude protein (CP), fat (CF), dry matter (DM), nitrogen-free extract (NFE), fiber (F), gross energy (BE) and ash (ash) obtained. Table 2 shows the data reported by author and stage of development of the common cricket; it also shows the analysis of the chemical composition of soybean meal and fishmeal. In this table can be seen that house cricket is normally studied in two stages of development, adult and nymph, reporting an average protein content of 68% for adult and 61% for nymph; It shows that the percentage of ash in crickets house is 7% adult and nymph is 5.5% on average. Another fact we can get from the table is the content of gross energy (BE) which alone is reported in adulthood with 22.4 MJ / kg [21] and 19.16 MJ / kg [22].

Although knowing the amount of protein contained is a good start point, it is also necessary to know the amino acids present in it, since it gives not only quantity, but the nutritional quality of the protein as well. The table 3 shows the compiled information of the content of amino acids in house cricket, meal soybean and fishmeal, reported by different authors, where we can observe the content of 18 amino acids, a row named average (AVG) where the average content, in g / kg DM, for each amino acid of the house cricket is shown, being glutamate (GLU) the one with greater amount (about 77 g / kg DM), followed by alanine (ALA) with 59 g / kg DM, while those in fewer quantity are cysteine (CYS), methionine (MET) and Tryptophane (TRP) with 5.6, 9.9 and 4.8 g / kg DM, respectively.

The same table shows the contents of the 18 amino acids in meal soybean and the fishmeal, high and low protein. It can be observed that the more present amino acid in the meal soybean high-protein is glutamate (GLU) with 95 g / kg DM, followed by aspartate (ASP) with 61 g / kg DM; similar behavior to that presented in the content amino acids in fishmeal high protein, which presents with 95 g / kg DM for glutamate and 65 g / kg DM ASP [23].

G. Chemical composition of other insects of the order Orthoptera.

Data reported in the chemical composition of other insects of the order Orthoptera migratory locust (*Locusta migratoria*) and grasshopper common (*Zonocerus variegatus*), is shown in Table 4 in which we can found that the protein content in the migratory locust is 55% while the grasshopper common ranges between 61 and 58%, in the content of gross energy (BE) there's only data on the migratory locust which contains 24MJ / kg of energy. No data was found reported gross energy content for common grasshopper; the migratory locust shows an ash content of 3.5% while the common grasshopper 4.3%.

TABLE 3. AMINO ACID CONTENT IN DRY MATTER (DM) OF HOUSE CRICKET, SOYBEAN MEAL AND FISHMEAL (SOURCES ARE SHOWN IN TABLE).

name	scientific name	stage	Amino acid content (g/kg DM)																		references	
			Asp	Thr	Ser	Glu	Ala	Gly	Cys	Met	Ile	Leu	Tyr	Phe	His	Lys	Arg	Pro	Trp	Val		
House cricket	<i>Acheta domesticus</i>	adult	x	25.4	x	x	x	x	x	x	11.3	28.2	46.6	x	22.6	24	40.9	40.2	x	x	40.2	Bosch et al., 2014
		adult	55.8	24	33.12	69.8	58.4	33.8	5.5	9.7	30.5	66.6	32.5	21.1	15.6	35.7	40.6	37.34	4.22	34.7	Finke, 2002	
		adult	53.7	25.8	28	91	59.7	37.6	x	x	26.5	48.6	x	x	15.5	39	47.9	39.8	6.6	40.5	Yi et al., 2013	
Soybean meal		nymph	47.6	24	27.9	69.9	59.7	35.4	5.7	8.73	28.8	64.2	37.1	18.8	14.8	36.2	41	37.1	3.5	33.2	Finke, 2002	
		low prot.	58.5	20.2	25.9	91.7	22.8	21.8	7.8	7.3	23.9	38.9	18.1	25.9	13.5	31.6	38.3	25.38	6.7	24.9	Heuzé et al., 2015	
Fish meal		high prot.	61	20.3	24.6	95.8	23	22.5	8.6	7.5	24.6	41.2	18.7	27.3	14.5	33.7	39	26.8	7.5	25.7	Heuzé et al., 2015	
		high prot.	65.6	30.9	30.2	95	46	44.5	6	21.1	32.4	52.8	21.9	28.7	16.6	56.6	43.7	28.7	8.3	37	Heuzé et al., 2015	
		low prot.	46.5	19.4	17	61	30	33.9	5.8	12.6	19.9	36.3	15.5	19.4	11.6	33.9	25.2	23.2	x	25.2	Heuzé et al., 2015	

mealworm and dubia roach have average protein content between 3.9 and 4.4%.

TABLE 4 CHEMICAL COMPOSITION OF OTHER INSECTS OF THE ORDER ORTHOPTERA (SOURCES ARE SHOWN INTABLE).

name	scientific name	stage	DM (g/kg)	CP (g/kg)	CF (g/kg)	Ash (g/kg)	NFE (g/kg)	BE (Mj/kg)	references
Langusta migratoria	<i>Locusta migratoria</i>	adult	343	555	296	33	x	24	Oonincx, 2011
Common grasshopper	<i>Zonocerus variegatus</i>	adult	291	555	247	37	x	23	Oonincx, 2011
		mix	x	615	69	43	243	x	Alegbeleye et al., 2012
		mix	x	580	155	x	x	x	Olusola et al., 2003

H. Chemical composition of other insects

Values of the chemical composition of other insects were found and presented in table 5, that are worth mentioning in this review in order to generate a comparison with the house cricket, among other insects found. The mealworm (*Tenebrio molitor*), belonging to the order Coleoptera, the dubia roach (*Blaptica dubia*) of the order of Blatrania, and musca common (*Musca domestica*) of the order Diptera are described; these three insects like the house cricket, were studied in their different stages of development: adult, pupae, larvae, nymph and maggot. The results are shown in table 5, where we observed that on average *Musca common* had the highest protein content, with 63% followed by dubia roach, with 60% protein and finally, the mealworm average containing 59% protein.

The contents of gross energy (BE) reported for the three insects have a similar range between 20 and 23 Mj / kg. Another thing that should be noted is the ash content being *Musca common* the one with higher average (5%), the

TABLE 5 CHEMICAL COMPOSITION OF OTHER INSECTS (SOURCES ARE SHOWN INTABLE).

name	scientific name	stage	DM (g/kg)	CP (g/kg)	CF (g/kg)	Ash (g/kg)	NFE (g/kg)	BE (Mj/kg)	references
Mealworm	<i>Tenebrio molitor</i>	adult	386	637	184	31	x	24	Bernard et al., 1997
		adult	363	653	149	33	38	16	Finke, 2002
		adult	388	676	177	72	x	x	Oonincx, 2012
		pupae	390	513	366	32	19	27	Bernard et al., 1997
		pupae	X	531	366	32	19	23	Ramos, 2007
		larvae	376	527	328	39	x	27	Barker et al., 1998
Dubia roach	<i>Blaptica dubia</i>	adult	x	644	245	44	x	x	Bosch et al., 2014
		adult	374	630	214	49	43	19	Kulma et al., 2015
		adult	326	590	236	x	x	x	Yi et al., 2013
		nymph	422	525	328	40	42	22	Kulma et al., 2015
		pupae	x	762	144	x	x	20	Pretorius, 2011
<i>Musca common</i>	<i>Musca domestica</i>	pupae	x	799	183	11	x	x	St-Hilaire et al., 2007
		maggot	x	675	256	54	13.2	23	Hwangbo et al., 2009
		maggot	x	389	205	x	16	21	Ogunji et al., 2007
		larvae	x	597	224	67	x	x	Aniebo and Owen, 2010
		larvae	x	568	200	68	x	25	Bernard et al., 1997

IV. COPARISON AND DISCUSSION

As previously mentioned, soybean meal and fish meal are the most widely source material used for the production of feed for livestock such as cattle, poultry, and fish protein due to its high proteic input.

Table 2 shows results of proximal analysis of house cricket obtained by different authors in different stages. As it is seen, the average protein content in the adult cricket is 68%, with a maximum of 73.6% [22], while in the nymph stage, an average content of 61% is presented; the high-protein meal soybean shows a content of 53.5% [23] which is a less than the one presented by the house cricket in adulthood, reported by Yi et al., 20%; although the high-protein fish meal has 75.4% [15], it is not far above from that of the house cricket (68%). The crude protein content of the latter is higher than the presented

in soybean meal and fish meal in their versions of low protein by around 16%.

Another fact that can be rescued from the same table (2) is the ash content, various authors reported an average of 6.4 g / kg DM for the different stages of development of cricket, compared to the ash content of the soybean meal which is approximately 7 g / kg DM [23]. Regardless of whether it is low or high protein, the difference is not large, only 1.4 g / kg DM; compared to the fishmeal, the difference whether it is low-protein or high flour is not large. The first is five times higher than the ash content of the house cricket with 35 g / kg DM, and the second is two times with 13.6 g / kg DM. Knowing the values of ashes is important because it is a percentage of food that is not exploited in any way by the animal consuming.

In respect of gross energy content, the house cricket has two values: one of 22.4 MJ / kg DM [21] and other of 19.16 Mj / kg DM [22]. Values between these are the values reported by Heuzé et al. for meal soybean low and high protein, with 19.7 Mj / kg DM and low and high-protein fishmeal of 19 and 21.9 MJ / kg DM respectively, so we can say that there is no difference in content of gross energy to be meaningful.

The second guideline that should be taken into consideration is the quality of the protein, and the content of amino acid. Therefore, table 3 shows a comparison of the quality of protein house cricket, meal soybean and fishmeal. In this table the contents of 18 amino acids in g / kg DM are shown. A comparison between high-protein meal soybean and house cricket demonstrate that the latter has a considerably higher content of alanine (Ala), glycine (Gly), leucine (Leu), tyrosine (Tyr), but shows deficient glutamate (Glu). If the comparison is made with high-protein fishmeal, house cricket has higher content of Ala, proline (Pro) and Tyr, but lower content of aspartic acid (Asp), Glu, methionine (Met) and lysine (Lys). However if we compare the amino acid content of the house cricket with low-protein fishmeal the house cricket has higher content of all amino acids, particularly alanine (Ala) with a difference of 29.3 g / kg DM, tyrosine (Tyr) a difference of 19.3 g / kg DM and arginine (Arg) with 17.2 g / kg DM.

In recent years, other insects have been studied in search for a protein source for balanced food, this review shows in table 4 data on the chemical composition of other insects from the family of Orthoptera, as the migratory langusta and common grasshopper. Although it is from the same order of insects, crude protein content is less than 68%, which is lower than the house cricket, immigration presents langusta 55.5% [24], while the common grasshopper 60% on average. As for the ash content both migratory grasshopper lagusta as common shows less content than the house cricket. The content of crude BE energy between the three insects is similar, ranging from 20 to 24 MJ / kg DM.

Table 5 displays the chemical content of some insects from different orders that are important for their protein content,

which have been studied and reported by different authors, among them are the mealworm (*Tenebrio molitor*), dubia roach (*Blaptica dubia*) and Musca common (*Musca domestica*), the average protein content of any of these insects is less than the house cricket, being the musca common that more is about 63%, 5% less than the average reported to housecricket, but still can be considered as an optional source of protein for balanced meals. The ash content is less than in the house cricket while reported gross energy is similar in the four insects.

V. CONCLUSION

Undoubtedly global population growth requires the supply of food for human consumption, which quantity and quality should be maintained; many of the foods consumed by human need balanced nourishment. The main components of these balanced meals are the meal soybean and fishmeal, however, production of these flours translates as overexploitation of the seas and farmland, therefore it is necessary to search a new source of high-quality protein and easily-produced food. As shown throughout this review a very attractive option is the protein from house cricket (*Acheta domesticus*) thanks to its protein content which is on average greater than conventionally used flour, their similarity in amino acid content is another important factor to flip, in order to consider the house cricket as a raw material in the production of flours that provide protein pet foods, thus reducing the exploiting of seas and farmlands.

ACKNOWLEDGMENT (Heading 5)

I greatly thank to National Council of Science and Technology (CONACYT) for the financial support given which helped in the achievement of this article. As well I deeply appreciate the support given by Mrs. Rebeca Rosas Medina and Ximena Vargas.

REFERENCES

1. FAO/WHO. Protein quality evaluation: Report of joint FAO/WHO expert consultation, Food and Nutrition Paper 51. FAO, 1991.
2. Deydier E, Guilet R, Sarda S, Sharrock P (2005). Physical and chemical characterization of crude meat and bone meal combustion residue: "waste or raw material?". Journal of Hazardous Materials. 121: 141 – 148.
3. Statistics and information from the Department of Fisheries and Aquaculture 2014 FAORome/Roma, FAO.
4. CONAPESCA, Statistical yearbook of aquaculture and fishery, <<https://www.conapesca.sagarpa.gob.mx/estadistico-de-pesca>> [Consultado: octubre 2016]
5. P. Van Wyk, M. Davis-Hodgkins, C.R. Laramore, K.L. Main, J. Mountain, and J. Scarpa [1999], Farming Marine Shrimp in Recirculating Freshwater Systems, FDACS Contract M520. Florida Department of Agriculture and Consumer Services, Tallahassee, FL.



6. Avnimelech, Y. (2005). Tilapia harvest microbial flocs in active suspension research pond. *Global Aquaculture Advocate*, 8(5), 57-58.
7. Rumpold BA, Schlüter OK (2013). Potential and challenges of insects as an innovative source for food and feed production. *Innovative Food Science and Emerging Technologies*. 17: 11 – 13.
8. Erickson, R. (Ed), *Practical Handbook of Soybean Processing and Utilization*. Estados Unidos: AOCS/US B, 1995.
9. Crouse, JR. et al. A randomized trial comparing the effect of casein with that of soy protein containing varying amounts of isoflavones on plasma concentrations of lipids and lipoproteins, *Arch Intern Med*. 159, 2070-2076, 1999.
10. Rynek Pasz. (September,2010). Stan i perspektywy. *IERiG* ISSN 1428-1228
11. Ensminger, M. E. 1980. *Poultry science*, 2nd ed. Interstate, Danville, Ill.
12. Van Eys, J.E., Offner, A., & Bach, A. (2004). *Chemical Analysis. Manual of Quality Analysis for Soybean Products in the Feed Industry*. American Soybean Association. http://www.asa-europe.org/Library/library_e.htm.
13. Enamul Hoq, M., Bhuiyan, A. K. M. A., & Mansur, M. A. (1995). Quality aspects of fish silage and fish meal from marine trash fish. *Indian journal of marine sciences*, 24(3), 158-161.
14. Heuzé V, Tran G, Kaushik S (2015a). Fish meal. *Feedipedia*, a programme by INRA, CIRAD, AFZ and FAO. <http://www.feedipedia.org/node/208>. Last updated on May 11, 2015, 14:32.
15. Retrieved [11,20,2016], from the Integrated Taxonomic Information System (ITIS) (<http://www.itis.gov>).
16. McFarlane, I. E., Steeves, E., & Alli, I. (1983). Aggregation of larvae of the house cricket, *Acheta domesticus* (L.), by propionic acid present in the excreta. *Journal of chemical ecology*, 9(9), 1307-1315.
17. Garibay, R. (2007). *Zootecnia del grillo*. Tesis, Universidad Michoacana de San Nicolás de Hidalgo, Facultad de medicina veterinaria y zootecnia, Morelia.
18. Territorio salvaje. (2009). *Acheta domesticus*. <<http://www.territoriosalvaje.com/t331-ficha-acheta-domesticus>> [Consultado: noviembre 2016]
19. Wang D, Zhai SW, Zhang CX, Bai YY, An SH, Xu YN. (2005). Evaluation on nutritional value of field crickets as a poultry feedstuff. *Asian-aust. J. anim. Sci*. 18: 667-670.
20. Bernard JB, Allen ME, Ullrey DE (1997). Feeding Captive Insectivorous Animals Nutritional aspects of Insects as Food. Nutrition Advisory group. Handbook. Fact sheet 003. Scientific Advisory Group to the American Zoo and Aquarium Association.
21. Yi L, Lakemond CM, Sagis LM, Eisner-Schadler V, van Huis A, van Boekel MA (2013). Extraction and characterisation of protein fractions from five insect species. *Food Chem*. 141: 3341-3348.
22. Heuzé V, Tran G, Kaushik S (2015b). Soybean meal. *Feedipedia*, a programme by INRA, CIRAD, AFZ and FAO. <http://www.feedipedia.org/node/674> Last updated on May 19, 2015, 15:44
23. Oonincx DGAB, van der Poel AFB (2011). Effects of Diet on the Chemical Composition of Migratory Locusts (*Locusta migratoria*). *Zoo. Biol*. 30: 9–16.
24. Barker D, Fitzpatrick MP, Dierenfeld ES (1998). Nutrient composition of selected whole invertebrates. *Zoo. Biol*. 17: 123-134.
25. Bosch G, Zhang S, Oonincx DGAB, Hendriks WH (2014). Protein quality of insects as potential ingredients for dog and cat foods. *Journal of Nutritional Science*. 3(e29): 1-4.
26. Finke M D (2002). Complete nutrient composition of commercially raised invertebrates used as food for insectivores. *Zoo. Biol*. 21: 269-285.
27. Nagasaki BJ, DeFoliart GR (1987). Protein quality of the house cricket *Acheta domesticus* when fed to rooster chicks. *Poult. Sci*. 66: 1367-1371.
28. Banaskiewicz T (2011). Nutritional value of Soybean meal. Pp. 1-20. In: El-Shemy, H. (ed.). *Soybean and Nutrition*. In Tech, Rijeka, 476 pp. Available from: <http://www.intechopen.com/books/soybean-andnutrition/nutritional-value-of-soybean-meal>
29. Alegebeye WO, Obasa SO, Olude OO, Otubu K, Jimoh W (2012). Preliminary evaluation of the nutritive value of the variegated grasshopper (*Zonocerus variegatus* L) for African catfish *Claria gariepinus* (Burchell, 1822) fingerlings. *Aquacult. res*. 43: 412-420.
30. Olusola L, Solomon M, Maduka H (2003). Proximate Chemical Analysis of *Zonocerus variegatus* (Giant Grasshopper). *Nig. J. of Biotech*. 14: 42-45.
31. Ramos-Elorduy J, Medeiros-Costa E, Ferreira-Santos J, Pino-Moreno JM, Landero-Torres L, Angeles-Campos SC, García- Pérez A (2006). Estudio comparativo del valor nutritivo de varios coleopteran comestibles de México y *Pachymerus nucleorum* (Fabricius, 1792) (Bruchidae) de Brasil. *Interciencia*. 31: 512-516.
32. Kulma M, Plachý V, Vrabc V, Bubová T, Orsák M in prep. Nutritional composition differences between three species of subadult and adult cockroaches.
33. Pretorius Q (2011). The Evaluation of Larvae of *Musca domestica* (Common House Fly) as Protein Source for Broiler Production. M.Sc. Thesis. University of Stellenbosch.
34. St-Hilaire S, Sheppard C, Tomberlin JK, Irving S, Newton L, McGuire MA, Mosley EE, Hardy RW, Sealey W (2007). Fly Prepupae as a Feedstuff for Rainbow Trout, *Oncorhynchus mykiss*. *Jour. World Aquacult. Soc*. 38(1): 59-67.
35. Hwangbo J, Hong EC, Jang A, Kang HK, Oh JS, Kim BW, Park BS (2009). Utilization of house fly-maggots, a feed supplement in the production of broiler chickens. *Journal of Environmental Biology*. 30(4): 609-614.
36. Ogunji JO, Nimptsch J, Wiegand C, Schulz C 2007. Evaluation of the influence of housefly maggot meal (maggot meal) diets on catalase, glutathione S-transferase and

glycogen concentration in the liver of *Oreochromis niloticus* fingerling. *Comp. Biochem. Physiol.* 147: 942–947.

37. Aniebo AO, Owen OJ (2010). Effects of age and method of drying on the proximate composition of housefly larvae

(*Musca domestica* Linnaeus) meal (HFLM). *Pak. J. Nut.* 9: 485-487.



Design of a domestic irrigation system for a green roof

Bruno Azael Lazarini De La Fuente
Engineering department.
Universidad Autónoma de Querétaro.
Querétaro, México.

Emiliano Ponce López
Engineering department.
Universidad Autónoma de Querétaro.
Querétaro, México.

Juan Román Sánchez Gómez
Engineering department.
Universidad Autónoma de Querétaro.
Querétaro, México.

Dr. Omar Chávez Alegría
Engineering department.
Universidad Autónoma de Querétaro.
Querétaro, México.

Dr. José Gabriel Ríos Moreno
Engineering department.
Universidad Autónoma de Querétaro.
Querétaro, México.

Dr. Mario Trejo Perea
Engineering department.
Universidad Autónoma de Querétaro.
Querétaro, México.

ABSTRACT

Due to the need to find a solution for excessive water consumption, a way has been sought to maximize the use of this resource. That is why it was planned to design an irrigation system for a green roof located in the engineering faculty, with the aim of maintaining the vegetation by reusing the water that comes from the toilets of a building that is located uphill. By doing the research and calculations necessary, the appropriate design will be made using materials that are within the scope of the faculty budget. With an automatic irrigation system, the cost of water is reduced by 50%, energy is reduced by 13% and labor is reduced by 96%, practically nonexistent, this in the first six months.

Keywords - Irrigation system, Ecology, Adequate design, Garden, water reuse.

I. INTRODUCTION

Throughout the history of the Autonomous University of Querétaro, has always been seen to carry out the creativity of its students for the development of the same, especially for the engineering faculty, which seeks to solve the various problems that are presented over time. On this occasion it is intended to design an irrigation system suitable for a green

area corresponding to this faculty, focused on the problem of saving and reusing water.

This is possible because the water supply comes from the toilets that are located uphill from the area that is proposed to irrigate. And with the help of a filtering process, we obtain gray waters that are suitable for the development of this project. Initially there is already a tank that is responsible for storing and at the same time filtering said water. And later, there is a design that involves the use of sprinklers, pipes and pumps, which fit the budget of the university. Since the irrigation area is relatively small we can focus on a model of three main feed pipes that are distributed in the lateral and central parts of the garden. Later with previous information on the demand, evapotranspiration of the plants and the surrounding vegetation we are guided to know the time that is needed to water.

As it is known that already exist different and very varied designs of systems and also diverse techniques of irrigation. That is why you plan to get the best of each to have a better result.

The sprinklers have a range of more than 6 m, ie they throw water from 6 meters onwards, depending on whether they have more or less pressure and the type of nozzle, these sprinklers can be divided into 2 types; Emerging: They rise from the ground when irrigation is opened and when it stops, they retract, movable: They are attached to the end of

a hose and positioning from one place to another according to their need. [10].

Hydroponics is a method of growing plants in a medium that is not traditional (earth), but artificial, and which is based on applying, in rational practice, the theory that minerals are the main food of plants. These minerals are supplied through a solution of water and salts (nutrient solution).

There are three main systems for performing hydroponics; Growing in water: Plants live directly in the water, in which nutrients, which are in contact with the roots of the plant, have been dissolved. Substrate cultivation: The plants grow in a solid, inert and free of Nutrients that is the substrate, this helps to fix to the root of the plant serving as support, Aeroponic culture: In this system the roots are not in a substrate or directly on the water, the roots are suspended in a nutrient haze Where they take in the nutrients and considerably improve their oxygenation, which is a fundamental factor for the development of the plant. [1]

The innovation of this system consists precisely in that the plants are suspended inside a panel, their roots are free in the air, therefore, the oxygen supply is permanently assured. [2]

At present, the aeroponia is practiced commercially in different countries like the United States, Japan and Germany, having reached a different development according to the places. In Israel, the company Adj Ltd demonstrated in 1982 that the aeroponic system was commercially viable. But users found it relatively complex, expensive and it did not reach maturity until 2003.

In Asia research is continuing to improve the technique, so some companies have put up for sale units based on pilot models, which have an integrated environmental control system, however, these have a price that fluctuates Between \$ 1000 and \$ 1500. [3]

There are several reasons why it is thought that in future the application of this technique will be generalized. One of the reasons is the high productivity of crops compared to those obtained with traditional crops, even surpassing other hydroponic systems.

In this system the plants are developed in a closed system. Its roots are constantly sprayed with a mist or nutrient-rich micro-droplets, and can grow suspended and enclosed in a dark and wide box or container, which, as light does not pass into the interior, prevents the growth of algae .

Research on aeroponics has two aspects: Reformulation of the nutrient solution and generation of nutrient mist. [2].

Drip irrigation consists of providing the water so it is located right at the foot of each plant. Drippers or emitters are in charge of this. These can be integrated into the pipe or button, which are inserted into the pipe, these types of irrigation have the advantage of having a low water consumption. [4]. Underground irrigation is one of the most modern methods. It is even used for lawns instead of sprinklers and diffusers on small surfaces burying a network

of pipes. These are perforated pipes that are buried in the soil at a certain depth (5 and 50 cm) depending on the plant to be watered and depending on whether the soil is more sandy or clayey.

The advantages of this system, such as the reduction of losses due to exposure to air, the reduction of weeds, since the surface is kept dry, is more aesthetic, the pipes being buried last longer because they do not give the sun, and Avoid vandalism problems. It can also present drawbacks due to binding in perforations due to causes such as lime, or roots, for which herbicides are recommended. [5]. The exudation tapes are pipes of porous material that distribute the water continuously through the pores, which results in the formation of a continuous strip of moisture, which makes them very suitable for the irrigation of crops in line. They moisten a great surface and it is especially interesting in sandy soil and can be used in the irrigation of trees.

The working pressures are lower than those of the drippers. This makes it necessary to use special pressure regulators or flow microlimitators. Exudation tapes may become clogged due to algae and lime deposits (limestone). Therefore, they require maintenance treatments. [6]. Microspeakers are preferable for sandy texture, because they cover more surface than traditional drippers, for example, to irrigate fruit. This irrigation system is ideal for flower beds, roses, small areas, etc. [7]. Irrigation with a hose means having it in your hand for many hours. For the lawn it is clear that it is the worst system. In addition it does not get a good uniformity, some places they drop more water than others.

The central pivot irrigation is named after the circular movement around a central point called pivot. At present, it is one of the most efficient irrigation systems. It also has the capacity to distribute fertilizers and herbicides. The ability of a central pivot system to irrigate flat terrain like rolling terrain has given it the distinction of being the most significant instrument of change in the concept of agriculture since the invention of the tractor.

The most important characteristic of central pivot irrigation is its ability to irrigate uniformly, which is conceived with the installation of sprinklers along the main pipe, the nozzles of the sprinklers vary with respect to the distance from the central point since Greater radius, they will have to irrigate a larger area. [8].

With the realization of this research, a solution is proposed to the problematic that we face, offering options that are within reach of the students and mainly of the faculty.

On the other hand it is intended to maintain the integrity of the garden taking into account the demand requirements that the local vegetation needs, maintaining a suitable humidity index and implemented by the relatively automatic system of the system.

Subsequently the main idea is that through the documentation of the project have practical bases as theoretical in the future if you want, remodel or remaster the system, or are planned to give some maintenance.

II. THEORETICAL CONSIDERATIONS

Green Roofs have become a very important component of sustainable urban development within the last 30 years. Growing environmental awareness and the striking economical and ecological advantages are the driving forces for this great success. At present, Green Roofs, sky gardens and rooftop gardens can be found in nearly all big cities around the world, benefiting the urban environment and their inhabitants. Landscaped roofs provide many positive effects for the life expectancy and the energy balance of a building.

The word Green Roof has come to describe a roof which is green in the economic sense. In other words it is energy efficient or sustainable.

Basically, it is a living roof which is placed on a building instead of a conventional roof. There are various components that are necessary plus the main structure of the building must be tested before any attempt to put a green roof onto a large expanse of roof. There are numerous benefits surrounding green roofs including, helping to control water in areas of flash flooding as it absorbs more water slowing the release of rainwater. It can be used as a filtration method capturing the run off water and using it for other uses such as brown water (flushing toilets etc). Experiments have shown that a green roof can help both with insulation during colder months and a cooling effect during hotter times.

When the demand curve of a distribution network in an irrigation system is constant (fixed demand), the drive system only needs a careful design to optimize its operation, but does not require any regulation when working on them Conditions. On the contrary, when the demand of the network to which it feeds is variable, taking into account different operating criteria, it is essential to regulate the system, seeking in each situation the best operating conditions.

The regulation of a pumping system is normally carried out by measuring the outlet pressure (gauge control), measuring the flow (flow control) or measuring both (manoca-flow metering), choosing one or another type according to the needs, To guarantee the supply, in the necessary conditions, in all the points of the installation.

The use of groups of pumps in parallel in which some operate in nominal and others through variable speed groups, are very interesting solutions from the hydraulic point of view, with the following main advantages:

Minimum hydraulic losses when adapting the system to the demand curve of the network.

Constant maintenance of near-optimal performance, with improved efficiency in the use of electric power.

Decrease in number of pumps required.

Elimination of overpressures and depressions in starts and stops, avoiding, in most cases, other devices to control the water hammer.

As main drawback we can mention, the higher price of these facilities with automated regulation compared to conventional ones.

Finally, to indicate that any automatic control system of a process must have a series of internal alarms and controls, besides the monitoring and surveillance that can be done by the irrigator itself, to detect possible problems and stop the installation in case of detecting important anomalies, For example, pressure drops that indicate breakage, filtration problems due to lack of cleaning due to failure of some actuator, rearming of the system in the event of power outages, etc. [9]. One of the fundamental equations that we use for the realization of this project is the Darcy-Weisbach equation (1), which allows us to determine the main elements that act within an irrigation system.

$$h_f = f \cdot \frac{L}{D} \cdot \frac{V^2}{2g} \quad (1)$$

III. METHODOLOGY

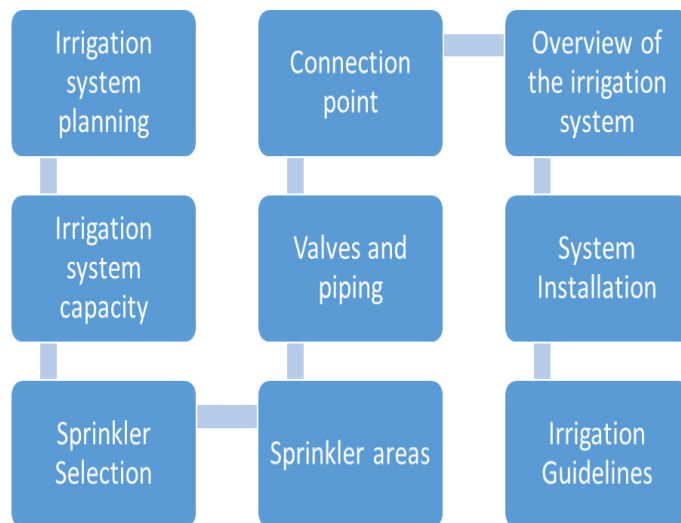


Figure 1. Block diagram of the Hunter's methodology

First we need to know the area and locate the source of water supply, which in this case is the cistern, figure 2. Very specifically we are working on the area between building I and the classrooms of architectural students. In the faculty of engineering, figure 3.



Figure 2. Cistern used for storage.



Figure 1. G building, engineering faculty.

Since the terrain on which the three important points for the flow of water (sanitary, cistern, garden) are sloping slope, we proceed to make a survey to determine the levels and thus find the heights that are going to be elementary to The selection of the pump. [11].

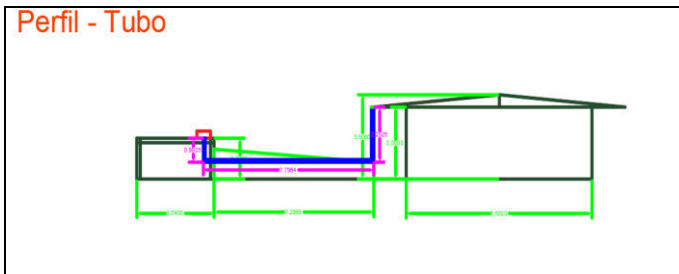


Figure 4. Profile of cisterna and the building in question

Figure 4 shows the profile of the area in which the cistern is located and then the building with the green roof that is planned to be irrigated, taking into account the dimensions of both elements (green lines).

Cistern: Length: 3.54 m, Height: 1.7m

Spacing between cistern and building: 7.29 m

As the green roof is gable there is a difference in heights, which are: Lowest point: 3m, Highest point: 3.5m, Width of building: 3.5m

The pink lines describe the path of the pipe and the depth that will reach the pichancha.

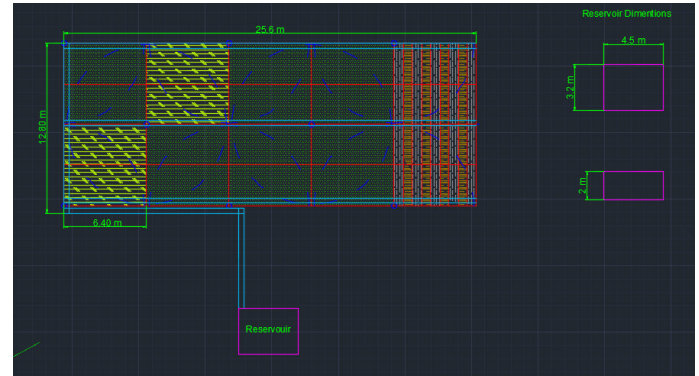


Figure 5. Profile in plan of the irrigation zone.

Figure 5 shows the irrigation zone in plan, which gives us an area of 31.5m x 11.46m. Which will help us determine which sprinklers and how many we will occupy. As well as the structuring of the pipe.

Once recognized the terrain and having the respective plans. We proceed to design the system which we are tentatively left in the following way:

A. Description And Selection Of Materials.

As the project is supported by the budget of the engineering faculty, the selection of materials had to be adapted to it, for that reason is that for the question of pump selection was determined as follows:

B. Pump

The scenario we have is: It is required to calculate the power of a pump that needs to carry the water to a height of 3.5 m (maximum height of the building) and the depth of the cistern is 1.7 m and if both are at the same level of floor and The pump is placed on the roof of the same tank, then the actual height to raise the pump is:

$H_{real} = \max.$ Of the building - height of the cistern

$$Actual H = 3.5 m - 1.7 m = 1.8 m$$

As the height is small, there are not many losses, in the pipeline and therefore the efficiency of the pump would increase. Which gives us to use a pump of 1HP and even one of 1.5HP which was previously quoted and approved.

This will work with a Evans pump of 1.5 HP.

As the pump is superficial the ideal will be to place it in the ceiling of the cistern making a small incision that enters

the chamber of the filtered water. The specifications of the pump are shown in figure 6.

Motor	
Tipo de Motor	Eléctrico
Marca del motor	Simens/Weg
Potencia del motor	1.50 hp
RPM del motor	3450 RPM
Voltaje	127/220 V
Fases del motor	Monofásico
Protección térmica	Si

Bomba	
Tipo de bomba	Superficie
Flujo óptimo	127.00 LPM
Altura óptima	31.00 m
Número de etapas	1 etapa
Diámetro de succión	1.50 pulgadas
Diámetro de descarga	1.25 pulgadas
Tipo de impulsor	Cerrado
Material de cuerpo	Hierro fundido

Figure 6. Pump specifications

C. Pipe And Unions

Another part that we need to cover is the part of pipes, and due to its properties and its low cost it has been decided to work with PVC pipeline 40. Obviously respecting the diameter measures at the entrance and exit of the pump, which are 1.5, and 1.25 inches, respectively, as well as elbows and plugs for pipe path changes and flow interruption for the pipes feeding the sprinklers. [11]

D. Installation

First we need to place the pump right next to the chamber of the filtered water in the top of the tank, proceed to make a small incision that fits the suction pipe to be connected to the pump., We will try to use galvanized pipe in that Part of the connection to prevent ruptures by movement. Later we will describe the trajectory of the outlet pipe by the top of the cistern and with the help of the elbows or connections we will give changes of direction to it, the point is to make a kind of bridge from above that reaches one of the sides Of the garden so that afterwards the sprinkler feeder pipes can flow out.

The point of passing the pipe from the top is to save material and avoid accidents by overlapping the pipe down the hallway of the building.

Once the side pipe is installed, we will take another three along the garden so that there are two sides and a central one, through which the series of sprinklers will pass.

Before we know that the sprinklers have a radius of coverage, that is why we will place these, at the appropriate distance according to the specifications of the manufacturer and as we already have the configuration of placement of the plane previously shown. Just rest the rest of the sprinklers.

Once placed, we will put the plugs at the end ends of each feeder tube of the sprinklers, obviously so that the circuit is closed and water can flow through them.

It should be noted that all this has to be done, making the necessary excavations inside the garden and later, to replace the grass on the excavation previously made. [11]

IV. RESULTS

In Fig. 7 we can see the distribution of the pressures of each of the sprinklers represented by each node within the system. Using the Epanet program for pipe simulation.

On the other hand, in the figure 8 and 9 the report is found by means of tables of the specifications of the system as are the elevation with respect to the topographic survey, the water demand in each one of the sprinklers, as well as the roughness, length , Diameter and flow of the pipes.

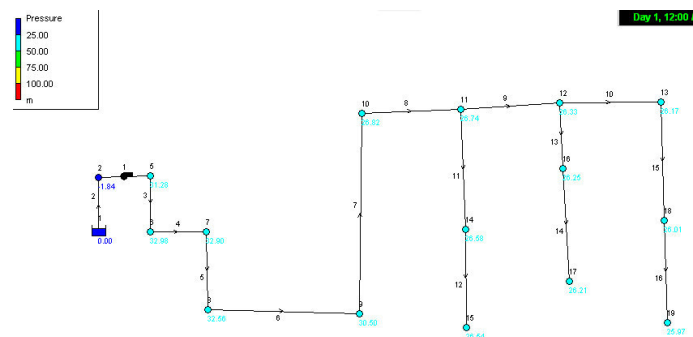


Figure 7. Distribution of pressures

Node ID	Elevation m	Base Demand LPS	Demand LPS	Head m	Pressure m
Junc 2	3	0	0.00	-0.01	-3.01
Junc 3	3	0	0.00	18.37	15.37
Junc 4	1.2	0	0.00	18.36	17.16
Junc 5	1.2	0	0.00	18.35	17.15
Junc 6	.2	0	0.00	18.24	18.04
Junc 7	.2	0	0.00	18.04	17.84
Junc 8	3.4	0	0.00	17.99	14.59
Junc 9	3.4	0.075	0.08	17.90	14.50
Junc 10	3.4	0.075	0.08	17.83	14.43
Junc 11	3.4	0	0.00	17.79	14.39
Junc 12	3.2	0.075	0.08	17.78	14.58
Junc 13	3.2	0.075	0.08	17.78	14.58
Junc 14	3.4	0.075	0.08	17.77	14.37
Junc 15	3.4	0.075	0.08	17.77	14.37
Resvr 1	0	#N/A	-0.45	0.00	0.00

Figure 8. Report nodes

Link ID	Length m	Diameter mm	Roughness mm	Flow LPS	Velocity m/s	Unit Headloss m/km	Friction Factor
Pipe 1		38.1	.03	0.45	0.39	6.15	0.030
Pipe 3	1	31.75	.03	0.45	0.57	14.88	0.029
Pipe 4	.5	31.75	.03	0.45	0.57	14.88	0.029
Pipe 5	7.5	31.75	.03	0.45	0.57	14.88	0.029
Pipe 6	13.5	31.75	.03	0.45	0.57	14.88	0.029
Pipe 7	3.2	31.75	.03	0.45	0.57	14.88	0.029
Pipe 8	6.2	31.75	.03	0.45	0.57	14.88	0.029
Pipe 9	6.2	31.75	.03	0.38	0.47	10.74	0.030
Pipe 10	6.2	31.75	.03	0.30	0.38	7.22	0.031
Pipe 11	6.2	31.75	.03	0.15	0.19	2.15	0.037
Pipe 12	6.2	31.75	.03	0.08	0.09	0.47	0.033
Pipe 13	6.2	31.75	.03	0.08	0.09	0.47	0.033
Pipe 14	6.2	31.75	.03	0.08	0.09	0.47	0.033
Pump 2	#N/A	#N/A	#N/A	0.45	0.00	-18.38	0.000

Figure 9. Pipe reporting

Evaluations of Uniformity of Distribution, Coefficient of Uniformity and discharge Efficiency are performed for different sprinkler height and wind speed conditions, table 1.

Table 1. Irrigation quality parameters according to wind speed. Wind <1.0 m / s Wind> 3,60m / 2

Alt. Emisor (m)	UD(%)	CU(%)	Ed(%)	UD(%)	CU(%)	Ed(%)
0,70	78,15	84,42	60,71	45,83	56,39	51,87
0,40	80,30	86,18	70,42	51,90	58,84	58,09
0,00	66,30	58,80	52,35	39,48	38,72	42,09

During irrigation with low wind speed the UD achieves acceptable results with the emitter located at 1.00 m in height and satisfactory with the emitter located at 0.40 m, while without height it is unacceptable according to Merriam and Keller (1978). UCs are satisfactory when sprinkler heights are used and bad when they are not used (Christiansen, 1942; Keller and Bliesner, 1990), while Ed only reaches acceptable values with a height of 0.40 m (Merriam and Keller 1978).

The increase in wind velocity brings with it a reduction of all the parameters of irrigation quality, obtaining in all

cases the category of unacceptable ones, being worse still the results when the height is eliminated.

The results indicate that this system of irrigation is very susceptible to the effect of the wind, obtaining a quality of the bad irrigation and producing considerable losses of water when the speed of the wind increases.

Table 2. Effect of pressure on irrigation quality.

Presión (kPa)	CU(%)	Ed(%)
25	84,42	60,71
20	78,17	61,80
30	81,88	53,42

The results, table 2, indicate a reduction of the Ed by increasing the working pressure, which is attributable to a greater effect of the wind on the smaller drops, the variation of the pressure has a negative effect on the uniformity by a change in the Model of water distribution.

Low values of the CU indicate an incorrect combination of the aspersion with the nozzle diameter, working pressure and watering frame.

The cost of an irrigation system varies for many reasons because no system is the same as another, but the average price in the region per 100 m² is approximately \$ 4,000, decreasing somewhat in relation to larger areas.

On the other hand, for the same area, the cost of irrigating it through a traditional irrigation system monthly is approximately \$ 340, but with a sprinkler irrigation system the cost is approximately \$ 170. If to this difference we add the saving in labor, it is evident the advantage in the economic field that has a sprinkler irrigation system over a traditional one.

V. CONCLUSIONS

With an automatic irrigation system, the cost of water is reduced by 50%, energy is reduced by 13% and labor is reduced by 96%, practically nonexistent, this in the first six months.

On the other hand, the economical percentage that increases when implementing this procedure, in relation to the traditional irrigation, is of 16.22%, proportion recovered in only the first year with the decrease in labor.

Finally we must not forget that it is a partially ecological irrigation system due to the reuse of water, ie the percentage of water consumption decreases even more, and although the area is very small and demand too, this serves as To a scale model for future approaches at larger scales. Which gives rise to systems of greater magnitude and that in the future may be used in more places of the faculty and why not, the entire university.

REFERENCES

- [1] Samperio Ruiz, G. (2007). Hidroponía Básica. 10 ed. Editorial: Diana.
- [2] José Álvaro Vázquez Rivera, (2012). Diseño De Un Sistema De Riego Aeropónico Automatizado. Programa De Maestría Y Doctorado En Ingeniería. Universidad Nacional Autónoma De México.
- [3] Junlong Fang, Fulu Wang (2011). Design of greenhouse remote monitoring system based on Labview.
- [4] hogarutil.com. 2011. hogarutil.com. [En línea] 2011. [Citado el: 24 de Octubre de 2016.] <http://www.hogarutil.com/jardineria/mantenimiento/herramientas-accesorios/201106/sistema-riego-goteo-9066.html>.
- [5] Infojardin. 2009. Infojardin. [En línea] 2009. [Citado el: 24 de Octubre de 2016.] <http://articulos.infojardin.com/articulos/sistemas-riego-jardin.htm>.
- [6] Penuela, Viveros la. 2009. Viveros la penuela. [En línea] 2009. [Citado el: 24 de Octubre de 2016.] http://www.viveroslapenuela.com/sistemas_riego_goteo_exudacion.asp.
- [7] Inta. 2002. Inta. [En línea] 2002. [Citado el: 24 de Octubre de 2016.] http://www.inta.gov.ar/region/ mesa/galeria/riego_03.htm.
- [8] Traxco. Traxco. [En línea] [Citado el: 24 de Octubre de 2016.] <http://www.traxco.es/pages/posts/informacion-general-del-pivot-central177.php>.
- [9] Ortega Álvarez J.F., Carrión Pérez P., Montero Martínez J., Tarjuelo Martín-Benito J.M.. (Enero 2001). Las nuevas tecnologías aplicadas al control automático del riego. *Mecanización*, 24, 6.
- [10] Tarjuelo J.M. 1999. El riego por aspersión y su tecnología (2º Edición). Mundi-Prensa S.A. Madrid, España.
- [11] Hunter Industries Incorporated. (2013). Una Introducción Paso a Paso al Diseño e Instalación. Manual de Diseño de un Sistema de Riego Residencial, 9, 20.





Biological System Modelling

Breast Cancer Marker Electrics Properties

Silvana Valencia Rodríguez.

División de Investigación y Posgrado.

Facultad de Ingeniería Campus Centro Universitario.

Santiago de Querétaro, México.

svalencial1@alumnos.uaq.mx

José Jesús Bernal Alvarado.

Departamento de Ingeniería Física

División de Ciencias e Ingeniería Campus León.

León, México.

bernal@fisica.ugto.mx

José Francisco Gómez Aguilar.

CONACyT-Centro Nacional de Investigación y
Desarrollo Tecnológico.

Tecnológico Nacional de México.

Cuernavaca, México.

jfranciscogoma@hotmail.com

Abstract—Around the world, the breast cancer is the first cause of death in women. There are many biomedical lab tests that they allow to sort out in stages. Nevertheless, that lab tests are late to confirm the level. Biological systems can be characterized by the parameters of an equivalent electric circuit when subjected to alternating current stimulation, particularly protein suspensions in saline solutions. The following paper shows an analysis electrical properties of breast cancer marker proliferating cell nuclear antigen (PCNA) of three steps with Electrical Impedance (Z) that it permits to make an experimental characterization and an original theoretical methodology.

Keywords—Breast cancer; Electrical Impedance; Proliferating cell nuclear antigen; Fractional calculation Ohm law; Cole-Cole model.

I. INTRODUCTION.

During the last years, breast cancer has been placed as one of the first causes of death around the Mexico. There exist different criteria to make a detection method efficient, among these characteristics said method must be comfortable for the patient, it must be precise, sensitive, specific, achievable, low cost and quick in its sampling.

There are two categories detection methods the tumour structure: non-invasive and invasive methods. Microwaves and Infrared Thermography are noninvasive methods. These methods are advances in detecting breast cancer. They are good but do not sort out the disease.

Electrical impedance spectroscopy (EIS) has shown to give characteristic patterns in tissue from invasive carcinomas of the cervix in comparison to the patterns from healthy cervical tissue. Therefore, this technique could be applied for early cancer diagnosis, due to its high sensibility and quick response when subjected to physical and mathematical analysis.

Nowadays, there is little research that applies this technique for the diagnosis of different diseases and clinical pictures related to breast cancer; neither has there been a trend or correlation of proliferating cell nuclear antigen (PCNA) along the 4 stages of the disease. Studies have only been performed around the cell cycle of these tumor cells. Given the scenario described, and as one of the objectives, this paper aims to validate the functionality of EIS for the study of breast cancer through the spectroscopic study of PCNA protein.

Fractional calculus (FC) provides more accurate models of the physical systems than ordinary calculus does. Fractional derivatives provide an excellent instrument for the description of memory and hereditary properties of various materials and processes.

The main objective of this research is to study the electrical properties of the PCNA protein using electrical impedance spectroscopy, the test is based on five typical samples of the studied protein, under the Cole-Cole model and the fractional

Ohm law model. With this, it is expected to contribute to a more accurate knowledge of this cancer marker.

II.METHODOLOGY.

Before studying the structure and mechanism of action of a protein, it is essential to purify it. It is not possible to use a single method for the extraction of all the different proteins, due to its different sizes, charges and levels of water solubility. A total of 30 samples of breast tissue with ductal and lobular carcinoma were counted, this samples corresponded to women between 29 and 70 years old. Once the five protein samples (PCNA) were selected, capillary tubes, of 75mm long, were used as containers. A pair of platinum electrodes were connected at the ends of each tube.

In order to establish the electrical properties of the proliferating cell nuclear antigen (PCNA) as a marker of breast cancer, the electrical impedance spectroscopy technique was applied, said technique consists on applying an alternating voltage on the electrodes. This way, a low power alternating current passes through a sample, taking this input as a reference to compare it with the current and voltage measurements taken at the output. By using a representation in the complex plane of the Ohm Law, the value for the electrical impedance, in amplitude and phase, can be obtained. Lastly, a frequency sweep results in the characteristic spectrum of the sample.

Commonly, the impedance spectrums are analyzed by electrical circuits, whose components are resistances (R), capacitances (C), inductances (L), etc., the combination of these components allows to reproduce the measured impedance spectrums, generating equivalent electrical circuits. The equipment used was an impedance spectrometer by Solartron, model 1260, and the software used for the analysis of the spectrum was the Zview® software. The frequency range in which the samples were analyzed goes from 1 to 32 Hz, applying a regulated voltage lower than 20mV. One of the simplest and most used circuits on the test of biological tissues, is a parallel resistance – capacitor circuit (RC). It also has a series resistance, R_s , which reflects the electrical resistance of the sample-electrode interface. This research uses an algebraic representation of the RC circuit in the adjustment to the impedance spectrums with the modification for the Cole-Cole model and its total impedance is expressed as:

$$Z=R_s + R/(1+RC(j\omega)^P], \quad (1)$$

where $j=\sqrt{-1}$ represents the imaginary unit and ω is the angular frequency of the alternating current used as excitation, P represents the average value of the different electrical paths of the electrodes, obtained using the relaxations times statistical distribution.

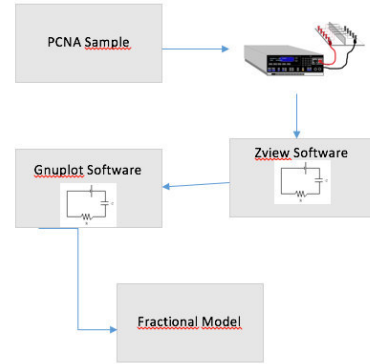


Fig. 1. Representation of the methodology for the experiment.

Figure 1 show a diagram to follow for the experiment. First step is introducing the sample into the Capillary tube, at the ends it is connected with the Solartron®. Next steps is analyzed by the different software.

III.RESULTS.

Figures shown the comparison between the different adjustments obtain using the Zview® and Gnuplot software. These Figures describes the behavior of the electrical elements present on the PCNA protein samples.

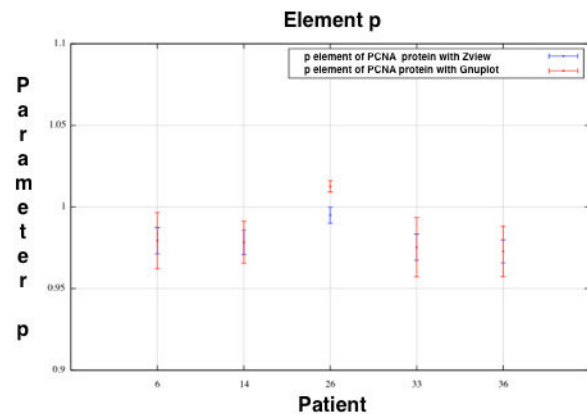


Fig. 2. Representation of the adjustment of the Cole – Cole model. The data in blue represents the values of adjustment obtain from Zview®, the values on red were obtained using Gnuplot.

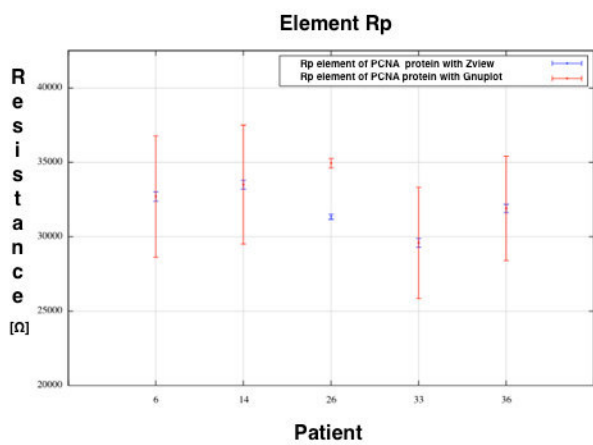


Fig. 3. Representation of the Rp element from the Cole – Cole model. Values in blue were obtain using Zview®, values on red were obtained using Gnuplot.

Number patient	6	14	26	33	36
Element circuit electric.					
$C_p(\Omega F^p)$	3.64E-12	3.64E-12	2.93E-12	3.64E-12	3.8E-12
$\Delta C_p(\Omega F^p)$	4E-13	4E-13	2E-13	4E-13	5E-13
$\% \Delta C_p(\Omega F^p)$	12.2	11.2	7.3	12.6	10.6
P	0.97937	0.97843	0.99499	0.97536	0.97278
ΔP	0.008841	0.0074869	0.004945	0.008873	0.00769
$\% \Delta P$	0.82544	0.7652	0.49292	0.82916	0.72585
$R_p(\Omega)$	32696	33496	31335	29583	3191
$\Delta R_p(\Omega)$	321.443	292.76	180.78	305.56	275.42
$\% \Delta R_p(\Omega)$	0.9838	0.8741	0.57693	1.329	0.86336

Table 1. Characteristic value of each of the electrical parameters measured with the adjustment of the Cole – Cole model, using Zview®.

Number patient	6	14	26	33	36
Element circuit electric.					
$C_p(\Omega F^p)$	3.74E-12	2.2E-12	2.14E-12	3.91E-12	3.91E-12
$\Delta C_p(\Omega F^p)$	1E-12	1E-13	1E-13	1E-12	1E-12
$\% \Delta C_p(\Omega F^p)$	35.5	6.2	5.4	36.5	31.3
P	0.97943	0.97843	1.01267	0.97536	0.97278
ΔP	0.01726	0.01286	0.003562	0.0182	0.01547
$\% \Delta P$	1.764	1.314	0.3517	1.866	1.59
$R_p(\Omega)$	32696	33496	34945.6	29583	3191
$\Delta R_p(\Omega)$	4080	4002	3133	3739	3500
$\% \Delta R_p(\Omega)$	12.46	11.95	0.8965	12.64	10.97

Table 2. Values of the elements for the samples which patient's keys are shown on row 1 (Gnuplot Cole-Cole).

Table 1 shows the characteristic values of the Cole – Cole model working with Zview® software. The results obtain using Gnuplot software of the adjustments to the cole – cole model are shown on Table 2.

There exists a constant phase element in the Cole-Cole (1) model, which does not have the units of a capacitor. Fractional calculus has become a powerfully used tool to improve modeling and the process of control in many areas of science and engineering. This kind of calculus is a natural generalization of traditional calculus, and involves integrals of a non-integer order. The equation for the Cole – Cole model, maintaining the consistency of the units involved on the parameters is given by

$$Z = R_s + R_p / [1 + (R_p C_p / \sigma^{1-\gamma})(j\omega)^\gamma], \quad (2)$$

where the Eq. (2) is the result of applying the fractional temporary operator to the equivalent equation of the RC circuit, this generic formula includes an arbitrary constant σ and, as a particular case, when $\sigma = R_p C_p$ the Cole model is reduced. In this particular case, C_p has now the units of a capacitor. On the other hand, when $\gamma = 1$, the RC circuit becomes the ideal one.

When said equation is modeled using the Gnuplot, the software provides the units corrections. Table 3 presents those results.

Number patient / Element circuit electric.	6	14	33	36
$C_r(F)$	2.64E-12	2.69E-12	2.46E-12	2.51E-12
$\Delta C_r(F)$	2E-13	3E-13	2E-13	2E-13
$\% \Delta C_r(F)$	9.287	9.5210	8.665	7.885
P	0.97937	0.9287	0.97536	0.97278
ΔP	0.01655	0.01262	0.01789	0.01519
$\% \Delta P$	1.69	1.29	1.834	1.561
$R_r(\Omega)$	32696	33496	29583	3191
$\Delta R_r(\Omega)$	4120	4223	3875	3616
$\% \Delta R_r(\Omega)$	12.6	12.31	13.1	11.34

Table 3. Results of Gnuplot modeling of equation (2).

IV. DISCUSSIONS.

The samples belong to different stages of cancer. In the three tables shown it can be seen that there is a significant difference between the samples. This could help to have different parameters for different stages of cancer.

Zview® software gives the instantaneous adjustments by default, not allowing to make changes. However, Gnuplot software allows to make the necessary changes on each model. These results can be in figures (1) and (2), where both fits have the same value for the parameters.

Zview® does not meet the correction of capacitor units, however it is accepted by the program to have those units. By changing from a commercial to a free software, aside from comparing the compatibility between them, is possible to model the fractional Ohm Law and make adjustments to the capacitor units on the Cole – Cole model.

V. FINAL THOUGHTS

Electrical impedance is a technique that has been applied to biological components, considering that, this research works with the electrical characteristics of the PCNA protein. On an experimental montage of capillary tubes and considering the electrical characteristics of the PCNA, certain electrical parameters of the cancer marker were found. Said parameters

include resistance, capacitance and distributive electrical elements.

Numerical analysis was presented statistically, in order to cover the biological variability of individuals whose samples were taken. The group of individuals analyzed was made up of female adults over 29 years old.

The bioelectric parameters were reported on tables. This tables include different data, such as the uncertainty of the resistance and capacitance, and elements of the constant phase. In addition, the least square analysis was performed using two independent programs: the commercial software Zview® and the free software Gnuplot, this last one whit the capability to handle complex variables.

A comparative analysis between the two algorithms of least square adjustments, allowed to validate the free software, with the objective of applying generic model through it and apply it to the same kind of samples.

The theoretical generalization that was used was based on Ohm's fractional law applied to an RC circuit. This analysis led to two important contributions to this work, the first is to establish a physical interpretation to the fractional order derivative that is related in Ohm's law, and the second is to establish a mathematical model consisting of units that are applicable to tests of electrical impedance. This corrects fundamental flaws in the methodologies based on the Cole-Cole model.

This research allowed us to characterize the traditional analysis of biological samples using the electrical impedance technique and to establish a modern and correct methodology applicable to bioelectric techniques in general.

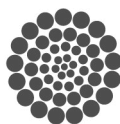
ACKNOWLEDGMENT

Special thanks to Dr. Francisco Gómez Aguilar for his support and for providing the necessary tool to conclude this research and my friend Daniela Hernández for her help, without her I could not be able to finish on time.

REFERENCES

- [1] G. Olarte, W. Aristizabal, G. Osorio. et al. Espectroscopia de impedancia eléctrica en cáncer invasivo del cuello uterino en mujeres de caldas (colombia), 2008-2009. Colombia. Vol. 61. N° 1, 2010.
- [2] F. Hernández, C. Guerrero, J. Bernal. Determinación de las propiedades eléctricas en tejido sanguíneo. México. Octubre-Diciembre 2005.
- [3] H. Lodish, A. Berk, P. Matsudaira. et al. Estructura y función de las proteínas. Biología Celular y Molecular. 5 edición. Editorial: Médica Panamericana. Buenos Aires, México: 2005, reimpresión 2006-2009. p. 59-99.
- [4] J. Mendoza, R. Durán, J. Genescá. Espectroscopia de impedancia electroquímica en corrosión. Instituto del Petróleo. Facultad de Química, UNAM.
- [5] J. Barreda. Tejido sanguíneo de donadores sanos y pacientes diabéticos mediante espectroscopia de impedancia eléctrica y la sedimentación de

- eritrocitos. Nuevo León. 2007. 175p. Presentada en Universidad Autónoma de Nuevo León para obtención del grado de Licenciatura.
- [6] INEGI Secretaría de Salud.DGIS, 2008. Elaborado a partir de base de datos de defunciones 2008 y CONAPO, 2006. Proyecciones de Población de México 2005-2050. Consultado: <http://sinais.salud.gob.mx/mortalidad/>
- [7] M. Otero Identificación y cuantificación de la proteína PCNA en muestras de carcinoma mamario y su correlación con espectroscopia RAMAN. Silao de la Victoria, Guanajuato, México. 2012. 71 p. Presentada en la Unidad Profesional Interdisciplinaria de Ingeniería Campus Guanajuato del Instituto Politécnico Nacional, para obtención del grado de Ingeniero Farmacéutico.
- [8] OMS Nota descriptiva N° 334 Noviembre 2009 [en línea] Consultado: <http://www.who.int/mediacentre/factsheets/fs334/es/index.html>
- [9] Espinosa, R. O. Inmunología (de memoria) (3ra Ed.). Médica Panamericana. España. Capítulo 16. 2001.
- [10] Lodish, Berk, Matsudaira. et al. Biología Celular y Molecular. Panamericana. 5 Edición.
- [11] L. M. Vinagre Martínez. Guía clínica de cirugía de la mama. Capitulo 1: Anatomía quirúrgica de la mama.
- [12] Institutos Nacionales de Salud de EE. UU. Cáncer de seno(mama): Tratamiento. 5 de septiembre de 2013. <http://www.cancer.gov/espanol/pdq/tratamiento/seno/Patient/page5/AllPages/Print>.
- [13] El Mundo. Cáncer de mama. Disponible en: <http://www.dmedicina.com/enfermedades/cancer/cancer-mama>.
- [14] C. Sánchez, E. Sánchez y R. Gerson Tratado de las enfermedades de la glándula mamaria. Ed. El Manual Moderno. México, D. F. 2003.
- [15] MedLinePlus.Cáncer de mama. Información de salud (versión impresa). Disponible en: <http://www.nlm.nih.gov/medlineplus/spanish/ency/article/000913.htm>
- [16] Zenon, Rayter. Janine Mansi. History of breast cancer. Medical therapy of breast cancer. October 2008. p. 1-10.
- [17] Claudia Arce, Enrique Bargalló, et al. Onco Guía. Instituto nacional de cancerología. <http://www.cancer.gov/espanol/cancer/que-es>
- [18] J.Oscar Casas Piedrafitá. Contribución a la obtención de imágenes paramétricas en tomografía de impedancia eléctrica para la caracterización de tejidos biológicos. Barcelona. Septiembre de 1998.
- [19] J. Ross Macdonald. Impedance Spectroscopy. Annals of Biomedical Engineering, Vol. 20, pp. 289-305. 1992. Department of Physics and Astronomy. University of North Carolina.
- [20] E. Sallent. Alessandro Volta: Sobre la electricidad excitada por el simple contacto de sustancias conductoras de distintas especies. Barcelona. Octubre de 2000.
- [21] Daria Vladikova. "a,b,c" Impedance. IEES-BAS. Centre of Excellence.
- [22] Carlos A. Herrera Cuadros. Aplicación de la técnica de espectroscopia de impedancia en el estudio del comportamiento electroquímico del sistema acero-concreto bajo inmersión parcial aireada. Bucaramanga. 2004
- [24] F. Hernández, C. Guerrero, J. Bernal. Determinación de las propiedades eléctricas en tejido sanguíneo. México. Octubre-Diciembre 2005.
- [25] R. Valenzuela. Caracterización de materiales por espectroscopia de impedancia. Cuba. Vol. 19, N° 2, 2002.
- [26] F. Gómez, J. Bernal, J. Rosales. et al. Caracterización eléctrica de tejido sanguíneo mediante función de transferencia. México. Vol. 20, N° 3, Diciembre 2010.
- [27] A. Alzate, P. Noreña, B. Segura. et al. Estudio de la manzana mediante la técnica de espectroscopia de impedancia eléctrica. Colombia. Vol. 41, N° 1, Enero 2009.
- [28] A. Peláiz, E. Barranco, O. García. et al. Utilidad de la espectroscopia de impedancias para la determinación de la composición corporal en humanos. Cuba. Vol. 23, N° 1, 2006.
- [29] G. Olarte, W. Aristizábal, G. Osorio. et al. Detección precoz de lesiones intraepiteliales del cuello uterino en mujeres de caldas -Colombia- mediante la técnica de espectroscopia de impedancia eléctrica. Colombia. Vol. 58, N° 1, 2007.
- [30] I. Stoimenov, T. Helleday. PCNA on the crossroad of cancer. Inglaterra. Biochemical Society Annual Symposium N. 76. 2009.
- [31] C. Sittel, S. Ruiz, P. Volling, H.M. Kvasnicka, M. JungehuE Ising, H.E. Eckel. Prognostic significance of Ki-67 (MIB1), PCNA and p53 in cancer of the oropharynx and oral cavity. Germany. Oral Oncology 1999.
- [32] H. Lodish, A. Berk, P. Matsudaira. et al. Estructura y función de las proteínas. Biología Celular y Molecular. 5° edición. Editorial: Médica Panamericana. Buenos Aires, México: 2005, reimpresión 2006-2009. p. 59-99.
- [33] E. Fernández, A. Galván. Métodos para la cuantificación de proteínas. Departamento de Bioquímica y Biología Molecular, Campus Universitario de Rabanales, Córdoba, España.
- [34] L. Baquero, J. Castro, C. Narváez Catalasa, peroxidasa y polifenoloxidasa en pitaya amarilla. Acta Biológica Colombiana. Vol. 10. N° 2. 2005.
- [35] M. Arrechea, F. Vicente et al Subtipos moleculares del cáncer de mama: implicaciones pronósticas y características clínicas e inmunohistoquímicas. Chile. An. Sist. Sanit. Navar. 2011, Vol. 34, N. 2, Mayo-Agosto.
- [36] A. Rosciani, W. Merlo, et al Determinación del antígeno de proliferación celular (PCNA) y de apoptosis en neoplasias malignas de la glándula mamaria canina. Argentina. Facultad de Ciencias Veterinarias(UNNE). 2008.
- [37] S. Martínez, A. Raventós, et al Expresión de antígenos HMB-45 y antígenos nuclear de proliferación celular (PCNA) como posibles factores pronóstico en los nevus displásicos. Estudio inmunohistoquímico en dos hermanas gemelas. España. Universidad Autónoma de Barcelona. 1996.
- [38] F. Gómen, J. Bernal, J. Rosales y T. Córdova. Modeling and simulation of equivalent circuits in description of biological systems a fractional calculus approach. Journal of electrical bioimpedance. Vol. 3. July 2012. pp 2-11.
- [39] I. Podlubny Fractional differential equations . Academic Press, New York, 1999.



CONACYT

Consejo Nacional de Ciencia y Tecnología



CONCYTEQ

Optimization of scheduling problems by coloring

Planning Time Slots for Courses offered by the School of Engineering: A case study

Montuffar Otero Hansel A.

School of Informatics
Autonomous University of Queretaro
Queretaro, Mexico
hans_mntfr@hotmail.com

Gonzalez-Gutierrez Arturo, Gonzalez-Gutierrez
Fidel, Sosa-Garza Carmen

School of Engineering
Autonomous University of Queretaro
Queretaro, Mexico
{aglez, fglez, carsg}@uaq.mx

Abstract— The chromatic polynomial is studied in algebraic graph theory as a branch of mathematics. It counts the number of graph colorings as a function of the number of colors. The minimum number of colors required to color a graph is called chromatic number. This problem is referred as the Coloring Graph Problem. In this paper, we present a study case to schedule the courses offered by the School of Engineering as an interesting application of the Coloring Graph Problem. We show that the graph model corresponding to the twelve undergraduate programs for the case when the students follow appropriately their study plan, the greedy algorithm produces the result in no more than one second, and the resulting chromatic number is 15. In other words, it is needed no more than 15 time-slots to offer all the courses, such that there does not exist intersection among courses taken by any typical student. The greedy algorithm was proven to be efficient in determining the chromatic number of the graph that models the set of courses offered by the School of Engineering.

Keywords— coloring graphs; scheduling problem; chromatic number; planning; optimization.

I. INTRODUCTION

A graph $G = (V(G), E(G))$ is an ordered pair where $V(G)$ is a finite, not empty set of elements which are called vertices, and $E(G)$ is a set of subsets of cardinality of 2 from $V(G)$, which are called edges [1]. A Graph Coloring is an assignment of labels, called colors, to the vertices of a graph such that no two adjacent vertices share the same color [2]. The optimal coloring of graph G is a coloring of the vertices of G using the fewest possible number of colors. The chromatic polynomial counts the number of ways a graph can be colored using no more than a given number of colors [3]. The chromatic polynomial is a polynomial studied in algebraic graph theory, a branch of mathematics, and was defined in 1912 by George David Birkhoff for planar graphs, in an attempt to prove the four-color theorem. If $P(G, k)$ denotes the number of proper colorings of G with k colors, then one could establish the four-color theorem by showing $P(G, 4) > 0$ for all planar graphs G .

In this way, Birkhoff applied the powerful tools of analysis and algebra for studying the roots of polynomials to the combinatorial coloring problem. Hassler Whitney generalized the polynomial of Birkhoff from the planar case to general graphs in 1932. In 1968 Read came up with the question about the existence of more than one chromatic polynomial for a given graph, a question that remains open, and introduced the concept of chromatically equivalent graphs [4]. The coloring graph problem has several uses and applications such as creating schedules taking two or more events that happen at the same time as vertices related by edges [5]. There exist different algorithms to solve the chromatic polynomial. We use in this paper a greedy approach to determine the minimal number of colors that a graph needs to color it properly. This algorithm is efficient but in general there is no way to determine if the result it provides corresponds to the optimal solution. The greedy algorithm is as follows:

Given the set of vertices $V(G)$:

- Assign the first color(c_1) to the first vertex(v_1)
- **while** there are none colored vertices in G **do**
 - if**
Next vertex (v_i) is not adjacent to previous vertex(v_k), v_i is colored with color(c_i)
 - else**
 v_i is assigned another color(c_k)

This algorithm differs from the traditional manner because it only checks if the vertex currently being evaluated has neighbors that have been previously evaluated while the traditional method checks if the vertex relates to all the vertices previously evaluated [3]

II. METHODOLOGY

This work is divided in three phases



Fig. 1. First semester of automatization viewed as a graph

1. Recovering of information regarding to the courses assigned with the twelve undergraduate programs which are offered by the school of engineering
2. Modeling the requirements of the courses on a graph
3. Implementation of the greedy algorithm

It should be noted that we keep the name of the courses in Spanish in order to be precise in our communication with the administrative personnel of the School of Engineering.

III. MODELING WITH A GRAPH

The autonomous university of Queretaro (UAQ) currently has 14 faculties with diverse programs and each program offers different areas of focus and also offers different areas that the students can specialize in, however the case of study only considers the engineering faculty which by February 2017 offers 12 different careers (agroindustrial engineering, architecture, automatization engineering, biomedical engineering, civil engineering, industrial design, industrial and manufacture engineering, electromechanical engineering, physics engineering, applied mathematics, mechanical and automotive engineering and nanotechnology engineering) however architecture is divided in 3 areas so in total 14 different academical programs were considered, each program is divided by semester and each semester generally holds anywhere from 5 to 8 subjects specially in the first semesters where each career is required to offer courses that the whole university shares, for example here is a list of the subjects that all the different careers take in the first semester

1. Licenciatura en Matemáticas Aplicadas
Cálculo 1, Álgebra Superior 1, Geometría Analítica 1, Lengua Adicional 1, Cultura Física 1, Universidad y Sociedad, Programación
2. Ingeniería en Automatización
Álgebra lineal, Cálculo Diferencial, Química, Lengua Adicional 1, Cultura Física 1, Universidad y Sociedad, Probabilidad Y Estadística, Diseño Asistido por Computadora

3. Ingeniería Agroindustrial
Álgebra lineal, Cálculo Diferencial, Química Inorgánica, Lengua Adicional 1, Cultura Física 1, Biología, Introducción a la Ingeniería Agroindustrial, Diseño Asistido por Computadora

4. Arquitectura
Diseño Arquitectónico, Dibujo Técnico, Modelos y Maquetas, Lengua Adicional 1, Conceptos Básicos de Arquitectura, Universidad y Sociedad, Estática, Deportes 1

5. Ingeniería Biomédica
Álgebra lineal, Cálculo Diferencial, Probabilidad Y Estadística, Química Inorgánica, Universidad y Sociedad, Biología, Deportes 1, Ingles 1

6. Ingeniería Civil
Álgebra lineal, Cálculo Diferencial, Química, Probabilidad Y Estadística, Diseño Asistido por Computadora, Lengua Adicional 1, Cultura Física 1, Universidad y Sociedad

7. Ingeniería en Diseño Industrial
Fundamentos del Diseño 1, Modelos 1, Geometría, Dibujo 1, Dibujo Técnico, Lengua Adicional 1, Cultura Física 1, Universidad y Sociedad, Creatividad

8. Ingeniería Industrial y Manufactura
Diseño Asistido por Computadora, Álgebra lineal, Cálculo Diferencial, Química, Probabilidad Y Estadística, Lengua Adicional 1, Cultura Física 1, Universidad y Sociedad

9. Ingeniería Electromecánica
Diseño Asistido por Computadora, Álgebra lineal, Cálculo Diferencial, Química, Probabilidad Y Estadística, Lengua Adicional 1, Cultura Física 1, Universidad y Sociedad, Taller de Electromecánica

10. Ingeniería Física
Álgebra lineal, Cálculo Diferencial, Química, Cultura Física 1, Universidad y Sociedad, Física 1, Laboratorio de Química, Ingles 1, Taller Optativa

11. Ingeniería en Mecánica Automotriz
Álgebra lineal, Cálculo Diferencial, Química, Universidad y Sociedad, Cultura Física 1, Probabilidad Y Estadística, Diseño Asistido por Computadora, Laboratorio Automotriz, Lengua Adicional 1

12. Ingeniería en Nanotecnología
Álgebra lineal, Cálculo Diferencial, Química, Cultura Física 1, Universidad y Sociedad, Física 1, Introducción a la Nanotecnología, Lengua Adicional 1

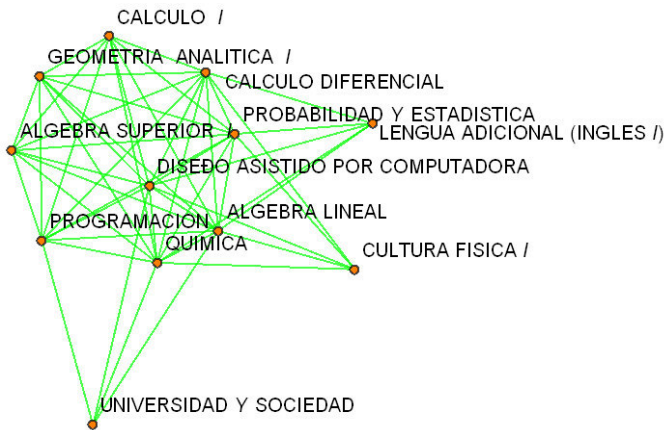


Fig. 2. First and second semester of automatization viewed as a graph

As it can be appreciated the different programs share subjects or in some cases the programs have the exact same subjects, this situation creates a logistic problem, if the school decided to open a single class for every subject of every program then the amount of classes would be exponentially bigger than if there were a way to minimize the number of subjects such as our protocol proposes, since these subjects need to be taken by the student in the same semester at the same time each semester is interpreted as complete non directed graph with each vertex being one of the subjects a student would be required to course this is assuming that the students follow the designed program that offers the subjects in a progressional manner so that the students have courses that they can understand based on the knowledge they gain, a complete graph implies that it's chromatic number would be the same as the number of vertices because all of its vertices are connected therefore they will always be connected to a vertex that already has a color assigned, for example Figure 1 refers to the first semester of the automatization career, since the first semester some careers share subjects with other careers, so now the semester is

interpreted as a non directed graph with cliques, each clique is the complete graph of every student coursing the semester of the different programs of the school of engineering, for example adding the first semesters of both automatization and mathematics as Figure 2 illustrates. Interpreting the semester this way provides information that helps reduce the size of the graph, for example the fact that both automatization engineering and civil engineering share the exact same subjects in the first semester so instead of adding the subjects twice they are considered as the same clique, Figure 3 illustrates how the graph for the first semester is constructed.

IV. RESULTS

Using this method the number of subjects, which is the number of vertices in the graph, was reduced from 1139 subjects to 529 subjects, due to the shared courses, this makes the graph substantially smaller so any algorithm used to get the chromatic number would be faster, after all the subjects of all the semesters were defined and converted to a graph it was possible to observe that with the expectation of two semesters, (the 9th semesters of automatization and industrial design that are analyzed as two separated graphs), all semesters can be interpreted as a one graph with several cliques such as all the different subjects and semesters are related in some way, even in the final semesters it can still be appreciated how some careers share a common core this is, again, due to the fact that the university offers classes that need to be taken regardless of the career such as the language courses, this common core implies that none of those subjects can be taken at the same time so in the graph they need to be colored with a different color. Figure 4 illustrates how the complete graph of all the programs of the school of engineering would be visualized, in this graph it can be seen that there are some subjects that only have relations with a common subject but they have no relation with each other, this is because of some careers like architecture that have different areas or different terminal lines that make it so that only the subjects that are shared need to be in the same time slot, this also implies that those subjects that are in different terminal lines can have the same color and can be taken at the same time. When defining the graph there

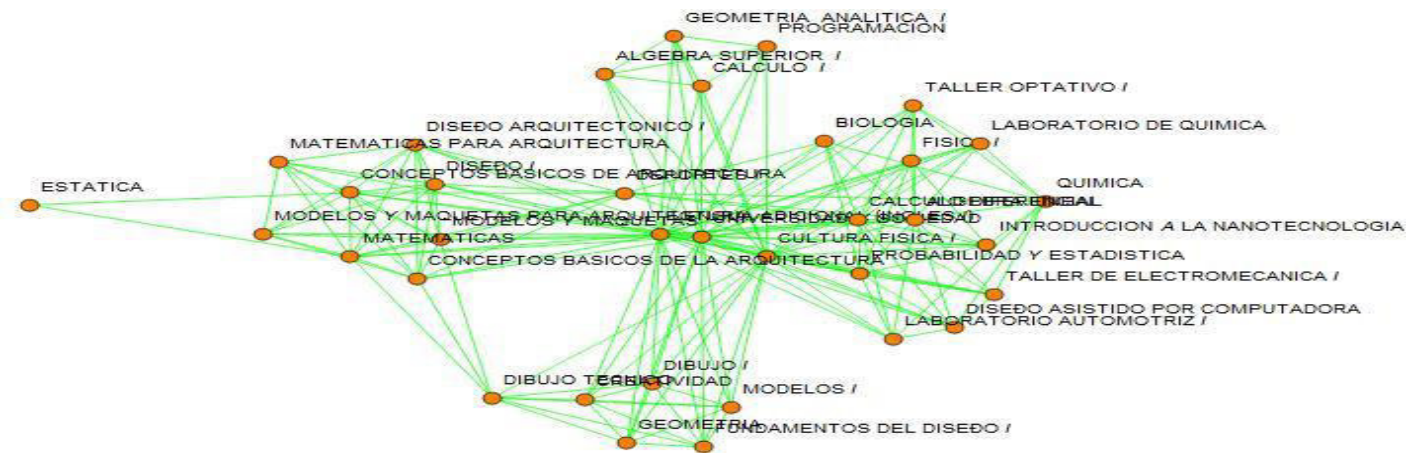


Fig. 3. First semester of all the careers in the School of Engineering viewed as graph

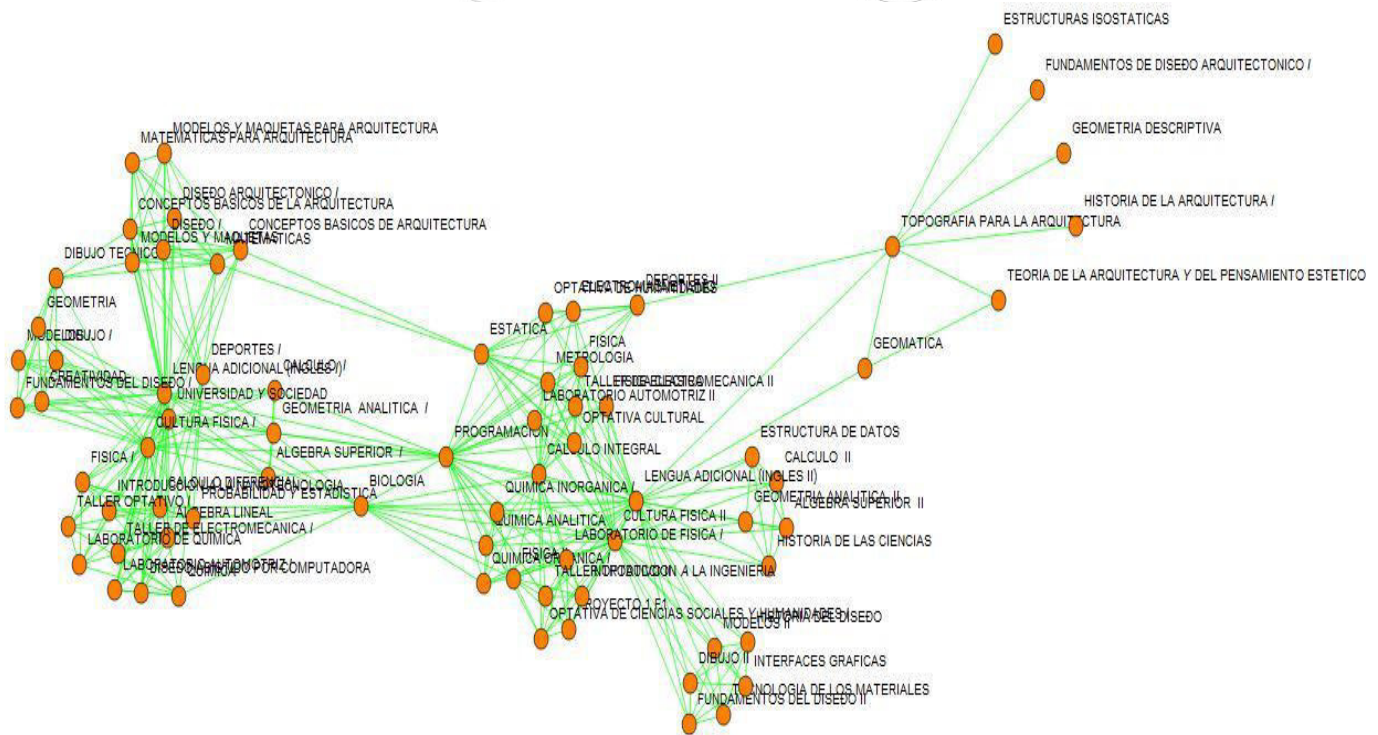


Fig. 4. All the semesters of the careers in the school of engineering viewed as a graph

are some filters to ensure that the graph is properly defined such as a filter to eliminate repeated connections, in the case that there are careers with the same classes, and an inverse filter for when the information presented gives an edge that is equivalent to another, for example the edge (a,b) is equivalent to the edge (b,a) since the graphs needed for this study are not directed this sort of situation would create 2 edges within the same vertices that would potentially create problems for the algorithm. After the graph is defined it is put through the greedy algorithm to find the result of the chromatic number and the color that each vertex will be assigned, the color is referred to as a number since there are no preference for the actual color that would be used, in the particular case of the school of engineering it was found that its graph has a chromatic color of 15, so its only needed 15 time slots for all the subjects which is possible assuming that there are 7 or 8 classes a day repeated in two days of the week, and the result was found in 720 milliseconds using a program developed in Python that analyzed the graph as a 2 dimension array that had the relations as 2 elements for each subject in the internal arrays as previously mentioned this array was reduced in size since some subjects are repeated or are presented as an inverse relation. It should be noted that this is the result obtained in the second compilation, the second compilation of a program in Python is normally faster than the first one, this is because of the way that python programs are translated to machine language. The time in which the result is found is efficient enough to be applied in a real world application which is the intention of this project.

CONCLUSIONS

The greedy algorithm was proven to be effective in determining the chromatic number of the graph generated with a timing that is fast enough so that it can be used, now that it is known which vertex belong to which color the colors can be referred as a space of time that can be shared with vertices that were assigned the same color. This study proved to be effective in designing a graph that can visually representate the schedule of the engineering faculty, said graph, that can be viewed in Figure 4, is helpful to illustrate how the graph coloring problem can be used in schedules. Future work will involve the development of a system that has a graphical user interface so that users with any level of skill regarding computers can build an schedule that does not have any kind of interferences, it will also involve adding all the other faculties of the autonomous university of queretaro and consider any other challenges that these faculties can present such as their corresponding areas and different terminal lines in which the students can specialize.

ACKNOWLEDGMENTS

We would like to thank the administrative personnel of the School of Engineering from the Autonomous University of Queretaro for providing information regarding the undergraduate programs. Without them as a source of information it wouldn't have been possible to guarantee the reliability of the information processed



REFERENCES

- [1] Ramón Espinosa Armenta, *Matemáticas Discretas*, 1st ed, Mexico, pp. 380
- [2] Tom Leighton, *6.042J / 18.062J Mathematics for Computer Science*, Fall 2010. (Massachusetts Institute of Technology: MIT OpenCourseWare), <http://ocw.mit.edu> (Accessed February 12 2017). License: Creative Commons BY-NC-SA
- [3] Peter Tannenbaum, *Excursions In Modern Mathematics with Mini-Excursions*, 6th Edition, pp B1-B14
- [4] George D. Birkhoff. A determinant formula for the number of ways of coloring a map. *The Annals of Mathematics*, 14(1/4):42–46, 1912
- [5] F. Thomson Leighton, *A Graph Coloring Algorithm for Large Scheduling Problems.*, *JOURNAL OF RESEARCH of the National Bureau of Standards* Vol. 84, No.6, November- December 1979.



Estimating the basic reproductive number, using differential equations, for Dengue.

L.M.A. Gabriela Herrera Trejo

Posgrado de Ingeniería, Maestría en Ciencias.
Universidad Autónoma de Querétaro
Querétaro, Querétaro.
gabriela.herrera.trejo@gmail.com

Dr. Jorge X. Velasco Hernández

Instituto de Matemáticas
Universidad Nacional Autónoma de México, Juriquilla.
Querétaro, Querétaro.
jx.velasco@im.unam.mx

Abstract— this research is about the estimation of the basic reproductive number, defined as the number of new cases that produce an infected individual during your period of infection on a susceptible population. Will be applied to the estimation of the basic reproductive number of Dengue in the State of Guerrero, to know the behavior of the disease in the future.

Keywords—(Number reproductive, attack Rate, Epidemic, Dengue)

I. INTRODUCTION

Throughout the history of man, there has been a variety of explanations and proposals to understand the cause and spread of disease outbreaks. From those who consider them of divine punishment, up to the current, which is known to be due to the presence of bacteria, viruses and other pathogens in the body.

Infectious diseases remain a major problem, The acquired immunodeficiency syndrome(AIDS) epidemic, the Plague, outbreaks of new diseases such as Ebola, are events that concern many people. Malaria and Dengue are endemic(they are all the time) in many regions of the world and significantly affect the population that suffer from them[1].

On the 20th of April, 1760, the mathematician swiss Daniel Bernoulli presented at the Royal Academy of Sciences of Paris, a mathematical analysis about the risks and benefits of vaccination of smallpox, by the variolacion, which is the exposure of a healthy person to an inoculum(enter in the body by artificial means the virus or the bacteria of a contagious disease) infection of an infected person[2].

Ronald Ross, used the principle of mass action in a model of continuous time, in his classic work on the dynamics of malaria, published in 1908. In the structured model of Ross, was used for the first time a mathematical theory, as a powerful research tool in epidemiology. The ideas of Hamer and Ross were expanded in more detail by H. Soper in 1929, who deduced fundamental mechanisms of the periodicity in the incidence of several infectious diseases[3].

R. Anderson and R. M. May published in 1982, an article in the prestigious magazine “Science”, in which they succeeded in the estimation of the spread of infectious diseases in human communities, as well as the basic reproductive number of the infection, denoted by R_0 , and the use of this measure, to determine the immunization levels necessary to control and even eradicate diseases preventable by vaccination[4].

After the Second World War, it became necessary to improve the understanding of the probabilistic processes, and many new advances, were stochastic processes. At the end of the decade of 1990. Was when the physical began to get interested in the topics of epidemiology, to understand the rapid spread of infectious diseases, as was the case with the severe acute respiratory syndrome(SRGA) in 2001, which appeared in Hong Kong, spread to north America and Europe and has claimed a large number of lives in a period of 15 days[5].

Implementation: this investigation is based on the article: The R_0 package: a toolbox to estimate reproduction numbers for epidemic outbreaks of Thomas Obadia, Roman Haneé and Pierre-Yves.

II. DEFINITION OF MATHEMATICAL MODEL.

A mathematical model is a description, in mathematical language, an object that exists in a universe non-mathematical.

In general terms, in all mathematical model we can determine three phases[6]:

1. Construction of the model, the transformation of the object non-mathematical in mathematical language.
2. Analysis of the model, study of the mathematical model.

3. Interpretation of the mathematical analysis, application of the results of the study of mathematics to the initial object is not mathematical.

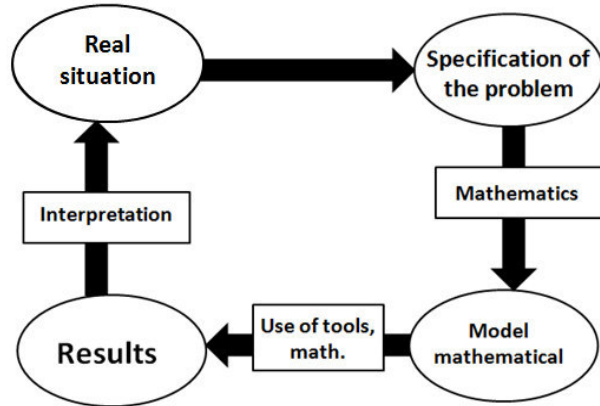


Fig. 1. Process to develop a method of mathematical.

III. DEFINITION OF THE BASIC REPRODUCTIVE NUMBER.

The symbol R_0 denotes the basic reproductive number, which is defined as the number of secondary infections that an individual infectious typical produces, in a population consisting of susceptible individuals only[20]. The interpretation to the basic reproductive number is given depending on the value that is:

- $R_0 < 1$ the infection dies after a long period of time
- $R_0 = 1$ each individual infectious simply be replaced same well and not produce an epidemic.
- $R_0 > 1$ the infection can get spread widely among the population.

IV. ESTIMATE: ATTACK RATE(AR).

The attack rate is a particular case of the incidence rate. Corresponds to the number of people who have a disease, related to the number of people exposed to the risk of the disease in a limited period of time and in special conditions such as in an epidemic[18].

$$AR = \frac{I}{S_0} \quad (1)$$

Where I represents the number of people infected and S_0 the number of the total population.

For example the attack rate for Dengue fever in Acapulco in the year 1999, we have 1998 deaths and a denominator, given by the population that is exposed to such an event, 673479 people. This way, you get a ratio that represents the mathematical probability of the occurrence of an event in a population and a defined time. In the example, the rate earned estimated the risk of each habitant of Acapulco to die of Dengue.

$$AR = \frac{1998}{673479} \times 1000 = 2.96668493 \quad (2)$$

This means that for every 1000 habitant of the municipality of Acapulco, we will have about three people that will die from Dengue. In the classic model SIR that examines the transmission of the disease, the attack rate (AR: the percentage of the infected population over time) is linked to the number of the basic reproductive R_0 by the following equation:

$$R_0 = \frac{\log\left(\frac{1-AR}{S_0}\right)}{AR-(1-S_0)} \quad (3)$$

Where S_0 is the percentage of the initial susceptible population, or well as we drove it earlier, the total number of the population that is exposed to the disease.

The assumptions required are:

- Constant population
- No intervention during the outbreak (this is not to apply vaccines or some type of treatment to help the recovery of the disease).

If they had interventions during the process would be inconvenient to use the method susceptible, infected and recovered (SIR), as you would have more variables and it would be best to change the mathematical model to make a better approximation of the basic reproductive number R_0 .

Doing a few steps of algebra and by setting certain assumptions, we will be able to do the following.

Let $a = \frac{I}{S_0}$ we have:

$$R_0[a - (1 - S_0)] = -\ln(1 - a) \quad (4)$$

$$R_0[a - (1 - S_0)] = (\ln(1 - a))^{-1} \quad (5)$$

$$e^{R_0[a - (1 - S_0)]} = e^{(\ln(1 - a))^{-1}} \quad (6)$$

$$e^{R_0\left[\frac{I}{S_0} - (1 - S_0)\right]} = e^{(\ln\left(1 - \frac{I}{S_0}\right))^{-1}} \quad (7)$$

We also suppose that $S_0 \sim N = 1$

$$e^{R_0\left[\frac{I}{N} - (1 - N)\right]} = e^{(\ln\left(1 - \frac{I}{N}\right))^{-1}}$$

$$e^{R_0\left[-\left(1 - \frac{I}{N}\right) + N\right]} = \frac{1}{1 - \frac{I}{N}}$$

Now $1 - \frac{I}{N}$ is a proportion of the population less infected people, to this proportion, I will denote by S^* .

$$e^{R_0(-S^* + N)} = \frac{1}{S^*} \quad (8)$$

$$S^* e^{R_0(-S^* + N)} = 1 \quad (9)$$

But now $N - S^*$ are the infected i

$$e^{R_0 i} = \frac{1}{S^*} \quad (10)$$

$$S^* e^{R_0 i} = 1 \quad (11)$$

So to solve this equation:

$$\frac{dS}{dt} = R_0 S S = S^* \quad (12)$$

We will have

$$S(1) = S^* e^{Ri} \quad (13)$$

Thus we can summarize that to be our equation equal to 1, it meant that the virus will spread throughout the population, which sounds logical to the point of thinking that we are talking about diseases that they come to produce epidemics.

V. ESTIMATION OF THE BASIC REPRODUCTIVE NUMBER OF DENGUE, ACAPULCO, GUERRERO DEFINITION OF THE BASIC REPRODUCTIVE NUMBER.

It has a database of Dengue, provided by the National Institute of Public Health from the years 2002 to 2009, with the collaboration of Dr. Jorge X. Velasco Hernández will give us a guideline of how to being the research, what has been collected at this time and be able to work in the job objective. The database with he worked was from the state of Guerrero, which had a total of 7586 of Dengue fever cases registered, did a debugging of data to form a new database that is outside of Acapulco, we took into account that it was the town where there were more cases of Dengue with 2543 cases are registered.

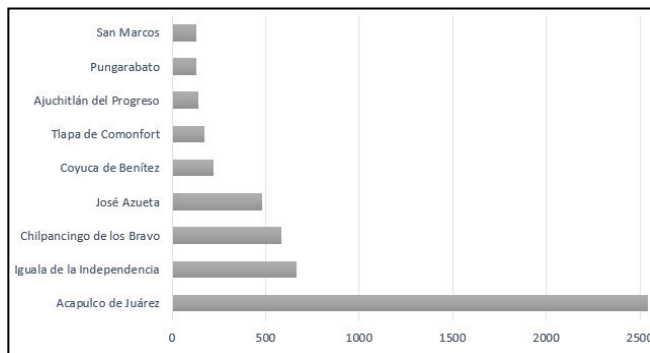


Fig. 2. Number of registered cases of Dengue fever by municipality in Guerrero from the years 2002 to 2009.

VI. RESULTS: R_0 DENGUE OF ACAPULCO.

The initial inspection of the data shows that the period of growth takes place from week 32 until week 41 which suffers a decline in the graph, having several disturbances to the week 51, but following the line of descent in the number of cases registered per week.



Fig. 3. Dispersion of the data recorded by week of Dengue fever in Acapulco in the years 2002 to 2009.

A sensivity analysis will help to refine the choice of a time window that is optimal for the exponential growth, which will be discussed below, Using the software r-project, especially the package R0, is made the analysis of the data.

In the following table show the results for the method of AR as well as its confidence interval.

TABLE I. RESULTS WITH THE METHOD AR

Method	R_0	I.C. min	I.C. máx
AR	1.00189	1.00181	1.00196

For the method of AR, the confidence interval had a variation of 0.000147, which is very small, that is to say that estimate is very good.

VII. CONCLUSIONS.

The reproductive number in an epidemic is of interest when the disease is transmitted in reality among the subjects, either directly or indirectly. This is for example the case of the flu, childhood diseases, but not in the epidemics of foodborne illness caused by environmental exposure to a pathogen.

The implemented methods should be used for acute diseases with short intervals of series. The analysis of diseases with incubation time very long requires methods that are more specialized.

While there are several methods to estimate the reproduction numbers, sometimes with code provided by its authors there is a common framework available to allow the comparison easy and direct results.

An implicit assumption in all methods is that all cases are recorded and are united by a chain of transmission.

However, you will encounter the following problems:

- Lack of early cases
- Cases that are not reported
- Report delays

The method of this type of attack requires less information, but is only usable when the epidemic has finished, and in addition requires that any intervention is established over the entire course of an outbreak.

Therefore, its use is usually restricted to particular environments such as schools or the platoons of the army. In conclusion, our R_0 calculated is backed by the news that we had back then, which is concerned that it will become an epidemic.

Now we know that if it came to be. Although they have developed many mathematical models to estimate several types of reproduction numbers during epidemic outbreaks, there exists a unique framework.

We apply this method to a disease that today is of the utmost importance, by the number of deaths you have had. As a result of Dengue fever.

We try to give an overview of the method suggested for the estimation of R_0 , and also gave a small introduction of what is a mathematical models.

I hope that this work will serve to people interested in the subject, and also for those that are just dabbling in the field of epidemiology.

REFERENCES

- [1] Escrito por Marta Talise, Licenciada en medicina y análisis clínico. "Ebola". www.webconsultas.com
- [2] Enfermedad por el virus del Ebola", Nota descriptiva n.103,Abril de 2014. Organización Mundial de la Salud.
- [3] "Dengue y dengue grave",Nota descriptiva n.117, Mayo de 2015. Organización Mundial de la Salud.
- [4] "Las peores epidemias de la humanidad" <http://www.taringa.net/posts/ciencia-educacion/13503426/Las-peoresepidemias-de-la-humanidad.html>
- [5] "Fundacion Polar, El mundo de la matemática, Modelos Matemáticos" <http://www.mat.uson.mx/jldiaz/Documents/Funcion/modelos-fasciculo17.pdf>
- [6] Hernández, J. X. V. (1999). Sobre enfermedades infecciosas. *Miscelánea Matemática*, 29, 51-57.
- [7] "Como modelar una epidemia: el caso de la influenza", ACADEMIA DE CIENCIAS DE MORELOS, A.C. Lunes 8 de Junio de 2009.

- [8] "Juan Alberto Rodríguez Velázquez y Cristina Steegmann Pascual, MODELOS MATEMÁTICOS, UOC. ["http://www.uoc.edu/in3/emath/docs/"](http://www.uoc.edu/in3/emath/docs/)
- [9] "Sitio web: de_nicion.de, Definicion de modelo matemático" http://de_nicion.de/modelo-matematico/
- [10] Academia.edu, uploaded by: Judith Esparza, "QUE ES UN MODELO MATEMÁTICOS?". ["http://www.academia.edu/9253640/"](http://www.academia.edu/9253640/)
- [11] "Pehman Rohani, Departamento de Zoología,Universidad de Cambridge. Juniode 2001. *Biología Matemática. Un Enfoque Desde los Sistemas Dinámicos*"
- [12] Osval Antonio Montesinos-López, Carlos Moisés Hernández-Suárez, *Modelos matemáticos para enfermedades infecciosas, Salud P_blica M_ex 2007; Vol. 49(3):218-226"*
- [13] .Ep_onimos medicos, Biogra_as medicas, Ronald Ross(1857-1932)" <http://www.historiadelamedicina.org/ross.htm>
- [14] "Biología Matemática. Un Enfoque Desde los Sistemas Dinámicos, August 26, 2011"<http://www.fenomec.unam.mx>
- [15] *Revista Cubana de Informática Médica, Modelo ?SIR? para epidemias: Persistencia en el tiempo y nuevos retos en la era de la Inform_atica y las pandemias. Autores: Karell R. V_azquez Argote. Instituto Nacional de Higiene, Epidemiología y Microbiología. INHEM."*
- [16] Unless noted R0 values are from: History and Epidemiology of Global Smallpox Eradication From the training course titled "Smallpox: Disease, Prevention, and Intervention" The CDC and the World Health Organization. Slide
- [17] "Wallinga J, Teunis P (2004). ((Di_erent epidemic curves for severe acute respiratory syndrome reveal similar impacts of control measures)). *Am. J. Epidemiol*"
- [18] "The R0 package: a toolbox to estimate reproduction numbers for epidemic outbreaks,Thomas Obadia, Romana Haneef and Pierre-Yves Bo_elle"
- [19] "Dietz K: The estimation of the basic reproduction number for infectious diseases. *Statistical Methods in Medical Research* 1993."
- [20] "Wallinga J, Lipsitch M: How generation intervals shape the relationship between growth rates and reproductive numbers. *Proceedings of the Royal Society B: Biological Sciences* 2007."
- [21] "Forsberg White L, Pagano M: A likelihood-based method for real-time estimation of the serial interval and reproductive number of an epidemic. *Statist. Med* 2008"

Uses and applications of expanded polystyrene in construction

Ing. Aarón Victor Manuel Galván Rodríguez

Student of Masters in Sciences (Construction)

Engineering Faculty, Autonomous University of Queretaro
Queretaro, Qro.

aaron_tmm@hotmail.com

Dr. Juan Bosco Hernández Zaragoza; Dr. Jose Luis
Reyes Araiza

Teacher- Researcher, Engineering Faculty
Engineering Faculty, Autonomous University of Queretaro
Queretaro, Qro.

Abstract—Within the field of construction, and throughout history, numerous materials have been developed for building, always seeking the objective of developing resistant materials, economic, innovative and contributing to sustainable development, for this reason is the importance of experimenting with recycled materials as components of materials and building elements. This work focuses on the use of expanded polystyrene derived from the recycling of waste products, to obtain liquid polystyrene to be used as a cement between particles and thereby achieve a sustainable material with properties similar to conventional mixtures of hydraulic concrete which are used in the construction industry.

Keywords - Sustainable development; Expanded polystyrene; Liquid polystyrene; Conventional mixtures; Hydraulic concrete.

I. INTRODUCTION.

The 21st century has involved an almost unlimited use of plastics; the products made with these materials are present everyday as part of objects such as furniture, toys, car parts, pens, clothes and food containers, just to name a few. However, with the development of the plastics industry, the use of "disposable" containers for transporting and containing all kinds of articles, which after a very short lifetime become trash, contributing to deteriorate the environment, since when degraded (which can happen in three months or even 500 years) enter the food chains of animals, plants and the same human being. Obviously this has led to an environmental crisis that results in an unsustainable development that at present reaches global dimensions [1].

More than 350 thousand tons per year of polystyrene are produced in Mexico. Expanded Polystyrene (EPS) is a rigid plastic, made from the molding of pre-expanded beads which has a closed cellular structure filled with air. Production in Mexico is estimated to be 350 thousand tons of EPS per year, of which less than 1% is recycled, and the rest is confined to sanitary landfills where it reaches 15% of the total volume. According to the National Institute of Ecology, the waste that reaches the landfill is more than 50% organic, about 40% of the waste in the cities are made up of containers and packaging, thirdly the EPS, the remaining 10% are difficult to recycle products [2].

Cement production has undergone tremendous development since its inception some 2000 years ago. Although the use of

cement in concrete has a long history, industrial production of cement began in the mid-nineteenth century. Today's global annual cement production is estimated at 2.8 billion tons, and is expected to rise to about 4 billion tons per year [3]. Further growth is expected in countries such as China and India, as well as in regions such as the Middle East and North Africa. At the same time, the cement industry faces challenges such as rising costs of energy supply, requirements to reduce CO₂ emissions and supply of raw materials in sufficient quality and quantity. The World Council of Enterprises for Sustainable Development (WBCSD) and its Cement Sustainability Initiative, made up of cement producers around the world, have launched the "Getting the right numbers" project, which for the first time provides a data for most of the global cement industry regarding CO₂ production and energy efficiency. Cement production is currently responsible for 6% of global anthropogenic CO₂ emissions and 7% for industrial fuels [4]. The purpose of this research is to use EPS debris as a cement material between concrete particles and mortars to partially or totally replace hydraulic cement added to conventional mixtures used in construction.

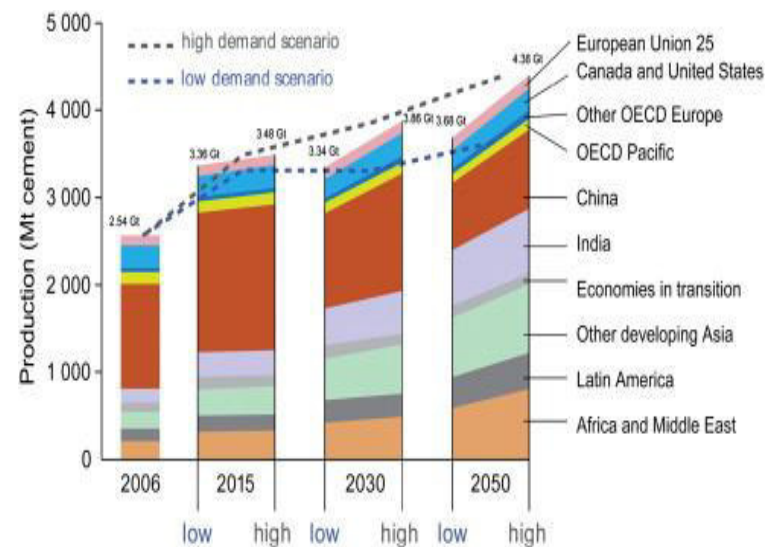


Figure 1. Cement production at global level [3].

II. BACKGROUND.

Various compounds have been developed and used in the industry to improve concrete mixtures in construction, such as cellular concretes and mortars, the use of these has several advantages such as: significant reduction of dead loads of the structures, as well as the reduction of cross-sections and the size of foundations. Generally, the use of a lightweight concrete helps to reduce the damages caused by an earthquake because the acceleration and its magnitude depends largely on the weight of the structure. Low density, high strength/weight ratio, lower thermal conductivity coefficients, better fire resistance, improved durability properties and better sound insulation capacity are factors that increase with the use of lightweight concrete.

The effects and the way in which EPS particles contribute to various factors such as fire resistance, thermal conductivity and compressive strength of cellular concretes have been studied.

Cellular concrete and polystyrene foam concrete were designed for densities ranging from 1200 kg/m³ to 150 kg/m³ with a volume range of EPS of 0 to 82.22% and a water-cement ratio of 0.33. Cellular concrete with a density of 800 kg/m³ and a volume of EPS of 0% was designed as a reference for the foamed polystyrene concrete. The results indicated that the increase in the volume of EPS causes a significant reduction of the thermal conductivity obtaining values up to 0.084 W/m·K, fire resistance up to 1450 °C without severe damage and compressive strength of 93.6 kg/cm² [5].

Other studies have been carried out on the manufacture of low density bricks of dimensions of 10x20x6 cm where

Portland cement, water and recycled polystyrene material were used, the results were that the bricks developed in the research showed to have efficient mechanical properties and that could be used as a masonry element in construction since this material meets the required parameters in masonry elements in Mexico. The pieces are composed of recycled EPS as a commercial aggregate and Portland cement as a binder. Unlike most papers published in the literature, this mortar did not use additional pozzolans, additives or additives.

Unlike concrete (with coarse aggregate), failure trajectories always follow the interfaces of the polystyrene aggregate particles and are cut through the cement paste and the aggregate particles themselves. The cracks in the polystyrene bricks are similar to the concrete cracks reported in the compression and stress test.

The sustainable use of EPS in cellular concrete bricks was very favorable with respect to those existing in the market. The material obtained was lighter, which facilitates its rapid elaboration, quality control and transport.

Its production is simpler and the final product is less permeable, which helps prevent moisture formation from affecting its strength due to the increased adhesion shown with dry polystyrene. In addition, it is more resilient and flexible, which makes walls less vulnerable to cracking caused by ground movements. Finally, this material is cheaper because it uses recycled materials and has properties that prevent its deterioration thus increasing its useful life. The use of completely dry EPS is recommended to obtain the best properties of the final pieces [6].

Table 1. Comparative properties of samples A and B compared to reported parameters [6].

Properties	Brick A	Brick B	Baked clay brick	Mortar brick
Dimensions: thickness, width and length (cm)	6, 10, 20	6, 10, 20	5.5, 11.5, 23	18, 12, 38
Volumetric weight (kg/m ³)	1568	1236	1580	1890
Average percent of absorption (%)	9.3	4.3	17.8	25.2
Compression strength (MPa)	9.69	6.92	11.16	4.69
Average breaking stress (MPa)	2.94	1.65	0.755	0.794

In 2002, in a study carried out at Babylon University College of Engineering, some of the mechanical properties of polystyrene concrete were investigated by destructive and non-destructive methods. The experimental results of the non-destructive test were correlated with the compressive strength, tensile strength, flexural strength, impact strength and cracking patterns. The result of the test showed that the mechanical properties of the concrete improve with the addition of EPS up to a ratio of 1/3 (percentage of cement/polystyrene). On the other hand, it was noted that increasing EPS in the proportion of cement increases the flexural strength and abrasion resistance for concrete [7].

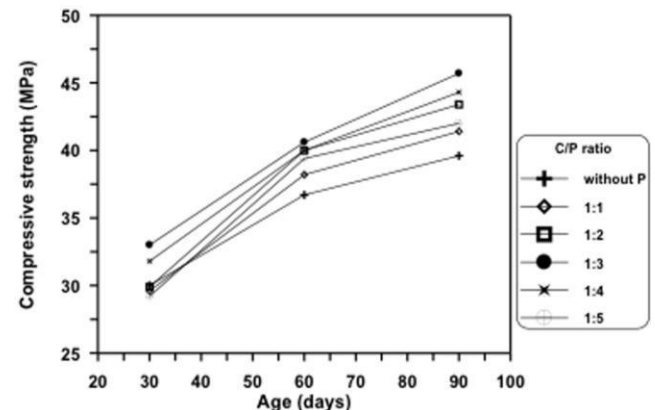


Figure 2. The effect of PE on the compressive strength of concrete at different ages [7].

In a study conducted in Vilnius, Lithuania; EPS foam residues were used, as well as fine and coarse residues of EPS and fine blown EPS particles; to produce the filler material of a light heat insulation compound, of which the matrix is a EPS base cement. Investigation of the contact zone between the EPS base cement and the EPS granules showed no fractures or microcracks. The adhesion of the two components depends on the size and shape of the granules used. When a polystyrene bead is stripped from the EPS base cement, the created hole repeats the granule structure as if it were a mold and the granule leaves polystyrene residues in the hole. This demonstrates the fact that the EPS base cement has a stronger contact zone than the polystyrene material of the granule. When fine granules of EPS are used, they disintegrate along the contact zone. This material has a lower adhesion strength, however, it is stronger compared to a composite material, made with different EPS foam pellets, provided with a better macrostructure. The strength and thermal conductivity of the composite depends on its density, the matrix mixture, its arrangement, and the amount used, all this was defined by means of regression equations [8].

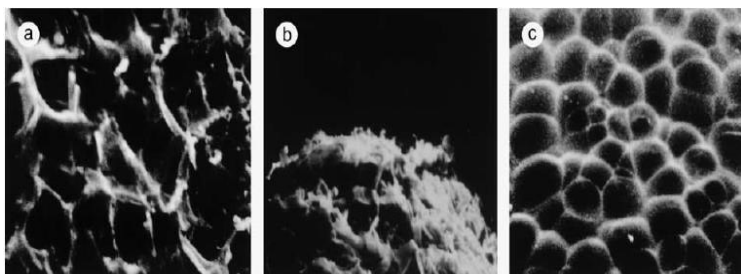


Figure 3. Microstructure of polystyrene granule (X120): a) large particle, b) crumbled particle, c) fine particle [8].

In 2011, a work was done using recycled EPS through the melting and/or dissolution of this material in acetone as a solvent and was used for the production/manufacture of integrated circuit boards. The material obtained was characterized by flexural tests according to ASTM D 790 and the results were compared with phenolite, traditionally used. Fractures of the specimens were observed by scanning electron microscopy in order to establish patterns. The EPS as phenolite were analyzed by thermogravimetric analysis (TGA) and differential scanning calorimetry (DSC). The method used for the dissolution gave very fragile material results. The melt method used did not show void formation or increase brittleness of the material. The recycled EPS has a significantly lower resistance value than the phenolite, this is a reduction of about 60% of its flexural strength. From this it can be concluded that by itself, the laminated and hardened liquid polystyrene does not have good flexural properties [9].

After all the above it is possible to conclude that it is feasible to add EPS to the concrete and mortar mixtures since in most cases their mechanical and insulating

properties are improved for the sought purposes, in the last paragraph it is mentioned that it is not the use of the hardened liquid polystyrene matrix in bending tests is no feasible when does not have stony aggregates because the matrix works only as a binder material and therefore lacks consistency.

III. WORK DESCRIPTION.

In this work, we are looking for the elaboration of mixtures based on common aggregates used in construction (gravel and sand) embedded in a cement matrix composed of Liquid Polystyrene (LPS) that satisfies the needs of the construction industry and for the purpose to contribute to the recycling of products that are harmful to the environment. It is sought that the mixtures obtained have similar properties in resistance to conventional mixtures made from hydraulic cement to be used in bonding of masonry pieces in the case of mortars and in structures such as floors, slabs, walls, foundations, sidewalks and fittings for the case of concretes. Destructive and non-destructive tests in LPS base and hydraulic cement mixtures will be performed in order to compare results, such as: fresh volumetric weight, slump, absorption, simple compression and pure bending.

IV. MATERIALS.

- Ordinary Portland cement (OPC) that meets the standard N-CMT-2-02-001-02 [10].
- Gravel and sand that meets the standard NMX-C-111-ONNCCE-2004 [11].
- Expanded polystyrene, which was originally used as packaging of various articles, which will be used as recycling material.
- Industrial grade acetone as solvent for expanded polystyrene.
- Industrial grade ethyl acetate as solvent for expanded polystyrene.

V. METHODOLOGY.

- Obtaining materials.

To begin, we will proceed to the purchase of the base materials for the preparation of concrete and mortar (gravel-sand) to subsequently extract the sufficient amount of material to carry out the evaluation of the stony aggregates; For the case of the polymer will be obtained expanded polystyrene of waste materials such as: packaging waste, waste of light bulb used in construction, among others.

- Characterization of sustainable polymer (liquid polystyrene).

Once the waste product is obtained, it will be dissolved in acetone and ethyl acetate (50/50 ratio) to form 6 cylindrical specimens measuring 5 cm X 10 cm to later measure properties such as volume, weight, density, specific gravity, setting time, compressive strength, etc.

- Evaluation of aggregates.

In order to evaluate the quality of the materials in some way, a series of tests will be made to the aggregates like:

- Obtaining moisture from materials.
- Determination of volumetric weight, this in dry and loose conditions.
- The elaboration of granulometric curves.
- Organic matter content in sands.
- Los Angeles test in the case of gravel.

- Design of mixtures.

3 designs of mixtures will be tested, 100%, 50%, and 0% cementing material (Sustainable Polymer) and the complementary percentage of hydraulic cement will be tested. The dosages for concrete will be made based on the regulation ACI 211.1-97 [12]. The dosages for mortar will be made based on the Complementary Technical Standards for Design and Construction of Masonry Elements for a type III mortar.

- Elaboration of specimens.

Once the design of mixtures will be made, the production of specimens will proceed; which will be:

- Cylinders of 10 cm in diameter and 20 cm in height for the case of concrete mixtures.
- Cubes of 5 cm of base and 5 cm of height for the case of the mixtures of mortar.
- 9 specimens will be cast for each mixing ratio, with a total of 27 concrete cylinders and 27 mortar cubes.
- Beams of 15X15X60 cm, 3 for each mix. They will be tested 28 days after curing.

- Specimen testing.

- Fresh volumetric weight.

A 10-liter volumetric metal bucket will be filled with three layers of concrete. Strain each layer with 25 strokes of rod and tap the outside of the bucket; taking care not to beat in excess to avoid that the mixture is disaggregated. The last layer is covered with a steel ruler, the exterior surface is cleaned and finally the weight is taken. The volumetric weight is obtained: w / v . The same procedure is performed 3 times to obtain an average.

- Slump.

A slump test shall be performed on each different type of mixture following the procedure established by NMX-C-156-2010 [13].

- Absorption.

This test will be performed only on 28-day specimens for each type of mixture. It consists in submerging the 3 pieces in a container with water at room temperature for 24 hours.

Absorption at 24 hours is performed according to ASTM-C-67-03 [14] and equation 1 is used.

$$Absorption = \frac{W_{24h} - W_s}{W_s} \times 100 \quad (1)$$

Where:

W_{24h} = Weight of the specimen after being submerged in cold water for 24 hours, (kg).

W_s = weight of the specimen in the dry state, (kg).

- Simple Compression.

For each mixture 3 specimens will be tested at 7 days, 3 to 14 days and 3 to 28 days. After the curing of the specimens the nodding of the specimens will be carried out, this will be done with a sulfur base mortar with a resistance of approximately 527 kg/cm², so that the forces are evenly distributed on both sides of the cylinders. The cylinders shall be placed on a steel plate and in turn in each test a ball-and-socket joint shall be placed on the upper face of the specimen to absorb the uniformities of the cylinder. Subsequently you will start with the load application. The entire procedure will be executed under the parameters of the standard NMX-C-083-ONNCCCE-2002 [15]. To obtain the compressive strength of the test pieces, equation 2 is used.

$$R_c = \frac{F_c}{S} \quad (2)$$

Where:

R_c = compressive strength of the specimen, (kgf/cm²).

F_c = maximum load supported during the test, (kgf).

S = cross section of the specimen, (cm²).

- Pure bending.

A bending test shall be performed on each different type of mixture following the procedure established by ASTM C-78-02 [16], which indicates that a beam shall be loaded as shown in the diagram. Only beams will be tested for 28 days after casting. The flexural strength will be calculated with equations 3 and 4. If the fracture starts at the tensioned surface and at the middle third of the separation between supports the equation 3 will be used.

$$R = PL/bd^2 \quad (3)$$

Where:

R = modulus of rupture, (psi or MPa).

P = maximum load applied indicated by the universal machine, (lbf or N).

L = separation between supports, (in or mm).

b = average specimen width, (in or mm), in the fracture, and

d = average specimen depth, (in mm), in the fracture

If the fracture occurs on the tensile surface and outside the middle third of the spacing between supports and not more than 5% of the distance between supports, equation 4 will be used.

$$R = 3Pa/bd^2 \quad (4)$$

Where:

a = average distance between the fracture line and the closest support measured at the beam tensile surface (in or mm).

If the fracture occurs on the tensile surface outside the middle third of the distance between supports by more than 5% of the distance between supports, the results of the test are discarded.

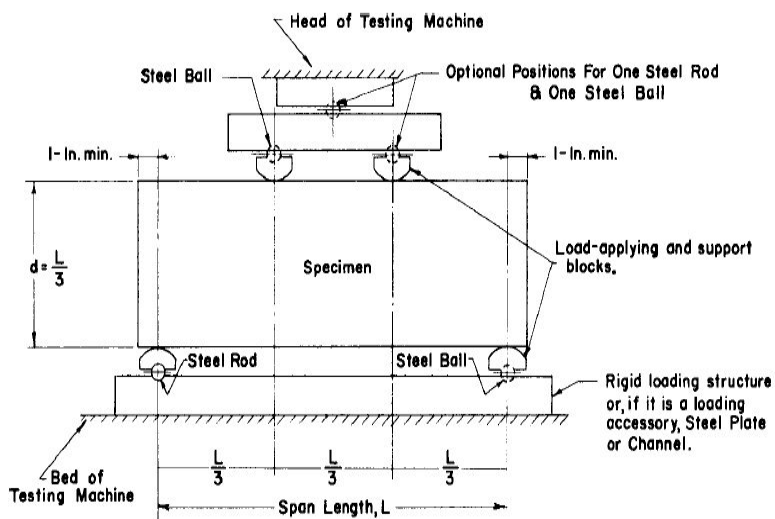


Figure 4. Pure flexion test diagram [16].

VI. EXPECTED RESULTS.

When EPS is used as the particle binder material, it is expected to characterize the cementitious material as a product of EPS waste, to obtain low density mixtures compared to traditional concrete and mortar mixtures, to reach that such mixtures are impermeable and resistant to weathering; as well as to improve the thermal and acoustic insulation capacities for a possible use inside buildings and with this, to decrease the use and cost of heating and air conditioning systems.

VII. REFERENCES.

[1] Hernández, J. B., López, T., Martínez, G., & Menchaca, C. (2005). *Materiales Sustentables y Reciclados en la Construcción* (Omniascience). Barcelona, España.

[2] Araiza, L. (2012). *Producción y contaminación de unicele en México*. El Sol de León. <http://www.oem.com.mx/elsoldeleon/notas/n2793509.htm> (Last query 01/11/2016).

[3] Schneider, M., Romer, M., Tschudin, M., & Bolio, H. (2011). Cement and Concrete Research Sustainable cement production — present and future. *Cement and Concrete Research*, 41(7), 642–650. <http://doi.org/10.1016/j.cemconres.2011.03.019>

[4] Habert, G. (2013). *Environmental impact of Portland cement production 2013 Eco-Efficient Concrete.pdf*. Zürich, Switzerland. <http://doi.org/10.1533/9780857098993.1.3>

[5] Sayadi, A. A., Tapia, J. V., Neitzert, T. R., & Clifton, G. C. (2016). Effects of expanded polystyrene (EPS) particles on fire resistance, thermal conductivity and compressive strength of foamed concrete. *Construction and Building Materials*, 112, 716–724. <http://doi.org/10.1016/j.conbuildmat.2016.02.218>

[6] Hernández-Zaragoza, J. B., López-Lara, T., Horta-Rangel, J., López-Cajún, C., Rojas-González, E., & Adué, J. (2013). Cellular Concrete Bricks with Recycled Expanded Polystyrene Aggregate. *Advances in Materials Science and Engineering*, 2013. Retrieved from <http://dx.doi.org/10.1155/2013/160162>

[7] Mansour, M., & Mohammed, K. (2002). Study the Effect of Polystyrene on Some Mechanical Properties of Concrete. Retrieved from http://repository.uobabylon.edu.iq/journal_view.aspx?dpp=207

[8] Laukaitis, A., Zurauskas, R., & Kerien, J. (2005). The effect of foam polystyrene granules on cement composite properties, 27, 41–47. <http://doi.org/10.1016/j.cemconcomp.2003.09.004>

[9] Schmidt, P. N. S., Cioffi, M. O. H., Voorwald, H. J. C., & L, J. (2011). Flexural Test On Recycled Polystyrene. *Procedia Engineering*, 10, 930–935. <http://doi.org/10.1016/j.proeng.2011.04.153>

[10] N-CMT-2-02-001-02 (2002). *Características de los materiales. Materiales para estructuras. Materiales para Concreto Hidráulico. 001 Calidad del Cemento Portland*.

[11] NMX-C-111-ONNCCE-2004 (2004). *Industria de la Construcción. Agregados para Concreto Hidráulico, especificaciones y métodos de prueba*.

[12] ACI 211.1-97 (2002). *Standard Practice for Selecting Proportions for Normal, Heavyweight, and Mass Concrete*.

[13] NMX-C-156-2010 (2010). *Industria de la Construcción. Concreto Hidráulico. Determinación del Revenimiento del Concreto Fresco*.

[14] ASTM-C-67-03 (2003). *Standard Test Methods for Sampling and Testing Brick and Structural Clay Tile*.

[15] NMX-C-083-ONNCCE-2002 (2002). *Industria de la Construcción. Concreto Hidráulico. Determinación de la resistencia a la compresión de cilindros de concreto. Método de Prueba*.

[16] ASTM C-78-02 (2002). *Standard Test Method for Flexural Strength of Concrete (Using Simple Beam with Third-Point Loading)*.

Production of Bean Straw Pellets with Maximum Energy Content

D. Trejo-Zamudio¹, C. Gutiérrez-Antonio¹, J.F. García-Trejo²

¹ Facultad de Química, Universidad Autónoma de Querétaro, Querétaro, Querétaro, México. dtreza15d.t@gmail.com

² Facultad de Ingeniería, Universidad Autónoma de Querétaro, Querétaro, Querétaro, México.

Abstract— The increase in energy demand over the years has been the cause of the searching for new energy alternatives, which can provide clean and sustainable energy. Research has been launched for the development of second generation biofuels, which uses crops and wastes that are not for human or animal consumption. In this context, one of the less studied residues to produce biofuel is bean straw, which has a high production in Mexico, derived from its importance in the Mexican diet. The densification of this waste can provide a clean, sustainable biofuel that complies with the standards, and allows the reduction of solid waste.

Keywords— *Pellets, bean straw, biofuels, agroindustrial waste.*

I. INTRODUCTION

Over the years, the population has been increasing, resulting in a major demand for goods and services. Energy is one of the services with the greatest increase in demand; since 1990, primary energy requirements have augmented by approximately 38% [1].

Fossil fuels, such as oil, coal and natural gas, represent the world's major energy sources; approximately 80% of the energy currently consumed comes from these sources [2]; however, the combustion of these fuels has produced pollutant emissions, which have also caused an increase in terrestrial temperature due to the greenhouse effect.

Among the greenhouse gases, CO₂ is one of them. During 2013, there were 32,189.7 million tons of CO₂ derived from the burning of fuels in the world; from this total 46% came from coal combustion, 33% from oil combustion, 20% from gas, and the remaining 1% was produced by other energy sources [3].

Many strategies to reduce CO₂ emissions have been proposed, including nuclear energy and renewable energy; the last one includes solar, wind and biofuels. In particular, biofuels are defined as those fuels produced from biomass from plants. Biofuels, when burned, produces usable energy such as heat, light and movement in a similar manner that fossil fuels [4].

Biofuels are classified into generations: first, second and third; according to the type of raw material used to produce them. Thus, first generation biofuels refer to those that are elaborated from crops that have a food use. Second generation biofuels are biofuels produced from non-edible crops, which includes plants, crop residues, food processing residues and municipal organic waste [5]. Finally, third generation biofuels are those that are made from algae and micro algae.

Specifically, second-generation biofuels have the advantage of using raw materials from a variety of agricultural land and wood residues, without any direct claim [1]. In addition, second generation biofuels would make it possible to boost the economic development of rural areas, as well as job creation. It could also take advantage of what is sometimes considered a pollution factor. From these residues, can be produced biofuels in liquid, solid or gaseous state, through different processing routes.

In particular, solid biofuels include firewood, wood pellets and non-wood biomass pellets, as well as charcoal. Pellets are the most popular solid biofuels, since they have the advantage of using wood residues and straws from other plants. Pellets can be produced by mechanical extrusion, pelletized, obtaining biofuels of low humidity, high density and uniformity; pellets can be used in different applications, including domestic kitchens, boilers and power plants [6]. When the biomass is densified in a pellet its calorific value per unit volume improves, which facilitates its storage and distribution management [7].

Currently the pellets have been made from various raw materials, such as wood waste, rice crop residues, wheat straw and corn stubble. Other materials have been considered as potential bioenergy sources, which include bean straw and cotton stems but still without applications in the production of pellets; other materials have been studied in pellet production models such as alfalfa and pasture rod [8].

Bean is one of the most important products in the Mexican diet, from which the bean straw is produced; in 2006, 1.75 million tons of bean straw were generated in Mexico, being the second largest amount of cultivated land in the country [9]. This residue represents a potential biomass source for various

applications; since, although it is used as fodder, it does not have a strong demand. In many cases, the bean straw is burned or used as fertilizer in the fields; however, could be exploited in the production of a densified fuel, an application that has not been reported in the literature. For this reason, the present investigation focuses on the use of bean straw as raw material to produce solid biofuels, specifically pellets, of maximum energy content.

II. MATERIALS AND METHODS

A. Biomass selection

The raw material used was obtained from farmers in the municipality of Nopala de Villagran in the state of Hidalgo, Mexico.

The straw was obtained from the harvests of the year 2016, and it was dried in the sun and transported to carry out the investigation.

Figure 1 shows the bean straw, which is placed in bags to avoid degradation by moisture and facilitate transportation. The bean straw is composed of the stem and the pod of the plant, and both are harnessed in the densified process.



Fig. 1. Bean Straw.

B. Characterization

One of the most important factors during pellet production is moisture. So, it is necessary to determine the initial moisture content of the raw material, which is determined by gravimetric analysis of volatilization. By this method, the straw is subjected to heating above 100 ° C to vaporize the water; the sample is weighed before and after the heating process, and the moisture content is determined by the difference in weight.

The moisture content allows to identify if it is necessary the addition of water or the drying of the raw material, since the humidity must remain below 20%.

Straw characterization includes the determination of ash, carbon and nitrogen content, in order to predict the quantity and types of gases that can be obtained by burning the pellet; as well as determining whether straw residues can be used as fertilizer on farmland.

C. Pretreatment

By means of an experiment design, at least three moisture values and three particle size values are selected to determine whether the response behavior is linear.

In a first step, it is verified that the bean straw contains the moisture required for the experiment; otherwise it is dried with the aid of the sun or with a stove, depending on the amount of moisture to be removed. If moisture is required, the straw can be moistened using water spray or in the form of steam.

Bean straw is subjected to a grinding process using a hammer mill. The straw is passed through a sieve and distributed in three particle sizes, covering the range of 0.8 mm to 6 mm, which is equivalent to the average pellet diameter.

It is verified that the humidity of the straw is in the established intervals, and the biomass is placed in sealed bags to avoid the loss or gain of humidity. The bags are transported to the pelletizing equipment, and are not opened until the densification process.

D. Densification

The samples of ground straw are densified with a pelletizer, where the use of pressure and an increasing in temperature causes the lignin to melt; when the temperature drops, the pellet is formed. The temperature of the pellets when leaving the pelletizer is between 70 ° C and 80 ° C, so that a slight loss of moisture may be present.

Figure 2 shows the pelletizing equipment. The raw material with particle size and humidity controlled is placed in the upper part of the equipment; by means of rollers is subjected to a pressure increasing in the formed matrix, where acquires the shape and size of pellet.



Fig. 2. Pelletizing equipment.

Subsequently, the pellet is cooled to room temperature, and it is at this stage that the lignin hardens and the pellet acquires its final shape and strength. A sieve allows to eliminate the non-densified straw as well as the powder.

E. Pellet density

Pellets are identified by particle size and humidity used. With a vernier, the diameter D (cm) and the length L (cm) of the pellet are determined individually, and the volume V_p is calculated by applying equation (1). Then the pellet is weighed and the individual mass is obtained m_p . Using equation (2), the individual density of the pellet, in g/cm^3 , is obtained and the average of a sample is obtained.

$$V_p = \left(\frac{\pi D^2}{4}\right) * L \quad (1)$$

$$\rho_p = m_p / V_p \quad (2)$$

Figure 3 shows pellets of bean straw with powder. Density determinations must be made with clean pellets. In addition, the appearance of powder in the final product shows that the pellet has little resistance and usually low density.



Fig. 3. Pellets

F. Bulk density

The pellets are weighed and placed in a known volume vessel, their units can be g/cm^3 . Equation (3) is used:

$$\rho_g = m_g / V_g \quad (3)$$

Where:

m_g : Bulk mass (g)

V_g : known volume of a vessel (cm^3)

G. Durability

The durability is determined by the lost mass of the samples, after being subjected to a screening process. The pellets are weighed and placed in a vibrating sieve for 10 minutes; then reweighed and the lost mass during the test is determined. The loss of 2.5% of the initial mass indicates that

it is a fragile pellet, according to international references, as shown in the review of García-Marever et al.[10].

H. Calorific power

By means of a calorimeter the energy content of the pellets is determined, using benzoic acid as substance to calibrate the equipment.

The results of the test are recorded, and with them a mathematical model is constructed; this model considers the density and resistance of the pellet as factors of response to the variation of humidity and particle size.

Thus, higher density is expected to obtain higher calorific power, as well as lower humidity; however, a low humidity can have negative effects to the pellet giving it less resistance to handling and transportation. The model is validated with experimental data.

III. EXPECTED RESULTS

The methodology for obtaining pellets from residues of bean crops has been presented. The objective is obtaining as much energy as possible from this type of straw under the most favorable conditions, and comparing the results with other types of pellets. In the end, we intend to know the potential of this densified residue; especially against pellets of waste from the forest industry, which have been shown to have a high calorific value.

At the end of the research it is sought to determine the most favorable levels of moisture and particle size, in which the bean straw offers the greatest calorific value when densified and subsequently burned.

Previous studies have shown that a lower moisture content gives a higher amount of energy when burning the pellet; however, low moisture content can affect the resistance of the pellet, which is why it is important to know the most suitable conditions for this type of residue.

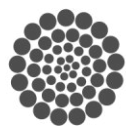
The aim is to find an alternative energy that can be used in the short term, and that can contribute to the reduction of greenhouse gas emissions.

Also, it is desirable that pellets can be integrated in rural communities, where the process can be source of employment.

Moreover, it is important the diversification of the raw materials used in the production of pellets, allowing the access of this technology to areas where other raw materials are few, or none of them can have a similar calorific power to other types of pellets that use straw as biomass to burn.

REFERENCES

- [1] K. Ullah, V. Kumar, S. Dhingra, G. Braccio, M. Ahmad, and S. Sofia, "Assessing the lignocellulosic biomass resources potential in developing countries : A critical review," *Renew. Sustain. Energy Rev.*, vol. 51, pp. 682–698, 2015.
- [2] R. Saidur, E. Abdelaziz, A. Demirbas, M. S. Hossain, and S. Mekhilef, "A review on biomass as a fuel for boilers," *Renew. Sustain. Energy Rev.*, vol. 15, no. 5, pp. 2262–2289, 2011.
- [3] International Energy Agency, *CO2 Emissions from fuel combustion. Highlights*, 2015th ed. 2015.
- [4] M. Guo, W. Song, and J. Buhain, "Bioenergy and biofuels : History , status , and perspective," vol. 42, pp. 712–725, 2015.
- [5] G. Taylor, "Biofuels and the biorefinery concept," *Energy Policy*, vol. 36, no. April 2008, pp. 4406–4409, 2010.
- [6] J. M. Castellano, M. Gómez, M. Fernández, L. S. Esteban, and J. E. Carrasco, "Study on the effects of raw materials composition and pelletization conditions on the quality and properties of pellets obtained from different woody and non woody biomasses," vol. 139, pp. 629–636, 2015.
- [7] W. B. Kusumaningrum and S. Sofyan-Munawar, "Prospect of Bio-pellet as an Alternative Energy to Substitute Solid Fuel Based," *Energy Procedia*, vol. 47, pp. 303–309, 2014.
- [8] A. Sultana and A. Kumar, "Ranking of biomass pellets by integration of economic , environmental and technical factors," *Biomass and Bioenergy*, vol. 39, pp. 344–355, 2012.
- [9] I. Valdez Vazquez, J. A. Acevedo Benítez, and C. Hernández Santiago, "Distribution and potential of bioenergy resources from agricultural activities in Mexico," *Renew. Sustain. Energy Rev.*, vol. 14, pp. 2147–2153, 2010.
- [10] A. García-Maraver, V. Popov, and M. Zamorano, "Data Bank A review of European standards for pellet quality," *Renew. Energy*, vol. 36, pp. 3537–3540, 2011.





Electrostatic fermentation system for the production of bioethanol

I. A. Gallegos-Almanza, A. Amaro-Reyes, J. N. Gracida-Rodríguez
Parque Biotecnológico
Facultad de Química, Universidad Autónoma de Querétaro, UAQ.
Querétaro, Qro., México.

G. Macías-Bobadilla
Facultad de Ingeniería, Universidad Autónoma de Querétaro, UAQ.
Querétaro, Qro., México.

Abstract—In recent times we have begun to see how gas, coal and hydrocarbons have ceased to be a viable energy option therefore directly involved in global warming. The irresponsible use and exploitation of fossil fuels makes it necessary to include new technologies that support both the economy, society and the environment. The management of microorganisms for the production of metabolites of interest provides benefits such as the use of industrial waste for the production of alternative energy such as second generation biofuels, a specific case of bioethanol. Recently fermentation techniques have managed to more selectively direct the production of primary metabolites through an electric current that is in direct contact with the yeast, one is what has defined as an electrostatic fermentation system. The proposal of this work focuses on the use of the electrostatic fermentation system for the production of bioethanol using strains of *Saccharomyces cerevisiae* that are subjected to electrical stimuli with different current intensity and duration while growing in yeast culture medium (YPD) and by fed-batch. Subsequently the production of the ethanol generated and the consumption of sugars is quantified.

Keywords; *Bioethanol, second generation biofuels, Electrostatic fermentation system, biomass.*

I. INTRODUCTION

The energy crisis and environmental pollution are two major environmental challenges facing the world today. For its part, energy is a key factor for every sector of the modern economy, which is derived mainly from fossil fuels, about 80% of the total energy supply in the world depend on this source [1]. Products derived from crude oil such as gasoline and diesel are the main fossil fuels used for power generation, which are used in the transportation, commercial, domestic and industrial sectors, and in agriculture, where, for example, about 98% of the energy consumed by the transport sector comes from this type of fuel [2].

Climatologists have observed that concentrations of carbon dioxide (CO₂) in the atmosphere have increased significantly during the last century, compared to the pre-industrial age (about 280 parts per million or ppm). The CO₂ concentration of 2014 (397 ppm) was approximately 40% higher than in the mid 1800s, with an average growth of 2 ppm / year in the last ten years. There have also been significant increases in levels of methane (CH₄) and nitrous oxide (N₂O). In 2013, global emissions reached 32.2 GtCO₂, an increase of 2.2% over 2012 levels. This growth was higher than in 2012 (0.6%), but lower than the annual average since 2000 (2.5%) [3]

Other evidence of the future energy crisis is global CO₂ emissions from non-renewable fuels, which were 5.5 Gigatonnes in 2013, 68% more than in 1990 [3]. This is another strong indication for switching to alternate forms of energy.

Among the energy alternatives that have been studied for the replacement of fossil fuels are hydrogen, natural gas, synthesis gas and biofuels, the latter being the most environmentally friendly source of energy, come from renewable sources, are biodegradable and their low gas emissions are acceptable [4, 5]

Biofuels, in conjunction to their positive carbon balance with regards to fossil fuels, represent a significant potential for sustainability and economic growth of industrialized countries because they can be generated from locally available renewable material. Biofuels are usually classified as; First-generation biofuels are directly related to a biomass that is generally edible; Second-generation biofuels are defined as fuels produced from a wide array of different feedstock, ranging from lignocellulosic feedstocks to municipal solid wastes. Meanwhile, third-generation biofuels which are, at this point, related to algal biomass but could to a certain extent be

linked to utilization of CO₂ as feedstock [6]. Among the most representative liquid biofuels we can find biodiesel and bioethanol.

Ethanol as a renewable and environmentally friendly fuel has attracted significant interest. In recent years ethanol production in the United States has increased from 4.89 billion gallons in 2006 to 14 billion gallons in 2011, indicating an almost threefold increase. Similar increases have occurred in other countries such as China and India [7]. General scheme of bioethanol production is shown in Fig. 1.

A key step for an efficient bioethanol production is the fermentation process [8,9]. Ethanol fermentation can be performed in batch, fed-batch, and continuous modes. The batch fermentation consist in a closed culture system, the fermentation mixture is added into fermenter without removal of media during fermentation, and products are collected at the end of the process. This method has some disadvantages, particularly when microorganisms have either strongly affected by substrate inhibition or have a slow growing [10]. The fed-batch mode is started as a batch mode with a small amount of biomass and substrate in the fermenter. Then, a feeding medium is fed, stepwise or continuously, to the fermenter when most of the initially added substrate has been consumed. This process can increase the total substrate content in the fermenter while maintaining a low substrate concentration during fermentation to reduce the negative effects of osmotic pressure on yeast. The advantages of this process include reduction of substrate inhibition, higher productivity, shortened fermentation time, and reduction of toxic effects of the medium components, which are present at high concentrations [11].

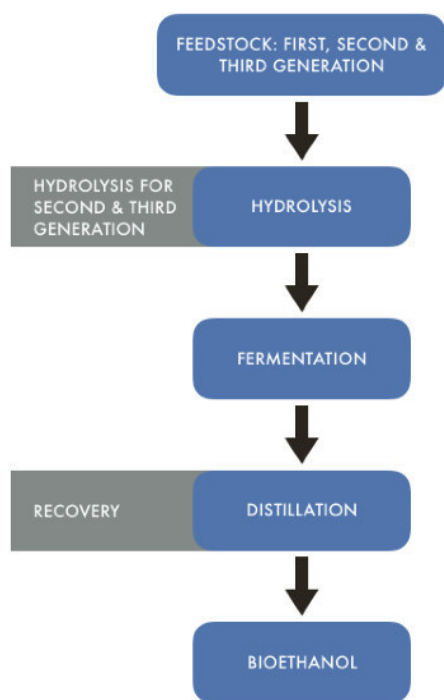


Figure 1. General scheme of bioethanol production.

Furthermore new technologies like electro-fermentation can optimize fermentation metabolisms by controlling imbalances due to substrate purity, redox / pH conditions, byproduct accumulation, etc., establish oxidative or reductive conditions to drive carbon chain breakdown or elongation; increase ATP synthesis and improve microbial biomass yield; and extract target products by selective membranes. [6] In principle to support metabolism, all organisms need an electron donor and acceptor. An alternative way is supplying or subtracting electrons through direct electrochemical means to the microbial cell metabolism [12,13]. Microorganisms able to use inorganic compounds as electron donors/acceptors are named lithotrophic (and depending on whether they use organic compounds or CO₂ as carbon source can be either lithoheterotrophic or lithoautotrophic, respectively) [12]. These organisms were demonstrated to have the particular capacity of using solid conductors as electron donors or acceptors [14]. This effect can be achieved via direct extracellular electron transfer (EET) and transmembrane transport, using nanowires, cytochromes, NADH-ubiquinone oxidoreductase, hydrogenase, and other membrane-bound enzymes [15–17]. EET, as well as transmembrane transport to the cytoplasm, can also be mediated by specific molecules [13,16]. Soluble redox mediators (e.g., thionin, neutral red, methyl viologen, riboflavins, humic acids, etc.) can act as electron shuttles from the electrode surface to the microorganism [12], and also can diffuse through the periplasm to the cytoplasm as reducing/oxidizing agents for the NAD/NADH couple [16]. Through this mechanism, chemo-organoheterotrophic organisms (which normally find electron donors/acceptors in the form of organic molecules and do not use EET as a means of ATP synthesis) can also be electrochemically active [17]

Taking into account the above described fermentation technologies which produce bioethanol, in the near future, should encompass the use of waste materials as potential substrates to extract high value compounds and complement the main industrial biomass utilization platforms [7]. Since electrofermentation is the technique that reports an increase both in ethanol yield and productivity [6]

II. METHODS

A. Reagents and materials

All reagents will be of analytical grade and will be obtained from the Sigma brand (St. Louis, MO, EU) except where noted. Two strains of *Saccharomyces cerevisiae* Will be put into experimentation: Monastery Ale Yeast WLP500 (White Labs, San Diego, CA, USA). and PF-2.

B. Inoculum

Viable *S. cerevisiae* cells will be determined per gram of lyophilized yeast in YPD (1% yeast extract, 2% casein peptone, and 2% glucose) medium at pH 5.5 supplemented with 2% agar by serial decimal dilutions. It will be maintained in 250 mL of YPD medium and then incubated to reach a cell density of 10⁷ or 10⁸ CFU/mL at 150 rpm and 30 ° C, then the cells will be centrifuged at 500 x g for 15 min.

C. Bioreactor design

The fermentation system consists of a modified model of the methodology of Mathews et al., [6] where an electrode and a fermentation mixture is contained in a sealed glass vessel. The electrode consists of a carbon fiber and a copper wire that covers it. The electrode is suspended from the vessel lid and connected to a voltage source (Fig. 2).

D. Fed Batch Fermentation

From results obtained in the fermentations by batch the best conditions will be used to start the culture by fed-batch. For small-scale batch fermentation, 500 mL initial batch (as shown in Figure 5) will be fed continuously at different rates (2-8 g L⁻¹ h⁻¹) with a different glucose solution C / N (10-50). The cultures will be incubated at the appropriate temperature for each yeast and will be static cultures (Fig. 3)

E. Analytical methods

Cell viability will be determined using the methylene blue method and a hemocytometer [18]. For biomass tests, the cells will be washed, filtered and dried at 70 °C to constant weight. The fermented broth will be centrifuged at 13,000 rpm for 10 minutes and the supernatant will be tested for total and reducing sugars by phenol-sulfuric acid method [19] and dinitrosalicylic acid method (DNS) [20], respectively. The sugar concentration will be calculated using standard curves and expressed in grams of sugar per liter. Ethanol production will be determined by simple distillation and by refractometry.

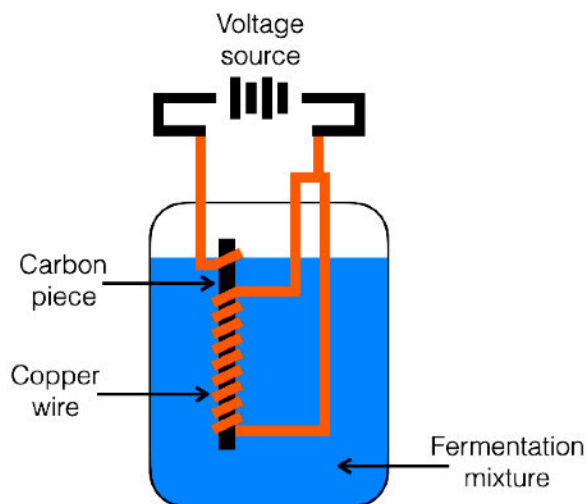


Figure 2. Proposed design for the electrostatic fermentation system.

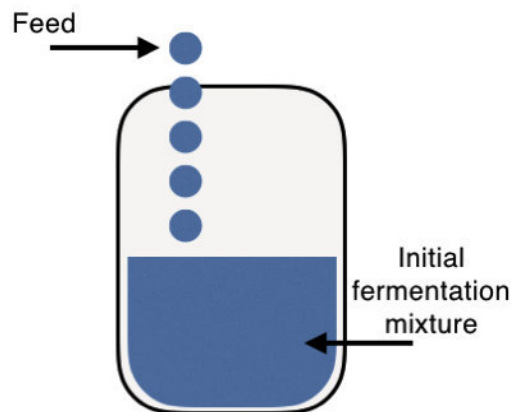


Figure 3. Fed-Batch illustration.

F. Statistic analysis

All determinations will be made in triplicate and reported as the mean of the trials. The experimental design and comparison of measures (with $p < 0.05$ as the significant minimum level) were performed using software J.M.P 5.0.1 (2002, SAS Institute Inc., Cary, NC, USA).

G. activity diagram

The activity diagram is planned for the part of experimentation and obtaining results (Fig. 4).

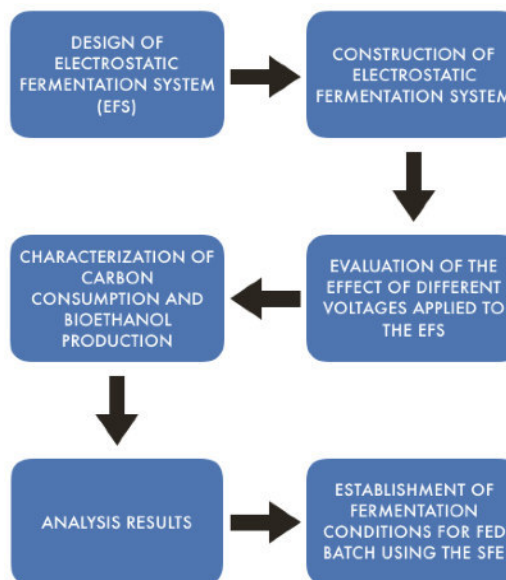


Figure 4. Activity diagram for experimentation and obtaining results.

The present work is the protocol proposal for master's thesis and results will be obtained soon. Based on the literature reviewed, investigations related to voltage-to-fermentation applications have succeeded in modulating the mechanism of yield and production of several metabolites that are attributed to extracellular electron transfer, a transmembrane transport, cytochromes, and other membrane-bound enzymes. However it is necessary to study in greater detail all the routes involved for a better understanding of the metabolic pathways involved [6]. On the other hand, the use of batch-fed fermentations has shown advantages over traditional fermentations such as increased bioethanol production and yield, lower concentration of residual sugars, as well as lower toxicity and greater cell viability [21]. An additional proposal to this research work is the generation of a repeated fed batch, that is to say, combining the different fermentation systems to know the yeast response to the carbon consumption, production and productivity of bioethanol.

REFERENCES

1. R. Potumarthi, R. R. Baadhe, and S. Bhattacharya, "Fermentable Sugars from Lignocellulosic Biomass: Technical Challenges," in *Biofuel Technologies: Recent Developments*, 2014, pp. 3–27.
2. W. H. Liew, M. H. Hassim, and D. K. S. Ng, "Review of evolution, technology and sustainability assessments of biofuel production," *J. Clean. Prod.*, vol. 71, pp. 11–29, 2014.
3. International Energy Agency (IEA), "CO₂ Emissions From Fuel Combustion," IEA Publ., 2015.
4. H. N. Bhatti, M. A. Hanif, M. Qasim, and Ata-ur-Rehman, "Biodiesel production from waste tallow," *Fuel*, vol. 87, no. 13–14, pp. 2961–2966, 2008.
5. P. S. Nigam and A. Singh, "Production of liquid biofuels from renewable resources," *Prog. Energy Combust. Sci.*, vol. 37, no. 1, pp. 52–68, 2011.
6. A. Schievano, T. P. Sciarria, K. Vanbroekhoven, H. De Wever, S. Puig, S. J. Andersen, K. Rabaey, and D. Pant, "Electro-Fermentation – Merging Electrochemistry with Fermentation in Industrial Applications," *Trends Biotechnol.*, vol. 34, no. 11, pp. 866–878, 2016.
7. A. S. Mathew, J. Wang, J. Luo, and S.-T. Yau, "Enhanced ethanol production via electrostatically accelerated fermentation of glucose using *Saccharomyces cerevisiae*," *Sci. Rep.*, vol. 5, no. October, p. 15713, 2015.
8. F. W. Bai, W. A. Anderson, and M. Moo-Young, "Ethanol fermentation technologies from sugar and starch feedstocks," *Biotechnol. Adv.*, vol. 26, no. 1, pp. 89–105, 2008.
9. L. Laopaiboon, P. Thanonkeo, P. Jaisil, and P. Laopaiboon, "Ethanol production from sweet sorghum juice in batch and fed-batch fermentations by *Saccharomyces cerevisiae*," *World J. Microbiol. Biotechnol.*, vol. 23, no. 10, pp. 1497–1501, 2007.
10. G. Najafpour, H. Younesi, and K. S. Ku Ismail, "Ethanol fermentation in an immobilized cell reactor using *Saccharomyces cerevisiae*," *Bioresour. Technol.*, vol. 92, no. 3, pp. 251–260, 2004.
11. N. Phukoetphim, A. Salakkam, P. Laopaiboon, and L. Laopaiboon, "Improvement of ethanol production from sweet sorghum juice under batch and fed-batch fermentations: Effects of sugar levels, nitrogen supplementation, and feeding regimes," *Electron. J. Biotechnol.*, vol. 26, pp. 84–92, 2017.
12. K. Rabaey and R. A. Rozendal, "Microbial electrosynthesis - revisiting the electrical route for microbial production," *Nat. Rev. Microbiol.*, vol. 8, no. 10, pp. 706–16, 2010.
13. J. C. Thrash and J. D. Coates, "Review : Direct and indirect electrical stimulation of microbial metabolism," *Crit. Rev.*, vol. 42, no. 11, pp. 3921–3931, 2008.
14. D. R. Lovley, "Powering microbes with electricity: Direct electron transfer from electrodes to microbes," *Environ. Microbiol. Rep.*, vol. 3, no. 1, pp. 27–35, 2011.
15. G. Reguera, K. D. McCarthy, T. Mehta, J. S. Nicoll, M. T. Tuominen, and D. R. Lovley, "Extracellular electron transfer via microbial nanowires," *Nature*, vol. 435, no. 7045, pp. 1098–1101, 2005.
16. F. Kracke and J. O. Krömer, "Identifying target processes for microbial electrosynthesis by elementary mode analysis," *BMC Bioinformatics*, vol. 15, no. 1, p. 410, 2014.
17. F. Kracke, I. Vassilev, and J. O. Krömer, "Microbial electron transport and energy conservation - The foundation for optimizing bioelectrochemical systems," *Front. Microbiol.*, vol. 6, no. JUN, pp. 1–18, 2015.
18. B. W. Zoecklein, K. C. Fugelsang, B. H. Gump, and F. S. Nury, *Wine Analysis and Production*. 1999.
19. M. Mecozzi, "Estimation of total carbohydrate amount in environmental samples by the phenol-sulphuric acid method assisted by multivariate calibration," *Chemom. Intell. Lab. Syst.*, vol. 79, no. 1–2, pp. 84–90, 2005.
20. G. L. Miller, "Use of Dinitrosalicylic Acid Reagent for Determination of Reducing Sugar," *Anal. Chem.*, vol. 31, no. 3, pp. 426–428, 1959.
21. H. Zabed, J. N. Sahu, A. Suely, A. N. Boyce, and G. Faruq, "Bioethanol production from renewable sources: Current perspectives and technological progress," *Renew. Sustain. Energy Rev.*, no. October 2015, pp. 1–27, 2017.

Simulation and Assessment of Cable Tension Forces in a Cable-Stayed Bridge

Anaya Díaz M.¹, Pérez Lara y Hernández M. A.¹, Quintana Rodríguez J. A.², Carrión Viramontes F. J.², Horta Rangel J. ¹, Arroyo Contreras M. ¹

¹ Facultad de Ingeniería, Universidad Autónoma de Querétaro, Querétaro, Querétaro. anayadiaz.uaq@gmail.com, migperez@uaq.mx, marroyoc@uaq.mx, jaimhorta@prodigy.net.mx

² Instituto Mexicano del Transporte, Sanfandila, Querétaro. jaquintana@imt.mx, carrión@imt.mx

Abstract-- One of the most important aspects to evaluate in a cable-stayed bridge is the performance of cables, in this paper is presented a vibration test procedure to determine the tension force in 24 cables of Mezcala Bridge, a cable-stayed bridge in Guerrero, Mexico. The results obtained from these experimental tests are used to calibrate a finite element model in order to obtain and evaluate the tension force in the remaining cables. Additionally, it is presented the employment of an iterative calibration procedure.

Keywords: Cable-stayed bridges, Ambient vibration tests, Finite element model calibration, Cable tension assessment.

I. INTRODUCTION

Accurate simulation of the behavior of real structures through the Finite Element Method (FEM) is a complex activity due the variability of material properties, the current geometry and dimensions could differ from those described in structural prints, presence of damage, construction defects and own limitations of the FEM software to simulate certain boundary conditions and/or the element physics. In order to obtain a precise finite element model of a real structure it is required a calibration procedure that permits to identify the most adequate structural parameters and an experimental procedure used to obtain the response of the structure.

Calibrated finite element models can be used to predict the static and dynamic response of the structure under new load scenarios, damage detection, repair actions management and to improve the remaining life predictions of the structure [1].

A considerable amount of research has been developed in the ambit of the assessment of cable-stayed bridges, mainly in the procedures used to obtain natural frequencies and modal shapes in order to evaluate the structure dynamic performance [2], the dynamic performance of a cable-stayed bridge was investigated by Brownjohn [3] where the ambient vibration testing showed to be the most appropriate for obtain the modal parameters for this kind of structures, another widely used procedure is the impact testing, where the structure is excited in certain locations of interest using impact hammers or another kind of devices [4]. From modal experimental procedures it can be obtained the natural frequencies of the stay cables, these are very important due they are related to the cable

tension force, the assessment of this forces are very important for the reliability and conservation of cable-stayed bridges [5-6].

For large systems it is very difficult or expensive to measure the entire cable natural frequencies thus it is required to simulate the entire structure behavior using a calibrated finite element model. The most used finite element calibration methods are the sensitivity based methods [7], where the parameter identification inverse problem is solved using Gauss-Newton algorithms, Huynh [8] used the dynamic response obtained from the Hwamyung Bridge health monitoring system under the action of two typhoons to identify the changes in structural parameters, Zhang [9] used the ambient vibration procedure and Gauss-Newton method to obtain and calibrate respectively the natural frequencies of Kap Shiu Mun Bridge and Quintana [4] calibrate Rio Papalopan Bridge focusing in wave propagation signals calibration, however, this algorithms are computationally expensive due for each iteration it is required to compute the implicit derivate (sensitivity) for each unknown parameter, thus in this work it is used an iteratively algorithm computationally less expensive than sensitivity based methods.

The main objective of this work is to describe the experimental procedure used to obtain cable tension forces of the instrumented cables of Mezcala Bridge, the finite element modelling, tension force calibration and simulation procedure of the remaining cables.

II. MEZCALA BRIDGE

It is a cable-stayed bridge located in km-221 of Autopista del Sol in the state of Guerrero, Mexico. It was inaugurated in 1993, it consists of six spans, the main span has a length of 312 m and the total bridge length is 940 m. Due its geographic location, vehicular flow and economical importance it is one of the most important bridges in Mexico. The bridge is located in the seismic zone "D", which is the zone with the most intense seismic events in Mexico, also, it is located in the influence zone of the hurricane winds of the Pacific Ocean. The bridge is shown in Fig. 1.



Fig.1. Mezcala Bridge

2.1. Structural Proprieties

The bridge has 140 cables distributed in 12 semi-harps, these are numerated from 1 to 12 and the cables are numerated from inside out the semi-harp. Each cable is composed of 19-31 ASTM A 416 grade 270 strings of 15 mm of individual diameter. The cables are anchored in a concrete H-shaped frame structure. The main deck has a width of 18.5 m and consists of a prestressed concrete slab of 0.30 m thickness supported by two main beams and secondary beams made of steel A-709 grade 50. The concrete compression resistance is 35 MPa.

The structural proprieties of the strings are shown in Tab.1.

TABLE I. STINGS STRUCTURAL PROPIERTIES

Property	Value	Units
Area	0.00014	m ²
Modulus of Elasticity	199.5	GPa
Density	7850	kg/m ³
Mass per unit length	1.102	kg/m
Ultimate Tensile Stress	1,900	MPa

2.2. Structural Health Monitoring

It consists of 36 accelerometers, 16 tiltmeters, 58 strain gages, 11 temperature sensors and 2 displacement sensors. To acquire the information of each sensor it is necessary an acquisition system wich consists of a computer that controls the dara acquisition frequency (125 Hz). The file size, data viewing and the equipment that acquires each sensor values in equally time periods. A scheme of the structural health monitoring system is shown in Fig. 2.

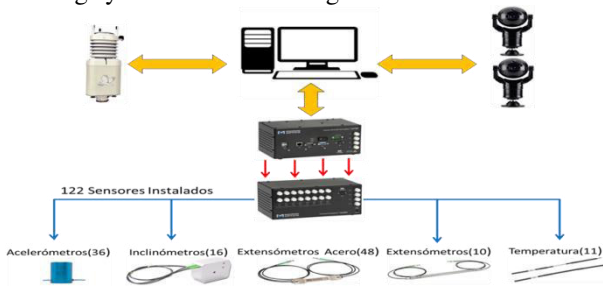


Fig.2. Structural Health Monitoring System of Mezcala Bridge

III. FINITE ELEMENT MODELLING

The finite element model of Mezcala Bridge was developed in the open software StaDyn [10], the principal advantage using this software is the ability of using it in batch mode. The model consist of 8, 804 elements and 3, 666 nodes, the main deck was modeled using triangular plate elements with 6 degrees of freedom in each node [11]. The steel beams, pylons and main piles were modeled using frame elements, each cable was modeled using 8 frame elements [12]. The boundary conditions for the piles was fixed at the base, the right side of the bridge (Acapulco direction) was considered fixed and the left side (Cuernava direction) was considered as a roller support. A view of the main piles No. 5 and 6 is shown in Fig.3.

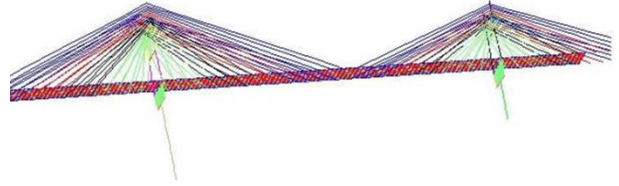


Fig.3. Finite element model of Mezcala Bridge (Main piles No.5 and 6)

IV. THEORICAL MODELS TO DETERMINE TENSION FORCE

The linear model is a vibration based mathematical approach that has demonstrated to be adequate to determine the tension force in cable-stayed bridges [5-6].

The fundamental duequation that describes the free vibration (y) of a rope or cable with a mass (m) submitted to a tension (T) is:

$$\frac{\partial^2 y}{\partial x^2} - \frac{m}{T} \frac{\partial^2 y}{\partial t^2} = 0 \quad (1)$$

From (1) is performed a modal analysis to determine the natural frequencies whose value is given by:

$$f_n = \frac{n}{2L} \sqrt{\frac{T}{m}} \quad (2)$$

Where L is the cable length and n is the associated mode. The tension force (T) in function of the first mode is given by:

$$T = m(2L f_1)^2 \quad (3)$$

For large deformations and to evaluate various levels of tension then the non-linear model can be used, however, it has been demonstrated that in cable-stayed bridges this model presents small variatios compared with the linear model (3%), thus in this work it will be used only the linear model to determine tension forces.

V. EXPERIMENTAL PROCEDURE

The procedure consisted in use the dynamic response of each instrumented cable under normal operation conditions of the bridge, the accelerometer used in cables is shown in Fig. 4.



Fig.4. Accelerometer in cable

The structural response of a time period of 15 days was analyzed obtaining a total of 10, 660 frequency data, the frequency distribution is shown in Fig.5. Each of this frequencies was obtained using a Fast Fourier Transform that analyzes an acceleration vector obtained in a time period of 2 minutes acquiring at 125 Hz.

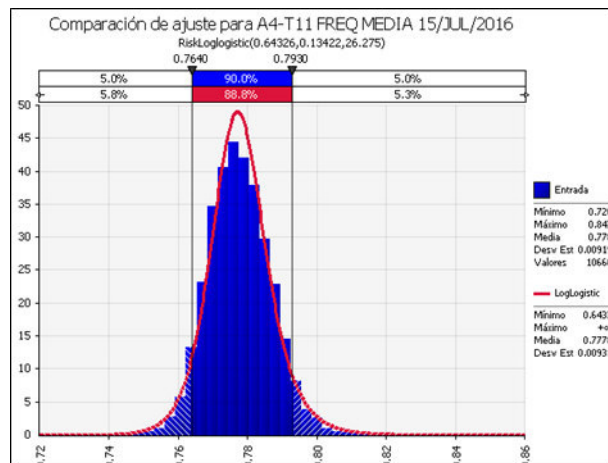


Fig.5 Statistical distribution of frequencies.

Using this procedure it was obtained the natural frequencies of the 24 instrumented cables, it is shown in Fig.5. The semi-harps S1 to S6 are located mainstream and S7 to S12 are located downstream.

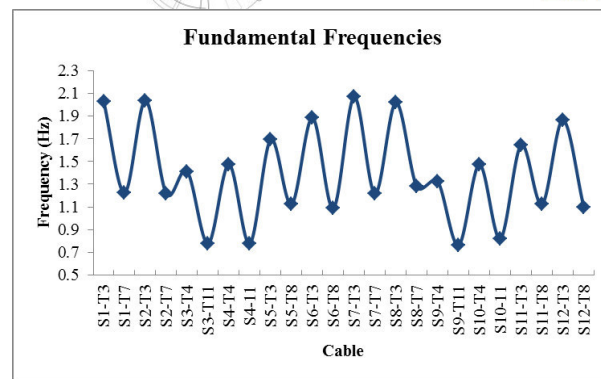


Fig.6 Measured fundamental frequency of instrumented cables.

5.1. Cable tension forces

To measure the cable tension forces it is necessary to know the structural properties of all the cable materials: strings, sheath and the filling. The strings properties were shown in Tab. (1), the sheaths are 20 cm diameter pipes made of Polyethylene with a density of 970 kg/m³ and the filling consists of an anticorrosive wax. Due the amount of wax in the cable is an uncertainty it is required to estimate it using the bibliography and the finite element model. Vila [13] reported that the influence of the wax in the cables of Tampico Bridge was nearly 20% of the cable weight, using these material properties in (3) it is calculated the tension force for each cable, a comparison between these computed forces and the finite element model is shown in Fig.7.

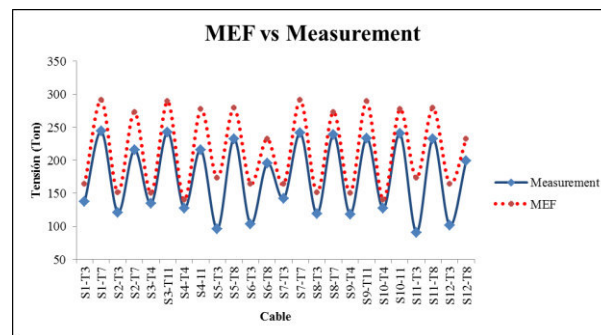


Fig. 7 Experimental tensions of Mezcala Bridge.

There exists considerable differences between the model and the measurements, these differences will be corrected in the model calibration procedure.

VI. FINITE ELEMENT MODEL CALIBRATION

In cable analysis, the cable force is taken to act along inclined cord although the cable sags slightly under its own weight. This flexibility is combined with changes in length to induce inelastic response [14]. For finite element analysis of cable-stayed bridges it is used a straight-line member to model the cables and the effects of sagging are introduced using an reduced cable modulus of elasticity given by:

$$E_{eq} = \frac{E}{1 + \left[\frac{(wL)^2 AE}{12T^3} \right]} \quad (4)$$

Where E is the cable material modulus, L is the horizontal projected length of the cable, w is the weight per unit length, A is the cross-sectional area of the cable, and T is the cable tension, this formula was proposed by Ernst in 1965 [15].

In the finite element model the cable stiffness is given by:

$$C_{stiffness} = \frac{EA}{L} \quad (5)$$

In which E is often replaced by E_{eq} of (4), but in finite element analysis of a real structure there exists other effects that affect the material properties that were previously discussed in the Introduction section, thus in our approach a value of E will be determined using the measurements and an iterative updating algorithm.

6.1. Iterative Algorithm

Traditional sensitivity based model updating seems to be computationally expensive in the sense of in each iteration there is the need of compute each unknown parameter sensitivity [16], in our approach the model calibration is performed through relative increments based in the difference between the measured and simulated tensions forces, this is addressed next:

Let R_i be the relative difference between the experimental and the simulated tension force of the i -th cable:

$$R_i = \left(\frac{T_{m_i} - T_{s_i}}{T_{m_i}} \right) \quad (6)$$

Using (6) it is computed the $n+1$ value for the modulus of elasticity of the i -th cable:

$$E_{i_{n+1}} = E_{i_n} + R_{i_n} * E_{i_n} \quad (7)$$

In each iteration it is computed a new value for E , then the finite element analysis is performed using the new set of updated values and it is evaluated the root mean square error function given by:

$$RMSE = \sqrt{\frac{\sum_{i=1}^N (T_{m_i} - T_{s_i})^2}{N}} \quad (8)$$

Using (8) it is determined a stopping criterion of convergence of the algorithm as:

$$\left| \frac{RMSE_n - RMSE_{n-1}}{RMSE_{ref}} \right| \leq \phi \quad (9)$$

Where $RMSE_{ref}$ is the initial value of the RMSE and ϕ is a very small value that could be taken as 0.001.

6.2. Calibrated tension forces.

The iterative updating algorithm converged in 5 iterations, the RMSE function value for each iteration is shown in Fig. 8.

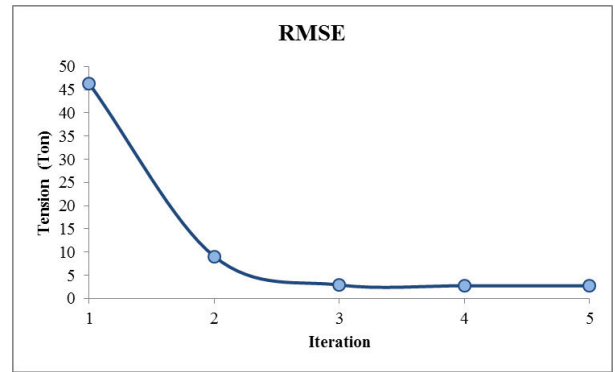


Fig.8. Values of the RMSE function.

The updated values for the cable modulus of elasticity are compared from those that would be obtained using (4), this comparison is shown in Fig.9.

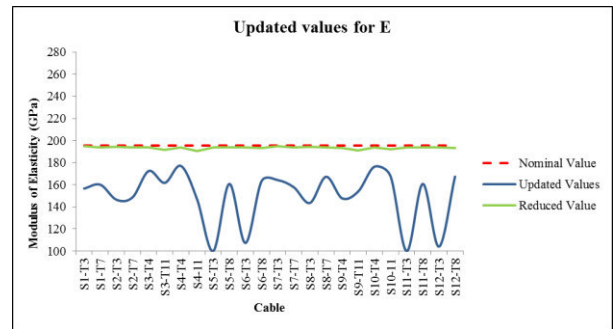


Fig.9. Values of the updated modulus of elasticity.

The effects of sagging seem to be negligible in Mezcala Bridge cable elements, and the updated values of the modulus of elasticity are those that better simulate the actual tension forces. The comparison between the measured and simulated tension forces is shown in Fig. 10.

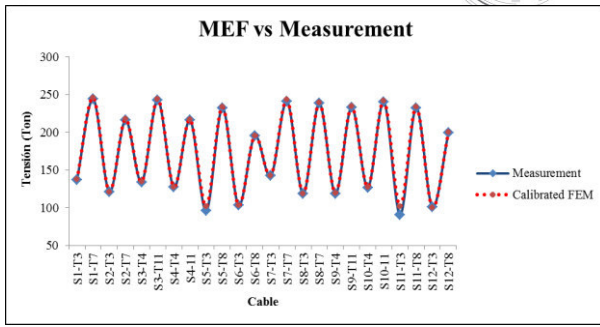


Fig.10. Comparison between the simulated and measured cable tension forces

6.3. Estimation of the remaining cables tension forces.

Based on the updated E values it was estimated the tension force on the 116 remaining cables, the main hypothesis is that the mean of the updated values is valid for all the cables and then there are established confidence interval (C. I.) limits based on the standard deviation as follows:

$$C.I. = mean \pm 2sdv \quad (10)$$

Fig. 11 shows the tension force values simulated in the finite element program and the estimated values of confidence.

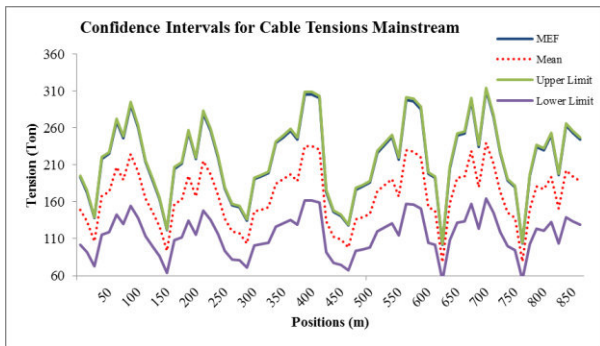


Fig.11a. Confidence intervals for cable tensions mainstream.

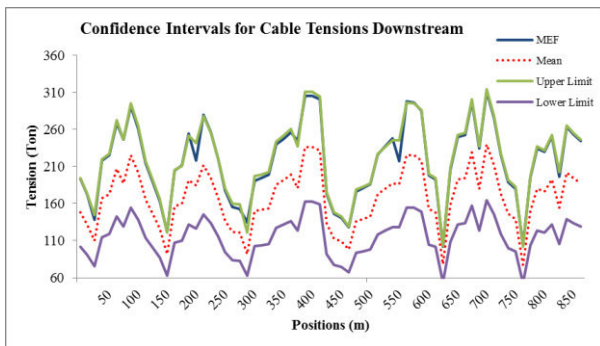


Fig.11b. Confidence intervals for cable tensions mainstream.

In our approach the upper limit confidence interval tension forces match with the finite element simulated tension forces, thus we consider the finite element simulated tensions as the

maximum values that can occur in the bridge based in a confidence interval.

VII. CABLE TENSION ASSESSMENT

Tension in the stay cables should remain within a recommended range of allowable values. A lower bound is necessary to ensure that unseating of a cable does not occur, and an upper bound provides a factor of safety to prevent failure of the cable [17]. The tension in the i -th cable may not exceed $0.7 Tu$ or fall below $0.2 Tu$ where Tu is the rupture tension force. The comparison between the simulated tensions and the critical values for the pile No.4 is shown in Fig. 12.

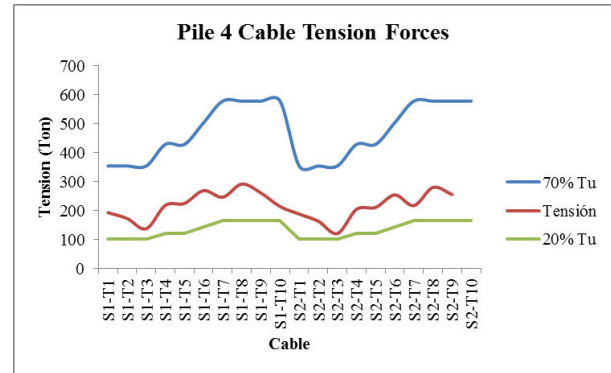


Fig. 12 Tension force comparison of pile no.4 cables.

This scenario is nearly constant on the six harps; all the finite element simulated cable tensions are below the critical and slightly above de minimum, the mean estimated values for cable tensions are above the minimum value of $0.20 Tu$, and the estimated lower limit tensions values are below the minimum value of $0.20 Tu$.

VIII. CONCLUTIONS

In this work it was explored the possibility to simulate the entire cable tension forces of a cable-stayed bridge using limited frequency measurements where it was used a confidence interval criterion based on calibrated values. In total it was analyzed the dynamic response of 24 stay cables of Mezcala Bridge during a time period of 15 days, then it was obtained the cable natural frequencies from this analysis in order to obtain the cable tension forces. The iterative updating algorithm has the potential to minimize the errors between FE simulation and measured tensions, however, it is necessary to validate the measured tensions with data obtained via load tests.

It is necessary yet to perform a dynamic model updating procedure, adjusting the deck, pylons and beams proprieties in order to improve the tension force calibration procedure exposed in this work.

ACKNOWLEDGMENTS

The author would like to express his gratitude to CONACYT and Universidad Autonoma de Queretaro for all the support and to Instituto Mexicano del Transporte for all the facilities, teachings and trust.

REFERENCES

- [1] T. Türker and A. Bayraktar, "Structural safety assessment of bowstring type RC arch bridges using ambient vibration testing and finite element model calibration", vol. 58, pp. 33–45, 2014.
- [2] J. M. W. Brownjohn, P.-Q. Xia, H. Hao, and Y. Xia, "Civil structure condition assessment by FE model updating: methodology and case studies," *Finite Elem. Anal. Des.*, vol. 37, no. 10, pp. 761–775, 2001.
- [3] J. M. W. Brownjohn, J. Lee, B. Cheong. "Dynamic performance of a curved cable-stayed bridge". *Engineering Structures*. p.p. 1015-1027, 1998.
- [4] J. A. Quintana, "Análisis del Método de Búsqueda Global para la detección de daño y monitoreo estructural de puentes", Instituto Mexicano del Transporte, Publicación Técnica. no. 367, 2012.
- [5] F. J. Carrion, J. R. Hernández, J. Teran, "Estudio Experimental De Un Puente Atirantado," Instituto Mexicano del Transporte, Publicación Técnica no. 265, 2005.
- [6] W. Ren, H. Liu, G. Chen. "Determination of cable tensions based on frequency differences". *Engineering Computations*, p.p. 172-189, 2007.
- [7] M.I. Friswell, J.E. Mottershead, "Finite Element Model Updating in Structural Dynamics," Springer Science, 1995.
- [8] T. Huynh, J. Park, and J. Kim, "Structural identification of cable-stayed bridge under back-to-back typhoons by wireless vibration monitoring," *Measurement*, vol. 88, pp. 385–401, 2016.
- [9] Q. W. Zhang, T. Y. P. Chang, C. C. Chang. "Finite-element model updating for the Kap Shiu Mun cable-stayed bridge". *Journal of Bridge Engineering*, p. p. 285–293, 2001.
- [10] J. F. Doyle. "Static and Dynamic Analysis of Structures". Kluwer Academic Publishers. 1991.
- [11] P. G. Bergan, C.A. Felippa. "A Triangular Membrane Element With Rotational Degrees of Freedom". *Computer Methods in Applied Mechanics and Engineering*. Vol. 50, pp. 25-29, 1983.
- [12] J. C. Wilson, W. G. Gravelle. "Modelling of a cable-stayed bridge for dynamic analysis". *Earthquake Engineering and Structural Dynamics*, Vol. 20, p.p. 707-721, 1991.
- [13] D.M. Vila, "Determinación de las características estructurales de los cables en dos puentes atirantados," *Sociedad Mexicana de Ingeniería Estructural*, no. Octubre, 2004.
- [14] P. P. Xanthakos. "Theory and Design of Bridges". John Wiley & Sons Inc., p.p. 837-855, 1995.
- [15] J. H. Ernst. "Der E-Modul von Seilen unter Berücksichtigung des Durchhanges". *Bauingenieur*, Vol. 40, No.2, p.p. 52-55, 1965.
- [16] J. F. Doyle, "Modern Experimental Stress Analysis", John Wiley & Sons Ltd, England, 2004.
- [17] J. M. Caicedo, S.J. Dyke, S. J. Moon, L. A. Bergman, G. Turan, S. Hague, "Phase II benchmark control problem for seismic response of cable stayed bridge", *Journal of Structural Control*, Vol. 10, p.p. 137–168, 2003.

Freight Trip Generation in Querétaro City, Mexico

*José Manuel Anza-Álvarez

Autonomous University of Querétaro
Querétaro, México
e-mail: jose.manuel.anzaa@gmail.com

Eduardo Betanzo-Quezada

Professor, Autonomous University of Querétaro
Querétaro, México
e-mail: betanzoe@uaq.mx

Abstract— The understanding of urban freight transport (UFT) and freight trip generation patterns plays a key role to improve its performance as a system. Establishment-based surveys are a specific data collection process helping to understand urban freight operations. We investigate the Freight Trip Generation (FTG) patterns on retail establishments in Querétaro City, México. A survey is applied allowing to carry out statistical analyses, as line/scatter plots and Ordinary Least Squares (OLS) linear regressions. The results show that the surface of the establishment has a stronger relation with FTG than the number of employees. Surveys based on the establishment can provide a considerable amount and variety of data to study the UFT and put in place specific measures.

Keywords—urban freight transport; freight trip generation; establishment-based survey, retail establishment

I. INTRODUCTION

The need of understanding freight travels in cities is due to the strong relationship between human requirements and the land use of the urban territory [1]. Urban freight transport (UFT) has recently become important because of its contributions to social and economic issues, but also because of its negative impacts as traffic congestion, energy consumption, pollution and accidents [2].

Characterizing the urban freight system is a prerequisite for the development of policies and programs to improve its performance. However, this task becomes a challenging attempt due to many factors involved in the freight transport system. Surveys or others forms of data collection are commonly used in public transport, but specific factors affect the effectiveness of freight trip generation studies [3]. Reference [3] provides a list of reasons behind this circumstance:

- a multiplicity of measure to define freight,
- a multiplicity of factors to measure the freight demand generation and freight trip generation,
- a multiplicity of economic agent involved, and

- every agent has its partial point of view of the freight system.

Consequently, researchers have implement different techniques to collect useful data, summarize as follows [4]:

- Establishment-based survey
- Vehicle observation survey
- Freight operator survey
- Parking survey
- GPS data
- Supplier survey
- Traffic counts
- Service provider survey

A prototype establishment-based survey designed to collect data related to off-street loading/unloading maneuvers on small groceries shops is applied. The method is expected to be a useful standard tool to analyze freight delivery patterns, to known the number of freight vehicles arriving to retail establishments, to measure loading/unloading times, and to know the characteristics of freight trips. One of the negative externalities of urban freight transport is the generation of heavy traffic, since the suppliers generally have problems finding a place to park in front of or near each establishment in a route distribution. In addition, we investigate how surface of the establishment influences the FTG, as well as the number of employees.

The proposed establishment-based survey was applied in a congested area of the historical center of Querétaro City, which may be useful for planning infrastructure purposes.

II. LITERATURE REVIEW

A. Establishment-based survey design

Even though the establishment-based surveys are very useful in the field of UFT, there is no technical standard about structure-content, sampling method or the implementation process of such kind of survey [5]. Allen and Browne [4] affirm that the lack of technical standard is due to the fact that many research reports are not available to the public or professional individuals and the difficulties to get access to scientific or applied literature. Although the studies could attempt similar purposes, the objectives may differ and the influence of the urban zone can be decisive, therefore the surveys need to be adjusted fitting to the researchers' purposes.

According to Ogden [6] the importance of getting UFT data depends on: topic study, the planning and policy framework in which the issue arises, the established model to get data and the previous availability of collected data. Routhier and Toilier [7] propose three basic requirements for the definition of an adequate data collection process: coherence, relevance and measurability. Alho and e Silva [5] affirm that the balance among these attributes will be the effectiveness in the chosen methodology. The perfect link between the objectives of the collection data process and the structure-content surveys is a reflection of coherence and relevance. Measuring capability is assumed to be implicit in the survey design. Hence, the factors defined by Ogden [6] are considered as determinant in the structure and content of a useful survey.

B. Two survey designs based on establishments

Holguín-Veras et al. proposed an example of this kind of survey in 2012 [8]. This survey was designed for stores that provide goods and services to their customers. The main objective of this survey was to generate information about the freight trip generation (FTG), as well as the origin or destination from the stores. Later, the survey analyzes the relation between the FTG and the size of the store according to the numbers of employees and area of the store, which are important determinants of the freight generation (FG).

Betanzo [9] designed a survey for Mexican cities in 2015. This survey was designed in the frame of a research project dealing with indicators for UFT performance in Mexican cities supporting energy and sustainable development policies. With a wider scope, the Betanzo's survey aims to be more comprehensive than others currently available. Betanzo's survey has a set of questions that give more essential information for this research, such as the amount of trucks arriving to the stores, size of the store measured by the number of employees and area, and so on.

Betanzo's survey is divided into four sections. The first section collects get general data from the retail store, in order to further use Geographic Information Systems. The second section pursues to gather information about the total number of freight vehicles and the mix traffic counts during off street observation periods. Betanzo suggests a thirty minutes of off-street observation since it's the usually spent time for loading and unloading operations. The third section gives a detailed

view of the contiguous road infrastructure where the retail store is situated, with the purpose of recognizing road infrastructure facilities, as off-street parking spaces or related signals. The last section deals with two variables commonly used to estimate freight trips: effective surface (area) of the establishment and the number of employees they have.

III. RESEARCH METHODOLOGY

A. Characteristics of Querétaro city

According to the National Council of Population (known as CONAPO in Mexico), Querétaro is ranked as the 10th more populated metropolitan area in the country [10]. Consequently, the urban good transport needs to be better organized and city planners have to address feasible strategies to cope with environmental impacts, and to enable more efficient supply goods to fulfill increasing consumer needs within this agglomeration.

In addition, the historical downtown enclose a great value monument zone acknowledged by the United Nations Educational, Scientific and Cultural Organization (UNESCO) since 1996. For this reason it is crucial to study the UFT in order to reduce the negative impacts generated by both commercial and service activities. The study area is bordered at North by Universidad Avenue, at South by Zaragoza Avenue, at east by Circunvalación Avenue and at west by Tecnológico Avenue. The Fig. 1 shows the delimited area of study.

B. Surveyed establishment

In order to choose the kind and number of establishment situated in the zone of study for the survey, first of all it was checked the North American Industry Classification System, Mexico (NAICS) [11], as it is a common classification system used in Canada, United State and Mexico. Since there is a common basis, it is possible to compare statistics among the three countries.

As literature reports that grocery shops have an important influence on the generation of freight traffic in a city, the survey focused on retail establishments of perishables such as milk, cheese, cream, sausages, sweets, cookies, bread, cake, snacks, fried foods, canned products, bottled purified water, soft drinks, wine and liquor packaged, cigars, egg, toilet paper, detergent, soap, paper napkins, and disposable kitchenware [11]. The NAICS structure to which it belongs can be seen in Table I.

TABLE I. NAICS STRUCTURE OF THE ESTABLISHMENT UNDER STUDY, WITH ACTIVITY CLASS CODE.

Level	Code	Titles of categories
Sector	46	Retail trade
Subsector	461	Retail trade of groceries, food, bevegares, ice and tobacco.
Industry sector	4611	Retail trade of groceries and food.
Industry	46111	Retail trade in grocery stores
National Industry	461110	Retail trade in grocery and miscellaneous stores.

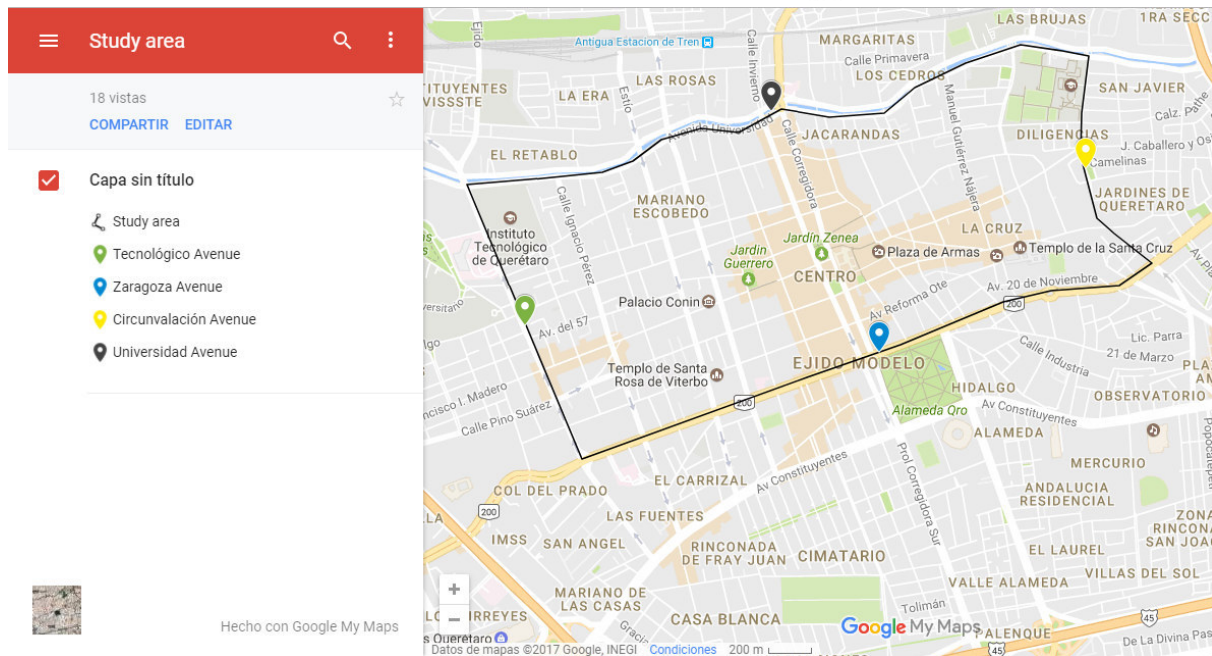


Fig. 1. Study Area (map courtesy of Google Maps)

The National Yearbook of Economic Units (known as DENUE in Mexico) was used to identify the establishments, classed as code 461110 located in the study area. According to DENUE [12] the total number of establishments within the study area was 106. However, we reduced that number at 103 due to duplicated registers. In addition, the DENUE also provided the name of the establishments, the geo-coding address of them. Once the prototype of survey was reviewed, the next step was to adapt it and to execute the field survey.

C. Design of the Establishment-based survey

Betanzo designed the prototype survey applied in 2016 [13]. This format was selected because it met the two objectives of the data collection process:

- Freight trip generation (FTG): assuming FTG as the number of vehicles arriving to commercial establishments with the purpose of unloading freight in a given period of time. The survey designed by Betanzo allows us know this information.
- Characterization of the establishment under study: the selected survey has a set of indicators addressing on the performance of the UFT, making possible to characterize the establishment under study.

Given that the original survey has a length that doesn't make not literally copy in this paper, a summarized description of its structure is presented:

- General data establishment: Name, street and number, neighborhood, municipality, zip code and X & Y geo-references.
- Specific characteristic of FTG and the establishments: number of delivery freight trips or unloading

operations, number of employees at shop, effective surface at shop in square meters.

- Loading and unloading patterns: Day of the week that freight vehicles arrives the most, hour of the day that freight vehicle arrives the most, loading and unloading time, and type of vehicle most used for freight trips.
- Face-to-face opinion about loading and unloading operations and its difficulties at the shop surrounding.
- Others as own parking space for loading/unloading operations, electronic devices for on-line shipping order, and so on.

D. Statistical Analysis

In order to treat, analyze and understand the data obtained in the survey, descriptive statistic was used as a basic method to provide a better interpretation of the data collected. Descriptive statistics covers tabular, graphical and numerical methods. Using those methods, the establishment indicators were characterized within the study area.

IV. RESULTS AND DISCUSSION

A. Overview of retail establishments

Providing an overview of the characteristics of retail establishments, allows us to better understand the case study, as well as to provide information for comparisons purposes among other research studies.

One hundred and three establishments were visited, thirty one of them were disposed to participate in the study, reaching a 30% of responses rate. The reasons expressed by the

employees of the establishments when they were not willing to participate were the following:

- Lack of time
- Establishment's Policies

The total establishments surveyed don't belong to any chain or franchises business, and its size is generally small; 84% of the establishments don't have an effective surface (area) bigger than 24 square meters. Also, none of the employees mention to have an exclusive area for products storage, so the stock available is on racks. The typical establishments have just one employee, in 52% of the establishments surveyed that person was the business owner. That information is important because these small establishments produce considerable FTG in a city [14].

A recurring problem for the establishments visited was that they don't have the sufficient parking infrastructure for trucks to unload delivered goods without affecting local traffic. Sixty-four percent of the people responded that their suppliers always have troubles to park in front or near the establishments. Thirteen percent also reported that their suppliers sometimes have the same problem. The above information confirm the conclusions of other researchers, which revealed figures ranging from 50% to 86% of illegally parked vehicles or likely situations disturbing side traffic in delivery actions [14] [15]. This situation blocks and delays the unloading maneuvers of the trucks. 55% of suppliers spend from 11 to 20 minutes to unload the goods, even 13% can spend from 21 to 30 minutes to do so.

Through the survey, it is also revealed that the most used trucks by the suppliers is commercial or light trucks, with 79% of the cases. This confirms the trend to use light trucks in urban zones. It can be argued that light vehicles are less intimidating that heavy vehicle in urban areas, as their size is more appropriate for the urban environment and street provisions. However, activity levels of light vehicles in urban areas are a reason to concern since it is associated with a number of negative impacts as more urban congestion, more consumption of fossil fuel, and more consumption of large quantities of materials in the manufacture, maintenance and disposal of the light vehicles than heavy vehicles [16]. Since several light vehicles represent only one heavy vehicle.

None of these establishments have parking permission on the roadside, for personal use as well as loading and unloading areas. This is a considerable proportion of establishments that shows dissatisfaction with the current urban support infrastructure.

One-hundred percent of the surveyed establishment perform visual inspections to assess stock levels. This is done is because they don't have optimal inventories, adequate control of how much items they have at hand and sell. Additionally, this could be associated with less than optimum sorting processes that generate a greater number of deliveries [5].

Every retail establishments receive goods directly from the wholesale suppliers, which highlight the tour nature of urban freight deliveries. Basically, this may suggest that while freight trip models can predict the number of freight vehicles that visit the establishments, the total number of vehicles circulating in a given urban area could be considerably lower, since each vehicle will likely make several stops [5].

Other important information observed is that establishments don't accept loading and unloading operations outside the public hour operation, which could be an obstacle to the implementation of out-of hours delivery policies if there is no incentive to change [17]. As well, in this type of establishments, deliveries are inspected on arrival, although it's not known if the carrier waits while this control task is being carried out. If so, this would increase delivery time and traffic disturbances.

On the other hand, 26% of people surveyed declares that the hour of greatest concentration of trucks at site is from 10:00 to 10:59 hours (see Fig. 2). The next two hours of the day don't differ the same amount of incidences. From 11:00 to 11:59 and 12:00 to 12:59 it is observed the same relative frequency ranging from 23% to 20% respectively. It can be inferred that the time from 10:00 to 12:59 reveals bigger concentration of vehicles arriving to establishments, since 69% of the surveyed people match with the same time.

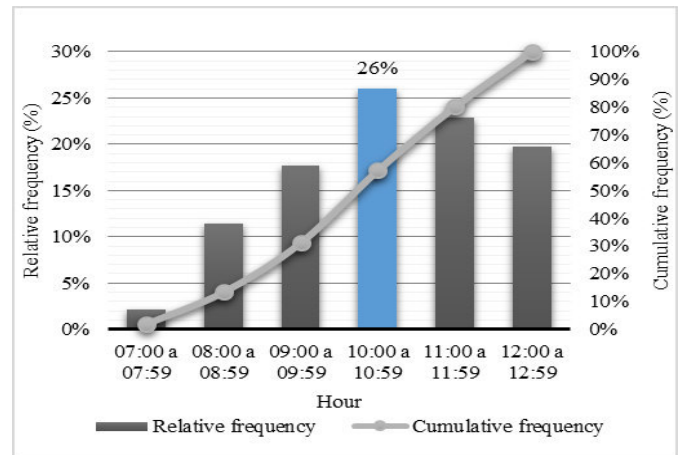


Fig. 2. Time of the day with greater concentration of arriving of trucks to the establishment. Source: Figure made by the author.

The day of the week with the highest concentration of arrivals of freight trucks to establishments is on Monday (see Fig. 3). However, on Tuesdays and Wednesdays they experience a considerable concentration of trucks arriving for delivery purposes. 75 % of the people surveyed answers that Monday, Tuesday or Wednesday are the days with the highest concentration of arrivals of freight trucks.

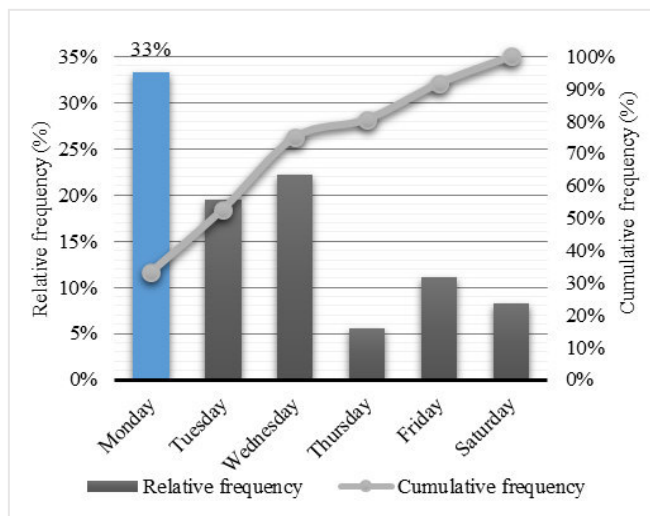


Fig. 3. Day of the week with the greater concentration of arriving freight trucks . Source. Figure made by the author.

B. FTG and its relation with the size of the establishment

Forty five percent of the establishments receive between 5 to 7 deliveries a day. The median of trips for each establishment was 6 a day, a minimum of 2 and a maximum of 12 vehicles. The standard deviation was 3.5.

Table II shows the average, the standard deviation and the correlation coefficient (CC) from the variables: FTG, effective surface (m2) and number of employees. In addition, it is presented the coefficient of determination (r^2) from the results of the linear regression between the total of FTG and the area and the number of employees. The exploration of the variables relation is a crucial step for the demand of freight trips, this make possible the existing parking infrastructure requirements to understand if it is adequate or not.

TABLE II. FTG, SURFACE (M2) AND NUMBER OF EMPLOYEES

		Establishment
Observations		31
FTG		
Average		6.67
Standard deviation		3.55
Coefficient of variation		53.22%
Surface (m2)		
Average		17.52
Standard deviation		7.49
Coefficient of variation (CV)		42.75%
Coefficient of determination (r^2) ^a		0.77
No de employees		
Average		1.74
standard deviation		0.89
Coefficient of variation (CV)		51.15%
Coefficient of determination (r^2) ^a		0.50

^a Regardless to the regressions with FTG as dependent variable.

Comparing the values of the average and the standard deviation, it can be seen that there is a considerable dispersion of data for the variables. The coefficient of variation (CV) confirms this, the area variable with less variability. The model with the lowest CV has predictions closer to the current values. Considering r^2 , the best predictor of FTG is the area of the establishment. However the variable number of employees obtained an r^2 of 0.50, which is not insignificant.

A scatter plot analysis in Figs. 4 and 5 allow a better understanding of the data presented in the Table II. Fig 4 shows how FTG increases along with the surface of the establishment. On the other hand, the number of employees has a weaker relation with FTG (Fig. 5).

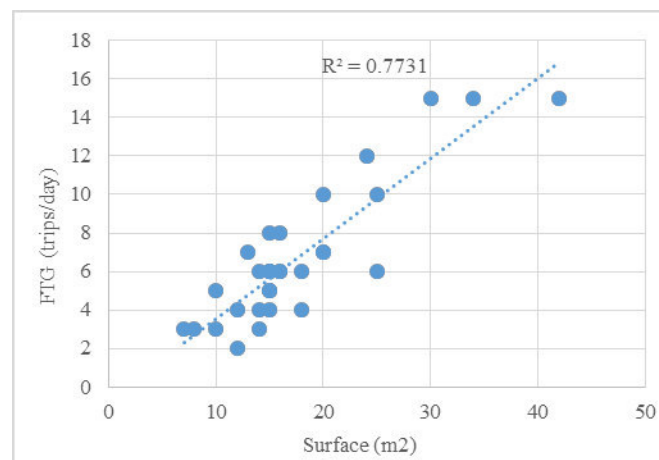


Fig. 4. Relation between the FTG and the effective surface of the establishment. Source: Figure made by the author.

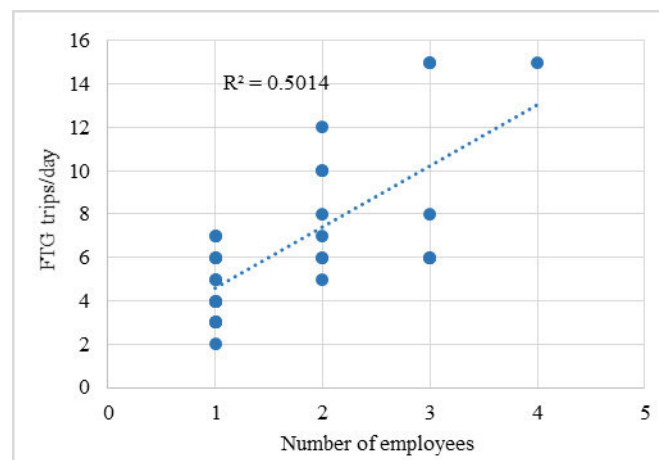


Fig. 5. Relation between FTG and the number of employees. Source: Figure made by the author.

V. CONCLUSIONS

It was confirmed that survey based on the establishment can provide both a considerable amount and a variety of important data to study the UFT. Several new ideas obtained in this study confirm the fact.

The retail trade branch within the Historical Center of Queretaro is mainly small both in the number of employees and business area. However, these establishments generate a considerable freight movement, with a median of 6 trips per day. Since the establishments don't have storage capacity the suppliers have to send goods more frequently.

For the establishment under study, the variable that proved to be the best predictor of FTG was the effective surface area of the establishment, with an r^2 of 0.77. It would be interesting to further compare the results of this survey with others ones worldwide to evaluate if this conclusions are consistent.

Consequently, it's suggested to implement a reconditioning the road infrastructure by reviewing the current parking infrastructure and the conditions under which loading/unloading operations are performed.

ACKNOWLEDGMENT

The National Council of Science and Technology of Mexico granted a scholarship. Professor Eduardo Betanzo Quezada offered additional guidance and support through his project "Indicators of Freight Transport in Mexican Cities to Design Energy and Sustainable Policies" (contract CONACYT PDCPN2013-01-212975). We also thank the Autonomous University of Queretaro (UAQ).

REFERENCES

- [1] C. Lawson, J. Holguín-Veras, I. Sánchez-Díaz, M. Jaller, S. Campbell, and E. L. Powers, "Estimated generation of freight trips based on land use," *Transportation Research Record: Journal of the Transportation Research Board*, no 2269, pp 65-72, 2012.
- [2] E. Betanzo-Quezada, J. A. Romero-Navarrete, and S. A. Obregón-Biosca, "An Index to Evaluate Public Policies in Urban Freight Transport," *Gestión y política pública*, vol. 22, no. 2, pp 313-354, (in Spanish), 2013.
- [3] J. Holguín-Veras, and M. Jaller, "Comprehensive freight demand data collection framework for large urban areas," in *Sustainable Urban Logistics: Concepts, Methods and Information Systems*, pp 91-112, 2014, Berlin Heidelberg: Springer.
- [4] J. Allen, and M. Browne, "Review of Survey Techniques in Urban Freight Studies," Project Report of the Green Logistics: Work Module, 9, 2008.
- [5] A. R. Alho, and J. e Silva, "Lisbon's Establishment-based Freight Survey: revealing retail establishments' characteristics, goods ordering and delivery processes," vol. 7, no. 2, pp 1-17, 2015.
- [6] K. W. Ogden, "Urban goods movement: a guide to policy and planning," 1992, United Kingdom: Ashgate Publishing.
- [7] J. L. Routhier, and F. Toilier, "FRETURB V3, a policy oriented software tool for modelling urban goods movement," in *11th WCTR*. Berkeley, United States, 2007.
- [8] J. Holguin-Veras, M. Jaller, I. Sanchez-Diaz, J. Wojtowicz, S. Campbell, H. Levinson, ... and L. Tavasszy, "Freight trip generation and land use," No. NCHRP Project 08-80, 2012.
- [9] E. Betanzo-Quezada, "Generación de Indicadores de desempeño del transporte de carga en ciudades mexicanas en apoyo al diseño de políticas energéticas y de desarrollo sustentable," in Universidad Autónoma de Querétaro. Querétaro, México: Informe de investigación, 2015.
- [10] Consejo Nacional de Población, INEGI, SEDESOL, Delimitación de las Zonas Metropolitanas de México 2010, Secretaría de Gobernación, México, (In Spanish), 2010.
- [11] INEGI, *Sistema de Clasificación Industrial de América del Norte, México SCLAN 2013*. Aguascalientes: Instituto Nacional de Estadística y Geografía, 2013.
- [12] INEGI. (11 de 12 de 2016). *Directorio Estadístico Nacional de Unidades Económicas*. Obtenido de Directorio Estadístico Nacional de Unidades Económicas: <http://www.beta.inegi.org.mx/app/mapa/denue/>
- [13] J. L. Silva, "Generación de datos sobre el transporte de carga en establecimientos comerciales en la ciudad de Querétaro", in Universidad Autónoma de Querétaro, México, Tesis, 2016
- [14] T. Cherrett, J. Allen, F. McLeod, S. Maynard, A. Hickford, and M. Browne, "Understanding urban freight activity – key issues for freight planning," *Journal of Transport Geography*, no. 24, pp. 22-32, 2012.
- [15] L. Delaitre, "A new approach to diagnose urban delivery areas plans," *Computers & Industrial Engineering* in International Conference on: IEEE, pp. 991-998, 2009.
- [16] M. Browne, J. Allen, T. Nemoto, and J. Visser, "Light goods vehicles in urban areas," *Procedia-Social and Behavioral Sciences*, vol. 2, no. 3, pp. 5911-5919, 2010.
- [17] J. Holguín-Veras, C. Wang, M. Browne, S. Hodge, and J. Wojtowicz, "The New York city off-hour delivery project: lessons for city logistics," *Procedia-Social and Behavioral Sciences*, vol. 125, pp. 36-48, 2014.

Random Number Generator based on electrical noise and implemented on FPGA

González-Abreu A. D., Jaen-Cuellar A.Y., de Santiago-Perez J.J. and Osornio-Ríos R.A.

Facultad de Ingeniería, Campus San Juan del Río.
Universidad Autónoma de Querétaro
San Juan del Río, Querétaro, México
Email: raor@uaq.mx

Abstract— Random numbers have applications in many areas: simulation, game-playing, cryptography, statistical sampling, computation in statistical physics, and modern control techniques applied to mechatronics systems, to name a few. In this paper, sequences of random numbers were generated from samples of electrical noise, the signal taken to seed the random number generator was processed in FPGA, the module implemented receives the analog signal from an electrical noise antenna and transmit the data quantized to the PC via USB in order to obtain the random number. Several experimental tests were performed in which random numbers were generated and stored. These datasets of random numbers were analyzed to prove their randomness; the tests to prove it consist of uniformity and independency. Finally, a statistical test of hypothesis was performed.

Keywords— Random Number Generator; FPGA; Statistical Test of Hypothesis, Electrical noise.

I. INTRODUCTION

Random numbers are essential elements in many applications such as simulation, education, cryptography, arts, numerical analysis, computer programming, testing, recreation, control applications or electronic design applied to mechatronics systems and sampling among others. In addition to the aforementioned, several modern heuristic techniques such as those bio-inspired like Genetic Algorithms (GA), Particle Swarm Optimization (PSO), Evolutionary Programming (EP), Ant Colony Optimization (ACO), Simulated Annealing (SA), among others, require into their procedure the use of random values in order to provide variability and diversity in their iterative processes [1] to the methodology. Moreover, some physical and tabular techniques are used for production of random sequences such is the case of congruential, shift register, lagged Fibonacci, inverse and cellular automata generators [2]. In order to function properly, these applications require many parallel streams of high quality, large periods, uncorrelated uniform random number generators as well as large processing power. FPGA optimized Random Number Generators (RNG) are a more efficient resource than other software RNGs because they utilize the

advantages of bitwise operations and parallelism of the FPGA [3].

There are some researches in the literature that involve different techniques or implementations of random number generators, for example the work presented by [4] is a fully digital high speed ASIC random number generator based on ring oscillators. However, this approach requires of a functionally specific circuitry and no flexibility to adjust the generator is possible for other applications. In the meantime, in [5] was developed a novel design method for discrete time chaos based on true random number generators using skew tent map as a case of study. Upon this approach, a complex scheme is considered making it more difficult to implement. Respect to Pseudo random number generators (PRNG), in [6] a PRNG is presented based on a hardware cryptographic architecture in quantum-dot cellular automata (QCA). For this work the proposed approach was validated by simulation. Otherwise in [7] a study on how certain families of aperiodic infinite words can be used to produce aperiodic pseudorandom number generator with good statistical behavior can be implemented. Regarding the randomness topic, in [8] a study in which an electroencephalogram signal can be treated as a pseudorandom number generator is presented. Meanwhile the work of [9] presents a high speed true random number generator based on open loop structures in FPGAs, this architecture allows higher bit rates while maintaining provable unconditional security, but special care must be taken when routing the delay chain wires. On the other hand, in [10] an approach is proposed to generate the pseudo random number sequences from a single generalized Lorenz chaotic system. This approach is complex and its implementation requires many resources in a digital system. On the other side, [11] proposes a new scheme for generating good pseudo random numbers, based on a quantum logistic map. As a particular observation, there are different methods or techniques to generate sequences of random numbers, the majority of the works take or implement the randomness by complex expressions and schemes. Also, their applicability seems to be compromised because their complexity and the amount of resources required in software or hardware.

In this paper is presented and validated a simple and low-cost RNG, in which the randomness is obtained by reading the electrical signal from a noise antenna. The reading of the noise antenna is performed through a digital-to-analog converter (ADC) and USB communication by describing the hardware modules that drive the ADC, the USB communication, a static random access memory (SRAM) to transmit the data to the PC, in order to obtain the sequence of random numbers. The system presented attempts to be a low cost and low complexity respect to the works mentioned before because this is based on simple elements easy to purchase and implement. The modules that integrate the RNG being described in hardware description language allow a fast data processing, parallel data processing, and re-configurability of the RNG to apply it on any mechatronic problem as required.

II. THEORETICAL BACKGROUND

A. Random Number Generators (RNG)

A random number is one that is drawn from a set of possible values, each of which is equally probable to be picked up, that means it poses a uniform distribution. When discussing a sequence of random numbers, each number draws from the set that must be statistically independent from the others [12]. Random number generators can be divided into two subcategories namely pseudo random (PRNG) or true random numbers (TRNG), which can be further categorized based on their implementation as generated by software or generated by hardware. Regarding the hardware RNGs they can also be separated in two categories as fully digital blocks, and analog blocks; for each one of them there exist various implementation methods. Fig. 1 shows the classification of random number generators according to [4]. PRNGs implement algorithms that use mathematical expressions or simply pre-calculate tables to produce sequences of numbers that appear randomly; TRNGs extract randomness from physical phenomena and introduce it into a computer. In this research, the generation of random numbers based in TRNG is adopted, inasmuch as it is ideal to count with a system simple and easy to use.

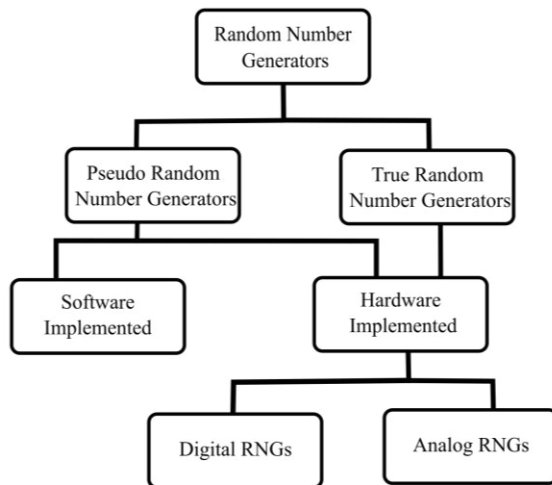


Fig. 1. Classification of random number generators

B. Random Noise Generator

A random-noise generator is just as its name implies: a generator that generates signals of random amplitude and frequency. The fact that these signals are totally unintelligible and unpredictable is the reason why they are simply referred to as noise [13]. Thermal noise is generated due to thermal effects resulting from the interaction between free electrons and the vibrating ions of a material in conduction. The result is an uneven flow of electrons through the medium, which will result in a varying potential across the medium. In most cases, these randomly generated signals are in the microvolt range. A second type of noise is called shot noise; this type of noise is also inherent to any physical substrate and it is caused by the charge of carriers randomly traversing gaps. Shot noise depends on the total amount of current flowing, hence on the voltage applied. It is important to note that shot noise is a result of randomly occurring discrete events, unlike thermal noise [14]. As shot noise source, the barrier typically used is a diode, and there are several noise sources in a reverse-biased diode:

Avalanche noise, is when the diode operates near the breakdown region. Depending on the diode type, two breakdown mechanisms exist, the Zener effect and the avalanche multiplication of carriers.

The Zener effect is mainly observed in highly doped diodes, with a very thin depleted layer. When the reverse voltage reaches several volts, the electric field is high enough to stimulate tunneling. This phenomenon, responsible for shot noise and very little excess noise is pertinent to Zener diodes operating at low voltages (less than about 5 V). Zener diodes are used as reference diodes in low-noise circuits and low – noise regulators [15]

C. Statical Test of Hypothesis

A statistical test of hypothesis consists of five parts:

1. The null hypothesis, denoted by H_0
2. The alternative hypothesis, denoted by H_a
3. The test statistic and its p -value
4. The rejection region
5. The conclusion

The two competing hypothesis are the alternative hypothesis H_a , generally the hypothesis that a researcher wishes to support, and the null hypothesis H_0 , a contradiction of the alternative hypothesis. The statistical test always begins by assuming that the null hypothesis is true. Therefore, the researcher uses the sampled data to decide whether the evidence favors H_a rather than H_0 and selects one of these two conclusions:

- Reject H_0 and conclude that H_a is true.
- Accept (do not reject) H_0 as true

The decision to reject or accept the null hypothesis is based on information contained in a simple drawn from the population of interest. This information takes these forms:

- Test statistic : a single number calculated from the sample data
- p -value: a probability calculated by using the test statistic

These measurements may act as a decision maker for the researcher and help him in deciding either to discard or to accept H_0 .

The entire set of values that the test statistic may assume is divided into two sets, or regions. One set, consisting of values that support the alternative hypothesis and lead to rejecting H_0 , is called the rejection region. The other, consisting of values that support the null hypothesis, is called the acceptance region.

If the test statistic falls into the rejection region, then the null hypothesis is rejected. If the test statistic falls into the acceptance region, then either the null hypothesis is accepted or the test is judged to be inconclusive.

To decide the critical values that separate the acceptance and rejection regions, depends on the amount of confidence that the researcher wants to attach to the test conclusions and the significance level α , the risk to take of making an incorrect decision.

This value α represents the maximum tolerable risk of incorrectly rejecting H_0 . Once this significance level is fixed, the rejection region can be set to allow the researcher to reject H_0 with a fixed degree of confidence in the decision. [16].

D. The Kolmogorov Goodness of Fit Test

A test for goodness of fit usually involves examining a random sample from some unknown distribution in order to test the null hypothesis but the unknown distribution function is in fact a known, specified function. This test is used in this proposed approach with the aim of validating the uniformity of the random values generated [17].

E. Runs Test

A “run” refers to a succession of similar events separated by different events. In this test a “run-up” is a monotonically increasing subsequence and a “run-down” is a monotonically decreasing subsequence. Intuitively, runs of longer lengths should be rare if the samples are random, so this test measures the randomness by examining the distribution of lengths of runs up and runs down. In this manuscript the run test is performed to validate the independency of the random values.

III. METHODOLOGY

The system proposed here to generate a sequence of random numbers is based on the generation of electrical noise

by hardware circuitry (noise antenna) and hardware architectures implemented into an FPGA to obtain this randomness. Fig. 2 shows the general block diagram of the proposed approach.

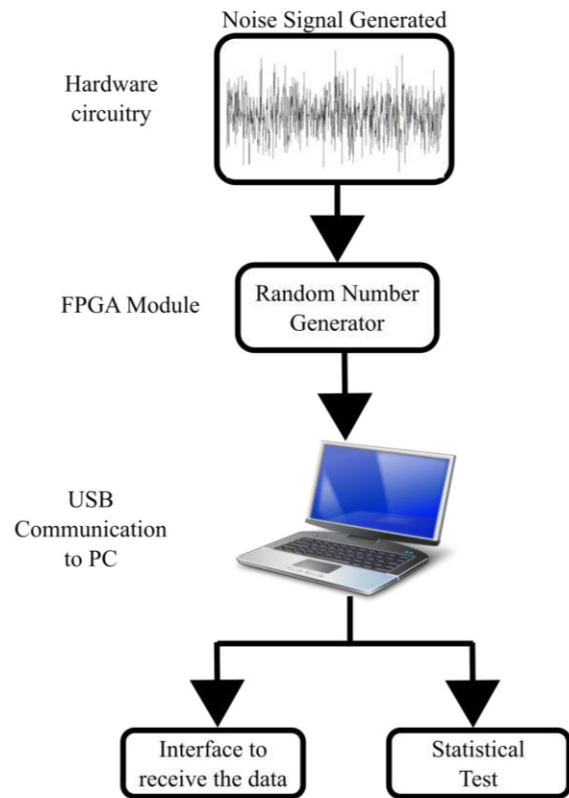


Fig. 2. General block diagram of the proposed methodology to generate random numbers

The first block is the noise signal generated by the hardware circuitry consisting of a noise antenna. In the second block, the electrical noise of the antenna is read and quantized by an ADC converter, leaving a 12 bit representation of the analog noise voltage. The digital read is stored in the FPGA and the random value obtained is then sent to the PC by the USB communication. The third and last block is in the PC, where a user interface is integrated to receive, store and decode the binary words from the FPGA to conform the random values in order to execute the validation. Finally, the randomness of the data is validated through statistical test hypothesis.

A. Noise Generator Circuit

The hardware module implemented to generate electrical noise is shown in Fig. 3, it consists only of two components, a Zener diode and a resistor of high value, the voltage in the resistor is the signal of noise that is desired to obtain.

Fig. 4 shows the physical implementation of this circuit with a resistor of 20 M Ω value, Zener diode 1N4740 and supply with 5V DC.

Fig. 5 shows the noise voltage signal measured and observed in an oscilloscope, it can be noted the random fluctuations of voltage on the signal. The fluctuation of this signal is acquired with the ADC, the levels of this signal based on the measurements observed in the oscilloscope are in the range from 0 to 100 mV or slightly higher values.

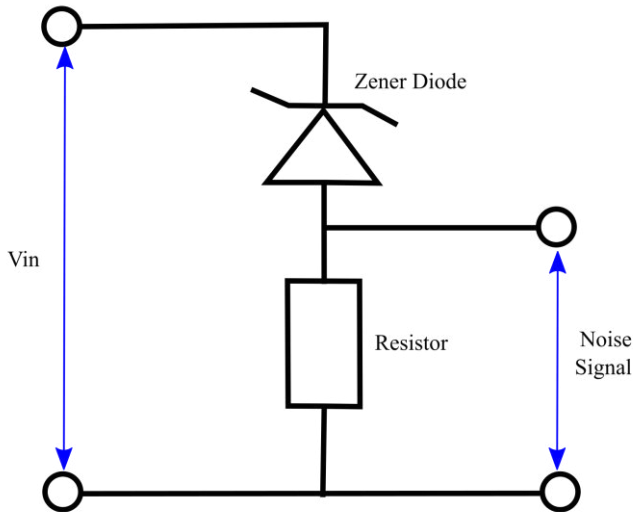


Fig. 3. Noise generator circuit diagram

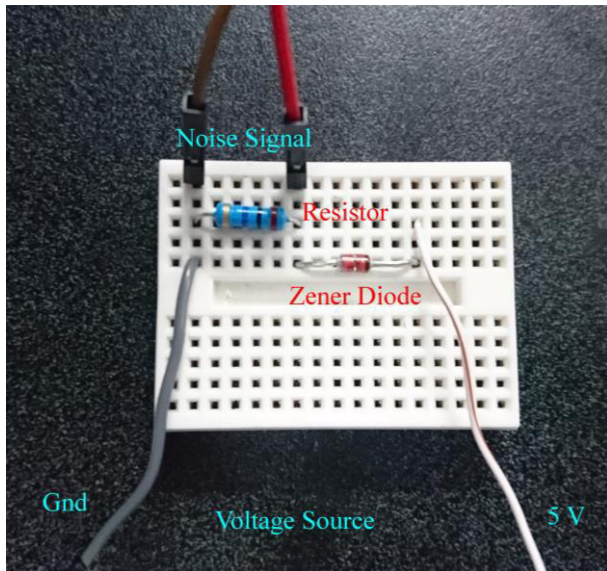


Fig. 4. Noise generator circuit implemented

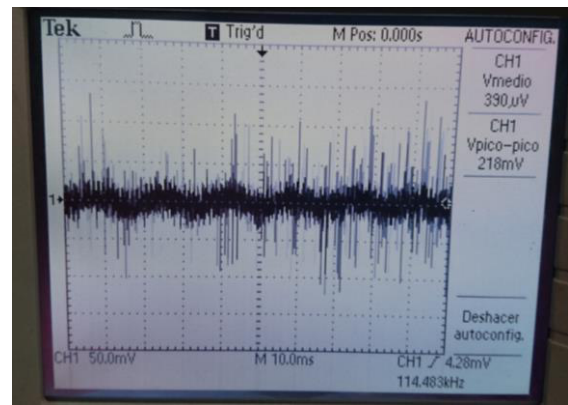


Fig. 5. Noise Signal

B. Random Number Generator in FPGA

The hardware architecture implemented on FPGA starts with the reading from an analog signal of electrical noise generated by a noise circuit, as presented in the last section. The voltage is taken in the resistor; this signal is converted into a digital signal represented in 12 bits of resolution through an analog-to-digital converter ADS7841. The quantized data are stored as the seed to conform the random number through the following procedure: from these 12 bits the interest lies on the four Least Significant Bits (lsb), which changes faster and more frequent due to the noise dynamic. Therefore, four readings from the analog-to-digital converter are stored in a SRAM and the four lsb of every one of the readings are concatenated to form a 16 bits length word, this process is repeated until the system stores the quantity of values needed. Once the SRAM is filled with the random numbers required, they are sent to PC by using a USB communication. Different tests were run in order to store random numbers at different sample frequencies and by using different resistor values for the noise antenna, the tests performed were to sample frequencies of: 1 ms, 10 ms and 100 ms; meanwhile the values of the resistor used in the noise generator circuit were of 6.8 M Ω and 20 M Ω ; three test of each combination were taken, in total 18 test of acquisition of data were executed. The entire hardware architecture integrated and synthesized in the FPGA was developed by using Very High Speed Hardware Description Language (VHDL), the Fig. 6 show the architecture implemented.

The digital structures that integrate the RNG system are controlled by a finite state machine (FSM) module "FSM_RNG", it controls the process and is interconnected with the other modules, there is a timer "Timer ADS" to enable the acquisition of the data through the driver of the ADC converter, named in figure as "drvADS" and a shift register, specified in figure as "Shift Register", take the four lsb mentioned before to form the 16 bit length word that represents the random number generated, an enable register, "Enable Register", allows the load of the 16 bit word and after that, it is stored in the SRAM module "drvSRAM", the quantities of values stored are defined in the address counter "Address Counter", when the SRAM is filled, there a timer, "Timer USB", and additional FSM module, "txFSM", is integrated to transmit the data previously acquired via USB communication, "drvUSB".

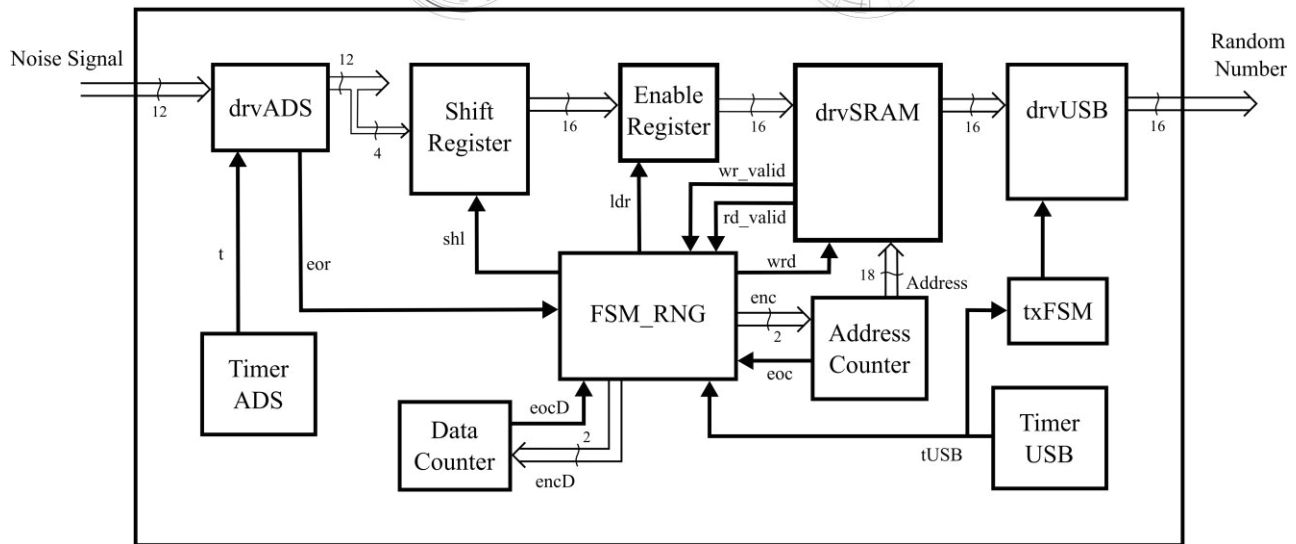


Fig. 6. FPGA hardware architecture for the Random Number Generation process

The module RNG here presented was described in Hardware Description Language (HDL) through Very high speed integrated circuit Hardware Description Language (VHDL) and the principal components used were the finite state machine to control the entire process, the static RAM to store the data and the USB driver for the transmission of the data.

Physically a proprietary FPGA board named DUA-I developed at the Universidad Autonoma de Queretaro was used; this board is oriented to servo systems control and for mechatronics applications in general. This target integrates in its hardware the elements needed to convert, store and transmit the signal of interest. The components used are an ADS7841, a SRAM and USB communication to send data to the PC. Fig.7 shows the physical connexion of the driver modules implemented, it can be seen the noise circuit generator connected to the DUA-I, which has the hardware description to generate the random numbers and later send to PC via USB.

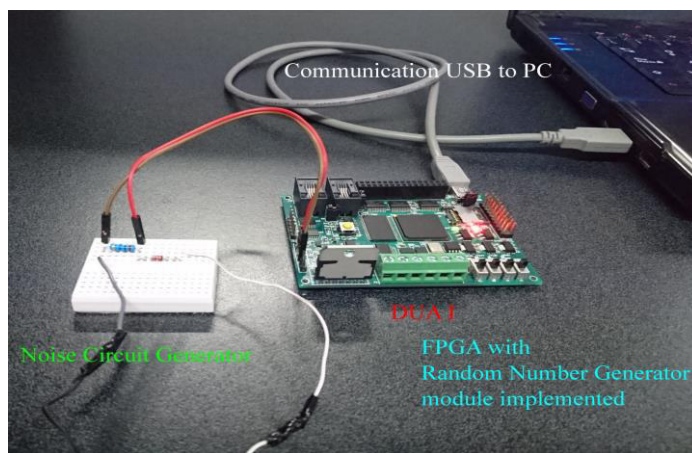


Fig. 7. Hardware implementation of random number generator

C. Communication USB to PC

For this work, a module USB was integrated described in hardware, the selection to integrate this module is due to the property board used have compatibility with the USB module developed.

The communication USB to PC for the transmission of data is also helped with a C++ user interface to recognize the device and send the random numbers. Fig. 8 and Fig 9 show the process when the transmission of data from the DUA-I to the PC is performed, the process first is waiting for data from the FPGA proprietary board, then it displays a message if an error occurs or not in the communication, the amount of data received and the value of data, first in a hexadecimal word, because the transmission is in a packet from of 64 bits word, but only 16 bits are sent. Finally the value in decimal format is shown, this value is the random number. All these numbers sent are stored in a text file.

```
Tipo de error No error
Dato Numero 6
Dato leido = 0 0 0 0 0 0 BE A7
Dato unido = 48807

Esperando por dato de FPGA
Tipo de error No error
Dato Numero 7
Dato leido = 0 0 0 0 0 0 7D D0
Dato unido = 32208

Esperando por dato de FPGA
Tipo de error No error
Dato Numero 8
Dato leido = 0 0 0 0 0 0 DF 5
Dato unido = 57093

Esperando por dato de FPGA
Tipo de error No error
Dato Numero 9
Dato leido = 0 0 0 0 0 0 30 FD
Dato unido = 12541

Esperando por dato de FPGA
```

Fig. 8 Process to transmission data by USB


```

Tipo de error No error
Dato Numero 75
Dato leido = 0 0 0 0 0 0 94 14
Dato unido = 37908

Esperando por dato de FPGA
Tipo de error No error
Dato Numero 76
Dato leido = 0 0 0 0 0 0 ED DE
Dato unido = 60894

Esperando por dato de FPGA
Tipo de error No error
Dato Numero 77
Dato leido = 0 0 0 0 0 0 7A BE
Dato unido = 31422

Esperando por dato de FPGA
Tipo de error No error
Dato Numero 78
Dato leido = 0 0 0 0 0 0 EA 45
Dato unido = 59973

Esperando por dato de FPGA

```

Fig. 9. Process to transmission data by USB

D. Test Hypothesis

The sequences of random numbers generated was of 200 numbers, to prove the randomness, each sequence was validated under two different tests, one of uniform and other to independence, which are the two principal properties to verify the randomness. First, for the uniform test, we used Kolmogorov goodness of fit test which was described in section II. For the independence test we used test runs also defined in section II. These tests were implemented in a script of Matlab software.

IV. RESULTS AND DISCUSSION

A. Result of RNG

The sequences obtained by the random number generator were stored in a text file. We take different sequences to change two parameters. The first was the value of resistor in the noise circuit and the second was the change of the value of sample time in the ADS module inside the FPGA. We store three sequences of data for each parameter change, so in total, 18 sequences of random numbers were stored.

The use of the PC is exclusively for monitoring purposes, in general the RNG is completely in hardware, so the randomness values generates are sent by the USB module to the PC to analyze their randomness characteristics.

B. Result for randomness test

A each sequence obtained was validated through the two test mentioned previously, each test has a test statistic, Table 1 shows the result from the test statistic for each sequence of random numbers in which a resistor value of 6.8MΩ was used. Table 2 shows the results by using a resistor of 20 MΩ.

Table 1. Results of test statistic from a resistor of 6.8MΩ

Resistor	6.8 MΩ	
Test	Kolmogorov	Runs
Ts	1 ms	
1	0.067494	0.129019
2	0.069924	4.575628
3	0.090782	6.712183
Ts	10 ms	
1	0.056709	4.653408
2	0.066729	0.175682
3	0.075824	3.052149
Ts	100 ms	
1	0.037763	3.940605
2	0.052876	2.38487
3	0.083813	2.110219

Table 2. Results of test statistic from a resistor of 6.8MΩ

Resistor	20 MΩ	
Test	Kolmogorov	Runs
Ts	1 ms	
1	0.066516	1.324404
2	0.050195	7.995677
3	0.05202	0.924402
Ts	10 ms	
1	0.074202	3.37998
2	0.052542	2.3021
3	0.069001	3.6363
Ts	100 ms	
1	0.045872	3.836475
2	0.035919	0.943018
3	0.076936	3.482749

The statistic value to determine the randomness of the sequences is taken from the inference tables for each test to the number of samples taken in this case 200 and with a level of significance of 5%, which is a good parameter to evaluate this tests [18]. Table 3 shows these values for each test.

Table 3. Test Statistics to level of significance of 5%

Kolmogorov	Runs
0.096167	233.9942

The statistic test obtained from the sequences is minor than the value in the table 3, and the hypothesis that the sequences are random sequences is accepted.

V. CONCLUSIONS

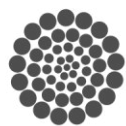
The random number generator presented was successfully tested because the results of the statistical tests indicated that the random numbers sequences obtained are random to a good significance level. The system to generate this randomness is a low-cost; the components that integrate are cheap and easy to purchase. Referring to its complexity, the implementation on FPGA permitted parallel processing, reconfigurability, understanding of language description and easiness of implementation. With these results, the RNG developed could be applied in different fields of engineering and investigation.

ACKNOWLEDGMENT

This work was partially supported by CONACyT scholarship number 783321/610468 and by project SEP-CONACyT 222453-2013.

REFERENCES

- [1] A.Y. Jaen Cuellar, "Diseño de arquitecturas basadas en FPGA para algoritmos genéticos, aplicado a la optimización de controladores en sistemas de posicionamiento", Universidad Autónoma de Querétaro, 2014.
- [2] Fatin Sezgin, Tevfik Metin Sezgin, Finding the best portable congruential random number generators, *Computer Physics Communications*, Volume 184, Issue 8, August 2013, Pages 1889-1897
- [3] Remya Justin, Binu K. Mathew, Susan Abe, FPGA Implementation of High Quality Random Number Generator Using LUT Based Shift Registers, *Procedia Technology*, Volume 24, 2016, Pages 1155-1162
- [4] Ülkühan Güler, Salih Ergün, A high speed, fully digital IC random number generator, *AEU - International Journal of Electronics and Communications*, Volume 66, Issue 2, February 2012, Pages 143-149
- [5] Ihsan Cicek, Ali Emre Pusane, Gunhan Dunder, A novel design method for discrete time chaos based true random number generators, *Integration, the VLSI Journal*, Volume 47, Issue 1, January 2014, Pages 38-47
- [6] Tamoghna Purkayastha, Debashis De, Kunal Das, A novel pseudo random number generator based cryptographic architecture using quantum-dot cellular automata, *Microprocessors and Microsystems*, Volume 45, Part A, August 2016, Pages 32-44
- [7] Lubomíra Balková, Michelangelo Bucci, Alessandro De Luca, Jiří Hladký, Svetlana Puzynina, Aperiodic pseudorandom number generators based on infinite words, *Theoretical Computer Science*, Volume 647, 27 September 2016, Pages 85-100,
- [8] Guangyi Chen, Are electroencephalogram (EEG) signals pseudo-random number generators?, *Journal of Computational and Applied Mathematics*, Volume 268, 1 October 2014, Pages 1-4
- [9] J.-L. Danger, S. Guilley, P. Hoogvorst, High speed true random number generator based on open loop structures in FPGAs, *Microelectronics Journal*, Volume 40, Issue 11, November 2009, Pages 1650-1656
- [10] Volodymyr Lynnyk, Noboru Sakamoto, Sergej Čelikovský, Pseudo random number generator based on the generalized Lorenz chaotic system, *IFAC-PapersOnLine*, Volume 48, Issue 18, 2015, Pages 257-261
- [11] A. Akhshani, A. Akhavan, A. Mobaraki, S.-C. Lim, Z. Hassan, Pseudo random number generator based on quantum chaotic map, *Communications in Nonlinear Science and Numerical Simulation*, Volume 19, Issue 1, January 2014, Pages 101-111
- [12] <https://www.random.org>
- [13] Boylestad, Robert L. and Louis Nashelsky. *Electronic devices and circuit theory*. Pearson, 2013.
- [14] Trefzer, Martin A. and Andy M. Tyrrell. *Evolvable Hardware: From Practice to Application*. Springer, 2015.
- [15] G. Vasilescu, *Electronic noise and interfering signals: principles and applications*, First Edition, Springer, 2005.
- [16] Mendenhall, William, Robert J. Beaver, and Barbara M. Beaver. *Introduction to Probability and Statistics*. Pacific Grove, Calif: Brooks/Cole, 2013.
- [17] Conover, W. J. *Practical Nonparametric Statistics*. New York: Wiley, 1999
- [18] Massey, F. J. "The Kolmogorov-Smirnov Test for Goodness of Fit." *Journal of the American Statistical Association*. Vol. 46, No. 253, 1951, pp. 68-78



CONACYT
Consejo Nacional de Ciencia y Tecnología



CONCYTEQ

Effect of density in leopard frog tadpoles (*Lithobates forreri*) under greenhouse

Diego Arné Robles Bustos, Jesus Josafat De León Ramírez, Juan Fernando García Trejo

Laboratorio de Bioingeniería, Campus Amazcala
Universidad Autónoma de Querétaro
Querétaro, México
diegoarnerb@hotmail.com

Abstract— One of the highest demanded species is the *Rana forreri*; this is due to its nutritional characteristics and its use in scientific developments. The current situation of this species is critical and it is under special protection in the Mexican norms. The captive production of *Rana forreri* has not been studied and it is necessary to know the characteristics for its development during its life cycle. For a frog culture the tadpole stage is crucial because it needs proper conditions, such as density. In this study, the density of the tadpoles was determined for captivity production using densities of 1 ind/3L, 1 ind/1.5L and 1 ind/L. The results show that in weight gain there is no significant difference; however it suggests that during the first month of sowing a density of 1 ind/3L is required. The highest survival rate, 98.1%, was obtained at the density of 1 ind/L, while the metamorphosis rate did not show statistical differences. The density of 1 ind/3L had the highest percentage with 37.5%. These results suggest that a treatment with 1 ind/3L is suitable for the handling of tadpoles in captivity.

Keywords—Metamorphosis rate; survival rate; Weight gain

I. INTRODUCTION

Lithobates forreri also known as “Rana pinta” or *Rana forreri* [1], forms part of the *Lithobates pipiens* complex [2-3]. It is located in the state of Sinaloa, in western Mexico [4], but there have been sightings in Jalisco, Nayarit, Costa Rica, Nicaragua, el Salvador, Guatemala and Honduras [5-6], it is distinguished from other frogs by having a pointed snout, dorsal folds that extend from the eye to the legs base and have dark spots on the back [7].

Thousands of these animals are used every year for research, human consumption and foreign education purposes [8]. Due to *Rana forreri* exploitation, its population has suffered a considerable decrease. Therefore, it has become necessary to condition the species in captivity for their exploitation and reintroduction to the environment in the future. Currently, there are no specialized centers in the production of this species. Plus, in Mexico, the *Rana forreri*

has been included in the Norm NOM-059-SEMARNAT-2010 in the list of special protection (Pr) [9].

However, the cultivation of *Rana forreri* (and of any frog) is complex, since each stage of its life cycle requires different cultivation techniques [10]. These have a close relationship with water during their life, from the lay to metamorphosis are completely aquatic, and once converted to frogs need water and soil [11].

A successful management of frogs requires adequate management during the tadpole stage, in order to maintain a high survival rate, as well as a metamorphosis in the shortest possible time [10]. The use of greenhouses for tadpoles breeding allows us to maintain a stable temperature, humidity and exclusion of predators [12].

In addition, there are several factors that affect the development of tadpoles such as: temperature, food, photoperiod and density [10, 13, 14, 15, and 16]. This last one acquires great importance at this stage, since a high density increases the metamorphosis rate, affecting the survival rate and growth [17, 18, and 19].

The density in *Rana forreri* has not been documented, but there are several studies where it has been studied in different species, for example in the bullfrog (*Rana catesbeiana*) Adams and Bruinsma (1987) propose a density of 1 to 2 ind/L, while Hayashi et al. (2004) indicated that 2.5 ind/L is adequate in ponds. Munguía et al. (2015) found that a density of 1 ind/3L is adequate; to minimize stress and optimize water refills [10, 18, and 20].

In studies with *Rana temporaria* from Egea-Serrano and Van Buskirk (2016), they propose the use of 2 ind/L. Woolrich-Piña et al. (2015) use a density of 1, 2 and 4 ind/L for two frog species (*Exerodonta xera* and *Incilius occidentalis*) [21-22].

The different densities in tadpole ponds affect their growth, survival and metamorphosis rate, so the objective of this work

is to determine the appropriate density for a tadpole culture of *Rana forreri* under greenhouse conditions.

II. METHODS

A. Place

This experiment was carried out in the Faculty of Engineering of the Universidad Autónoma de Querétaro in Campus Amazcala, Amazcala, El Marqués, Qro.

B. Biological material

Rana forreri tadpoles were used in stage 21 of the Gosner scale (1960) with a weight of 0.5358 ± 0.0046 g (Figure 1). These tadpoles were obtained from leopard frogs previously adapted to the greenhouse conditions [23].



Fig. 1. *Rana forreri* tadpole in stage 21 of Gosner scale.

C. Experimental desing

A randomized block design was used. The blocks were made using individuals of the same size per block to maintain the homogeneous system. Three treatments were performed with 3 replicates per treatment with an experimental unit of 30 individuals per treatment. Treatments are as follows: 1 ind/L, 1ind/1.5L and 1 ind/3L. The duration of the experiment was 120 days, performing biometrics (size and weight) every 12 days.

The animals were kept in grids within ponds of 91 X 60 X 50 cm (Fig 2), with the different described treatments and arranged at random. These tadpoles were subjected to the same 40% protein feed suggested by Olvera-Novoa et al. (2007), with constant daily recirculation [13].



Fig. 2. Pounds used for the experiment..

The response variables measured were: growth rate, survival and metamorphosis. To determine the significant differences between treatments, the data obtained during the tests were subjected to an analysis of variance (ANOVA) with 95% confidence.

III. RESULTS

A. Weight Gain

During the experimental period, in the first month, it was obtained that Treatment 1 tadpoles (1 ind/3L) had significant differences with respect to Treatments 2 and 3 (1 ind/1.5L and 1 ind/L respectively), however after the experimental time, in the next two months, no significance was observed between treatments. During the first month, tadpoles of 3.016 g were obtained in T1, 2.351 g in T2 and 2.153 g in T3 (See Fig 3). In the final part of the experiment, individuals of 4.147 g were obtained in T1, 3.877 g in T2 and 4.222 in T3. Thus obtaining that density does not affect tadpoles cultivation, except for the first stage of the tadpole which is 1 ind/3L.

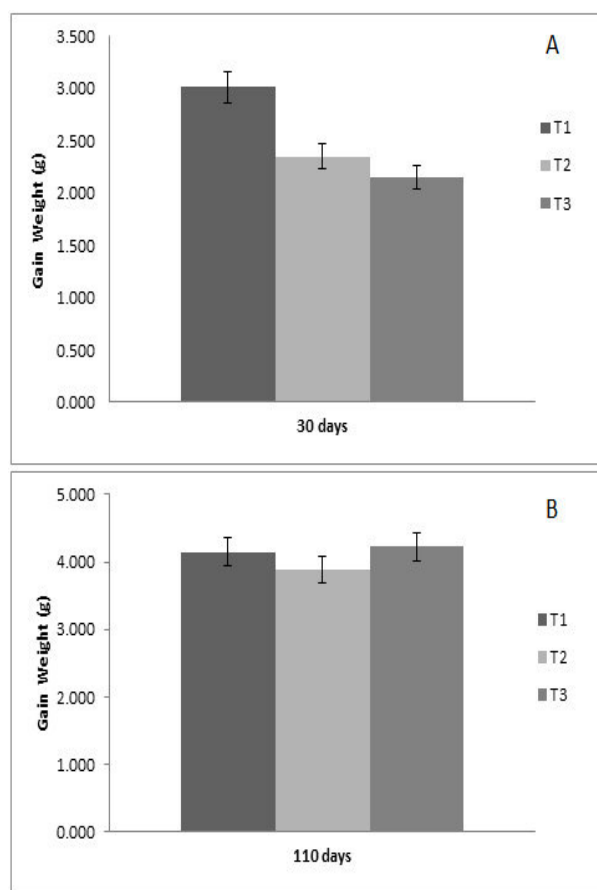


Fig. 3. A. During the first month of the experiment, significant differences were found between T1-T2 and T1-T3; however B. at the end of the experiment the treatments had no differences.

B. Survival Rate

The effect of density on the survival rate of the animals shows that a density of 1 ind/L (T3) is adequate for this since it has a rate of 98.1% and is statistically significant with respect to T1 and T2 (91.67% and 88.65%, respectively). Fig. 4 shows that from day 70, the tadpoles in treatments 1 and 2 began to decay reaching a point at which they kept their population stable until metamorphosis.

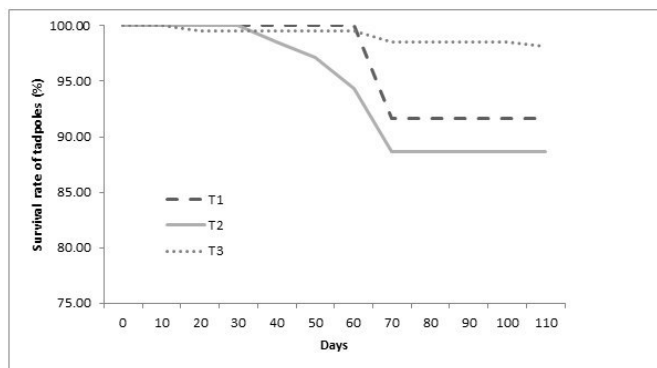


Fig. 4. Survival rate: in T1 and T2, from day 70 the population decayed but remained stable until the end of the experiment. Significant differences were found between T3-T1 and T3-T2.

C. Metamorphosis Rate

Fig. 5 shows the metamorphosis rate which for T1 was 37.5%, T2 of 21.28% and T3 of 9.05%. The T1 of 1 ind/3L is the treatment with the best performance in terms of metamorphosis, however when performing the statistical analysis it was found that there were no differences between treatments, but when relating the data, we obtain that the best treatment is T1 for weight gain at the beginning of the study (30 days) and metamorphic rate. Therefore, it can be inferred that there must be an adequate handling of the tadpoles at each of their stages on the Gosner scale [23].

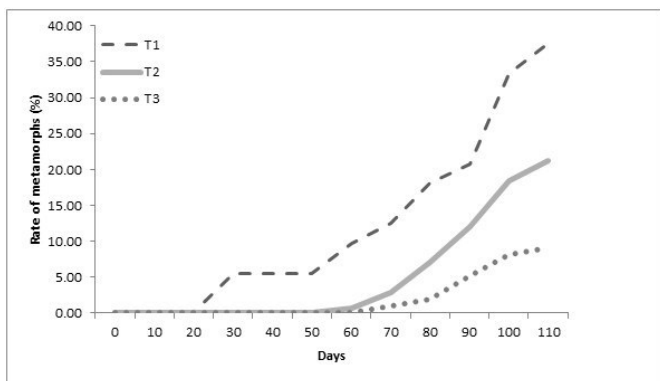


Fig. 5. Metamorphosis rate where T1 had the highest percentage. Significant differences were not found between treatments.

In Table 1 all data were generalized, according to their statistical analysis, showing that there are no statistically significant differences between treatments in weight gain. While in the survival rate treatment 3 shows a significant difference with respect to the others. In the metamorphosis rate no statistical difference is observed, but as shown in Fig. 4 treatment 1 has a higher metamorphic rate.

IV. DISCUSSION

The present study shows that the treatments in terms of weight gain do not have differences between them, however, when T1 (1 ind/3L) is observed in the first month of the experiment (See Fig. 2), there are significant differences between the T1 and T2, T3. It can be inferred that the lower the density the greater the growth, as mentioned by Mungía, *et al.* (2015) with *Rana catesbeiana*, so for our object of study is an initial point to be able to realize an appropriate handling of the animals. About why there was no statistically significant difference in weight gain, Kehr *et al.* (2013) give a trace that between larger water volumes, the tadpoles tend to increase their size and weight, this can be explained in Fig 3 and 4 where it is observed that the change to frog and the death of several individuals caused a slight increase in the total water volume per grid and consequently the weight gain is similar. The results in the final stage of the experiment can also be attributed to the feeding pause during metamorphosis climax, according to Crespi and Denver (2005) the tadpoles remain alive with the nutrients absorbed from the tail [10, 24 and 25].

TABLE I. GENERAL SUMMARY

Variable	Treatments		
	T1	T2	T3
Weight Gain (g)	5.062±0.534 ^a	3.939±0.621 ^a	5.398±0.405 ^a
Survival rate (%)	91.67±0.2 ^a	88.65±0.2 ^a	98.1±0.4 ^b
Metamorphosis rate (%)	37.5±0.2 ^a	21.28±0.1 ^b	9.05±0.1 ^c

Data with similar indices do not show statistically significant difference (p>0.05)

The survival rate (Fig. 3) of 98.1% in T3 and regarding to weight gain, the statistical analysis (P> 0.05) shows that there are statistically significant differences between treatments, it indicates that the higher the density, the weight will remain in a steadily rising trend, but with a greater survival. However, in Mungia *et al.* (2015) studies, the trend is reversed, in their study they indicate that at a density of 1ind/3L the survival rate is higher, but decreases as density increases. While in Bellakhal *et al.* (2014) studies, the density of 1 ind/L is higher compared to the lower densities. So our results suggest that in *Rana forreri* the higher the density the survival rate increases [10, 26].

The metamorphosis rate is linked to the gain and the fall of weight, according to Crespi and Denver (2005) tadpoles entering metamorphosis get their nutrients from the tail, causing a fall in their weight. Our results indicate that a density of 1 ind/3L is adequate to obtain a higher metamorphosis rate in this species. Bellakhal *et al.* (2014)

indicate that a density of 1 ind/L has a higher metamorphosis percentage. It was found in *Rana catesbeiana* that the higher the density, the metamorphic rate increases, but affects survival and size in weight, as we saw in this study (Mungia *et al.*, 2015). A density of 1 ind/L has greater survival rate, but a lower metamorphosis percentage, as well as a constant weight change. It should be taken in mind that the results of this study could open the gates to generate a manual of handling when breeding *Rana forreri* tadpoles, where the appropriate density for the handling of the animals is 1 ind/3L [10, 25, and 27].

V. CONCLUSIONS

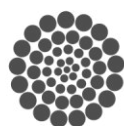
The effect of density on the development of *Rana forreri* tadpoles was defined by the comparison between three treatments and the difference in the first period of the experiment. This contrast can be compared to *Rana catesbeiana* tadpoles, but cannot be compared with frogs of different genus. We believe that this study is the first step in order to generate a manual of handling of this species in captivity to satisfy the demand and its possible repopulation in the wild.

ACKNOWLEDGMENT

The work group is grateful with the Universidad Autónoma de Querétaro for being participant in the offered field, with the students who supported the writing of this and with the advisor that without his help this text could not have been written. To the master's program in Biosystems that has a greater impact in the quality programs in the university and CONACYT for providing support to the students..

REFERENCES

- [1] Chávez, E. A., Ornelas, V. A. V., & Barragán, J. S. (1995). La explotación y disponibilidad de rana en el noroeste de México. *CIENCIA ergo-sum*, 2(3), 361-366.
- [2] Frost J. S. (1982) Functional Genetic Similarity between Geographically Separated Populations of Mexican Leopard Frogs (*Rana pipiens* complex). *Syst. Zool.* 31(1):57-67.
- [3] Hillis D. M. (1988) Systematics of the *Rana pipiens* complex: Puzzle and paradigm. *Ann. Re. Ecol. Syst.* 19:39-63.
- [4] Sanders, O., & Smith, H. M. (1971). Skin tags and ventral melanism in the Rio Grande leopard frog. *Journal of Herpetology*, 31-38.
- [5] Frost, J. S., & Bagnara, J. T. (1977). An analysis of reproductive isolation between *Rana magnaocularis* and *Rana berlandieri forreri* (*Rana pipiens* complex). *Journal of Experimental Zoology*, 202(3), 291-305.
- [6] Santos-Barrera, G., Chaves, G., Savage, J., Wilson, L.D. & Bolaños, F. (2008). *Lithobates forreri*. The IUCN Red List of Threatened Species 2008: e.T58599A11796501. <http://dx.doi.org/10.2305/IUCN.UK.2008.RLTS.T.58599A11796501.en>
- [7] Degenhardt W. G., Painter C. W., Price A. H.; 1996. Amphibians and reptiles of New Mexico. University of New Mexico Press. Albuquerque.
- [8] Altherr, S., Goyenechea, A., & Schubert, D. J. (2011). Canapés to Extinction: The International Trade in Frog's Legs and Its Ecological Impact. *Pro Wildlife*.
- [9] Norma Oficial Mexicana **NOM-059-SEMARNAT-2010**, Protección ambiental-Especies nativas de México de flora y fauna silvestres-Categorías de riesgo y especificaciones para su inclusión, exclusión o cambio- Lista de especies en riesgo. Diario Oficial de la Federación.
- [10] Munguia-Fragozo, P. V., Alatorre-Jacome, O., Aguirre-Becerra, H., García-Trejo, J. F., Soto-Zarazúa, G. M., & Rico-García, E. (2015). Growth and Metabolic Effects of Stocking Density in Bullfrog Tadpoles (*Rana catesbeiana*) under Greenhouse Conditions. *International Journal of Agriculture and Biology*, 17(4), 711-718.
- [11] Hernández B. F.; 1996. La rana cría y explotación 2da edición. Editorial Mundiprensa. Madrid.
- [12] Carmona-Osalde, C., Olvera-Novoa, M. A., Rodríguez-Serna, M., & Flores-Nava, A. (1996). Estimation of the protein requirement for bullfrog (*Rana catesbeiana*) tadpoles, and its effect on metamorphosis ratio. *Aquaculture*, 141(3), 223-231.
- [13] Olvera-Novoa, M. A., Ontiveros-Escutia, V. M., & Flores-Nava, A. (2007). Optimum protein level for growth in juvenile bullfrog (*Rana catesbeiana* Shaw, 1802). *Aquaculture*, 266(1), 191-199.
- [14] Figueiredo, M. R. C., Agostinho, C. A., Baêta, F. D. C., & Lima, S. L. (1999). Efeito da Temperatura sobre o Desempenho da Rã-touro (*Rana catesbeiana* Shaw, 1802). *Revista Brasileira de Zootecnia*, 28, 661-667.
- [15] Bambozzi, A. C., SEIXAS-FILHO, J. D., Thomaz, L. A., Oshiro, L. M. Y., Braga, L. G. T., & Lima, S. L. (2004). Efeito do fotoperíodo sobre o desenvolvimento de girinos de rã-touro (*Rana catesbeiana* Shaw, 1802). *Revista Brasileira de Zootecnia*, 1(1), 1-7.
- [16] Martínez, I. P., Álvarez, R., & Herráez, M. P. (1996). Growth and metamorphosis of *Rana perezi* larvae in culture: effects of larval density. *Aquaculture*, 142(3), 163-170.
- [17] Browne, R. K., Pomeroy, M., & Hamer, A. J. (2003). High density effects on the growth, development and survival of *Litoria aurea* tadpoles. *Aquaculture*, 215(1), 109-121.
- [18] Hayashi, C., Soares, C. M., Galdioli, E. M., Furuya, V. R. B., & Boscolo, W. R. (2004). Desenvolvimento de girinos de rã-touro (*Rana catesbeiana* Shaw, 1802) cultivados em diferentes densidades de estocagem em tanques-rede. *Revista brasileira de zootecnia*, 33(1), 14-20.
- [19] Dash, M. C., & Hota, A. K. (1980). Density effects on the survival, growth rate, and metamorphosis of *Rana tigrina* tadpoles. *Ecology*, 61(5), 1025-1028.
- [20] Adams, I. K., & Bruinsma, E. C. (1987). Intensive commercial bullfrog culture: a Brazilian experience. *Aquaculture management*, 358(4), 28-44.
- [21] Egea-Serrano, A., & Van Buskirk, J. (2016). Responses to nitrate pollution, warming and density in common frog tadpoles (*Rana temporaria*). *Amphibia-Reptilia*, 37(1), 45-54.
- [22] Woolrich-Piña, G. A., Smith, G. R., & Lemos-Espinal, J. A. (2015). Effects of salinity and density on tadpoles of two anurans from the Rio Salado, Puebla, Mexico. *Journal of Herpetology*, 49(1), 17-22.
- [23] Gosner, K. L. (1960). A simplified table for staging anuran embryos and larvae with notes on identification. *Herpetologica*, 16(3), 183-190.
- [24] Kehr, A. I., Schaefer, E. F., Dure, M. I., & Gómez, V. I. (2014). Influence of light intensity, water volume and density in tadpoles raised in mesocosm experiments. *Journal of Zoology*, 293(1), 33-39.
- [25] Crespi, E. J., & Denver, R. J. (2005). Roles of stress hormones in food intake regulation in anuran amphibians throughout the life cycle. *Comparative Biochemistry and Physiology Part A: Molecular & Integrative Physiology*, 141(4), 381-390.
- [26] Gromko, M. H., Mason, F. S., & Smith-Gill, S. J. (1973). Analysis of the crowding effect in *Rana pipiens* tadpoles. *Journal of Experimental Zoology Part A: Ecological Genetics and Physiology*, 186(1), 63-71.
- [27] Bellakhal, M., Neveu, A., Fartouna-Bellakhal, M., Missaoui, H., & Aleya, L. (2014). Effects of temperature, density and food quality on larval growth and metamorphosis in the north African green frog *Pelophylax saharicus*. *Journal of thermal biology*, 45, 81-86.



A hydroinformatics tool for data management and IDW interpolation.

Jaime Alberto Arteaga Vargas

Facultad de Ingeniería, Universidad Autónoma de
Querétaro
Santiago de Querétaro, México
jaime_av@hotmail.com

Samuel Rodriguez Flores

Facultad de Ingeniería, Universidad Autónoma de
Querétaro
Santiago de Querétaro, México
srsam@hotmail.com

Abstract—Inverse Distance Weighting interpolation gives us the possibility of estimating unknown values in certain points in which we doesn't have measurements. Data measurement and availability are some of the main problems engineers have to deal, most of the time we found data from different sources and different formats. These research was made to solve the problems mentioned below by using computational routines.

Keywords—Hydroinformatics, Spatial Analysis, IDW, Matlab

I. INTRODUCTION

With the advent of increased computational power, the capabilities of computer-based modelling have expanded considerably. Numerical simulation methods based on well established physical conservation principles are at the heart of present day research and consultancy (Arthur E. Mynett. 2004).

The usage of computational tools afford us a broader and more reliable outlook about how meteorological phenomena act. The geographical information systems (GIS) combined with numerical analyst tools, become essential in the hydrological modeling. With these tools we know simultaneous and in real-time the geomorphological characteristic of a basin and the meteorological events happening over it. However, the shortage of data is a common problem in hydrology, becoming necessary the optimization of the available data in certain geographic area (Pelczar et. al. 2007).

Taking advantage of these increased computational power this paper shows the benefits of using computational routines to solve and make efficient tasks when we make hydrological studies from the first step of collecting data and its management to the processing and interpolation of missing rainfall data, this algorithms let us finish tasks that used to take days in a few minutes.

The role of meteorological variables such as precipitation, temperature, evaporation, solar radiation, etc. is crucial for

understanding the variation of nature along a basin. (Elias and Castellvi 2001).

With the population increase and global warming affecting climates it is necessary to plan and design with the greatest amount of data we can, this will increase the precision of our estimations and having done that we can proceed to the next step, optimization. Once we have choose a method we use computational routines to perform complex operations or just repeat the same operation thousand of times.

II. MATERIALS AND METHODS

Mexico has about 5300 pluviometric stations but only 2685 work in good conditions also we have 96 Automatic Meteorological Stations distributed in national territory. These stations send information every 10 minutes making this net the most reliable on the country but unfortunately we don't have a full coverage of the territory making interpolation imminent to solve the problem as shown on *Fig. 1*.

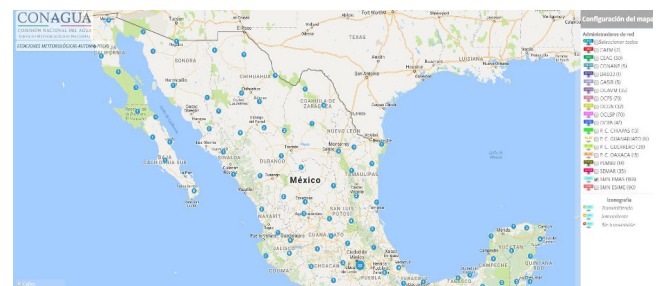


Fig. 1. Distribution of Weather Stations in Mexico.

As we said before most of the times we wont find the whole information we need from only one source so in order to get a better precision we will have to fill missing information from other sources facing us to the problem of homogenized data, measured in different intervals of time or just downloaded with other formats of date.

The tool presented in this paper is integrated by two modules programmed on Matlab, each one with its own graphical user interface to achieve a quick and easy usage compiled and distributed as an “.exe.” file compatible with windows even if you don’t have Matlab installed.

The first step before using this modules is to choose the criteria we will be working with in order to select the most representative weather stations near to the zone of study *Fig. 2*. We have to choose a representative area taking considering topography between weather stations. For the next step and once we have selected the representative stations we have to analyze data and choose a common period of time for the whole database according to the amount of measurements. In order to do this we have to download data and save it on a general database using the first module “Data Management”.

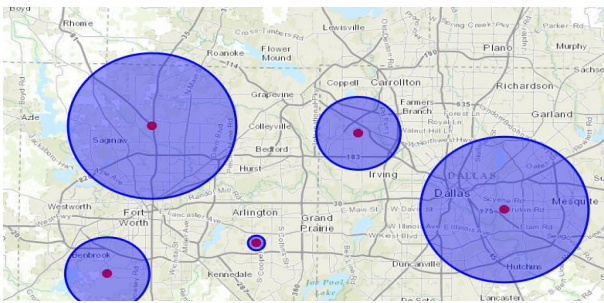


Fig. 2. Example of criteria for choosing representative weather stations localized inside of the buffer.

The first module *Fig. 3* is an algorithm that converts our data from each selected station near to the study zone from its own format to an standardized one compatible with “Microsoft Excel”, on the first columns we have date, on the second one the time with an interval of 10 minutes and on the next columns values of precipitation of each weather station it also has a simple tool that allows us to compare time series measured by other organizations by calculating the Pearsons Correlation Coefficient.

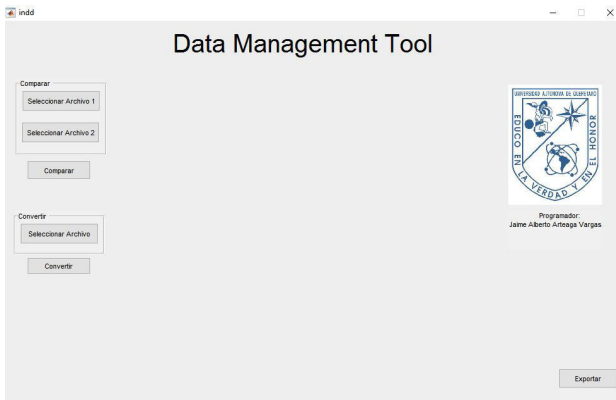


Fig. 3. Graphical User Interface of Module 1 “Data Management Tool”.

As we said before when we chose to compare two time series on the first module the algorithm also estimates the Pearson correlation coefficient to determine how similar are they and if we found good matches between both sources we could take the decision of using a non-official data source for scientific issues as a validation input or discard the source and work with the official one, *equation (1)*.

$$Z(x) = \frac{n \sum_{i=1}^n x_i y_i - \sum_{i=1}^n x_i \sum_{i=1}^n y_i}{\sqrt{\sum_{i=1}^n x_i^2 - (\sum_{i=1}^n x_i)^2} \sqrt{\sum_{i=1}^n y_i^2 - (\sum_{i=1}^n y_i)^2}} \quad (1)$$

At this point after we have discarded useless data and selected the good one using the first module we will be capable to save all the weather station measurements on a “.csv” or “.xls” file.

Once we have prepared our database if we are lucky we will have information of our area of interest but if we don’t the only way we have to get data of this area will be filling gaps of missing information using an interpolation method, in this case we will be using an Inverse Distance Weighting (IDW) interpolation algorithm programmed in Matlab.

Inverse Distance Weighting method weights the points in which we have measurements so in these way the influence of a point with other decreases depending on the distance to the point we want to interpolate, *Fig. 4*. This weighting is assigned to each point with a coefficient that controls the influence of each point during the interpolation.

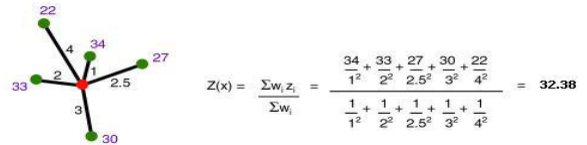


Fig. 4. Weighting depending of distances between green and red points.

The second module presented on this paper estimates coefficient of weight for each measured point depending on the distance between each weather station on the complete database to the point of interest using *equations (2) and (3)*.

$$Z(x) = \frac{\sum_{i=1}^n (W_i)(Z_i)}{\sum_{i=1}^n W_i} \quad (2)$$

$$W_i = \frac{1}{d_i} \quad (3)$$

After selecting the common period we have to select it on the calendars interface carefully because if we don't have data on that day the program will throw a message of error, typing these we just have to click on the button "Run" Fig. 5 and after a few minutes the program will save the full interpolated database for the period selected before.

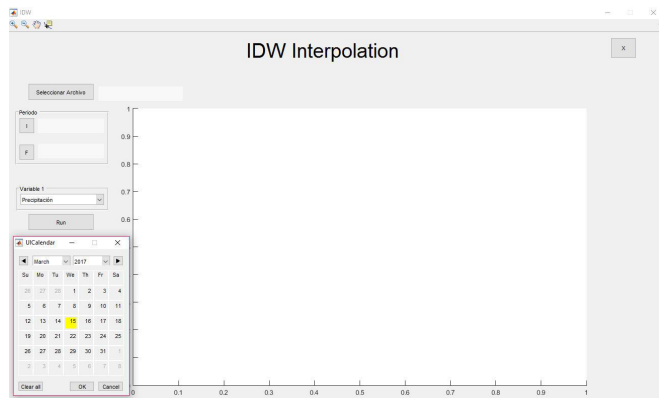


Fig. 5. Graphical User Interface of Module 2 "IDW interpolation".

It's easy to use this tool, with just one click the full database will be completed using IDW interpolation. It looks easy and that is the idea, if we look inside the algorithm we can see that for each iteration we calculate an independent weight for each available data and estimate the unknown value with equations (2) and (3).

III. RESULTS

For the first tool we use it for compare an official time series "CEA-Weather Station" with a private Wather Station net "CIAQ-RadioUAQ" we found that Pearsons coefficient has a value of 0.726, with these value we conclude that both time series are not as similar as we need if we where thinking to use CIAQ weather stations for official projects, in conclusion it won't be a good idea but it will if we are looking for more detailed information and also if we want to work with a group of 20 weather Stations instead of the 2 or three official stations its the perfect solution Fig. 6.

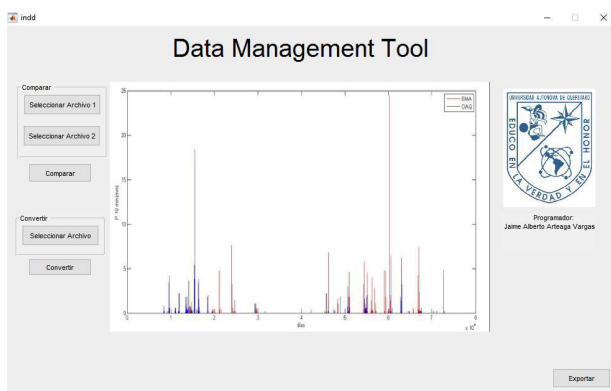


Fig. 6. Comparison between ESIME Querétaro CEA-CIAQ Radio UAQ .

We saw an application for the first module for taking decisions and talking about the second module we mentioned the processing advantages of a computer son as an example we applied this module for 5 Weather Station located in Chihuahua "Maguarichi", "Basaseachi", "CD.Cuahtemoc", "Urique" and "Chinipas for 14 year, a 275,489 lines of measured data with 5 columns each one corresponds to one weather station, this module was able to interpolate the whole database in just 3 minutes line by line, on Fig. 6 we can see an example of the usage of these module as a visualisation data, we choose three days of measurements for the first weather station and this tool plot the values corresponding to temperature for those days.

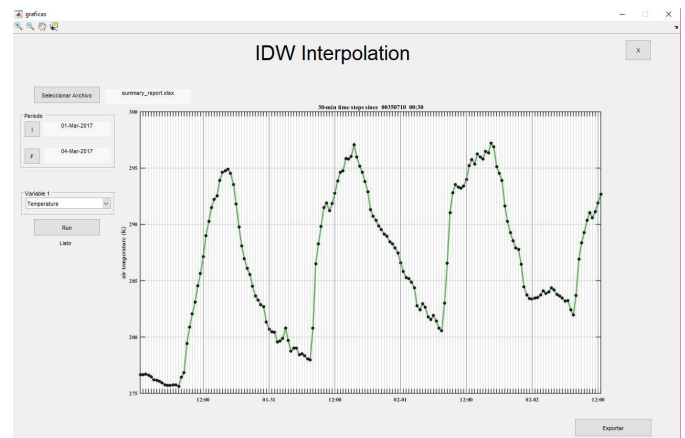


Fig. 7. Graphical User Interface of Module 2 "IDW interpolation".

As we can see its easy to use both tools for data management and interpolation and that is main idea but while the user just press two or three buttons the algorithms are complex and efficient, they are capable to interpolate database of about 300,000 lines applying the corresponding equations and interpolate the missing data in just a couple of minutes and on the other side it is possible to compare two time series and get an homogenized data with just one click instead of wasting time extracting information from each one of the available sources.

IV. DISCUSSION AND CONCLUSIONS

It's important to say that precision of the IDW method depends on the distribution of the the measured data in addition the maximums and the minimums will be determined by the global values of the parameters on the database so if there is a value over the maximum of the measured data we wont be able to estimate it, also we have to be careful choosing the criteria for selecting the weather stations inside a representative zone because long distances between stations will increase the error during the interpolation method.

There are lots of interpolation methods and IDW interpolation is one of the easiest one but experience shows that the most part of the time it gave us good results, if we are

not sure of the results self experience will help to take decisions.

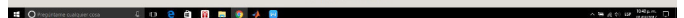
Data management is always a mess and a long task that could even take weeks, make an homogenized database and then estimate the missing gaps line by line, by my own experience we have reduced processing time from weeks to hours or even just some minutes.

Using Graphical User Interfaces helps users to understand in a visual way inputs and outputs of the algorithm saving them from trying to understand and learn a programming language, it is also important to mention that this tool is presented as an executable program that includes a compiler and in that way people who has “Windows” as operative system will be able to install and run the tool without having installed Matlab.

Finally the program give us the possibility to save this file with the hole interpolated data as a .csv or .xls extension so we can manipulate the information on Microsoft Excel whenever we wants and on a more friendly environment.

REFERENCES

- [1] Arthur E. Mynett, “Hydroinformatics Tools for Ecohydraulics Modelling, World Scientific Publishing Co. Pte. Ltd., Singapore, pp. 3, June 2004.
- [2] Pelczer, I., Ramos, J., Domínguez, R. and González,.”Establishment of regional homogeneous zones in a watershed using clustering algorithms”, Proc. IAHR, Venice, Italy, 2007.
- [3] Elías, F. and Castellvi, F., “Medio Ambiente y Ciencias del Suelo”,Ed. Mundi-Prensa, Madrid, Spain, pp. 517, 2001



Effect of grazing time and natural feed additives on the quality of Ross 308 chicken meat

Torres Martínez, Alma Vianet; Robles Bustos, Diego Arné; Flores Tejeida, Laura Berenice; De León Ramirez, Jesús Josafat; García Pérez, Javier.

Faculty of Engineering
Autonomous University of Querétaro
Querétaro, México
ind.vtorres@gmail.com

Abstract— Chicken farming consists of fattening fast growing birds in confined spaces with a high population density, a reduced rest time, and with a high control of feeding and environment. This has generated an important reduction in the physical activity of the birds, and, therefore, an increase in the deposition of abdominal fat. This is related to the nutritional and sensorial quality of the meat. Therefore, an experimental design is proposed to determine the influence of those factors considered essential in the development of adipose tissue in the bird. The proposed design aims to determine the relationship of the time of locomotor activity of the birds and the thyme supplementation in the diet, with the generation of fat and in turn of this with the protein percentage, the coloration, the texture and the water-holding capacity of meat.

Keywords— *quality meat; fat content; feeding program; rearing system*.

I. INTRODUCTION

Poultry meat is one of the most demanding meat products in our country, since consumers are looking for nutritious, easy-to-prepare foods at a low cost [1,2]. Chickens for fattening have a great capacity for development and growth, and are determined as a commercial strain of high productivity [3]. Chicken meat is the most consumed in Mexico [4], however, to meet the demand demand, production systems have been modified and have brought with it environmental contamination and an increase in fat percentage, affecting both the health of the Bird as the quality of the meat obtained. The quality of the meat can be determined from its nutritional content, mainly through the determination of the percentage of fat, protein and cholesterol; And by their sensorial and physicochemical characteristics, through pH, water-holding capacity (WHC), color and texture [5 - 11]. The percentage of fat in today's chicken breeds constitutes up to 21.7% of the total tissue of the bird, and only 6.2% is found in muscle tissue; however, the remaining 15.5% is found in the skin and abdomen of the bird [12 - 14]. The disadvantage of this fat is

that it contains saturated fats that can not be easily metabolized [15]. This affects some aspects of meat quality, including protein percentage; Rizzi and Chiericato [16] mentioned that as the percentage of fat decreases the protein percentage increases and decreases the color intensity while increasing the water retention capacity [17], all this causes changes in the juiciness and texture of the meat [6]. These three aspects of quality are related with the nutritional quality through the fat content, and can determine the level of acceptance of the product [9, 10].

The percentage of fat in poultry is attributed in addition to the genetic aspect of the birds, the modification in the rearing systems [1,16] and the modern poultry feed programs [18, 19]. These modifications have been made through with respect to the type of ship or storage shed, the environmental control and the space available by bird. This is the main variable to be modified, since it has been observed that, by increasing the availability of space in open grazing areas, the fat content can be reduced [1, 8, 11, 16, 20 - 22]. The feeding programs have three fundamental pillars which can modify the fat profile of birds: food restriction, protein-energy balance and the use of additives [18, 19, 23]. Additives can be added either in the food or drink water and are involved mainly in the process of fatty acid synthesis (lipogenesis) and do not modify the composition of the diet, they also work as facilitators in the process of obtaining Energy (glycolysis) [24]. Thyme (*Thymus vulgaris*) is a natural additive used in poultry farming due of its antioxidant and antimicrobial effects [25], and because its saponin content has been used as an additive in reducing abdominal fat [26]. Due to the demand for higher quality meat, the tendency to maintain the welfare of the animals, as well as the effects on the environment during the livestock exploitation, new animal husbandry policies have emerged, which focus on improving nutritional and sensory attributes of meat by accessing the outdoors and using special feeding programs [27 - 30]. However, nowadays, the poultry industry has focused primarily on improving pre-slaughter and post-slaughter processes, studying fasting time [10, 31] the loading

and transport process to the processing plant [28, 32], the marinating or value-added treatments of meat [33], and modern production systems and feeding plans [21, 34, 35], without explaining in a concrete way the factors involved in the nutritional composition of meat during the fattening period and its relation with the sensorial and physicochemical quality, leaving in door to the investigation of factors that affect both its protein content and its percentage of fat. The objective of the present work is to determine the factors involved in the deposition of fat and to establish a production process that allows to decrease it.

II. METHODOLOGY

To determine the effect of factors involved in the fattening of the chicken, it is proposed to establish a rearing system in free grazing, providing the birds with a shelter area and a grazing area with controlled access (8 and 6 h), balanced feed in three periods: 15-21, 22-35 and 36-49 days, with a protein percentage of 21, 20 and 18% respectively, [2] , 0.10 and 0.15% of thyme powder will be supplied in the first Two feeding stages. A factorial design 3², with experimental units of 10 birds with 3 replicates with a total of 150 birds as described in Table 1 will be utilized in this experiment.

TABLE 1. TREATMENTS OF THE EXPERIMENT, (OWN ELABORATION).

Treatments	Grassing time (h)			Thyme (%)		
	Age(days)					
	15-21	22-35	36-49	15-21	22-35	36-49
C	0	0	0	0	0	0
T ₁	0	6	6	1	1	0
T ₂	0	8	8	1.5	1.5	0
T ₃	0	6	6	1	1	0
T ₄	0	8	8	1.5	1.5	0

Ross 308 male chicks of 15 days old will be used, and will be housed with a density of 10 birds / m² in the shelter area and 4 birds / m² in the grazing area. During fattening period, weight and feed intake will be monitored, and a vaccination program will be applied according to current regulations [36].

To obtain the data, 6 birds will be taken from each treatment, sacrificed by standardized procedures in a type TIF trail [11]. The abdominal fat, the breast and the legs with skin will be weighed and placed in labeled individual bags and kept in refrigeration for 24 h at 4 ° C [10, 37]. Once the post-mortem process is completed, the breast and leg muscles will be sampled to determine the nutritional and sensory quality under the methods listed below.

A. Determination of nutritional quality

Fat it will be determined by means of extraction of lipids by microwaves with the equipment Multiwave Pro by the method EPA 3546.

Protein will be determined by the method of Kjeldahl in a Digesdahl equipment, spectrophotometer model DR6000 of the mark HACH.

B. Determination of sensorial quality

Color will be done by reflectance spectrometry with the equipment CR 410 model CR 410 brand Cokonica Minolta after removing the skin and exposing the surface to oxygen for 30 min at 4 ° C.

Water-holding capacity will be determined by fresh weight difference with cooking weight as indicated [38].

Texture will be determinate in meat samples before and after cooking by a cut-resistance test with a Warner-Bratzler knife adapted to a Stable Textile Meter Micro Systems model TAXTPLUS / 30 [31].

C. Analysis

The analysis of the effects of each of the factors on both sensory and nutritional characteristics will be carried out through an analysis of variance (ANOVA) using the R Studio software as analysis tool.

III. RESULTS

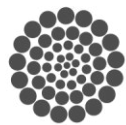
At the end of the proposed experiment, it is expected to determine the grazing time and percentage of thyme required to modify the percentage of abdominal fat and thus to establish a competitive production system producing chicken meat with less than 6% abdominal fat, as well as obtaining manuals for implementation and training of the production system.

REFERENCES

- [1] M. del P. Castañeda, "Factores involucrados en la calidad de la carne de pollo," 2011.
- [2] A. C. Barroeta, D. Izquierdo, and J. F. Pérez, "Manual de avicultura. Breve manual de aproximación a la empresa avícola para estudiantes de veterinaria," p. 60, 2014.
- [3] C. Villanueva, Manual de producción y manejo de aves de patio Manual de producción y manejo de aves de patio. 2015.
- [4] UNA, "Compendio de Indicadores Económicos del Sector Avícola 2016.," 2016.
- [5] S. G. Kannan, G., C. B. Chawan, B. Kouakou, "Influence of packaging method and storage time on shear value and mechanical strength of intramuscular connective tissue of chevon. Journal of Animal Science," 80:2383, 2002.
- [6] D. Braña et al., Manual de Análisis de Calidad en Muestras de Carne. 2011.
- [7] M. de L. Pérez and E. Ponce, "Tecnología de Carnes Manual de prácticas de laboratorio," p. 110, 2013.
- [8] K. H. Wang, S. R. Shi, T. C. Dou, and H. J. Sun, "Effect of a free-range raising system on growth performance, carcass yield, and meat quality of slow-growing chicken.," Poult. Sci., vol. 88, no. 10, pp. 2219–2223, 2009.
- [9] Diego Braña Varela, A. V. Izquierdo, J. A. E. G. G. M. L. M. M. P. Díaz, J. L. J. Barrera, G. M. Trejo, and A. L. E. Carrillo, Calidad en puntos de venta de Carne, no. 22. 2012.
- [10] Y. Bautista, "Colegio de postgraduados," Control, vol. 34, no. 1, pp. 741–746, 2013.
- [11] C. Y. Lin, H. Y. Kuo, and T. C. Wan, "Effect of free-Range rearing on meat composition, physical properties and sensory evaluation in taiwan game hens," Asian-Australasian J. Anim. Sci., vol. 27, no. 6, pp. 880–885, 2014.
- [12] A. E. . P. R. G. & M. J. S. CARDEN, "Efecto de sexo y raza sobre la composición corporal en pollos parrilleros 2: Distribución del músculo y de la grasa.," 1978.



- [13] et al. Sañudo C, Albertí P, Franco J, Olleta JL, Campo MM, Panea B, “Calidad instrumental de la carne de siete razas bovinas españolas,” *Eurocarne*; 73 37-54., 1999.
- [14] USDA, “Organic Production,” 2007.
- [15] USAPEEC México, “Contenido Nutricional de Carne de Pollo,” 2013.
- [16] C. Rizzi and G. M. Chiericato, “Chemical composition of meat and egg yolk of hybrid and Italian breed hens reared using an organic production system.,” *Poult. Sci.*, vol. 89, no. 6, pp. 1239–1251, 2010.
- [17] A. C. Fanatico, P. B. Pillai, L. C. Cavitt, C. M. Owens, and J. L. Emmert, “Evaluation of slow-growing broiler genotypes grown with and without outdoor access: Growth performance and carcass yield,” 2005.
- [18] D. E. Le Bihan, M. N, and R. H., “Broiler meat quality: effect of selection for increased carcass quality and estimates of genetic parameters,” *Poult. Sci.*, 1999.
- [19] I. Lopes, V. JL, L. J. DV, Z. J. Freitas, and E. Souza, “Meat quality and color of abdominal fat of broilers fed diets containing cashew nut meal treated with antioxidant,” *Acta Sci. Technol.*, 2013.
- [20] V. C. Resconi, M. M. Campo, M. Font i Furnols, F. Montossi, and C. Sañudo, “Sensory quality of beef from different finishing diets,” *Meat Sci.*, vol. 86, no. 3, pp. 865–869, 2010.
- [21] E. N. Sossidou, A. DAL BOSCO, C. CASTELLINI, and M. A. GRASHORN, “Effects of pasture management on poultry welfare and meat quality in organic poultry production systems,” *Worlds. Poult. Sci. J.*, vol. 71, no. 2, pp. 375–384, 2015.
- [22] C. Castellini, C. Mugnai, and A. Dal Bosco, “Meat quality of three chicken genotypes reared according to the organic system,” *Ital. J. Food Sci.*, vol. 14, no. 4, pp. 401–412, 2002.
- [23] A. M. F. and H. K. El-Senousey, “Nutritional Factors Affecting Abdominal Fat Deposition in Poultry: A Review,” *Asian Australas. J. Anim. Sci.*, vol. 27, no. 7, pp. 1057–1068, 2014.
- [24] and C. E. E. Qureshi, A. A., Z. Z. Din, N. Abuirmeleh, W. C. Burger, Y. Ahmad, “Suppression of cholesterologenesis and reduction of LDL cholesterol by dietary ginseng and its fractions in chicken liver. Atherosclerosis,” 48:81-94., 1983.
- [25] and V. L. Khan, R. U., S. Naz, Z. Nikousefat, V. Tufarelli, “*Thymus vulgaris*: alternative to antibiotics in poultry feed.,” *World’s Poult. Sci. J.* 68401-408., 2012.
- [26] and A. A. Abdulkarimi, R., M. Daneshyar, “Thyme (*Thymus vulgaris*) extract consumption darkens liver, lowers blood cholesterol, proportional liver and abdominal fat weights in broiler chickens.,” *Ital. J. Anim. Sci.* 10101-105., 2011.
- [27] Food and Agriculture Organization of the United Nations (FAO), “Principios de producción orgánica.,” Depósito Doc. la FAO, FAO., 2015.
- [28] E. J. Van Loo, V. Caputo, R. M. Nayga, M. Canavari, and S. C. Ricke, *Organic Meat Production and Processing*. 2012.
- [29] A. Vázquez, F. P. Lang-ovalle, I. Peralta-Garay, and F. J. Aguirre-Peréz, “PERCEPCIÓN DEL CONSUMIDOR Y PRODUCTOR DE Perception among consumers and producers of organic food: The Ocelotl market in Xalapa , Ver . Mexico,” pp. 20–29, 2012.
- [30] G. Castromán, M. Del Puerto, and A. Ramos, “Organic and Conventional Chicken Meat Produced In Uruguay: Colour, Ph, Fatty Acids Composition and Oxidative Status,” *Am. J. Food Nutr.*, vol. 1, no. 2, pp. 12–21, 2013.
- [31] Y. Bautista et al., “Efecto del estrés por calor y tiempo de espera ante mortem en las características fisicoquímicas y la calidad de la carne de pollo,” vol. 48, no. 1, pp. 89–97, 2016.
- [32] B. L. Schneider, R. A. Renema, M. Betti, V. L. Carney, and M. J. Zuidhof, “Effect of holding temperature, shackling, sex, and age on broiler breast meat quality.,” *Poult. Sci.*, vol. 91, no. 2, pp. 468–77, 2012.
- [33] N. M. Harper and K. J. K. Getty, “Effect of salt reduction on growth of *Listeria monocytogenes* in meat and poultry systems.,” *J. Food Sci.*, vol. 77, no. 12, pp. M669-74, 2012.
- [34] J. L. T. Heerkens et al., “Specific characteristics of the aviary housing system affect plumage condition , mortality and production in laying hens,” pp. 2008–2017, 2012.
- [35] P. M. de C. C. Pereira and A. F. dos R. B. Vicente, “Meat nutritional composition and nutritive role in the human diet,” *Meat Sci.*, vol. 93, no. 3, pp. 586–592, 2013.
- [36] J. Gonzales, “Manual de Buenas Prácticas Pecuarias,” *Senascia*, vol. 1. pp. 1–112, 2009.
- [37] J. K. Qiao, M., Fletcher D. L., Smith, D.P., and Northcutt, “Effect of Raw Breast Meat Color Variation on Cooked Meat Quality,” *Poult. Sci.*, vol. 81, pp. 276–280, 2002.
- [38] Suarez, “Evaluación de dos factores que intervienen en la calidad de la canal de pollo: sistemas de captura y programas de restricción alimenticia,” 2005.
- [39] C. Rizzi and G. M. Chiericato, “Chemical composition of meat and egg yolk of hybrid and Italian breed hens reared using an organic production system.,” *Poult. Sci.*, vol. 89, no. 6, pp. 1239–1251, 2010.



CONACYT
Consejo Nacional de Ciencia y Tecnología



CONCYTEQ

Antimicrobial activity of habanero pepper extracts under the influence of hydrogen peroxide

MARCELA VARGAS HERNÁNDEZ, ISRAEL MACIAS BOBADILLA, PERLA MUNGUÍA FRAGOZO, ROSALIA OCAMPO VELÁZQUEZ, ENRIQUE RICO GARCÍA, RAMÓN GERARDO GUEVARA GONZÁLEZ, IRINEO TORRES PACHECO.

Faculty of Engineering, C.U. Cerro de las Campanas
Autonomous University of Queretaro
Santiago de Querétaro, Queretaro, Mexico.

Abstract— Habanero pepper possesses diverse secondary compounds with different biological activities. The objective of this research is to study the antimicrobial effect of the habanero chili extract elicited with 18 mM hydrogen peroxide over time against *E. coli* and *S. aureus*. For the above, a growth curve of the microorganisms inoculated with extracts of habanero was carried out. The results indicate that the extract has the effect of inhibiting the growth of the two microorganisms for approximately 6 hours. It is concluded that habanero peppers elicited with 18 mM hydrogen peroxide induce the synthesis of antimicrobial compounds against pathogens related to human health.

Keywords—Habanero, antimicrobial activity, extracts, *Staphylococcus aureus* ATCC, *Escherichia coli* ATCC.

I. INTRODUCTION

Pepper is part of the culinary tradition of Mexico, archaeological excavations in Mesoamerican locations have found seeds, tissues and fruit remains [1]. The genus *capsicum* belongs to the solanaceous family which contains about 27 species of which 5 have been domesticated: *C. annum* L., *C. frutescens* L., *C. pubescens* Ruiz & Pav., *C. baccatum* L. y *C. chinense* Jacq [2]. The fruits of chile have great variability in form, color, size, pungency among others. *Capsicum chinense* is characterized by a high content of capsaicin in the fruit which causes pungency and is of importance in the pharmaceutical and food industry [3].

The genus *Capsicum* also has other types of bioactive compounds such as phenols and flavonoids, vitamin C, calcium among others [4]. Diverse Studies shows that the amount of these compounds can be increased under the effect of hydrogen

peroxide, in addition, these compounds exhibit antimicrobial activity [5].

Staphylococcus aureus and *Escherichia coli* stands out as important human pathogens, producing infections. *S. aureus* is a gram-positive coccus forming spherical to ovoid cells about 1 μm diameter [6] while *E. coli* belongs to gram-negative microorganisms is a rod-shaped, coliform bacterium [7]. Both *S. aureus* and *E. coli* are the most common source of infections [6]. Due to the above, it is important to search for new sources of antimicrobial compounds, plants comprise a wide range of secondary metabolites with a wide range of structures that provide different biological activities.

The objective of this work is to observe the antimicrobial effect of the habanero pepper extract elicited with 18 mM hydrogen peroxide over time against *E. coli* and *S. aureus*.

II. METHODOLOGY

A. Pepper growth

The cultivation of pepper *Capsicum chinense* var. Jaguar was established in a greenhouse of 108 m², located in the Campus Amazcala of the Autonomous University of Queretaro, between 20 ° 31 'and 20 ° 58' Latitude and between 100 ° 09 'and 100 ° 24' in length to 1 850 m SNM.

Seeds were immersed in a 200 ppm KNO₃ solution for 24 hours and subsequently placed on wet absorbent paper inside a large vessel. After 48 hours of germination, the seedlings were transferred to unicel containers (measure JM-29) and substrate peat moss (or peat moss). The seven-month plants were

III. RESULTS AND DISCUSSION

transported to the experimental greenhouse 219 days after germination. During the first three days, the plants were allowed to acclimatize inside the experimental area and the transplant was then carried out in black bags of 10 l volume with tezontle substrate.

In this stage, the seedlings were fertirrigated with solution Steiner (1984) to 100% each week with irrigations every third day.

The pepper were sprayed with a 18 mM hydrogen peroxide solution weekly until harvest for control no treatment were aplicated. Some parameters of the plant were measured weekly during its development, lenght and diameter.

B. Obtention of pepper extracts

At 3 months after transplanting in greenhouse (recommended harvest time with the variety of pepper to be used), the fruits were harvested. The peppers were then frozen with liquid nitrogen and ground with dry ice to obtain the fresh matter, it will be stored at -80 °C until its later use. The extraction of the compounds was carried out by the maceration method, using as solvent methanol in a ratio of 1:10 fresh matter and ethanol respectively, according to previous reports in our group for purposes of evaluating. In addition, the results of the present study are presented. The concentration of the methanolic extracts was carried out on a rotary evaporator of the brand Heidolph at a temperature of 40 ° C in order to avoid degradation of the compounds.

C. Antimicrobial activity

Staphylococcus aureus ATCC and *Escherichia coli* ATCC strains were activated in half trypticase soy broth for 24 h at 37 ° C. Soy agar tripticasein agar was then stained on agar and incubated for 24 h at 37 ° C. Clones were isolated and transferred to blood agar, again incubated 24 h at 37 ° C. The grown strains are those that will be used for the antimicrobial test.

Strains grown on the blood agar were inoculated in trypticasein soy broth medium until obtaining a concentration of 1×10^7 CFU. The strains were inoculated into medium tubes with a concentration of 200 mg/ml of habanero pepper extract and incubated at 37 ° C. The growth curve was determined by means of plate casting at 0, 1, 2, 3, 4, 5, 6, 8, 10, 12 hours, the solutions used were: direct, 1st dilution and 2nd dilution. The colonies were counted on the agar plates and the growth curves were performed.

A. Pepper growth parameters.

Physiological parameters of plants were measured under the effect of hydrogen peroxide 18 mM. It is observed that the plants with the treatment have significantly lower height than the control (Figure 1). There are some studies that demonstrate increases in growth under different stressors [8], in this case at the concentration evaluated there is a decrease in growth, therefore, it is important to evaluate more concentrations of the elicitor.

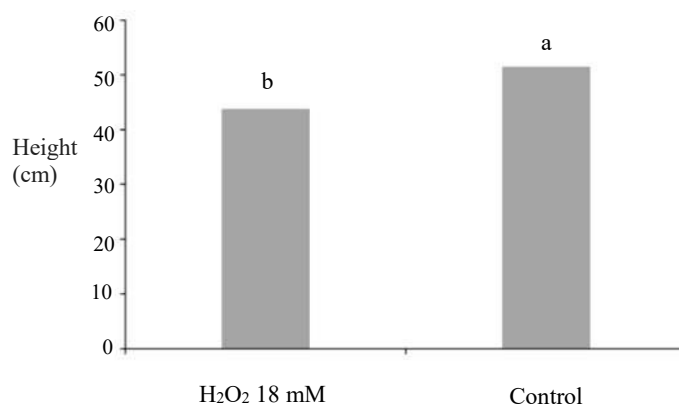


Fig. 1. Height of habanero pepper elicited with hydrogen peroxide 18 mM.

With respect to the basal diameter of the pepper, there is no significant difference between control and treatment with hydrogen peroxide (Figure 2).

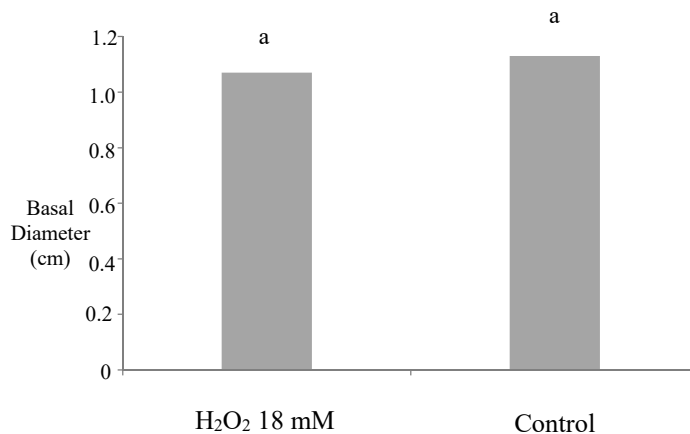


Fig. 2. Basal diameter of habanero pepper elicited with hydrogen peroxide 18 mM.

B. Antimicrobial activity against *E. coli* and *S. aureus*.

Figure 3 shows the antimicrobial activity of the extracts elicited with 18 mM hydrogen peroxide, the first lines indicate that the *S. aureus* bacteria have a phase in which they do not grow, however, after 4 hours bacteria growth exponentially. When seeded in the plates it can be observed that the lowest concentration of bacteria has a more delayed growth, this is due to the fact that the sample is more diluted.

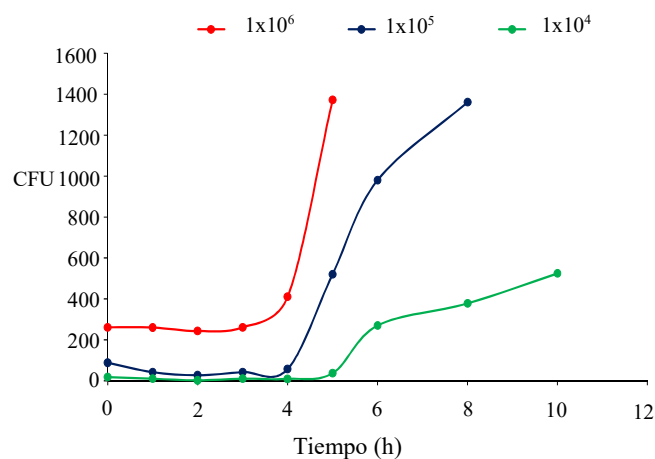


Fig. 3. Growth curve of *S. aureus* under the extracts of habanero pepper elicited with hydrogen peroxide 18 mM.

With respect to the growth of *E. coli* can be observed that it has less antimicrobial activity because it began to grow from the beginning in the concentration 1×10^6 . However, it is observed that the solutions 1×10^5 and 1×10^4 the bacteria grows at 6 and 8 hours (Figure 4).

The methanolic extracts of pepper under the effect of hydrogen peroxide had low antimicrobial activity after this time bacteria grew to a concentration so high that they could not be counted.

The above indicates that the extracts have a bacteriostatic effect because they do not completely inhibit the growth of the organism, but delays it.

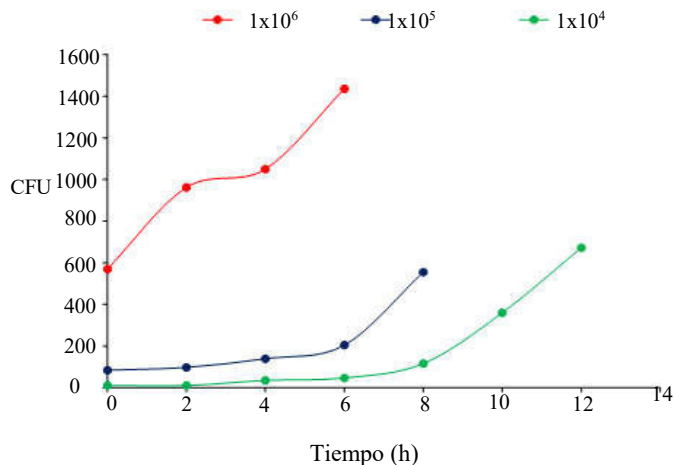


Fig 4. Growth curve of *E. coli* under the extracts of habanero pepper elicited with hydrogen peroxide 18 mM.

The presence of several compounds in the extracts poses the activity to inhibit the growth of the microorganisms. Therefore it is important to take into account the microorganisms concentrations and the compounds which possess the antimicrobial activity such as the capsaicin which has been reported to have an antimicrobial effect against various microorganisms [9] as well as, other secondary metabolites.

IV. CONCLUSION

Hydrogen peroxide induces the synthesis of antimicrobial compounds in *Capsicum chinense* which can be used in both the pharmaceutical and food industries for a wide range of microorganisms, however densities of microorganisms have a direct effect on the antimicrobial activities. The application of stress factors to the plant can be a very important tool for the production of different metabolites of interest.

ACKNOWLEDGES

M. Vargas-Hernández thanks to FOPEFI 2016 for the grant provided. Authors acknowledges.

REFERENCES

- [1] B. Pickersgill. Domestication of Plants in the Americas: Insights from Mendelian and Molecular Genetics. *Annals of Botany*, 2007, pp. 925-940.
- [2] P. M. Aguilera, H. J. Debat, M. A. Scaldaferrro, D. A. Martí, M. I. Grabile. FISH-mapping of the 5S rDNA locus in chili peppers (*Capsicum-Solanaceae*). *An Acad Bras Cienc.*, 2016, PP. 117-25.

- [3] M. Sganzerlaa, J. Pereira Coutinhoa, A. Marchi Tavares de Melob, H. Teixeira Godoy. Fast method for capsaicinoids analysis from *Capsicum chinense* fruits. Food Research International. 2014, pp. 718–725.
- [4] S. N. Jimenez-Garcia, M. A. Vazquez-Cruz, R. G. Guevara-Gonzalez. I. Torres-Pacheco, A. Cruz-Hernandez, A. A. Feregrino-Perez. Current Approaches for Enhanced Expression of Secondary Metabolites as Bioactive Compounds in Plants for Agronomic and Human Health Purposes. Pol J Food Nutr Sci., 2013, 67–78.
- [5] M. Vargas-Hernandez, I. Torres-Pacheco, F. Gautier, B. Álvarez-Mayorga, A. Cruz-Hernández, L. García-Mier, S. N. Jiménez-García, R. V. Ocampo-Velázquez, A. A. Feregrino-Perez, R. G. Guevara-Gonzalez, Influence of Hydrogen Peroxide Foliar Applications on in vitro Antimicrobial Activity in *Capsicum chinense* Jacq. Plant Biosyst. 2016, pp. 1-7.
- [6] G. Bachir-raho, B. Abouni. Escherichia coli and Staphylococcus aureus most common source of infection. The Battle Against Microbial Pathogens: Basic Science, Technological Advances and Educational Programs (A. Méndez-Vilas, Ed.). pp. 637-648.
- [7] A. Y. Peleg, D. C. Hooper. Hospital-Acquired Infections Due to Gram-Negative Bacteria. The New England journal of medicine. 2010, pp. 1804-1813.
- [8] J. Xiong, Y. Yang, G. Fu, L. Tao. Novel roles of hydrogen peroxide (H₂O₂) in regulating pectin synthesis and demethylesterification in the cell wall of rice (*Oryza sativa*) root tips. New Phytol. 2015, 118-26.
- [9] E. Marini, G. Magi, M. Mingoia, A. Pugnali, B. Facinelli, Antimicrobial and Anti-Virulence Activity of Capsaicin Against Erythromycin-Resistant, Cell-Invasive Group A Streptococci. Frontiers in Microbiology. 2015, pp. 1281.



Sustainability in the Construction Industry: A Review of Recent Developments in Modular Systems

S. Urrutia-Reyes
Civil Engineering/Masters in Sciences
Universidad Autónoma de Querétaro
Querétaro, México.
silvia_cei06@hotmail.com

J. L. Reyes-Araiza, J.B. Hernández-
Zaragoza, R. Ramírez-Jiménez
Engineering Civil /Masters in Sciences
Universidad Autónoma de Querétaro
Querétaro, México.
lreyes@uaq.mx / bosco@uaq.mx /
ruraji@uaq.mx

Abstract- The present work brings together researches about the recent progress of the modular systems in the construction industry, with the aim of raising an antecedent for a future research, which promotes the continuity and feedback of future research related to the modular systems. Recently the theme of sustainability in construction has taken on great importance. By using sustainable alternatives such as the modular system, it is possible to improve social, economic and sustainability indicators. In the first instance, it reviews the concepts related to the modular system, focuses on methodologies and the tools used in the present environment. Second, this paper explains and discusses the technical and economic differences between the conventional construction process and the use of a modular system. Finally, this work can be used by stakeholders as an important reference in the use of modular systems including the updated literature on approaches and methodologies for sustainability in the environment. The present review has tried to collect and reflect relevant information of the subject in the last six years of 2010 to 2016. In summary, it can be affirmed that the application of modular systems is fundamental for the sustainability in the construction and edification, also it promotes the increase of the productivity and competitiveness of construction markets, for this reason, this review examines the use of sustainable alternatives, in this case particularly modular systems, because to its wide international acceptance as a means to improve environmental processes, and in consequence, the quality of life.

Keywords- Modular systems, Sustainability, Sustainable development, Construction industry, Sustainable alternatives.

1. Introduction

The term sustainable development can be described as improving the quality of life and thus enabling people to live in a healthy environment and improve social and environmental conditions for present and future generations (Ortiz, Castells, & Sonnemann, 2009). The General Assembly of the United Nations coined the most well-known definition of sustainable development, being that development meets the needs of the present without compromising the ability of future generations to meet their own needs (CMMAD, 1987: 24).

It is noteworthy that sustainable development does not refer to an immutable state of nature and natural resources, but it does incorporate a perspective of moderation in their management, mitigates the "exploitation" of natural resources, leading to a "management" of these; also emphasizes the need for solidarity with current and future generations and promotes intergenerational equity.

It should be mentioned that the construction industry is the sector that offers the most profitable option in the implementation of alternatives that promote sustainability. Social, economic and environmental indicators do a call on the construction sector, which is an emerging sector and a highly active industry in developing countries.

In Mexico, the Undersecretary for Employment and Labor Productivity stated that more than 8% of the economically active population work directly in the sector, exceeding 13%, incorporating indirect personnel, ranking fourth as the generator of employment by branch of economic activity (Empleo & Laboral, 2017). The participation of construction in GDP, exceeds 7% being the fifth most representative sector in the share of GDP construction (Segovia Guerrero, Garcia Soto, & PROFECO, 2012).

Conversely, it is a critical sector in energy consumption, waste generation, excessive emissions of gases into the atmosphere and depletion of natural resources.

In order to mitigate the growing concern over the depletion of resources and incorporate some environmental criteria in both, developed and developing countries, the construction industry has been exposed to the industrialization process in recent decades and has experienced different construction methods, where the modular system takes importance as a highly viable alternative to improve the sustainability of construction.

The objective of this review is to systematically analyze the development of modular systems in the construction sector, to examine the current situation and to plan the main latent challenges in the use of this sustainable alternative. First, this document provides details, methodologies and tools that have been carried out in previous research. Second, the review explores and evaluates the different ways of implementing the modular system, including materials and combination of investigated components.

Next we present the discussion of the perceived advantages and limitations of the execution of modular systems and, finally, it is precise in the perspectives and challenges for the investigation of the use of this system and determining some conclusions.

2. Basic Concepts of Modular Systems.

Modular construction is one of the most efficient off-site construction methods. In this method, the different components of a building are designed and manufactured outside the construction site in factories as one or more modules, and then assembled on site to form the final product (Kamali & Hewage, 2016b).

Based on the degree of work outside the construction site, they can be classified as: unidirectional, bidirectional and tridirectional, being interpreted that they can be linear (skeletons), planes (plates) and volumetric (modules) (Novas Cabrera, 2010).

For the module element, the work to be carried out is to anchor it on the floor or on top of another box, in this system, the installations and finishes are made in the factory in order to cover production from start to finish.

The skeleton system allows more freedom than the previous one in terms of design and individual choice, however it has the disadvantage that the assembly is not in the factory and the work is carried out in the work site in the traditional way. In the same line of the constructive systems are the system of plates and the system of panels, which are similar and its basic difference is the scale, the systems of panels are commonly used in buildings of low height, whereas in the plate system, the components can become as large as a specific space requires.

About 85-90% of the modular construction takes place outside the construction site and the rest of the work (10-15%), including foundations and utility connections, is done on site (Kawecki, 2010).



Figure 1. Example of modules and plates.

It should be mentioned that a panel system is different from the modular system. The modular system is defined as the system that is partially built in a plant, sent to the development site and placed on a base, where the roof structure and exterior finishes are completed. The panel system is a similar construction technique that uses wall panels manufactured in a controlled environment, sent to the construction site and installed in the prepared base (Siggner, 2011).

The fundamental difference between the two systems is the prefabricated unit, for the first system are structural modules and for the second system are complete box panels, including the roof structure and exterior finishes and sometimes represent the functional units of the home (Elitzer, 2015). The quantitative results of a comparative study between the two systems showed that the modular construction method is scarcely more profitable than the panel construction method under the managed circumstances (Lopez & Froese, 2016).

The modular system is an efficient option for buildings that represent repetitive activities, however only a small percentage choose to use the modular system, one reason for customers' reluctance to accept new construction techniques lies in the difficulty of determining the benefits that offsite construction provides to the entire project.

It is stated that modular construction provides a wide range of environmental, economic and social advantages; therefore, can contribute to the achievement of sustainability objectives (Boafo, Kim, & Kim, 2016). These indicators may justify the use of modular construction as a viable alternative. To facilitate the understanding of the advantages of the modular system it is necessary to investigate the sustainability performance that the modular buildings provide throughout their life cycle. Therefore, the main objective of the review is to critically analyze the development of modular systems highlighting the main benefits and challenges of using such systems in construction.

3. Method: state of technique of the modular systems.

In this review of the application of modular systems to the construction industry focuses on cost analysis and the advantages of the modular prefabricated system as well as the industrialization of modular systems. It has been demonstrated that the module-based system allows for better quality control practices. When the modules arrive at the site, fewer operations are involved in the installation of the building, and the amount of work they have to do and the time they have to invest in the site is also reduced (Lopez & Froese, 2016).

Mohammad, Baharin, Musa, & Yusof (2016)

In the study, surveys were carried out between the manufacturers of the IBS modular system and the contractors of Klang Valley, Selangor. In order to establish a significant sample, a survey was conducted with approximately 40 participants. The purpose of the questionnaire was to obtain the answers about the acceptance of the Modular System in IBS projects. The results of the questionnaire survey indicated that the modular system may be able to reduce overall construction time and minimize construction waste considerably. However, the high initial cost and lack of technical expertise are among the obstacles in the implementation of the Modular System.

Musa, Mohammad, Yusof, & Ahmad (2016)

The objective of the research was to develop and validate an organizational preparation framework of industrialized building system IBSMS modular system for contractors and manufacturers in Malaysia. The methodology was the review of the literature and interview sessions with the people involved in this topic. Three modular systems was chosen, developed by manufacturers/contractors and a particular manufacturer selected for the study. The study explored and identified the elements of preparation and criteria for the major components of the framework. Through this framework, organizations that execute modular construction or IBSMS will be competent to execute the construction efficiently.

Generalova, Generalov, & Kuznetsova (2016)

The article highlights that modular construction has the potential to shorten design and engineering, reduce costs and improve construction productivity, and the installation of modular buildings is profitable, safe and environmentally friendly.

The research results of the article show that the development of modern systems of modular construction, provides to the population with comfortable and sustainable buildings. The document also describes the prospects and importance of the introduction of modular prefabricated units not only in low-rise buildings but also can be used in the construction of large buildings while providing improvements in the construction process.

Kamali & Hewage (2016)

In this search a methodology is used to identify and select the indicators of performance SPI appropriate to the life cycle. The contrasts of the modular and conventional construction were evaluated. Through an exhaustive bibliographical review, sustainability performance indicators identified in conventional and modular buildings were identified, a survey was designed and carried out. Subsequently, the perceptions of construction professionals on the applicability of these sustainability indicators were captured on a 5-point Likert scale. The reliability of the questionnaire was analyzed using Cronbach's alpha measure. Then, all SPI are classified according to their severity index (SI) values ranging from 20 to 100% corresponding to a severity scale from "very low" to "extremely high" levels of importance. Everybody

SPIs were classified, as well as within their associated sustainability categories. Analyzes show that 33% of environmental RLS, 67% of economic RLS and 42% of RLS were ranked equal to or greater than "high" on the severity scale. This paper contributes by highlighting the most applicable indicators for comparison and sustainability of modular construction and conventional construction.

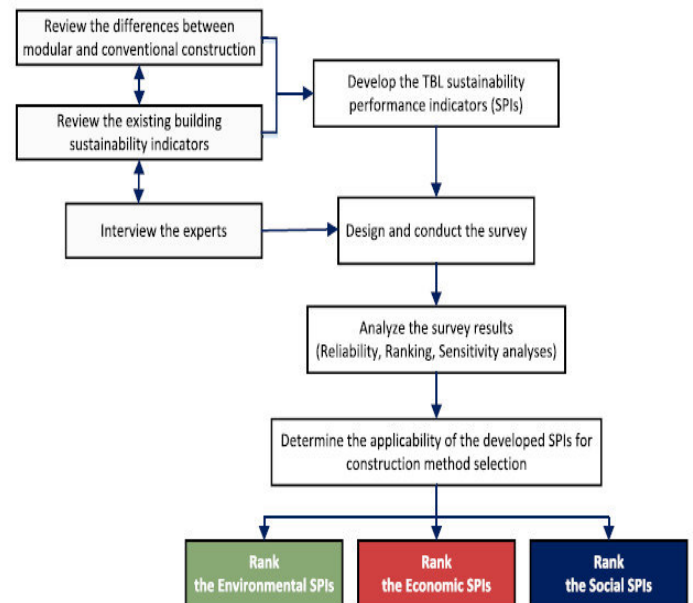


Fig. 2. The research methodology adopted in this study

4. Discussion of perceived advantages and limitations of modular systems

Due to the growing interest in the construction industry in the area of sustainability, modular construction has advantages that improve the indicators related to the same, faster construction, improved productivity and high quality in the workforce, which is reflected in cost savings, greater security in the work, control of inputs and mitigation negative environmental impacts. In addition, modular construction techniques present greater potential to reuse a considerable amount after the end of the life cycle of the work, which leads to the reduction of waste generated in the demolition phase. Among the main causes of the little implementation of the modular system, which are scenarios too to be improved for the acceptance of new construction techniques, are: transportation restrictions, engineering and planning processes are more sophisticated, the greater coordination and communication, among relevant Points there are to request a much greater investment than conventional construction project, and most importantly, negative perceptions of people toward new construction methods.

Most of the research indicated in the results, Both positive and negative, are qualitative but not quantitative, which gives rise to uncertainty in the choice of works in this constructive process, there is no analysis of clear and concrete costs, however the life cycle cost, sample that modular buildings are preferable when you compare with traditional buildings with economic similarity. As mentioned above, there are other benefits besides the economic factor, which is value added, such as work speed, productivity, safety, etc.

As an important deduction, an effective measurement method or an overall framework is needed in which the various benefits are contrasted with the challenges presented by the modular construction process, to be clearly defined and weighted the sustainability performance criteria in a qualitative and quantitative way.

Few studies have been carried out to assess the environmental impacts of the modular system, one reason could be the fact that the modular construction method is relatively new compared to conventional methods that have an invaluable amount of time in practice therefore, there is little information and data based on real projects supported by manufacturers of modular buildings. A major priority to improve environmental performance is to reduce energy consumption during the phase of the operation of the building, this objective can achieve by designing and building new systems, buildings as low energy consumption, particularly in the phases of production of construction material. Indirect built-in energy is used to acquire and process the production of building materials, while direct built-in energy is the one used to transport the building modules to the site, and then assemble the Modules the place the modular system allows to use friendly materials with low energy consumption during the life cycle.

Future research may contribute to the assessment of the economic and social performance of modular buildings. In addition, ways of addressing all dimensions of sustainability in a united framework can be investigated to comparatively assess the overall sustainability of modular and conventional buildings (Kamali & Hewage, 2016b).

The design and manufacture of a limited number of modules allow the configuration of living spaces, which means cost savings due to the repetition of processes and a wide range of final product offerings.

5. Conclusions

It has been confirmed that modular buildings provide superior life cycle performance, for example, the energy performance of a building, among others. Further life cycle studies are suggested, taking into account all dimensions of sustainable construction, in order to develop the solid image of the sustainability of modular construction.

Sustainable construction is increasingly important due to the constraints of natural resources. The use of new construction methods, ie off-site techniques, can be an effective alternative to conventional techniques in the search for greater sustainability.

The objectives of this work were to critically review the studies related to the modular construction process, thus delving into the benefits and challenges of modular construction compared to its conventional counterpart. The review of the literature carried out in this study did not address all dimensions of sustainability (environmental, economic and social).

References

- Boafo, F. E., Kim, J. H., & Kim, J. T. (2016). Performance of modular prefabricated architecture: Case study-based review and future pathways. *Sustainability (Switzerland)*, 8(6), 1–16. <https://doi.org/10.3390/su8060558>
- CMMAD. Comisión Mundial del Medio Ambiente y del Desarrollo de las Naciones Unidas. Brundtland report. <<http://sds.uanl.mx/el-concepto-desarrollo-sustentable/>>;1987 [accessed 20.02.17]
- Elitzer, J. ¿Sabe usted la diferencia entre casas prefabricadas y fabricados? [Internet]. EE.UU.: Los propietarios de viviendas modulares; 2015 [citado 2015 20 DEC]. Disponible de: <http://modularhomeowners.com/do-you-know-the-difference-between-prefab-and-manufactured-homes/>
- Empleo, D. E., & Laboral, P. (2017). MÉXICO.
- Generalova, E. M., Generalov, V. P., & Kuznetsova, A. A. (2016). Modular Buildings in Modern Construction. *Procedia Engineering*, 153, 167–172. <https://doi.org/10.1016/j.proeng.2016.08.098>
- Kamali, M., & Hewage, K. (2016a). Development of performance criteria for sustainability evaluation of modular versus conventional construction methods. *Journal of Cleaner Production*, 142, 3592–3606. <https://doi.org/10.1016/j.jclepro.2016.10.108>
- Kamali, M., & Hewage, K. (2016b). Life cycle performance of modular buildings: A critical review. *Renewable and Sustainable Energy Reviews*, 62, 1171–1183. <https://doi.org/10.1016/j.rser.2016.05.031>
- Kawecki, L. R. (2010). Environmental Performance of Modular Fabrication: Calculating the Carbon Footprint of Energy Used in the Construction of a Modular Home.
- Lopez, D., & Froese, T. M. (2016). Analysis of Costs and Benefits of Panelized and Modular Prefabricated Homes. *Procedia Engineering*, 145, 1291–1297. <https://doi.org/10.1016/j.proeng.2016.04.166>
- ModularandPrefabricatedHousing.pdf. (n.d.).
- Mohammad, M. F., Baharin, A. S., Musa, M. F., & Yusof, M. R. (2016). The Potential Application of IBS Modular System in the Construction of Housing Scheme in Malaysia. *Procedia - Social and Behavioral Sciences*, 222, 75–82. <https://doi.org/10.1016/j.sbspro.2016.05.189>
- Musa, M. F., Mohammad, M. F., Yusof, M. R., & Ahmad, R. (2016). Industrialised Building System Modular System (IBSMS) Organisational Readiness Framework. *Procedia - Social and Behavioral Sciences*, 222, 83–92. <https://doi.org/10.1016/j.sbspro.2016.05.191>
- Novas Cabrera, J. a. (2010). Sistemas Constructivos Prefabricados Aplicables a La Construcción De Edificaciones En Países En Desarrollo. *Proyecto Fin de Master Universidad Politecnica de Madrid*, 62. Retrieved from http://oa.upm.es/4514/1/TESIS_MASTER_JOEL_NOVAS_CABRERA.pdf
- Ortiz, O., Castells, F., & Sonnemann, G. (2009). Sustainability in the construction industry: A review of recent developments based on LCA. *Construction and Building Materials*, 23(1), 28–39. <https://doi.org/10.1016/j.conbuildmat.2007.11.012>
- Segovia Gorrero, A., Garcia Soto, C. E., & PROFECO. (2012). El sector inmobiliario en México. *Brujula de Compra*, 1–14. Retrieved from http://www.profeco.gob.mx/encuesta/brujula/bruj_2012/bol228_sec_inmobiliario.asp
- Siggner, R. Vivienda Modular: Beneficios, desafíos y lecciones aprendidas [Internet]. Columbia Británica, Canadá: BC Vivienda; 2011 [citado 2015 20 DEC]. Disponible a partir de: https://www.bchousing.org/resources/About%20BC%20Housing/Research_Reports/Modular-Housing-Research.pdf
- Tse-Lun Chiu, el análisis de S. Una de: el potencial de la industria de la construcción prefabricada [Internet]. Columbia Británica, Canadá: UBC Investigación de Pregrado; 2012 [citado 2015 20 DEC]. Disponible a partir de la UBC biblioteca abierta Colecciones: <https://open.library.ubc.ca/cIRcle/collections/undergraduateresearch/1042/items/1.0103132>

Diagnostic Methodology Based on Extraction of Statistical Indicators for Detection of Bearing Fault in Induction Motors

Francisco Arellano-Espitia,
Juan José Saucedo-Dorantes,
Roque Alfredo Osornio-Rios
HSPdigital, CA-Mecatronica
Engineering Faculty, Autonomous
University of Queretaro
San Juan del Rio 76806, Mexico
francisco_arellano_fae@live.com.mx.
jsaucedo@hspdigital.org
raosornio@hspdigital.org

Rene J. Romero-Troncoso
HSPdigital CA-Telematica
DICIS, University of Guanajuato
Salamanca 36885, Mexico
troncoso@hspdigital.org

Abstract— A bearing fault diagnosis method has been proposed based on the calculation of a statistical-time set of features applied to detect different faults in the bearing in an induction motor. Vibration signals are taken into account for calculating its statistical-time features and perform the characterization analysis of fault conditions. Then, the features are subjected to a reduction through Principal Components Analysis. Finally a Fuzzy- based classifier is implement to diagnosis of the different status. Analysis were conducted on electrical motor bearings with three different fault categories and several levels of fault severity. The experimental results shown that the proposed methodology cannot only reliably discriminate between different fault categories, but classifier the level of fault severity. Due to the performance of the proposed methodology, this is applicable in different industrial areas.

Keywords—*Induction Motors, Fault Diagnosis, Principal Components Analysis, Vibration Measurement.*

I. INTRODUCTION

INDUCTION motors (IM) influence all areas of modern life at both the domestic and industrial level. The average modern home in the world contains 20-30 electric motors in the range 0-1 kW for clocks, toys, domestic appliances, air conditioning or heating systems. Modern cars use electric motors for windows, windscreen wipers, starting and now even for propulsion in hybrid vehicles. In the industry, water systems are also driven by electrical machines, as are the processes that produce the raw materials for the agricultural, chemical and pharmaceutical industries [1]. Environmental changes and load conditions applied to motors can cause a malfunction and reduce the efficiency of the motors, leading to repair expenses and financial loss due to unexpected downtime. Common faults in induction motors are: 1) air-gap eccentricity;

2) rotor bar damage; 3) bearing damage; and 4) stator winding imbalance [2]. These faults are often progressive and eventually cause more breakdowns inside the machine. A suitable methodology for continuous condition monitoring can detect the appearance of faults besides its implementation may help to identify the origin of faults and prevent subsequent failures.

One of the main faults in IM that have been analyzed are related to bearings. Within these related faults there exist three different types of faults: inner race damage, outer race damage and ball damage [2]. Commonly the physical magnitudes used for the detection of failure in bearings are: vibrations, current measurement and acoustic emission. Some applications that have been used vibration measurement to provide the condition and the fault diagnosis are focused on the diagnosis of pitting corrosion faults in rolling bearings [3]. Also, condition monitoring using vibration analysis have been applied to hybrid motors and cars in automobile industry for detecting or anticipating faults [4]. Most of the analysis based on stator current are based on calculation of characteristic frequencies in bearings fault, in order to locate the spectral components of the faults [5]. The condition monitoring analysis through acoustic emission may provide a reliable assessment of the presence of specific fault condition in an induction motor with a single fault present through the study of a sound signal [6]. In addition to the measurement of these variables, several analyzes are performed as classical spectral analysis (such as fast Fourier transform). Another type of time-frequency analysis that is used is Wavelet transforms [7] and Hilbert transform [8]. Although the aforementioned methodologies are quite reliable in fault detection, these are only useful for the study of a single type of failure in bearings, limiting to study each type of failure separately.

This paper present a methodology based on the extraction of statistical indicators aiming to perform the detection of bearing faults in an induction motor.

In this methodology, an analysis though PCA (Principal Component Analysis) technique is carried out in order to obtain a classification of different bearing faults, as well as the classification of different severities of the same fault using vibration signals. In this work are addressed the bearing faults of: inner race damage, outer race damage and ball damage. The application of the proposed diagnosis methodology to bearing faults resulting in a reliable classification and detection of different failures and different severity of bearing faults.

II. BACKGROUND THEORETICAL

This part deals with the theoretical relationships for the predictable of failures in bearings in induction motors, as well as the tool that is used for the detection of such failures.

A. Extraction of Fault Frequencies

Bearing faults can be classified according to the fault location (outer race, inner race and ball) and the type of defect (cyclic or noncyclic).

A single-point (cyclic) defect produces an impact between the ball and the raceway and generates a detectable vibration. Various theoretical frequencies can be calculated such as the inner and outer race element pass frequencies and ball rotational frequency. The occurrence of vibrations may help to predict the fault-related frequencies depending on which surface of the bearing contains the fault, on the geometrical dimensions of the bearing, and on the rotational speed of the rotor f_r . Such specific vibration frequencies is the follows [9]:

$$\text{Outer race: } f_o = N/2 f_r (1-d/D \cos(\alpha)) \quad (1)$$

$$\text{Inner race: } f_i = N/2 f_r (1+d/D \cos(\alpha)) \quad (2)$$

$$\text{Ball: } f_b = N/2d f_r (1-(d/D)^2 \cos^2(\alpha)) \quad (3)$$

where N is the number of balls, d is the ball diameter, D is the bearing pitch diameter, and α is the ball contact angle (typically equal to 0°). Fig. 1 shows the variables in the bearing geometry. For simplicity, the outer and inner race characteristic frequencies can be approximated for most bearings with between 6 and 12 balls by

$$f_o = 0.4 N f_r \quad (4)$$

$$f_i = 0.6 N f_r \quad (5)$$

Another method of detecting bearing faults can be obtained by noting that bearing vibration typically leads to variations in the motor torque which is related to the current drawn by the motor. Thus, the current harmonics at the specific frequencies will be affected by bearing vibration. The current spectrum can also be used to detect bearing failures as follows:

$$\text{Outer race: } f_{\text{current}} = f_s \pm k f_c \quad (6)$$

However, these analyzes usually include information of other damages inside the machine, so it is necessary to eliminate this information with other techniques, such as Wiener filter-based noise cancellation [10] and statistical approaches [11].

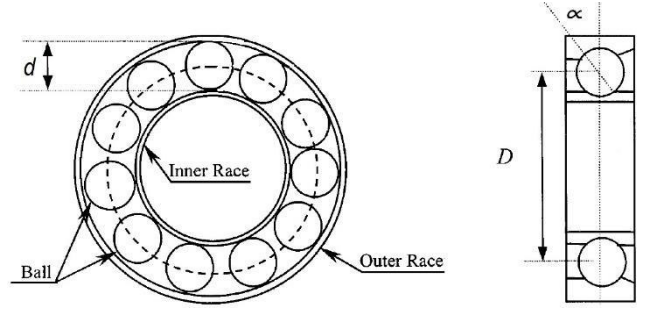


Fig. 1. Structure of a ball bearing.

B. Feature Reduction using PCA

The best way to realize a good classification of faults is by means of a set of features. However, a reduced number of features will not contain enough information to describe and to characterize the machine working conditions. Therefore, the addition of new features is an option to increase the capability of discrimination, and improve the classification performance. However, working with a high-dimensional set of features it could complicate the classification process, since may not offer additional information to the machine condition. In addition to having redundant information, misclassifications can be obtained and have a high computational cost, compromising the proper convergence of the algorithms [12]. For that reason, techniques of feature reduction are implemented in condition monitoring schemes [13]. Mainly, it is possible to remove redundant or non-discriminative features by means of two reduction type of analysis: feature selection and feature extraction.

The implementation of feature selection strategies in condition monitoring schemes is used to preserve the most discriminative characteristic. On the other hand, features characteristic extraction differs in the question of whether a technique is supervised or unsupervised. The main difference between both techniques is the availability of labels to distinguish the different classes. PCA is a well-known and the most common used technique for unsupervised dimensionality reduction and feature extraction [14]. Because it is an unsupervised technique, PCA becomes convenient with respect to other types of techniques of extraction of features, because these increasing the number of observations diminish their effectiveness due to theirs increasing of related variables of an observation. PCA is a mathematical procedure for multivariate analysis using an orthogonal transform to convert a set of observation variables correlated with a set of variable values linearly uncorrelated denominated as principal component. The reduction from the number of variables is not performed by a variable selection, but the generation of new variables by linear combination from the original variables. PCA is based on statistical analysis and even though it does not concern in the separation of different classes, it has advantage in feature extraction due to preserving the variability of the data. Therefore, the use of PCA analysis is useful in the study of the condition to discard redundant information that is not required to detect faults in a system.

A basic algorithm of PCA is as follows [15]: For a given set of observations A_1, A_2, \dots, A_n , where each observation is characterized by a vector of length m , and the dataset is represented by a matrix $A_{m \times n}$.

$$A_{m \times n} = \begin{pmatrix} a_{1,1} & a_{1,2} & \dots & a_{1,n} \\ a_{2,1} & a_{2,2} & \dots & a_{2,n} \\ \vdots & \vdots & \ddots & \vdots \\ a_{m,1} & a_{m,2} & \dots & a_{m,n} \end{pmatrix} \quad (7)$$

$$= (A_1 \ A_2 \ \dots \ A_n)$$

The average observation is defined as follows:

$$\mu = \begin{pmatrix} \bar{a}_1 \\ \vdots \\ \bar{a}_j \\ \vdots \\ \bar{a}_m \end{pmatrix} = \begin{pmatrix} \frac{1}{n} \sum_{i=1}^n a_{1i} \\ \vdots \\ \frac{1}{n} \sum_{i=1}^n a_{ji} \\ \vdots \\ \frac{1}{n} \sum_{i=1}^n a_{mi} \end{pmatrix} \quad (8)$$

While the deviation from the average is defined by Eq. 9:

$$\varphi_i = A_i - \mu \quad (9)$$

Then, the covariance matrix of each data sample is defined by Eq. 10:

$$V_{m \times m} = \frac{1}{n} \sum_{i=1}^n \varphi_i \varphi_i^t = \frac{1}{n} \sum_{i=1}^n (A_i - \mu)(A_i - \mu)^t \quad (10)$$

Where φ^t refers to the transpose matrix of φ .

The covariance measures the linear correspondence between two random variables. A wide positive value indicates positively correlated data. Similarly, great negative values denotes poor correlated data. Thus, the covariance matrix V provides the first view concerning the spread of data in the dataset. In the application of PCA for dimensional data reduction, eigenvalues and corresponding eigenvectors of the sample covariance matrix V are computed by the Singular Value Decomposition (SVD).

Considering that $(\lambda_1, \vartheta_1), \dots, (\lambda_g, \vartheta_g), \dots, (\lambda_m, \vartheta_m)$ are m eigenvalue-eigenvector pairs of the sample covariance matrix. Thus, chosen g eigenvectors corresponding to the largest eigenvalues. g is the inherent dimensionality of the subspace governing the signal, while the remaining $(m-g)$ dimensions usually contain redundant information. Creating a $m \times g$ matrix U whose columns refers to g eigenvectors. Then, data representation by principal components is based on projecting the data onto the g -dimensional subspace w_g as follows:

$$Y_i = U_t \varphi_i = T_t (A_i - \mu) \quad (11)$$

Specifically, in this work, the PCA is applied to reduce the dimensionality of the vectors of the estimated statistical features. The employment of the technique allowed to reduce the input matrix to only 7 significant statistical features which originally had 15 statistical features.

III. DIAGNOSIS PROCEDURE

The proposed methodology for the detection of faults in bearings is composed of the five steps shown in Fig 2. First, the vibration signals are extracted from Case Western Reserve University (CWRU) Bearing Data Center Website [16].

The experimental test bench used in CWRU for testing the different conditions are shown in Fig. 3. It consists of a 2 hp Reliance Electric motor driving a shaft on which a torque transducer and encoder are mounted. Torque is applied to the shaft via a dynamometer and electronic control system [17]. The database has healthy signals, too data sets for rolling element faults and inner and outer race faults, with the outer race faults themselves grouped into three categories according to the fault position relative to the load zone: ‘centred’, ‘orthogonal’ and ‘opposite’.

Second, the feature calculation. Estimate is made a set of 7 significant statistical features. For the calculation, the measurements are taken into account are in the fan-end bearing housing (FE) and on the motor supporting base plate (BA). For each considered measure it is estimated a set of 14 numerical statistical features, 7 statistical features per each vibration signal. The proposed statistical-time features are: maximum value, Root mean square (RMS), skewness, latitude factor, crest factor, kurtosis, and sixth moment. These statistical-time features and their corresponding equations are listed in Table I. Where: x is the total set of samples, n the number of samples, \bar{x} is the mean x_k each of the samples, σ the standard deviation and SRM corresponds to the value of Square Root Mean.

The third step is the feature extraction. The estimated sets of statistical features representing the different working conditions are subjected to a compression process and extraction of principal components by means of PCA analysis. Through extraction process a final set of new features from the previous estimated sets of statistical features is obtained. The new extracted set of features is projected in a 2-dimensional space allowing a visual interpretation of the considered conditions, facilitating the classification task.

Finally, the last step is the classification where extracted set of features is evaluated under a structure of a Fuzzy-based classifier to implement a diagnosis of the different status.

IV. RESULTS AND DISCUSSION

The results shown in this section are obtained by applying the proposed methodology. The application of this methodology is performed under Matlab for the processing of the vibration signals and the classification of the conditions. As it has been mentioned, the analysis was performed by taking the vibration signals from CWRU considering the measurement at two sites in the kinematic chain, in the fan-end bearing housing and on the supporting motor base plate. The available information was obtained at an operating frequency of 12 KHz and consists of ten seconds for each condition considered, then, each one of the acquired signals is segmented in one hundred parts with the objective to generate a set of consecutive samples.

Then, it was performed the calculation of the 7 statistical-time features from each one of the two vibration signals. As a result, the vibration signals are now characterized by fourteen statistical-time features with 100 samples to represent each of the conditions, with the aim of having a better characterization of healthy and failures conditions. These estimated sets of features are then used for extracting a new subset of features.

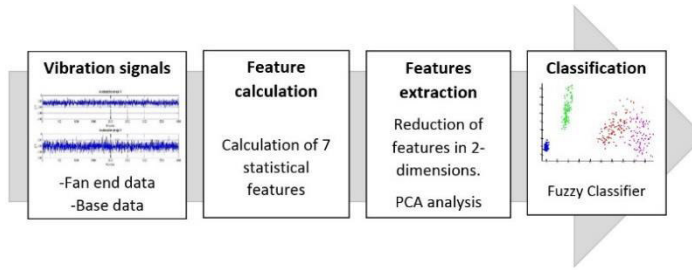


Fig. 2. Proposed diagnosis methodology based on extraction of statistical indicators for detection of bearing fault.

TABLE I
STATISTICAL TIME-BASED FEATURES

Maximum value	$\hat{x} = \max(x)$	(1)
Root mean square	$RMS = \sqrt{\frac{1}{n} \cdot \sum_{k=1}^n (x_k)^2}$	(2)
Skewness	$S_k = \frac{E[(x_k - \bar{x})^3]}{\sigma^3}$	(3)
Latitude factor	$LF = \frac{\hat{x}}{SRM}$	(4)
Crest factor	$CF = \frac{\hat{x}}{RMS}$	(5)
Kurtosis	$k = \frac{E[(x_k - \bar{x})^4]}{\sigma^4}$	(6)
Sixth moment	$6thM = \frac{E[(x_k - \bar{x})^6]}{\sigma^6}$	(7)

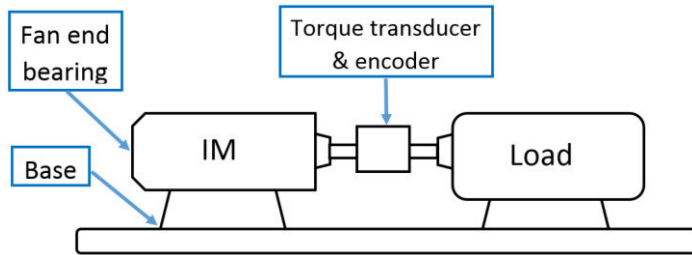


Fig. 3. Flow chart of the CWRU test bench.

The extraction of the new features is carried out by PCA. The PCA analysis aims to find a new projection in a smaller dimensionality trying to maximize the separation between the considered conditions. Then, it obtain a new subset of extracted features, which contain functions with greater variability and relevant information related to the fault conditions considered. With these sets of features is possible a visual representation of the conditions considered in a two-dimensional space. It should be noticed that the faulty conditions are faced to the healthy condition. Thus, in Fig. 4 are shown the projection of the extracted set of features computed by the PCA considering only one vibration signal in motor supporting base plate.

As a justification for the use of two measurements to improve fault classification, a comparison is made between the sets of features extracted considering a single measurement in FE and the sets of extracted features measured in FE and BA. Then, we proceed to the estimation of the set of seven statistical-time features and then to the projection and extraction of indicators is performed through PCA.

The projected in a 2-dimensional space of the extracted set of features computed by analysis of PCA for measurement in FE are shown in Fig 5.

The main problem that occurs when considering only a measurement of vibration in the kinetic chain is that some of the projections resulting from the considered conditions overlap. As can be seen, the ball fault condition is very near to the fault in outer race. This nearness or overlap in the features extracted from the conditions can lead to a misclassification. Although there is some spreading of some points within the considerations, it should note a greater separation between the classes of faults.

For classification a fuzzy-based classifier is used to diagnose the types of faults and to generate the output classes. When considering two signals of vibration one has a greater separation of the classes, this facilitates in much the classification, for which, a simple structure considered in the classifier allows obtaining good results without an excessive use of computational resources. For a statistically significant result, the classifier is trained and tested under a 5-fold cross-validation scheme. In this scheme for classification, the samples of the conditions are subdivided into two types: data used for training and data used for testing. The original database is composed by 360 samples, 90 samples per condition. For training is used 288 samples, 72 samples per condition; for testing purposes is used 72 samples, 18 samples per condition.

To analyze the performance of the classification proposed by the methodology, we proceed to train and test the same structure of the fuzzy-based classifier, five classification ratios are obtained as a result of the iterations generated by the 5-fold-cross-validation scheme, then, these classification ratios are averaged and a classification ratio for the training is obtained. First, with the extracted sets of features obtained only in the measurement of the motor supporting base. Thus, the classification ratio achieved during the test of the fuzzy-classifier by considering only measurement of the motor supporting base are approximately 73.5%. Meanwhile, when vibrations are used both in supporting base and fan-end bearing housing, have been obtained a classification ratio of 93.6%. Table II summarizes the classification ratios achieved during the test of the fuzzy-classifier of the extracted sets of features by considering only one and two vibration signals.

Therefore, it is shown that the overall classification ratio using two vibration signals is improved by about 20% compared when considering a single vibration signal in the analysis. According to the results obtained, proves the performance of the two vibration signals in the progress of condition monitoring for rolling elements in induction motors.

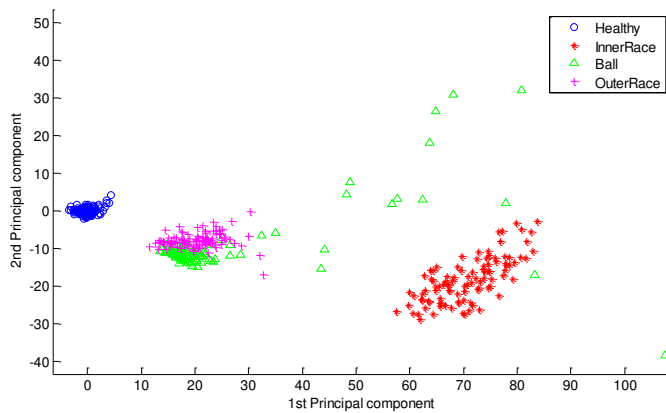


Fig. 4. Projection of the extracted set of feature computed by the PCA considering a set of statistical features estimated from only one vibration signal.

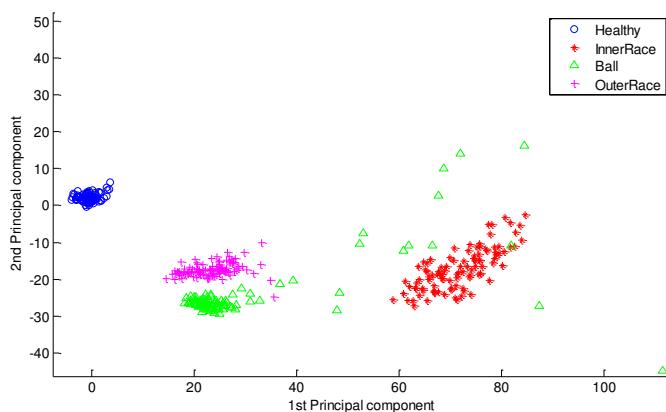


Fig. 5. Projection of the extracted set of feature computed by the PCA considering a set of statistical features estimated from two vibration signals.

TABLE III
CLASSIFICATION RATIOS OBTAINED DURING THE TEST OF THE FUZZY-CLASSIFIER

Number of vibration signals	1 vibration signal	2 vibration signals
Classification ratios achieved	73.5%	93.6%

V. CONCLUSIONS

In this work, a bearing fault diagnosis approach has been developed based on vibration signals using the calculation of the 7 statistical-time features: maximum value, Root mean square, skewness, latitude factor, crest factor, kurtosis, and sixth moment, also, the feature extraction by PCA. Through PCA it is possible to represent the statistical-time features into a 2-dimensional space where the different considered faults are represented. Regarding to the use of one and two vibration signals, the results show an improvement when two vibration signals are used. The experimental results indicate that Fuzzy-based classifier may exhibit a higher diagnostic accuracy when

is used two vibration signals than only one vibration signal, the accuracy increases significantly to 20%.

Four different conditions have been considered, including the healthy and faulty states. The experimental results show that the proposed methodology is suitable to be applied for fault diagnosis of bearings in induction motor. Further, some perspectives of this work is to expand the classification analysis for other types of kinetic chain faults.

REFERENCES

- [1] "United States Industrial Electric Motor Systems Market Opportunities Assessment." U.S. Dept. of Energy, Washington, DC, USA, 1998.
- [2] E. T. Esfahani, "Multisensor wireless system for eccentricity and bearing fault detection in induction motors," IEEE/ASME Transactions on Mechatronics, vol. 19, no 3, pp. 818-826, 2014
- [3] K. Zhang, Y., Shi, H., Zhou, X., Zheng, Z., 2015, "Vibration Analysis Approach for Corrosion Pitting Detection Based on SVDD and PCA," The 5th Annual IEEE International Conference on Cyber Technology in Automation, Control and Intelligent Systems, June 8-12, 2015, Shenyang, China.
- [4] K. Jafarian, M. Darjani, and Z. Honarkar, 2016, "Vibration Analysis for Fault Detection of Automobile Engine Using PCA Technique," 4th International Conference on Control, Instrumentation, and Automation (ICCIA) 27-28 January 2016, Qazvin Islamic Azad University, Qazvin, Iran.
- [5] J. J. Saucedo-Dorantes, M. Delgado-Prieto, J. A. Ortega-Redondo, R. A. Osorio-Rios and R. J. Romero-Troncoso, 2016, "Multiple Fault Detection Methodology Based on Vibration and Current Analysis Applied to Bearings in Induction Motors and Gearboxes on the Kinematic Chain," Hindawi Publishing Corporation Shock and Vibrationm Volume 2016, Article ID 5467643.
- [6] A. G. Perez, R. J. Troncoso, E. C. Yopez, R. O. Rios, and J. L. Martinez, "Application of high-resolution spectral-analysis for identifying faults in induction motors by means of sound," J. Vib. Control, vol. 18, no. 11, pp. 15851594, 2012.
- [7] K. I. Rodopoulos and I. A. Antoniadis, "Instantaneous Fault Frequencies Estimation in Roller Bearings Via Wavelet Structures," Journal of Sound and Vibration 383(2016) 446463, July 2016.
- [8] L. Leh-Sung, K. Jong-Hyun, L. Willey and L. Sun-Kyu, "An Approach Based on Wavelet Packet Decomposition and HilbertHuang Transform (WPDHHT)for Spindle Bearings Condition Monitoring," Mechanical Systems and Signal Processing 33 (2012) 197211, July 2012.
- [9] Bo L., Mo-Yuen C., Yodyium T. and Hung J. C. "Neural-Network-Based Motor Rolling Bearing Fault Diagnosis," IEEE Trans. Ind. Electron., vol. 47, no. 5, October 2000.
- [10] W. Zhou, T. Habetler, and R. Harley, "Bearing fault detection via stator current noise cancellation and statistical control," IEEE Trans. Ind. Electron., vol. 55, no. 12, pp. 42604269, Dec. 2008.
- [11] F. Immovilli, M. Cocconcelli, A. Bellini, and R. Rubini, "Detection of generalized-roughness bearing fault by spectral-kurtosis energy of vibration or current signals," IEEE Trans. Ind. Electron., vol. 56, no. 11, pp. 47104717, Nov. 2009.
- [12] X. Wan, D. Wang, P. W. Tse, G. Xu, Q. Zhang, "A critical study of different dimensionality reduction methods for gear crack degradation under different operating conditions," Measurement, vol. 78, pp. 138-150, 2016.
- [13] F. Li, J. Wang, M. K. Chyu and B. Tang, "Weak fault diagnosis of rotating machinery based on feature reduction with Supervised Orthogonal Local Fisher Discriminant Analysis," Neurocomputing, vol. 168, pp. 505-519, 2015.
- [14] R. H. Cunha Palacios, A. Goedtel, W. F. Godoy and J. A. Fabri, "Fault identification in the stator winding of induction motors using PCA with artificial neural networks," Journal of Control, Automation and Electrical Systems, vol4, no. 20, 2016.
- [15] Jolliffe, I. T. (2002). Principal Component Analysis (2nd ed.). New York, Springer.

[16] Case Western Reserve University Bearing Data Center Website
<http://csegroups.case.edu/bearingdatacenter/home>.

[17] W. A. Smith, R B. Randall “Rolling element bearing diagnostics using the Case Western Reserve University data: A benchmark study,” Mechanical System and Signal Processing 64-65 , 2015.



Analysis of Spatial Variability of Short-duration Storms for the Northwest Region of Querétaro City and the Metropolitan Area

Nadia Ingrid Alburquerque-González.

División de Estudios de Posgrado, Facultad de Ingeniería
Universidad Autónoma de Querétaro
Querétaro, Qro., México
ingrid.alburquerque@live.com.mx

Pablo Talamantes Contreras.

División de Estudios de Posgrado, Facultad de Ingeniería
Universidad Autónoma de Querétaro
Querétaro, Qro., México
tpabloc@uaq.mx

Abstract— The impact of the storm spatial structure should be studied for achieving more realistic hydrologic models, in this study the data from 5 meteorological stations is analyzed so it could be possible to find a pattern of typical storms for the north region of Querétaro City, Mexico. The rainy season in Querétaro city occurs between the months of June and August, it is a semi-arid zone characterized by torrential rain that last a few minutes. Torrential storms from 5 to 30 minutes were prevalent for the year of 2014, also there was 2 longer storms of 40-60 minutes with high intensity which were analyzed as well. The semi variogram function for the storms show a deep relationship between the intensity of the stations which helps the Kriging interpolation to be more accurate. This study focuses only in the spatial variability of the intensity of the rain, for the northwest region of the Queretaro city for simultaneous rain stages.

Keywords—Semivariogram, Kriging function, Short Duration Storms.

I. INTRODUCTION

The relevance of the study of the occurrence of the storms for hydrology studies has a big weight. The most important factor of runoff generation is the variability of the storm, that is why the magnitude of more precise variability studies of storms e.g. [1,2] It has been Highly documented that the response of the drainage network has a solid relation with the structure of the storm. Also, as stronger is the intensity near the basin output, more severe it is the response of the catchment, leading to riskier flows e.g.[3,4]. Even when Geographic information systems has approach solutions for various spatial hydrologic items, the technology of the devices used in the

field has had little progress. Since real-time transmission devices are high cost, the use of meteorological and hydrological models have spread in undeveloped countries. It's common to use spatial interpolation methods for working with rainfall-runoff modelling, methods like Thiessen polygons, Inverse Distance Weighting, Multiquadric functions fitting, kriging techniques are widely use because of their simplicity, but those models are not really accurate because of their lineal approach or their Gaussian normal assumptions. Also, daily measurements that has being highly analyzed and used for hydrologic models does not brings out enlightenment about intensity and translation of the rain, information that is useful for a better understanding of the basin behavior, since the geomorphologic characteristics in combination with the occurrence of the storm brings resolutions about the runoff regime. This may charge more weight in urban settlements, which are commonly founded in the valleys and low points of the basins, so it is for mountain catchments that may present a different department.

II. MATERIALS AND METHODS

A. Meteorological station network conditions

The meteorological station network data was given for the RED-CIAQ devices, RED-CIAQ it is a network property of the Autonomous University of Querétaro. It has 15 meteorological stations spread in the state of Querétaro, most of them are located in the city and the metropolitan area. They have been working since august 2012, and offers 1-minute interval data.

B. Availability of data

After a careful audit of the availability of record data, we look forward to work with high density data. For the year 2014, we found excellent information about most of the storms that took place in the rain season, thus eliminating the uncertainties that may affect the interpretation of the algorithms of the rain behavior for this region of the city. The stations that show a big correlation between them and that includes the region we are interested in, were; the number 1 station “Chulavista”, the number 2 station “Belen”, number 3 station “Real del Parque”, the number 9 station “El Refugio”, the number 12 station “Geociencias”. In the table 1 we can appreciate the duration and intensity in the stations for various events.

C. Statistical analyses.

The rainfall patterns are well organized structures in space and time [5], variogram is commonly used to identify the mean quadratic deviation between each pair of punctual data, the correlogram are fitted by 3 parameters; which are the range, the anisotropy ratio, and the direction, this model gives information about the distribution of the intensity of the precipitation in this case, so it is feasible to find values in ungauged zones.

Even when a combination of several factors causes rain, it has been proven that it may show a uniform behavior when talking about time and space. The main idea of this study is to find the spatial correlation for any rain, especially for short-duration events with high intensity, since those cause the biggest damage in the city.

An arrange of spatially distributed data are dependent between somehow, this dependency maybe stronger in a specific scale, also, when biggest the density better the understanding of the stage.

The variogram theory shows that given an aleatory cloud of punctual data, some pairs may have a bigger dependency, the function of dependency will be given in terms of the variable distance h and in function of the 2D distribution, there could be

a direction in which the correlation may be stronger, this anisotropic approach comes from the idea of the predominant orientation of many physical processes.

Semi variogram is given by half of the square difference of a pair of stations [6] separated by an h distance and given a certain variable, in this case that variable will be the rain.

$$\gamma(h) = \frac{1}{2} E \left[\{Z(\mathbf{x} + h) - Z(\mathbf{x})\}^2 \right] \tag{1}$$

Z(x) is a random variable which represents the phenomena of study and that has a position in a 2D system Z(x, y)

h is the distance between two experimental points.

III. RESULTS

The standard deviation and variance is shown in the table 2, some high variation can be observed, this occurs because of the information that wasn't normalized, still this high variation helps in order to find the spatial anisotropy. The geospatial analysis of the data shows, that in all the events of rain in 2014, the behavior of the precipitation in the space was anisotropic and has some common directions, an example can be seen in Fig1. Also, as the table 3 shows, the predominant direction of the rain was between 70° - 90° for this zone in the city while two storms have another direction 130° - 150° but still in the same range, remember that the variogram has a tolerance in the direction, in which the variance between pairs at specific distance may be found. In no case was possible to fit a model equation to an omnidirectional distribution, as can be seen in the Figure 2. Conjointly the reduction of the nugget effect or the error, according with the theory of the semivariogram, of the directional models with respect to the omnidirectional ones also explains why the model that could better adjust the

TABLE 1. Rain intensity and rain duration values for the events of study in the Stations of interest

Event	Station	Chulavista	Belen	Real del Parque	El Refugio	Geociencias
June 19, 2014	Intensity	30.15	43.92	36.85	34.24	36.00
	Duration	39.00	25.00	21.00	24.00	33.00
June 19, 2014*	Intensity	6.43	20.00	12.88	27.60	33.40
	Duration	14.00	9.00	7.00	10.00	46.00
June 24, 2014	Intensity	18.00	18.67	8.67	22.00	24.55
	Duration	38.00	9.00	9.00	9.00	54.00
July 8, 2014	Intensity	12.00	28.15	6.00	6.00	62.04
	Duration	32.00	13.00	5.00	13.00	44.00
July 24, 2014	Intensity	21.00	22.00	11.00	8.00	9.70
	Duration	18.00	11.00	18.00	21.00	13.00
August 8, 2014	Intensity	12.00	28.15	6.00	6.00	62.04
	Duration	32.00	13.00	5.00	13.00	44.00
August 9, 2014	Intensity	21.00	22.00	11.00	0.00	9.70
	Duration	18.00	11.00	18.00	0.00	13.00

TABLE 2. Standard deviation and variance for the Rain Intensity and Rain Duration statistics

Rain Event	Rain Intensity Sample Statistics		Rain Duration Sample Statistics	
	Standard Deviation	Variance	Standard Deviation	Variance
June 19, 2014	2.81	47.94	5.01	25.2
June 19, 2014*	3.4	111.59	15.5	240.3
June 24, 2014	6.04	36.42	4.09	16.7
July 8, 2014	6.47	441.8	12.03	144.7
July 24, 2014	4.11	416.88	4.086	16.7
August 8, 2014	6.47	441.8	12.03	144.7
August 9, 2014	7.44	455.41	3.19	410.2

behavior of the intensity of the rain in the space must be directional .

In the other hand, rain duration (Table 4) shows an erratic behavior in general, even when the totality of the events where better adjusted in directional semi variogram.

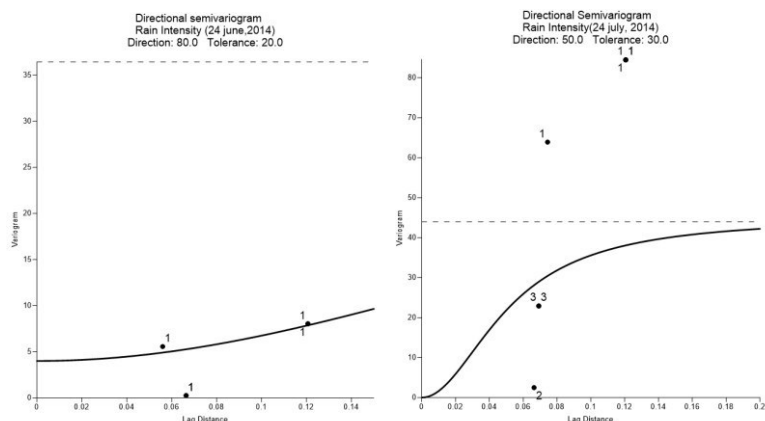


Fig. 1 Directional Semi variogram Examples for Rain Intensity, to the left is shown the directional semi variogram for the event of 24 July, 2014, and to the right is shown the semi variogram for the event of 24 June, 2014.

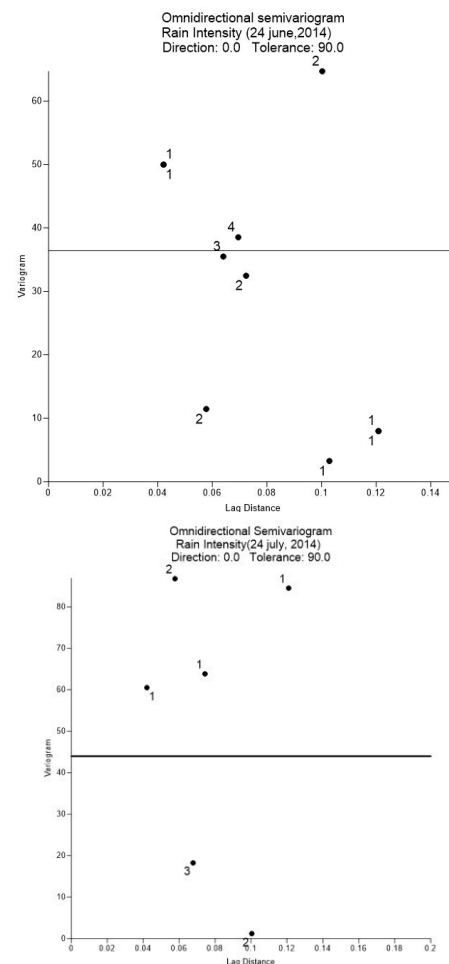


Fig. 2 Omnidirectional Semi variogram Examples for Rain Intensity, (Up) omnidirectional semi variogram for rain intensity of the event of 19 June, 2014, (Down) omnidirectional semi variogram for rain intensity of the event of 24 June, 2014.

TABLE 3. Results of Anisotropy in each event, Direction, Tolerance and Best fit Model.

Rain Event	Rain Intensity			Rain Duration		
	Direction	Tolerance	Model	Direction	Tolerance	Model
June 19, 2014	30	30	Wave	160	45	Rational Quadratic
June 19, 2014*	70	45	Spherical	90	30	Spherical
June 24, 2014	80	20	Rational Quadratic	50	30	Rational Quadratic
July 8, 2014	130	45	Rational Quadratic	10	45	Rational Quadratic
July 24, 2014	80	30	Rational Quadratic	160	45	Rational Quadratic
August 8, 2014	150	45	Rational Quadratic	50	30	Rational Quadratic
August 9, 2014	90	30	Spherical	100	45	Rational Quadratic

TABLE 4. Fit factors for each model and any Intensity semi variogram event, Nugget, Scale (Variance), Length (Distance h), Anisotropy ratio and angle.

Rain Event	Directional Semivariogram					Omnidirectional Semivariogram		
	Nugget	Scale	Lenght (h)	Anisotropy Ratio	Anisotropy Angle	Nugget	Scale	Lenght (h)
June 19, 2014	2.81	13	3.5	300	5	25	-	-
June 19, 2014*	10.86	100	0.06	0.9	0	11	-	-
June 24,2014	4	36.42	0.35	1	0	36.42	-	-
July 8,2014	6.47	560	0.25	7.1	0	561	-	-
July 24,2014	0	45	0.2	5	0	43.98	-	-
August 8,2014	150	450	8	20.7	0	563	-	-
August 9,2014	7.44	55.41	0.2	1.6	0	82.14	-	-

TABLE 5. Fit factors for each model and any Duration semi variogram event, Nugget, Scale (Variance), Length (Distance h), Anisotropy ratio and angle.

Rain Event	Directional Semivariogram					Omnidirectional Semivariogram		
	Nugget	Scale	Lenght (h)	Anisotropy Ratio	Anisotropy Angle	Nugget	Scale	Lenght (h)
June 19, 2014	5	60	0.04	0.5	65	55	-	-
June 19, 2014*	0	30	3	20	0	265.7	-	-
June 24,2014	40	422.7	2	16.6	0	441	-	-
July 8,2014	12	144	0.15	4.8	0	12	-	-
July 24,2014	2.88	18	0.1	0	0	16.6	-	-
August 8,2014	50	200	5	50.7	0	258	-	-
August 9,2014	3.19	40	10	185	0	54.5	-	-

In the Table 6 the distance h is considering since it is the distance from which we can find the highest density of the pairs of points that are correlated, it means the points that will define the mathematical model of semivariogram. Also, the concept of range indicates the distance in the axis h in which the curve reaches its sill, indicating then, the distance from which, no longer exists correlation between pairs of points in the defined direction and tolerance.

TABLE 6. Range of the semiovariogram model and distance h between pairs of points to plot for rain events.

Rain Event	Rain Intensity		Rain Duration	
	Range	Distance h	Range	Distance h
June 19, 2014	>0.08	0.01	0.1	0.01
June 19, 2014*	0.15	0.02	0.12	0.02
June 24,2014	>0.15	0.02	0.15	0.02
July 8,2014	0.14	0.02	>0.12	0.01
July 24,2014	0.2	0.02	0.15	0.02
August 8,2014	0.2	0.02	>0.15	0.02
August 9,2014	0.11	0.02	0.13	0.02

The distance h used for plotting the pairs is very small in most of the case. Then the range are pretty small, but not in some cases, were the symbol “>” or “bigger than” is used, this is the case of the models that has a very high variance and then the model will take quite a lot of distance to reach the line of the variance in the graph, or the line at which, there is no correlation between points.

IV. RESULTS

The information processed in this article indicates that for the rain events of high intensity for the summer of 2014, there is a prevalence in the direction 70° - 90° and an acceptable tolerance between 30° - 45°, still is not possible to assume a similar conclusion for the behavior of rain duration. Additionally directional plots shows a bigger number of pairs with small variance than omnidirectional plots, as well the indicator of error (nugget) shows a great diminution when working in directional paths instead of the general assumption of same variability in all directions, that proves that a method that doesn't take into consideration the variation in an specific path bigger than in the others is not useful for this region of the



V. REFERENCES

city.

Since the stations coordinates are given in decimal grades of latitude and longitude, also the calculus of distance between pairs is given in this unit, the distance h for plotting was tested to reach the bigger number of pairs to fit to a semidirectional variogram, and therefore the intensity rain shows a bigger correlation at longer distances than most of the duration rain semivariogram. This is a measure of the low relation that rain duration has between one point and another, so it may be related to other factors than distance, even when in this paper, we can not affirm which are these factors, another analysis should be done.

The range at which the pairs of points have still relation is quite small for most of the models, but there is still some models where is hard to calculate the distance at which the sill starts, in that cases de symbol ">" were used, but this do not mean that the pairs of data that has big distance between them is correlated, it means that since no points appears, there is a lack in measurements.

About the curves adjusted to the data, it was found that most of them are missing information about connection between pairs at small distance, this means that the transition information is needing more feed, in consequence any estimation in an ungauged point may be highly sensitive to this lack in the data.

Even though this data is not enough to build a kriging map with confidence, yet it is possible to affirm that the rain follows a specific directional path.

- [1] S.M.S. Shah., P.E. O'connell, and J.R.M. Hosking, "Formulation and calibration of a stochastic rainfall field model", Modelling the effects of spatial variability in rainfall on catchment response. Jour. of hydrology, volume 175 pp.67-88, February 1986
- [2] Marie-Laure Segond, Howard S. Wheater and Christian Onof, "The significance of spatial rainfall representation for flood runoff estimation: A numerical evaluation based on the Lee catchment, UK". Jour. of hydrology, volume 347, pp. 116-131, December 2007.
- [3] I. Rodríguez-Iturbe, and J. B. Valdés. "The geomorphologic structure of hydrologic response". *Water Resour. Res.* **15**(6):1409-1420.1979
- [4] D.H Pilgrim," Travel times and nonlinearity of flood runoff from tracer measurements on a small watershed". *Water Resour. Res.*, 12 (3):487-496.1976.
- [5] Zoubeida Kebaili and Andràs Bardossy, "Modeling short duration extreme precipitation patterns using copula and generalized maximum pseudo-likelihood estimation with censoring", *Advances in Water Resources*, volume 84, pp 1-13, October 2015.
- [6] Sebastian Voss, Beate Zimmermann and Alexander Zimmermann, "Detecting spatial structures in throughfall data: The effect of extent, sample size, sampling design, and variogram estimation method", *Jour. of hydrology*, volume 540, pp. 527-537, September, 2016.

Characterization of Mortar with Mineral Additives

Rebeca Visairo Méndez
Faculty of Engineering, UAQ
Santiago de Querétaro, Querétaro, México
rvisairom@gmail.com

Andrés A. Torres Acosta
Instituto Mexicano del Transporte (IMT)
Sanfandila, Querétaro, México
atorres@imt.mx

Luis Alfonso García Cortés
SICGA S.A. de C.V.
alfonso.garcias@sicga.com.mx

Lucero Altamirano Serrano
MOVINCO S.A. de C.V.
movinco@hotmail.com.mx

Roberto Alvarado Cárdenas
Faculty of Engineering, UAQ
Santiago de Querétaro, Querétaro, México
ralvaradocardenas@gmail.com

It has been an increase on the number of concrete structures with corrosion induced damage in Mexico in recent years. There are many studies trying to understand the mechanic and electrochemical behavior in structure elements affected by corrosion [1, 2]. The Ibero-american Thematic Network DURAR confirm that the concept of durability includes the lifetime of a structure [3]. The main problem has been the period of residual life of the structure because in this period the structures are repaired in case of damage. It has been proved that the load capacity and the displacements get affected considerably with corrosion damage [4]. The repair in reinforced concrete beams has been studied considering mechanic and electrochemical behavior. The most important repair is with different proportions of mortar but it has been proved that the corrosion never disappears completely. Actually, there are few studies about this theme considering the durability concept. Therefore, this investigation includes an evaluation of mortar to increase its electrical and ionic conductivity to increase the efficiency of the entire hybrid system (mechanic and electrochemical behavior). Additions include carbon, zinc and alumina powders, and this investigation presents preliminary experimental results obtained from the tested mortars (i.e. mortar physical characterization: electrical resistivity, ultrasonic pulse velocity, and total void content).

Mortar, corrosion, repair, reinforced concrete.

I. INTRODUCTION

Reinforced concrete is the most used material in construction industry nowadays. Nonetheless, it presents the disadvantage of being susceptible to corrosion failure [4].

When reinforcing steel bars (rebars) corrode, a passive layer of the steel surface is consumed, and corrosion products (iron oxides or hydroxides) grow on the rebar perimeter. The volume occupied by the expansive oxides (hydroxides) is bigger than the original steel, creating pressures against the surrounding concrete. These tensile pressures cause cracks, concrete delaminations and finally the structural element resistance decreases [4].

There are many studies about economic and structural lost due to corrosion and it has been proved that the 25 % of the damage could be avoid applying techniques for repair structure elements [5].

Different repair and rehabilitation methods have been tested elsewhere in deteriorated structures in general. An author found that the best proportion using additives was about 15 %p/p, which recover an 89 % in regard to beams without corrosion [6].

There is few information about recovery in structural elements using mortar [6, 7, 8]. The authors concluded that mechanic behavior improves with time but the corrosion could continue. Therefore, it is important to confirm if a repair system increases the load capacity after corrosion damage and different ages.

This publication includes the first part of an experimental procedure, which is the physical performance of the mortar fabricated.

II. EXPERIMENTAL PROCEDURE

A. Materials

Mortar mixture was fabricated from commercial mix mortar (SICGA S.A de C.V)¹ used to fabricate specimens in IMT's Laboratory. Mortar for addition mixtures was prepared considering Mexican and international regulations [9, 10, 11].

B. Specimen geometry

Twelve cylinders with dimensions 10 x 20 cm (diameter x height) were fabricated. Also, 36 plain mortar cubes with dimensions 5 x 5 x 5 cm (height x length x width) were fabricated. All the specimens were divided into two series and it was considered the main finally tests in the periods of 30 days; 60 days; and 90 days for each series. After casting, the specimens were kept in a high humidity chamber (~95% relative humidity, RH) for a 28-day curing period. They were then transferred into closed plastic containers until analysis.

C. Physical Characterization

All trials were run in the same laboratory environment (22±6 °C, ~60% RH). Five consecutive tests were done in the following order: (a) total void content; (b) electrical wet resistivity; (c) pulse velocity; (d) capillary absorption; and (e) compressive strength. Since this is an ongoing investigation, the present publication will only show the results up to date, which correspond to test characterizations (a), (b), and (c) for the first series. Test characterizations (d) and (e) will be presented in the near future.

D. Electrical Wet Resistivity

Mortar electrical wet resistance (R_w) was measured after the second wet cycle using a Model 400 Nilsson Soil Resistance Meter following the DURAR Manual procedure [3]. Each test was done using external stainless steel plates with sponge pads. The sponges were placed between the stainless steel plates and the cube surface, and special clamps used to attach the plates to the mortar cube without causing electrical interference. Electrical wet resistivity (ρ_w) was estimated with the formula $\rho_w = C_C \cdot R_w$, where R_w is measured wet resistance (in kilo ohms, $k\Omega$) and $C_C = 5$ cm, the cell constant. Preparatory measurements were taken after oven drying at 50 °C until constant mass. Then a first measurement was taken and designated as dry resistivity (ρ_D). The cubes were placed in a high humidity plastic container and measurements taken continuously until the resistivity value was constant, at which point a final ρ_w measurement was taken.

E. Ultrasonic Pulse Velocity

After electrical resistance analysis, the same cubes were tested with the Ultrasonic Pulse Velocity (UPV) technique. This parameter was measured using a CONTROLS Model E48 ultrasonic pulse velocity testing device following ASTM C-597 [12].

F. Total Void Content

Total void content was measured following the ASTM C-642 procedure [13]. After drying at 50 °C until constant mass (from 21 to 35 days), an initial measurement was taken and designated as dry mass (m_D). Then the specimens were placed in a high humidity plastic container and measurements taken constantly until reaching constant mass, when a final m_W was recorded. The water-saturated cubes were weighed inside the water to measure saturated-submerged mass (m_{SS}).

III. RESULTS AND DISCUSSION

Results and their discussion presented in this publication include only electrical wet resistivity, ultrasonic pulse velocity, and total void content percentage.

A. Electrical Wet Resistivity

Electrical resistivity quantifies pore interconnection within granular (i.e. soils) and porous materials. In porous materials such as mortar or concrete, electrical resistivity depends on degree of pore saturation and, to a lesser extent, on paste hydration or the presence of dissolved salts in the aqueous phase. Mortar containing normal moisture levels has a ρ_w on the order of 20-60 $k\Omega \cdot cm$.

Values ranged from 46.98 to 97.89 $k\Omega \cdot cm$ (Fig. 1). Electrical resistivity also depends on movable ion content, not just on material porosity and tortuosity. Inclusion of compounds in cement will increase its ionic content, and consequently its ion mobility (conductivity).

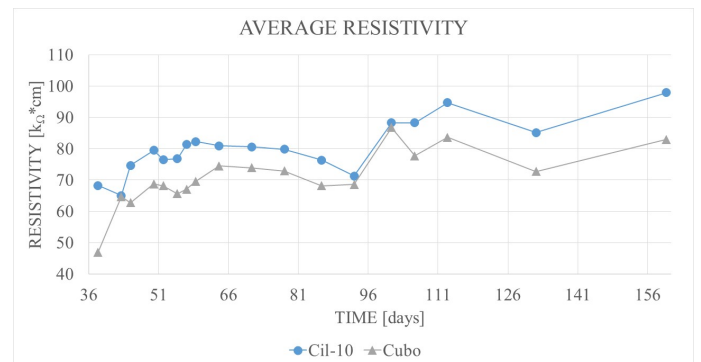


Fig. 1 Average values of Electrical Wet Resistivity

B. Ultrasonic Pulse Velocity (UPV)

This technique is an indirect method for quantifying homogeneity in cement-based materials. An emitter sends an ultrasonic pulse through the tested material to a receptor, and the distance between the emitter and receiver divided by elapsed wave travel time is known as UPV. Values ranged from 4.67 to 4.95 km/s for cylinders and 3.65 to 4.14 km/s for cubes (Fig. 2).

¹ Servicios Integrales (SICGA S.A de C.V.)

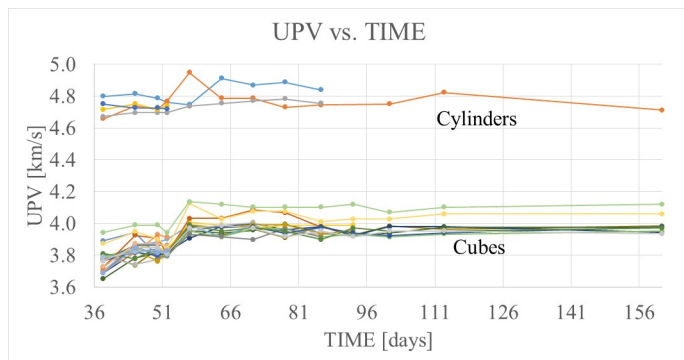


Fig. 2 Ultrasonic Pulse Velocity (UPV)

C. Total Void Content

The total void content test corroborated the ρ_w and UPV test results (Table I).

TABLE I RESULTS FOR AVERAGE OF TOTAL VOID CONTENT

SPECIMEN	Total Void Content (%)
Cylinders	5.35
Cubes	5.82

Of all the physical properties measured here, the most important result is the effective porosity, also called connective porosity. This physical characteristic will be tested using capillary water absorption procedure, which will be ready in the near future together with the compressive strength of the mortar mixtures tested in this experimental program.

IV. CONCLUSIONS

From a previous investigation performed by the present authors, it is assumed that the mortar in this study has physical characteristics that improve any structural element with corrosion damage. In conclusion, the durability of this mortar specimens is good enough for being used in reinforced concrete structures and avoid these type of damage. It is important to continue with the other evaluations and with more types of mortar. In consequence, this mortar will be proven in the next evaluations for rehabilitation of concrete reinforced beams for Doctoral research.

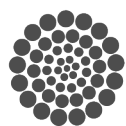
ACKNOWLEDGMENT

This research was supported by the Universidad Autónoma de Querétaro (UAQ), Instituto Mexicano del Transporte (IMT),

Servicios Integrales (SICGA S.A de C.V.) and the National Council of Science and Technology (CONACYT) through financial support and research scholarship to M.E. Visairo-Méndez. The opinions and findings in this paper are those of the author and not necessarily those of the funding agencies.

REFERENCES

- [1] Guevara, B., Juárez, C., Fajardo, G., & Castro Borges, P. (2009). "Comportamiento a cortante en vigas de concreto reforzado con deterioro por corrosión en los estribos". *Ingeniería de Construcción*, 24(3), 259-270.
- [2] Wang, L., Li, C., & Yi, J. (2015). "An experiment study on behavior of corrosion RC beams with different concrete strength". *Journal of Coastal Research*(73), 259-264.
- [3] DURAR, R. (1997). "Manual de inspección, evaluación y diagnóstico de corrosión en estructuras de hormigón armado". CYTED. Maracaibo, Venezuela: Programa iberoamericano de ciencia y tecnología para el desarrollo, subprograma XV corrosión / impacto ambiental sobre materiales.
- [4] Torres Acosta, A., Martínez Madrid, M., & Muñoz Noval, A. (2003). "Capacidad remanente en vigas de hormigón que presentan corrosión localizada en el acero de refuerzo". *Mater Construcc*, 53(271-172), 125-133.
- [5] Vázquez Castillo, C. D. (1998). "Diagnóstico de la corrosión del puente de Celestún". Tesis. Mérida, Yucatán, México: Facultad de Ingeniería, Universidad Autónoma de Yucatán.
- [6] Hernández López, Y. E. (2009). "Evaluación de microsilíce en la reparación de vigas de hormigón armado contaminado con cloruros". Universidad de Granada, Departamento de Ingeniería Civil, Área de Ingeniería de la Construcción, E.T.S. de Ingenieros de Caminos, Canales y Puertos. Granada: Universidad de Granada.
- [7] Malumbela, G., Alexander, M., & Moyo, P. (2010). "Variation of steel loss and its effect on the ultimate flexural capacity of RC beams corroded and repaired under load". *Construction and Building Materials*(24), 1051-1059.
- [8] Muñoz Noval, A. (2009). "Comportamiento de vigas hiperestáticas de hormigón armado corroídas y reparadas con mortero. Pérdida de propiedades mecánicas del acero de refuerzo y fisuración del recubrimiento de hormigón por corrosión". Madrid, España: Universidad Politécnica de Madrid.
- [9] NMX-C-030-ONNCCE-2004. (2004). *Industria de la construcción - Agregados - Muestreo*. Diario Oficial de la Federación. México, D.F.: Organismo Nacional de Normalización y Certificación de la Construcción y Edificación, S.C.
- [10] ASTM E 230-12. (2012). *Standard Specification and Temperature-Electromotive Force (emf) Tables for Standardized Thermocouples*. American Society for Testing and Materials (ASTM).
- [11] ASTM C 305-14. (2014). *Standard Practice for Mechanical Mixing of Hydraulic Cement Pastes and Mortars of Plastic Consistency*. American Society for Testing and Materials (ASTM).
- [12] ASTM C 597-16. (2016). *Standard Test Method for Pulse Velocity Through Concrete*. American Society for Testing and Materials (ASTM).
- [13] ASTM C 642-97. (2006). *Standard Test Method for Density, Absorption, and Voids in Hardened Concrete*. U.S.A.: American Society for Testing and Materials (ASTM).



Living walls:

A little review through this technology and the opportunities to innovate

Martinez Alvarez, E.D.

Posgraduate Department, MSc. Construction
Universidad Autonoma de Querétaro.
Querétaro, Qro.
daniel_m.a@outlook.com

Rico Garcia, E.

Posgraduate Department, Phd.
Universidad Autonoma de Querétaro.
Querétaro, Qro.

Abstract—Today, although the living walls technique is a referent in sustainable construction, there is a lack of information about it. The benefits are very known but there is a problem in the difference between one type of technique to another and the lack of technical data makes difficult to evaluate correctly the use of them. The innovation developed through many investigations around the world has little of publicity and that makes harder to establish what kind of technology has an option to minimize the impact of the construction activity correctly. This article wants to establish some very important points about the development of the living walls and the progress of investigation to create a more accessible and standardized option to the building industry.

Keywords: living walls systems, sustainable construction, living walls last innovations.

I. INTRODUCTION: WHAT IS A LIVING WALL?

Based on [1], living walls are systems which integrates the vegetation into the vertical surface of a construction (like walls and columns) with a specific choice of plants and also a growing media which provides the necessary to the development of the plant. This concept is sometimes short and merely incomplete because it does not describe correctly all the parts of the living wall and the difference with other type of technologies (traditional green walls, green façade, extensive or intensive, passive or active, among others). Based on [2], we can complete this definition like a system in which vegetation not only is attached to a building façade but also is fully integrated into the façade construction where the plants and planting media are both placed on the vertical surface. Just in this point, we could see a difference in the definition of the term “living wall”, in one side, the consideration of the growing media, type of plants and location could define correctly a living wall, meanwhile by others, it is necessary to say additionally the location in the construction (indoor or outdoor) and the type of support system. Completing these considerations, we can not only define, but also, select the correct type of living wall for our construction requirements.

The aim of this paper is to provide insights on how to construct successful living wall systems, exposing recent research also the advances on the technical requirements. This

not only creates a less complex understanding but also, respond the cited criticism like “too expensive [3]”, “too complicated [4]”, “too decorative and superficial [5]”.

II. TYPES OF LIVING WALLS

A. Important aspects of living wall to define

Using the description given by [2], the components of the living walls are primarily three: the support system, the plant selection and the type of maintenance (Fig. 1). This could give us a better response to select the correct type of living wall and adjust the budget related to this.

1) *Support system:* Is where the living wall going to grow and live. It is the most important part of the technology because, considering the characteristics of the building (structural, integrity of wall surface material, among others) and the budget, we can define the type of living wall what we going to use in our project[6].

2) *Plant selection:* It is another important point to define in our project. This selection should be appropriate for the weather conditions and climate conditions of the project. [2],[7] recommend that native hardy plant species are the most suitable to any kind of project. Plants which still green in ever season are more appropriate related to cooling effects in warmer and hot climates, also, deciduous plants are more acceptable to cooling in summer and passive heater in winter, just like in temperate and colder climates[8].

3) *Maintenance system:* This depends primarily of the scope of the project. Type of irrigation and fertilization could be an important factor because those are regularly automated systems and require skilled hand for the maintenance. Also, the periodical examination of the living wall could help to know about the plant health and also, avoid possible damage on the building caused for the humidity of the system and leakage on the irrigation system.



Fig. 1. General aspects of the living wall

B. Classification of living walls

We need to put aside the term “green wall”. Green wall is only the application of vegetation into a vertical surface, no matter what kind of support, plant or growing media use to. Also, the vegetation is not only attached to the building but also integrated into. We can generalize at the beginning to help us to difference between one to another. In the fig. 2, Manso [7] classifies the different types of green walls accord to the construction method to understand the differences between the “green wall” and “living wall” terms.

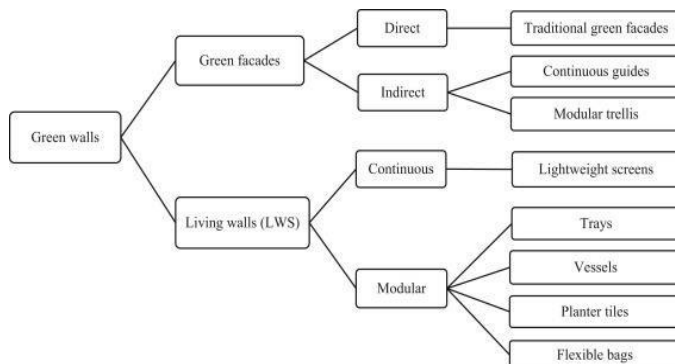


Fig. 2. Classification of green walls, according to their construction characteristics (Manso, 2015)

Also in annex A), we can check an overview of all vertical systems with their characteristics.

III. PROS AND CONS

After all, there is a lot of ignorance about the application of this technologies. Those allegations are based merely on observations and a lack of technical information about the systems. Primarily are three: cost, implementation and only had an aesthetic application in the building.

A. Cost

In a construction project, the budget a fundamental tool to make decision. The cost of this technologies varies between one project to another (from 150 dollars to 400 dollars per square meter). Also, we need to consider the cost of maintenance, which in many times, is not consider into the project budget and makes the correct implementation fail [9].

B. Implementation and success of the system

The living wall system, as a “living” system needs water. The consumption and cost of this resource makes a criticism aimed at living walls from within the design profession [10]. There is very little information published on this topic, but some off-the-record figures were shocking. Occasionally the topic is addressed[11], but more transparency is needed if living walls are to become a sustainable construction system. Some researchers are responding to this need. There is a growing list of published research on sustainable living walls and their irrigation, noteworthily from Spain [12]. On today’s market the most efficient living wall exterior systems consume 1 liter of water per m²/day[13].

C. Aesthetic applications

Green walls can reclaim disregarded space by providing aesthetic stimulation where it would not otherwise be found. They can also serve to create privacy and a sense of enclosure while limiting the negative psychological effects associated with property demarcation.

Certainly, the living walls are a feasible option to urban media, not only because the technologies make a sustainable construction and adapts to any kind of surface and/or/without building, but also has a lot of benefits like:

- Reduction in energy consumptions and greenhouse emissions [2, 14, 15].
- Urban heat island effect reduction [16].
- An increase of thermal performance which follows as a reduction of energy cost in the building [12].
- Positive effect in the urban hydrology and water quality[17].
- Improves the air quality[18].

- Acoustic improvement of the surface [19].
- Biodiversity improvement and increase in a urban media [20].
- Improves comfort and health quality [21].

Based on the allegations, we can discover a lot of innovations and examples around the living wall technologies. On Annex B), we could see a different overview of this kind of technology.

IV. CONCLUSIONS

Vertical gardening is basically about growing your plants upwards on vertical surfaces, be it on the wall of a home or a large facade of a building. As space is a constraint for many urban areas these days, having a vertical garden is certainly an option to still include some greenery in the house/building. Vertical gardening is more than just aesthetics; it can help to cool and insulate buildings, reducing the need and cost for air-conditioning. Growing plants in the building can also help to filter air particulates and improve air quality as well as add some humidity to centrally cooled offices at the same time. Vertical gardening requires little maintenance/trimming and mostly does not use soil. It also helps to save water by reducing the need for irrigation and watering. With vertical greenery, it also helps to soften the grey, hard and cold look of concrete especially in concrete urban jungles.

REFERENCES

Uncategorized References

1. Newton, J., et al., *Building Greener: Guidance on the use of green roofs, green walls and complementary features on buildings*. 2007, London: CIRIA.
2. Susorova, I., *Green facades and living walls: vertical vegetation as a construction material to reduce building cooling loads*, in *Eco-efficient Materials for Mitigating Building Cooling Needs*. 2015, Woodhead: Uk. p. 132.
3. Fulcher, M., *The Paradise Park fallout: Are living walls worth it?* Architecture Journal, 2009. N°18.
4. Shevory, K., *Taking Greenery Straight Up*. N. Y. Times, 2010.
5. White, J., *Greenwalls or greenwash?* Landscape Journal 2013.
6. Hindle, R.L., *A vertical garden: origins of the Vegetation-Bearing Architectonic Structure and System (1938)*. Studies in the History of Gardens & Designed Landscapes, 2012. 32(2): p. 99-110.
7. Manso, M.C.-G., João, *Green wall systems: A review of their characteristics*. Renewable and Sustainable Energy Reviews, 2015. 41: p. 863-871.
8. E.A. Eumorfopoulou, K.J.K., *Experimental approach to the contribution of plant-covered walls to the thermal behaviour of building envelopes*. Building and Environment, 2009(44): p. 1024-1038.
9. Veisten, K., Smyrnova, Y., Klæboe, R., Hornikx, M., Mosslemi, M., Kang, J., *Valuation of Green Walls and Green Roofs as Soundscape Measures: Including Monetised Amenity Values Together with Noise-attenuation Values in a Cost-benefit Analysis of a Green Wall Affecting Courtyards*. Int. J. Environ. Res. Public Health., 2012(9): p. 3770-3788.
10. Rosenblum, C., *Please Weed the Wallpaper*, in *N. Y. Times* 2013: N. Y.
11. Green, E., *The Dry Garden: A skeptic's view of vertical gardens*, in *Los Angeles Times*. 2010: Los Angeles, CA.
12. Perez Urrestarazu, L., et al., *Influence of an active living wall on indoor temperature and humidity conditions*. Ecological Engineering, 2016. 90: p. 120-124.
13. TREEBOX, T.G.W. *Living Wall | Urban Greening, TREEBOX Green Walls Living Wall Urban Green*. 2016; Available from: <http://www.treebox.co.uk/index.html>.
14. Wong, I. and A.N. Baldwin, *Investigating the potential of applying vertical green walls to high-rise residential buildings for energy-saving in sub-tropical region*. Building and Environment, 2016. 97: p. 34-39.
15. Coma, J., et al., *New Green Facades as Passive Systems for Energy Savings on Buildings*. 2014. 57: p. 1851-1859.
16. Otte, M., et al., *Comparative life cycle analysis for green façades and living wall systems*. Energy and Buildings, 2011: p. 3419-3429.
17. Ostendorf, M., Retzlaff, W., Thompson, K., Woolbright, M., Morgan, S., Celik, S., *Storm water runoff from green retaining wall systems*, in *Cities Alive!: Ninth Annual Green Roof and Wall Conference*. 2011.
18. Feng, H. and K. Hewage, *Lifecycle assessment of living walls: air purification and energy performance*. Journal of Cleaner Production, 2014. 69: p. 91-99.
19. Ismail, M.R., *Quiet environment: Acoustics of vertical green wall systems of the Islamic urban form*. Frontiers of Architectural Research, 2013. 2(2): p. 162-177.
20. Madre, F., et al., *Global Ecology and Conservation*. Building biodiversity: Vegetated façades as habitats for spider and beetle assemblages, 2015. 3: p. 222-233.
21. Sheweka, S. and N. Magdy, *The Living walls as an Approach for a Healthy Urban Environment*. Energy Procedia, 2011: p. 592-599.

Annex A): Overview of all vertical systems with their characteristics

Vertical green type	green façade				wall vegetation		living wall system (LWS)				
	type	direct*	direct	indirect*	indirect	natural	concrete panel	planter boxes*	foam based*	mineral wool based*	felt layers*
Schematic representation											
System properties											
rooting space	in the ground	planter box	in the ground	planter box	wall	panel	planter boxes	box	plate	pockets	
substrate	soil	soil	soil	soil	façade material	soil	soil	aminoplast	rock wool	felt	
supporting system	--	--	for plants	for plants	--	for module	for module	for module	for module	for module	
plant specie	climbing plant	climbing plant	climbing plant	climbing plant	shrubs	small shrubs	shrubs	shrubs	shrubs	shrubs	
air cavity (mm)	0	0	3000≥50	3000≥50	0	0	≈50	≈50	≈50	≈50	
total thickness greening system (mm)	200	200	100	100	≤300	≤350	≤450	≤500	≤400	≤350	
maximum greening height (m)	30	30	30	30	depending to plant specie	unlimited	unlimited	unlimited	unlimited	unlimited	
plants	≤4/m ¹	≤4/m ¹	≤4/m ¹	≤4/m ¹	--	<10	30/m ²	22-25/m ²	27/m ²	25/m ²	
system weight kg/m ²	>5.5	>5.5	>4.3	>4.3	--	>300	>150	100-120	40-60	100	
natural rainwater/irrigation system	natural rainwater	irrigation system	natural rainwater	irrigation system	natural rainwater	natural rainwater	irrigation system	irrigation system	irrigation system	irrigation system	
plant life expectation (Y)	50	50	50	50	≈100	50	10	3.5	3.5	3.5	
biodegradable	yes	yes	plant-yes	plant-yes	plant-yes	plant-yes	plant-yes	foam and plant-yes	plant-yes	plant-yes	
maintenance	pruning	pruning	pruning	pruning	--	pruning	replacement/pruning	replacement/pruning	replacement/pruning	replacement/pruning	
realization time (Y)	≈30	≈2-3	≈30	≈2-3	--	≈1	<1	<1	<1	<1	
price (€/m ²)	30-45	≈200	40-75	100-800	--	--	400-600	750-1200	500-750	350-750	
prefabricated/in situ	insitu	prefabricated/in situ	insitu	prefabricated/insitu	insitu	prefabricated	prefabricated	prefabricated	prefabricated	prefabricated/insitu	

* measured in experimental set up (hotbox).

Annex B): Overview of vertical greening systems pros and cons based on cited literature

vertical green type	green façade				wall vegetation		living wall system (LWS)				
	type	direct	direct	indirect	indirect	natural	concrete panel	planter boxes	foam based	mineral wool based	felt layers
schematic representation											
advantages and disadvantages											
reducing heat island effect (UHI)	xx	xx	xx	xx	x	x	xxx	xxx	xxx	xxx	xxx
adsorption fine dust particles	xx	xx	xx	xx	x	x	xxx	xxx	xxx	xxx	xxx
increasing of biodiversity	xx	xx	xx	xx	x	x	xx	xx	xx	xx	xx
moderating buildings internal temperature via external shading	xx	xx	xx	xx	x	xx	xxx	xxx	xxx	xxx	xxx
sound insulation	xx	xx	xx	xx	x	xx	xxx	xxx	xxx	xxx	xxx
creating micro climate	xx	xx	xx	xx	x	x	xx	xx	xx	xx	xx
improved aesthetic value	xx	xx	xx	xx	--	x	xxx	xxx	xxx	xxx	xxx
improved insulation property	x	x	x	x	--	--	xx	xx	xx	xx	xx
greening system costs	x	x	xx	xx	--	x	xxx	xxx	xxx	xxx	xxx
maintenance costs	x	x	xx	xx	--	--	xxx	xxx	xxx	xxx	xxx
irrigation system required	--	x	--	x	--	--	xx	xx	xx	xx	xx
short period of covering	--	x	--	x	--	--	xxx	xxx	xxx	xxx	xxx
full covering of the façade	x	x	x	x	--	--	xxx	xxx	xxx	xxx	xxx
chance of moisture problems on solid walls (without air cavity)	xx	xx	--	--	x	x	--	--	--	--	--
penetration of roots in the wall	xx	xx	--	--	xx	xx	--	--	--	--	--
indoor application	--	--	x	x	--	--	xx	xx	xx	xx	xx
technical expertise needed	--	x	xx	xx	--	xx	xxx	xxx	xxx	xxx	xxx
replacement of panels	--	--	--	x	--	--	x	xx	xx	xx	xx
replacement of died plants	--	x	--	x	--	--	xx	xx	xx	xx	xx

x poor
xx good
xxx better
-- not applicable

Estimation of a probabilistic model for the count rate of a two stages outbound call center

J. Antonio Villeda-Reséndiz

División de Posgrado, Facultad de Ingeniería
Universidad Autónoma de Querétaro
Querétaro, Qro., México
antoniovilleda@gmail.com

Eduardo Castaño-Tostado

División de Posgrado, Facultad de Química
Universidad Autónoma de Querétaro
Querétaro, Qro., México
ecastano@uaq.mx

Abstract— *Models for inbound or outbound call centers typically assume that there is only one stage, so there are little results for call centers in which calls are transferred to a secondary area, this is basically a two stages call center. In this article a probabilistic model for the rates of the number of calls that arrives to an inbound call center is applied to a two stages outbound call center as the first step to estimate workforce for the second stage.*

Keywords— arrival rate; autoregressive model; call center; forecast; inbound; management; outbound; time series; two stages call center; workforce.

I. INTRODUCTION

Call centers (CCs) are companies in the service sector that operate via telephone; are a primary contact between service providers and their clients [1]. There are two main types of CC: *inbound* (IBCC) and *outbound* (OBCC). In a IBCC calls are received from people that want to get product or services via telephone, for example a bank or Internet provider customer care center, the contact service to buy a product advertised on TV or an emergency contact such as “911” or the telephone number of a insurance company in case of an accident. In the other case calls are made in a OBCC, the most common reasons for this calls are surveys or telemarketing.

At first glance operation of CCs seems a simple system, but the truth is that in order to study them and solve their inner problems sophisticated theory and tools are needed such as queue theory, stochastic process, inference in stochastic processes, stochastic optimization, simulation, time series among others.

The common path that follows a call in a IBCC is: first a person that need some service calls a CC, then she is connected with an interactive voice machine, where she can perform some self-service transactions; the call can finish in that moment, but if the customer needs another kind of services if there is a free agent and is capable to execute the asked service, then the customer is served immediately, but if there is no free

agent, the call enters in a invisible queue. Eventually the client is served by an agent or the customer abandons the call before being served if his waiting tolerance is overcome [2], [1].

The common path that follows a call in an OBCC starts when a telephone agent indicates that he is free, then an automatic dialer pick-ups a number from a phone book of potential clients and dials the number; if somebody answers the call is immediately transferred to the free agent whom is going to offer a product /service or apply a survey [3].

The most important factors involved in a CC are the level of customer satisfaction and the reduction of operation costs. The most satisfied is the client with the service, the most revenue for the company but also and an adequate manage of workforce is needed in order to reduce the operation costs. An excess or lack of agents affects the conditions of a CC; in the case of an IBCC a lack of agents can result in a bad experience for the customer with an uncertain future if he would use the service again [4]. In the case of an OBCC it is needed that agents being convincing but not so insistent in order to reduce the rejection level.

Then the three main problems in the CC business are agent workforce forecast to have optimal operations, reduction of the amount of abandoned calls, estimation and modeling of the customer waiting tolerance time. This problems are intrinsically related [5], [6]. In the previous decade about 70% percent of CC expenses were to paying wage for the staff [1], that is the reason workforce forecasting is so important for the adequate management of a CC.

The first automatic call distributor appeared in the 1950s to handle central operator inquiries at main telephone companies [7] and until the 2000s the management was almost completely empirical. In the first half of that decade some researchers noticed the complexity and challenge that the management of a CC involves and started to develop more analytical tools or at least heavily based on data analysis [1]. The first challenge that researcher discovered was the lack of quality data, because all

CC only saved poor reports consisting of summary information for intervals of 15 or 30 minutes along the day, so the first step in CC modern research was to establish what kind of data are important and the requirement of call by call data, because a CC study starts with a careful data analysis [5]. In spite of this exposed necessity the practice of partial reports still spawns the business.

In the case of IBCC the first works focused on compare them with classic queue systems[Shen2010], but this was inaccurate because in this kind of systems the arrival count is a Poisson process with constant rate, the service times are exponential with the same rate and the client never abandon the queue; but in a call the arrival count is not an homogeneous Poisson process if there is overdispersion, this is the variance is bigger than the mean, there is non homogeneous behavior for time intervals of the same that means different rates for different time intervals and seasonal effects over hours, days of the week or months [8] .

Most outbound CCs in Mexico dedicated to telemarketing have two stages, one for promoting and selling products or services, and the other, to check if data of the potential buyer or client are correct and if he is capable of buying the product or service offered. This means that the call of a potential client after responding that he would buy the product is transferred to another area of the CC and the transfer creates an invisible queue where the potential client waits until some can validate his data. The problem arises because there are more sales operators than validation operators and in some moments of the day the waiting time in queue is bigger than the potential client patience and he hang up the call. This is a problem because a sell operation almost closed finished abruptly and it is highly possible that in the near future the potential client would change his mind about buying the product or service. This kind of CC with two stages are presented in many regions of the world, but there are not serious studies about them as it is exposed on [9] and there are not defined analytical methodologies for the management of them. In this article a statistical analysis process for IBCCs is used to estimate a model for the counts of clients that completed the first stage of the OBCC, just before being transferred to the second stage. This model is required to estimate the workforce needed for the second stage. In the first part of the article a precise description of the two-stage CC and their problem are made, in the second part of the article the methodology to estimate the model for the first stage is established, the third part of the article shows how good is the model applied to a data. Finally the conclusions.

II. PROBLEM STATEMENT

The idea behind this work came from a CC company that came to seek advice from a group of mathematicians. The process for this OBCC in reality has three stages, in the first and automatic dial caller (ADC) picks up a telephone number from a data base, if a sell agent indicates that is free the ADC dials the number, if somebody answers, then the call is transferred to the free sell agent, this is the sales stage. Here the agent offers to the potential client a product or service, the time in this stage is stochastic, there are many factor involved in the duration such as the skills of the agent and the nature of the

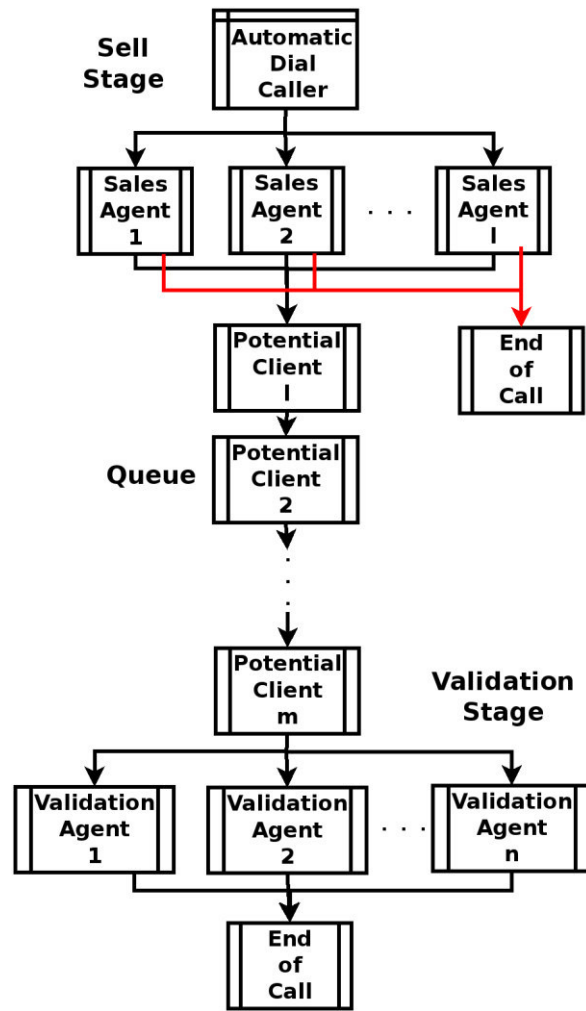


Fig. 1. Two stages CC diagram.

potential client. Managers of this CC said that there is also a seasonal effect that depends on the time and the day, even the month. Then if the client refuse the product the call ends, but if he decides to buy the call is transferred to the validation stage where the potential client data are check, at the end of this stage the purchase can be refused if there are any requirements from the provider not satisfied, if not then the sale has been made and the CC would receive a payment. Sell and validation stages are separated because in the past there were bad practices from the agents that caused some problems, this is what makes different this kind CC from typical OBCCs and they are pretty common in Mexico. It is not financially viable to have the same number of sell agents and validation agents, so there are less for the second, but this asymmetry originates other problem, in a some moment of the day if there are many potential clients purchasing the product or service then the queue they enter when transferred to the validation stage can be long and if the waiting time is bigger than his tolerance time then potential client hung up the call. The purchase operation is not completed and the time inversion made by the sell agent is lost; it is feasible to call the potential client to finish the operation, but this generates extra expenses and the potential

client can change his mind and not buy the product. When the system is overloaded for a specific product or service the managers increment the number of validation agent but this action is posterior to the abandonment of some potential clients, even this measure can be useless because the congestion could have been finished before. There is no system that forecast the workforce for the validation stage or that indicates that an overload is near.

Typical OBCC have been studied in the past and an important contribution for their optimal operation is the management of the ADC with is considered solved [3], so instead of three stages it considered that the first stage is the sell stage and the second is the validation stage. Fig. 1 shows a diagram for call process in the system.

III. METHODOLOGY

The CC studied is outbound, but the validation stage can be seen as an IBCC inside it, then this kind of CC is like a hybrid, so it is reasonably to estimate the number of calls that are transferred to the validation stage applying IBCC techniques to estimate the arrival counts. An important issue with the CC company that inspired this work is that there are not call by call data, there are only registers for 15 minutes between lapses as a typical CC, but in this case in [10] was developed a model to forecast the workforce for an IBCC with this kind of data. A random model for the arrival rate count is used from [11] and [2], then a forecast for the workforce is done. This model was applied in the present research to estimate the random rate of the number of potential clients transferred to the validation stage, as follows:

For a certain day d let be $\{S_t^{(d)} : t \geq 0\}$ the number of calls where the potential client accept to buy the product at time t , $\{V_t^{(d)} : t \geq 0\}$ the number of calls that finished validation stage at time t and $\{A_t^{(d)} : t \geq 0\}$ the number of abandoned calls while waiting at time t . $V_t^{(d)}$ and $A_t^{(d)}$ are Poisson processes of rate $n\mu$, δ , where n is the number of validation agents. $S_t^{(d)}$ is double stochastic Poisson Process with random rate $A_t^{(d)}$, this rate is another continuous time stochastic process that is locally stable, that is has the same value for time intervals of reasonable length. Let be $[0, T]$ the daily operation time, $d \in D = \{0, \dots, D\}$ the day index for D days of activity, $I \in I = \{0, \dots, I\}$ the lapse index such that $I \times m = T$, where m is the size of the lapses, $l_d = \{0, 1, \dots, 6\}$ is the day of the week, where $0 = \text{monday}$ and $\gamma_{d,i} = S_{(i+1)m}^{(d)} - S_{im}^{(d)}$ is the number of calls transferred to validation stage in lapse i on day d . Then $\gamma_{d,i} \sim \text{Poisson}(m\lambda_{im}^{(d)})$. Let be $\lambda_{d,i} = m\lambda_{im}^{(d)}$ and $\lambda_d = (\lambda_{d,1}, \dots, \lambda_{d,I})$. If $\lambda_{d,i}$ is enough big

then $Y_{d,i} = \sqrt{\gamma_{d,i} + 1/4} \sim N(\sqrt{\lambda_{d,i}}, 1/4)$. Then this transformations establish a hidden arrival-rate process:

$$\begin{aligned} \omega_d - \alpha_{l_d} &= \beta(\omega_{d-1} - \alpha_{l_{d-1}}) + \eta_d, \eta_d \sim N(0, \phi^2), \\ \theta_{l_d,i} &0, \sum_{i=1}^I \theta_{l_d,i} = 1, \\ \sqrt{\lambda_{l_d,i}} &= \omega_d \theta_{l_d,i}, \\ Y_{d,i} &= \sqrt{\lambda_{l_d,i}} + \varepsilon_{d,i}, \varepsilon_{d,i} \sim N(0, \sigma^2). \end{aligned} \quad (1)$$

Where ω_d is the total daily arrival rate for day d , α_{l_d} is the seasonal factor that centers in zero the total arrival rate, $\theta_{l_d,i}$ is the proportion of the total daily arrival rate due to lapse i and the day of the week l_d for day d and $\lambda_{d,i}$ is the arrival rate for lapse i and day d for the counts $\gamma_{d,i}$. It is noticed that $Y_{d,i} \approx N(\sqrt{\lambda_{d,i}}, 1/4)$, because there is distribution convergence. So $\omega_d - \alpha_{l_d}$ follows an autoregressive model of order one and the random variables of the sequence $\{\omega_d \theta_{l_d,i} : i = 1, \dots, I\}$ are also Normal. Finally $\{\theta_{l_d,i} : i = 1, \dots, I\}$ is the distribution of total daily rate along the lapses.

Now there is a model for the unobserved rates $\lambda_{d,i}$, this kind of model is called space state Gaussian model and their parameter can be estimated via maximum likelihood: if $\{y_{d,i}\}$ are the observed square rooted call counts, then the maximum likelihood estimators are:

$$\begin{aligned} \hat{\omega}_d &= \sum_i y_{d,i}, \\ \hat{\alpha}_{l_d} &= \frac{\sum_{\{d': l_{d'}=l\}} \sum_i y_{d',i}}{\|\{d' : l_{d'}=l\}\|}, \\ \hat{\theta}_{l_d,i} &= \frac{\sum_{\{d': l_{d'}=l\}} y_{d',i}}{\sum_{\{d': l_{d'}=l\}} \sum_i y_{d',i}}, d = 1, \dots, D, i = 1, \dots, I. \end{aligned} \quad (2)$$

Now β can be estimated with linear regression and then the estimates for σ^2 and ϕ^2 can be obtained with the residual sum of squares, so the random model for rate is ready to be used for workforce forecasting.

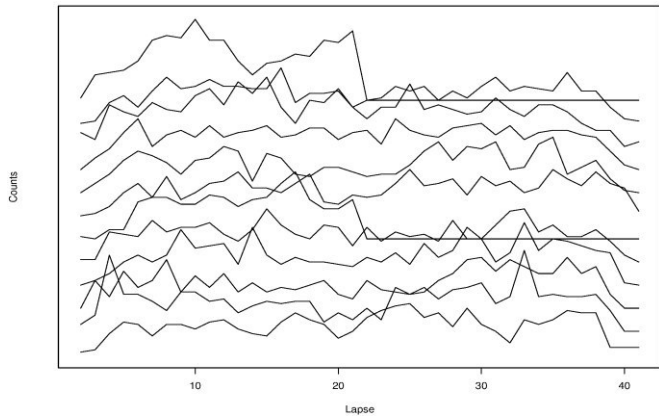


Fig. 2. Number of calls transferred to validation stage over lapses for days between February 9 and February 21, 2015.

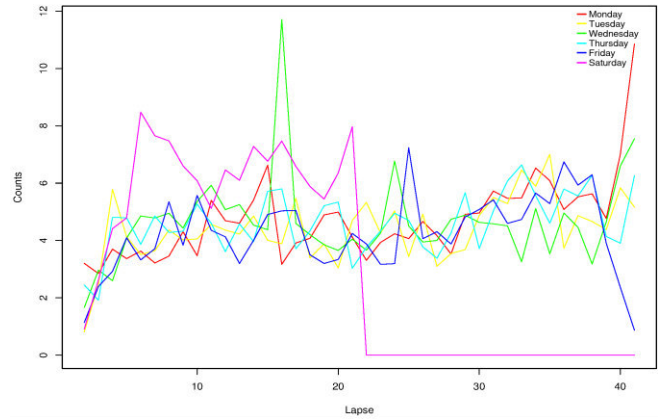


Fig. 4. Standard deviations of calls transferred to validation stage across all same days of the week over lapses.

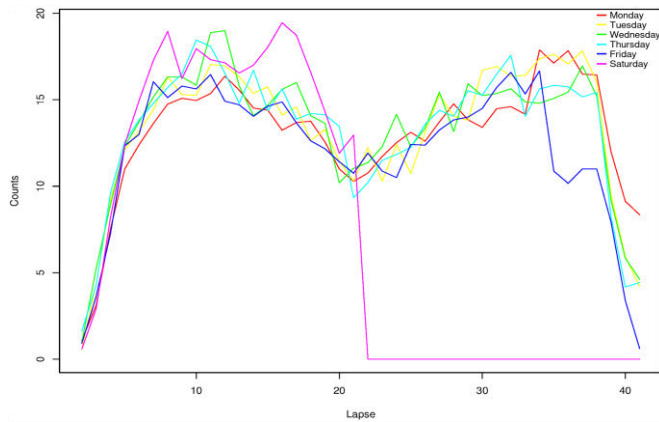


Fig. 3. Averages of calls transferred to validation stage across all same days of the week over lapses.

IV. RESULTS

Data were gathered at an OBCC between December 22, 2014 and June 30, 2015, for each there are reports for lapses of 15 minutes between 9:00 and 19:00 hours for weekdays and between 9:00 and 14:00 hours for Saturdays, there are no operations on Sundays. The variables in reports are campaign (two campaigns, one for each product), number calls transferred to the validation stage, number of answered calls in validation stage, percentage of number of transferred calls, mean abandonment times, average waiting time, average selling time, average validation time, number of hung up call that wait in queue more than 10 seconds, mean call time, this is since the call starts until is hung. There are 28 days without date because of holidays and a week of maintenance, because the maintenance period is a whole week it was just discarded, but the holy days were treated as zeroes.

The counts of transferred calls over all lapses of the day presented a similar qualitative behavior: for week days the counts increased in function of time until a peak around 10:00 hours (lapse number 6), then declined until around 14:00 hours (lapse number 22) and again the count increased until a peak around 18:00 hours (lapse number 38), then fall until the

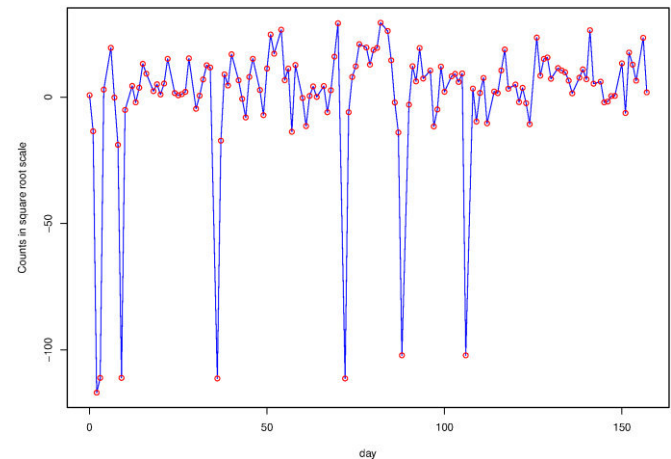


Fig. 5. Time series for the total number of calls in square root scale for each day without week day seasonal effect.

closing of operation at 19:00 hours. In the case of Saturdays there are two peaks, the first around 10:00 hours (lapse number 6) and the second around 12:45 hours (lapse number 17). Fig. 2 displays the counts for 12 days between February 9 and February 21, 2015. Fig. 3 displays the averages across all same days of the week over lapses and Fig. 4 displays the standard deviations across all same days of the week over lapses, each represent a different day. With this three graphs it was concluded that Saturdays and weekdays are qualitatively different, because of the two peaks and higher variance. This three graphs offered some empirical evidence to apply model (1) because they were similar to the graphs of the data in [10] and [11]. In order to apply model (1) it is important to check the $AR(1)$ assumptions for $\hat{\omega}_d - \hat{\alpha}_{l_d}$, so Fig. 5 shows the time series for the total number of calls in square root scale for each day without week day seasonal effect, there are values smaller than the rest, this values are caused because the holy days with count zero, the other values shows an acceptable stationary behavior according to [12].

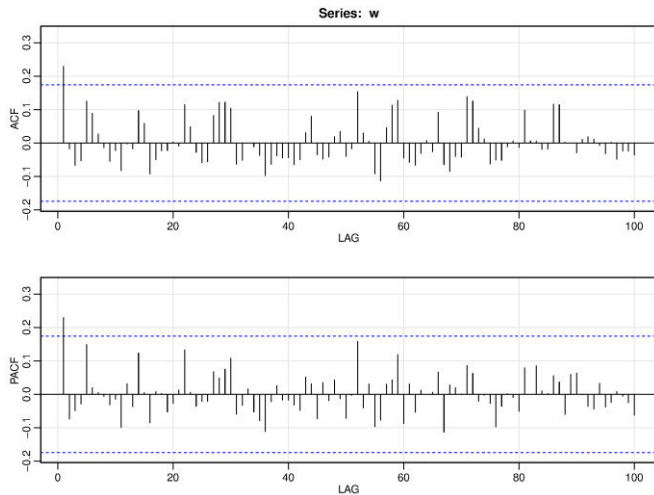


Fig. 6. Autocorrelation function (ACF) and partial autocorrelation function (PACF) for the total number of calls in square root scale for each day without week day seasonal effect.

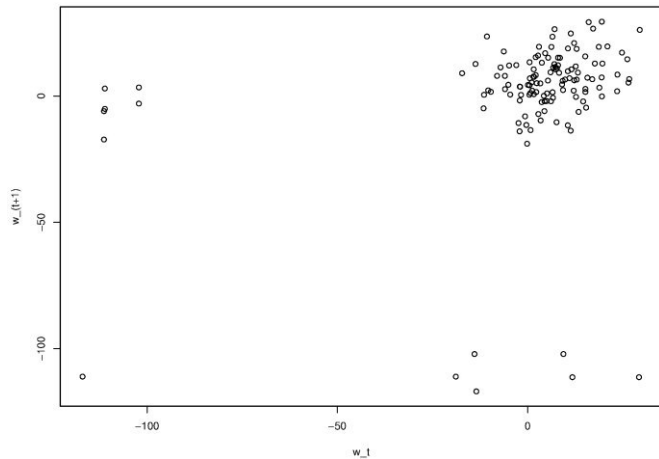


Fig. 7. Scatter plot for $\hat{\omega}_d - \hat{\alpha}_{l_d}$ and $\hat{\omega}_{d+1} - \hat{\alpha}_{l_{d+1}}$.

Fig. 6 shows the autocorrelation function (ACF) and partial autocorrelation function (PACF), the PACF said that the only significant lag effect for $\hat{\omega}_d - \hat{\alpha}_{l_d}$ was $\hat{\omega}_{d-1} - \hat{\alpha}_{l_{d-1}}$ and this means according to [12] that an $AR(1)$ could be applied. Then to estimate β linear regression is required, but it is necessary to diagnose if the model is acceptable, so Fig. 7 displays the scatter plot between $\hat{\omega}_d - \hat{\alpha}_{l_d}$ and $\hat{\omega}_{d+1} - \hat{\alpha}_{l_{d+1}}$, in this there are three groups of data, the ones that is in the superior left corner and in the inferior right corner are due to the holy days with count zero, it would be a good idea take them off. Then the regression with all the data said that $\hat{\beta} = 0.2290$, the p-value for the t-statistic of the coefficient was 0.0083,

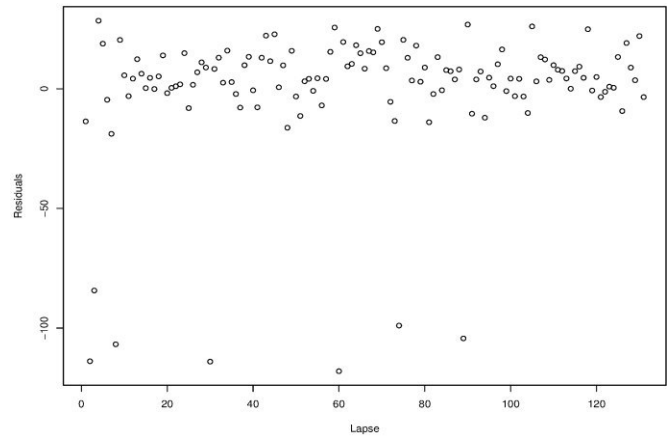


Fig. 8. Residuals.

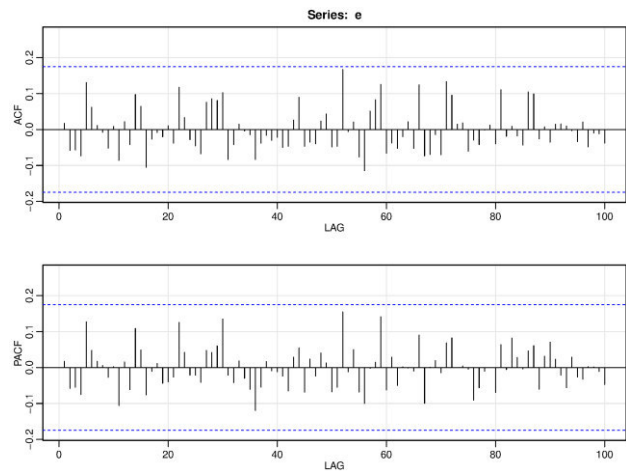


Fig. 9. Autocorrelation and partial autocorrelation functions for residuals.

which is small, so is significant, but R^2 and corrected R^2 statistics were 0.0525 and 0.0452, respectively which means a bad fit. The regression without the holidays values said that $\hat{\beta} = 0.4453$, the p-value for the t-statistic of the coefficient was 1.96^{-7} which means that is significant because is small but the R^2 and corrected R^2 statistics were 0.0525 and 0.1917, respectively. They are better than the ones for the complete data, but still is a bad fit. It important to notice that the second estimates came from a better fit but it almost duplicate the first, but to take out date is not simple, because to estimate ω_d , α_{l_d} and $\theta_{l_d,i}$ whole weeks are needed. Fig. 8 displays the residual for the fit, this graph makes more evident that it would be good to take off the holidays data, but something good is that the autocorrelation function and the partial autocorrelation functions had non-significant pattern as display in Fig. 9.

Another interesting finding is that if ω_d is estimated including Saturdays and divided by the number of hours that the CC operates on day d ; 10 for week days and 5 for Saturdays, it is

$$\hat{\omega}_d = \begin{cases} \frac{1}{10} \sum_i y_{d,i}, & \text{if } l_d \neq 5 \\ \frac{1}{5} \sum_i y_{d,i}, & \text{if } l_d = 5. \end{cases}$$

Then $\hat{\omega}_d$ are in the same scale for all days of the week and then all days are comparable. The ACF displayed in Fig. 10 shows seasonal behavior because of the weeks, but the PACF also shows a hidden behavior that manifest around every thirteen days, this behavior can be an effect of payday, that is usually every 15 days, or in this case every 12 days because this model does not consider Sundays.

V. CONCLUSIONS

The model applied to the data seems reasonable, but the fitted autoregressive model was not good, it can be improved if the weeks with holidays are excluded as fit for $\hat{\omega}_d$ without holidays was better, but in that case the holidays must be excluded at the beginning of the estimation of ω_d , α_{l_d} and $\theta_{l_d,i}$, that would be a good next step on this investigation. After that workforce estimation for validation stage can be performed, but it is important to be sure if the assumptions are accomplished, because there are not correct models, only useful ones. You can always apply a model to whatever data you have, but that does not mean that the results would be good. In the best scenario if assumptions for the model are satisfied there is a high probability that you would get enough good results to confront reality, that what is called statistical engineering.

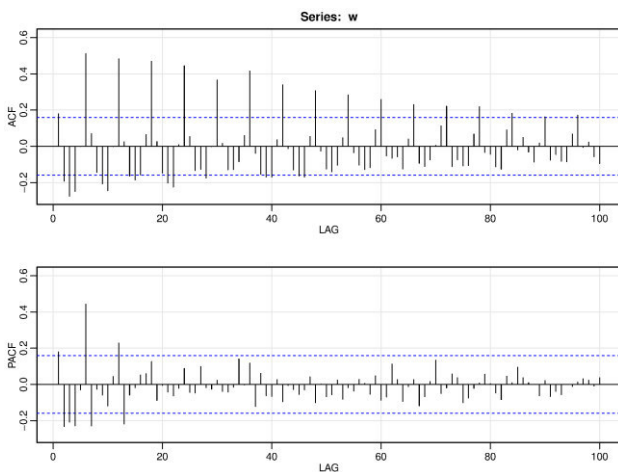


Fig. 10. Autocorrelation function (ACF) and partial autocorrelation function (PACF) for residuals.

ACKNOWLEDGMENT

A. Villeda wants to thank División de Posgrado of Facultad de Ingeniería of Universidad Autónoma de Querétaro for all the facilities and support. This work was partially financed by CONACyT for awarding the scholarship 424697 for M.S. studies of the first author.

REFERENCES

- [1] H. Shen, "Statistical Analysis of Call-Center Operational Data: Forecasting Call Arrivals, and Analyzing Customer Patience and Agent Service," *Wiley Encycl. Oper. Res. Manag. Sci.*, pp. 1–10, 2010.
- [2] L. Brown *et al.*, "Statistical Analysis of a Telephone Call Center: A Queueing-Science Perspective," *J. Am. Stat. Assoc.*, vol. 100, no. 469, pp. 36–50, 2005.
- [3] P. J. De Freitas Filho, G. F. Da Cruz, R. Sea Ra, and G. Steinmann, "Using simulation to predict market behavior for outbound call centers," *Proc. - Winter Simul. Conf.*, pp. 2247–2251, 2007.
- [4] P. Chuchual, N. Chongpravatisakul, T. Kusolmanomai, and S. Komolavanij, "Inbound and outbound calls assignment for an efficient call center," *2010 7th Int. Conf. Serv. Syst. Serv. Manag. Proc. ICSSSM' 10*, vol. 66, no. 0, pp. 468–471, 2010.
- [5] N. Gans, G. Koole, and A. Mandelbaum, "Telephone Call Centers: Tutorial, Review, and Research Prospects," *Manuf. Serv. Oper. Manag.*, vol. 5, no. 2, pp. 79–141, 2003.
- [6] A. Mandelbaum, "Call centers (centres): Research bibliography with abstracts," *Version*, 2002.
- [7] "The History of the Call Centre." [Online]. Available: <https://www.callcentrehelper.com/the-history-of-the-call-centre-15085.htm>. [Accessed: 01-Mar-2017].
- [8] A. N. Avramidis, A. Deslauriers, and P. L'Ecuyer, "Modeling Daily Arrivals to a Telephone Call Center," *Manage. Sci.*, vol. 50, no. 7, pp. 896–908, 2004.
- [9] J. Woo and S. Chan, "Outsourcing strategy in two-stage call centers," *Comput. Oper. Res.*, vol. 37, pp. 790–805, 2010.
- [10] N. Gans, H. Shen, Y.-P. Zhou, N. Korolev, A. McCord, and H. Ristock, "Parametric Stochastic Programming Models for Call-Center Workforce Scheduling," *Manuf. Serv. Oper. Manag.*, no. July, pp. 1–33, 2015.
- [11] H. Shen and J. Z. Huang, "Interday Forecasting and Intraday Updating of Call Center Arrivals," *Manuf. Serv. Oper. Manag.*, vol. 10, no. 3, pp. 391–410, 2008.
- [12] R. H. Shumway and D. S. Stoffer, *Time Series Analysis and its Applications: With R Examples*. Springer, 2015.

Test of Lightweight Panel based on non standard steel profiles under AISC-05LFRD and ANSI-01 LRFD

Sosa-Guerrero FE¹, Escalante-Valvidia JA², Arroyo-Contreras GM^{2,3}, Pérez-Lara y Hernández MA²,
Reyes-Araiza JL², López-Cajún CS²

¹Engineering Faculty
Autonomous University of Querétaro
Querétaro, Qro
fesg3108@hotmail.com

^{2,3} Research and Postgraduate Division, Engineering
Faculty
Autonomous University of Querétaro
Querétaro, Qro
marroyoc@uaq.mx

Abstract— The present research aims to show the technical aspects associated to the lightweight panel test based on non standard steel profiles under the AISC-05LFRD and ANSI-01 LRFD standards as part of the Master's Degree in Design of Lightweight Steel Structures, Prefabricated, Detachable and Modulable in House Room (Escalante-Valvidia, 2017; personal communication) in which I participated as student of the Laboratory of the subject of Design of Structures of Steel that is imparted in the Engineering Faculty in the career of Civil Engineering of the Autonomous University of Querétaro. The objective of the test consisted in testing two panels based on non standard steel open-web profiles to demonstrate that they guarantee the limits of Resistance and Service established by the structural design regulations AISC-05 LRFD and ANSI-01 LRFD, With the objective of proposing a new system of structuring to replace the materials commonly used in the construction of house rooms, such as masonry and reinforced concrete. It is noted that the materials approved for this purpose have low quality control standards and considerably increase the time and cost in the execution of the work.

Keywords— *Structuring system; Execution times; Open web profiles, Lightweight panel; Non standard steel profile; AISC-05LFRD; ANSI-01 LRFD.*

I. INTRODUCTION

At present, constructive systems in general are limited to implementing temporary structural systems (while they continue permanently seated) which in many cases play a negative role with the surrounding environment. Since they depend on expensive foundation systems which in some cases Individuals cause great impact to the soil in which they are settled and are a material loss once the structure fulfilled its useful life since they are not recoverable.

In Mexico as in many other Latin American countries, the construction sector focused on the building of house-type structures that has been relegated to simple structuring systems from the point of view of modern architecture, because the geometry of those buildings do not allow the use of flexible forms and spaces pleasing to the human and environment senses. Additionally to the lack of flexibility, those buildings are linked to uncertain results in relation to the mechanical properties therefore, the final product shows no standards for the manufacture because the mechanical properties of materials depending on the Region where the building production is carried out. In another context, housing construction in Mexico tends to be done handcrafted, since there are great uncertainties with materials that are commonly used and because the labor force in this sector sometimes has not enough training nor the necessary equipment for the correct realization of the different constructive processes stipulated in the stage of structural projection. (1).

Steel as a structural element has considerable advantages compared to other building materials; since its real mechanical behavior is the closest to the theoretical behavior that is assumed in the design process for the determination of the cross section that restores the demands to which the study structure is subjected. (2).

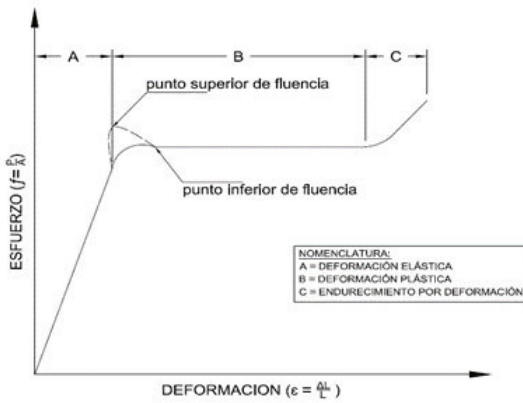


Fig. I. Deformation-strain diagram of a sweet or low carbon structural steel at room temperature (2).

Now a days, the steel structures show a large sustainable properties compared to other materials used in the construction industry such as cement, brick and aluminum (3), because throughout different chemical processes, it is possible to recover practically 100% of some structural component, thereby reducing the production of greenhouse gases and the excessive consumption of non-renewable energies because the production of those structural profiles (4).

The Solar Decathlon competition, to be held in October 2017, allowed the development of various proposals by the Autonomous University of Queretaro, from which the project for the Design of Lightweight, Prefabricated, Demountable and Modulable Steel Structures Houses Room. Because this proposal, it was necessary to test two panels based on non standardized open steel profiles and to demonstrate that they warranty the limits of Resistance and Service established by the regulations for the structural design, AISC-05 LRFD and ANSI- 01 LRFD, reported in this paper.

II. ELECTION OF THE STRUCTURAL SYSTEM AND MANUFACTURING PROCESS

The structure for the house that was chosen for the experimental test was the following, as Escalante-Valvidia (5) says in his thesis:

Orthogonal structure of 7.00m x 7.00m approximately, with an average height of 3.34m above the level of the slope of the natural terrain; The structural elements that make up the super structure will be based on square profiles "PTR" working together with horizontal elements and concentric contraventeo in specific areas in order to rigidizar the horizontal displacements produced by the accidental actions to which will be subjected the structure of study (Wind and earthquake). The boundary conditions of the structure will be of the articulated type, restricting the horizontal displacements in the x and z planes, but allowing rotation in both directions in order to minimize the thickness and depth of the foundation system. (Fig. II).

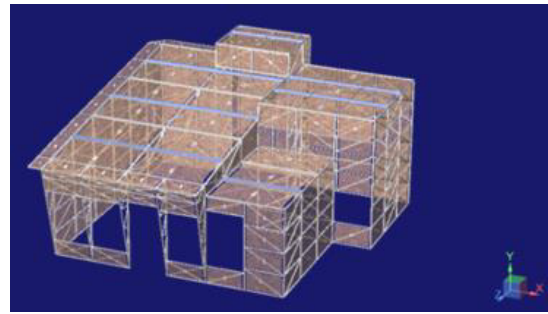


Fig. II. Reticular structure of 7.00m x 7.00m approximately with an average height of 3.34m (south facade). (5).

Manufacturing Process (5).

- Development of base plates and joining plates.
- Manufacture of posts and / or vertical panel elements
- Manufacture of horizontal and diagonal bracing elements
- Boring of Base Plates and Joining Plates
- Construction of joints between components
- Assembly and presentation of the panel in workshop
- Identification of parts for disassembly, transfer and subsequent on-site assembly

Fig. III shows a front view of the panel used in the construction process proposed by Escalante Valvidia (5), base of the lightweight panel test based on non standard profiles.

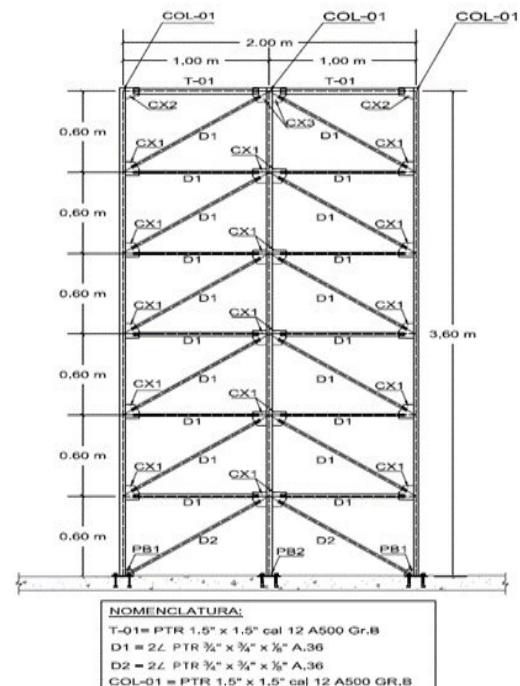


Fig. III. Proposal of structuring based on simple panel of ordinary frames with concentric counter-venting (OCBF) ASCE / SEI 7-05. (5).

II. DESIGN COMBINATIONS OF RESISTANCE AND SERVICE

The design criterion of the different elements that make up the super structure as the substructure will be as follows (5):

III.a Resistance Limit State

In order to design an effect involving the interaction of gravitational forces, the combinations of design that allow to calculate the resistance of the different elements that make up the global structure are those indicated in Table I.

TABLE I. LOAD COMBINATIONS FOR DESIGN BY PERMANENT AND VARIABLE ACTIONS.

Condition	Description	Regulation	State
D1	1.4DL	(ASCE, 2005)	Resistance
D2	1.2DL+1.6LL	(ASCE, 2005)	Resistance
D17	1.4DL+1.4LL	(NTC, 2004)	Resistance

DL=Dead load and LL= Maximum live load

The design that take into account the wind actions on the structure in both orthogonal directions, and the design combinations of the overall structuring system will be carried out by the combinations indicated in Table II.

TABLE II. LOAD COMBINATIONS FOR WIND

Condition	Description	Regulation	State
D3	1.2DL+0.8WPX	(ASCE, 2005)	Resistance
D4	1.2DL+0.8WPZ	(ASCE, 2005)	Resistance
D5	1.2DL+1.6WPX	(ASCE, 2005)	Resistance
D6	1.2DL+1.6WPZ	(ASCE, 2005)	Resistance
D7	1.2DL+ILL+1.6WPX	(ASCE, 2005)	Resistance
D8	1.2DL+ILL+1.6WPZ	(ASCE, 2005)	Resistance
D13	0.9DL+1.6WPX	(ASCE, 2005)	Resistance
D14	0.9DL+1.6WPZ	(ASCE, 2005)	Resistance

DL=Dead Load, ILL= Instant live load, WPX=Wind pressure in direction "X" and WPZ= Wind pressure in direction "Z".

For the design of accidental actions derived from the earthquake applied in both orthogonal directions of the global structuring system, design combinations that allow the calculation of the available resistances will be carried out using the combinations indicated in Table III.

TABLE III. LOAD COMBINATIONS BY EARTHQUAKE

Condition	Description	Regulation	State
D9	1.2DL+EX+0.3EZ	(ASCE, 2005)	Resistance
D10	1.2DL+0.3EX+EZ	(ASCE, 2005)	Resistance
D11	1.2DL+ILL+EX+0.3EZ	(ASCE, 2005)	Resistance
D12	1.2DL+ILL+0.3EX+EZ	(ASCE, 2005)	Resistance
D15	0.9DL+EX+0.3EZ	(ASCE, 2005)	Resistance
D16	0.9DL+0.3EX+EZ	(ASCE, 2005)	Resistance

DL=Dead Load, ILL= Instant live load, EX=Earthquake action in direction "X" and EZ= Earthquake action in direction "Z".

III.b Service Limit State

Based on the service limit state before gravitational loads, the calculation of the acting deformations will be carried out by the implementation of the load combination of Table IV.

TABLE IV. LOAD COMBINATIONS FOR REVISION OF PERMISSIBLE DEFORMATIONS

Condition	Description	Regulation	State
D18	DL+LL	(ASCE, 2005), (NTC, 2004)	Service

DL=Dead load and LL= Maximum live load

For the calculation of maximum distortion to restrict lateral displacements between adjacent floor systems, the following relationship was used in Table V.

TABLE V. PERMISSIBLE MEZZANINE DISTORTIONS

Structural System	Distortion
Steel or concrete frames with concentric windshields	0.015

Source: NTC, 2004 (6)

Once the design loads were analyzed, the structure was reported with the following characteristics (5):

Area = 49.58m²

Generating Area = 30.47m²

Perimeter = 30.20m

Average Height = 3.34m

Wall System Weight = 50kg / m²

Mass Estimate Total Dead Load 1.96ton

Total Instant Live Load 2.00ton

Covering Elements	0.510ton
Walls (Lightweight System)	4,843ton
Solar Panels	0.750ton
Total.....	10.063ton

III. EXPERIMENTATION

A.MOVE OF STRUCTURAL ELEMENTS AND ASSEMBLY

The experimental test of the panel required three months of previous preparation for its correct execution. This test began by transporting the missing structural elements such as the auxiliary support structure, the base of the panel together with its corresponding stud bolts and screws, the PTR profiles formed from angles to assemble the second panel, transferred from the manufacturing workshop to the Autonomous University of Queretaro and place said elements in the reaction slab located in front of the Biotechnology park of the university (Image I).

The slab and reaction wall were cleared in order to be able to place and fix the base structure to the slab, placing its studs in the corresponding holes so that the panel was at the correct distance from the reaction wall to the point where it was intended to load. (Image II and III).

The first panel was placed on its secondary structure base, in which certain difficulties arose since the steel shop made an incorrect drilling in the base plates of the panel, reason why this detail had to be corrected later to be able to fix the whole Panel to the reaction slab (Image IV).

The auxiliary structure was also fixed to stop the panel when it was being loaded laterally. (Image V).



Image I. Move of auxiliary structure for lightweight panel.



Image II. Secondary base structure for fixing the panel. (5).



Image III. Placement of stud bolts to fix panel base.



Image IV. Fixing the first lightweight panel.

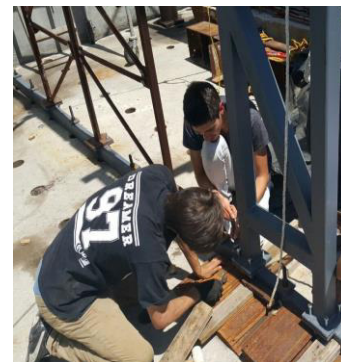


Image V. Laying of auxiliary structure.

B. TUNING DETAILS FOR EXPERIMENTAL TESTS

The loading piston of the reaction wall was placed at the correct height so as to be able to load the panel on its upper left side (front view), at a height of about 3.6 meters. (Images VI and VII).

While we quoted the solution for the drilling of the base of the panels, the second lightweight panel was armed to have all the ready for the experimental tests. (Image VIII).

The people who had made the steel profiles were called to correct the drilling error, drilled holes were drilled at the relevant distances of the plane and the corresponding diameter to be fixed, water was added to the plate each minute while the holes were being made since the materials were heated considerably by the friction of the drill with the base plates. (Image IX).



Image IX. Correction of drilling.



Image VI. Placing the load piston at the correct height.



Image VII. Reaction wall loading piston.



Image VIII. Arming the second panel.

C. SIMULATION OF DESIGN LOADS AT REAL SCALE

In order to simulate the load combinations using IPR profiles provided by Reyes-Araiza (2016; personal communication), it was measured with a digital vernier to obtain the cross-sectional area in m^2 . This result was multiplied by the volumetric weight of the steel ($7.8 \text{ Ton} / m^3$), (5) and a uniform load was obtained in Ton / m (weight per linear meter of the profiles), the combination of total load corresponding to the live load and dead load calculated in Escalante-Valvidia (5) was $0.0725 \text{ Ton} / m$ in clearer units $72.5 \text{ kg} / m$. Based on this information, we calculated the linear profile meters that we needed, in total there were two IPR profiles of 2m and two IPR of 70cm, and with these measures were continued to cut them with a special saw for steel. (Image X).

Then we moved them to the CEDIT (Center for Design and Technological Innovation) located next to the biotechnology park of the Autonomous University of Querétaro to join them with welding and electrodes type E 70 18 and in this way will remain a single piece of the uniformly distributed load. (Image XI).

Once the load for the panel was obtained, a $\frac{1}{4}$ -inch steel spindle reel and knots were purchased; this material was used to tension the panel, which was previously leveled with a lead and clamped three different points on the panel. To tense the lightweight panel we used strands cut every 7m approximately attached to concrete blocks that were in the reaction slab, this so that the panel remained straight and rigid in the plane of load. (Image XII and XIII).

Initially it was thought to place the load on the panel with the help of a few ptr anchored to the columns but consulting to Arroyo-Contreras (2016; personal communication) whom contributed the solution of using the toron that we already had so that it would not be dangerous at the time of Perform the test, because if the panel failed abruptly this load could fall and cause an accident during the experimentation.

Once the panel was leveled, the load was placed and it was fastened to the top of the structure using the steel spindle reel and knots so that it was hanging at the sides. (Image XIV).



Image X. IPR profiles cut to the required measurements.



Image XIII. 1/4 inch steel spindle reel and box of knots.



Image XI. Welding for IPR profiles at CEDIT.



Image XIV. Leveling of gravitational loads in a simple panel-based structuring system. (5).



Image XII. Leveling and tensing the panel.

D. LIGHT PANEL INSTRUMENTATION AND PUSH OVER ANALYSIS

Once the first panel was correctly assembled and leveled, and the load was placed, everything necessary to perform the relevant measurements was started. The main question was to measure the lateral load applied to the panel with the help of the piston and the displacements that were presented in its plane with the aid of a micrometer. Both measurements were taken electronically by a computer which tabulated the data at every second. (Image XVI).

In order to load laterally the panel, a small connection was added with a PTR profile and a plate with holes to be able to fix the piston to the panel. It should be noted that the load cell was previously calibrated. (Image XVII).

In order to measure the displacements in the plane of failure of the structure a small ring was added to one of the columns of the lightweight panel to be able to place the wire that measured the displacements, a small hole was made with a drill and the device was placed in the auxiliary structure. (Image XVIII).



Image XVI. Instrumentation complements for the measurement of applied load and displacements.



Image XVII. Connection of the piston to the lightweight panel.



Image XVIII. Micrometer of thread fixed to the auxiliary structure.

In the following image you can see all the instrumentation used for the experimental lightweight panel number one. (Image XIX).



Image XIX. Instrumentation for the first lightweight panel test.

A Push Over analysis was carried out, in which the real scale panel was modeled with all the connections that were in it and all the elements that constituted it to have an analytical graph prior to as it was the behavior of the panel being loaded laterally. This analysis not only gave a graphic behavior, but also said which element of the panel (diagonals, columns and horizontal) would be the first to fail plastically once the test started and which later in relation to the piston runs (load application lateral on the panel) which degraded the overall stiffness matrix of the entire structure with each increase of load.

To do this, two previous analyzes for the structure called Analysis of first order and second order were conducted and they consisted of the following:

D.a First Order Analysis

Also known as static analysis of the structure that involves the solution of a set of linear equations which is represented as follows (7):

$$\{F\} = [K]*\{D\} \quad (1)$$

Where:

{F} = Vector of loads and / or actions on the structure.

[K] = Global stiffness matrix of the structure.

{D}= Vector displacement product stock on the structure.

For the construction of this matrix it was necessary to determine the local stiffness matrices of each element of the structure and thus to be able to assemble the global stiffness matrix (the whole structure) taking into account the boundary conditions of each element (support conditions). The boundary conditions of the elements were as follows:

Columns → Articulated-Articulated

Diagonals → Articulated-Articulated

Horizontals → Simply Supported

An example of an element with its local stiffness matrix is shown in Fig. IV and V.

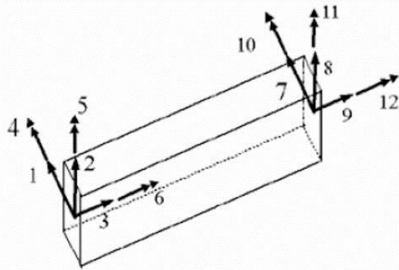


Fig. IV. The Linear element with its corresponding freedom degrees design. (7).

$$\begin{bmatrix} \frac{AE}{L} & 0 & 0 & -\frac{AE}{L} & 0 & 0 \\ 0 & \frac{12EI}{L^3} & \frac{6EI}{L^2} & 0 & -\frac{12EI}{L^3} & \frac{6EI}{L^2} \\ 0 & \frac{6EI}{L^2} & \frac{4EI}{L} & 0 & -\frac{6EI}{L^2} & \frac{2EI}{L} \\ -\frac{AE}{L} & 0 & 0 & \frac{AE}{L} & 0 & 0 \\ 0 & -\frac{12EI}{L^3} & -\frac{6EI}{L^2} & 0 & \frac{12EI}{L^3} & -\frac{6EI}{L^2} \\ 0 & \frac{6EI}{L^2} & \frac{2EI}{L} & 0 & -\frac{6EI}{L^2} & \frac{4EI}{L} \end{bmatrix}$$

Fig. V. Rigidity matrix of elements with six freedom degrees (2D). (7).

D.b Elasto-plastic analysis (push over analysis)

An elasto-plastic analysis was performed on the structural system; in Figure VI the results of this analysis and the displacements are shown with data in table VI.

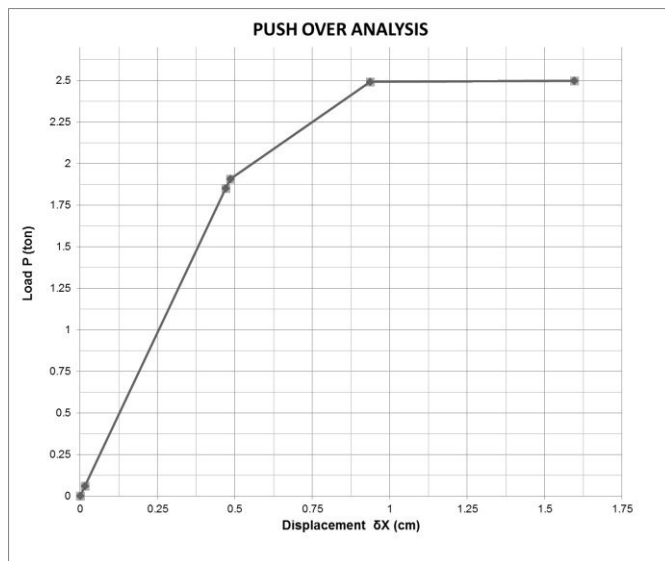


Fig. VI. Analysis standard of behavior of the simple panel-based structuring system as a result of the implementation of an Elasto-plastic analysis or "Push Over". (5).

Escalante-Valvidia (5) points out in his thesis the tools that he used to perform the analytical model of the structure:

The structural analysis and design software RamElements v13.00.22 was used for the modeling, analysis and design of the different elements that make up the analytical model representative of the two structuring proposals. (5).

A summary of the results obtained from the analysis and in Figure VII the behavior of these data are shown in Table VI below.

TABLE VI. DISPLACEMENT SUMMARY VS LOAD INCREMENTS PRODUCT OF THE IMPLEMENTATION OF A "PUSH OVER" ANALYSIS TO THE SIMPLE PANEL BASED STRUCTURING SYSTEM. (5).

	P (ton)
0	0
0.01548	0.061
0.46982	1.85135
0.48528	1.90689
0.93627	2.49231
1.59625	2.5

The behavior of the lightweight panel in ideal conditions is elastic up to 1.85 Tons: *The structuring system has a behavior within the elastic range approximately until an increase of lateral load of 1.85 tons applied in the plane of the structuring system in interaction with the Service loads (dead load + live load).* (5).

E. LIGHTWEIGHT PANEL RESULTS NUMBER ONE

With all the necessary instrumentation to perform the test, on January 12, 2017, the experimental test of the first panel was performed at 6:00 pm at the Universidad Autónoma de Querétaro; For this the blocks that supported the uniformly distributed load (IPR profiles) were removed and the experimentation started. The test did not last more than 15 minutes and the data collected were recorded in Excel, which were later cleaned to be able to have the loads corresponding to the above mentioned Push Over analysis and to perform the graphs against the deformation of the experimental test.

The images XX and XXI show that the structure underwent a very important deformation outside its plane, even greater than that of the plane of load where its displacements were measured. This phenomenon is explained below, which was also reported in (Escalante-Valvidia, 2017; thesis) (5).

A point of relevance within the experimental test was the fact that the elements that integrate the structural system adequately transmitted the actions as the lateral load increased and that together the elements that make up the structural specimen work as a composite column and not as isolated elements properly. Since the fail happened when the system was loaded with the collapse load, it provoked the failure of the system in relation to the weak axis of the same.

It could be observed that, like a column-like element, the compression capacity of the structure is entirely in relation to the weakness inertia of these elements, so it was proceed to calculate the design capacity to the compression of the system

based on single panel using the LRFD-2005 design expressions for elements subjected to pure compression.



Image XX. Single panel system completely loaded with a side load of 2.70 tons on average. (5).



Image XXI. Plastic deformation outside the plane (residual) of one inch in average as a result of the total discharge of the structural system. (5).

Table VII and Figure VII show the results obtained from the experimental lightweight panel number one, which indicate us analytically and graphically that the test was successfully modeled since the panel shows an elastic behavior and displacements in its Plan similar to those of the Push Over model.

TABLE VII. EXPERIMENTAL TEST RESULTS NUMBER ONE. LOAD VS DISPLACEMENT. (5).

Δx (cm)	P (ton)
0	0
0.016	0.0631342
0.309	1.859179
0.589	1.917606
1.079	2.47267
1.739	2.531098

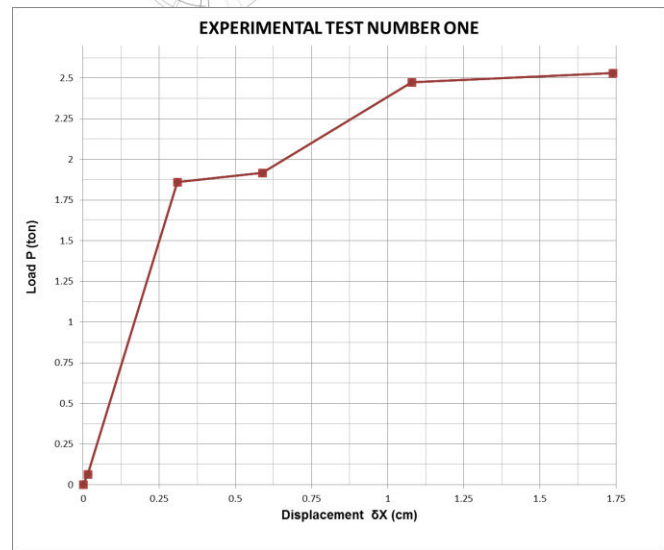


Fig. VII. Behavior of simple panel-based structuring system as a result of experimental test number one. (5).

F. LIGHTWEIGHT PANEL RESULTS NUMBER TWO

Based on the experience gained with the first panel, the inertia of the armored section was calculated, as well as other necessary parameters that are used to calculate the compression capacity of the panel, which is now considered as a column element, Table VIII shows the results obtained from the experimental test and the compressive capacity of panel two in Fig. VIII..

Once these results were obtained, we proceeded to disassemble the lightweight panel number one and mount the lightweight panel number two, taking into account that we are now expected to move out of the plane of the structure since it was observed that the panel works as a column element, a micrometer was mounted on a fixed base was added to the reaction slab measuring lateral displacement (out of plane) to the middle of the same column in which the micrometer of experimental test one was placed. (Image XXII and XXIII).

TABLE VIII. CALCULATION OF THE SLENDERNESS RATIO OF THE SIMPLE PANEL CROSS SECTION. (5).

I_x	26.6647 cm ⁴	Inertia of the armored section about the x-axis
I_x	0.6406 in ⁴	
A_g	11.3124 cm ²	Gross cross-sectional area
A_g	1.75342551 in ²	
r_x	0.60443528 in	Turning radius around the weak axis
L	3.6 m	Length without stranding of the element under compression
L	141.73 in	
k	1	Effective length factor
KL/r	234.48	Slenderness ratio

$$\phi P_{nc} = 7.2038 \text{ klb} \rightarrow 3.27 \text{ ton}$$

Fig. VIII. Compression capacity of light panel number two analyzed as a composite column. (5).



Image XXII. Fixed base to the reaction slab for secondary micrometer.



Image XXIII. Placement of micrometer to column to measure displacements outside the plane of the second panel.

Once the instrumentation of lightweight panel number two was finished, on January 27, 2017, the experimental test was performed at 5:00 pm, just as in the previous test the panel was loaded to the same magnitude indicated in the Push Over analysis, since from this load the panel became practically unstable and could happen some accident if it continued being loaded more. The results obtained with test number two are shown below (Table IX, Figure IX and X), where it is again observed that the number two test was represented in real scale successfully since the panel had a behavior quite similar to the ideal, in addition to that a graphical comparative between the three behaviors reviewed.

TABLE IX. EXPERIMENTAL TEST RESULTS NUMBER TWO. LOAD VS DISPLACEMENT. (5).

Δx (cm)	P (ton)
0	0
0.0174	0.07345
0.293	1.829
0.626	1.946
1.045	2.327
1.7035	2.5174

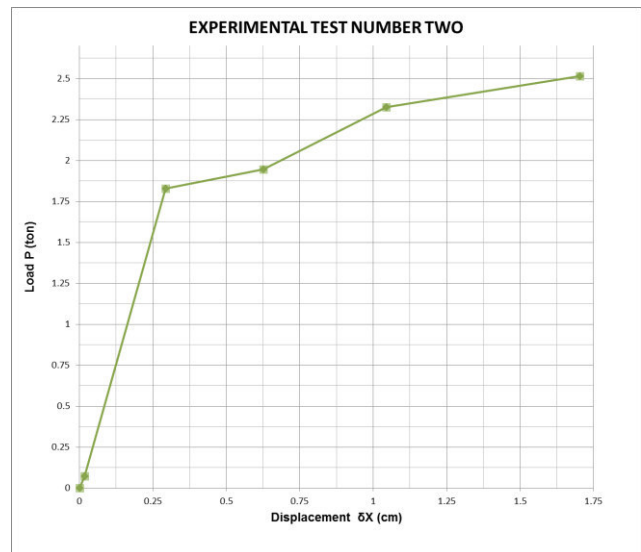


Fig. IX. Behavior of simple panel-based structuring system as a result of experimental test number two. (5).

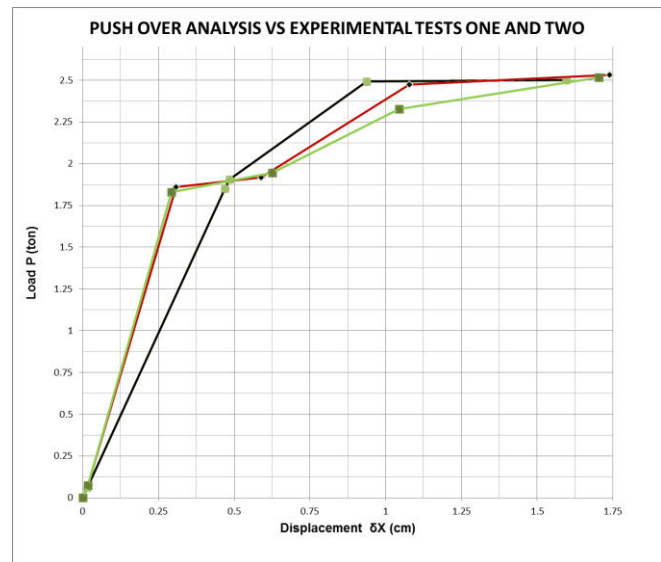


Fig. X. Comparative of behavior analysis product to last capacity "Push Over" vs experimental tests. (5).

IV. CONCLUSIONS AND RECOMMENDATIONS

Based on the results obtained with both experimental tests and the Push Over analysis of the structuring system, it is concluded that the real-scale model of both proposed lightweight panels worked perfectly together as a structural system, which is reflected in Fig. VII "load against displacement" of the Push Over analysis carried out and the results obtained from the tests, showed quite similar graphs which indicates that the connections, welding, screwing, simulation of design loads and instrumentation were used correctly, without leaving aside the correct analytical model. The proposed structuring system fulfilled with the structural design regulations AISC-05LRFD and ANSI-01 LRFD and

can be used for the construction of dwelling houses where simple panels meet the design requirements AISC-05LRFD and ANSI-01 LRFD. The regulations used as standards are referred to the limit states of resistance and service which allowed a viable structuring from the point of structural design for light habitable spaces of the house of social interest type. (5).

Given the limitations of the available infrastructure of the Structures laboratory, the instrumentation and results of 100% experimental tests can not be guaranteed, however there is a great correlation between the results of the analytical models and the results of the instrumentation of the test Of load to final capacity of the structural system type panel, that underpin the conclusions of this work.

It is observed that the structure was dimensioned with steel profiles, commonly used for blacksmithing, since the required strengths are very small, and there are no steel structural profiles for such low demands. These types of profiles are not covered by the standard for Steel Structures. On the other hand, given the thicknesses so thin of low caliber, of this type of profiles that the tiler was engineered to realize and guarantee said welds. Finally, the available resistances were much higher than required, even using the available minimum and weldable profiles. For all of the above, the panel's capacity under design loads is 10% of its ultimate capacity.

There are very few antecedents, of houses results as proposed in this work. The necessity and exigency of having to mount and dismantle easily the support structure of the house, it is opted for a structuring with steel profiles, similar to the conception of industrial buildings, metal structures or temporary structures, to mention.

One of the objectives reached in the development of these structuring systems was to promote a systematic or industrialized construction. It was concluded that the proposal of simple panel-based structuring encourages fully industrialized construction procedures, with a process of manufacturing the structural system in controlled

environments, thus ensuring and improving quality indices compared to conventional systems built *in situ*. (5).

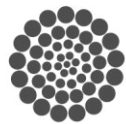
However, it was concluded that there is a need to ensure the quality of the materials and thus the mechanical properties according to the specifications A500 Gr. B for square and rectangular sections, A36 for angled and connecting plate sections as well as guarantee the correct application of welding that conforms to the specifications of the AWS (American Welding Society) regarding the correct application and resistance of the same. (5).

ACKNOWLEDGMENT

F.E. Sosa Guerrero appreciates the opportunity to participate in the Master Thesis project by Ing. J.A. Escalante Valvidia, as well as the confidence in the writing of the present work. We are grateful for funding from the National Council of Science and Technology CONACyT and the management of Dr. Manuel Toledano Ayala, head of the Research and Postgraduate Division of the Faculty of Engineering. Finally we thank the critical reading of the article to Dr. Hilda Romero Zepeda.

REFERENCES

- [1] Aparicio Torres, L.E., 2007. Prototipo de Casa Habitación Hecha de Perfiles Ligeros. Universidad Autónoma De Querétaro.
- [2] McCormac, J. C., & Csernak, S. F. (2013). Diseño de Estructuras de Acero. (A. G. Editor, Ed.) (5th ed.). Mexico D.F.
- [3] Casañas, V., 2011. La Energía Como Indicador del Impacto Ambiental en los Sistemas Constructivos, Conformados a Partir de Materiales de Producción Nacional. Universidad Federal de Rio Grande del Sur-Universidad de la Republicana.
- [4] Novas-Cabreras, J.A., 2010. Sistemas Constructivos Prefabricados Aplicables a la Construcción de Edificaciones en Países en Desarrollo. Universidad Politécnica de Madrid.
- [5] Escalante Valividia, J.A. (2017). Diseño de Estructuras de Acero Ligeras, Prefabricadas, Desmontables y Modulables en Casa Habitación. Tesis de Maestría. (Ing. Civil). Universidad Autónoma de Querétaro
- [6] NTC. (2004). Las Normas Técnicas Complementarias Del Reglamento De Construcciones Para El Distrito Federal. Gaceta Oficial Del Distrito Federal.
- [7] 2012 Bentley Systems, I. (2012). RAM Elements V8 i.
- [8] AISC. (2005). AISC 13th EDITION.
- [9] ASCE, S. (2005). Minimum Design Loads for Buildings and Other Structures. Reston, Virginia 20191.



CONACYT

Consejo Nacional de Ciencia y Tecnología



CONCYTEQ

Physical properties analysis of strawberry grown in aquaponic culture.

Girón Ovalle Elizabeth, García Trejo Juan Fernando.
División de Investigación y Posgrado de la Facultad de Ingeniería.
Universidad Autónoma de Querétaro, UAQ.
Santiago de Querétaro, México.
egiron19@gmail.com

Abstract— Strawberry growth and quality parameters were evaluated in aquaponic systems, as well as physical properties like equatorial diameter, color, wet weight in aquaponic system. System was made of a 1m³ fish tank and a vertical tubular system. Fish were feed three times a day at 8:00 am, 13:00 pm and 16:00 pm with Api-Tilapia 1 MaltaCleyton Brand adjusted to 8% of total biomass at the beginning and 5% at the end. Quality water parameters, pH, dissolved oxygen, conductivity and temperature, were obtained three times at week and nitrate (NO₃) nitrite (NO₂) ammonium (NH₄) twice a month. Fruits were harvested at 75% ripeness base on red color. The parameters of quality present in the strawberry were measured as equatorial diameter, fresh weight and color and the results obtained from an aquaponic culture and soil culture were compared. The equatorial diameter and the wet weight was better in the soil culture than in the aquaponic culture. There was a smaller variation in the dissolved oxygen and the pH in the water of the tank 1 and in tank 2 there was a lower pH variability.

Keywords—aquaponics culture; water parameters; strawberry parameters.

I. INTRODUCTION

According to [1] aquaponics refers to the culture of fish and plants in a closed recirculation system, which is the result of the integration of techniques used in hydroponics and aquaculture. These systems have been widely used throughout the history of mankind, because all great civilizations had been established near rivers or the sea, generating tools and techniques for fishing and aquaculture, as an example the Chinese culture has a tradition of more than 3000 years regarding fish farming refers [2]. Aquaponics try to build systems that resemble natural conditions in a lake or river where the waste produced by an aquatic organism serve as a nutrient source for plants. Of course, this requires the action of intermediary microorganisms as nitrifying bacteria that facilitate the flow of essential nutrients like nitrogen. Plants turn these compounds into nitrates that they can assimilate, by taking them clean the water avoiding crop eutrophication. The basic components of an aquaponic system are: aquatic organisms, plants and recirculation system.

Reference [3] says that aquaponics is gaining attention as a biointegrated food production system, which is done in closed recirculation aquaculture systems. Reference [4] indicates that this is due to the advantages of the system which includes:

prolonged water reuse and minimizing discharges; further integration of the production systems of fish and plants allows cost savings so that the profitability of aquaculture systems is improved. Reference [1] indicates that technological advances in recirculating aquaculture systems stimulated a big interest in it as a potential means to increase profits while some of the waste products are used. In this regard [5] report that conventional treatments of aquaculture discharges represent a significant additional cost; thus aquaponics becomes an alternative treatment of discharges from aquaculture, more economical and profitable.

Also Reference [6] indicates that the aquaculture effluent typically supplies 10 of the 13 required plant nutrients in adequate amounts, with only Ca, K and Fe needing supplementation. Continuous generation of nutrients from fish waste prevents nutrient depletion while uptake of nutrients by the plants prevents nutrient accumulation, extends water use, and reduces discharge to the environment. So that the objective of the present work was to analyze the physical properties of strawberries cultivated in an aquaponic crop without nutrients.

II. MATERIALS AND METHODS

A. Location of the Experiment

The experiment was conducted under greenhouse conditions. The greenhouse was located in Campus Amazcala with dimensions of 15 m long x 7 m wide and where two black plastic tanks were installed with a capacity of 2 m³ equipped with submersible pump of 1/6 hp boyu for water recirculation and the aeration was provided with an oxygen generator ecopet of 1 hp. The experiment was conducted over a period of 23 weeks.

B. Biological Material

Bare-rooted transplants of strawberry “Florida Festival (Fragaria xananassa)” from Zamora Michoacan were grown for horticultural and also were used for aquaculture Nile tilapia (*Oreochromis niloticus. var. Spring*) organisms over 23 weeks.

Each tank initially received 40 tilapia of 10 g mean wet weight and each culture tubular initially received 15 plants of strawberry while for the traditional crop is soil 30 plants of strawberries in pots.

C. Design of Experiments

The experimental design was a 2 x 2 design, where the two treatments interact. The number of replicates per treatment was one (or two experimental units by type of crop) to finally have a total of four experimental units.

Experimental unit consisted of:

a) T1. *Tilapia-strawberry aquaponic system using nutrient film technique (NFT) without nutrients.*

b) T2. *Cutivo in soil irrigated with the water of the fish tank of the aquaponic system.*

D. Associated variables with the measurement of physical-chemical parameters of water.

Determinations of the different forms of nitrogen in water were made, such as; ammonium nitrogen (NH₄), nitrate (NO₃), nitrite (NO₂) every twice a month and the pH, O₂ dissolved, conductivity and temperature determining them systematically three times at week.

E. Associated variables with strawberry biometrics

Response variables in strawberry culture were performed through biometrics, initially all organisms that were in treatment were measured, the measures taken were: Equatorial diameter in millimeters, wet weight in grams and color in hue angle (H). Systematically the same data were taken in a period of 23 weeks.

F. Analysis of collected data

A descriptive analysis expressed as the mean and standard deviation of strawberry harvested (wet weight, equatorial diameter and color in hue angle) in aquaponic systems was performed.

The same procedure was used for quality water in aquaponic systems and these data were plotted in excel.

III. RESULTS

A. Water Quality

A sample was taken every three times at week during the experiment; the data collected is shown in Table 1. The results of the analysis show that the water conductivity has a greater variability than all the other parameters. Reference [7] says that the optimum pH values are between 7 and 9; the temperature between 22 and 29°C, dissolved oxygen greater than 3 mg/L and ammonium higher than 0.05 mg/L.

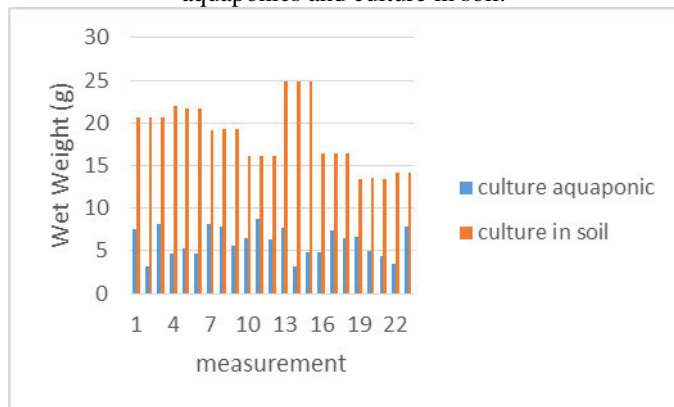
C. Strawberry Culture

The diameter of the strawberries and the weight in an aquaponic culture compared to a crop in soil (graph 1 and graph 2). The graphs show that the strawberries have a better weight and equatorial diameter in the traditional culture in the soil than the aquaponic culture.

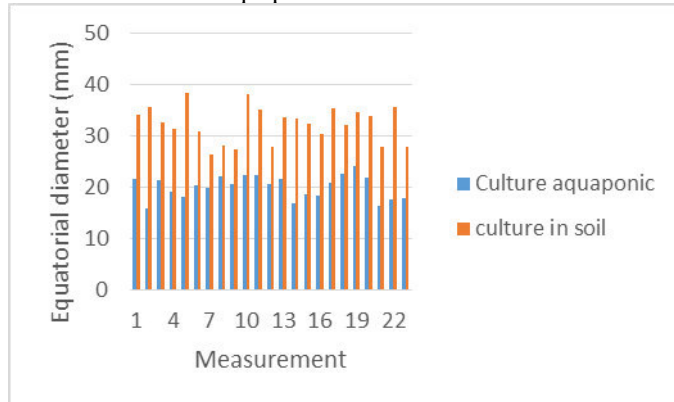
Table 1. Values of physicochemical parameters of water in different treatments during the experiment. Minimum (Min), maximum (Max) average (Avg) and Standard deviation (Std.D.)

Parameters	Tank 1				Tank 2			
	Average	Std. D.	max	Min	Average	Std. D.	Max	Min
Dissolved oxygen (mg/L)	6.79	0.34	7.38	5.69	6.18	0.68	6.9	3.95
Temperature (°C)	20.87	2.24	25.2	16.5	21.59	2.29	26.2	16
Hydrogen potential (pH)	6.88	0.38	7.46	6.08	6.88	0.3	7.32	6.29
Conductivity (mS/cm)	405.96	75.58	604	261	385.91	43.66	446	270
Nitrate (NO ₃ mg/L)	7.3	4	12.1	1.2	4.04	1.01	5.8	2.9
Nitrite (NO ₂ mg/L)	0.037	0.019	0.062	0.018	0.059	0.03	0.09	0.011
Ammonium (NH ₄ mg/L)	0.574	0.31	1.1	0.35	0.83	0.08	0.92	0.72

Graph 1. Strawberry wet weight parameters in a culture aquaponics and culture in soil.



Graph 2. Strawberry equatorial diameter parameters in a culture aquaponics and culture in soil.



IV. DISCUSSION

The dissolved oxygen and de the pH had a lower variation in tank 1 and in tank 2 there was a lower variability in the values of pH. Reference [7] says that the optimum pH values are between 7 and 9; the temperature between 22 and 29°C, dissolved oxygen greater than 3 mg/L and ammonium higher than 0.05 mg/L. It is worth mentioning that the optimum values of pH (7 - 9) are for tilapia cultivation although smaller values are required for the production of strawberries.

Color in hue angle obtained in the aquaponic culture was 3.14 on the red scale; which means that between the farther it is of zero the less red color will be present in the fruit.

Wet weight and equatorial diameter were better in strawberries harvested from a soil crop; suggesting that nutrients have to be added in the aquaponic culture in order to increase their values. Reference [8] mentions that if you have an equatorial diameter less than 32mm the quality of the cutter will be classified as type B, reason why its price in the market will be diminished. Although the temperature measured in the tanks within the optimum values suggested by the literature, reference [9] mentions that the high temperatures cause an

impact on the growth and development of the strawberries; o it is recommended to have a temperature between 10 and 15°C.

It is necessary to perform a mineral analysis of both the water contained in the tank and in the strawberry to be able to see where it is deficient.

It is also important to perform a statistical analysis to determine which of the variables measured in water has a greater significant contribution in the quality of the harvested fruit.

V. CONCLUSION

With the present work it was concluded that it is recommended to make an aquaponic culture supplemented to be able to match the values obtained from the equatorial diameter and the fresh weight in strawberries harvested from a traditional crop in the soil. It is important to do an analysis to see which of the minerals supplemented is the one that will have a greater contribution to the size, color and weight of the strawberries obtained.

ACKNOWLEDGMENT

I greatly thank to National Council of Science and Technology (CONACYT) for the financial support given which helped in the achievement of this article. As well I deeply appreciate the support given by Dr. Juan Fernando García Trejo.

REFERENCES

- [1] J. Rakocy, The status of aquaponics, part 1. Aquaculture Magazine 25: 83-88, 1999.
- [2] R. Pillay, Aquaculture and the Environmen. John Wiley and Sons, Inc, New York, NY, 1992.
- [3] S. Diver, Pond aquaponics: new pathways to sustainable integrate aquaculture and agriculture. Aquanews;34: :10-11, 2006.
- [4] M. Masser, Hydroponics integration with aquaculture. First Ed. Alabama: 23, 2002.
- [5] P.R. Adler, J. K. Harper, E. M. Wade , F. Takeda, and S. T. Summerfelt, Economic analysis of an aquaponic system for the integrated production of rainbow trout and plants. International Journal of Recirculating Aquaculture. 1: 10-13, 2000.
- [6] J.E. Rakocy, R. C. Shultz, D. S. Bailey, and E. S. Thoman, Aquaponic production of tilapia and basil: comparing a batch and staggered cropping system. Acta Horticulturae (ISHS) 648: 63-69, 2004.
- [7] Mjoun, K., and K. A. Rosentrater. 2010. Tilapia: Enviromental Biology and nutritional requirements. North Central Agricultural Research Laboratory, USDA-Agricultural Research Service Michael L. Brown. Department of Wildlife and Fisheries Sciences, South Dakota State University.
- [8] NMX-FF-062-1987. FRUTA FRESCA. FRESA (*FRAGARIA VESCA*). ESPECIFICACIONES. FRESH FRUIT. STRAWBERRY (*FRAGARIA VESCA*). SPECIFICATIONS. NORMAS

MEXICANAS. DIRECCIÓN GENERAL DE
NORMAS.

- [9] Choi, H. G., B. Y. Moon, and N. J. Kang. 2016. Correlation between Strawberry (*Fragaria ananassa* Duch.) Productivity and Photosynthesis-Related

Parameters under Various Growth Conditions. *Frontiers in Plant Science* 7.



Mathematical modeling of leptospirosis in multiple hosts

L.M.A. Hugo Emanuel Sánchez Hernández
Universidad Autónoma de Querétaro
División de Investigación y Posgrado Facultad de
Ingeniería
Querétaro, México
hesh.3765@gmail.com

Dr. Jorge X. Velasco Hernández
Universidad Nacional Autónoma de México
Campus Juriquilla
Instituto de Matemáticas
Querétaro, México
jx.velasco@gmail.com

Abstract: The research of this article is to predict the behavior of an infectious disease called leptospirosis. This disease is commonly transmitted from animals to humans. Transmission among humans is very unusual; it rarely spreads from human to human. Therefore, this article develops a qualitative and quantitative analysis of a mathematical model that simulates the behavior of leptospirosis among animals. In mathematical epidemiology, a fundamental result is the basic reproductive number, since this number indicates on average how many individuals will get infected in a population completely susceptible when is introduced an infected individual. Therefore, article aims to calculate this number and provide a biological interpretation. Finally, using computer software, it simulates the model with the objective of exemplify real cases of infection.

Keywords: dynamical system, leptospirosis, epidemiology.

I. INTRODUCTION

Viruses and bacteria that are found in our body and the environment are, in general, the main cause of infectious diseases. Various methods have been used to their study, such as biologists, physical and mathematical. More than 2000 years ago, Hippocrates had the idea that environmental factors influenced the appearance of new diseases. Later, in the 19th century it began to have anxiety of wanting to eliminate a disease which, at that time, contagious throughout a population. Therefore many investigations were carried out, trying to eliminate, or at least predict where there will be an outbreak of infection and which parameters depends on. These investigations marked the beginning of a discipline dedicated to study infectious diseases and it was until the beginning of the 20th century when the construction of a more formal approach to these diseases began [2].

During the years of 1346 and 1361 an epidemic plague, perhaps the more devastating in the history of humanity hit, in Europe, killing about one-third of the continental population [3]. In 1760, Daniel Bernoulli published a treatise on the

epidemic plague that strongly affected Europe. Later, during 20th century quantitative methods began to apply to biology and physics. A very important result of applying these methods was discovered in 1906, when Hamer formulated the law of mass action which states that the number of infectious contacts per unit time is proportional to the number of contacts among infectious and healthy individuals, this was a very important contribution to mathematical epidemiology. However, it was until 1927, when Kermack and McKendrick made a first mathematical model that could predict the behavior or the dynamics of disease transmission. The model they raised was the famous model SIR, which served as the studio for the epidemic of the bubonic plague that India suffered in 1906 [4].

From that moment, we have studied many infectious diseases, such as measles, smallpox, influenza, SARS and HIV among others. However, there are some diseases which, due to its difficult detection, its study through mathematical tools has not been performed with the desired depth. Such as leptospirosis, zoonosis of world distribution, caused by a bacterium called leptospira (see Figure 1).

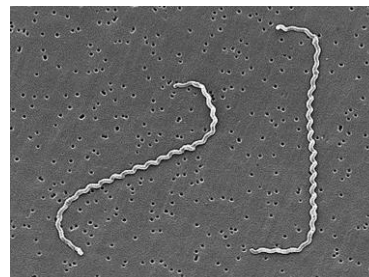


Figure 1. *Leptospira interrogans* is a bacterium in spiral that belongs to the family Leptospiraceae. Its shape is helical, limbs are open and its size is approximately 6.20 x 0.1 microns (National Institute of safety and hygiene at work, 2013). Source: [www.insht.es/RiesgosBiologicos/Contenidos/Fichas%](http://www.insht.es/RiesgosBiologicos/Contenidos/Fichas%20de%20Riesgo)

One of the first references of leptospirosis dates back to ancient times, although this disease continues affecting significantly the health of humans and animals. This produces an infection that can evolve from an inapparent form to so severe forms that require hospitalization [5].

Mathematical models are often used to observe the consequences that an infectious disease would have in a given population. In June 2015, Ohm wrote an (unpublished) study which showed a mathematical model of antibiotic treatment for leptospirosis. In this chapter a similar mathematical model shall be deemed, however, on some terms of the model, are amended in order to be able to observe the effect when leptospirosis is spread from multiple hosts. Subsequently, it will be analyzed with different methods and will show the basic reproductive number obtained by the method of van den Driessche and some derivatives of eliminating certain parameters.

II. MATHEMATICAL MODEL

Dynamic systems that model epidemics are based on the division of the host population in a certain number of compartments, each containing individuals that are identical in terms of their states regarding the disease in question, in our case, leptospirosis. The system covered in this section can have different biological interpretations, depending on the individuals that are considered. For example, leptospirosis is an infectious disease that is commonly spread in animals, then we can consider that the model consists of some animal species that can acquire leptospirosis, because in humans it is just like the contagious, when the human has contact with some infected animal.

In the next system there are eight compartments, we can assume in the first seven equations that they are compartments consisting of animals, ie, cows, dogs, cats, rodents, etc. And the last equation, refers to bacteria in the environment.

- Susceptible (S), individuals who do not have immunity to the infectious agent, therefore, can become infected if they are exposed to the virus.
- Susceptible in treatment (S_T), individuals who have taken a certain amount of antibiotics and have antibodies that protect against leptospirosis.
- Latent of leptospira (L_1), individuals living with the leptospira bacterium, however, still do not present symptoms.
- Latent to another infection (L_2), individuals living infected with another virus and still have no symptoms of them.
- Infectious leptospira (I_1), individuals who are currently infected with leptospira and can transmit the infection to susceptible individuals with whom they have contact.
- Infectious of another bacterium (I_2), individuals who are currently infected with another bacterium and could transmit it to susceptible individuals with whom they have contact.
- Treatment (T), individuals who have received some type of treatment for leptospirosis.

- Environment (E), the population of infectious bacteria, either leptospirosis or bacteria in the environment, including animal hosts.

The resulting mathematical model is shown in equation (1). Mathematical models that consist of many variables are sometimes more explicit if we see them graphically. This behavior can be seen in Figure 2. The dynamics of this model begins as everything, by the birth of susceptible individuals. The compartment of susceptible individuals (S) has a rate of input Δ , representing births per day. With the passage of time, those susceptible individuals have contact, directly or indirectly, with the Leptospira bacteria; either that, by accident, they are in touch with black waters contaminated by rodent urine or any other animal infected with leptospirosis. So, these susceptible individuals can develop infection, however, entering a period of latency (L_1) at a rate $\beta \frac{E^\xi}{E^\xi + \kappa}$ until they show symptoms that reveal that they are infected, where $E(t)$ represents the population of Leptospira in the environment at the time t . After a latency period ends, individuals enter the infectious compartment I_1 and, is here, where the symptoms of the infection can be transmitted to another individual who is susceptible to becoming infected. Finally, infected individuals are treated with some type of antibiotic entering to compartment (T). The compartments (I_2) and L_2 work in a similar way to I_1 and L_1 , respectively, but with any other infectious disease.

$$\begin{aligned}
 \dot{S} &= \Delta + \omega\gamma'T + \eta\mathcal{I}_2 - (\beta + \beta') \frac{E^\xi}{E^\xi + \kappa} S - (1-k)rS - \mu S \\
 \dot{S}_T &= (1-k)r[S + L_1 + I_1] + (1-\eta)\mathcal{I}_2 + (1-\omega)\gamma' - \\
 &\quad \beta'' \frac{E^\xi}{E^\xi + \kappa} S_T - \mu S_T \\
 \dot{L}_1 &= \beta \frac{E^\xi}{E^\xi + \kappa} S - (r + c_1 + \mu)I_1 \\
 \dot{L}_2 &= \frac{E^\xi}{E^\xi + \kappa} (\beta'S + \beta''S_T) - (c_2 + \mu)I_2 \\
 \dot{I}_1 &= c_1L_1 - (r + \mu)I_1 \\
 \dot{I}_2 &= c_2L_2 - (\gamma + \mu)I_1 \\
 \dot{T} &= kr[L_1 + I_1] - (\gamma' + \mu)T \\
 \dot{E} &= \theta(I_1 + I_2) - \delta E
 \end{aligned} \tag{1}$$

III. EQUILIBRIUM POINTS

From common theory of differential equations we know that critic point, equilibrium or steady of a system of differential equations is of great importance, because it is in them where the model presents different kinds of stability, either stable, semi-stable, asymptotically stable or unstable; and to find them, we have to solve the system of equations

equaled to zero. In Mathematical models that simulate an infectious disease, the equilibrium points can be classified into two types:

- Disease-free equilibrium point and
- Endemic infection equilibrium point.

Disease-free equilibrium point is matching the state variables containing individuals that influence the spread of the infection to zero and solving the resulting system, usually this procedure, is not very complicated. However, to find the equilibrium point of endemic infection all the state variables of the model must be contemplated and solve the system. Therefore, if you have a system that contains many non-linear equations, this procedure is not easy to make and often computer software are used to find them.

In this section, we will find disease-free equilibrium point, considering model in (1) and overriding state variables L_1, L_2, I_1, I_2, T and E ; we found disease-free equilibrium point. This point of equilibrium has the following form:

$$E^* = \left(\frac{\Delta}{(1-k)r + \mu}, \frac{(1-k)\Delta}{\mu((1-k)r + \mu)}, 0, 0, 0, 0, 0 \right). \quad (2)$$

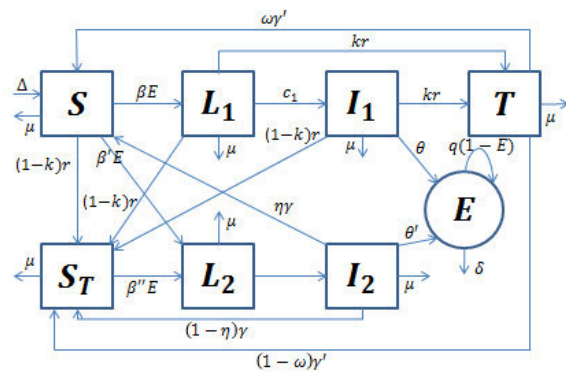


Figure 2. Diagram of leptospirosis model compartments.

IV. BASIC REPRODUCTIVE NUMBER

The basic reproductive number R_0 , is one of the most important results in the study of infectious diseases. This number provides very valuable information regarding the equilibrium points of the model. In this section we will follow closely the van den Driessche method. This method consists of rewriting the mathematical model into two matrices, one containing all terms that generate new infections and the other infections generated by individuals traveling from one compartment to another. We calculate the Jacobian matrix of each one, calling the array of new infections F and the other V . Finally, the basic reproductive number will be the Spectral radius of FV^{-1} , also known as the matrix of next generation. For more details on this method, the reader can see the article "Reproduction numbers and sub-threshold endemic equilibria for compartmental models of disease transmission" by Pauline van den Driessche, [1].

The next-generation matrix has a very interesting interpretation. Each entry (j, k) of the matrix V^{-1} is the average length of time spent by each individual in the j

compartment during its lifetime. And the entry (i, j) of F is the rate at which infected individuals in the compartment j cause new infections in the i compartment. Therefore, the (i, k) entry of the FV^{-1} is the expected number of new infections in the i compartment produced by an infected individual originally introduced from the k compartment. This matrix has the following form:

$$FV^{-1} = \begin{pmatrix} M_{11} & M_{12} & 0 & 0 & M_{15} \\ M_{21} & M_{22} & 0 & 0 & M_{25} \\ 0 & 0 & 0 & 0 & 0 \\ 0 & 0 & 0 & 0 & 0 \\ 0 & 0 & 0 & 0 & 0 \end{pmatrix} \quad (3)$$

$$\text{where } M_{11} = \frac{\beta\theta\Delta}{\delta\kappa((1-k)r + \mu)(r + \mu + c_1)}, \quad (4)$$

$$M_{12} = \frac{\beta\theta\Delta}{\delta\kappa((1-k)r + \mu)(\mu + c_2)}, \quad (5)$$

$$M_{15} = \frac{\beta\Delta}{-kr\delta\kappa + r\delta\kappa + \mu\delta\kappa}, \quad (6)$$

$$M_{21} = \frac{\theta\Delta(\mu\beta_1 + (1-k)r\beta_2)}{\delta\kappa((1-k)r + \mu)(r + \mu + c_1)}, \quad (7)$$

$$M_{22} = \frac{\theta\Delta(\mu\beta_1 + (1-k)r\beta_2)}{\delta\kappa((1-k)r + \mu)(\mu + c_2)} \text{ and} \quad (8)$$

$$M_{25} = \frac{\Delta(\mu\beta_1 + (1-k)r\beta_2)}{-kr\delta\kappa + r\delta\kappa + \mu\delta\kappa}. \quad (9)$$

Then, $R_0 = \rho(FV^{-1})$, where ρ denotes the spectral radius of the matrix FV^{-1} , we can find the basic reproductive number. Thus,

$$R_0 = \frac{\theta\Delta(\beta\mu(c_2 + \mu) + (r(1-k)\beta'' + \mu\beta')(c_1 + \mu + r))}{\delta\kappa\mu(c_2 + \mu)(c_1 + \mu + r)((1-k)r + \mu)} \quad (10)$$

We can say that this R_0 is always positive, since it was expressed in terms of sums and multiplications of positive values, since all parameters of the model are positive and $k < 1$. If $R_0 < 1$, the system has only the disease-free equilibrium point, and this is asymptotically stable, that is, that each solution approaches the disease-free equilibrium point. Then we say that the disease will die.

Conversely, if $R_0 > 1$, then the disease-free equilibrium point is unstable, but there is an endemic point of infection that is asymptotically stable. We say then that the disease will be endemic.

As you can see, the basic reproductive number is a result of great importance, and it is its biological interpretation that shows its true reason. To understand this interpretation we associate the R_0 in more explanatory terms. This is,

$$R_0 = \frac{\theta\beta c_1}{\delta\kappa(r+\mu)(c_1+\mu+r)}S^* + \frac{\theta\beta'}{\delta\kappa(c_2+\mu)}S^* + \frac{\theta\beta''}{\delta\kappa(c_2+\mu)}S_T^* \quad (11)$$

Note that this association can be simplified as follows $R_0 = R_{0,l} + R_{0,c} + R_{0,r}$, where

$$R_{0,l} = \frac{\theta\beta\mu c_1}{\delta\kappa\mu(r+\mu)(c_1+\mu+r)}S^*, R_{0,c} = \frac{\theta\beta'}{\delta\kappa(c_2+\mu)}$$

and $R_{0,r} = \frac{\theta\beta''}{\delta\kappa(c_2+\mu)}S_T^*$. It may be noted that the

terms $R_{0,l}$ and $R_{0,c}$ represents the contribution to overall disease proliferation from leptospirosis and $R_{0,r}$ represents the contribution from other bacterial infections.

V. NUMERIC SIMULATIONS

The simulations of model (1) were performed using an iteration algorithm for differential equations called odeint, using the Python 2.7 program. This function, odeint, solves the initial value problem for systems of ordinary differential equations using the LSODA function of the FORTRAN odepack library.

Therefore, in this section the complete mathematical model will be solved, using the values of the parameters of Table 1. In this Table, some parameters are assumed since there is still no research that supports them. Each of these values has its biological interpretation. For example, Δ is the birth rate per day, so the value of 0.01435 indicates that if we treat a population of, say 100 individuals, then on average 1.43 individual will be born per day. However, we can see that the natural mortality rate is the same value as the birth rate, therefore, this generates a population balances which makes that the population stays constant.

TABLE I. PARAMETERS DESCRIPTION

Parameter	Value	Units	Source
Δ	0.01435	Individuals per day	(assumed)
μ	0.01435	Per day	(assumed)
β	5.5×10^{-6}	Bacteria*	(assumed)
β'	5.5×10^{-6}	Bacteria*	(assumed)
β''	5.5×10^{-6}	Bacteria*	(assumed)

Parameter	Value	Units	Source
r	0.175	Per day	[9]
γ	0.04751	Per day	[10,11]
γ'	0.03333	Per day	[12]
θ	100.0	Bacteria*	[13]
k	0.8	Proportion	(assumed)
κ	0.01	Porportion	(assumed)
η	0.8	Proportion	(assumed)
ω	0.8	Proportion	(assumed)
c_1	0.275	Per day	[9,12]
c_2	0.19	Per day	[8]
δ	0.03333	Per day	[12]

*Millones de bacterias por día.

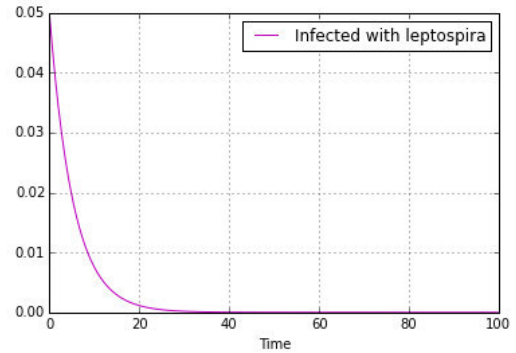


Figura 2. Simulaciones del modelo, tomando $S(0) = 0.95$, $S_T(0) = 0$, $L_1(0) = 0$, $L_2(0) = 0$, $I_1(0) = 0.05$, $I_2(0) = 0$, $T(0) = 0$, y $E(0) = 0.1$ como nuestras condiciones iniciales.

By using the software, Figure 2 is obtained. The purpose of this Figure is to exemplify a real case of leptospirosis infection. This is, supposing we are treating the contagion of leptospirosis in rodents. So S represents the compartment of all healthy rodents capable of contracting the infection, ie, susceptible rodents. S_T represents rodents that have taken a certain amount of antibiotics and have antibodies that protect against leptospirosis. L_1 , rodents living with the leptospira bacteria, however, still without symptoms. L_2 , rodents living infected with another virus and still do not have symptoms of these. I_1 , rodents that are currently infected with leptospira and can transmit the infection to rodents or other susceptible animals with whom they have contact. I_2 , rodents that are currently infected with another bacterium and can transmit it to other susceptible animals with which they have contact. T , rodents that have received some type of treatment for leptospirosis and E , the population of infectious bacteria, both leptospirosis and other bacteria in the environment, including host animals of the infection. The value of the initial condition S , indicates that we are considering (at scale) a population of 0.95 susceptible rodents, however, if to that population of susceptible rodents will enter a small population of 0.05 infected rodents with leptospirosis (initial condition of I_1)

Then there will be no outbreak of infection, this is, leptospirosis does not spread. This result is not only due to the initial conditions taken, but also to the values of the parameters that were assigned.

VI. LATIN HYPERCUBE SAMPLING

When we want to simulate a mathematical model there is uncertainty, we don't know if the values of the parameters are adequate to get results attached to real life. Then we gave the task of simulating several cases, we wanted to give different values to the parameters in a conventional way, and it is precisely the latin hypercube sampling that can provide these values, because we haven't any data we can assign a probability distribution to all parameters and then these would take the values that the distribution provides [7].

Latin hypercube sampling is, in general, a statistical method that is used to generate samples from values that have some probability distribution [6]. In the study of mathematical models this type of sampling is mixed with the sensitivity analysis, this analysis is a very useful method or tool that allows you to explore the full space of parameters of a mathematical model [7].

The mathematical model presented in equation (1), consists of 16 parameters, of which 15 are uncertain, because no study has been done for the correct assignment of these values. However, it is possible to perform simulations and observe the behavior of the leptospirosis dynamics depending on the variation of the parameters. In this section we will perform the steps that are described in Chapter 2 of the Boloye Gomero master's thesis entitled "Latin Hypercube Sampling and Partial Rank Correlation Coefficient Analysis Applied to an Optimal Control Problem".

We perform an analysis for sixteen of the seventeen full model parameters, using Latin Hypercube Sampling to simulate the model 100 times with 100 different parameter combinations. We continue to use an uniform distribution for all parameters.

Once again, the aim is to exemplify cases of contagion and spread of leptospirosis. In the previous section it was mentioned, for example, that individuals were rodents, but this concept can be generalized to several animals, such as cows, dogs, cats, etc; because they are the animals with which the human lives in a more direct way and then they could accidentally infect him with leptospirosis if the human is exposed to the bacteria.

The results of these simulations is shown in Figure 3. To assimilate this graph with a real case of leptospirosis contagion, suppose that a natural disaster occurred in certain population, say a flood. Then the probability of infection is altered quickly and growing. Then, if we restrict the population to only 0.05 individuals infected with leptospirosis and suppose that there isn't infected from any other disease, then we can see that values that took parameters infection of

leptospirosis (blue color) do not spread, however was not the case for other diseases (red color).

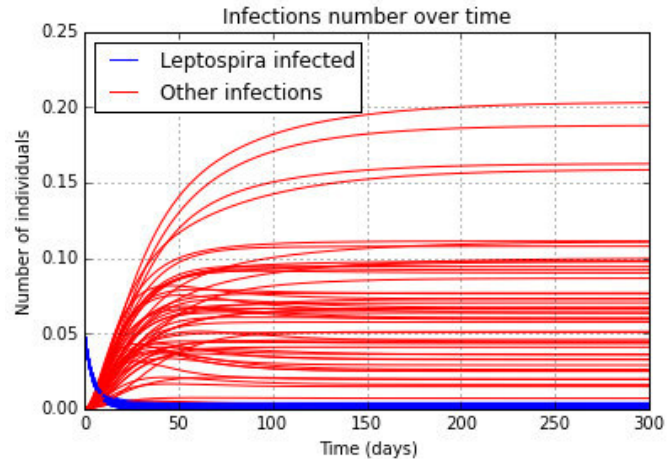


Figure 3. Simulations of the model using the Latin hypercube sampling method, taking $S(0) = 0.95$, $S_T(0) = 0$, $L_1(0) = 0$, $L_2(0) = 0$, $I_1(0) = 0.05$, $I_2(0) = 0$, $T(0) = 0$ and $E(0) = 0.1$ as our initial conditions.

VII. CONCLUSION

For each of the simulations performed the basic reproductive number can be obtained, and then we can know, when it is greater than one, that there will be an outbreak of leptospirosis. To observe the importance of the parameters in the basic reproductive number, Table 2 was generated. We can conclude that when the parameters have an uniform distribution, we have an approximate classical probability of 0.05 that there is an epidemic outbreak, considering that were 100 simulations of which five were less than one.

TABLE II. R_0 STATISTICS

R_0	
Minimum	0.4010
Maximum	9.7565
Mean	2.9659

Therefore, there is a higher probability of epidemic outbreak, which is due to the distribution of the parameters. That is a very interesting observation because in everyday life an effective measure of control can be applied for the prevention of leptospirosis and to be able to prevent epidemic outbreaks in the animals and thus, to avoid humans are infected. Figure 3 shows the simulations performed by latin hypercube sampling, this in order, again, to exemplify a case of infection in some animal host of the infection.

This research is an attribution to epidemiology through mathematics. We can observe that if biology, medicine and mathematics are combined in any way, very important results

will be obtained in terms of the eradication and control of infectious diseases.

Perhaps the fundamental use of this work is to be presented in research centers dedicated to the control of epidemics; because we could contribute that mathematics enrich this area and we could predict trends that present infectious diseases in a long term.

REFERENCES

- [1] Pauline Van den Driessche and James Watmough. Reproduction numbers and sub-threshold endemic equilibria for compartmental models of disease transmission. *Mathematical biosciences*, 180(1):29–48, 2002.
- [2] Ruth Bonita, Robert Beaglehole, and Tord Kjellström. *Epidemiologia básica*, 2008.
- [3] Sean Martin. *The Black Death*. Oldcastle Books, 2011.
- [4] Jorge X Velasco Hernández. *Modelos matemáticos en epidemiología: enfoques y alcances*. 2007.
- [5] Omelio Rodríguez Cepero, Ricardo Oses, and Ramón Cardoso. *Modelación matemática en la predicción de la leptospirosis*. 2013.
- [6] N Baron. *Técnicas estadísticas avanzadas en el análisis de grandes modelos computacionales*. In *Congreso latinoamericano de métodos computacionales para Ingeniería*. Argentina, 1999.
- [7] Boloye Gomero. Latin hypercube sampling and partial rank correlation coefficient analysis applied to an optimal control problem. 2012.
- [8] Jan Kluytmans, Alex Van Belkum, and Henri Verbrugh. Nasal carriage of staphylococcus aureus: epidemiology, underlying mechanisms, and associated risks. *Clinical microbiology reviews*, 10(3):505-520, 1997.
- [9] Alan R Katz, Vernon E Ansdell, Paul V E_er, Charles R Middleton, and David M Sasaki. Assessment of the clinical presentation and treatment of 353 cases of laboratory-con_rmed leptospirosis in hawaii, 1974{1998. *Clinical infectious diseases*, 33(11):1834-1841, 2001.
- [10] Sara E Cosgrove and Vance G Fowler. Management of methicillinesistant staphylococcus aureus bacteremia. *Clinical infectious diseases*, 46 (Supplement 5):S386-S393, 2008.
- [11] Vance G Fowler Jr, Helen W Boucher, G Ralph Corey, Elias Abrutyn, Adolf W Karchmer, Mark E Rupp, Donald P Levine, Henry F Chambers, Francis P Tally, Gloria A Vigliani, et al. Daptomycin versus standard therapy for bacteremia and endocarditis caused by taphylococcus aureus. *New England Journal of Medicine*, 355(7):653-665, 2006.
- [12] Paul N. Levett. Leptospirosis. *Clinical Microbiology Reviews*, 14(2):296-326, 2001.
- [13] Islay Rodríguez, Iuley Rodríguez, Carmen Fernández, José E Rodríguez, and Jorge Cantillo. Detection of leptospire from infected urine and tissue samples in vitro by modified fontana silver stain. *Jornal Brasileiro de Patologia e Medicina Laboratorial*, 49(1):39-45, 2013.



Tour Planning for the Small Unmanned Meteorological Observer

Licon-Gutierrez Diego A. , Gonzalez-Gutierrez Arturo, Morales-Velazquez Luis
School of Engineering
Autonomous University of Queretaro
Queretaro, MEXICO
dlicon16@alumnos.uaq.mx, aglez@uaq.mx, lmoales@hspdigital.org

Abstract—This work describes the tour planning for Small Unmanned Meteorological Observer (SUMO). The paper present a method to produce the tour planning based on the Traveler Salesperson Person (TSP), which uses greedy heuristic, Christofides algorithm and tour improvement (2-opt and 3-opt).

Keywords—wireless sensor networks; meta-heuristics algorithms; traveling salesperson problem; small unmanned meteorological observer

I. INTRODUCTION

Currently the measurements of meteorological variables are carried out by electronic sensors, which acquire a physical variable and represent its magnitude with an electrical equivalent, either digital or analog. There is a large number of observing systems, for example, automatic weather stations, balloon techniques, aeronautic meteorological stations, aircraft observations, etc. [1].

Meteorological prediction has improved significantly in recent years with advances in observational methods, data assimilation and modeling techniques[2]. Meteorological multicopter represent an economical and flexible platform for measurements of temperature and humidity in the atmospheric boundary layer [3].

Multicopter is a multirotor unmanned aircraft system (UAS). UAS are known under various different names and acronyms, such as “Unmanned Aerial Vehicle” (UAV), “aerial robot” or simply “drone”[4].

Multicopters are similar to helicopters but should be treated as a separate group of flying objects. They have higher maneuverability due to engines with fixed pitch propeller. Each motor is controlled independently by the flight controller, this feature allows a better precision than rotor standard helicopters [5].

As quadrotors become increasingly common, capable, and affordable, their utility as a mobile sensor platform continues to grow. Accordingly, this platform has potential applications in wind field estimation for urban planning and climatology, dispersion studies, atmospheric measurement, wind turbine site analysis, and structure design[6].

Either fixed wing or multicopters aircraft have been used for monitoring meteorological variables, withstanding a maximum wind speed of 8 m/s [7]–[10]. Although environmental research with airborne equipment is becoming very popular, professional literature on small multirotor devices subject is still extremely scarce, and is still on a hobbyist grade[11], [12].

In reference [7], it is established that an UAV with the capability to perform measurements of temperature, relative humidity and atmospheric pressure are denominated as Small Unmanned Meteorological Observer (SUMO).

However, making measurements with a SUMO adds problems inherent to UAV, as the performance of the battery and the aircraft control. Typically a drone has about 20 minutes of flight time, and the fuel cells downtime currently required for recharging between flights goes from one to two hours[13].

Experience shows that a careful design of the aircraft trajectory (waypoints, strips, speed, attitude, etc.) and a flexible real-time mission management capacity (sensor configuration, triggering events, flying directions, etc.) are essential in achieving productive and safe acquisition missions[10].

In addition, there is still the problem of the mission planner. The mission planner must sort the points of interest, minimizing the total length of the tour. Mission planning and real-time mission management subsystems are the key to a competitive exploitation of UAS for photogrammetry and remote sensing[4].

In references [7]–[9], it is established that the UAV has a Region of Interest (ROI) with a set of points that need to be visited. All the points must be visited, and normally these points are visited only once. These characteristics have a great similarity with the Traveling Salesperson Problem (TSP).

This paper offers a solution for the mission planner, computing the minimal tour using a set of metaheuristic algorithms.

II. PROBLEM

The TSP consist of graph $G = (C, D)$. The set $C = \{c_1, c_2, \dots, c_N\}$ of cities is the vertex set, and for each pair (c_i, c_j) of distinct cities a distance (edge) $D = \{(i, j) : i, j \in C, i < j\}$ that represents the cost of travelling from c_i to c_j . A cost matrix $C = (c_{ij})$ is defined on D . The cost matrix satisfies the triangle inequality whenever $c_{ij} \leq c_{ik} + c_{kj}$, for all i, j, k .

The TSP consist in finding the best possible way of visiting all the cities and returning to the starting point, minimizing the total travel cost (or travel distance). The goal is to find an ordering σ of the cities that minimizes the total tour length, as follows:

$$\text{Minimize } \sum_{i=1}^{N-1} d(c_{\sigma(i)}, c_{\sigma(i+1)}) + d(c_{\sigma(N)}, c_{\sigma(1)}) \quad (1)$$

Let n be the number of cities to be visited, then the total number of possible tours covering all cities, as a set of feasible solutions for the TSP, and is given by $n!$. The TSP is a well-known NP-Hard problem. Normally solving the TSP optimally takes a considerable amount of time, instead usually uses approximation algorithms, or heuristics[14].

In reference [15], it is established that the TSP is classified as symmetric TSP (sTSP), asymmetric TSP (aTSP), and multi TSP (mTSP). Following we describe briefly described each of categories;

sTSP: Let $C = \{c_1, c_2, \dots, c_N\}$ be a set of cities, $A = \{(c_i, c_j) : c_i, c_j \in C\}$ be the edge set, and $d(c_i, c_j) = d(c_j, c_i)$ be a cost measure associated with edge $(c_i, c_j) \in A$. In the particular case of planar problems for which the vertices are points $P_i = (x_i, y_i)$ in the plane, and the Euclidean distance between c_i and c_j is given by;

$$d(c_i, c_j) = \sqrt{(x_j - x_i)^2 + (y_j - y_i)^2} \quad (2)$$

aTSP: If $d(c_i, c_j) \neq d(c_j, c_i)$ for at least one (c_i, c_j) then the TSP becomes an aTSP.

mTSP: The mTSP is defined as: In a given set of nodes, let there are m salesmen located at a single depot node. The remaining nodes (cities) that are to be visited are intermediate nodes. Then, the mTSP consists of finding tours for all m salesmen, who all start and end at the depot, such that each intermediate node is visited exactly once and the total cost of

visiting all nodes is minimized. The cost metric can be defined in terms of distance, time, etc.

In this paper when we speak of TSP, we will refer to the sTSP.

III. METAHEURISTIC ALGORITHMS

We use three different approaches to solve our planning flight: Local Search, Greedy Strategy, and Approximation Algorithm. For the first case, we propose the 2-opt and 3-opt meta-heuristics, which consist of 2 or 3 permutations as the search is performed in the solution neighborhood.

We propose also a greedy algorithm according to the criterion of the shortest path connecting two points during the construction of the tour. Finally, we use the famous Christofides Approximation Algorithm [16], which produces solutions within 1.5 times the optimal solution. As follows we provide more detail of these algorithms.

A. Greedy

The Greedy heuristic gradually constructs a tour by repeatedly selecting the shortest edge and adding it to the tour as long as it doesn't create a cycle with less than N edges, or increases the degree of any node to more than 2. It must not add the same edge twice of course. Complexity of the greedy heuristic is $O(n^2 \log_2(n))$. Steps of Greedy approach are:

1. Sort all edges.
2. Select the shortest edge and add it to our tour if it doesn't violate any of the above constraints.
3. Do we have N edges in our tour? If not, repeat step 2.

The Greedy algorithm normally keeps solution within 15-20% of the Held-Karp lower bound [17].

B. Cristofides algorithm

Most heuristics can only guarantee a feasible solution or a fair near optimal solution. Christofides extended one of these heuristic approaches which is known as Christofides heuristic. Complexity of this approach is $O(n^3)$. The steps are given below:

1. Build a minimal spanning tree from the set of all cities.
2. Create a minimum-weight matching (MWM) on the set of nodes having an odd degree. Add the MST together with the MWM.
3. Create an Euler cycle from the combined graph, and traverse it taking shortcuts to avoid visited nodes.

C. Tour improvement (2-opt and 3-opt)

After generating the tour using any tour construction heuristic, an improvement heuristic can be further applied to improve the quality of the tour generated. Popularly, 2-opt and 3-opt exchange heuristic is applied for improving the solution. The performance of 2-opt or 3-opt heuristic basically depends on the tour generated by the tour construction heuristic.

IV. METODOLOGY

The 2-opt algorithm removes randomly two edges from the already generated tour, and reconnects the new two paths created. This is referred as a 2-opt move. The reconnecting is done such a way to keep the tour valid (see Fig 1 (c)). This is done only if the new tour is shorter than older. This is continued till no further improvement is possible. The resulting tour is now 2 optimal.

The 3-opt algorithm works in a similar fashion, but instead of removing the two edges it removes three edges. This means there are two ways of reconnecting the three paths into a valid tour (see Fig. 1(d)). Search is completed when no more 3-opt moves can improve the tour quality.

Running the 2-opt move often results in a tour with a length less than 5% above the Held-Karp bound. The improvements of a 3-opt move usually generates a tour about 3% above the Held-Karp bound [17]

D. Simulated Annealing

Simulated Annealing (SA) is basically a randomized local search algorithm that do not allow path exchange that deteriorates the solution. In general SA, uses 2-opt exchange mechanism for searching better solution in a neighborhood-search. A problem with simple neighborhood search approach i.e. only 2-opt or 3-opt exchange heuristic is that these can easily get stuck in a local optimum.

E. The Held-Karp lower bound

This lower bound is the common way of testing the performance of any new TSP heuristic. A Held-Karp (HK) lower bound averages about 0.8% below the optimal tour length [17]. For more details regarding the HK lower bound, paper by [17] can be referred.

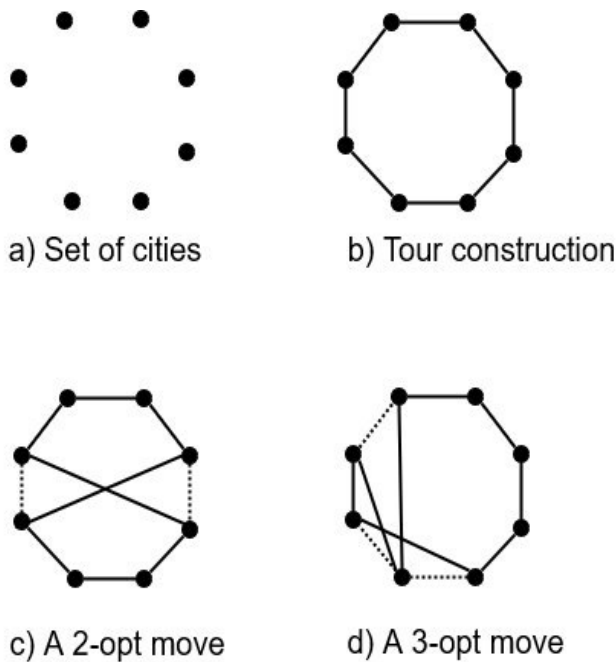


Fig. 1. A 2-opt and 3-opt move.

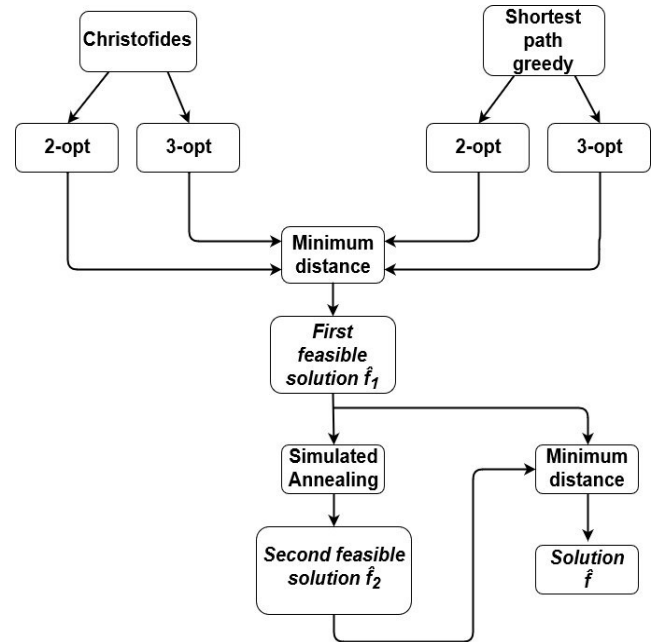


Fig. 2. Methodology to implement.

In Fig. 2 it is shown the flowchart of an approximate approach, an approximate approach never guarantee an optimal solution but gives near optimal solution in a reasonable computational effort[15]. It starts with two paths, first with the Christofides algorithm, which ensures at most 3/2 than optimal TSP solution[16].

All tour construction algorithms stop when a solution is found and never tries to improve it. It is believed that tour construction algorithms find solution within 10-15% of optimality [15], due to this, an enhancement is sought, the tour improvement to implement will be the 2-opt and 3-opt local search algorithms.

On the other hand, the second path starts with the greedy heuristic. Once the tour has been generated, a tour enhancement is applied. The tour improvement will be the 2-opt and 3-opt local search algorithms, just like on the first path. It is believed that tour construction algorithms find solution within 10-15% of optimality

At this point, there are 4 possible solutions, whereby a minimum distance filter is applied, this will be select the option with the minimum distance, giving the first feasible solution \hat{f}_1 .

Once \hat{f}_1 is calculated, the algorithm try to find an enhancement, applying a simulated annealing (SA). Although SA is also a local search algorithm, allows to visit moves not visited by the other local search algorithms, due to SA allows moves with negative gain. The SA give a second feasible solution \hat{f}_2 . By last, a minimum distance filter is applied, selecting the option with the minimum distance between \hat{f}_1 and \hat{f}_2 , giving the feasible solution \hat{f} as result.

V. STUDY CASE

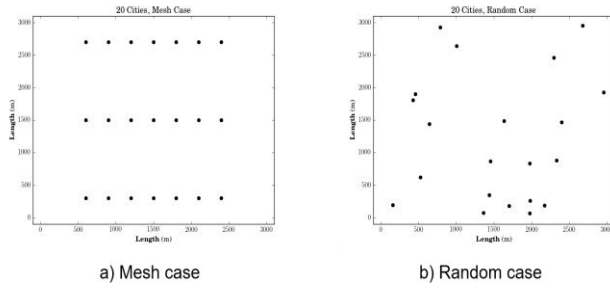


Fig. 3. Study cases.

In references [4], [5], [9], it is established that multicopters typically have an endurance of 15 to 30 minutes, and a maximum speed of 10 m/s over ground. This paper supposed a region of interest (ROI) with 20 points, starting with a point that does not belong to the ROI, an average speed of 10 m/s and an endurance of 20 minutes.

Due to this the quadcopter, will have an overcoming distance of approximately 12000 m. Thus, the total length of the planning flight must be less of 12000 m, and cover the 20 points of interest. In our study case we will supposed that the ROI have a square shaped figure with 3000 meters per side and an area of 9000 m².

A. Mesh case

This case consists on a starting point, and 20 points inside of the ROI. These points are generated by trying to cover as much surface area as possible of the ROI (see Fig 3 (a)).

B. Random case

This case consists on a starting point, and 20 points inside of the ROI. These points are generated randomly and suppose the case in which the user doesn't care the cover area of the points (see Fig 3 (b)).

VI. PERFORMANCE

Below it is show the validation of the method using a set of points clustered neatly, trying to cover as much surface area as possible of the ROI, this represents the worst-case .

The Figure 5 shows that the methods have 21 points, due to it consider the starting position of the UAV. The method start with two paths, one branch start with Christofides algorithm, and apply the 2-opt tour improvement. In our case the 2-opt algorithm doesn't find a better solution for Christofides algorithm.

On the other branch the greedy strategy find a worse solution than the Christofides algorithm, this is due to Christofides is an approximation algorithm produces solutions within 1.5 times the optimal solution, and in this case the greedy strategy has a higher tour length. However, the 2-opt find a solution better than greedy strategy

Finally, the simulated annealing find the better solution of the method, the initial temperature began at 100, and the rate of decrease was 0.9995 times. The Table 1 shows the performance for each method.

Initial Path	Test of methods			
	Tour improvement	f_1	f_2	f
10434 m. ¹	10431.0 m. ³	10431.6m. ⁵	10341.6 m. ⁶	10341.6 m. ⁷
10800 m. ²	10620.9 m. ³			

1. Christofides algorithm.
2. Greedy strategy.
3. 2-opt.
4. \min [Christofides->2-opt, Greedy->2-opt]
5. Simulated Annealing.
6. \min [Christofides->2-opt, Greedy->2-opt, Simulated Annealing].

Fig. 4. Results of the test on a mesh case.

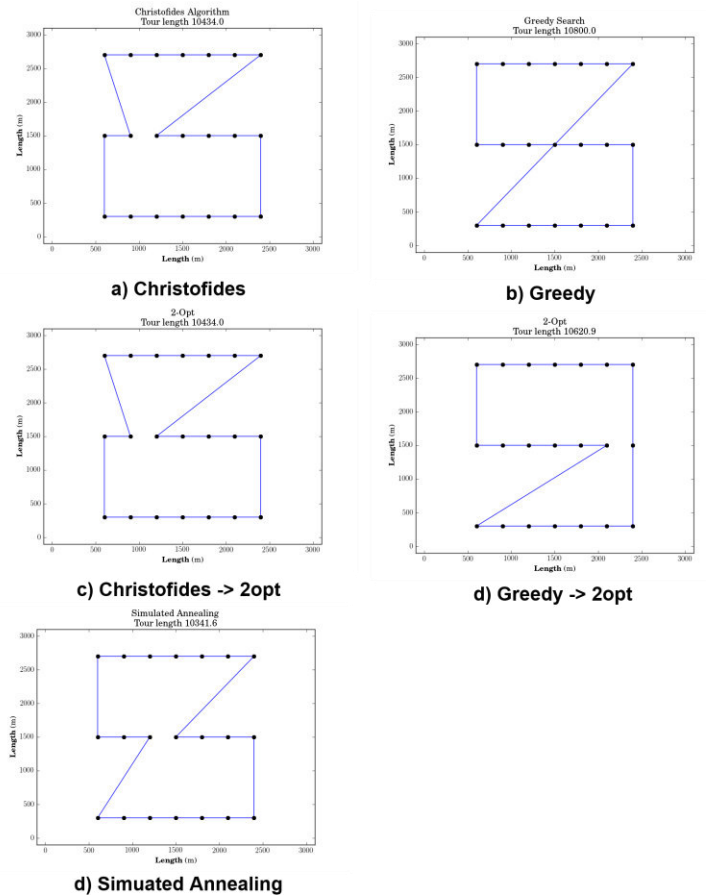


Fig. 5. Mesh case performance.

VII. CONCLUSIONS

The results show that the methodology implemented minimizes the total length of the flight plan, improving gradually as the method progresses. The initial value began with 10800 meters and ended with 10341.6 meters, representing a reduction of 458.6 meters and an improvement of 4.25%. On the other branch the initial value began with 10434 meters and ended with 10341.6 meters, representing a reduction of 92.4 meters and an improvement of 0.88%.

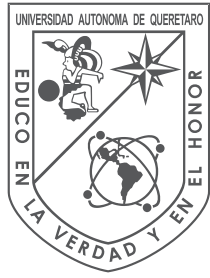
The preliminary results obtained from the tests indicate a better performance than Christofides algorithm which is an approximation algorithm, such algorithm produces solutions within 1.5 times the optimal solution. Therefore, our method is below 1.5 times the optimal solution.

ACKNOWLEDGMENT

We wish to thank Autonomous University of Queretaro (UAQ) for the infrastructure and academic support for this project research and CONACYT for the financial support.

REFERENCES

- [1] W. M. Organization, *Guide to Meteorological Instruments and Methods of Observation*, Seventh. Geneva, Switzerland: Charperson, Publication Board, 2008.
- [2] A. J. Simmons and A. Hollingsworth, "Some aspects of the improvement in skill of numerical weather prediction," *Q. J. R. Meteorol. Soc.*, vol. 128, no. 580, pp. 647–677, 2002.
- [3] S. Mayer, M. Jonassen, A. Sandvik, and J. Reuder, "The meteorological UAV SUMO: A new perspective for the evaluation of atmospheric boundary layer schemes in fine-scale atmospheric models," *Assembly*, vol. 11, p. 2009, 2009.
- [4] I. Colomina and P. Molina, "Unmanned aerial systems for photogrammetry and remote sensing: A review," *ISPRS J. Photogramm. Remote Sens.*, vol. 92, pp. 79–97, 2014.
- [5] S. Anweiler and D. Piwowarski, "Multicopter platform prototype for environmental monitoring," *J. Clean. Prod.*, vol. xxx, Oct. 2016.
- [6] P. Bruschi, M. Piotta, F. D. Agnello, J. Ware, and N. Roy, "Wind speed and direction detection by means of solid-state anemometers embedded on small quadcopters," *Procedia Eng.*, vol. 168, pp. 802–805, 2016.
- [7] J. Reuder and M. O. Jonassen, "First results of turbulence measurements in a wind park with the Small Unmanned Meteorological Observer SUMO," *Energy Procedia*, vol. 24, no. January, pp. 176–185, 2012.
- [8] P. P. Neumann and M. Bartholmai, "Real-time wind estimation on a micro unmanned aerial vehicle using its inertial measurement unit," *Sensors Actuators, A Phys.*, vol. 235, pp. 300–310, 2015.
- [9] P. P. Neumann, S. Asadi, V. H. Bennetts, and A. J. Lilienthal, "Monitoring of CCS Areas using Micro Unmanned Aerial Vehicles (MUAVs)," *Energy Procedia*, vol. 37, pp. 4182–4190, 2013.
- [10] W. Mayr, "UAV-MAPPING – A USER REPORT," *Int. Arch. Photogramm. Remote Sens. Spat. Inf. Sci.*, vol. XXXVIII, pp. 1–6, 2011.
- [11] S. Energy, A. Plans, and S. Francisco, "Sustainable development of energy, water and environment systems index for Southeast European cities," vol. 130, pp. 222–234, 2016.
- [12] C. Nicol, C. J. B. Macnab, and A. Ramirez-serrano, "Mechatronics Robust adaptive control of a quadrotor helicopter," *Mechatronics*, vol. 21, no. 6, pp. 927–938, 2011.
- [13] "Intelligent Energy fuel cells significantly boost drone flight time expand Indonesia R & D," no. January, p. 2016, 2016.
- [14] C. Nilsson, "Heuristics for the Traveling Salesman Problem."
- [15] R. Matai, S. P. Singh, and M. L. Mittal, "Traveling Salesman Problem: An Overview of Applications, Formulations, and Solution Approaches," 1976.
- [16] N. Christofides, "WORST-CASE ANALYSIS OF A NEW HEURISTIC FOR THE TRAVELLING SALESMAN PROBLEM," Report 388, Graduate School of Industrial Administration, Carnegie Mellon University, 1976.
- [17] D. S. J. L. A. Mcgeoch and E. E. Rothberg, "Asymptotic Experimental Analysis for the Held-Karp Traveling Salesman Bound."



UNIVERSIDAD
AUTÓNOMA DE
QUERÉTARO

